ACTA CHIMICA

ACADEMIAE SCIENTIARUM HUNGARICAE

TOMUS 103 FASCICULUS 1

AKADÉMIAI KIADÓ, BUDAPEST

1980

ACTA CHIM. ACAD. SCI. HUNG. ACASA2 103 (1) 1–109 (1980)

ACTA CHIMICA

A MAGYAR TUDOMÁNYOS AKADÉMIA KÉMIAI TUDOMÁNYOK OSZTÁLYÁNAK IDEGEN NYELVŰ KÖZLEMÉNYEI

Acta Chimica is a journal for the publication of papers on all aspects of chemistry in English, German, French and Russian.

Acta Chimica is published in 3 volumes per year. Each volume consists of 4 issues of varying size.

Manuscripts should be sent to

Acta Chimica
Budapest, P.O. Box 67, H-1450, Hungary

Correspondence with the editors should be sent to the same address. Manuscripts are not returned to the authors.

Subscription: $ 36.00 per volume.

Hungarian subscribers should order from Akadémiai Kiadó, 1363 Budapest, P.O. Box 24. Account No. 215 11488.

Orders from other countries are to be sent to "Kultura" Foreign Trading Company (H-1389 Budapest 62, P.O. Box 149. Account No. 218 10990) or its representatives abroad.

ACTA CHIMICA

ACADEMIAE SCIENTIARUM HUNGARICAE

TOMUS 103

AKADÉMIAI KIADÓ, BUDAPEST

1980

ACTA CHIMICA

TOMUS 103

Fasciculus 1

Fasciculus 2

Fasciculus 3

Fasciculus 4

INDEX

Acta Chimica Academiae Scientiarum Hungaricae, Tomus 103 (1), pp. 1—8 (1980)

EFFECT OF MERCURY ON THE ANODIC BEHAVIOUR OF GALLIUM

K. SZABÓ and K. G. SÓLYMOS

(Department of Physical Chemistry and Radiology, Eötvös L. University, Budapest)

Received 13 December 1978

Accepted for publication February 13, 1979

In a 1 mol dm^{-3} solution of hydrogen chloride the dissolution of liquid and solid gallium anodes has been studied as a function of mercury present as an impurity. Already at a concentration of 9.7×10^{-5} at.%, mercury alters the rate of dissolution of a solid gallium anode in both its active and passive regions. In contrast, a liquid gallium anode is dissolved at a rate which remains virtually unchanged even in the presence of 1.7×10^{-2} at.% mercury. The rate, $\lg j$, of the dissolution of a solid gallium anode with a small mercury contamination (10^{-4}—10^{-3} at.%) is linearly increased in both the passive and active regions, with increasing concentration of mercury ($\lg C_{Hg}$). This increase caused by mercury is reduced when its concentration increases, *i.e.* $\frac{\partial \lg j}{\partial \lg C_{Hg}}$ decreases.

Presumably the atoms of mercury present as an impurity adsorbed on the surface of solid gallium weaken the bonding of gallium atoms adjacent to them and thus break up the oxide layer, which is present also in the active region on the solid gallium surface and inhibits its dissolution, in consequence of this, anodic dissolution is enhanced.

The changes of some electrochemical properties of gallium as a function of the purity of this metal can be measured accurately. Thus, for instance, p.p.m. metal impurities of gallium are either adsorbed on its surface (Hg, Pb), or change its lattice parameters (Ag), both affecting the hydrogen overvoltage [1].

It may be expected that changes in the surface state or the crystal structure of the electrode metal in its also affect the anodic behaviour of gallium. There is ample indication in the literature that also slight amounts of alloying metals significantly change the anodic behaviour of metals. According to studies carried out by IVANOV *et al.* [2], 0.8% mercury in aluminium shifts the restpotential of the latter towards negative values. Small amounts of gallium, indium or thallium (0.01—0.02%) significantly affect the anodic behaviour of aluminium; its restpotential is shifted to negative values and, compared with results for pure aluminium, the rate of its anodic dissolution is significantly increased [3]. Similar results are described [4] in the cases of aluminium and indium, or aluminium and tin alloys, if the quantity of alloying indium or tin is between 0.5 and 6.0%.

In a review by KHOLOTYRKIN [5], mention is made of a connection between the purity of the metal and its rate of auto-dissolution: according

to this, the rate of auto-dissolution of pure iron and that of iron electrodes which contain some alloying metal differ by 0.5—1.0 order of magnitude. Also in the case of anodes in galvanic cells the effect of metal contaminants has been thoroughly studied. The rate of auto-dissolution of the negative plate of a lead cell is substantially increased by one p.p.m. platinum; though to a lesser degree, also copper, bismuth and silver impurities accelerate the auto-dissolution of lead [6].

The effects of the various alloying metals in steel or in other structural metals are extensively studied also with regard to their resistance to corrosion [7]. The hydrogen overvoltage of gallium is significantly increased by mercury impurities. This might be explained by the adsorption of mercury on the gallium surface, which covers one part decreases the area of free surface [8]. It might be supposed that impurities well adsorbing on the surface affect also the anodic behaviour of gallium by changing the state of the electrode surface. Earlier studies [8] show that gallium is easily contaminated with mercury and that the concentration of the latter can be adjusted precisely. Thus it seemed expedient to study the effect of mercury on the anodic behaviour of gallium.

Experimental

In a cell described in an earlier paper [9], solid or liquid electrodes of high-purity (99.9999%) gallium contaminated with amounts of mercury between 9.7×10^{-5} and 1.7×10^{-2} at.% were immersed in a 1 mol dm^{-3} solution of hydrogen chloride, saturated with hydrogen. The liquid electrode was kept at 32 °C, the solid gallium electrode at 28 °C.

The gallium samples with mercury impurities were prepared as described in a previous communication [8].

A PAR—170 type instrument was used for the recording of I and E data [10], at scan rates of 2, 10 and 100 mV/s against the normal hydrogen electrode. The rate of potential change (V) does not significantly affect the shape of the I *vs.* E curves are shown in Fig. 1 for liquid and solid electrodes of high-purity gallium, and of gallium with 1.7×10^{-2} at.% mercury. The maximum rate of anodic dissolution (j_{max}) of high-purity gallium as a liquid electrode is greater than that of the solid electrode; in contrast, the j_{max} values recorded for gallium with 1.7×10^{-2} at.% mercury were greater in the case of the solid electrode. The maximum rate of active dissolution of a solid gallium electrode with 1.7×10^{-2} at.% mercury is greater by three orders of magnitude than that of a solid gallium electrode of 99.9999% purity. The j_{max} found for a liquid electrode of pure gallium differs but slightly from the j_{max} found for a similar electrode with 1.7×10^{-2} at.% mercury. It is only in the case of solid gallium that mercury affects the rate of anodic dissolution to a significant degree, therefore, experiments carried out with solid electrodes will be discussed first. Figure 2 shows that at E = const., there is a linear correlation between $\lg j$ and $\lg C_{Hg}$ for low mercury concentrations of 10^{-4} to 10^{-5} at.% in the active section, and that the slope $\left(\frac{\partial \lg j}{\partial \lg C}\right)_E$ varies in the range from 1.09 to 1.19 (*cf.* Table I). However, at greater concentrations of mercury, the curve deviates from the straight line: the increase of the rate of active dissolution is diminished at greater concentrations of mercury *i.e.* the value of $\left(\frac{\partial \lg j}{\partial \lg C}\right)$ decreases.

It must be noted that also in the case of solid gallium electrodes containing mercury, the reproducibility of I *vs.* E curves is worse than with liquid electrodes, as found in the case of high-purity solid gallium electrodes [10]. The $\lg j$ values were determined by a computer from the experimental $I - E$ pairs. Repeated melting and freezing of gallium samples con-

taining mercury may alter the composition of the surface layer of the electrode: this is another detrimental feature as reproducibility is concerned. Our tests have shown that re-melting and freezing do not significantly affect the parameters of the polarization curves of solid gallium. Nevertheless, in order to achieve a better comparability, the lg j *vs.* E curves were plotted using data obtained after the first freezing of gallium electrodes containing mercury.

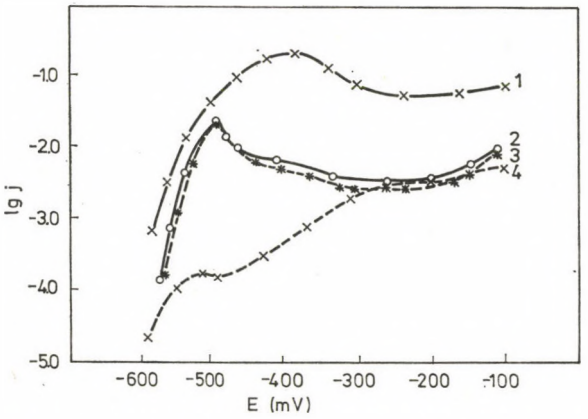

Fig. 1. lg j *vs.* E curves (1) for a solid gallium electrode with 1.7×10^{-2} at.% mercury, (2) for a liquid gallium electrode with the same amount of mercury, (3) for a solid, high-purity gallium electrode, (4) for a liquid, high purity gallium electrode, all in a 1 mol dm^{-3} solution of hydrochloric acid. Rate of potential change $v = 100$ mV sec^{-1}

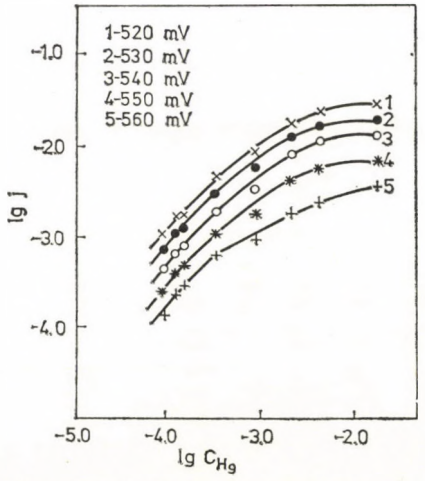

Fig. 2. lg j *vs.* C_{Hg} curves for a solid gallium electrode in a 1 mol dm^{-3} solution of hydrochloric acid, at a potential of (1) −520 mV, (2) −530 mV, (3) −540 mV, (4) −550 mV, and (5) −560 mV. C_{Hg} is the concentration mercury in at.%

Table I

E (mV)	$\left(\frac{\partial \lg j}{\partial \lg C_{Hg}}\right)_E^*$
−520	1.09
−530	1.16
−540	1.14
−550	1.16
−560	1.19

* Slope in the active phase when E = constant

Slope of the $\lg j_{max}$ *vs.* $\lg C_{Hg}$ curve, $E \neq$ constant

$$\frac{\partial \lg j_{max}}{\partial \lg C_{Hg}} = 1.50$$

Slope of the $\lg j_p$ *vs.* $\lg C_{Hg}$ curve plotted for the passive region; $E \neq$ constant

$$\frac{\partial \lg j_p}{\partial \lg C_{Hg}} = 1.76$$

Discussion

When E is constant, greater amounts of mercury in the solid gallium anode increase the rate of dissolution in both the active and passive region. We suppose that mercury is adsorbed on the surface of the gallium electrode [8] and covers its fraction Θ_{Hg}. More mercury reduces the number of free sites for dissolution $(1 - \Theta_{Hg})$ and the result to be expected is a decrease of the rate of dissolution when the mercury content increases. However, experimental data show that with more mercury present on the solid anode, the anodic dissolution is enhanced, while on the liquid gallium anode no such effect is noticeable: the rate of anodic dissolution is not affected by changes in the amount of mercury present. If the adsorption of mercury is supposed to occur, the increase of the rate of dissolution may be explained by the assumption that the mercury atoms adsorbed on the gallium surface loosening the bonding of gallium atoms since a part of Ga ↔ Ga interactions are replaced in part by weaker Ga* ↔ Hg interactions.

This weakening effect supposedly exerted by mercury atoms in their vicinity removes the oxide layer, otherwise present on solid gallium electrodes also in their active phase [11], which prevents dissolution. Thus the escape of the more weakly bonded and more active gallium atoms from the electrode surface needs a lower activation energy, consequently, the rate of anodic dissolution becomes greater as a result of this weakening effect. In the course of adsorption of mercury, a fraction Θ_{Hg} of the surface becomes covered with

mercury and this diminishes the rate of anodic dissolution. The dissolution-enhancing effect due to bond weakening by adsorbed mercury atoms on solid gallium is, however, much greater, hence more mercury increases the rate of anodic dissolution.

In order to understand the mechanism by which mercury affects dissolution, we suppose that the amount Θ_{Hg} of mercury adsorbed on the gallium surface governs the amount Θ_{Ga*} of weakly bonded gallium atoms on the oxide-free surface areas: $\Theta_{Ga*} \sim \Theta_{Hg}$. The rate of dissolution on surface areas free of mercury and of weakly bonded gallium atoms is $j' = j^\circ (1 - \Theta_{Hg} - \Theta_{Ga*})$, where j° is the rate of anodic dissolution when $\Theta_{Hg} = 0$ and $\Theta_{Ga*} = 0$.

The rate of dissolution on a surface covered with loosened gallium atoms is j^*. Θ_{Ga*}, where j^* is the rate of dissolution when $\Theta_{Ga*} = 1$.

Generally, *i.e.* when $0 < \Theta_{Hg} < 1$, the rate of dissolution of a solid gallium anode is

$$j = j^\circ(1 - \Theta_{Hg} - \Theta_{Ga*}) + j^* \Theta_{Ga*} \tag{1}$$

If we suppose that at low C_{Hg}, the $\Theta_{Ga*} = k\ \Theta_{Hg}$, where k is independent of the concentration of mercury, Eq. (1) can be rearranged to

$$j - j^\circ = \left[(j^* - j^\circ)\left(1 + \frac{1}{k}\right)\right] k\Theta_{Hg}. \tag{2}$$

If $j^* \gg j^\circ$, and in the range where $j \gg j^\circ$, the equation is

$$j \approx j^*\, \Theta_{Hg}\, k \tag{3}$$

It is supposed that the isotherm

$$\Theta_{Hg} \approx BC_{Hg} \tag{4}$$

describes the connection between the coverage by mercury Θ_{Hg} and the concentration of mercury C_{Hg}; if this is subtituted into Eq. (3), the result is

$$j \approx j^* kBC_{Hg} \tag{5}$$

or, with the constants collected in one term: $j^* kB = A$, and taking logarithms,

$$\lg j \approx \lg A + \lg C_{Hg}$$

i.e. $\lg j$, the logarithm of the anodic dissolution rate increases linearly with $\lg C_{Hg}$.

This is in agreement with the finding that at low concentrations (10^{-4} to 10^{-3} at.%) of mercury, $\lg j$ is a linear function of $lg\, C_{Hg}$ when E is kept constant. Deviations occur from this linearity when the concentration of mercury becomes greater (*cf.* Fig. 2), consequently, at greater C_{Hg}, the simplifying assumption of $\Theta_{Ga*} \approx k\ \Theta_{Hg}$ is not valid and also the $\Theta = f(C_{Hg})$ isotherm is more complicated. The precipitation of mercury on the gallium surface when the concentration of this contaminant becomes great is also possible.

The current j_{max} also increases when C_{Hg} increases; at low concentrations of mercury also the $\lg j_{max}$ *vs.* $\lg C_{Hg}$ curve is linear. From this straight line, deviations occur when C_{Hg} becomes greater (Fig. 3). The potential corresponding to the point where j_{max} is the greatest is changed towards positive values when the mercury concentration increases. This phenomenon may be interpreted as being a consequence of the formation of a passivating layer being hindered rather more on a gallium surface contaminated with mercury than on a pure gallium surface. Since the chemisorption of oxygen or water, preceding the formation of a passivating layer is energetically less favoured on a gallium surface that carries some mercury than on pure gallium, thus the passivation of gallium is shifted to the more positive potentials the more of mercury is on the gallium surface. In the case of the $\lg j_{max}$ *vs.* $\lg C_{Hg}$ curve shown in Fig. 3, the condition of E being constant does not apply.

Most probably, this is the reason why the slope of the curve is greater (1.5) at low concentrations of mercury than that of the $\lg j$ *vs.* $\lg C_{Hg}$ curve in the active section at E = constant (*cf.* Table I).

As shown in Fig. 4, the shape of the $\lg j_p$ *vs.* $\lg C_{Hg}$ curve, plotted for experimental points, in the passive section, is similar to that of the corresponding curve for the active section, and to that of the $\lg j_{max}$ *vs.* $\lg C_{Hg}$ curve. The $\lg j_p$ values indicate the lowest rates of dissolution in the passive section of the $\lg j_p$ *vs.* E curve. The condition that E is constant does not apply here either; also the slope (1.76) is greater than that in the active section (*cf.* Table I).

The latter experimental finding suggests that the mechanism of action of mercury is similar in the active and the passive phases. A correlation between the change of the rate of anodic dissolution due to changes in the concentration of mercury and the effect that weakens the bonding of gallium atoms adjacent to adsorbed mercury atoms and thus causes the partial destruction of the oxide layer was suggested; therefore, we may ascribe the correlation between the change of dissolution rate in the passive region with the mercury concentration to the same weakening effect, to the diminution of the protective effect of the passive layer. The study of the effect of impurities on the rate of anodic dissolution may help to elucidate more accurately the mechanism of passive dissolution.

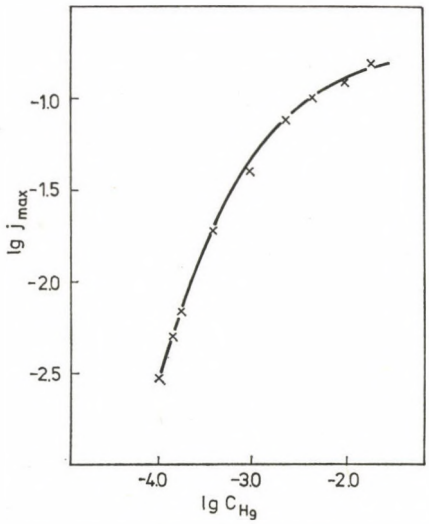

Fig. 3. $\lg j_{max}$ *vs.* $\lg C_{Hg}$ curve for a solid gallium electrode in a 1 mol dm^{-3} solution of hydrochloric acid

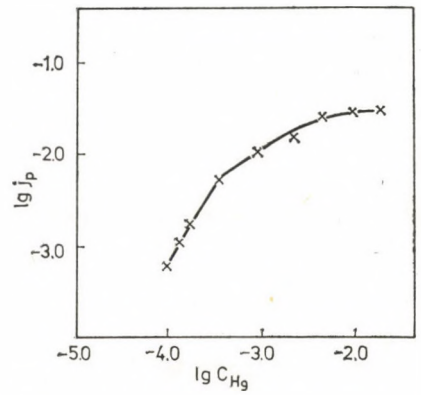

Fig. 4. $\lg j_p$ *vs.* $\lg C_{Hg}$ curve for a solid gallium electrode in a 1 mol dm^{-3} solution of hydrochloric acid

Experiments have shown that no significant effect is exerted by mercury, as an impurity, on the rate of anodic dissolution of liquid gallium: this means that the effect of adsorbed mercury atoms is much weaker upon the surface atoms of liquid gallium than upon those on solid gallium.

This dependence of the effect of contaminant mercury on the state of gallium may be ascribed to the fact that solid gallium has a rhombic, pseudo-tetragonal, looser lattice structure than has liquid gallium, which is more compact. Thus the loosening effect of mercury atoms is greater on the less

compact solid gallium electrodes than in on the liquid ones. Due to the stronger loosening effect, mercury atoms on the surface of solid gallium electrodes decompose in their vicinity the oxide layer — already present in the active state — which inhibits dissolution. This causes a substantial increase of the rate of anodic dissolution in both the active and the passive states. In contrast, when the gallium anode is liquid, the slight loosening effect causes hardly any increase in the rate of anodic dissolution in the active phase when the surface of the liquid gallium may be considered free from oxide. Also, due to the slightness of the loosening effect, the oxide layer which works against dissolution will not be decomposed in the passive states, thus no substantial increase of anodic dissolution will occur here either.

REFERENCES

[1] Szabó, K., Mihályi, L., Mika, J.: Elektrokhimiya, **12,** 756 (1976)
[2] Ivanov, E. G., Berkman, E. A., Petrova, G. M.: Sbornik rabot po khimicheskim istochnikam toka. Energiya, **9,** 186 (1974)
[3] Despic, A. R., Purenovic, M. M., Cikovic, N.: J. Appl. Electrochem., **6,** 527 (1976)
[4] Titova, J. E., Sadchikova, N. J.: Zh. Prikl. Khim., **47,** 2342 (1974)
[5] Kholotyrkin, Ya. M., Florianovich, G. M.: Itogi Nauki Elektrokhimiya, p. 5. Moskva 1971
[6] Jasinki, R.: High-Energy Batteries, p. 162. Plenum Press, New York 1967
[7] Skorchelletti, V.: Teoreticheskie Osnovy Korrozii Metallov, p. 255. Izd. Khim., Leningrad 1973
[8] Szabó, K., Mihályi, L., Mika, J.: Acta Chim. (Budapest) **74,** 185 (1972)
[9] Szabó, K.: Magy. Kém. Foly., **73,** 174 (1967)
[10] Szabó, K., Sólymos, G. K.: Magy. Kém. Foly., **83,** 216 (1977)
[11] Belaschk, D.: Z. Phys. Chem., **234,** 258 (1967)

Kálmán Szabó H-1088 Budapest, Puskin u. 11—13.
Kamilla G. Sólymos H-1088 Budapest, Múzeum krt. 4/a

Acta Chimica Academiae Scientiarum Hungaricae, Tomus 103 (1), pp. 9—15 (1980)

HIGH RESOLUTION MASS-SPECTROMETRIC INVESTIGATION OF HETEROCYCLIC COMPOUNDS CONTAINING S—Si—S BONDS

T. MÜLLER,[1] M. EL-KERSH,[2] K. BECKER-PÁLOSSY[2] and J. BALLA[1]

(Technical University of Budapest, [1]Institute of General and Analytical Chemistry, [2]Institute of Inorganic Chemistry)

Received August 7, 1978
Accepted for publication February 15, 1979

The investigation of mass spectra of some newly synthesized dithio-silacyclopentane compounds was carried out. Both low and high resolution spectra were taken and beside the molecular ions the most characteristic fragment ions were also identified by photoplate detection and high precision mass measurement. The respective fragmentation processes were suggested. Some information on properties of the S—Si—S bond, and the respective heterocyclic ring, were obtained too.

Introduction

In the last few years a number of heterocyclic compounds containing silicon (or germanium, tin, lead) and sulphur have been prepared, which contain one or more Me—S bonds (Me = Si, Ge, Sn, Pb) in the heterocyclic ring. The investigation of these types of compounds may provide interesting informations on the (p — d)π character of the Si—S bond. The investigation of the molecular structure of these compounds is especially useful since due to the relative rigidity of the rings the number of the possible conformers is limited and the quantummechanical treatment is, accordingly, simpler. Various types of these compounds have been investigated by mass spectrometry, too [1, 2, 3]. In this paper the results of a mass-spectroscopic study of some new compounds synthesized in our laboratory, are presented. The compounds investigated and their mass spectra are shown in Figs 1—4.

Experimental

A double focusing mass spectrometer/graph of the type JEOL JMS—01SG—2 was used for recording the low and high resolution mass spectra. The pressure in the electron impact ion source was $1-2.10^{-6}$ torr, in the analyzer it was lower than 1.10^{-7} torr. Ion-accelerating voltage of 10 kV, electron energy of 75 eV, and ionizing electron current of 200 μA were applied.

The low resolution spectra were taken and evaluated by the on-line data system of the instrument. The high resolution spectra were recorded on photoplates ILFORD Q—2. The low and high resolution measurements were carried out using a resolving power of 1500 and $\sim$20 000, respectively. The accuracy of the mass measurement was mostly better than 15 ppm. Continuous sample-flow technique was applied. The preparation and purification of the compounds have been described earlier [4].

Results and Discussion

a) *Investigation of the molecular ions*

Both silicon and sulphur have several isotopes [5] and, accordingly, molecular ions of various isotopic composition are to be found, even if only the isotopes of considerable abundance are taken into account. Due to this fact, the spectra are more complicated, but, on the other hand, the isotope peaks can be used to check the reliability of the identification of the ions in question. For the calculation of ionic masses the mass table of DIETZE's book [5] was used.

Table I

Molecular ions of compounds **I**—**IV**

Rel. int. %	*m/e*	Chemical formula	Mass: calc.	Mass: meas.	Required resolution
Compound **I**					
49.7	164	$C_5H_{12}S_2Si$	164.015	164.016	
5.6	165	$^{13}CC_4H_{12}S_2Si$ $C_5H_{13}S_2Si$	165.018 165.023	165.021	~37.000
6.1	166	$^{13}CC_4H_{13}S_2Si$	166.026	166.025	
0.9	167	$^{13}CC_4H_{13}S_2{}^{29}Si$	167.026	167.026	
Compound **II**					
63.7	226	$C_{10}H_{14}S_2Si$	226.031	226.031	
11.0	227	$^{13}CC_9H_{14}S_2Si$	227.034	227.035	
8.1	228	$C_{10}H_{14}{}^{34}SSSi$ $C_{10}H_{14}S_2{}^{30}Si$	228.026 228.027	228.028	~220.000
1.7	229	$^{13}CC_9H_{14}{}^{34}SSSi$ $^{13}CC_9H_{14}S_2{}^{30}Si$	229.030 229.031	229.031	~220.000
0.4	230	$C_{10}H_{14}{}^{34}S_2Si$ $C_{10}H_{14}{}^{34}SS^{30}Si$	230.022 230.023	230.022	~220.000
Compound **III**					
100.0	288	$C_{15}H_{16}S_2Si$	288.046	288.047	
22.5	289	$^{13}CC_{14}H_{16}S_2Si$	289.050	289.048	
13.8	290	$C_{15}H_{16}S_2{}^{30}Si$ $C_{15}H_{16}{}^{34}SSSi$	290.043 290.042	290.045	~280.000
2.6	291	$^{13}CC_{14}H_{16}S_2{}^{30}Si$ $^{13}CC_{14}H_{16}{}^{34}SSSi$	291.046 291.045	291.047	~280.000
0.8	292	$C_{15}H_{16}{}^{34}SS^{30}Si$	292.039	292.043	
Compound **IV**					
100.0	240	$C_6H_{12}S_4Si$	239.959	239.961	
14.4	241	$C_6H_{13}S_4Si$ $^{13}CC_5H_{12}S_4Si$	240.967 240.962	240.967	~ 54.000
21.4	242	$C_6H_{12}{}^{34}SS_2Si$ $C_6H_{12}S_4{}^{30}Si$	241.955 241.956	241.957	~230.000

The expected and measured isotopic molecular ions are summarized in Table I. Of course, not all theoretically possible combinations of isotopes have been considered, only those, giving sufficiently intensive lines on the photoplate.

It is to be mentioned, that most of the spectral lines measured are in fact very close doublets not separated by the resolving power available. For this reason the accuracy of the mass measurement is not as high as usually, and the intensity data are also uncertain to some extent. Nevertheless, the reliability of the identification of the ionic species investigated is completely satisfactory. Several peaks of low intensity ($<1\%$) and omitted in the low resolution spectra presented, have been reliably identified using photoplate detection.

b) *The characteristic fragment ions and the fragmentation processes*

The expected and measured mass values of the fragment ions considered characteristic are presented in Table II. The base peak of compounds **I** and **II** is the peak of the $M-CH_3^+$ fragment ion,

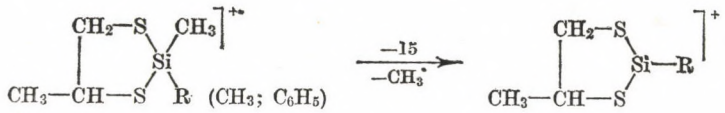

while that of compound **III** is the peak of the $M^{+\cdot}$ molecular ion. Thus it can be concluded, that the cleavage of the $Si-CH_3$ bond occurs most easily [6], and the five membered ring containing the sulphur atoms *i.e.* the S—Si—S bond is rather stable. This stability can be explained by the overlap of the p_π and d_π orbitals in the S—Si bond. The stability of the molecular ion of compound **III** can be interpreted by the interaction between the delocalized π electrons of the phenyl groups and the d-orbitals of the silicon atom.

Another characteristic fragmentation process is the successive loss of a H_2S molecule (rather common for sulphur compounds) most probably in the following way:

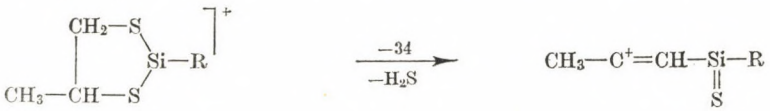

Further characteristic process is the additional loss of the C_3H_4 group:

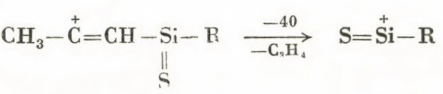

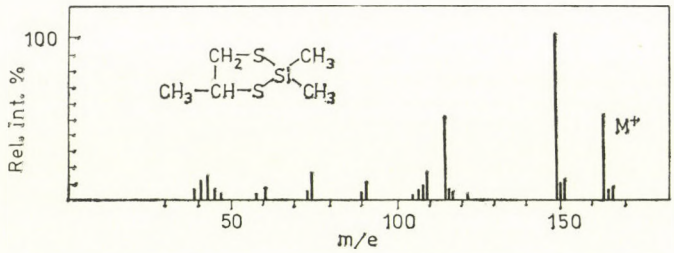

Fig. 1. Mass spectrum of 1,1,3-trimethyl-2,5-dithio-1-silacyclopentane; Compound **I**

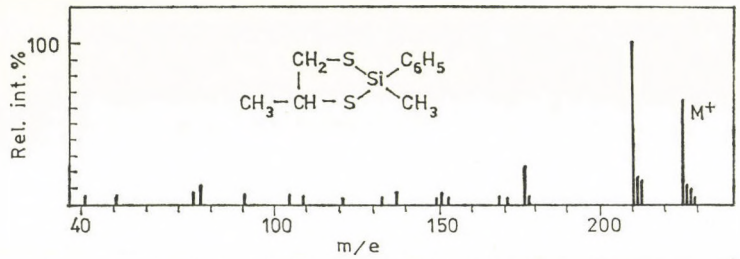

Fig. 2. Mass spectrum of 1,3-dimethyl-1-phenyl-2,5-dithio-1-silacyclopentane; Compound **II**

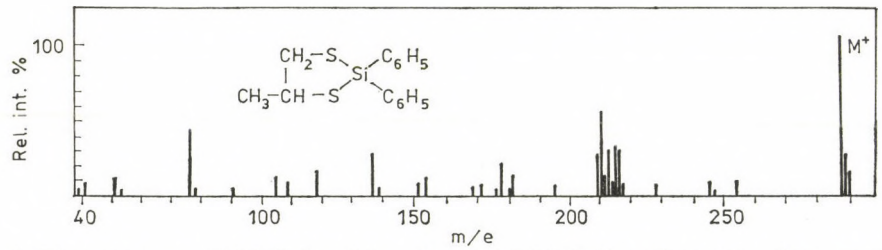

Fig. 3. Mass spectrum of 1,1-diphenyl-3-methyl-2,5-dithio-1-silacyclopentane; Compound **III**

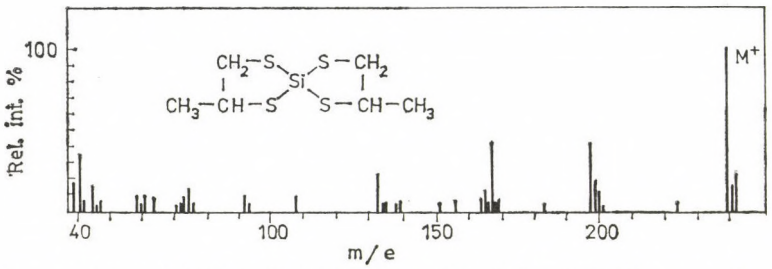

Fig. 4. Mass spectrum of 2,7-dimethyl-1,4,6,9-tetrathio-5-silaspiro[4.4]nonane; Compound **IV**

The most intensive peaks in the spectrum of compound **IV** (beside that of the molecular ion) appear at mass numbers 198 and 165 indicating the successive loss of the C_3H_6 group and $HS^{\cdot}$ radical, respectively, for which the following fragmentation and rearrangement processes may be suggested:

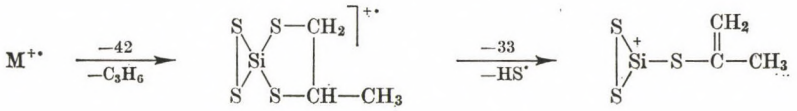

Table II

High resolution mass spectral data of compound **I** *(fragments)*

m/e	Chemical formula	calc.	meas.
		Mass	
149	$C_4H_9S_2Si$	148.992	148.995
119	$C_2H_3S_2Si$	118.945	118.943
115	C_4H_7SSi	115.004	115.005
109	CH_5S_2Si	108.960	108.962
105	CHS_2Si	104.929	104.932
	C_3H_9SSi	105.016	105.021
91	C_2H_7SSi	91.004	91.007
75	CH_3SSi	74.972	74.981
61	$HSSi$	60.957	60.956
58	C_2H_6Si	58.024	58.025
	C_2H_2S	57.988	57.988
47	CH_3S	46.996	46.996
45	CHS	44.980	44.982
43	CH_3Si	43.000	43.003
	C_3H_7	43.055	45.056
41	$CHSi$	40.985	—
	C_3H_5	41.039	41.038

Another peak of relatively high intensity is found at mass number 133, the elemental composition of which is given by the formula $C_3H_5S_2Si$. It is quite interesting, that the SiS_4^+ ion is also found in the spectrum at mass number 156, presenting another evidence for the strength of the S—Si bond.

*

The authors are indebted to Dr. I. CORNIDES for helpful discussions and suggestions. Furthermore, we would like to express our thank to Mr. J. BRLIK for his technical assistance.

Table II. (cont.)

High resolution mass spectral data of compound **II** *(fragments)*

m/e	Chemical formula	calc.	meas.
		Mass	
211	$C_9H_{11}S_2Si$	211.007	211.006
177	C_9H_9SSi	177.019	177.020
171	$C_6H_7S_2Si$	170.976	170.980
149	$C_4H_9S_2Si$	148.991	148.990
137	C_6H_5SSi	136.988	136.986
133	$C_3H_5S_2Si$	132.960	132.957
121	C_7H_9Si	121.047	121.049
		of compound **III** (fragments)	
254	$C_{15}H_{14}SSi$	250.059	254.056
246	$C_{12}H_{10}S_2Si$	245.999	245.998
228	$C_{13}H_{12}SSi$	228.043	228.043
216	$C_{12}H_{12}SSi$	216.043	216.042
214	$C_{12}H_{10}SSi$	214.027	214.027
212	$C_9H_{11}S_2{}^{29}Si$	212.007	212.006
211	$C_9H_{11}S_2Si$	211.007	211.008
210	$C_9H_{10}S_2Si$	209.999	209.999
181	$C_{12}H_9Si$	181.047	181.050
177	C_9H_9SiS	177.019	177.024
171	$C_6H_7S_2Si$	170.976	170.981
154	$C_7H_{10}SSi$	154.027	154.025
137	C_6H_5SSi	136.988	136.997
118	C_9H_{10}	118.078	118.078
109	C_6H_5S	109.011	109.012
105	C_6H_5Si	105.016	105.019
77	C_6H_5	77.039	—
		of compound **IV** (fragments)	
225	$C_5H_9S_4Si$	224.936	224.944
198	$C_3H_6S_4Si$	197.912	197.916
183	$C_2H_3S_4Si$	182.889	182.893
167	$C_3H_7S_3Si$	166.932	166.949
165	$C_3H_5S_3Si$	164.932	164.931
156	S_4Si	155.865	155.864
151	$C_2H_3S_3Si$	150.917	150.917
133	$C_3H_5S_2Si$	132.960	132.962

REFERENCES

[1] DISTEFANO, G., RICCI, A., DANIELI, R., FOFFANI, A., INNORTA, G., TORRONI, S.: J. Organometallic Chem., **65,** 205 (1974)
[2] GRAGG, R. M., TAYLOR, A.: J. Organometallic Chem., **99,** 391 (1975)
[3] LAPPERT, M. F., PEDLEY, J. B., SIMPSON, J., SPALDING, T. R.: J. Organometallic Chem., **29,** 195 (1971)
[4] EL-KERSH, M., BECKER-PÁLOSSY, K., NAGY, J., MÜLLER, T.: Acta Chim. Acad. Sci. Hung. (in press)
[5] DIETZE, H. J.: Massenspektroskopische Spurenanalyse, Akademische Verlagsgesellschaft, Leipzig, 1975. p. 204
[6] Analysis of Silicones. Ed.: A. Lee SMITH (Wiley Series of Monographs on Analytical Chemistry, Vol. **41**) Wiley Interscience, New York, 1974. p. 325—348

Tibor MÜLLER
Mokhtar EL-KERSH
Katalin BECKER-PÁLOSSY
József BALLA

H-1111 Budapest, Gellért tér 4.

Acta Chimica Academiae Scientiarum Hungaricae, Tomus 103 (1), pp. 17—25 (1980)

ON THE STUDY OF TRIPLE ION FORMATION. SODIUM IODIDE IN 1-OCTANOL AT 25 °C

P. BERONIUS[1] and L. PATAKI[2]

([1]Department of Physical Chemistry, University of Umeå, S-901 87 Umeå, Sweden, [2]Institute of Inorganic and Analytical Chemistry, Eötvös L. University of Budapest, Budapest)

Received November 28, 1978
Accepted for publication February 15, 1979

Triple ion formation of sodium iodide in 1-octanol at 25 °C has been studied by electrical conductance measurements over the concentration range of 0.5×10^{-4}—56×10^{-4} M. The data were analyzed by means of a conductance equation including ion atmosphere effects on ionic mobility. The equation used involves the limiting molar conductivity of the triple ions, Λ^{T}_{∞}, and implicitly the triple ion association constant, K_T, as adjustable parameters. Equal probabilities of forming the two different kinds of triple ions, Na_2I^+ and NaI_2^-, were assumed in the calculations. Triple ion formation was found to be negligible at concentrations less than 3.6×10^{-4} M, which is in good agreement with the theory. The best fit of the conductance equation to the experimental points was obtained for $K_T = 97\ M^{-1}$ and $\Lambda^{T}_{\infty} = 0.48\ \Lambda_{\infty}$, where Λ_{∞} is the limiting molar conductivity of the simple ions.

As part of an investigation [1] on the reactivities of various species, simple ions, ion pairs, and triple ions, as nucleophilic reagents the agglomeration of sodium iodide in 1-octanol at 25 °C was studied by measurements of electrical conductance. The objective of the present article is to discuss the results of the conductometric investigation, in which a recently developed method [2] for evaluation of the triple ion association constant and the limiting conductivity of the triple ions is used.

Experimental

The water content of the solvent used (1-octanol, Riedel De Haen AG) was found to be less than 0.02 vol.% according to titration by the Karl Fisher method. The solvent was flushed for 3 h with dry nitrogen to remove dissolved oxygen. Its density at 25.00 ± 0.02 °C, corrected for the buoyancy effect of the air, was 0.82167 g cm^{-3} using a Lipkin type pycnometer [3]. The electrolytic conductivity was less than 4×10^{-9} Ω^{-1} cm^{-1}. The values, $\varepsilon = 9.85$ for the relative permittivity [4] and $\eta = 0.073$ P for the viscosity [4], were used in the calculations.

Sodium iodide (Merck, *suprapur*) was predried for 2 h at 110 °C. Immediately before use it was dried again under these conditions.

Stock solutions of sodium iodide in 1-octanol were prepared by weight. The density of the solutions, determined as above, was found to vary linearly with the concentration of the salt according to Fig. 1.

Measurements of electrolytic conductivity were carried out using a conductivity cell of the DAGGETT—BAIR—KRAUS type [5] fitted with bright platinum electrodes and connected to a Leeds and Northrup 4666 conductivity bridge. The cell, which was of 1300 ml capacity, was kept at 25.00 ± 0.02 °C in a constant temperature kerosene bath. Aqueous potassium chloride solutions were used for calibration [6] of the cell. The cell constant, established by several calibration, was 0.062026 cm^{-1}.

Using a calibrated precision buret (Metrohm Herisau, Dosimat E 535), kept in an air thermostat at 25.00 ± 0.02 °C, portions of a stock sodium iodide solution were successively added to the cell initially containing a known amount of the pure solvent. The solution was agitated by a magnetic stirrer. After each addition the cell resistance was determined at different frequencies between 2–3.3 kHz and extrapolated to infinite frequency. A 20 kΩ precision resistor was connected in parallel with the cell because the cell resistance was, for most concentrations investigated, outside the range of the conductivity bridge.

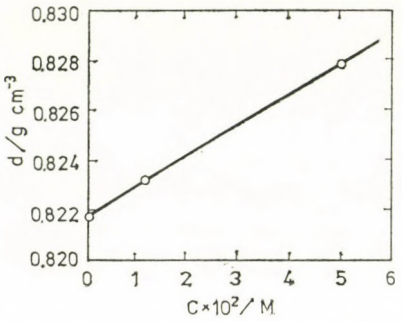

Fig. 1. Dependence of density on electrolyte concentration for solutions of NaI in 1-octanol at 25 °C

Results

Two series of measurements were performed. The results are given in Table I in which the molar conductivity, Λ, corrected for the conductivity of the solvent, is given at several different concentrations, c.

Discussion

Equations

It appears most reasonable to assume equal probabilities of forming the two different kinds of triple ions, Na_2I^+ and NaI_2^+. The following equilibria will be considered.

$$Na^+ + I^- \rightleftharpoons NaI \qquad (1)$$

$$NaI + Na^+ \rightleftharpoons Na_2I^+ \qquad (2a)$$

$$NaI + I^- \rightleftharpoons NaI_2^- \qquad (2b)$$

The equilibrium constant of (1), *i.e.* that of ion pair formation, is denoted K_A, while those of (2a) and (2b), being equal on the assumption above, are denoted K_T.

Denoting by $c\alpha$ the concentrations of Na^+ and I^-, respectively, and by $c\alpha_T$ the concentrations of Na_2I^+ and NaI_2^-, respectively, we have,

$$K_A = (1 - \alpha - 3\alpha_T)/(c\alpha^2\gamma^2) \quad (3)$$

$$K_T = \alpha_T/[c\alpha(1 - \alpha - 3\alpha_T) \quad (4)$$

where γ is the mean molar activity coefficient, which was calculated from the Debye—Hückel equation [7],

$$\ln \gamma \simeq \ln f = -\beta\varkappa/[2(1 + \varkappa R] \quad (5)$$

Table I

Electrical conductance data for NaI in 1-octanol at 25 °C

Series A		Series B	
$c \times 10^4$ M	Λ cm² Ω^{-1} mol^{-1}	$c \times 10^4$ M	Λ cm² Ω^{-1} mol^{-1}
0.54937	2.2333	0.62619	2.1529
1.0937	1.7793	0.83114	1.9624
1.6331	1.5412	1.0342	1.8192
2.1676	1.3868	1.2355	1.7096
2.6973	1.2769	1.4350	1.6203
3.2223	1.1922	1.6327	1.5450
3.7425	1.1251	1.8287	1.4810
5.9870	0.93687	2.0229	1.4255
10.417	0.75658	2.2154	1.3774
14.769	0.66312	2.4062	1.3347
21.158	0.58117	2.5954	1.2967
25.325	0.54496	2.7830	1.2625
29.422	0.51688	2.9689	1.2312
33.450	0.49451	3.1532	1.2030
37.411	0.47609	3.3359	1.1770
41.307	0.46061		
47.031	0.44160		
52.616	0.42617		
56.265	0.41741		

where f is the mean rational activity coefficient, R is a distance parameter, and β and $\varkappa$ have their usual meanings.

In the presence of both simple ions and triple ions the molar conductivity may be expressed,

$$\Lambda = m(\alpha\Lambda_\infty + \alpha_T\Lambda_\infty^T) \quad (6)$$

where m is a mobility correction factor, which corrects Λ for ion atmosphere effects and,

$$\Lambda_\infty = \lambda_T(Na^+) + \lambda_\infty(I^-) \tag{7}$$

$$\Lambda_\infty^T = \lambda_T(Na_2I^+) + \lambda_\infty(NaI_2^-) \tag{8}$$

According to the conductance equation of FUOSS and HSIA [8, 9] in the form of FERNÁNDEZ-PRINI [10] the mobility correction factor may be expressed,

$$m = (\Lambda_\infty - Sc_i^{1/2} + Ec_i^{10} \log c_i + J_1 c_i - J_2 c_i^{3/2})/\Lambda_\infty \tag{9}$$

where S and E are coefficients which depend on Λ_∞, ε, η, and temperature while J_1 and J_2 depend, in addition, on the distance parameter, R. The total ionic concentration, c_i, is given by the expression,

$$c_i = c(\alpha + \alpha_T) \tag{10}$$

Concentration range for ion pair formation

The present method of calculating triple ion association constants [2] requires access to the ion pair association constant, K_A, and the limiting molar conductivity of simple ions, Λ_∞. To obtain these quantities the concentration range for negligible triple ion formation was established by the following procedure.

The conductance equation for pairwise associated symmetrical electrolytes [8—10],

$$\Lambda = \Lambda_\infty - Sc_i^{1/2} + Ec_i^{10} \log c_i + J_1 c_i - J_2 c_i^{3/2} - K_A c\alpha\gamma^2\Lambda \tag{11}$$

where the symbols have the same meanings as in Eq. (9), was fitted to the four lowest concentration points (c, Λ) of Series A in Table I using a previously described computer programme [11]. By this means values of K_A, Λ_∞, and $\sigma(\Lambda)$, *i.e.* the standard deviation between experimental and computed Λ-values, were obtained. This curve fitting was repeated upon increasing step by step the upper limit of the concentration range, *i.e.* Eq. (11) was aplied to the five, six, *etc.* lowest concentration points.

A graph of the dependence of $\sigma(\Lambda)$ on the maximum sodium iodide concentration is shown in Fig. 2. It can be seen that the fit of Eq. (11) to the experimental points deteriorates markedly at concentrations above approximately 3.6×10^{-4} M indicating the presence of non-negligible amounts of triple ions at concentrations above this value. This observation is in very good agreement with theory [12] according to which triple ion formation of 1 : 1-electrolytes in 1-octanol at 25 °C is negligible at concentrations below 3.1×10^{-4} M.

In the following the concentration range above the experimentally determined concentration limit of 3.6×10^{-4} M will be referred to as the "triple ion range" while that below this limit will be referred to as the "ion pair range".

The six lowest concentration points of Series A and the points of Series B (Table I), which are all within the ion-pair range, were used to determine K_A

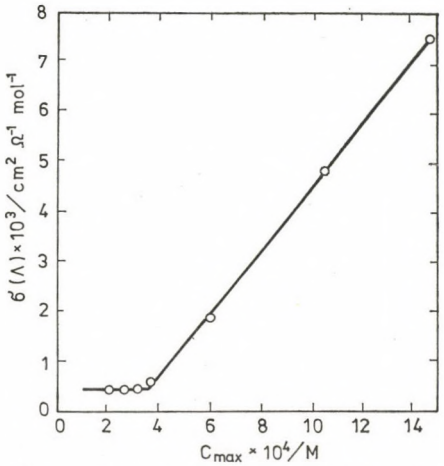

Fig. 2. Dependence of $\sigma(\Lambda)$ on maximum salt concentration for application of Eq. (11) to conductance data of NaI in 1-octanol at 25 °C

and Λ_∞. With the distance parameter, R, in Eqs (5) and (11) set equal to the Bjerrum radius, $q = 28.45$ Å, the following values of the constants in Eq. (11) were obtained: $\Lambda_\infty = 4.4674$ cm^2 Ω^{-1} mol^{-1}; $S = 43.88$; $E = 1036.4$; $J_1 = 5823$; $J_2 = 67\,100$; and $K_A = 39\,860$ (M^{-1}).

Triple ion formation

The following procedure was used to calculate the triple ion association constant, K_T, and the limiting conductivity, Λ_∞^T, from the 13 highest concentration points of Series A.

(i) For each experimental point (c, Λ) a first approximation for α was obtained from Eq. (3) and the K_T-value derived above approximating γ by unity and α_T by zero.

(ii) Using a preselected value of K_T a second approximation for α_T was calculated from Eq. (4).

(iii) A second approximation for γ was derived from Eq. (5) using c_i according to Eq. (10).

(iv) A better estimate for α was obtained by inserting the values of α_T according to (ii) and γ according to (iii) in Eq. (3).

This procedure was repeated until successive α-values as well as successive α_T-values differed by less than 1×10^{-6}.

The final values of α and α_T, which yield c_i, and the values of Λ_∞, S, E, J_1, and J_2 derived above were used to calculate, by means of Eq. (9), the mobility correction term.

Eq. (6) and a preselected value of Λ_∞^T were used to obtain a calculated value of Λ and, hence, the difference,

$$\Delta\Lambda = \Lambda(\text{exp}) - \Lambda(\text{calc}) \tag{12}$$

for each experimental point. The standard deviation, $\sigma(\Lambda)$, between experimental and calculated Λ-values was obtained from the expression,

$$\varrho(\Lambda) = \left(\frac{\Sigma(\Delta\Lambda)^2}{N-2}\right)^{1/2} \tag{13}$$

where N is the number of experimental points.

The procedure outlined was repeated by means of a Cyber 172 computer for different combinations of K_T and Λ_∞^T to find the values of these parameters which minimize $\sigma(\Lambda)$, *i.e.* which result in the best fit of Eq. (6) to the experimental points in the triple ion range.

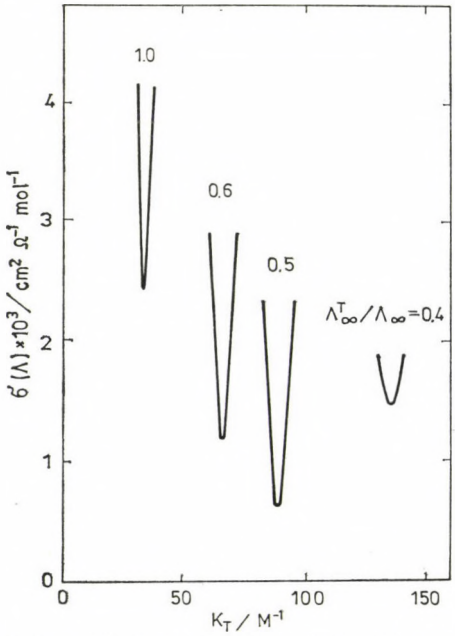

Fig. 3. Dependence of $\sigma(\Lambda)$ on K_T for application of Eq. (6) to conductance data for NaI in 1-octanol at 25 °C in the triple ion range

Some results of these calculations are shown in Fig. 3 in which $\sigma(\Lambda)$ has been plotted as a function of K_T for different values of the quotient, $\Lambda_\infty^T/\Lambda_\infty$.

To obtain that value of Λ_∞^T which results in the best fit of Eq. (6) to the experimental points the conditional minimum value of $\sigma(\Lambda)$ of several curves of the kind shown in Fig. 3 was plotted *vs.* $\Lambda_\infty^T/\Lambda_\infty$ in Fig. 4. This procedure resulted in a curve with a minimum at $\Lambda_\infty^T/\Lambda_\infty = 0.48$ suggesting that the mobility of the triple ions is slightly less than half that of the simple ions. It may be noted that almost exactly the same result was obtained for lithium bromide [2] in 1-octanol at 25 °C for which $\Lambda_\infty^T/\Lambda_\infty = 0.43$ was derived. This close agreement suggests that the present method might be useful to

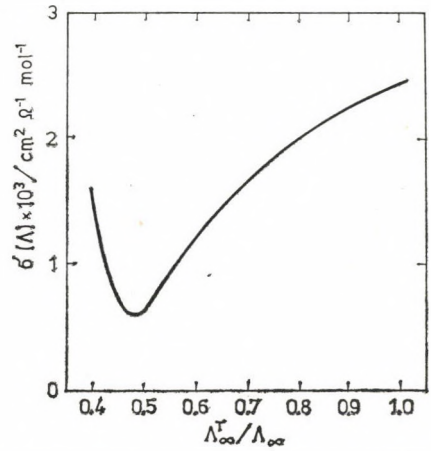

Fig. 4. Dependence of conditional minimum $\sigma(\Lambda)$, *cf.* Fig. 3, on the ratio, $\Lambda_\infty^T/\Lambda_\infty$, for NaI in 1-octanol at 25 °C

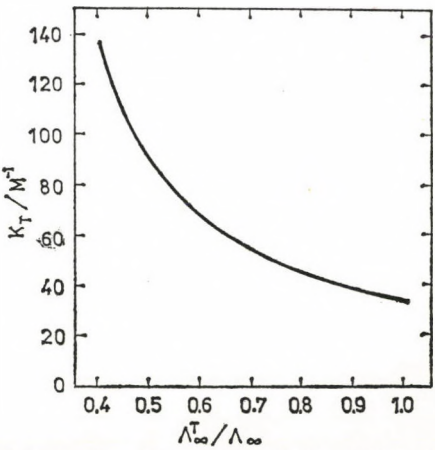

Fig. 5. Effect of the ratio, $\Lambda_\infty^T/\Lambda_\infty$, on K_T for NaI in 1-octanol at 25 °C

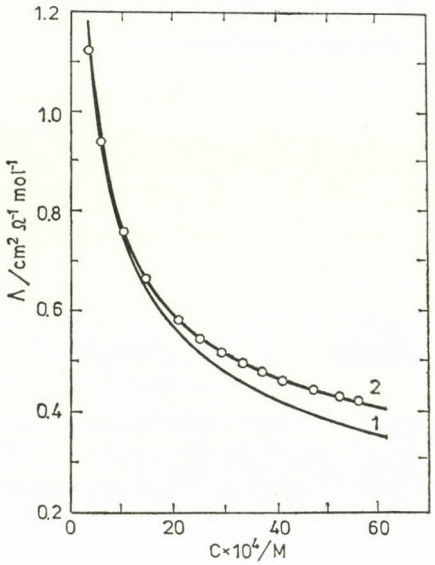

Fig. 6. Experimental values of Λ in the triple ion range as a function of the analytical concentration of NaI in 1-octanol at 25 °C. Curve 1: extrapolation of the equation for pairwise association, Eq. (11), to the triple ion range. Curve 2: best fit of Eq. (6)

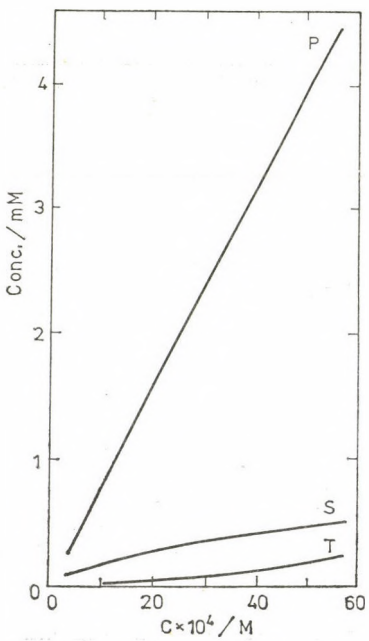

Fig. 7. Concentrations of simple ions (S), ion pairs (P), and triple ions (T) as a function of the analytical concentration of NaI in 1-octanol at 25 °C. $K_A = 39\,860$ (M^{-1}); $K_T = 97$ M^{-1}; $\Lambda_\infty^T/\Lambda_\infty = 0.48$

obtain information regarding triple ion mobilities. Previously, rather arbitrary *a priori* assumptions concerning triple ion mobilities have been made. For instance, the values 1/3 and 2/3 for $\Lambda_\infty^T/\Lambda_\infty$ have been used [7, 13].

The curve in Fig. 5 demonstrates how the assumption concerning the triple ion mobility affects the triple ion association constant. For $\Lambda_\infty^T/\Lambda_\infty =$ $= 0.48$, corresponding to $\sigma(\Lambda) =$ minimum, $K_T = 97\ M^{-1}$. This value may be compared with $K_T = 80\ M^{-1}$ for lithium bromide [2] in the present solvent at 25 °C.

In Fig. 6 the measured Λ-values in the triple ion range have been plotted as a function of the analytical sodium iodide concentration. Curve 1 represents an extrapolation of the conductance equation for pairwise association, Eq. (11), to the triple ion range. Curve 2 represents Eq. (6) with K_T and $\Lambda_\infty^T/\Lambda_\infty$ set equal to the values 97 M^{-1} and 0.48, respectively, arrived at above. It can be seen that Eq. (6) yields an excellent fit to the experimental points.

By Fig. 7 it is demonstrated how the concentrations of the various species, simple ions, ion pairs, and triple ions vary with the analytical concentration of the salt. Extension of the upper concentration limit of the salt taking quadrupole formation in account in analyzing the conductance data is a matter of further research.

*

The authors thank Mrs. M. Ögren for technical assistance and the Swedish Natural Science Research Council for financial support.

REFERENCES

[1] Pataki, L., unpublished results
[2] Beronius, P., Lindbäck, T.: Acta Chem. Scand., **A 32,** 423 (1978)
[3] Bauer, N., Lewin, S. Z.: in Weissberger, A., Ed., Physical Methods of Organic Chemistry, 3rd Ed., Interscience, New York 1959, Vol. I, Part *I*, Chapter IV
[4] Shkodin, A. M., Sadnovnichaya, L. P., Podolyanko, V. A.: Ukr. Khim. Zh., **35,** 144 (1969)
[5] Daggett Jr., H. M., Bair, E. J., Kraus, C. A.: J. Am. Chem. Soc., **73,** 799 (1951)
[6] Lind Jr., J. E., Zwolenik, J. J., Fuoss, R. M.: J. Am. Chem. Soc., **81,** 1557 (1959)
[7] Robinson, R. A., Stokes, R. H.: Electrolyte Solutions, Butterworths, London 1965
[8] Fuoss, R. M., Hsia, K.-L.: Proc. Natl. Acad. Sci., U.S.A., **57,** 1550 (1967)
[9] Fuoss, R. M., Hsia, K.-L.: Proc. Natl. Acad. Sci., U.S.A., **58,** 1818 (1968)
[10] Fernández-Prini, R.: Trans. Faraday Soc., **65,** 3311 (1969)
[11] Beronius, P.: Acta Chem. Scand., **A 28,** 77 (1974)
[12] Fuoss, R. M., Accascina, F.: Electrolytic Conductance, Interscience, New York 1959, Chapter 18
[13] Ralph, E. K., Gilkerson, W. R.: J. Am. Chem. Soc., **86,** 4783 (1964)

Per Beronius Department of Physical Chemistry, University of Umeå, S-901 87 Umeå, Sweden
László Pataki H-1088 Budapest, Múzeum krt. 4/b.

Acta Chimica Academiae Scientiarum Hungaricae, Tomus 103 (1), pp. 27—32 (1980)

OXAZEPINES AND THIAZEPINES, VII*

SYNTHESIS AND CIRCULAR DICHROISM OF 2,3-DIHYDRO-2,4-DIPHENYL-1,5-BENZOTHIAZEPINE GLYCOSIDES

A. LÉVAI,[1] R. BOGNÁR[1] and J. KAJTÁR[2]

([1]Institute of Organic Chemistry, Kossuth Lajos University, Debrecen and [2]Institute of Organic Chemistry, Eötvös Loránd University, Budapest)

Received November 2, 1978
Accepted for publication February 26, 1979

2,3-Dihydro-2,4-diphenyl-1,5-benzothiazepine glycoside acetates (**VII—X**) have been synthesized by the reaction of 2-aminothiophenol and chalcone glycoside acetates (**III—VI**), and the corresponding free glycosides (**XI—XIV**) were obtained on saponification. The chiroptical properties of the compounds prepared have been studied.

One of the interesting groups of benzothiazepines comprises the 2,4-disubstituted 2,3-dihydro-1,5-benzothiazepines obtained by the reaction of 2-aminothiophenol with α,β-unsaturated ketones [1—6]. We formerly synthesized such compounds starting from chalcones [5, 6] and their naphthyl analogues [20]. In the course of these investigations it was found that the reaction was significantly affected by both the electron density at the β-carbon atom of the α,β-unsaturated ketone and steric factors. In the knowledge of these effects it has become possible to establish such reaction conditions which can be widely used for the synthesis of the above-mentioned benzothiazepines.

Although numerous benzothiazepine derivatives have been described during the last two decades, to our knowledge, benzothiazepine glycoside have not yet been mentioned in the literature. Our studies have now been extended to the reactions of 2-aminothiophenol with chalcone glycosides, and the synthesis and circular dichroism of 2,3-dihydro-2,4-diphenyl-1,5-benzothiazepine glycosides will be reported in the present paper.

Chalcone glycoside acetates (**III—VI**) were synthesized from 4-hydroxy- (**I**) and 4′-hydroxychalcone (**II**) with α-acetobromoglucose or α-acetobromocellobiose according to the modified Koenigs—Knorr method. Compounds **III—VI** were allowed to react with 2-aminothiophenol in hot anhydrous toluene as described for chalcones [5, 6]. Since after evaporation of the solvent a jelly-like material was obtained, the residue was boiled in a mixture of anhydrous methanol and acetic acid. By means of this treatment, any β-(2-aminophenylmercapto)ketone glycoside possibly present in the reaction mixture is converted into the corresponding benzothiazepine glycoside. 2,3-Dihydro-2,4-

* For Part VI, see Ref. [7].

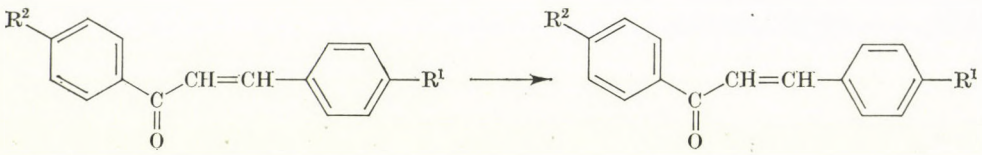

I: $R^1 = OH$, $R^2 = H$
II: $R^1 = H$, $R^2 = OH$

III: $R^1 = OGl(Ac)_4$, $R^2 = H$
IV: $R^1 = H$, $R^2 = OGl(Ac)_4$
V: $R^1 = OCb(Ac)_7$, $R^2 = H$
VI: $R^1 = H$, $R^2 = OCb(Ac)_7$

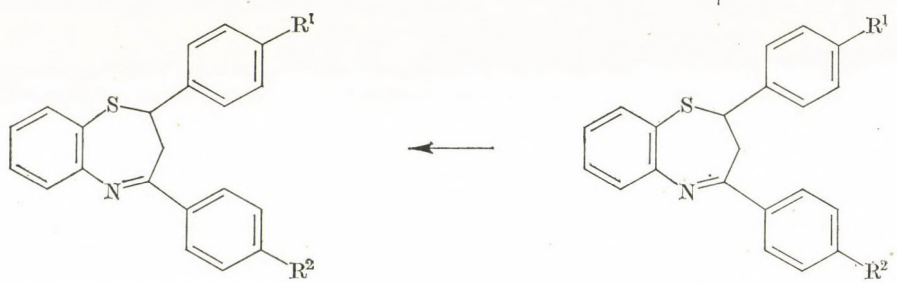

XI: $R^1 = OGl$, $R^2 = H$
XII: $R^1 = H$, $R^2 = OGl$
XIII: $R^1 = OCb$, $R^2 = H$
XIV: $R^1 = H$, $R^2 = OCb$

VII: $R^1 = OGl(Ac)_4$, $R^2 = H$
VIII: $R^1 = H$, $R^2 = OGl(Ac)_4$
IX: $R^1 = OCb(Ac)_7$, $R^2 = H$
X: $R^1 = H$, $R^2 = OCb(Ac)_7$

Gl = β-D-glucosyl; $Gl(Ac)_4$ = tetra-*O*-acetyl-β-D-glucosyl; Cb = β-cellobiosyl; $Cb(Ac)_7$ = hepta-*O*-acetyl-β-cellobiosyl.

diphenyl-1,5-benzothiazepine glycoside acetates (**VII**—**X**) were thus obtained in quite pure state. The acetates gave the free glycosides (**XI**—**XIV**) on saponification. On the basis of these results it can be stated that the conditions used in the reaction of 2-aminothiophenol with chalcones can also be applied for the same reaction of chalcone glycoside acetates, *i.e.* benzothiazepine glycoside acetates can readily be synthesized in this way (Table I).

The sign of the two CD bands ($^1B_{2u}$ and $^1B_{1u}$) of the simple phenyl glycosides [8—14] is determined by the type of the glycosidic linkage: both are negative for β-glycosides and positive for the α-anomers. In the case of glycosides having more complicated aglycones, where various chromophores are present in the molecule, *e.g.* flavonoids [15—17], the correlation is not so simple, since the chiroptical properties are significantly influenced also by the position of the glycosidic linkage. On this basis it was expected that the chiroptical properties of the 2,3-dihydro-2,4-diphenyl-1,5-benzothiazepine glycosides would somewhat depend upon the position of the sugar moiety.

Table I

Physical constants and analyses of the compounds prepared

	M.p., °C	Yield, %	Overall formula	Mol. weight	Analysis, %			
					Calculated		Found	
					C	H	C	H
III	148—149	24.3	$C_{29}H_{30}O_{11}$	554.53	62.81	5.41	63.02	5.54
IV	173—174	26.0	$C_{29}H_{30}O_{11}$	554.53	62.81	5.41	63.07	5.45
V	207—208	26.01	$C_{41}H_{46}O_{19}$	842.78	58.43	5.46	58.64	5.35
VI	225—226	28.3	$C_{41}H_{46}O_{19}$	842.78	58.43	5.46	58.56	5.33
VII	190—191	51.6	$C_{35}H_{35}O_{10}NS$	661.63	63.54	5.29	63.39	5.19
VIII	160—161	46.6	$C_{35}H_{35}O_{10}NS$	661.63	63.54	5.29	63.69	5.34
IX	188—189	79.1	$C_{47}H_{51}O_{18}NS$	949.88	59.36	5.36	60.02	5.48
X	163—164	72.3	$C_{47}H_{51}O_{18}NS$	949.88	59.36	5.36	59.18	5.39
XI	196—197	81.0	$C_{27}H_{27}O_6NS \cdot 2H_2O$	529.49	61.24	5.48	60.28	5.75
XII	187—189	87.8	$C_{27}H_{27}O_6NS$	493.49	65.72	5.47	64.86	5.51
XIII	226—228	78.4	$C_{33}H_{37}O_{11}NS$	655.63	60.45	5.64	59.51	5.71
XIV	216—217	58.8	$C_{33}H_{37}O_{11}NS$	655.63	60.45	5.64	59.71	5.52

In the UV spectra of the compounds under investigation (**VII—XIV**) three intense maxima are found in the 342—312, 278—258 and 231—220 nm regions. The UV spectra show no differences, probably owing to the fact that the sugar part is attached to a phenyl group located at position 2 or 4 of the hetero ring.

As far as the chiroptical properties are concerned, it must, above all, be mentioned that these compounds are strongly chiral: the magnitude of

Table II

IR and UV spectral data of 2,3-*dihydro*-2,4-*diphenyl*-1,5-*benzothiazepine glycosides*

	IR $\nu C{=}N$, cm^{-1}	UV λ_{max} [nm] (log ε)
VII	1609	322 (3.70), 260 (4.36), 224sh (4.37)
VIII	1608	312 (4.30), 278 (4.28), 220sh (4.29)
IX	1610	322 (3.87), 258 (4.31), 224sh (4.35)
X	1604	318 (4.12), 276 (4.28), 224sh (4.28)
XI	1610	318 (3.60), 265 (4.17), 231 (4.30)
XII	1600	342sh (3.75), 278 (4.28), 222sh (4.29)
XIII	1600	318 (3.46), 258 (4.11), 224sh (4.16)
XIV	1610	326sh (4.00), 278 (4.45), 226sh (4.39)

their $[\alpha]_D$ value is several hundreds. This is in accordance with the high rotational strength of their CD maxima. Contrary to the UV spectra, the shapes of the CD spectra are characteristically different depending on whether the sugar component is linked to the C-2 or C-4 phenyl group. However, the fact that the sugar moiety is a monosaccharide or disaccharide, acetylated or free sugar, results only in minor changes in the magnitude of the Cotton effects (Table III).

Table III

Chiroptical data of the compounds prepared

	$[\alpha]_D$ (in pyridine)	CD λ_{max} [nm] ($\Delta\varepsilon$)
III	− 29.0° (c = 0.86)	−
IV	− 20.0° (c = 0.70)	−
V	− 27.5° (c = 1.2)	−
VI	− 28.0° (c = 0.75)	−
VII	− 814.9° (c = 0.35)	327 (−27.76), 284 (−35.44), 257sh (+9.74), 244 (+11.22), 233sh (+7.97), 221 (−7.38), 208 (+33.96)
VIII	− 493.1° (c = 0.53)	330 (−19.42), 292sh (−14.13), 260 (+4.38), 233 (+7.54), 207 (+16.73)
IX	− 524.8° (c = 0.27)	328 (−22.28), 285 (−29.52), 256sh (+7.52) 245 (+8.35), 233sh (+6.13), 222 (−6.13), 208 (+25.35)
X	− 353.4° (c = 0.23)	328 (−27.32), 289sh (−17.94), 258 (+3.86), 233 (+6.62), 207 (+20.15)
XI	− 853.9° (c = 0.23)	332 (−20.56), 286 (−28.13), 258 (+8.51), 247 (+9.22), 224 (−9.45), 210 (+26.94)
XII	−1170.5° (c = 0.06)	325 (−37.74), 289sh (−18.13), 257 (+7.40), 233 (+14.06), 206 (+34.4J)
XIII	− 853.9° (c = 0.23)	327 (−20.96), 285 (−28.99), 248 (+8.47), 222 (−8.03), 207 (+20.74)
XIV	− 740.7° (c = 0.13)	328 (−31.48), 289sh (−17.04), 257 (+6.41), 232 (+12.63), 201 (+8.06)

The C-2 atom of these benzothiazepines is a chiral centre, but the aglycone of compounds under investigation exist in racemic form. This is shown by the fact that the CD spectra of compound **VII** prepared from the chalcone glucoside acetate **III** or by glycosylation of the corresponding hydroxyphenyl benzothiazepine (**XVI**) are practically the same.

In view of the complexity of the chromophore, interpretation of the relationships between the electron transitions and the CD maxima must await the investigation of further examples.

Experimental

M.p.'s are uncorrected.

IR spectra were obtained in KBr discs with a UNICAM SP 200G instrument. UV spectra were recorded in ethanolic solutions with a UNICAM SP 800 apparatus. CD spectra were measured with a JOBIN YVON dichrograph at 10^{-5} or $5 \cdot 10^{-6}$ sensitivity values in ethanolic solution at concentrations of about 1 mg/ml in 0.5 mm cells at room temperature.

The chalcones (**I** and **II**) were prepared as described in the literature [18, 19].

Chalcone glycosides (III—VI)

The chalcone (**I** or **II**) (25 mmoles) was dissolved in acetone (100 ml), and the appropriate α-acetobromo sugar (30 mmoles) and 2.0 *N* NaOH solution (13 ml) were added. The mixture was shaken for 24 h at room temperature, then poured into water and the solution neutralized with 10% acetic acid. Crystallization from ethanol of the separated oily substance gave the product as white crystals (Tables I—III).

2,3-Dihydro-2,4-diphenyl-1,5-benzothiazepine glycoside acetates (VII—X)

The chalcone glycoside (**III**—**VI**) (2.5 mmoles) and 2-aminothiophenol (3.0 mmoles) were dissolved in dry toluene (35 ml) and refluxed for 3 h in an apparatus provided with a water separator; the solvent was then removed under reduced pressure. The residue was refluxed for 1 h in a mixture of anhydrous methanol (100 ml) and glacial acetic acid (1.0 ml). The product which separated after cooling was recrystallized from methanol to obtain white crystalline material (Tables I—III).

2,3-Dihydro-2,4-diphenyl-1,5-benzothiazepine glycosides (XI—XIV)

2,3-Dihydro-2,4-diphenyl-1,5-benzothiazepine glycoside acetate (**VII**—**X**) (2.5 mmoles) was boiled for 10 min in a mixture of methanol (50 ml) and 1.0 *N* NaOH (10 ml), and the solution neutralized with 10% acetic acid. The solid which precipitated from the solution was filtered off and recrystallized from methanol to afford white crystalline substance (Tables I—III).

β-(4-Hydroxyphenyl)-β-(2-aminophenylmercapto)-propiophenone (XV)

4-Hydroxychalcone (10.0 g) and 2-aminothiophenol (7.0 ml) in anhydrous toluene (200 ml) were refluxed for 3 h. The solvent was then evaporated in vacuum and the residue crystallized from ethanol to yield 11.5 g (74.1%) of the product, m.p. 146—147 °C.

IR: νC=O 1669; νNH_2 3343 and 3440 cm^{-1}.

$C_{21}H_{19}O_2NS$ (349.36). Calcd. C 72.20; H 5.44. Found C 72.27; H 5.41%.

2,3-Dihydro-2-(4-hydroxyphenyl)-4-phenyl-1,5-benzothiazepine (XVI)

Compound **XV** (10.0 g) was boiled for 1 h in a mixture of *abs.* ethanol (500 ml) and glacial acetic acid (5 ml). The solid material which separated on cooling was recrystallized from methanol to obtain 7.1 g (75.5%) of a crystalline substance, m.p. 166—167 °C.

IR: νC=N 1610 cm^{-1}.

$C_{21}H_{17}ONS$ (331.35). Calcd. C 76.13; H 5.13. Found C 76.0; H 5.20%.

2,3-Dihydro-2-[4-(tetra-*O*-acetyl-β-D-glucosyloxy)-phenyl]-4-phenyl-1,5-benzothiazepine (VII)

A mixture of compound **XVI** (3.3 g), α-acetobromoglucose (5.0 g), 2.0 *N* NaOH (6.0 ml) and acetone (50 ml) was stirred for 24 h at room temperature, then poured into water and the solution neutralized with 10% acetic acid. The separated oily product was crystallized from ethanol to afford 2.1 g (31.7%) of white crystals, m.p. 189—190 °C, $[\alpha]_D$-805.6 (in pyridine, $c = 0.53$).

IR: νC=N 1610 cm^{-1}.

CD: λ_{max}[nm] [$\Delta\varepsilon$]; 326 (−29.27); 284 (−38.06); 256sh (+9.37); 245 (+10.83); 233sh (+7.90); 221 (−9.37); 208 (+33.37).

$C_{35}H_{35}O_{10}NS$ (661.63). Calcd. C 63.54; H 5.29. Found C 63.69; H 5.32%.

*

The authors' thanks are due to Drs. É. R. DÁVID and S. SZABÓ for the UV and IR spectra, to Mrs. E. HAJNAL for the valuable assistance in the experimental work. The present study was sponsored by the Hungarian Academy of Sciences for which our gratitude is expressed.

REFERENCES

[1] RIED, W., MARX, W.: Ber., **90,** 2683 (1957)
[2] MUSKALO, L. K.: Obsch. Khim., **28,** 507 (1958)
[3] STEPHENS, W. D., FIELD, L.: J. Org. Chem., **24,** 1576 (1959)
[4] HIDEG-HANKOVSZKY, O., HIDEG, K.: Acta Chim. Acad. Sci. Hung., **68,** 403 (1971)
[5] LÉVAI, A., BOGNÁR, R.: Acta Chim. (Budapest) **88,** 293 (1976)
[6] LÉVAI, A., BOGNÁR, R.: Acta Chim. (Budapest) **92,** 415 (1977)
[7] LÉVAI, A.: Acta Chim. Acad Sci. Hung. **102,** 141 (1979)
[8] STICZAY, T., PECIAR, C., BAUER, S.: Tetrahedron Letters, **1968,** 2407
[9] STICZAY, T., PECIAR, C., BAUER, S.: Tetrahedron, **25,** 3521 (1969)
[10] TSUZUKI, Y., KOYAMA, M., AOKI, K., KATO, T., TANABE, K.: Bull. Chem. Soc. Japan, **42,** 1052 (1969)
[11] TSUZUKI, Y., KATAOKA, S., FUNAYAMA, M., SATSUMABAYASHI, K.: Bull. Chem. Soc. Japan, **44,** 526 (1971)
[12] LÉVAI, A., TŐKÉS, A. L., BOGNÁR, R., STICZAY, T., PECIAR, C., BAUER, S.: Magyar Kém. Foly., **79,** 197 (1973)
[13] STICZAY, T., PECIAR, C., BAUER, S., TŐKÉS, A. L., LÉVAI, A., BOGNÁR, R.: Chem. zvesti, **28,** 90 (1974)
[14] LÉVAI, A., LIPTÁK, A., PINTÉR, I., SNATZKE, G.: Acta Chim. (Budapest) **84,** 99 (1975)
[15] LÉVAI, A., BOGNÁR, R., PECIAR, C., BYSTRICKY, S., STICZAY, T.: Acta Chim. (Budapest) **79,** 365 (1973)
[16] STICZAY, T., BYSTRICKY, S., PECIAR, C., LÉVAI, A., BOGNÁR, R.: Chem. zvesti, **29,** 538 (1975)
[17] LÉVAI, A.: in "Flavonoids and Bioflavonoids: Current Research Trends" (ed. L. FARKAS, M. GÁBOR, F. KÁLLAY), Akadémiai Kiadó, Budapest 1977, pp. 295—306
[18] VORLÄNDER, D.: Ber., **58,** 118 (1925)
[19] SHRINER, R. L., KUROSAWA, T.: J. Am. Chem. Soc., **52,** 2538 (1930)
[20] LÉVAI, A.: Pharmazie, **34,** 439 (1979)

Albert LÉVAI
Rezső BOGNÁR } H-4010 Debrecen, P.O. Box 20

Judit KAJTÁR H-1088 Budapest, Múzeum krt. 4/b

Acta Chimica Academiae Scientiarum Hungaricae, Tomus 103 (1), pp. 33—42 (1980)

HOMOGENEOUS CATALYTIC HYDROGENATION OF DIOLEFINS AND ALKYNES IN THE PRESENCE OF PALLADIUM(II) COMPLEXES

A. SISAK, I. JABLONKAI and F. UNGVÁRY*

(Institute of Organic Chemistry of the University of Chemical Industries, Veszprém)

Received December 4, 1978
In revised form February 16, 1979
Accepted for publication February 28, 1979

Palladium(II)chloride in dimethylformamide catalyzes the hydrogenation of conjugated diolefins and alkynes in homogeneous solution. Monoolefins are formed selectively.

Introduction

Palladium compounds are versatile reagents and catalysts for organic synthesis [1]. In comparison to other transition metal complexes such as those of rhodium, very few hydrogenations have been reported with soluble palladium complexes as catalysts.

Principally two kinds of soluble palladium catalysts are known depending upon the oxidation state of the metal as can be seen in Table I. The first group consists of Pd(O) complexes such as $Pd(Ph_3P)_4$ or complexes prepared *in situ* by the reduction of Pd(II) compounds. The second group comprises various Pd(II) complexes. The activity of Pd(O) containing catalysts can be generally enhanced by oxidation with air or oxygen.

We were interested in the simple catalyst system $PdCl_2$ in dimethylformamide (DMF), which was reported by RYLANDER and coworkers [11] to hydrogenate dicyclopentadiene in homogeneous solution. Normally, the solutions of $PdCl_2$ in DMF react with H_2 very rapidly and finely dispersed black Pd metal is formed almost instantaneously. Dicyclopentadiene is an appropriate stabilizing ligand and the complex in solution is able to catalyze its hydrogenation.

We found that from $PdCl_2$ in DMF a catalyst is formed in the presence of conjugated diolefins and alkynes [12] which hydrogenates these unsaturated compounds selectively to monoolefins. In the absence of hydrogen, alkynes and diolefins react with $PdCl_2$ in DMF under the formation of Pd complexes with oligomeric alkynes and dienes as ligands. These complexes are also effective homogeneous catalysts for selective hydrogenation [22].

Now we report on experiments with a number of unsaturated substrates using $PdCl_2$ in DMF.

Table I

Palladium complexes as homogeneous hydrogenation catalysts

Pd(0) complexes	Ref.	Pd(II) complexes	Ref.
$Pd(Ph_3P)_4$	[2]	$PdCl_2$	[10]
$Pd(Ph_2PCH_2CH_2PPh_2)_2$	[3]	$PdCl_2(DMF)_2$	[11, 12]
$PdX_2L_2 + NH_2NH_2$	[4]	$PdCl_2(DMSO)_2$	[13, 14]
$PdX_2L_2 + NaBH_4$	[5, 6, 7, 8]	$PdCl_2(Ph_3P)_2$	[4, 6, 15, 16]
$PdX_2L_2 + R_3Al$	[9]	$Pd(CN)_2(Ph_3P)_2$	[16, 17]
where X = Cl, Br, I, CN		Pd(salen)	[18]
L = Ph_3P, Bu_3P,		$Pd(acac)_2$	[19]
NMP, DMSO		$C_3H_5PdCl(PEt_3)_2$	[20]
		oxidized Pd(O) compl.	[3, 6, 7, 21]

DMF = dimethylformamide, DMSO = dimethyl sulfoxide, NMP = *N*-methyl-2-pyrrolidone, salen = ethylenebis(salicylimine)

Experimental

For the experiments we used commercial $PdCl_2$ without purification or $PdCl_2(DMF)_2$ prepared as described by UGO and coworkers [23].

The propargylethers were prepared as described in the literature [24]. Other alkynes and dienes and the solvent dimethylformamide were commercial products which were freshly distilled under argon before use.

The catalytic experiments were run at room temperature in a small scale glass autoclave [25], starting the reaction by introducing H_2 under pressure and agitating the mixture of 2 mmol substrate, 2.5 ml DMF and 0.01 mmol $PdCl_2$ or $PdCl_2(DMF)_2$. The pressure drop was followed with a manometer. After the desired H_2 uptake, the pressure was released and the composition of the mixture analyzed by gaschromatography using standard compounds and retention data from the literature [26, 27]. For aliphatic alkynes and dienes: 10% 2,2′-oxydipropionitrile on 60—80 mesh Chromosorb P, 4 m, 4 mm ∅, 1.4 l H_2/hour, HWD, 30—50 °C. In the case of pentadienes and their hydrogenated products: 2,2′-oxydipropionitrile in a 50 m capillary column, 2 ml argon/min, FID. For phenylacetylene and its hydrogenated products: 10% polyethylene glycol 20 M on 80—100 mesh Chromosorb P, 3 m, 3 mm ∅, 3.1 l H_2/hour, HWD, 100 °C. In the case of heteroatom containing alkynes and their hydrogenated products: polyethylene glycol 1500 in a 50 m capillary column, 2 ml argon/min, FID, 100—150 °C.

Results and Discussion

$PdCl_2$ in DMF proved to be stable under H_2 in the presence of several dienes and alkynes. These compounds prevent Pd deposition and the colour of the solutions remains orange or changes to yellow. Rapid H_2 uptake by the homogeneous solutions could be observed with both types of substrates at room temperature under 25 bar H_2 pressure. Mostly, the bright yellow or orange colour of the reaction mixture was convincing for homogeneity, and could be observed visually working with the glass autoclave. To prove the homo-

geneity of the reaction mixture also by another independent way we added thiophene, a strong poison for heterogeneous catalysts. Up to 2 mol of thiophene per mol Pd did not change the rate of the catalytic reaction. At 100 mol thiophene per mol Pd, the colour of the raction mixture became somewhat

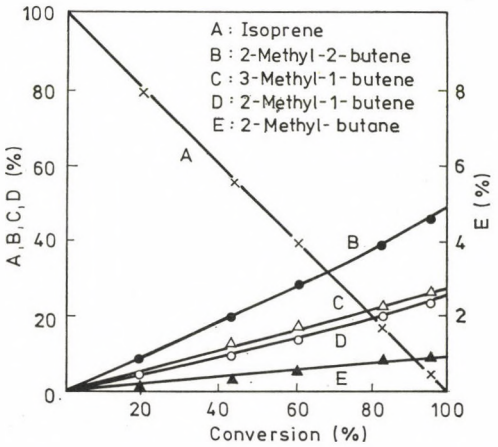

Fig. 1. Products of isoprene hydrogenation at various conversions using $PdCl_2$ in DMF solution

lighter yellow than without added thiophene and hydrogenation took place only after an induction period of about 10 min.

In this homogeneous hydrogenation of dienes the corresponding monoolefins are formed with high selectivity, as can be seen from Table II. Isomerization of the olefinic products does not take place. The ratio of products remains practically unchanged during the whole experiment as can be seen in Fig. 1 in the case of isoprene.

A preferential complexing of dienes as compared to monoolefins is evident: after all the diolefin has been consumed the stabilizing effect vanishes and Pd metal appears. The Pd metal so formed catalyzes the slow hydrogenation of the olefins to alkanes. From this point on the composition of the olefins is changed due to isomerization on metallic Pd.

With butadiene, isoprene and 2,3-dimethyl-1,3-butadiene as well, considerably less than equilibrium 2-butene, 2-methyl-2-butene and 2,3-dimethyl-2-butene formation indicates substantial 1,2 addition of H_2 besides 1,4 addition.

Mainly 1,2 and 2,3 addition of H_2 accounts for the product composition from 3-methyl-1,2-butadiene. Isomerization is practically negligible as can be seen from the small quantity of 2-methyl-1-butene.

A mixture of diolefins was hydrogenated to determine relative reactivities. The order found: *cis*-1,3-pentadiene > *trans*-1,3-pentadiene > isoprene >

Table II

Homogeneous hydrogenation of diolefins (2 mmol) in DMF (2.5 ml) using $PdCl_2$ or $[PdCl_2(DMF)_2]$ (0.01 mmol) as catalyst precursor

$P_{H_2} = 25$ bar; RT

Substrate	Conversion (%)	Conversion (min)	Products (%)				Selectivity (%) $\left(\frac{\text{olefins} \cdot 100}{\text{olefins} + \text{alkane}}\right)$
	39.0	15		22.5		0.5	98.7
				14.0			
				2.0			
	76.5	23		50.0		1.0	98.7
				23.0			
				2.5			
	41.9	4		11.5		0.3	99.1
				10.7			
				19.3			
	82.0	7		22.0		0.8	99.0
				20.5			
				38.5			
	100 Pd ↓	10		5.9		7.5	
				20.3			
				66.3			
	46.5	8		25.1		0.04	>99.9
				21.4			

Table II (cont.)

	91.5	15		52.2	 0.05	>99.9
				39.3		
	38.7	3		12.4	 0.4	99.0
			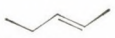	15.5		
			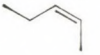	10.5		
	89.7	6		28.7	 0.8	99.1
			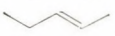	34.2		
			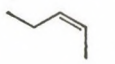	26.0		
	31.3	2	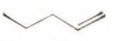	5.0	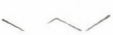 0.3	99.0
				21.9		
				4.1		
	90.2	7		15.3	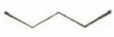 1.2	98.7
				62.1		
				11.7		
	42.0	10		42.0	 ~0.03	>99.9
	95.6	20		95.6	 ~0.05	>99.9
3-Methyl-1,2-butadiene	40.2	4		11.3	 0.5	98.8
				~0.05		
				28.4		
	84.0	8		25.2	 1.2	98.6
				0.1		
				57.5		

2,3-dimethyl-1,3-butadiene > 1,3-cyclohexadiene > 1,3-butadiene, is in accord with the rates measured individually.

The proton NMR spectra (Fig. 2) of the 1 : 1 reaction mixture of 2,3-dimethyl-1,3-butadiene and $PdCl_2$ in heptadeutero-DMF under argon, show the signals of methyl protons characteristic for a π-allyl type complex beside the strong methyl proton signal of unreacted 2,3-dimethyl-1,3-butadiene. When

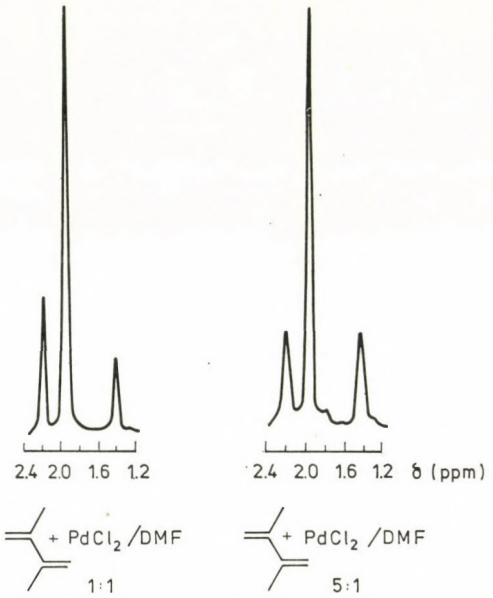

Fig. 2. Part of the 60 MHz ^{1}H-NMR spectra of 2,3-dimethyl-1,3-butadiene and $PdCl_2$ in DMF-d_7

the ratio of diene to $PdCl_2$ was raised to 5 : 1, the signals of the methyl protons in the π-allyl complex became broader — probably owing to the insertion of other dienes into the Pd—C bond [22]. In the presence of hydrogen and a large excess of dienes, the oligomerization of the substrates occurs only to a minor extent. Most probably, hydrogenation takes place by hydrogenolysis in the simple π-allyl stage.

From 1,3-pentadienes several kinds of π-allyl-Pd complexes may be formed which should yield different olefins by hydrogenolysis (Fig. 3). A product distribution was calculated based on the statistical formation of the π-allyl type complexes neglecting any steric or electronic differences. For *cis*-1,3-pentadiene the experimental data agree reasonably with these simple calculations. With *trans*-1,3-pentadiene, however, this is not the case possibly due to the preferential formation of the symmetrical π-allyl complex yielding *trans*-2-pentene as product.

Other diolefins such as 1,5-hexadiene, norbornadiene and 6,6-dimethylfulvene can be readily hydrogenated in homogeneous solution using $PdCl_2$ in DMF as well, but without selectivity. Alkanes from olefins are formed at nearly the same rate as olefins from the dienes. No isomerization of 1,5-hexadiene could be detected in the homogeneous stage of the reaction. Cyclopenta-

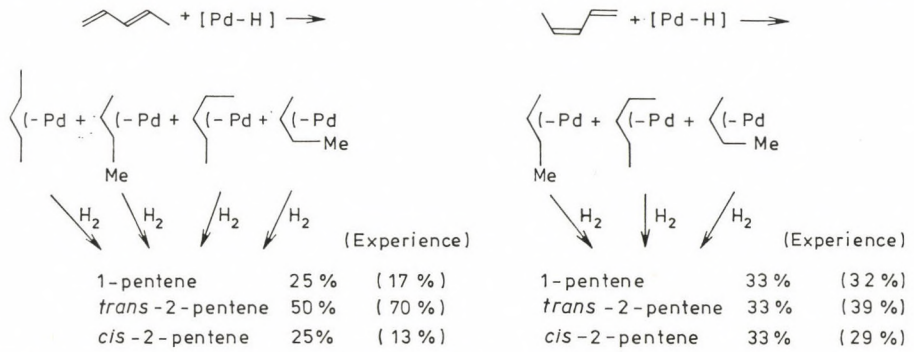

Fig. 3. Assumed statistical formation of π-allyl type complexes from 1,3-pentadienes and $PdCl_2$ in DMF and their products after hydrogenolysis

diene, α,β-unsaturated carbonyl compounds and furane derivatives could not be hydrogenated in homogeneous solution.

The other group of substrates for which $PdCl_2$ in DMF is effective are alkynes (see Tables III and IV).

As can be seen from the composition of products in the case of pentynes, heptyne and phenylacetylene hydrogenation, olefin formation is preferred with high selectivity. It is of interest that 2-pentyne reacts faster then 1-pentyne. On heterogeneous catalysts internal alkynes are usually hydrogenated slower than primary alkynes, probably because a terminal triple bond is less hindered than an internal one. A possible explanation for our observation may be that the easier complexation of the less hindered 1-pentyne is not favourable for hydrogenation. The same effect may account for the relatively low rate of hydrogenation with butadiene (Table II).

With simple alkynes like pentynes and heptyne the composition of alkenes *e.g.* the ratio of 1-alkene to 2-alkenes or the *cis-trans* ratio of internal olefins does not change during the hydrogenation reaction up to 99% conversion. It is well known that in the presence of palladium metal, isomerizations both kinds occur under such conditions. After all alkyne has been consumed, the yellow colour of the solution (orange in the case of phenylacetylene) turns black due to formation of finely dispersed Pd metal. At this point the isomerization of olefins begins and heterogeneous hydrogenation to alkane takes place slowly.

Table III

Homogeneous hydrogenation of alkynes (2 mmol) in DMF (2.5 ml) using $PdCl_2$ (0.01 mmol) as catalyst precursor

$P_{H_2} = 25$ bar; RT

Substrate	Conversion (%)	Conversion (min)	Products (%)				Selectivity (%) $\left(\frac{\text{olefins} \cdot 100}{\text{olefins} + \text{alkane}}\right)$
1-Pentyne	3.23	7	1-Pentene	31.5	Pentane	0.8	97.7
			2-Pentene	0.1			
	81.1	18	1-Pentene	78.5	Pentane	2.4	96.8
			2-Pentene	0.1			
2-Pentyne	34.3	5	*cis*-2-Pentene	33.8	Pentane	0.3	99.0
			tr-2-Pentene	0.1			
	85.7	13	*cis*-2-Pentene	82.7	Pentane	1.4	98.3
			tr-Pentene	1.7			
1-Heptyne	49.0	12	1-Heptene	48.0	Heptane	0.9	97.9
			2-Heptene	0.1			
	100 (Pd ↓)	25	1-Heptene	89.0	Heptane	6.3	
			2-Heptene	2.9			
			3-Heptene	1.8			
Ethynylbenzene	80.0	56	Styrene	75.8	Ethylbenzene	4.2	94.7

Table IV

Homogeneous hydrogenation of oxygen, nitrogen or halogen containing alkynes (2 mmol) in DMF (2.5 ml) using $PdCl_2$ (0.01 mmol) as catalyst precursor

$P_{H_2} = 25$ bar; RT

Substrate	Conversion (%)	Conversion (min)	Products (%)		Selectivity (%) $\left(\frac{\text{olefins} \cdot 100}{\text{olefins} + \text{alkane}}\right)$
Propargyl-alcohol	78.9	19	Allyl alcohol 76.3	1-Propanol 2.6	96.7
2-Methyl-3-butyn-2-ol	93.0	18	2-Methyl-3-buten-2-ol 91.0	2-Methyl-butan-2-ol 2.0	97.7
	32.8	6	31.8	1.0	97.0
Propargyl methyl ether	70.4	40	Allyl methyl ether 68.4	1-Propyl methyl ether 2.0	97.0
	26.8	15	26.0	0.8	97.1
Propargyl 2-tetrahydropyranyl ether	96.7	30	Allyl 2-tetrahydropyranyl ether 86.3	1-Propyl 2-tetrahydropyranyl ether 10.4	89.2
	24.0	8	22.6	1.4	94.2

The effect of heteroatoms in alkynes on hydrogenation varies. The triple bond in propargylalcohol, 2-methyl-3-butyn-2-ol and in two propargylethers can be hydrogenated to the corresponding double bond with high selectivity in homogeneous solution as can be seen in Table IV.

3-heptyn-2-ol and *N,N*-diethyl-1-propyn-3-amine are not able to stabilize $PdCl_2$ and the solution becomes heterogeneous. Despite the orange colour of the mixture no H_2 uptake could be achieved with propargylbromide. Neither volatile products nor unchanged propargylbromide could be found by GC. Most probably, polymerization occurred.

Unsaturated amines, oximes and nitro compounds stabilize $PdCl_2$ in H_2 atmosphere at RT but no H_2 uptake could be achieved even at higher temperatures. Aliphatic oximino compounds in a 2 or 3 fold excess cause an induction period and hydrogenation slows down but the sudden deposition of Pd at the end of hydrogenation can be retarded. The same effect could be achieved with 8-hydroxyquinoline and salen. The ratio of hydrogenation dropped 30 fold at a mole ratio of 1 : 1. At mole ratios higher than 1 : 1 for salen and 1 : 2 for 8-hydroxyquinoline the catalytic activity completely vanished.

Phosphines poisoned the catalyst formed from $PdCl_2(DMF)_2$ at a 1 : 1 mole ratio. Dienes could not be hydrogenated and the reaction with alkynes became extremly slow. If the order of addition was reversed and trialkylphosphines were added to the reaction mixture of $PdCl_2$, isoprene and DMF, then after an induction period of 5 to 15 min, hydrogenation did take place. This catalyst also produces olefins selectively, but among the olefins 2-methyl-2-butene is formed in nearly the thermodynamically expected amount.

*

The authors are grateful to Prof. L. MARKÓ for support and valuable discussions.

REFERENCES

[1] MAITLIS, P. M.: The Organic Chemistry of Palladium, Vol. 2. Academic Press, New York 1971
[2] WILLOTT, M. C. K., JOSHI, K. K., DUNNING, R. W., OLDHAM, A. R.: Brit. Pat. 1,154,937; C. A., **71,** 49213b (1969)
[3] STERN, E. W., MAPLES, P. K.: J. Catal., **27,** 120 (1972)
[4] BELOSLIUDOVA, T. M., ILINA, L. A.: Kinet. Katal., **16,** 788 (1975)
[5] FREIDLIN, L. Kh., KOPITCEV, Yu. A., NAZAROVA, N. M.: Izv. Akad. Nauk SSSR, Ser. Khim., **1974,** 604
[6] BERENBLUM, A. S., LAKHMAN, L. I., MOISEEV, I. I., RADCHENKO, E. D.: Izv. Akad. Nauk SSSR, Ser. Khim., **1975,** 2417
[7] NAZAROVA, N. M., KOPITCEV, Yu. A., SCHERBAKOVA, S. I., FREIDLIN, L. Kh.: Izv. Akad. Nauk SSSR, Ser. Khim., **1975,** 2589
[8] HECK, R. F.: U. S. Pat. 3,270,087; C. A., **65,** 16857d (1966)
[9] SLOAN, M. F., MATLACK, A. S., BRESLOW, D. S.: J. Am. Chem. Soc., **85,** 4014 (1963)
[10] MAXTED, E. B., ISMAIL, S. M.: J. Chem. Soc., **1964,** 1750
[11] RYLANDER, P. N., HIMELSTEIN, N., DUANE, B. S., KREIDL, J.: Engelhard Industries Inc., Techn. Bull., **3,** 61 (1962)

[12] SISAK, A., UNGVÁRY, F.: Chem. Ber., **109,** 531 (1976)
[13] FREIDLIN, L. Kh., KOPITCEV, Yu. A., NAZAROVA, N. M.: Izv. Akad. Nauk SSSR, Ser. Khim., **1972,** 700
[14] FREIDLIN, L. Kh., KOPITCEV, Yu. A., NAZAROVA, N. M.: Neftekhimiya, **13,** 369 (1973)
[15] ABLEY, P., MCQUILLIN, F. J.: Disc. Faraday Soc., **46,** 31 (1968)
[16] ITATANI, H., BAILAR, J. C., Jr.: J. Am. Oil Chem. Soc., **44,** 147 (1967); Ind. Eng. Chem. Prod. Res. Dev., **11,** 146 (1972)
[17] TAYIM, H. A., BAILAR, J. C., Jr.: J. Am. Chem. Soc., **89,** 4330 (1967)
[18] OLIVÉ, G. H., OLIVÉ, S.: Angew. Chem., **86,** 561 (1974); J. Molecular Cat., **1,** 121 (1975/76)
[19] DATTA, M. C., SAHA, C. R., SEN, D.: Chem. Ind., **1975,** 1057
[20] KANAI, M., MIYAKE, A.: Jap. Pat. 71 29,127; C. A., **75,** 150891d (1971)
[21] ROZHDESTVENSKAYA, I. D., TELESHEV, A. T., KUCHEROV, A. V., SLINKIN, A. A., NIFANTEV, E. E.: Koord. Khim., **1977,** 1226
[22] SISAK, A., UNGVÁRY, F.: Acta Chim. Acad. Sci. Hung., **99,** 209 (1978)
[23] DONATI, M., MERELLI, G., CONTI, F., UGO, R.: Chim. Ind., **50,** 231 (1968)
[24] BRANDSMA, L.: Preparative Acetylenic Chemistry, pp. 29, 65, 103, 172. Elsevier Publ. Co. 1971
[25] UNGVÁRY, F., SISAK, A.: Magy. Kém. Foly., **83,** 285 (1977)
[26] SMITH, B., RAGNAR, O., LARSON, G.: Acta Chem. Scand., **17,** 463 (1963)
[27] DIETZ, W. A.: J. Gas Chrom., **5,** 68 (1967)

Attila SISAK
István JABLONKAI
Ferenc UNGVÁRY
H-8201 Veszprém, Schönherz Z. u. 12.

Acta Chimica Academiae Scientiarum Hungaricae, Tomus 103 (1), pp. 43—50 (1980)

APPLICATION OF THE KUHN—MARK—HOUWINK CONSTANTS IN THE UNIVERSAL CALIBRATION OF GEL PERMEATION CHROMATOGRAPHY

G. SAMAY and L. FÜZES
(Research Institute for Plastics Industry)

Received January 18, 1979
Accepted for publication February 28, 1979

In this report investigations are made on how the choice of the Kuhn—Mark—Houwink constants taken from the literature affects the accuracy of the calibration curves obtained on the basis of universal calibration in gel permeation chromatography. It was found that the difference in the calibrations obtained using different Kuhn—Mark—Houwink constants is small, *i.e.* the effect of the choice is also small. For correct calculations the universal calibration curve must be constructed in the elution range of the low molecular weight too; for low-molecular-weight calibrating materials the intrinsic viscosity can be calculated using the "theta data" for Kuhn—Mark—Houwink constants.

In our previous paper [1] some measurements were made to determine the Kuhn—Mark—Houwink constants (KMH constants) for some homo- and copolymers. With the help of these data, BENOIT's [2] universal calibration was constructed for two differently working gel permeation chromatograph (GPC) systems. The validity of the calibration was confirmed and it was shown that universal calibration permits determination of the molecular weight in the case of different materials if (i) the viscosity of the GPC eluate is measured continuously and automatically, or (ii) if the KMH constants are known for the material tested.

If the intrinsic viscosity cannot be measured at many points of the elution region by an automatic viscometer, the knowledge of the KMH constants is necessary for data processing in GPC practice using universal calibration. The measurement of the KMH constants is time-consuming and requires narrow fractions of known absolute molecular weights, therefore, they are often taken from the literature. However, there are many different relations published for the same material under the same conditions. This fact seems to make the correct calculation very difficult or even impossible, as was assumed by CERVENKA [3].

The aim of the present paper is to obtain information about the effect of the choice of published KMH constants on the accuracy of the GPC method, if the universal calibration is used in data evaluation.

Experimental

Two GPC set-ups were used for the measurements, one was operated at 403 K with 1,2,4-trichlorobenzene (TCB), while the other apparatus at ambient temperature with tetrahydrofuran (THF) as solvent. The details of the systems have been described [1], together with the respective universal calibration curves.

Results and Discussion

First of all the published KMH constants were collected for several polymers for the conditions, used in our GPC instruments and listed in Table I. As is seen from Table I, the value of a varies within a wide range for a given material under the given conditions. Thus it might be supposed that highly different molecular weights can be obtained for the same measurement if the different KMH constants are used together with universal calibration. To characterize this effect through the whole elution range, we have constructed the log M *vs.* elution volume (V) calibration curve, f(V), with the help of direct measurements of narrow fractions, and calculated them from the universal (log M *vs.* V) calibration — F(V) — with the different KMH constants in Table I on the basis of Eq. (1):

$$f(V) = \frac{F(V) - \log K}{a + 1} \tag{1}$$

where K and a are the KMH constants.

Thus a set of calibration curves can be constructed for a certain material using the universal calibration. In Figs 1—5 the log M *vs.* V calibration curves are shown for the two GPC instruments as constructed using the universal calibration and the KMH constants in Table I. In those cases where too many data were at disposal [polyethylene, TCB, 403 K and poly(vinylchloride), THF, 298 K] only the regions are shown where the calibration curves are located, together with the directly measured calibrating points. The curves run very close to each other and to the experimental points. In the case of polyethylene (PE) also the calibration referring to the "theta" conditions was constructed (pointed line) which nearly coincides with the true calibration if the molecular weight is low. This fact supports the assumption that in the case of small molecules the approximation $a = 0.5$ is valid [4]. In Fig. 1 the two thick lines show the confidence limits of the curve calculated from the measured points at a 95% significance level. (The calibration curves were approximated by second order polynomials fitted to the experimental points by the least squares method.) The calibrations constructed on the basis of Table I fall inside the region of these confidence limits. This means that at least in this case the uncertainity of direct calibration is higher than that of

Table I

Kuhn—Mark—Houwink constants for several polymer types taken from the literature and measured on our laboratory

Polymer	Conditions	$K \times 10^2$ cm³/g	a	Reference	
PS	TCB, 403 K	0.89	0.727	Boni	[4]
		2.80	0.64		[1]
	408 K	1.21	0.707	Coll	[5]
PS	THF, 296 K	0.682	0.766	Boni	[4]
	298 K	1.17	0.726	Goedhardt	[6]
		1.14	0.72	Otocka	[7]
		0.609	0.768		[1]
PE	TCB, 408 K	4.34	0.724	Coll	[5]
	403 K	7.1	0.67	Cote	[8]
		12.7	0.61	Prechner	[9]
		4.6	0.725	Mendelson	[10]
		5.23	0.70	Crouset	[11]
		9.54	0.64	Williamson	[12]
		4.48	0.718	Cervenka	[3]
		5.1	0.706	Otocka	[7]
		3.92	0.725	Wagner	[13]
		5.26	0.70	Peyrouset	[14]
		16.9	0.591	Panaris	[15]
		6.14	0.678		[1]
PP	TCB, 408 K	1.37	0.75	Coll	[5]
	403 K	0.74	0.83		[1]
PVC	THF, 298 K	1.6	0.77	Goedhardt	[6]
		4.98	0.69	Freemann	[16]
		1.63	0.77	Freemann	[16]
		1.5	0.77	Endo	[17]
		5.32	0.67	Baijal	[18]
		4.48	0.70		[1]
	303 K	1.27	0.82	Bohdanecky	[19]
		12.9	0.54	Kobayashi	[20]

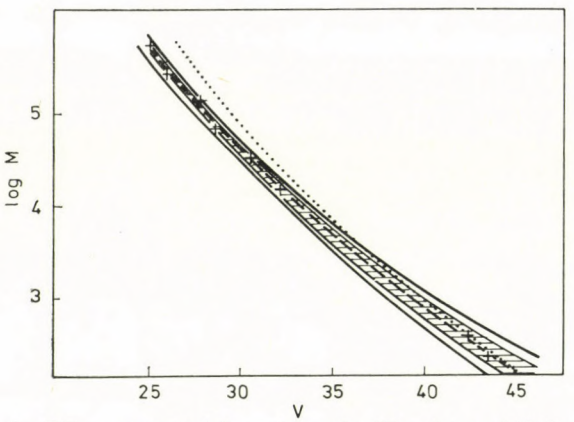

Fig. 1. Calibration for PE as computed by universal calibration and Kuhn—Mark—Houwink constants (TCB, 403 K). The shaded band is the area where the lines fall, the crosses are the measured points, the dotted line is the least squares fit to these points, the thick lines are the confidence limits of this fit and the pointed line is the calibration using data corresponding to theta conditions

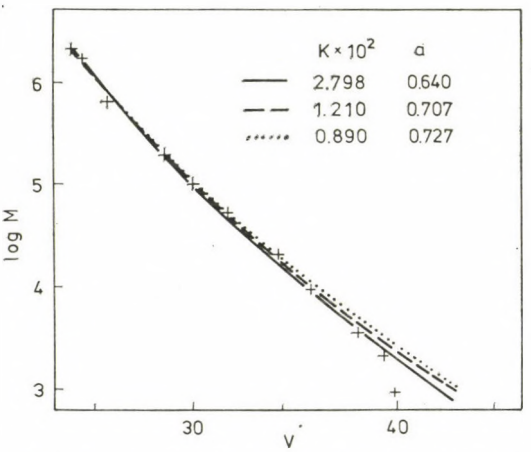

Fig. 2. Calibrations for PS as calculated by means of the universal calibration and Kuhn—Mark—Houwink constants (TCB, 403 K)

the line computed on the basis of the universal calibration using different KMH constants taken from the literature.

The universal calibration may be used only in the molecular weight region where measured points are at disposal. However, it is difficult to measure the intrinsic viscosity for low molecular weight samples, therefore, experimental points are mostly not at disposal for high values of elution volumes. Nevertheless, according to Boni *et al.* [4] and Kurata and Stockmayer [21], the values for low molecular weight materials do not differ from those in

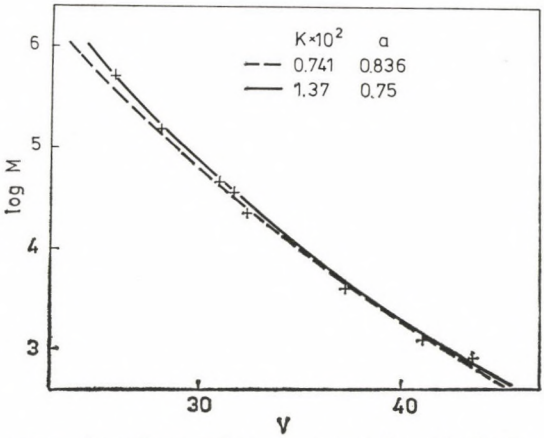

Fig. 3. Calibration curves for polypropylene, constructed on the basis of universal calibration and the Kuhn—Mark—Houwink constants (TCB, 403 K)

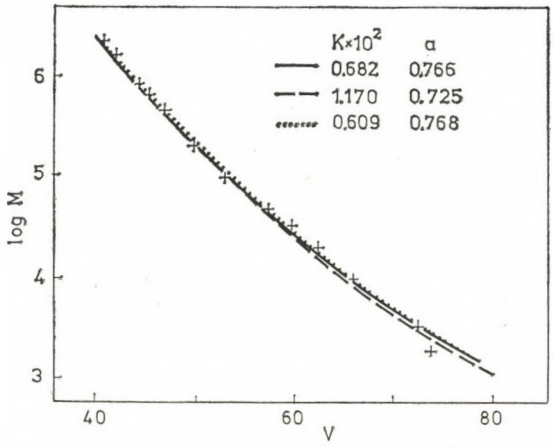

Fig. 4. Calibrations for PS, computed by means of universal calibration and the Kuhn—Mark—Houwink constants (THF, 298 K)

"theta" solutions, *i.e.* they can be estimated with using the "theta" data. In this way the universal calibration can be extended to higher elution volumes. Figure 6 shows the effect of the above approximation on the reliability of calculation in the case of the high temperature GPC. The crosses in Fig. 6 represent the experimental points for PE standards and *n*-paraffins in the log M *vs.* V plot. The full line is the calibration curve computed using Eq. (1) ($a = 0.61$, $K = 0.127$ were used in Eq. (1)) from the universal calibration curve without points in the low molecular weight region, while the dotted line

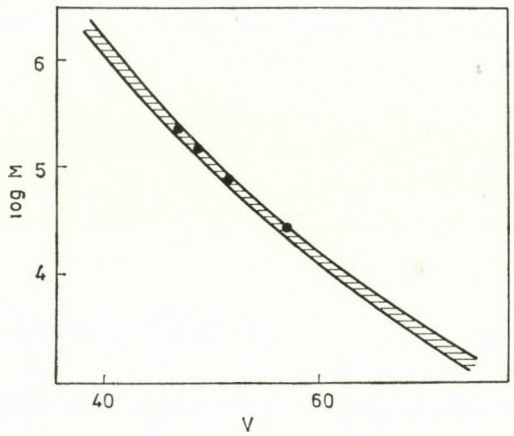

Fig. 5. Calibration for PVC (THF, 298 K), computed on the basis of universal calibration and Kuhn—Mark—Houwink constants. The shaded band is the area where the calibration lies and the points are measured experimentally

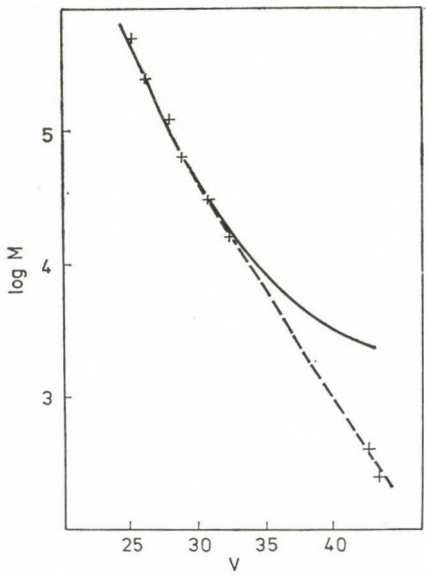

Fig. 6. Comparison between the calibration curves constructed by means of the universal calibration, if the small molecules are not taken into account (full line) and if they are (dotted line) (TCB, 403 K)

is similarly obtained if low molecular weight samples are also included into universal calibration using the above approximation.

The curves in Fig. 6 coincide in the high molecular weight region (where calibrating points were used in both cases), but below the molecular weight of about 2×10^4 only the dotted line represents a good fit to the experimental data (it was obtained from the universal calibration with points in the high elution volume range).

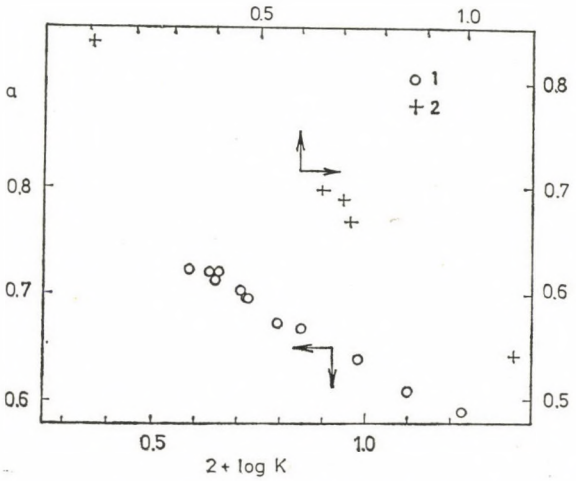

Fig. 7. Relation between the Kuhn—Mark—Houwink constants in Table I for polyethylene (1) and poly(vinyl chloride) (2)

These investigations show that the choice of KMH constants from the published data does not affect the accuracy of data processing with universal calibration to a marked degree. The reason for this is probably that different KMH constants may lead to a good agreement of viscometric data and molecular weights if a certain relation holds between the K and a, as was shown by others (*e.g.* [22]). If the measurements are free from gross experimental errors — as can be expected in the case of published data — the data obtained obey this relation, and supposedly can be used for calculations in both viscometry and gel permeation chromatography. In Fig. 7 the a values are plotted against $\log K$ (see [22]) for polyethylene and poly(vinyl chloride), and a nearly linear dependence can be observed.

For correct calculations the universal calibration must be constructed for the whole range of elution volumes available; with low molecular weight samples the "theta" data of KMH constants can be used for this purpose.

REFERENCES

[1] SAMAY, G.: Acta Chim. Acad. Sci., Hung. (In press)
[2] BENOIT, H., GRUBISIC-GALLOT, Z., REMPP, P., DECKER, D., ZILLOIX, J. G.: J. Chim. Phys., **63,** 1507 (1966)
[3] CERVENKA, A.: Makromol. Chem., **170,** 239 (1970)
[4] BONI, K. A., SLIEMERS, F. A., STICKNEY, P. B.: J. Polym. Sci., A-2, **6,** 1579 (1968)
[5] COLL, H., GILDING, D. K.: J. Polym. Sci., A-2, **8,** 89 (1970)
[6] GOEDHARD, D. J., OPSCHOOR, A., AKZO, T.: J. Polym. Sci., A-2, **8,** 1227 (1970)
[7] OTOCKA, E. O., ROE, R. J.: Macromolecules, **4,** 507 (1971)
[8] COTE, J. A., SHIDA, M.: J. Polym. Sci., A-2, **9,** 421 (1971)
[9] PRECHNER, R., PANARIS, R.: Report on the Working Party on Macromolecular Characterisation of Polyethylenes. C.R.N.S., Strasbourg, France, March 12, 1971
[10] MENDELSON, R. A., BOWLES, W. A., FINGER, F. I.: J. Polym. Sci., A-2, **8,** 105 (1970
[11] CROUZET, P., MARTENS, A., MARGIN, P.: 7th Int. Seminar on GPC. Monte Carlo, 1969
[12] WILLIAMSON, G. R., CERVENKA, A.: Eur. Polym. J., **8,** 1009 (1972)
[13] WAGNER, H. J., HOERE, C. A. J.: J. Polym. Sci., Polym. Phys., **11,** 1189 (1973)
[14] PEYRUOSET, A., PRECHNER, R.: J. Appl. Polym. Sci., **19,** 1363 (1975)
[15] PANARIS, R., PRECHNER, R.: 7th Int. Seminar on GPC. Monte Carlo, 1969
[16] FREEMAN, M., MANNING, P. P.: J. Polym. Sci. A-2, 2017 (1964)
[17] ENDO, R., GOTO, R., TAKEDA, M.: Kobunshi Kagaku, **22,** 405 (1965)
[18] BAIJAL, M. D., KAUPILA, K. M.: Polym. Eng. Sci., **11,** 181 (1971)
[19] BOHDANECKY, M., SOLC, K.: J. Polym. Sci., A-2, **5,** 343 (1965)
[20] KOBAYASHI, T.: Bull. Chem. Soc. Japan, **35,** 726 (1962)
[21] STOCKMAYER, W. H., KURATA, M.: Fortschr. Hochpolym. Forsch., **3,** 196 (1963)
[22] AHARONI, S. M.: J. Appl. Polym. Sci., **21,** 1323 (1977)

Géza SAMAY
László FÜZES } H-1950 Budapest, Hungária krt. 114.

Acta Chimica Academiae Scientiarum Hungaricae, Tomus 103 (1), pp. 51—58 (1980)

ACIDITY CONSTANTS OF 1,2,3-CYCLOHEXANE TRIONE DIOXIME (1,3) AND OF 1,2,3-CYCLOHEXANE TRIONE TRIOXIME

J. ZSAKÓ, A. BENKŐ, J. HORÁK and Cs. VÁRHELYI

(Faculty of Chem. Technology, Babeş-Bolyai University, Cluj-Napoca, Romania)

Received November 17, 1978
Accepted for publication March 9, 1979

1,2,3-Cyclohexane trione dioxime (1,3) **(I)** and 1,2,3-cyclohexane trione trioxime **(II)** were synthesized. Their acidity constants were determined both by potentiometric and spectrophotometric methods, at 20 °C and ionic strength of $\mu = 0.1$ *M*. UV and visible absorption spectra are presented. The correlation between acidity and molecular structure is discussed.

Due to the electron-attractive effect of the C=N double bond, the oximes are weak acids. The pK value of the acetoxime [1] is 12.22. The substitution of the methyl group, or of the hydrogen, for more electron-withdrawing groups leads to the increase of the acidity. Thus, the pK value of acetophenoneoxime [2] is 11.48, that of the benzophenoneoxime 11.30. The aromatic aldoximes are even stronger acids, especially in their α-form. In the case of α-benzaldoxime pK = 10.06 [3].

The presence of a C=O group in α position increases the acidity of the oxime group [4]. A similar effect can be observed with α-dione dioximes, *e.g.* the pK_1 value of the dimethyl-glyoxime [5] is 10.55. Such an increase of the acidity is due to the delocalization of the C—N π-bond. In the case of the α-dione dioximes a larger delocalized π-bond system leads to further increase of the acidity. Thus the pK_1 value of the α-benzyldioxime is 10.12, that of α-furyldioxime 9.80 [5].

In the case of the 1,2-cyclohexane dione dioxime literature pK_1 data are between 10.41 and 10.75 [5—9]. For the corresponding pK_2 values 12.16 [5] and 12.40 [7] have been reported.

As the acidity of the 1,2,3-cyclohexane trione dioxime (1,3) **(I)** and of the 1,2,3-cyclohexanetrione trioxime **(II)** studied in the present paper, are concerned, the presence of a CO group between the oxime groups must increase sensibly both acidity constants of **(I)** and the acidity of the oxime group of **(II)** in position 2 must be even higher.

One can expect the pK_2 value of **(II)** to be a little lower, the pK_3 value of **(II)** to be a little higher than the pK_2 value of the 1,2-cyclohexane dione dioxime.

In this paper the acidity constants of (I) and (II) have been determined, both by potentiometric and spectrophotometric methods.

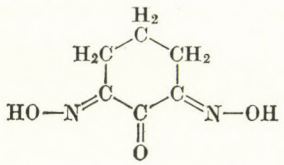

I

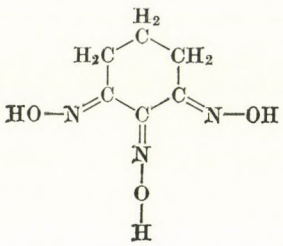

II

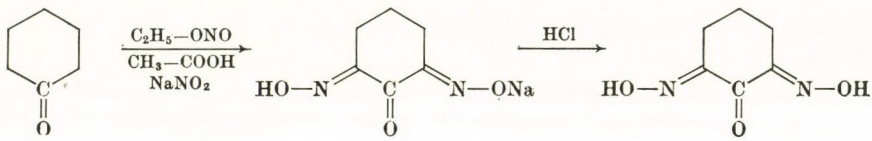

Experimental

By the izonitrozation of cyclohexanone with ethyl nitrite in the presence of acetic acid TREIBS and KUHN [10] obtained the sodium salt of 1,2,3-cyclohexane trione dioxime (1,3) according to the reaction.

The corresponding trioxime was obtained from this with an excess of hydroxylamine.

In the present paper a modification of the above method is proposed, which allows the purification of the products and the increasing of the yields.

Synthesis of 1,2,3-cyclohexane trione dioxime (1,3)

410 g $NaNO_2$ is dissolved in approx. 800 ml water, 170 ml ethyl alcohol and then further water added to make 1700 ml. Separately 170 ml conc. H_2SO_4 ($d = 1.84$) is dissolved in 800 ml water and 170 ml alcohol added, then diluted with water up to 1700 ml. The acidic alcoholic solution is added drop by drop to the nitrite solution. The ethyl nitrite gas evolved is bubbled through 180 ml cyclohexanone acidified with 10 ml *conc.* hydrochloric acid for 5—6 hours, below 10 °C, under continuous stirring. After 5—6 hours of standing, the yellow precipitate formed is filtered, washed with dil. alcohol (1 : 1). The crude product is recrystallized from hot alcohol. Yield: 175 g, m.p. 224 °C.

$C_6H_8O_3N_2$ (156.1). Calcd. N 17.9. Found 18.1%.

Synthesis of 1,2,3-cyclohexane trione trioxime

60 g 1,2,3-cyclohexane trione dioxime (1,3) is dissolved in 350—400 ml methanol and treated with an excess of hydroxylamine hydrochloride (75 g). The mixture is refluxed for 4—5 hours. The trioxime separates on evaporation as pink microcrystals. The crude product is recrystallized from a small volume of water. Yield: 60%, m.p. 176—177 °C.

$C_6H_9O_3N_3$ (171.2). Calcd. N 24.6, Found 24.5%.

Potentiometric measurements

Samples of about 0.01 *M* solutions of (I) and (II) were titrated with 0.1 *M* NaOH solution, potentiometrically, by using an universal glass electrode. Measurements were performed at 20 °C and the ionic strength of the samples was $\mu = 0.1$ *M*, obtained by adding appropriate amounts of $NaClO_4$.

Spectrophotometric measurements

The UV and visible spectra of **(I)** and **(II)** were recorded at different pH values, on a SPECORD recording spectrophotometer.

In order to derive acidity constants different phosphate buffers were prepared with pH values between 5 and 13. The ionic strength was adjusted to $\mu = 0.1$ by adding an appropriate amount of a $NaClO_4$ solution. Samples were kept in ultrathermostat at 20 °C. Absorbance measurements were performed on a VSU—2 spectrophotometer in 1 cm path cells, against the same buffer solution, without dioxime.

Results

The potentiometric titration curves are presented in Fig. 1.

As seen from curve I, practically no potential jump is obtained in the case of **(I)**. The pH value in the point corresponding to the neutralization of a half of the first hydrogen ($pH_{1/2}$, indicated by an arrow in Fig. 1) is equal

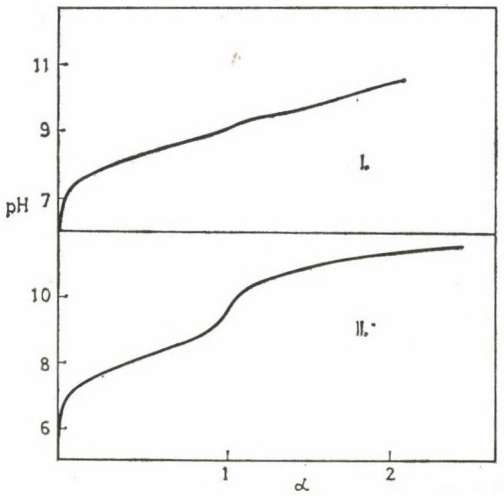

Fig. 1. Potentiometric titration curves of 1,2,3-cyclohexane trione dioxime (1,3) **(I)** and of 1,2,3-cyclohexane trione trioxime **(II)** with 0.1 M NaOH solution; $t = 20$ °C, $\mu = 0.1$ *M*, $c = 0.01$ *M*

to 8.36. This means, that the pK_1 value must be very close to this $pH_{1/2}$ value. The first portion of the titration curve, up to 25 per cent neutralization of the first hydrogen ($\alpha \leq 0.25$), was used to calculate K_1 as described earlier [11].

The second acidity constant was derived from the points of the titration curves, corresponding to $\alpha > 0.8$, by using the K_1 value derived from the first portion of the same titration curve. Calculations were performed as earlier [11].

The mean values of pK_1 and pK_2 derived from different points of the titration curves are presented in Table I.

Table I

Acidity constants derived from potentiometric titration curves, $t = 20$ °C, $\mu = 1$ M

Substance	pK_1	pK_2	pK_3
1,2,3-cyclohexane trione dioxime (1,3)	8.40 ± 0.03	9.83 ± 0.07	—
1,2,3-cyclohexane trione trioxime	8.16 ± 0.06	11.11 ± 0.07	12.19 ± 0.25

As seen, the pK_1 value is very close indeed to the above given $pH_{1/2}$ value.

Curve II of Fig. 1 shows a clear potential jump at the first equivalence point. Since $pH_{1/2} < 10$, its value (8.16) can be taken for pK_1 [12]. By using the first portion of the titration curves, up to $\alpha = 0.9$, different experimental points gave a practically constant value for K_1. As expected, the mean value of pK_1, given in Table I, is practically identical with the $pH_{1/2}$ value. The second acidity constant has been derived from the portion of the titration curves corresponding to $1 < \alpha < 1.4$, and its mean value is presented in Table I.

The third acidity constant has been derived from the points of the titration curves, corresponding to $\alpha > 1.8$, by using the above obtained K_1 and K_2 values.

The arithmetical mean of the results obtained are presented also in Table I.

In order to see the possibilities to derive the acidity constants, the UV and visible spectra of (**I**) and (**II**) were recorded at different pH values. In Fig. 2 three representative spectra are presented for both compounds, reflecting the general features of these spectra. Curves *a* were obtained in acidic solutions (pH $\approx$ 3), curves *c* in basic ones (pH $\approx$ 12) and curves *b* at a lower pH value than curves *c*.

On the basis of these curves several wave lengths were chosen in order to obtain experimentally the pH dependence of the absorbance. These wave lengths are indicated by arrows in Fig. 2. Results obtained are presented in Figs 3 and 4.

As seen from Fig. 3, curve 2 recorded at $\lambda = 292$ nm has a maximum corresponding to pH = 9.15. This allows us to use our trial and error procedure proposed earlier [11] and to derive K_1 and K_2. Results are given in Table II.

In the case of compound (**II**) curve 1 of Fig. 4 suggests the idea that at 211 nm the molar absorptivities of the 3 ionic species have practically the same value, *i.e.* $\varepsilon_1 = \varepsilon_2 = \varepsilon_3$, where ε_i stands for the absorptivity of the species $H_{3-i}X^{i-}$ resulting from the ionization of the acid H_3X studied. Thus, the variation of the absorbance is governed exclusively by K_1. On the basis

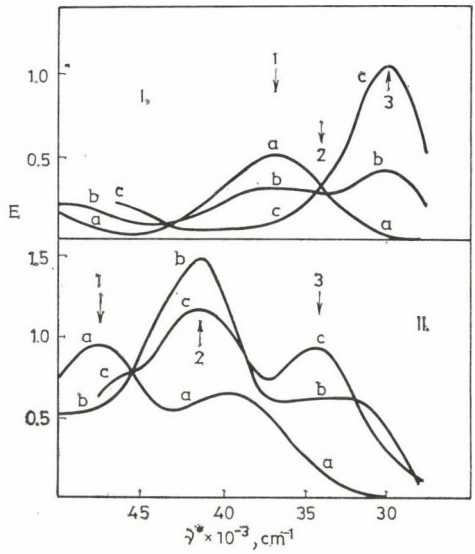

Fig. 2. UV and visible absorption spectra of 1,2,3-cyclohexane trione dioxime (1,3) **(I)** and of 1,2,3-cyclohexane trione trioxime **(II)**; $c = 5 \times 10^{-5}$ *M*, 1 cm path cell; **(I)** a — pH = 2.95, b — pH = 8.76, c — pH = 12.7; **(II)** a — pH = 2.95, b — pH = 9.82, c — pH = 12.8

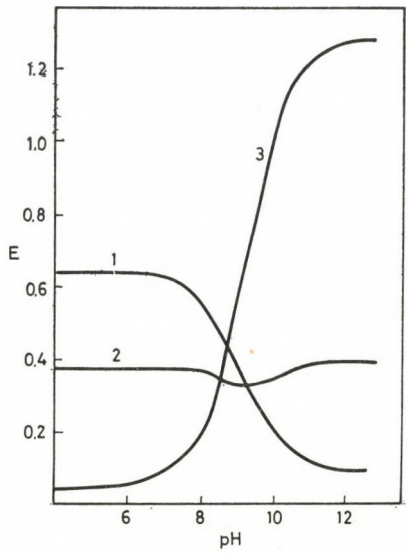

Fig. 3. Absorbance —pH curves of 1,2,3-cyclohexane trione dioxime (1,3), $c = 6 \times 10^{-5}$ *M*, $\mu = 0.1$ *M*, $t = 20$ °C; 1 — $\lambda = 270$ nm, 2 — $\lambda = 292$ nm, 3 — $\lambda = 332$ nm

of this presumption K_1 can be derived as with monovalent acids. The mean value of K_1 obtained in this way is given in Table II.

The curve 2 shows a clear maximum at pH = 9.95 and E has a practically constant value at higher pH, suggesting the idea that $\varepsilon_2 \approx \varepsilon_3$, allows the application of the above mentioned trial and error method to derive both K_1 and K_2 from the experimental E values (up to pH = 10.6). Results are presented also in Table II.

Since curve 3 shows a variation of E even at higher pH values than curve 2, the last portion of curve 3 allows us to derive the K_3 value, too.

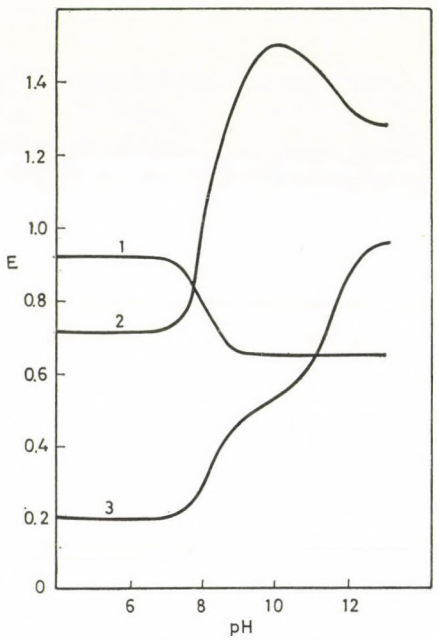

Fig. 4. Absorbance — pH curves of 1,2,3-cyclohexane trione trioxime, $c = 10^{-5}$ M, $\mu = 0.1$ M, $t = 20$ °C; 1 — $\lambda = 211$ nm, 2 — $\lambda = 241$ nm, 3 — $\lambda = 290$ nm

Table II

Acidity constants obtained spectrophotometrically, $t = 20$ °C, $\mu = 0.1$ M

Substance	pK_1	pK_2	pK_3	λ nm
1,2,3-cyclohexane trione dioxime (1,3)	8.50 ± 0.05	9.91 ± 0.05	—	292
1,2,3-cyclohexane trione trioxime	8.14 ± 0.07	—	—	211
	8.38 ± 0.02	10.93 ± 0.02	—	241
	—	—	11.96 ± 0.09	290

The absorbance of a trivalent acid H_3X can be given as

$$E = \frac{H^3 \varepsilon_0 + K_1 H^2 \varepsilon_1 + K_1 K_2 H \varepsilon_2 + K_1 K_2 K_3 \varepsilon_3}{\Sigma} \; cd \tag{1}$$

where

$$\Sigma = H^3 + K_1 H^2 + K_1 K_2 H + K_1 K_2 K_3 \tag{2}$$

where H stands for the concentration of the hydrogen ions, c for the analytical concentration of the acid, and d for the path of the light beam in the solution.

The absorbance ε_0 can be derived directly from curve 3, *viz.* from the absorbance at low pH values. In order to derive ε_1 and ε_2, the following procedure has been used:

From each experimental point the fractions of the species $H_3X(\alpha_0)$, $H_2X^-(\alpha_1)$, $HX^{2-}(\alpha_2)$ and $X^{3-}(\alpha_3)$ were calculated from the following expressions [13]

$$\alpha_0 = \frac{H^2}{\Sigma}; \; \alpha_1 = \frac{K_1 H^2}{\Sigma}; \; \alpha_2 = \frac{K_1 K_2 H}{\Sigma}; \; \alpha_3 = \frac{K_1 K_2 K_3}{\Sigma} \tag{3}$$

K_1 and K_2 were obtained from curves 1 and 2, and for K_3 an approximate value of 10^{-12} was taken.

In the case of the first portion of curve 3, $\alpha_3 < 0.01$, *i.e.* the contribution of X^{3-} to the absorbance can be neglected, and from (1) the following expression can be obtained:

$$\frac{\varepsilon_1 cd}{b} + \frac{\varepsilon_2 cd}{e} = 1 \quad \text{with} \quad b = \frac{E - \varepsilon_0 cd \alpha_0}{\alpha_1}; \; e = \frac{E - \varepsilon_0 cd \alpha_0}{\alpha_2} \tag{4}$$

Equation (4) allows us to derive ε_1 and ε_2 from the intersection of a number of straight lines, corresponding each one to an experimental point [14].

By means of this graphical method ε_1 could be well derived, but ε_2 values were rather scattered. By taking the experimental points corresponding to $0.02 < \alpha_2 < 0.3$ a practically constant value could be obtained for ε_2 by means of the formula

$$\varepsilon_2 = \frac{E - (\varepsilon_0 \alpha_0 + \varepsilon_1 \alpha_1) cd}{\alpha_2 cd} \tag{5}$$

The acidity constant K_3 and the absorptivity ε_3 were derived from the last portion of curve 3, by means of (1) and by using the above described trial and error method. Results are presented in Table II.

Discussion

As seen from Tables I and II, the potentiometric and spectrophotometric methods give almost the same values for the acidity constants. At any rate, differences between the pK values derived by means of both methods are not higher than differences obtained by deriving pK spectrophotometrically from curves corresponding to different wave lengths.

The acidity of the oxime groups is exactly as expected on the basis of the molecular structure.

In the case of compound (**I**) the presence of the carbonyl group increases the acidity of both oximes. The electronrepulsing effect of the electric charge of HX^- is not very important, since it is localized on a group linked to the C atom in β-position.

In the first ionization step (**II**) is stronger acid, than (**I**), but in the second one it is a rather weak acid, since the electric charge of H_2X^- is localized on a group linked to the C atom in α-position. This is why the first hydrogen can be titrated separately. The difference between pK_2 and pK_3 is much less, since the new charge in HX^{2-} appears in β-position, as in the case of (**I**).

REFERENCES

[1] LUNDÉN, H.: Z. physik. Chem., **54,** 532 (1906)
[2] BRADY, O. L., CHOKSHI, N. M.: J. Chem. Soc., **1929,** 946
[3] BRADY, O. L., GOLDSTEIN, R. F.: J. Chem. Soc., **1926,** 1918
[4] GANDINI, A., STRANEO, C.: Gazz. chim. Ital., **67,** 104 (1937)
[5] SAVOSTINA, V. M., ASTAKHOVA, E. K., PESHKOVA, V. M.: Zhur. neorgan. Khim., **9,** 80 (1964)
[6] BANKS, C. V., ANDERSON, S.: J. Inorg. Chem., **2,** 112 (1963)
[7] BANKS, C. V., CARLSON, A.: Anal. Chim. Acta, **7,** 291 (1952)
[8] BANKS, C. V., BARNUM, D. V.: J. Am. Chem. Soc., **80,** 3579 (1958)
[9] HARRIS, R., RYAN, D., CHANEY, G.: J. Am. Chem. Soc., **84,** 1149 (1962)
[10] TREIBS, A., KUHN, A.: Chem. Ber., **90,** 1691 (1957)
[11] ZSAKÓ, J., HORÁK, J., FINTA, Z., VÁRHELYI, Cs., MITRACHE, I.: Microchim. Acta, **1979** I, 405
[12] ZSAKÓ, J., ALMÁSI, L., GIURGIU, M., HANTZ, A.: Studii si Cercet. Chim. Cluj, **14,** 271 (1963)
[13] ZSAKÓ, J.: Studia Univ. Babeș-Bolyai, Chem., **11,** 13 (1960)
[14] IRVING, H. M. N. H.: Analyst, **93,** 273 (1968)

János ZSAKÓ
András BENKŐ
József HORÁK
Csaba VÁRHELYI

Faculty of Chemical Technology, Babeș-Bolyai University, 3400 Cluj-Napoca, Str. Arany János 11, Romania.

Acta Chimica Academiae Scientiarum Hungaricae, Tomus 103 (1), pp. 59—69 (1980)

SEMIEMPIRICAL QUANTUMCHEMICAL CALCULATIONS ON THE C_7 CONFIGURATION OF SOME 7-SUBSTITUTED 3-KETO-4-ENE STEROIDS

P. NAGY and Gy. BEER

(Chemical Works of Gedeon Richter Ltd., Budapest)

Received January 3, 1979
Accepted for publication March 9, 1979

The nucleophilic addition to 3-keto-4,6-diene steroids results in 7-substituted, 3-keto-4-ene steroids. The position of the substituent depending on the nature of the nucleophilic agent is generally axial (α). PCILO calculations support these experimental experiences. The study of the reasons leading to the formation of the given configuration suggests that the degree of the steric interactions between the substituent and the steroid skeleton governs primarily the configuration to be realized.

It has been well-known for a long time that the 3-keto-4,6-diene steroids undergo nucleophilic additions to the $C_6—C_7$ double bond. It is interesting in this case that in the great majority of examples published in the literature the obtained compounds have an *axial* (α) 7-substituent (Fig. 1).

DODSON and TWEIT [1, 2] carried out the first thioacetic acid addition to 3-keto-4,6-diene steroids of androstane and pregnane types (struct. 1). The reaction took place by refluxing in excess of thioacetic acid applying UV irradiation as well. According to their investigations the acetylthio group enters the *axial* position of the conjugated system, so 7α-acetylthio-3-keto-4-ene steroid was formed.

SCHAUB *et al.* [3] carried out the addition to 3-keto-4,6-diene steroids in concentrated acetic acid using HCl as a catalyst. The nucleophilic reagents were thioacetic acid, methylmercaptan, thiocyanic acid and the reactions resulted in 3-keto-4-ene steroids, having the aforementioned sulphur containing substituents in 7α position.

In cases of 3-keto-4-ene steroids having other 7-substituents the experiences were similar. RINGOLD and BOWERS [4, 5] prepared 7-cyano, 3-keto-4-ene steroids the product was a mixture of 7α and 7β-cyano derivatives. CAMBELL and BABCOCK [6] prepared 7-methyl, 3-keto-4-ene steroids producing 7α derivative, 7β epimer occurred only in the presence of a 11-hydroxy group.

Investigating the addition by the preparation of the spironolactone [7α-acetylthio-17α-(2′-carboxyethyl)-17β-hydroxy-androst-4-ene-3-one lactone] CELLA and TWEIT [7] established that a little amount of 7β, equatorially substituted epimer also was yielded though the main product was the spironolactone. Since this latter one contained 7α-acetylthio group it was stated that the thioacetic acid addition to the $C_6—C_7$ double bond was *trans diaxial* addition.

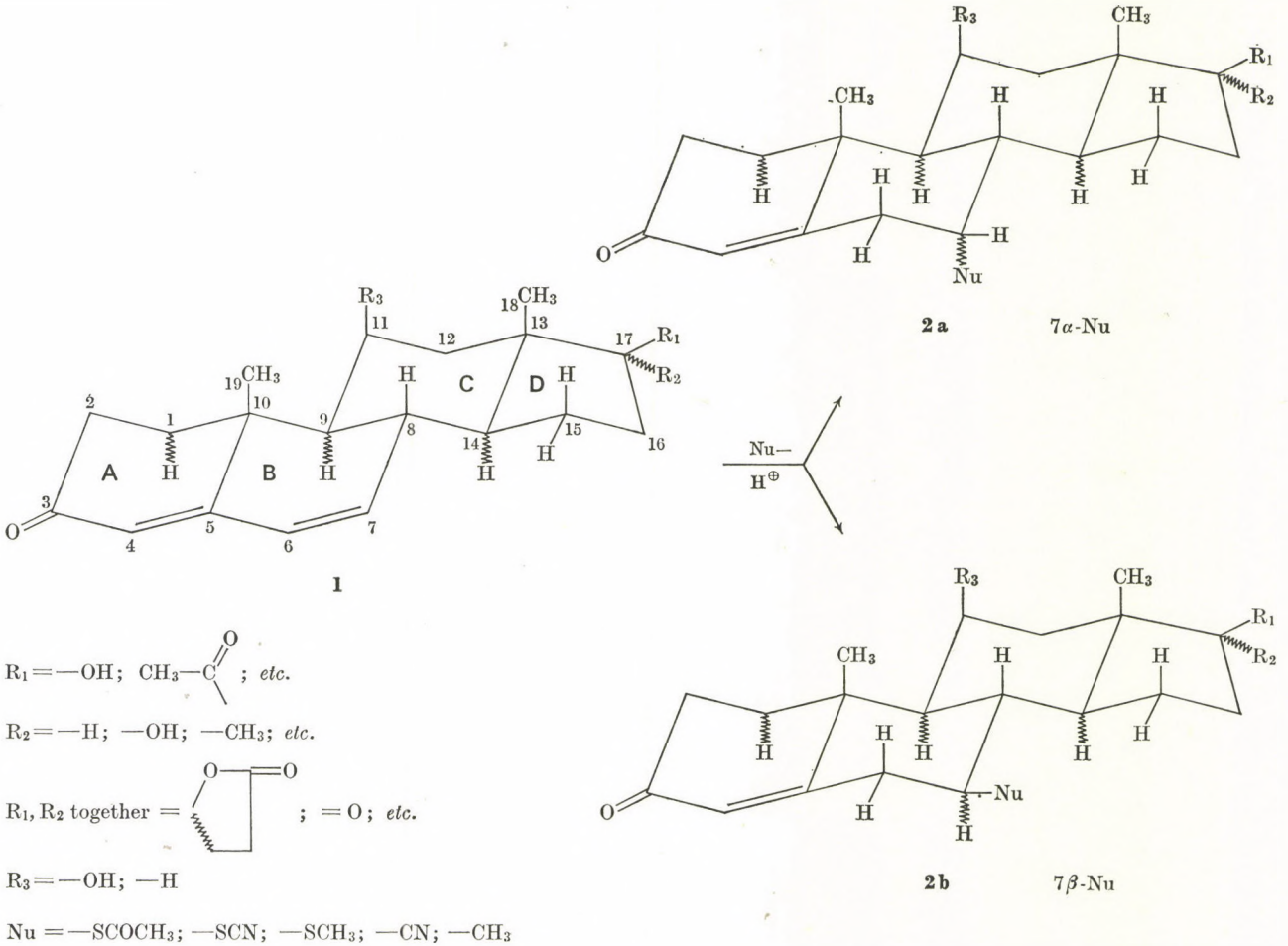

Fig. 1. The reaction scheme of the nucleophilic addition of 3-keto-4,6-diene steroids

TWEIT's [8] effort to get a greater part of the β epimer either by the isomerization of the α one or by changing the conditions of the reaction remained unsuccessful. He supposed that under the conditions necessary to the isomerization thioacetic acid elimination may occur as a side reaction.

The available experiences caution us to take steric interactions between the 7-substituent and the steroid skeleton into consideration.

The degree of these interactions depends mainly on the size and shape of the substituent. It is thought this is the dominant factor in the formation of the thermodynamically preferred 7-substituted, 3-keto-4-ene steroid epimer.

Model and calculations

The PCILO method [9—12] (Perturbation Configuration Interactions using Localized Orbitals) was used in the CNDO/2 hypothesis to study the above questions. The corresponding QCPE program [16] used in our calculations was modified by Th. WELLER.

The PCILO method proved useful in earlier calculations [13—15] to investigate molecular conformations so it was hoped the experimental results could be interpreted in our case too.

However, we had to carry out the calculations on model compounds since due to our limited possibilities we could not make calculations on the whole molecules. The calculations were made on an ICL 1903/A computer having a maximum storage capacity of 55 K words available.

The basic 3-keto-4,6-diene steroid (struct. 1) yields 7-substituted, 3-keto-4-ene steroids (struct. **2a**, **b**) in nucleophilic accidition. In the 7-substituted compound the Nu group may take *axial* (α, **2a**) or *equatorial* (β, **2b**) position.

First we investigated the electronic structure of compound 1 for checking the nucleophilic site, then the total energy differences of the 7-substituted epimeric pairs were calculated.

The reactions took place in polar medium so it was necessary to calculate also the charge distribution in the steroid molecule protonated on the carbonyl oxygen.

To the calculation of the electronic structure of compound 1 and its protonated form model compounds were chosen. The models (3**a**—**d**) and their calculated charge distributions are shown in Fig. 2.

Since no data have been found referring to the molecular geometry of compound 1 reasonable geometry was assumed on the basis of X-ray [17] and electron diffraction [18] investigations on 4-pregnene-17α, 21-diol-3,20-dione and cyclohexene, respectively. The O—H length was assumed to be 1 Å (3**c**, **d**).

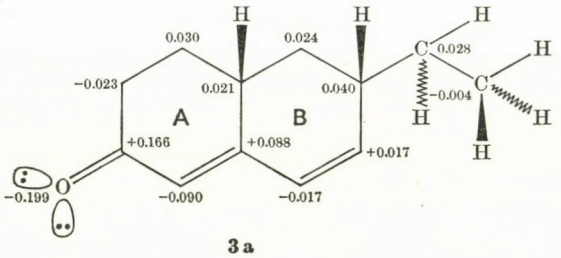

3a

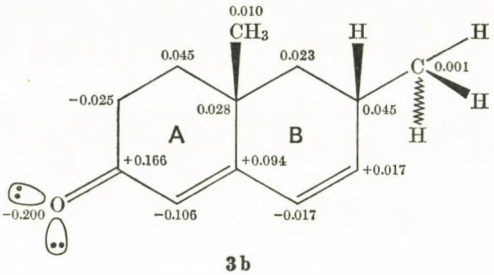

3b

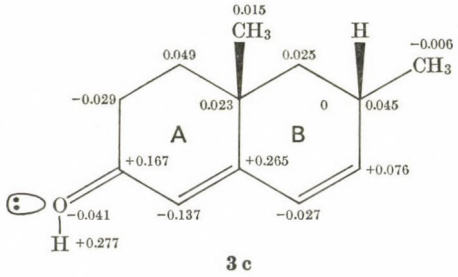

3c

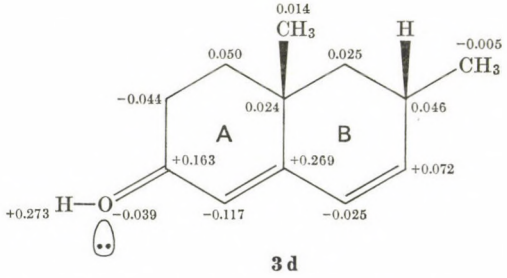

3d

Fig. 2. The calculated charge distribution of the 3**a**—**d** model compounds. The charges indicated at the methyl groups refer to the C atoms

In the following the energy differences of the epimeric pairs were investigated in the 7-substituted, 3-keto-4-ene steroids. To these calculations model 4 was chosen. This choice may be verified by the assumption that the influence of the 3-keto group is approximatively equal on the electronic structure of the 7α and 7β epimers. Furthermore there can not exist significant steric interaction between the 3-keto group and the 7-substituent being the two groups

rather far from each other. So it is assumed implicitly that the total energy difference of the epimeric pairs depends decisively on the interactions existing in the vicinity of the substituted molecular site.

The geometry of model 4, which is a model of the ring B and the interesting part of the rings C and D of the steroid molecule, was assumed on the basis of the X-ray investigations of DUPONT *et al.* [17]. Some C—C bonds of

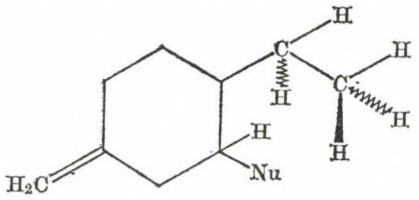

4

the steroid skeleton were replaced by C—H bonds the directions of which coincided with the original ones.

Some of the original HCH and CCH angles were very far from the tetrahedral value. The experimental C—H bond lengths varied from 0.89 to 1.19 Å. Instead of the X-ray data referring to bonds containing H, we assumed more realistic C—H bond lengths of 1.095 Å and 1.07 Å for C—C—H and C=C—H bonds, respectively, as well near tetrahedral angles. The following substituents (symbolized in general with Nu) were investigated: —CN, —Cl, $-CH_3$, $-SCOCH_3$. The necessary geometric data were taken from the literature [20]. The H—C_7—Nu angle angle was not optimized, it was accepted in every case to be near tetrahedral. The error made is estimated in the discussion. The sulphur-carbon distance in the acetylthio group was assumed being between the C—S and C=S bond lengths. This choice based on the similar situation existing in the oxygen containing esters. The accepted value of the C—S bond length was 1.77 Å. The geometry of the groups connecting to the C_7 atom is shown in Fig. 3. The total energy differences were calculated for every substituent both in *axial* and *equatorial* positions. In the case of the methyl group a rotation of 60° was made about the C_7—S axis that is both the staggered and eclipsed conformations were calculated. In the case of $-SCOCH_3$ substituent potential curves were examined rotating the substituent group about the C_7—S axis, both in α and β positions. The potential curves can be seen on Fig. 4. A clockwise rotation about the C_7—S axis from the view point of the C_7 atom was assumed. The origin corresponds to an arrangement where the H—C_7—S—CO—C atoms are in the same plane, the C_7—S and C=O, as well the H—C_7 and C=O bonds are in *cis* position.

The energy differences of the α and β epimers and the experimentally found configurations are given in Table I.

Table I

The energy differences of the epimeric pairs in kcal/mol and the experimentally found configurations (references in parentheses)

	$E_\alpha - E_\beta$ (kcal/mol)	Exp. configuration
$-CN$	$+0.2$	α, β [4, 5]
$-Cl$	-1.3	no exp. data
$-SCOCH_3$	-1.6	α [1, 2, 3]
$-CH_{3stag}$	-5.6	α [6]
$-CH_{3ecl}$	-4.5	α [6]

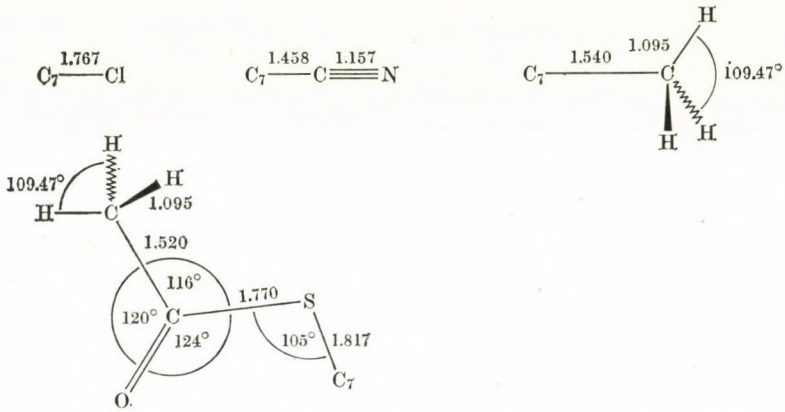

Fig. 3. The geometry of the substituents connecting to the C_7 atom

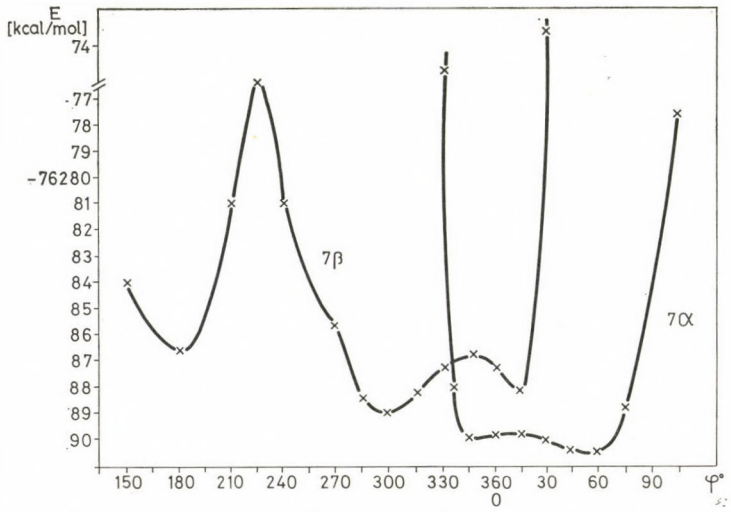

Fig. 4. The total energy of the 7α and 7β acetylthio derivatives as a function of the rotation angle about the C_7—S axis

Discussion

The aim of the present calculations is to compare the energy differences of 7 axially and equatorially substituted 3-keto-4-ene steroids having different substituents. Furthermore, we are going to interpret these ΔE values as compared to experiment. Before making it, however, some remarks are necessary on the calculated charge distributions.

As it can be seen the positive and negative charges alternate in the conjugated parts of models 3**a**—**d**. Though while the carbonyl group bears the greatest charges in the models of the ground state (3**a**, **b**), the C_4, C_5 atoms become the most positive and negative centers in the transition ion (3**c**, **d**). Nevertheless, both types of the models show a greater electrophilicity of the C_5 atom as compared to C_7. This result suggests that the addition should take place rather on the C_4—C_5 double bond leading to the formation of a C_5—Nu σ bond. On contrary, the experiments proved that the addition takes place always at the C_6—C_7 double bond. Taking the calculated charge distributions into account the experimental fact may be explained by steric hindrance.

The σ bond connencting to the C_5 atom may only have an axial position. (The C_7 atom can form principally both *axial* and *equatorial* bonds.) The nucleophilic attack from the region above the general plane of rings A and B is hindered by the C_{19}-methyl group. The approach under the general plane is easier but it suffers from the repulsive 1,3 *diaxial* interactions with the *axial* hydrogens of C_1 and C_9 atoms and the total steric interaction with the atoms of the rings A and B. The formation of a 7-*axial* bond is hindered also by the 1,3-*diaxial* interactions with the *axial* hydrogens of C_9 and C_{14}. However, there is a greater possibility for a more convenient arrangement of the approaching nucleophilic group, since it gets in steric interactions almost exclusively with the ring B.

It must be pointed out the calculations are based on hypothetical molecular geometries. These geometries do not reflect the fine details of molecular structures. A little change in the molecular geometry does not alter qualitatively the charge distribution, but may increase significantly the steric hindrance to the formation of some new bonds.

Though it is believed that the assumed geometries are not far from the real ones (the most data are taken from experimental results referring to similar compounds), so the charge distributions should be qualitatively good.

In this case, however, we must suppose that the connection of a substituent to the C_5 atom is hindered by steric factors. This conclusion is strongly supported by the experience that the nucleophilic addition to the C_4—C_5 double bond is practically exluded in the 3-keto-4-ene steroids [19].

Returning to our original aims, it may be said that the conclusions can be drawn from the calculated energy differences of the 7-substituted steroids

are in fairly good agreement with the experiment. We have to take into account, of course, that the PCILO results are numerically uncertain if the energy difference is less than 0.5 kcal/mol [15, 16].

Another source of this uncertainty is the lack of the optimization of the H—C_7—Nu angle. Accepting a harmonic approximation the total energy increase may be given as follows: $\Delta E' \approx 1/2\, k\Delta q^2$, where Δq is the difference between the actual and optimized value of the angle mentioned, k is the bending force constant. Taking the value of k equal 1 mdynA/rad^2 [21] and a Δq value of 0.1 rad (that is a rather great value for the difference) $\Delta E'$ will be about 0.7 kcal/mol.

Taking into account that the optimization was neglected at the both members of the epimeric pairs, the errors in the total energy differences should be less than 0.7 kcal/mol.

These two sources of the uncertainty with respect to the energy differences at the different epimeric pairs suggest that we must not accept the total energy difference to be significant if it is less than 1 kcal/mol.

The $\Delta E = E_\alpha - E_\beta$ value is +0.2 kcal/mol between the cyano derivatives. This means that the α or β position of the cyano substituent does not cause a great change in the total energy, so there is not a really preferred configuration. This interpretation is in accordance with the experiences [6, 7]. The reaction yield was mentioned as a mixture of α and β epimers, without giving their ratio obtained.

Although the 0.2 kcal energy difference is not significant for preferring any configuration, a remark may be made. Since the calculated energies of the 7α and β cyano derivatives differ slightly, it is thought, this is due to the stretched shape of the CN group. This shape assures that there is not significant repulsion with the H_{15} atom (the hydrogen atom connecting to C_{15}) even in the *equatorial* position.

In other cases, however, the situation is quite different. The Cl atom is repulsed in *equatorial* position (its lone pairs get too close to the C_{15}—H bond). The S atom and the CO group of the *equatorial* —$SCOCH_3$, the hydrogens of the *equatorial* —CH_3 group are also close to H_{15}.

If the substituent is —$SCOCH_3$, the most favoured rotational position of the α and β epimers must be found, and the total energies should be compared at the minima of the potential curves. The calculated energy difference was 1.6 kcal/mol. This value helps us to understand why only a little amount of the 7β epimer is obtained in the thioacetic acid addition.

This interpretation of the calculations suggests it is accepted that the ratio of the products is regulated by thermodynamical factors. If it is so and equilibrium can be supposed, it means there are no significant potential barriers or at least these barriers are of similar magnitude in the two cases. To prove this idea we calculated the total energies of the two configurations

at different separations of the C_7 and S nuclei. This was taken as a crude model of the transition states of the additional reaction. We calculated the energies along a special reaction path: the geometries of the 4 model compounds differed only in the C_7—S separation.

The calculations were carried out in the range of 1.8—2.8 Å. At greater separation the PCILO method has not found acceptable bond polarity for the C_7—S covalent bond.

Both potential curves show a slight minimum at 2.0 Å, a steep and a slighter increase in the range of 2.0—2.6 Å and 2.6—2.8 Å, respectively.

Disregarding the place of minimum — the PCILO method does not give the length of the single bond correctly in general — the curves show too large energy increase. This is due to the restrictions on the reaction path, the lack of geometry optimization and the model in which the transition states were simply taken as some stretched states of the C_7—S covalent bond.

The total energy differences, however, give interesting information. The $\Delta E = E_\alpha - E_\beta$ values and the C_7—S separation are shown in Table II. It can be seen that the α position is preferred with 2.24 kcal/mol at 2.3 Å.

Table II

The total energy difference (in kcal/mol) of the 7α and 7β thioacetyl compound at different C_7—S separations

R_{C_7-S}/Å	1.817	2.0	2.3	2.6	2.7	2.8
$\Delta E = E_\alpha - E_\beta$	−1.57	−2.04	−2.24	−1.95	−1.76	−1.39

This can be explained with steric interactions influencing the α or β preference in the greatest measure at 2.3 Å. This explanation is supported by the values calculated for the greater separations: the greater the distance between the thioacetyl group and the steroid skeleton is, the less the energy difference is.

Despite many shortcomings of our model for the transition state the following may be concluded: the ΔE values show the α preference in the whole range investigated. The thioacetyl group approaching from the β direction suffers increasing steric hindrance as compared to the α one. This difference is maximal at the C_7—S distance of about 2.3 Å. Getting nearer to the steroid B ring the energy of "formation" of the C—S single bond stabilizes the β position too; the ΔE values decrease in the bonding region.

The methyl substituent may possess practically only α position since there is an even greater energy difference between the two configurations. The reason is, in this case too, the strong repulsion with the H_{15} atom.

Investigations were performed on the staggered and eclipsed conformations of the methyl group both in the α and β configurations. It is seen (Table I)

that there exists a difference ($\Delta\Delta E$) of 1.1 kcal/mol between the ΔE values of the different configurations due to the different methyl conformations. A rotation of 60° of the methyl group in the α epimer resulted in an energy change of 2.2 kcal/mol on favour of the staggered form. This value is very similar to the PCILO calculated rotational barrier of the ethane (appr. 2 kcal/mol [13, 16]). It suggests that the factors influencing the rotation of the α methyl group in the steroid derivative do not differ significantly from the ones in the ethane molecule.

In the equatorially substituted β epimer the methyl rotation resulted in an energy difference of 1.2 kcal/mol only. Though the staggered form was more favoured in this case too, the repulsive interactions with H_{15} had greater effect on the staggered than the eclipsed form. This reduced the energy gain of the preferred conformation.

These numerical results support the assumption that preference of the *axial* substitution over the *equatorial* one may be explained essentially by steric effects.

Conclusions

On the basis of the PCILO calculations referring to the 6,7 addition of 3-keto-4,6-diene steroids it was found that in the 7-cyano derivative the *equatorial* position is slightly preferred but the axially substituted epimer is significantly more stable in cases of substituents like $-Cl$, $-CH_3$, $-SCOCH_3$. These results are essentially due to steric effects. Some bulkier substituents can avoid to get too close to the H_{15} atom of the steroid D ring only in α, *axial* position. The conclusions drawn on the basis of the calculated energy differences of epimeric pairs are in good agreement with experiment. Upon addition of the cyano group a mixture of the epimers will be obtained, however, only the 7α epimer is awaitable practically in cases of $-Cl$, $-CH_3$, $-SCOCH_3$ substituents.

*

The authors wish to express their thanks to dr. KÉKESY for encouragement throughout this work and to dr. NÁRAY-SZABÓ for the valuable discussions. This work has been supported by the Chemical Works of Gedeon Richter Ltd.

REFERENCES

[1] DODSON, R. M., TWEIT, R. C.: J. Amer. Chem. Soc., **81,** 1224 (1959)
[2] DODSON, R. M., RIDGE, P., TWEIT, R. C.: U. S. Patent 2,904.560
[3] SCHAUB, R. E., WEISS, M. J.: J. Org. Chem., **26,** 3915 (1961)
[4] RINGOLD, H. J., BOWERS, A.: U. S. Patent 3,099.664
[5] BOWERS, A., RINGOLD, H. J.: U. S. Patent 3,050.534
[6] CAMBELL, J. A., BABCOCK, J. C.: J. Amer. Chem. Soc., **81,** 4069 (1959)
[7] CELLA, J. A., TWEIT, R. C.: J. Org. Chem., **24,** 1109 (1959)

[8] TWEIT, R. C.: J. Org. Chem., **27,** 3325 (1962)
[9] DINER, S., MALRIEU, J. P., CLAVERIE, P.: Theor. Chim. Acta, **13,** 1 (1969)
[10] MALRIEU, J. P., CLAVERIE, P., DINER, S.: Theor. Chim. Acta, **13,** 18 (1969)
[11] DINER, S., MALRIEU, J. P., JORDAN, F., GILBERT, M.: Theor. Chim. Acta, **15,** 100 (1969)
[12] JORDAN, F., GILBERT, M., MALRIEU, J. O., PINCELLI, U.: Theor. Chim. Acta, **15,** 221 (1969)
[13] WELLER, Th., KLÖPPER, D., KÖHLER, H. J.: Z. Chem., **14,** 278 (1974)
[14] KÖHLER, H. J., WELLER, Th., KLÖPPER, D.: Z. Chem., **15,** 224 (1975)
[15] PULLMAN, B., COURRIERE, Ph., COUBEILS, J. L.: Mol. Pharm., **7,** 397 (1971)
[16] "Notice for the PCILO program submitted to the QCPE." Quantum Chemistry Program Exchange, Program No. 220. Indiana University, Bloomington, Indiana
[17] DUPONT, P. L., DIDEBERG, O., CAMPSTEYN, H.: Acta Cryst., **B29,** 205 (1973)
[18] CHIANG, J. F., BAUER, S. H.: J. Amer. Chem. Soc., **91,** 1898 (1969)
[19] KOMENO, T.: U. S. Patent 3,016.386
[20] SUTTON, L. E.: "Tables of Interatomic Distances." The Chemical Society, London 1965
[21] See, *e.g.:* KANAKAVEL, M., CHANDRASEKHAR, J., SUBRAMANIAN, S., SINGH, S.: Theor. Chim. Acta, **43,** 185 (1976) and references therein

Péter NAGY
György BEER } H-1475 Budapest, P.O. Box 27.

Acta Chimica Academiae Scientiarum Hungaricae, Tomus 103 (1), pp. 71–85 (1980)

A STRUCTURE THEORY FOR CHEMICAL ENGINEERING

T. BLICKLE and G. FAY

(Research Institute for Chemical Engineering of the Hungarian Academy of Sciences, Veszprém)

Received June 12, 1978
In revised form March 9, 1979
Accepted for publication March 11, 1979

Giving a brief historical overview in investigations concerning the works on the logical structure of chemical engineering systems, carried out from the beginning of the seventies in Hungary, a possible way is demonstrated of how to treat logical relations, generally characterizing chemical engineering systems, by exact algebraic (lattice theoretical) means. The mathematical definitions of *properties*, *property classes* and the common occurrence of these properties, in one word the *possibilities* of chemical engineering systems are given. It is proved that these possibilities form a lattice (in an algebraic sense). The valuation of this lattice is introduced corresponding to the conservational transport theoretical substances in chemical engineering systems (mass, energy, volume, *etc.*). Thus chemical engineering problems may be investigated by lattice theoretical means and these investigations may also be computerized, especially in interactive, dialogue mode.

1. Introduction

The concept of structure has been introduced very early to chemistry with the structural formula. In chemical engineering, in order to survey connections of operational units, it also was developed very soon, by the 19th century.

The concept of structure in chemical engineering first appeared in the early sixties in independent sources and later in more and more integrated forms. Since the early 70's one even may speak of a "theory of chemical engineering graphs" or rather a kind of a "chemical engineering graph theory".

As to the relevant preliminaries and historical overview the reader is refered to [11].

The graph theory, as a special representation of the structure concept, appears under different synonyms in chemical engineering applications. Thus the Soviet school of KAFAROV refers to it as, "the topology of chemical industrial systems", the Hungarian KORACH school prefers the expression "technological graphs". In the Soviet Union the first important results of chemical engineering cybernetics appeared in the early 70's.

In this respect we feel that the results of KAFAROV and coworkers [10] stand close to our work. Reference [10], offers a summary of references.

The structure theory, to be introduced in the sequel, aims at finding the algebraic and logical structure of chemical engineering systems.

Motives of a "chemical engineering structure theory" do not differ from those of chemical industrial cybernetics nor of the graph theoretical approach: researchers are urged to investigate structures (no matter whether the structure is geometrical, algebraic or logical) by the recognition of the fact that the classical description methods using differential equations are no longer sufficient to treat modern chemical engineering systems.

During the last two decades the mathematical modelling of chemical operations has turned out to be more and more important and widespread.

The quantitative description of chemical engineering processes is based on the use of balance equations [1, 8]. While, however, in the case of examples found in textbooks (being often oversimplified for didactical purposes) a verbally conceptualized model is sufficient to set up the balance equations, then the construction of balance equations — the very establishment of the model — in practice cannot be carried out on a bare intuitive-verbal base. Literature does not refer to any type of logical techniques concerning the methodic "know-how" of establishing such models. The reasons for making certain assumptions and neglections in a given case generally remain "workshop secrets", and the clashes of interests also (for reasons, among others, of legal protection) produce obstacles for researchers, too, against dealing with logical methods of establishing models in chemical engineering.

The systematic investigation of the (logical) structures of chemical engineering systems was begun, to the best of our knowledge, first in the Research Institute of Chemical Engineering of the Hungarian Academy of Sciences (MTA MÜKKI, Veszprém, Hungary). References, partly having English and Russian summaries are: [3, 4, 5, 12, 14]. Needless to say the authors are completely aware of the fact that without the aid of a logic-oriented computer machinery the attempt of revealing the logical structure of realistic chemical engineering systems would be quite unrealistic.

Fortunately, today at least three sources are available, hopefully, to cope with the enormous logical treadmillwork to get practically usable results in the case of chemical engineering systems of real complexity.

First, there is "DILOS", a dialog system for information retrieval, computation and logical inference, developed by V. B. Briabrin, D. A. Pospelov and their group in the USSR [2]. The subsystem LP (logical processor) of DILOS was implemented there already in 1975. It gives the possibility of deducing new facts from existing axioms and temporary results. (Examples of axioms characterizing chemical engineering systems will be given later in this paper.)

Second, there is "GUHA" (General Unary Hypotheses Automation) being developed in the Czechoslovak Academy of Science, by P. Hájek and

his school since 1966, a method of mechanized formation of hypotheses, a computer system for finding logical relationships from empirically given data. A very detailed description with a complete reference list can be found in [9].

Third, there is "PROLOG" a programming language based on mathematical logic, developed by R. KOWALSKY in Edinburgh in 1974. This system was implemented in Hungary as early as 1975 and since then a number of applications have been achieved. Among the applications there are two, which have at the same time logical and chemical engineering character [6, 7]. Information on the implementation on several computers (such as ICL 1903 A, ICL 4/70, EMG 840, ODRA 1304, HONEYWELL 66/20, *etc.*) is available from NIMIGÜSzI, BUDAPEST, HUNGARY.

The present authors wish to use the expression "logical structure theory of chemical engineering systems", or "structure theory" for short. By using this terminology, differing from the previous two, we intend to express that, in our view, it is not the geometric connections of chemical industrial systems that are primary, but rather, in a more abstract way, the logical (or algebraic) connections, by which we propose to treat chemical engineering systems to be constructed for practical purposes.

As for the application of abstract algebraic methods in theoretical chemistry, they reach nearly as far back as the group-theoretical foundation of the quantum theory. While these investigations (on atomic, molecular and crystal phase levels) are actually structure-oriented, few results have been obtained by using algebra in the phenomenological description of chemical reactions.

2. Structure Theoretical Characterization of Chemical Engineering Systems

From now on, the term "Chemical Engineering System" will be abbreviated as "CE system".

The structure theory of CE systems starts with the following basic concepts and axioms, thought intuitively as immediately given. These essential statements are formalized in order to illustrate the working methods and results of structure theory, to calculate results by exact (formal logical) methods, and to concentrate our (qualitative) knowledge on CE systems.

In this paper — due to limited space — we cannot list all of these statements. Details of pure technical relevance (required only for the internal, logical development of the structure), are omitted here.

Our intuitive starting point is that CE systems can be characterized by three factors: a collection of CE *properties* denoted by A ("attribute"), a hierarchical *grouping* (or classification) of these properties (*e.g.* atoms, molecules, phases, phase systems, *etc.*) and the *possibilities* of the simultaneous

occurrence ("coexistence", "compatibility", co-occurrence) of these properties.

Once the *properties*, the *property classes* of a system, and the *possibilities* of property combinations are given, one can answer numerous practical questions, as will be shown in Chapter 3.

2.1 *Basic Concepts*

2.1.1. *Property*

For instance a property of a typical CE system is the (truth of the) following statement:
"In a given (*i.e.* given by a given model) CE system, in some point with x, y, z coordinates at time t, an HCl molecule can be found".

To define this concept, we start with the concept of the "elementary CE system" ("ECE system", for short) as a nondefined fundamental concept. An ECE system is denoted by the symbol S_{lj}, where S stands for the "System" and $l, j = 1, 2, \ldots$ are indices to distinguish the different groups of elementary systems. l is the *type index*, j is the *group index*. So S_{lj} denotes "the ECE system of type l in the class j".

Examples of this concept are shown in the following list. In a CE system producing dichloroethane, the following ECE systems can be found:

Property symbol	System ECE symbol	Meaning	Type $l=$	Class $j=$
d_1	S_{11}	chlorine atom	1	1
d_2	S_{21}	carbon atom	2	1
d_3	S_{31}	hydrogen atom	3	1
b_1	S_{12}	chlorine molecule	1	2
b_2	S_{22}	ethylene molecule	2	2
b_3	S_{32}	hydrochloric acid	3	2
b_4	S_{42}	dichlorethane	4	2
b_5	S_{52}	trichloroethane	5	2
c_1	S_{13}	liquid phase	1	3
c_2	S_{23}	gas phase	2	3
d_1	S_{14}	liquid phase	1	4
d_2	S_{24}	gas phase	2	4

After this, a *property* of a CE system of type l in the j-th class denoted by a_{ij} will be, by definition, equal to the following statement:

$$a_{ij} = (\exists \mathrm{R})\ STY\ \mathrm{RS}_{ij} \qquad \text{DEF}$$

Here $STY\ RS_{ij}$ is the formulation of the statement saying: "In a space time point R (of a given CE system) there exists an ECE system S_{ij} staying ($STaY$)."

$\exists R$ is the symbol for "there exists such an R that".

That is, in words, property a_{ij} means that in the space-time point R of the given CE system, there can be found an ECE system S_{ij}. It is often more convenient to use main symbols instead of class indices. As in the example, let $a_{11} = a_1$; $a_{21} = a_2$; $a_{31} = a_3$; $a_{12} = b_1$; $a_{22} = b_2$; $a_{32} = b_3$, *etc.* Thus we may talk about the property classes ("groups") A, B, C . . .

2.1.2. *Classification*

In intuitive terms, classification ("grouping") is nothing else but determining whether "properties X and Y belong to the same group". If this is symbolized by *SCL* XY (*SCL*: *S*ame *C*lass), then it is evident that always:

(1) $SCL\ XX = \text{true}$
(2) $SCL\ XY \leftrightarrow SCL\ YX$
(3) $(SCL\ XY \wedge XCL\ YZ) \rightarrow SCL\ XZ$

Where $\leftrightarrow$ means "if and only if"
$\wedge$ means "and"
and $\rightarrow$ means "if — then" (implies).

In this way (property) classification generates an equivalence relation [that is, a relation statisfying (1), (2) and (3)]. For example $SCLa_1a_2$ means that the property saying that a chlorine atom is staying in a (space — time) point and the one saying that a carbon atom is in a point (which may differ from the previous one!) belong to the same property class (naturally to the class of atoms). This does not, of course, mean that the two statements together must be true at the same time.

The classification of properties in structure theory is to be carried out through relations (rather then by determining all the classes themselves) since, in practice, the concept of property equivalence develops well before the very class concept! (Two chemical systems may have the same *smell* although we cannot tell what "class of smell" they belong to, simply because we have no noun to name the class itself.)

2.1.3. *Possibility*

Let us look at the next eight statements. In a CE system, con isting of a film reactor, producing dichloroethane, a hydrogen atom can be found:

1° in ethylene molecules in the liquid phase of the liquid film ("$a_3b_2c_1d_1$");
2° in ethylene molecules in the liquid phase of the spray ("$a_3b_2c_1d_2$")
3° in ethylene molecules in the gas phase of the spray ("$a_3b_2c_2d_2$");
4° in hydrochloric acid molecules in the liquid phase of the film ("$a_3b_3c_1d_1$");
5° in hydrochloric acid molecules in the liquid phase of the spray ("$a_3b_3c_1d_2$");
6° in dichloroethane molecules in the liquid film ("$a_3b_4c_1d_1$");
7° in trichloroethane molecules in the liquid film ("$a_3b_5c_1d_1$");
8° in trichloroethane molecules in the spray drops ("$a_3b_5c_1d_2$").

Each of these statements is considered to be a *possibility* for the hydrogen atom. In general, properties appearing together (occurring together) are called possibilities. (Its formal definition will be omitted here.)

In practice, the number of possibilities of a CE system may be extremely large, the number of possible property combinations is, however, even larger. In our example only the number of all the dual combinations amounts to 45.

The designer must have a reliable knowledge about these possibilities in order to set up, if this can be done at all, some quantitative model for the CE system in question.

Structure theory offers two ways for this. The first is based on the observation that, for the designer, there are well known, mutually excluding properties belonging to different property classes. These are the so-called "paired prohibitions". For example a carbon atom *cannot be* present in the hydrochloric acid molecule.

These paired prohibitions exclude a great number of possibilities and thus all the possibilities of a system can be determined by an algorithm (with the help of a computer [14]).

The basis of the other approach is that algebraic operations can be defined between possibilities, in other words, the logical "union" and "intersection" of possibilities can be formed. The "possibility algebra", developed in this manner, can be proved to be a "lattice", so that possibilities can be practically calculated. (As for lattice theory, see *e.g.* [9].)

In the following this latter approach is discussed.

2.2. *Possibility Algebra*

2.2.1. *Disjunction and Conjunction of Properties*

Properties of CE systems, "CE properties" for short, being formally statements — can be connected to each other by the help of logical operations in a very natural manner. Consider the following statements:

(b_2) "In a given state of a given film reactor, producing dichloroethane, in point x, y, z of the reactor at a given time, there exists an ethylene molecule."

Similarly, b_4 is the statement meaning (now more concisely),

(b_4) "There exists a (space-time) point x, y, z, t where a dichloroethane molecule is staying."

By expressing properties b_2 and b_4 explicitly, the next statement is the "union" of the statements b_2 and b_4:

($b_2 \vee b_4$) "There exists a point x, y, z, t where either an ethylene molecule (b_2) *or* a dichloroethane molecule (b_4) is, *or* both are, present."

It is obvious that the statement ($b_2 \vee b_4$) is to be considered as a property on the same grounds as statements b_2 and b_4 have been.

The above is easily generalized, postulated and formalized: Let a_{ij} and a_{kj} be two properties belonging to the same (j-th) group ($i, j, k = 1, 2, \ldots$) of a CE system $\mathbf{R} = \langle A, E, P \rangle$ with $E \subset A \times A$, $P \subset 2^A$.

If

$$a_{ij} = (\exists R)\ STY\ RS_{ij} \in A$$

and

$$a_{kj} = (\exists R)\ STY\ RS_{kj} \in A$$

then by definition,

$$a_{ij} \vee a_{kj} = (\exists R)\ [STY\ RS_{ij} \vee STY\ RS_{kj}] \qquad \text{DEF}$$

and

$$a_{ij} \vee a_{kj} \in A\ .$$

Where $\vee$ is the symbol for "or".

It is obvious that $a_{ij} \vee a_{kj}$ is also a statement just as a_{ij} and a_{kj} ($i, j, k = 1, 2 \ldots$), and it can be proved that the following (very important) conditions are fulfilled for all $i, j, k, l = 1, 2, \ldots$:

$$a_{ij} \vee a_{jk} = a_{kj} \vee a_{ij} \text{ (commutativity)}$$

$$a_{ij} \vee a_{ij} = a_{jl} \text{ (idempotency)}$$

$$a_{ij} \vee (a_{kj} \vee a_{lj}) = (a_{ij} \vee a_{kj}) \vee a_{lj} \text{ (associativity).}$$

This operation is called the *disjunction of properties.*

Again, it is self-evident that the statement formed only by substituting the operation "and" for the operation "or", is also a property. It is called the *conjunction* (or intersection) of properties.

So, formally, let

$$a_{ij} \wedge a_{kj} = (\exists R)\ (STY\ RS_{ij} \wedge STY\ RS_{kj}) \qquad \text{DEF}$$

for all $i, j, k = 1, 2, \ldots$, where $\wedge$ is the symbol of the (logical) conjuction ("and").

Like disjunction, this operation also turns out to be commutative, idempotent and p o s t u l a t e d to be associative. For all $j, k, l = 1, 2, \ldots$:

$$a_{ij} \wedge a_{kj} = a_{kj} \wedge a_{ij} \text{ (commutativity)}$$
$$a_{lj} \wedge a_{lj} = a_{lj} \text{ (idempotency)} \quad (2)$$
$$a_{ij} \wedge (a_{kj} \wedge a_j) = (a_{ij} \wedge a_{kj}) \wedge a_j \text{ (associativity)}$$

2.2.2. *Intersection and union of possibilities*

By defining the disjunction ($\vee$) and conjunction ($\wedge$) of *properties* we may introduce the concepts of union and intersection for *possibilities* too.

Definition: Let $a_{ik} \in A$, for $i, k = 1, 2, \ldots$
and $P_s = a_{s1}, a_{s2}, a_{s3} \ldots \in P_s = 1, 2, \ldots$
and $P_r = a_{r1}, a_{r2}, a_{r3} \ldots \in P_r = 1, 2, \ldots$
be possibilities of a system $\mathbf{R} = \langle A, E, P \rangle$ with $E \subset A \times A$, $P \subset 2^A$. The union (intersection) of the possibilities P_s and P_r is then

$$P_s \left|\bowtie\right| P_r = \{(a_{s1} \mathbin{XX} a_{r1}), (a_{s2} \mathbin{XX} a_{r2}), (a_{s3} \mathbin{XX} a_{r3}), \ldots\} \qquad \text{DEF}$$
$$P_s \left|\bowtie\right| P_r \in P$$
$\left|\bowtie\right| = \cup, \cap$; $XX = \wedge, \vee$
$\cup, \vee$ for union and $\cap, \wedge$ for intersection, respectively.

We assume further that operation $\cup$ and $\cap$ defined between properties $A \ni a_{ik}$ $(i, k = 1, 2, \ldots)$ are commutative, idempontential and associative (See 2.2.1. — (1), (2), (3)) and do not lead out from A, *i.e.* if $a, b \in A$ then $a \cap b$ and $a \cup b \in A$.

2.2.3. *Possibility lattice*

The concepts defined on the above algebraic background are not sufficient to develop the mathematical tools needed to *valuate* CE systems.

In order to construct a mathematically easy-to-handle efficient valuation function G(P), it is necessary to characterize further (like in [12] and [14]) the algebraic structure P, $(\cup, \cap)$ formed by the possibilities $P \in P$ of $\mathbf{R} = \langle A, E, P \rangle$.

The commutative, idempotent and associative character of the operations $\cup, \cap$ introduced above are not enough yet to tell anything useful about the valuation function. It requires some information about the *connection* of the two operations.

Notice that in (mathematical) logic there is a very simple connection between the operations $\wedge$ and $\vee$. Let a and b be arbitrary statements. If it

happens that $a \vee b = a$("=" meaning logical equivalence) then, necessarily $a \wedge b = b$.

That is if the disjunction of two statements is logically equal to *one* of the statements then their conjunction must be equal to the *other*.

If this crucial logical rule is employed to possibilities, we obtain that for any possibilities P_1 and P_2

$$\text{if } P_1 \cup P_2 = P_2 \text{ then } P_1 \cap P_2 = P_1.$$

Let us consider, for example, the following two possibilities.

$P_1 : \{a_1, b_3, c_1, d_2\}$, that is, a chlorine atom (a_1) is found in hydrochloric acid (b_3) in the liquid phase (c_1) of the spray (d_2)

and

$P_2 : \{a_1, b_3, c_2\}$, that is, a chlorine atom (a_1) is found in hydrochloric acid (b_3) in the liquid phase of some phase system (this means that property class D is not represented in the possibility).

In this case, what does the possibility $P_1 \cup P_2$ mean. Obviously, it means the very possibility P_2 since the statement "either spray or some phase system (or both) is present in R" means exactly that:

"Some phase system is present in R."

Therefore

$$P_1 \cup P_2 = P_2,$$

that is, here we actually arrive at a case where the union of two possibilities results in *one* of the possibilities (P_2). Therefore, we infer to that

$$P_1 \cap P_2 = P_1.$$

Notice that this is intuitively also true since the statement saying "the spray *and* an arbitrary phase system is present in R simultaneously" in this case means exactly that the spray is found in R.

In this consideration we explored the greatest advantage of the idea of structure theory saying that a property *not presented* in a possibility is *indifferent* to the possibility. If it is actually indifferent, let the arbitrary phase system be a spray. Then because of "spray and spray = spray", the statement above is obtained. Hereupon, the above dual connection will be postulated in general, as a principle, in the following form.

Principle of Duality: Let $\langle A, E, P \rangle$ be a CE system and $P \ni \mathrm{P}, \mathrm{Q}$ be two of its possibilities.

Then

$$\mathrm{P} \cup \mathrm{Q} = \mathrm{Q} \text{ if and only if } \mathrm{P} \cap \mathrm{Q} = \mathrm{P}.$$

On the basis of associativity, commutativity, and idempotency, the succeeding relationship can be proved presenting a useful connection between the union and intersection of possibilities.

For any possibilities $P \ni \mathrm{A}, \mathrm{B}$,

$$\mathrm{A} \cap (\mathrm{A} \cup \mathrm{B}) = \mathrm{A}. \tag{1}$$

Proof: Let

$$\mathrm{A} = \mathrm{P} \text{ and } \mathrm{A} \cup \mathrm{B} = \mathrm{Q} \tag{2}$$

then

$$\begin{aligned} &\mathrm{P} \cup \mathrm{Q} = \mathrm{A} \cup (\mathrm{A} \cup \mathrm{B}) \\ &\mathrm{P} \cup \mathrm{Q} = (\mathrm{A} \cup \mathrm{A}) \cup \mathrm{B} \quad \text{(by associativity)} \\ &\mathrm{P} \cup \mathrm{Q} = \mathrm{A} \cup \mathrm{B} \quad \text{(by idempotency)} \\ &\mathrm{P} \cup \mathrm{Q} = \mathrm{Q} \quad \text{[according to (2)]} \end{aligned}$$

According to the principle of duality,

$$\mathrm{P} \cap \mathrm{Q} = \mathrm{P}$$

by substitution from (2), we obtain

$$\mathrm{A} \cap (\mathrm{A} \cup \mathrm{B}) = \mathrm{A}$$

as claimed in (1).

Similarly we get:

$$\mathrm{A} \cup (\mathrm{A} \cap \mathrm{B}) = \mathrm{A} \tag{3}$$

Owing to their importance in algebra (especially in lattice theory) relations (1) and (3) are called the "*absorption laws*" [9].

Algebraic structures with two operations $\cap$, $\cup$, $(P, \cap, \cup)$, where both operations are commutative, associative, idempotent and absorptive are called lattices [17].

Our result so far is that we have managed to define lattice operations on the set P of possibilities, of a CE system.

In other words, we have proved that the possibilities of a chemical engineering system form a lattice (in algebraic sense). Having this, we may return to the problem of valuation of CE systems.

2.2.4. *Valuation and measure*

Traditionally, for the description of a CE system in chemical engineering, just as in theoretical chemistry, balance equations are used, expressing the conservation of substances. (Mass of different chemical components, energy, momentum, electric charge, *etc.*) In traditional transport theory the construction of balance equations is based on the consideration that the change of some substance in unit time, in a subspace bounded by a surface, is equal to the resultant of substance flowing in and out through the surface during unit time. This philosophy has been intensively developed in chemical engineering since 1936, starting with the works of DAMKÖHLER. Its references, mathematical aspects and a typical application are illustrated in [8] on a level of the middle sixties. LÁSZLÓ and BENEDEK give a complete survey of this subject in their book [1].

This view, as is well known, had to be essentially modified in the case of chemical reactions. Chemical reactions had to be taken into account by introducing source terms to the balance equations.

Naturally, the transport theory itself provides no information about how to find these terms. In consequence, no *method* is available for constructing balance equations in the case of chemical engineering processes occurring in practice, where bare intuition does not provide the necessary mental support any more.

Below, we outline the method provided by the structure theoretical approach for describing the conservation of chemical substances even in the case of chemical reactions of any kind.

Our basic idea is that the most essential feature of the substance is not that it is conserved (in the sense that they are, *e.g.* not absorbed or produced) but rather, that they can be traced from possibility to possibility.

To clarify this, let us return to the problem of producing dichloroethane, discussed on the previous pages and try to trace the hydrogen atoms. The following elementary statements are obviously true (although of course not in one-one correspondence with that of statements 1°—8° of 2.1.3.).

1. The ethylene molecule contains hydrogen atoms.
2. The hydrochloric acid contains a hydrogen atom.
3. The dichloroethane contains hydrogen atoms.
4. The trichloroethane molecule contains hydrogen atoms.

More possibilities on this hierarchic level (molecular level) are not possible, regardless of whether or not chemical reaction occur.

Furthermore:

a) The liquid phase may contain ethylene.
b) The gas phase may contain ethylene.
c) The liquid phase may contain hydrochloric acid.
d) The liquid phase may contain dichloroethane.
e) The liquid phase may contain trichloroethane.

More possibilities are not considered on this hierarchic level (phase level), again, independently of transport features such as sources.

Furthermore:

$\alpha)$ The phase system of liquid film contains liquid phase.
$\beta)$ The phase system spray contains liquid phase.
$\gamma)$ The phase system spray contains gas phase.

More possibilities are not considered on this hierarchic level (phase system level).

It follows that the occurrence of hydrogen atom has eight possibilities, those listed above under 1°—8°, and the gist of the description of the processes is that of the changes in the actualized possibilities.

To describe changes without any kind of differential equations is, admittedly, hard even to imagine. Still, there are well developed techniques for this under the heading of "iterative arrays" such as cellular automata, tesselation systems, parallel processing systems, *etc.*

By taking each possibility into account, we may determine the mass of hydrogen belonging to each possibility. The total mass of hydrogen atoms in the system is the *sum* of these partial masses. The point of doing this is that nothing is derived more than once and nothing is omitted from the calculations. If G_i denotes the mass of hydrogen atoms represented by the possibility symbol in braces, then total mass of hydrogen is obtained by the equation as follows:

$$\begin{aligned} G_i\{a_3\} = {} & G_i\{a_3, b_2, c_1, d_1\} + G_i\{a_3, b_2, c_1, d_2\} + \\ & + G_i\{a_3, b_3, c_2, d_2\} + G_i\{a_3, b_3, c_1, d_1\} + \\ & + G_i\{a_3, b_3, c_1, d_2\} + G_i\{a_3, b_4, c_1, d_1\} + \\ & + G_i\{a_3, b_4, c_1, d_2\} + G_i\{a_3, b_5, c_1, d_1\} + \\ & + G_i\{a_3, b_5, c_1, d_2\} \end{aligned}$$

By generalizing these ideas and summing up the earlier ones, the mathematical definition of the concept of CE systems can be given in the following way:

When we are talking about a CE system (more exactly about its mathematical model), we mean the following ordered triplet:

$$\mathbf{R} = \langle A, E, P \rangle,$$

where A is the set of R properties,

E is an equivalence relation, $\subset 2^A$,

$P = \langle P, \cap, \cup \rangle$ is an algebraic structure, the *possibility algebra* of **R**, where P is the set of all the possibilities of **R**, $\cap$ and $\cup$ are lattice operations defined in P. The possibility set $2^A \supset P$ is restricted by the following condition: for every $p \in P$ there exist attributes $a_i, a_j, \ldots$ such that

$$p = \{a_i, a_j, \ldots\} \; a_i \in A_i, a_j \in A_j, \ldots,$$

where $A_i, A_j \ldots$ are the equivalence classes of the set A determined by $E-$.

The *valuation of* the CE system **R** is a *function* defined in the possibility algebra P of the system **R**, assigning to each $p \in P$ a nonnegative real number

$$G\{p\} \quad p \in P$$

such that the following condition holds for every $p, q \in P$ (*c.f.* [13], chapter 39).

$$G\{p \cap q\} + G\{p \cup q\} = G\{p\} + G\{q\}$$

The valuation function is a *measure* by definition if

$$G\{\Phi\} = 0$$

where Φ is the "empty possibility". (Because of space shortage we shall not deal with its formalization.)

By introducing this measure concept we slightly differ from the term [13] otherwise considered to be our guide. There, "additive valuation" is used for what we call a measure, and the lattice in question in that valuation is presumed to be a Boolean algebra, see [13], chapter 47.

In CE systems, as many measures can be defined as many substances exist.

The most frequently occurring ones are:

— mass of different atomic components;
— mass of different molecular components;
— number of particles,
— linear size, surface, volume, *etc.*

Naturally, these measure concepts within the general concept must be defined for each concrete model.

3. Construction Principles of Structure Theory

The measure $G_i : P \rightarrow \mathbf{TR}$ (where **TR** is the set of nonnegative real numbers and $i = 1, 2, \ldots$) defined in the possibility lattice $P = \langle \mathrm{P}, \cap, \cup \rangle$ of the CE system $\mathbf{R} = \langle A, E, P \rangle$ makes it possible to introduce *homogeneous* and *heterogeneous* relative measure (ratio) with the following definitions for the *homogeneous relative measure* of possibilities P and Q:

$$\beta_i \{\mathrm{P}, \mathrm{Q}\} = \frac{G_i\{\mathrm{P}\}}{G_i\{\mathrm{Q}\}} \qquad \mathrm{Q} \neq \Phi \qquad \text{DEF}$$

The quotient of measures with subscripts i and j for possibility P (*e.g.* the quotient of mass to volume) is the *heterogeneous relative measure*:

$$\gamma_{ij} \{\mathrm{P}\} = \frac{G_i\{\mathrm{P}\}}{G_j\{\mathrm{P}\}} \qquad \mathrm{P} \neq \Phi \qquad \text{DEF}$$

In CE systems it often occurs and is very important that the homogeneous relative measures are *constant*, that is, they are independent of P and Q, and that the heterogeneous relative measures are *invariant*, that is independent of i and j.

The constancy of the homogeneous relative measures and the invariance of the heterogeneous relative measures provide an opportunity to develop algorithms to answer some essential questions concerning CE systems.

A characteristic feature of these algorithms is that dialogues between man and machine play an important role in computer aided operation designs of CE systems. A detailed report on these algorithms can be found in [14].

Typical inputs and outputs of the algorithms are:

Input	Output
— A (property set); — $A_1 A_2, \ldots$ property classes; — dual prohibitions; — measure types; — constant homogeneous relative measure; — invariant heterogeneous relative measure; — balance equations.	— all possibilities; — independent measures; — number of the independent variables; — independence tests.

The inherent dialogue-like characteristics of the algorithms are manifested in such a way that one algorithm has an input that is the output of another. These connections among algorithms, a type of feedback, are controlled through man—machine dialogues.

This is the point where structure theory is deeply connected to dialogue theory. In artificial intelligence research several cybernetical theories of dialogues have been elaborated [2].

REFERENCES

[1] Benedek, P., László, A.: Foundations of Chemical Engineering Sciences (in Hungarian). Műszaki Könyvkiadó, Budapest 1964
[2] Briabrin, W. M., Pospelov, D. A.: DILOS-Dialog System for Information Retrieval, Computation and Logical Inference. In: Conference on Artificial Intelligence: Question-Answering Systems. Laxenburg, Austria 1975, June 23—25. International Institute for Applied Systems Analysis, 2361 Laxenburg, Austria
[3] Blickle, T.: Algebraic Description of Chemical Engineering Systems. In: Advances in Chemistry (in Hungarian), Akadémiai Kiadó, Budapest 1973
[4] Blickle, T., Seitz, K.: Application of Modern Algebraic Methods in Chemical Engineering (in Hungarian). Műszaki Könyvkiadó, Budapest 1975
[5] Blickle, T. (ed.): Mathematical Models of Mass and Heat Transfer Systems (in Hungarian). Műszaki Könyvkiadó, Budapest 1977
[6] Darvas, F., Futó, I., Szeredi, P., Szeredi, I., Mátrai, Gy.: Application of Theorem-prover Based Machine Intelligence for Drug Design: PROLOG programs. Artificial Intelligence (to be published)
[7] Darvas, F., Futó, I., Szeredi, P.: Intern. Biomed. Comp. (to be published)
[8] Fay, L.: Acta Chim. Acad. Sci. Hung., **56**, 315 (1968)
[9] Hájek, P., Havránek, T.: Intern. J. Man-Machine Studies, **10**, (1) ... (1978)
[10] Кафаров, В. В., Перов, В. Л., Металкин, В. П.: Принципы математического моделирования химико-технологических систем. Химическая Кибернетика, Москва, Изд. «Химия» 1977
[11] Korach, M., Haskó, L.: Graph Theoretical Investigations of Chemical Engineering Systems (in Hungarian) Akadémiai Könyvkiadó, Budapest 1975
[12] Scientific Results of the Research Institute for Chemical Engineering of the Hungarian Academy of Sciences. II: Structure of Technical Chemical Systems (in Hungarian) MÜKKI, Veszprém 1974
[13] Szász, G.: Theorie des treillis. Akadémiai Kiadó, Budapest 1971 (English version also available)
[14] VEAB communications (Monographs of the Academic Committee of Veszprém, Hungary) I. 1975 (in Hungarian)

Tibor Blickle
Gyula Fáy
H-8200 Veszprém, Schönherz Z. u. 2.

Acta Chimica Academiae Scientiarum Hungaricae, Tomus 103 (1), pp. 87—94 (1980)

SYNTHESIS OF SOME 1,3,4-THIADIAZOLYLUREAS AND THEIR DERIVATIVES, II

Z. GYÖRFI and Gy. CSÁVÁSSY

(Department of Organic Synthesis, Oncological Institute, Cluj-Napoca, Romania)

Received September 22, 1978
In revised form February 9, 1979
Accepted for publication March 21, 1979

The synthesis and some chemical properties of a series of 1-(2-chloroethyl)-, 1-chloroacetyl-, and 1-dichloroacetyl-3-(5-alkyl- (or aryl) -1,3,4-thiadiazol-2-yl) ureas, obtained by the addition of 2-chloroethyl-, chloroacetyl- or dichloroacetyl isocyanates to 2-amino-5-alkyl- or -aryl-1,3,4-thiadiazoles, have been investigated. Some of the ureas were subsequently converted into the corresponding nitroso and/or hydantoin derivatives.

In continuation of our previous study in the thiadiazole series [1], we now report the syntheses of some 1,3,4-thiadiazol-2-yl-ureas and related compounds.

It is well known that derivatives of urea containing the 1,3,4-thiadiazole ring possess biological activity [2—4]. By introducing a 2-chloroethyl, chloroacetyl or dichloroacetyl group to one of the nitrogen atoms in urea, we expect that these thiadiazolyl-ureas should have antineoplastic properties.

The 1,3,4-thiadiazol-2-yl-ureas (**1**) were prepared by the reaction of 2-chloroethyl isocyanate [5] with the corresponding 2-amino-5-methyl- or -trifluoromethyl-1,3,4-thiadiazoles, in anhydrous *N*,*N*-dimethylformamide (DMF).

Compounds **1a** and **b** gave on nitrosation with sodium nitrite in 98—100% formic acid the corresponding 1-(2-chloroethyl)-3-(5-methyl- (**2a**), or -trifluoromethyl- (**2b**) -1,3,4-thiadiazol-2-yl)-1-nitrosoureas.

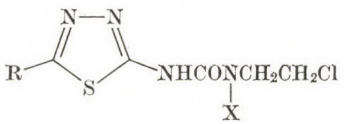

1a: R = CH_3; X = H **2a**: R = CH_3; X = NO

b: R = CF_3; X = H **b**: R = CF_3; X = NO

The simultaneous formation of 1-*N* and 3-*N*-nitroso derivatives has been reported in the nitrosation of *p*-(2-chloroethyl)-3-phenylurea with an aqueous solution of sodium nitrite [6]. When this reaction was effected with

Table I

No.	Formula (Mol. wt.)	Yield, % M.p., °C	Nitrogen, %		TLC R_f
			Calcd.	Found	
2a	$C_6H_8ClN_5O_2S$ (249.6)	44 124—125°	28.04	27.81	0.85 (1 : 1 ether/methanol)
2b	$C_6H_5ClF_3N_5O_2S$ (303.6)	50 77—80°	23.06	23.51	—

solid sodium nitrite, the 1-*N*-nitroso derivative resulted exclusively. We observed in our experiments that independently of the working conditions, only a single product was formed.

The position of the nitroso group in **2a** and **b** was established by comparing the ^{1}H-NMR spectra of the compounds with those of the corresponding parent ureas **1a** and **b**. The ^{1}H-NMR spectra of **1a** and **b** (in DMSO-d_6) (Table II) revealed A_2B_2 multiplets for the methylene protons, in both cases centered at $\delta = 3.70$. After nitrosation, the signal due to the protons adjacent to the

Table II

No.	IR spectra (cm^{-1}) in KB r pellets				NMR spectra (δ in ppm)		
	νNH	Amide I	Amide II	νN—NO	CH_3	CH_2	NH
1a	3100—2300	1690	1530	—	2.65 s	3.70 m	7.00 (N^1)
1b	3100—2500	1715	1580	—	—	3.70 m	7.20 (N^1) 11.80 (N^3)
2a	3300—2500	1700	1530	1530	2.65 s	3.70 t ($J = 6$ Hz) 4.28 t	— 10.00 (N^3)
2b	3300—2700	1705	1520	1520	—	3.68 t ($J = 6$ Hz) 4.23 t	— 10.00 (N^3)

N—N=O group has a downfield shift: $\delta = 4.28$ ($J = 6$ Hz) for **2a** and $\delta = 4.23$ ($J = 6$ Hz) for **2b**. The chemical shifts of the protons adjacent to the chlorine atom remain unchanged ($\delta = 3.70$ in **2a**) or are little changed ($\delta = 3.68$ in **2b**).

The IR spectra of compounds **2a** and **2b** show strong absorptions at 1700 cm^{-1} and 1705 cm^{-1}, respectively, due to the NH—CO group (Table II).

A series of 1-chloroacetyl- (**3**) and 1-dichloroacetyl- (**4**) -3-(5-alkyl-1,3,4-thiadiazol-2-yl)ureas were obtained by the reactions of 5-substituted-2-amino-1,3,4-thiadiazoles with mono- and dichloroacetyl isocyanates in tetrahydrofuran (THF) (Tables III and IV).

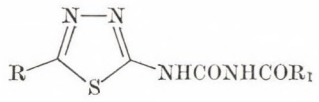

3; 4

	R_1	R					
		a	**b**	**c**	**d**	**e**	**f**
3	CH_2Cl	H	CH_3	C_2H_5	n-C_3H_7	iso-C_3H_7	n-C_4H_9
4	$CHCl_2$	H	CH_3	C_2H_5	n-C_3H_7	iso-C_3H_7	—

	R_1	R					
		g	**h**	**i**	**j**	**k**	**m**
3	CH_2Cl	iso-C_4H_9	—	n-C_5H_{11}	n-C_6H_{13}	n-C_7H_{15}	CF_3
4	$CHCl_2$	iso-C_4H_9	$C(CH_3)_3$	n-C_5H_{11}	n-C_6H_{13}	—	CF_3

The IR spectra of both derivatives **3** and **4** display two characteristic absorptions at 1735—1685 cm^{-1} (compounds **3**) and 1742—1675 cm^{-1} (compounds **4**), which belong to the vibrational group CO—NH—CO. In accordance with the data in the literature [7], the higher frequency band is ascribed to the $\nu_{asym}CO$, and that of lower frequency to $\nu_{sym}CO$. These data support the diketo structure RCONHCONHR of these compounds, hence neither the form RC(OH)=NCONHR nor RCONHC(OH)=NR_1 are present in the solid state.

Compounds **1a**, **1b** and **3m** when heated with anhydrous sodium acetate in DMF gave 2-(2-oxo-imidazolidin-2-yl)-5-methyl- (**5a**), -5-trifluoromethyl- (**5b**) -1,3,4-thiadiazole and 2-(2,4-dioxo-imidazolidin-1-yl)-5-trifluoromethyl-1,3,4-thiadiazole (**5m**), respectively.

1a, b and **3m** $\xrightarrow[DMF]{AcONa}$ 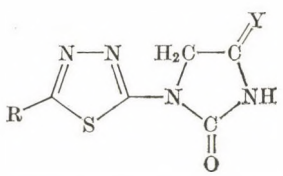

5 a: R = CH_3; Y = H_2

b: R = CF_3; Y = H_2

m: R = CF_3; Y = O

The IR spectra of amides **3m** and **4m** in carbon tetrachloride solutions show two groups of absorptions (3405—3400 cm^{-1} and 3305—3295 cm^{-1}) in the range of NH stretching vibrations, ascribed to free and bonded NH in

Table III

3	Formula (Mol. wt.)	M.p., °C (Recryst. solvent)	Yield, %	Nitrogen, %	
				Calcd.	Found s
a	$C_5H_5ClN_4O_2S$ (220.6)	197—199 dec. (acetic acid)	25	25.39	24.95
b	$C_6H_7ClN_4O_2S$ (234.6)	198—199 (acetic acid)	30	23.87	23.58
c	$C_7H_9ClN_4O_2S$ (248.6)	189—190 (acetic acid)	60	22.52	22.49
d	$C_8H_{11}ClN_4O_2S$ (262.7)	189—190 dec. (ethanol 96%)	51	21.28	20.55
e	$C_8H_{11}ClN_4O_2S$ (262.7)	191—192 (ethanol 96%)	32	21.28	21.36
f	$C_9H_{13}ClN_4O_2S$ (276.7)	187—188 dec. (THF)	32	20.24	19.98
g	$C_9H_{13}ClN_4O_2S$ (276.7)	189 dec. (THF)	40	20.24	20.36
i	$C_{10}H_{15}ClN_4O_2S$ (290.7)	195—196 (ethanol 96%)	22	19.26	19.01
j	$C_{11}H_{17}ClN_4O_2S$ (304.8)	196—197 (ethanol 96%)	22	18.38	18.01
k	$C_{12}H_{19}ClN_4O_2S$ (318.6)	194—195 (ethanol 96%)	32	17.58	17.48
m	$C_6H_4ClF_3N_4O_2S$ (288.6)	210—211 (ethanol 80%)	18	19.06	18.88

[a] overlapping with the thiadiazole ring frequencies
[b] d— doublet; t — triplet

secondary amides [8]. The lower frequencies are not influenced by progressive dilution; this confirms that they are due to intermolecular hydrogen bondings in a 6-membered ring.

Experimental

All m.p.'s are uncorrected. TLC was carried out on Kieselgel G-coated miscoscope slides, using Dragendorff reagent for detection. IR spectra were recorded in KBr pellets and in carbon tetrachloride solution with a UR—10 spectrophotometer (Carl Zeiss, Jena). ^{1}H-NMR spectra were determined with a Varian A—60D spectrometer in dimethylsulfoxide-d_6 solutions. The chemical shifts are expressed in δ units (ppm, TMS internal standard).

IR spectra (cm^{-1}) in Kbr pellets				NMR spectra (δ in ppm, J in Hz)[b]			
νNH	ν_{as} C=O ν_s C=O	Amide II (βNH)	aromatic ring frequencies	NH	CH_2Cl	CH	Other protons
3180 3090	1815 1685	1550— 1490[a]	1300, 1190 1140, 740	11.3	4.56	9.3 (CH)	—
3180 3090	1720 1695	1550— 1500[a]	1300, 1200 1170, 750	11.3	4.54	2.66 (CH_3)	—
3140	1720 1690	1550— 1490[a]	1300, 1190 1170, 745	11.3	4.55	1.37 t (CH_3) ($J = 7$)	—
3200	1715 1685	1570— 1500[a]	1300, 1195 1175, 745	11.3	4.55	0.90 t (CH_3) ($J = 7$)	3.00 t ($ArCH_2$)
3200	1715 1685	1550— 1490[a]	1290, 1200 1170, 750	11.3	4.52	1.39 d (CH_3) ($J = 7$)	—
3200	1730 1720 1685	1570— 1500[a]	1300, 1180 1140, 735	11.2	4.56	0.95 t (CH_3) ($J = 7$)	3.05 t ($ArCH_2$)
3195	1715 1685	1550— 1500[a]	1300, 1200 1170, 740	11.3	4.55	0.98 d (CH_3) ($J = 7$)	—
3200	1730 1720 1685	1570— 1500[a]	1300, 1170 1160, 730	11.3	4.55	0.90 t (CH_3) ($J = 7$)	3.03 t ($J = 7$)
3200	1730	1570— 1500[a]	1300, 1200 1170, 750	11.3	4.53	0.90 t (CH_3) ($J = 7$) 1.4 (CH_2)	3.02 t ($J = 7$) ($ArCH_2$)
3200	1730 1720 1685	1570— 1500[a]	1300, 1200 1170, 750	12.7	4.55	0.90 t (CH_3) ($J = 7$) 1.3 (CH_2)	3.02 t ($J = 7$) ($ArCH_2$)
3190	1735 1685	1550— 1480[a]	1300, 1200 1170, 750	11.5	4.55	—	—

1-(2-Chloroethyl)-3-(5-methyl-1,3,4-thiadiazol-2-yl)urea (1a)

To a suspension of 2-amino-5-methyl-1,3,4-thiadiazole (3.45 g; 0.03 mole) in 20 ml anhydrous DMF was added 2-chloroethyl isocyanate (2.6 ml; 0.03 mole) and the mixture was allowed to stand overnight at room temperature. The resulting solution was poured into water (80 ml), the solid filtered off, washed with ethanol and recrystallized from ethanol, to yield 4.2 g (65%) of the product, m.p. 173—174 °C; R_f 0.80 (1 : 1 ether/methanol).

$C_6H_9ClN_4OS$ (220.7). Calcd. N 25.16. Found 24.75%.

1-(2-Chloroethyl)-3-(5-trifluoromethyl)-1,3,4-thiadiazol-2-yl)urea (1b)

It was prepared in the same manner as **1a**. Yield: 67%, m.p. 128—129 °C (from 20% ethanol).

$C_6H_6F_3ClN_4OS$ (276.6). Calcd. N 20.24. Found N 20.17%.

Table IV

4	Formula (Mol. wt.)	M.p., °C (Recryst. solvent)	Yield, %	Nitrogen, %	
				Calcd.	Found
a	$C_5H_4Cl_2N_4O_2S$ (255.0)	213—215 (ethanol 96%)	54	21.92	21.69
b	$C_6H_6Cl_2N_4O_2S$ (296.1)	220—221 (acetic acid 80%)	77	20.81	21.01
c	$C_7H_8Cl_2N_4O_2S$ (283.1)	209—210 (ethanol 96%)	60	19.78	20.02
d	$C_8H_{10}Cl_2N_4O_2S$ (297.1)	200—201 (ethanol 96%)	62	18.84	18.95
e	$C_8H_{10}Cl_2N_4O_2S$ (297.1)	198—199 (erhanol 96%)	45	18.84	18.63
g	$C_9H_{12}Cl_2N_4O_2S$ (311.2)	197—198 (ethanol 40%)	48	18.00	17.92
h	$C_9H_{12}Cl_2N_4O_2S$ (325.2)	240—243 (acetic acid)	35	18.00	17.88
i	$C_{10}H_{14}Cl_2N_4O_2S$ (325.2)	171—172 (ethanol 50%)	42	17.22	17.11
j	$C_{11}H_{16}Cl_2N_4O_2S$ (339.2)	148—150 dec. (ethanol 60%)	52	16.51	16.41
m	$C_6H_3Cl_2F_3N_4O_2S$ (323.0)	144—145 (ethanol 80%)	50	17.34	17.12

[a] overlapping with the thiadiazole ring frequencies
[b] s — singlet; d — doublet; t — triplet; qu — quartet; sx — sextet; hpt — heptet; m — multiplet

1-(2-Chloroethyl)-3-(5-methyl- (2a) and -5-trifluoro-methyl- (2b) -1,3,4-thiadiazol-2-yl) -1-nitrosoureas

Sodium nitrite (1.72 g; 25 mmoles) was added in portions to a stirred solution of **1a** or **1b** (5 mmoles) in 20 ml formic acid (98—100%) during 10—15 min, at 0—5 °C. The yellow precipitate was collected, washed with ethanol and ether. The analytical data are summarized in Tables I and II.

1-Chloroacetyl-3-(5-alkyl-1,3,4-thiadiazol-2 -yl)ureas (3)

The appropiate 2-amino-5-alkyl-1,3,4-thiadiazole (0.01 mole) in 50 ml anhydrous THF, cooled to 5 °C, was treated dropwise, with stirring, with 1.19 g (0.01 mole) of chloroacetyl isocyanate. The mixture was allowed to stand overnight at room temperature, the precipitate was filtered off, washed with water and ethanol, and recrystallized from the proper solvent. The experimental data are given in Table III.

IR spectra (cm^{-1}) in Kbr pellets				NMR spectra in DMSO-d_6[b] (δ in ppm, J in Hz)			
νNH	ν_{as} C=O ν_s C=O	Amide II (βNH)	Aromatic ring frequencies	$CHCl_2$	CH_3	CH_2	CH
3180	1742 1710	1550— 1490[a]	1330, 1200 1170, 750	6.80	—	—	—
3180	1738 1710	1540— 1520[a]	1330, 1200 1170, 750	6.80	2.68 s	—	—
3185	1730 1710	1525	1330, 1190 1160, 750	6.80	1.38 t (J = 7.5)	3.03 qu	—
3195	1730 1715	1525	1330, 1200 — 760	6.80	1.00 t (J = 7)	1.80 sx	—
3195	1740 1698	1545— 1520[a]	1310, 1200 1170, 750	6.80	1.42 d (J = 7)	—	3.40 hpt
3200	1740 1695	1550— 1515[a]	1300, — 1175, 760	6.80	0.98 d (J = 6)	1.08— 2.00 m (6 H)	1.16— 2.33 m
3195	1738 1695	1550— 1515[a]	1300, — 1175, 760	6.81	1.46 s	—	—
3200	1738 1695	1550— 1515[a]	1290, — 1175, 760	6.80	0.90 t (J = 6)	1.08— 2.00 m (6 H)	—
3195	1738 1695	1550— 1515[a]	1300, — 1175, 760	6.80	0.90 t (J = 6)	1.08— 2.08 m (8 H) 3.00 t (2 H)	—
3460— 3200	1740 1700	1530	1280, — — 760	6.80	—	—	—

m—multiplet

1-Dichloroacetyl-3-(5-alkyl-1,3,4-thiadiazol-2-yl)ureas (4)

A suspension of the requisite 2-amino-5-alkyl-1,3,4-thiadiazole (0.01 mole) in 30 ml anhydrous THF (or 20 ml DMF) and 1.69 g (0.01 mole) of dichloroacetyl isocyanate was allowed to stand at room temperature. The precipitate was filtered off, washed with water and ethanol, and recrystallized. The experimental data are given in Table IV.

2-(2-Oxo-imidazolidin-2-yl)-5-methyl- (5a), -5-trifluoromethyl- (5b) -1,3,4-thiadiazole and 2-(2,4-dioxo-imidazolidin-1-yl)-5-trifluoromethyl-1,3,4-thiadiazole (5m)

Anhydrous sodium acetate (0.82 g; 10 mmoles) was added to a solution of 5 mmoles of **1a** or **3m** in 15 ml DMF. The mixture was heated at 110—115 °C for 1 h, then cooled and poured into water. The precipitate was filtered off and recrystallized from ethanol. The experimental data are given in Tables V and VI.

Table V

No.	Formula (Mol. wt.)	M.p., °C (Recryst. solvent)	Yield, %	TLC (R_f)	Nitrogen, %	
					Calcd.	Found
5a	$C_6H_8N_4OS$ (184.2)	252—253 (ethanol)	33	0.35 (8 : 2 ether/ methanol)	30.41	30.64
5b	$C_6H_5F_3N_4OS$ (238.2)	203—204 (ethanol)	67	—	23.52	23.33
5m	$C_6H_3F_3O_2S$ (252.1)	203—205 (water)	51	—	22.17	22.33

Table VI

No.	IR spectra (cm^{-1}) in KBr pellets				NMR spectra (δ ppm)		
	νNH	Amide I	Amide II	νCF	CH_3	CH_2	NH
5a	3350—2700	1720	1430	—	2.63 s	3.60 s 4.08 s	—
5b	3280—2800	1740	1490	1040	—	3.70 s 4.20 s	8.20 (N^1)
5m	3350—2700	1800—1730	1500	1035	—	4.65 s	—

*

The authors are indebted to Dr. D. POSTESCU for encouraging discussions and to Dr. P. SOHÁR for spectroscopic investigations.

REFERENCES

[1] GYÖRFI, Z., CSÁVÁSSY, GY.: Acta Chim. (Budapest) **82**, 91 (1974)
[2] ERMILI, A., CORTESE, I.: Il Farmaco, Ed. Sci., **22**, 393 (1967); Chem. Abstr., **68**, 2863m (1967)
[3] ERMILI, A., CAPUTO, A., BRUNORI, M.: Il Farmaco, Ed. Sci., **22**, 463 (1967)
[4] MAFII, G., TESTA, E., ETTORRE, R.: Il Farmaco, Ed. Sci., **13**, 188 (1958)
[5] JOHNSTON, C. K.: J. Org. Chem., **32**, 1508 (1967)
[6] JOHNSTON, TH. P., MCCALEB, G. S., OPLIGER, P. S., MONTGOMERY, J. A.: J. Med. Chem., **9**, 892 (1966)
[7] SOHÁR, P.: Magyar Kém. Folyóirat, **74**, 298 (1968)
[8] JOSE, C. I., PABRAI, P. R.: Spectrochim. Acta, **23A**, 734 (1967)

Zoltán GYÖRFI
György CSÁVÁSSY } 3400 Cluj-Napoca, Str. Republicii 34—36, Romania

Acta Chimica Academiae Scientiarum Hungaricae, Tomus 103 (1), pp. 95—100 (1980)

DETERMINATION OF THE CONFIGURATION AND CONFORMATION BY ^1H AND ^{13}C NMR SPECTROSCOPY OF TWO 2,4;3,5-DI-*O*-BENZYLIDENE-1,6-DIBROMO-1,6-DIDEOXY-D-MANNITOL DIASTEREOMERS

P. SOHÁR,* T. HORVÁTH and G. ÁBRAHÁM

(Institute for Drug Research, Budapest)

Received December 16, 1978
Accepted for publication March 21, 1979

The configuration and stable conformation of two 2,4;3,5-di-*O*-benzylidene-1,6-dibromo-1,6-dideoxy-D-mannitol diastereomers were established by ^1H and ^{13}C NMR spectroscopy.

Benzalation of 1,6-dibromo-1,6-dideoxy-D-mannitol in the presence of $ZnCl_2$ yields two mono- and two dibenzylidene derivatives [1]. One of the monobenzylidene derivatives (**1a**) proved to be a known compound [2], while the **2a** structure of the other one could be established by transforming it into a known derivative [1].

The two dibenzylidene derivatives can contain either two dioxolane, two dioxane or one dioxolane and one dioxepine ring, *i.e.* they possess bicyclic structures with (5 + 5)-, (6 + 6)- or (5 + 7)-membered rings. Due to the chirality of the benzylidene group, three diastereomers (*R*, *R*; *R*, *S*; *S*, *S*) of each type (2,3;4,5, 2,4;3,5- and 3,4;2,5-dibenzylidene derivatives) can be formed. The structure of the two isolated dibenzylidene derivatives of m.p. 161 °C and m.p. 165 °C, respectively, had to be selected from among these.

For this purpose their ^1H and ^{13}C NMR spectra were analyzed, using the diacetoxy derivatives (**1b** and **2b**) of **1a** and **2a**, as model compounds (Tables I and II).

Both dibenzylidene derivatives possess a symmetric structure; the protons and carbon atoms in positions 1,6, 2,5 and 3,4, as well as the benzylidene protons and carbons gave identical chemical shifts, hence all three diastereomers of the 5 + 7-membered bicyclic derivatives and also the asymmetric diastereomers of the bicyclic derivatives with two dioxolane and two dioxane rings could be excluded.

The ^{13}C NMR chemical shifts of the benzylidene carbon atoms excluded the presence of dioxolane rings, as the corresponding chemical shift of **2b**

* Present address: "EGYT" Pharmacochemical Works.

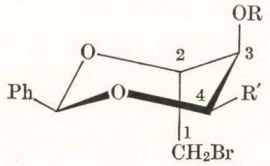

1

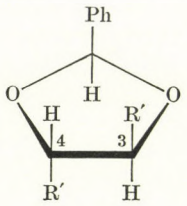

2

$$R' = -\overset{5}{C}H(OR)-\overset{6}{C}H_2Br$$

a: R = —H

b: R = —Ac

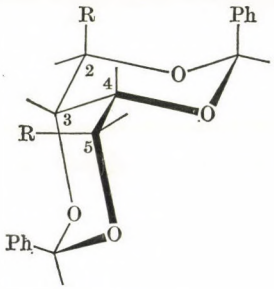

3a

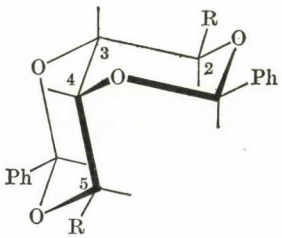

3b

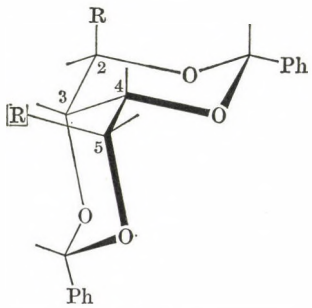

4a

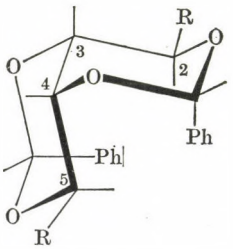

4b

$$R = -CH_2Br$$

Table I

^1H NMR data of compounds **1b**, **2b**, **3b** *and* **4a** *in $CDCl_3$ solution ($\delta_{TMS} = 0$ ppm) at 60 MHz*

Compound	δH−1,1',6,6'	δH−2,5	δH−3,4	δCH^x *s* (1H)	δArH (5H)	δCH$_3$(Ac) (3H)
1b	215−240* (4H)	250−275* (2H)$^{\neq}$ 300−330* (2H)$^{\bullet}$		5.90	435−465*	2.12+
2b	210−230* (4H)	290−330* (2H)	250−280* (2H)	5.95	~7.4 s	2.14 2.20
3b	3.44 (2H)$^{\ominus}$ 3.71 (2H)$^{\ominus}$	230−290* (4H)		5.70+	420−460*,+	—
4a	3.65 d° (4H)	4.20 t° (2H)	4.12 s (2H)	5.78+	420−460*,+	—

^{x} benzylidene proton
* multiplet in Hz
+double proton number
$^{\neq}$H−2,4
$^{\bullet}$H−3 *t*, overlapped with the H−5 multiplet, but is well identifiable
$^{\ominus}$Calculated from the *AB* part of the *ABX* multiplet
°J = 5 Hz
s: singlet
d: doublet
t: triplet

containing a dioxolane ring was much higher (104.4 ppm) than that measured for the two dibenzylidene derivatives (96.1 and 94.6 ppm). The latter values are, however, close to the chemical shift of the monobenzylidene derivative **1b** containing a dioxane ring (95.0 ppm).*

Thus both dibenzylidene derivatives contain two dioxane rings, consequently their structures can only be **3** (*S*,*S*) or **4** (*R*,*R*). Both of these structures can exist in two chair-chair conformations, among which, considering only the skeleton without substituents (*i.e.* the configuration of 1,3;2,4-di-*O*-methylene-L-threitol), the "*O*-inside"-conformer (**a**) is much more stable than its "*H*-inside" pair (**b**). The free energies of the two conformers are about 1.18 kcal/mole and 5.35 kcal/mole [6]. Considering, however, also the substituents, the two *axial* bromomethyl and two *axial* phenyl groups in conformer **3a** increase the free energy by about 5.8 kcal/mole [7] and 6.2 kcal/mole [8], respectively, resulting in a much higher value (13.2 kcal/mole) for **3a**. In the case of **3b** all substituents are *equatorial*, consequently the free energy is not increased. This is in accordance with our observation that the NMR spectrum of compound **3** is not temperature-dependent, suggesting a conformationally homogeneous system.

Both conformers of diastereomer **4** contain two identical substituents in *axial* position, conformer **a** the bromomethyl, and conformer **b** the phenyl

* Although according to numerous literature data (*e.g.* [3−5]) the ^1H NMR chemical shifts of the benzylidene protons in derivatives with dioxane or dioxolane rings show a characteristic difference, this is not valid for our compounds (*cf.* data of **1b** and **2b**, Table I); therefore the structures could not be elucidated by making use of this difference.

Table II

^{13}C *NMR chemical shifts of compounds* **1b**, **2b**, **3b** *and*

Compound	δC−1	δC−6	δC−2	δC−5	δC−3	δC−4
1b*	32.8	27.9	67.7	63.9	76.0	72.8
2b*	30.7	31.5	71.1	72.3	77.3	78.2
3b	32.4		69.3		72.6	
4a	29.1		68.1		75.3	

* In the case of the carbon atom pairs 1,6, 2,5 and 3,4 an alternative assignment is also possible,
+Benzylidene carbon atom
x Acetyl group
° Overlapped signals

groups. Since the *axial* phenyl or bromomethyl substituents cause a similar increase in the free energy, the original energy difference (about 3.8 kcal/mole) between the "*O*-inside" (**a**) and "*H*-inside" (**b**) forms of the skeleton would remain unchanged, but due to the steric hidrance between the two *endo* phenyl groups it is increased in the case of the **b** isomer. This difference is sufficiently high for considering also isomer **4** as a conformationally homogeneous system. However, in contrast with the diastereomer **3** existing in conformation **b**, in case of isomer **4** conformation **a** is more stable.

According to these considerations, the structures **3b** and **4a** were to be assigned to the isolated substances melting at 161 °C and 165 °C. This could be done on the basis of the values of the proton-proton coupling constants $J_{2,3} \equiv J_{4,5}$. In **3b** the corresponding dihedral angles are $\sim 180°$, while for isomer **4a** only $\sim 60°$.

The broad and complex H-2,5 and H-3,4 multiplets in the ^1H NMR spectrum of the substance melting at 161 °C affords evidence that the coupling constant $J_{2,3} \equiv J_{4,5}$ is large.

The H-3,4 signal of the substance melting at 165 °C is a singlet, and the H-2,5 signal being partly overlapped by this singlet is triplet-like, consequently the coupling constant $J_{2,3} \equiv J_{4,5}$ must be small, causing no significant splitting. Hence the structure of the substance melting at 161 °C is **3b** (*S*,*S*), while structure **4a** (*R*,*R*) can be assigned to the isomer melting at 165 °C. The coupling constants $J_{2,3} \equiv J_{4,5}$ of the former correspond thus to an *axial-axial* interaction, while this interaction is an *equatorial-axial* one for the latter, therefore $J_{2,3}$(**3b**) $\gg J_{2,3}$(**4a**).

This structure assignment based upon the ^1H NMR data was also confirmed by ^{13}C NMR spectroscopy. In the sterically more crowded isomer **4a**

4a *in* $CDCl_3$ *solution* ($\delta_{TMS} = 0$ ppm) *at* 25.16 *MHz*

δCH_3^X	δC^+	δC_{Ar}^s	δC_{Ar}^o	δC_{Ar}^m	δC_{Ar}^p	$\delta C{=}O^x$
20.7	95.0	136.9	126.1	128.4	129.3	169.5 170.2
20.8	104.4	135.9	126.6	128.4	129.8	169.6 169.7
—	96.1	136.9	126.3	128.6	129.6	—
—	94.6	137.6	126.1	128.9°	128.9°	—

but the one given here is more probable

containing *axial* bromomethyl groups, the chemical shifts of the carbon atoms 1,6-, 2,5- and the benzylidene carbon atoms are decreased by the field effect [9] by 3.3, 1.2 and 1.5 ppm, respectively (Table II).

By establishing the configurations and conformations of the compounds in question it could thus be proved that the two dibenzylidene derivatives represent a pair of diastereomers containing two dioxane rings each. To our knowledge, no example has been described so far in the literature for the simultaneous formation of 2,4;3,5-dibenzylidene type diastereomers.

Experimental

The preparation of the studied compounds, as well as the structure elucidation of compounds **1a, b** and **2a, b** were described elsewhere [1]. ^1H NMR spectra were recorded on a JEOL 60-HL, and ^{13}C NMR spectra on a VARIAN XL 100 FT-spectrometer, in $CDCl_3$ solutions, at room temperature, with tetramethylsilane as internal standard.

*

The authors thank Mrs. Judit CSÁKVÁRI and Mr. Attila FÜRJES for technical assistance

REFERENCES

[1] HORVÁTH, T., SOHÁR, P., ÁBRAHÁM, G.: Carbohyd. Res. **73,** 277 (1979)
[2] (a) KUSZMANN, J., VARGHA, L.: Carbohyd. Res., **17,** 309 (1971); (b) SOHÁR, P.: Nuclear Magnetic Resonance Spectroscopy (in Hungarian), Vol. **1,** p. 456. Akadémiai Kiadó, Budapest (1976)
[3] (a) BAGGET, N., BUCK, K. W., FOSTER, A. B., RANDALL, M. H., WEBBER, J. M.: J. Chem. Soc., **1965,** 3394, 3401; (b) Proc. Chem. Soc., **1964,** 118

[4] (a) FOSTER, A. B., HAINES, A. H., HOMER, J., LEHMANN, J., THOMAS, L. F.: J. Chem. Soc., **1961,** 5005; (b) FOSTER, A. B., RANDALL, M. H., WEBBER, J. M.: J. Chem. Soc., **1965,** 3388
[5] (a) GAREGG, P. J., MARON, L., SWAHN, C. G.: Acta Chem. Scand., **26,** 518 (1972); (b) GAREGG, P. J., SWAHN, C. G.: Acta Chem. Scand., **26,** 3895 (1972)
[6] STODDART, J. F.: Stereochemistry of Carbohydrates, p. 211. Wiley-Interscience, New York—London 1971
[7] See Ref. [6], p. 213
[8] See Ref. [6], *loc. cit.* 57, on p. 215
[9] GRANT, D. M., CHENEY, B. V.: J. Amer. Chem. Soc., **89,** 5315 (1967)

Pál SOHÁR H-1475 Budapest, P.O.B. 100
Tibor HORVÁTH, Gizella ÁBRAHÁM H-1325 Budapest-1, P.O.B. 82

RECENSIONES

Topics in Current Chemistry, Vol. 75
Organic Chemistry and Theory

Springer-Verlag, Berlin, Heidelberg, New York, 1978, 187 pages

The 75th volume of the series Topics in Current Chemistry is rather heterogeneous but, et least, it is a collection of multifarious papers. The first one is written by a research team of spectroscopists and electrochemists in Bologna, V. BAZANI and co-workers, and is entitled "Bimolecular Electron Transfer Reactions of the Excited States of Transition Metal Complexes". The topic is very interesting and timely. In the excited state of a molecule (*e.g.*, a metal complex) an electron is promoted to a higher energy level and simultaneously a "vacant site" having a relatively low energy level is also formed. The molecule in the excited state will possess a stronger reducing action owing to the presence of the electron of higher energy, while its oxidizing power is also enhanced by the presence of the vacant site of lower energy, as compared with the ground state. In oxidation-reduction systems excitation by light may produce such an electron transfer which will move the system far from the equilibrium corresponding to the components in the ground state. In this way the energy of light can be stored in the form of chemical energy of a redox system; this may have great practical importance in the conversion and utilization of solar energy. These questions are discussed very thoroughly and clearly in the paper which can be regarded as a significant source of scientific information, together with the several hundred references listed therein.

The second paper is of more limited interest. It contains the results in a well defined field, achieved by an American team of eight researchers headed by T. H. KOCH. The title of the paper is "Photochemical-Reactivity of Keto Imino Ethers. Type I Rearrangement and (2 + 2)-Photocycloaddition to the Carbon-Nitrogen Double Bond". The authors attempted the photodimerization of keto imino ethers which can readily be prepared from cyclic imides (*e.g.*, succinimide), and they found instead a rearrangement accompanied by ring contraction, which can be regarded as an intramolecular cycloaddition of the $[\sigma 2s + \pi 2s]$ type. Keto imino ethers in which this rearrangement does not take place can participate in cycloaddition reactions with olefins by means of the C=N bond. The paper gives a good picture of a relatively narrow field, but presents no extraordinary surprises.

The longest paper in the volume is a theoretical speciality. Two Czechoslovakian authors, I. HUBAČ and P. ČÁRSKY, one of them being a mathematician and the other a quantum chemist, present a broad survey of the theoretical problems and computational methods of electron correlation which are not negligible in quantum chemical calculations of higher level. The title of the paper is: "Computational Methods of Correlation Energy". The authors aimed at collecting and evaluating the results of the work done in the field of calculations of correlation energy, thus making them available for those who wish to use them in routine quantum chemical calculations. The paper thus deals with a field which is rather special even for quantum chemists, but inevitably important and useful and, according to quantum chemist colleagues, it offers a good summary.

The final paper is relatively short but substantial: it is concerned with an interesting theoretical stereochemical problem. The authors are Ivar UGI, professor of the Technical University Munich, and the members of his stereochemical research team. The title of the paper is:

"A Quantitative Measure of Chemical Chirality and Its Application to Asymmetric Synthesis." First they introduce and define the concept of chemical chirality. The geometric definition of chirality (a form not identical with its mirror image) holds for a fixed structure. From the chemical point of view, only such molecules can be regarded as chiral, which cannot be transformed into their mirror images by means of the intramolecular motions possible under the given conditions of the observation. (Let us consider, *e.g. gauche* butane, which is a chiral conformation, but at room temperature can easily transform into its mirror image.) The authors introduce the concept of chiral genus as a quantitative measure of chirality; this is related to the number of bonds to be split to achieve racemization of a given chiral molecule. This quantitative measure allows a classification of stereoselective reactions, and the quantitative characterization of asymmetric syntheses. The new concepts are explained by means of several examples.

The book containing a varied subject-matter provides much interesting and valuable information for chemists working in different fields.

M. KAJTÁR

I. HRONSZKY—M. VARGA: *Történeti-tudományelméleti megjegyzések a kémiáról*

(Historisch-wissenschaftstheoretische Bemerkungen über die Chemie)

Verlag der Ung. Akademie der Wissenschaften, Budapest, 1978, 180 S. (Ungarisch)

»Unserer Ansicht nach ist in der Analyse der heutigen Entwicklung der Chemie ihr gegenwärtiger Zustand als unabgeschlossene Geschichte zu betrachten. Die Gegenwart der Wissenschaft ist ebenfalls ein Vorgang, wo nicht zeitgenossische, jedoch zur selben Totalität gehörende Elemente zusammenleben . . .« — schreiben die Verfasser in der Einleitung. Dies ist sehr zu berücksichtigen. Meiner Meinung nach können die Naturwissenschaften nämlich nur historisch vorgetragen werden, einfach deshalb, weil sie sich geschichtlich entwickelten und sich weiter auch auf diese Weise entwickeln und verändern. Heute ist man geneigt die zu einem gegebenen Zeitpunkt bestehenden Kentnisse als abgegrundetes Ganzes zu behandeln und im Unterricht weiterzuvermitteln, wodurch ein gewisser Dogmatismus auf die Schülern übertragen wird, da sie den Eindruck erhalten, die Sache wäre komplett und unabänderlich.

Aus diesem Grund war es nützlich, dieses Buch zu veröffentlichen. Die Verfasser greifen aus der ferneren und nahen Vergangenheit der Chemie gewisse Probleme und Fragen heraus und untersuchen sie nach modernen wissenschaftstheoretischen Gesichtspunkten.

Das Buch ist sehr lehrreich, auch wenn der Leser vielleicht nicht mit jeder Behauptung der Verfasser einverstanden ist. Ich war es auch nicht immer. In der Geschichte sind jedoch nur die Ereignisse sicher (in der Wissenschaftsgeschichte manchmal auch diese nicht), das wie und warum läßt sich schon auf mancherlei Weise erklären. Untersuchungen über das Problem, wie und warum man zu einer neuen Erkenntnis gelangte, sind jedoch für den heutige Forscher nützlich, da er daraus viel zu erfahren vermag, was bei seiner eigenen Forschung von Nutzen ist. Er erfährt z. B., daß die Entwicklung der Chemie stillsteht, wenn man sich — was meistens nach dem Sturz bedeutender Hypothesen der Fall ist — keiner Hypothesen bedient. Es war vielleicht doch kein Zufall, daß der Name, mit dem die klassische organische Strukturtheorie verbunden ist, Kekulé und nicht Couper ist. Nach letzteren muß nämlich jede Theorie vom experimentellen und philosophischen Standpunkt aus richtig sein. Philosophische Richtungen gibt es aber verschiedene. Sehr unrichtig ist es, eine naturwissenschaftliche Theorie, deren Richtigkeit oder Unrichtigkeit erst durch die weitere Entwicklung bewiesen werden kann, von philosophischen Standpunkten aus sofort zu verurteilen, wie dies schon oft geschehen ist; bei der Resonanztheorie und Quantenchemie eben in der nahen Vergangenheit.

Interessant sind die Erörterungen über den Begriff des naturwissenschaftlichen Gesetzes. Manche behaupten nach Kant, Bedingung des Gesetzes ist mathematische Ausdrückbarkeit. So dachte auch Lothar Meyer. Deshalb ist nicht er der Entdecker des periodischen Gesetzes, sondern Mendelejew, nach dem der quantitative Charakter nur den Grad der Exaktheit ausdrückt. Man könnte noch zahlreiche solche interessante, an Beispielen orientierte Erörterungen aus dem Buch anführen.

Beim Lesen des Buches hat man den Eindruck als wären die Chemiker immer in der Rüstung der vollständigen Kentnis einer philosophischen Richtung zum Laboratorumstisch getreten, um zu forschen, und als hätten sie ihre Schlüsse nach gründlicher philosophisch-

wissenschaftstheoretischer Überlegung gezogen. Ich akzeptiere, daß herrschende Ideen eines Zeitalters auf die Forscher Einfluß ausgeübt haben, doch glaube ich, daß dies viel umbewußter geschah als es dem Buche nach den Anschein hat.

Das Buch ist Keine leichte Lektüre. Etwas Chemiegenschichte muß man schon kennen, um es verstehen zu können.

F. SZABADVÁRY

Metal Ions in Biological Systems, Vol. 7

SIGEL, H. (ed.) Marcel Dekker, New York and Basel, 1978, XVII, 417 pp.

Iron is the most important transition metal in living systems, being the metal constituent of a large variety of enzymes and proteins which play a part in different bioredox and electron transport processes, and some have oxygen-carrying properties. The biochemistry of iron is an enormously large field as it is also obvious from the series of monographs listed in Volume 7 of "Metal Ions in Biological Systems".

The introductory chapter written by M. T. BECK deals with the prebiotic coordination chemistry, *i.e.* the role of metal ions (among them that of iron) in the formation of compounds essential for biological evolution, and also with the possible role of transition metal complexes in the organization phase of chemical evolution. As to the first point, the author considers both the transition metal ions and the potential ligands (both inorganic and organic) present in the prebiotic soup, and discusses the influence of complex formation on both the reactivity of the ligands and the catalytic activity of the metal ion. A short survey is given on the role that metal ions might have played in the formation of amino acids, peptides, nucleobases and porphins. The author also deals with the biochemical function of transition metal ions and with the evolution of metalloenzymes.

The second review written by P. M. MAY, D. R. WILLIAMS and P. W. LONDER is entitled "Biological significance of low molecular weight iron(III) complexes". The monograph is centered around a very important problem, how low molecular weight complexes influence the iron metabolism in living systems. Iron is followed as it is transported through membranes and bound to different molecules within the cells. Sub-chapters are devoted also the chelation therapy and to the regulation of iron metabolism. Finally the authors show how computer simulation studies help us to gain insight into multicomponent equilibrium systems.

138 references close the review.

The third review, by T. EMERY, has the title "The storage and transport of iron". The author's main concern is microbial iron transport and storage, however, some discussion of plant and amimal systems is also presented. The author starts with iron solubilization and transport both in fungal and in bacterial systems. This is followed by a discussion of the stereochemistry of iron transport, and then comes back again to the iron pathway, dealing with the mechanisms of both reductive and hydrolytic iron release. The last two subchapters discuss the storage and transport of iron in higher plants and animal systems.

128 references are given.

The fourth review written by B. A. AVERILL and W. H. ORME-JOHNSON is entitled "Iron-sulfur proteins and their synthetic analogs". Iron-sulfur proteins (rubredoxins and ferredoxins) have an important role in many bioredox processes including photosynthesis and nitrogen fixation. The authors in their review deal with the properties of iron-sulfur proteins including their biological activities, chemical and physical characteristics, sequence homology and folding patterns. Then synthetic iron-sulfur systems (tetrameric and dimeric Fe—S cluster, monomeric FeS_4 systems) are discussed. This is followed by a description of the methods used to determine the type of Fe—S clusters in proteins. Two methods have been developed so far for analytical purposes: (*a*) the thiol displacement reaction and (*b*) the interprotein cluster transfer. The final part of this review is on iron-sulfur enzymes and on their function in different biological systems.

174 references are listed.

The fifth monograph authored by P. JONES and I. WILSON is concerned with "Catalases and iron complexes with catalase-like properties". In the introduction the authors deal with the formation of peroxide in organisms, and with the enzymic utilization of peroxides. This is followed by a discussion of catalases: the kinetic and mechanistic aspects of their catalytic action and particularly those aspects which permit comparison with the reactions of protein-

free ferrihemes. The review deals also with ferrihemes, their solution structures and aggregation equilibria, and with their catalatic and peroxidatic activities. The final chapter is on the comparative catalytic behaviour of iron(III)-centered catalysts.

194 references are listed.

The sixth review, by P. G. DEBRUNNER, I. C. GUNSALUS, S. G. SLIGAR and G. C. WAGNER, is entitled "Monooxygenase hemoproteins: Cytochromes P—450". The authors deal with the electronic structure of heme (electronic absorption and resonance Raman scattering spectra), with the electronic structure of iron (EPR and Mössbauer spectra) and with cytochrome m reaction states.

86 references close the review.

The seventh monograph entitled "Synthetic analogs of the oxygen binding hemoproteins" is authored by C. A. REED. The review begins with a brief description of the oxygen carrying hemoproteins and this continues with a discussion of deoxyhemoglobin analogs, oxyhemoglobin models, carbonmonoxyhemoglobin analogs and methemoglobin derivatives. The purpose of the author was to provide a basis on which the model approach of trying to understand the biochemistry of hemoproteins can be critically evaluated, and also to point out some of the remaining problems.

81 references are listed.

The next review in this volume, "Mechanisms for the modulation of hemoglobin oxygenation: A statistical mechanical analysis of equilibrium and kinetic data" was written by H. E. STANLEY, R. BANSIL and J. HERZFELD. In the first chapter the authors present a statistical-mechanical approach to the study of equilibrium and kinetic properties of allosteric proteins. This is followed by a quantitative description of the macroscopic behaviour expected from molecules conforming to a particular model. The authors make a thorough analysis of the oxygenation equilibrium of hemoglobin, and continue to deal with the kinetics of hemoglobin oxygenation.

33 references close the review.

The final review, by E. R. HUGHES, is entitled "Human iron metabolism". After a brief historical introduction of some events in understanding the function of iron in biology, the subsequent chapters discuss the fate of iron during metabolism. The main topics outlined in the present review are the absorption of iron, body iron kinetics and distribution and control mechanisms (including the role of intestinal mucosa, and storage and transport proteins). The final chapter discusses disorders of iron metabolism (iron deficiency and iron overload).

53 references are listed.

Volume 7 of this outstanding series dealing with the part played by metal ions in biological systems, provides the reader with a wealth of information on both the function and role of iron in living organisms, and on the models which have been constructed with the aim to arrive at a more thorough understanding of the molecular basis of biochemical-biological processes in which iron is involved.

E. KŐRÖS

Christian BIRR: *Aspects of the Merrifield Peptide Synthesis Reactivity and Structure in Organic Chemistry. Vol.* 8

Springer-Verlag, Berlin, Heidelberg, New York 1978, 102 pages, 62 figures, 6 tables

Ever since the introduction of the Merrifield peptide synthesis in 1962, it has been one of the most disputed fields of peptide chemistry. The author of the book has worked by the Merrifield method since the first years and several innovations have been associated with his name (use of symmetric anhydrides of amino acids, application of Ddz amino acids and 0.5% divinylbenzene-containing polystyrene resin in centrifugal reactors in the solid phase peptide synthesis).

Every line of this concise book written in an interesting style reflects great practice and theoretical knowledge of the author in the given field. Since in the past years several comprehensive monographs have been published dealing with the Merrifield method, the author omitted a detailed survey of the literature data of the sixties, rather the results of the seventies are discussed and the literature data critically treated. As expressed in the preface and closing lines, the purpose of the book was not to arrive at a final decision in the dispute between the followers and opposers of the Merrifield method but the author wanted to present a new

aspect of the method and a critical discussion of the methodological innovations introduced recently, which, of course, may again lead to further discussions.

There are five chapters in the book (The principle; Chemical details of the method; Automatization of the Merrifield peptide synthesis; Critical view on the applicability of the Merrifield synthesis; Conclusion). The discussion of the chemical details of the method is very interesting; evidently, all new literature methods have been tried in the laboratory of the author. Some new, surprising aspects are brought up, *e.g.*, that there is no difference in respect of chemical reactions between polystyrene gel containing 0.5% divinylbenzene and the polystyrene "liquid phase"; the so-called automatic peptide synthesizing apparatuses used heretofore have actually been only semiautomatic apparatuses because they give no indication about the reaction occurring, *etc.* A very valuable suggestion is forwarded for the construction of a *fully automated* peptide synthesizing apparatus utilizing spectrophotometric analysis of the reaction mixture.

A great virtue of the book is that, as a result of "daily confrontation" with the problems of the Merrifield method, the author is free from prejudices towards the various opinions. Of the 221 literature references 142 were published later than 1970. The figures and tables in the book are excellent.

In summary, this very readable, lucid and useful book can be recommended to all laboratories engaged in peptide chemistry, to researchers working in related fields and to chemists concerned with the synthesis of oligonucleotides.

B. PENKE

D. POLAND: *Cooperative Equilibria in Physical Biochemistry*

Clarendon Press, Oxford 1978, viii + 344 pp.

The development of the thermodynamics of multiple equilibria is an intriguing problem of history of science. Three practically independent paths can be noticed: the treatment of the stepwise formation of metal complexes, the complicated equilibria occurring in gaseous phase and the equilibria involving biopolymers. This book provided a most interesting, thought-provoking, although incomplete treatment of the multiple equilibria which undoubtedly play a crucial role in the understanding the function and behaviour of biochemical systems. POLAND's book provides a fresh approach of the complicated systems, stressing the deep analogy between the distribution of energy levels in quantum statistical ensembles and distribution of free energy states in chemical equilibria. (The partition function is analogues to the α function of the coordination chemists and symbolised by in this book. The microconstants of coordination chemists are treated as degeneracy of free energy levels.)

The first two chapters gives an excellent summary of the thermodynamical and statistical background furthermore a treatment of intermolecular forces necessary to understand the equilibria involving biopolymers by modelling them.

The third chapter is an application of the formerly formulated principles to the double-helix and triple-helix equilibria, while the fourth chapter outlines a matrix algebraic treatment of the partition functions of linear chain molecules. (A short review of matrix algebra is given in the appendix.)

The fifth chapter deals with problems of cooperativity when small molecules are bound to biopolymers; the concluding chapter gives an approach of the specific sequence to the conformational equilibria.

Notes and references are given at the end of each chapter. The list of the quoted papers is very limited and proves the validity of the first sentences of this review.

This stimulating book would be even more helpful if some informations concerning the experimental and computational treatment of multiple equilibria were given.

M. T. BECK

A. RUSANOV: *Phasengleichgewichte und Grenzflächenerscheinungen*

Herausgegeben von W. SCHIRMER. Akademie Verlag,
Berlin 1978. XVII + 465 pp, Preis 90 Mark

Bekanntlich gibt es zwei, voneinander prinzipiell verschiedene Möglichkeiten bzw. Aspekte, um heterogene Systeme, die außer den ausgedehnten Raumphasen noch sehr dünne Grenzschichten enthalten, thermodynamisch zu behandeln. Die eine Möglichkeit, der sich zuerst GIBBS in seinen klassischen Arbeiten bedient hatte, besteht darin, daß man das reale System mit einem solchen hypothetischen System vergleicht, in welchem die Grenzschicht durch eine fiktive mathematische Fläche, die sog. *Trennfläche* (dividing surface) ersetzt wird und dann jede Änderung der thermodynamischen Zustandsparameter, die im realen System gerade infolge der Existenz der wirklichen Grenzschicht endlicher Dicke und inhomogener Stoffverteilung gegenüber dem Referenzsystem auftritt, als Überschussgröße der Trennfläche zuordnet, darauf sozusagen "verschmiert". Durch diesen zwar nicht sehr anschaulichen, aber gedanklich vollkommen lückenfreien Formalismus versuchte GIBBS die Schwierigkeit zu umgehen, die sich daraus ergibt, daß die Zwischenschichten im Sinne des von ihm eingeführten Phasenbegriffs keine autonomen Phasen darstellen, da sie ja Raumanteile des Mehrphysensystems verkörpern, in denen diskontinuierliche Änderungen in den Eigenschaften auftreten, wenn man von einer Raumphase in die andere übergeht.

Die andere Betrachtungsweise geht auf VAN DER WAALS, BAKKER, VERSCHAFFELT, insbesondere aber GUGGENHEIM zurück. Im Gegensatz zum GIBBSschen Formalismus behandelt man hier auch die Grenzschichten als Phasen, denen bestimmte Werte der Zustansvariablen (Substanzmenge, Volumen, usw.) zugeordnet werden können, da sie zwar sehr dünn im Vergleich zu den Raumphasen sind, aber doch offensichtlich eine endliche Dicke, bestimmte Struktur usw. besitzen. Es ist sofort einzusehen, daß man sich dieser Betrachtung nur dann bedienen kann, wenn man die GIBBSsche Definition der Phase aufgibt und bewußt in Kauf nimmt, daß in der Grenzphase Inhomogenitäten bzw. Diskontinuitäten auftreten.

Im vorliegenden Werk hat sich RUSANOV die enorme Aufgabe gestellt, die Exaktheit des GIBBSschen Formalismus mit jener Realität in Einklang zu bringen, daß die Grenzschichten doch ausgedehnte Raumteile endlicher Dicke darstellen, die, wenn auch noch nicht immer, aber doch bereits in einigen Fällen der unmittelbaren experimentellen Untersuchung zugänglich sind. Daraus ergibt sich die Möglichkeit, die Theorie zu prüfen, wovon an Hand eigener Meßergebnisse auch Gebrauch gemacht wird.

Es sei nachdrücklich betont, daß es sich bei der "Versöhnung" der beiden Konzepte über Trennfläche bzw. Grenzphase um keinen Kompromiß handelt. RUSANOV hat die sich gestellte Aufgabe mit einer derartigen Klarheit und Konsequenz gemeistert, daß ein grundsätzlich neues logisches Bauwerk entstand, in das sich sowohl alle mögliche Besonderheiten (gekrümmte Grenzflächen, sehr kleine Teilchen, Dreiphasenlinien, usw.), wie auch praktische Problemstellungen (z. B. Stofftrennung durch Anreicherung an Grenzflächen) lückenlos einfügen lassen.

Aus der unten folgenden Übersicht der einzelnen Kapitel geht deutlich hervor, wie gründlich und vielseitig der gesamte Problemkreis behandelt wurde. (Dazu sei hier noch bemerkt, daß dieses Buch die von M. BÜLOW einwandfrei ins Deutsche übersetzte, vom Verfasser völlig überarbeitete Herausgebe des zuerst 1966 in russischer Sprache erschienenen Originalwerkes ist.) Die Einteilung der Monographie ist wie folgt:

1. Grundbegriffe; 2. Anwendung der Thermodynamik auf Grenzflächenschichten und heterogene Systeme; 3. Gleichgewicht zweier Phasen in Gegenwart einer ebenen Diskontinuitätsfläche; 4. Abhängigkeit der Grenzflächenspannung von der Temperatur; 5. Abhängigkeit der Grenzflächenspannung vom Druck; 6. Abhängigkeit der Grenzflächenspannung von der Zusammensetzung der koexistierenden Phasen; 7. Abhängigkeit der Grenzflächenspannung von den Hauptzustandsparametern; 8. Thermodynamik der Stofftrennung durch Anreicherung an Phasengrenzen; 9. Das Zweiphasengleichgewicht in Gegenwart einer gekrümmten Diskontinuitätsfläche; 10. Grenzflächenspannung gekrümmter Diskontinuitätsflächen; 11. Einfluß der Krümmung der Diskontinuitätsfläche auf die Hauptparameter des thermodynamischen Gleichgewichtes; 12. Zusammensetzung gekrümmter Grenzflächenschichten; 13. Besondere Beispiele für Gleichgewichte mit unvollständiger Komponentenverteilung; 14. Thermodynamik der Filme; 15. Grenzflächenerscheinungen in Festkörpern; 16. Adsorptionsfilme; 17. Benetzung und Dispergierung; 18. Energetik der Bildung neuer Phasen; 19. Gleichgewichte zweidimensionaler Phasen; 20. Methoden für die Behandlung kleiner Objekte und ihre Anwendbarkeitsgrenzen.

Kapitel 8 und 15 waren in der Originalmonographie noch nicht enthalten, sie wurden gesondert für diese Ausgabe vom Verfasser geschrieben, um der schellen Entwicklung auf diesen Gebieten gerecht zu werden. Die über 500 Literaturangaben (die jüngste aus dem Jahre 1976) befinden sich am Ende der einzelnen Kapitel. Ein Sachregister erleichtert die Orientierung.

Druck und Ausstattung ist von hoher Qualität. Der Preis ist angemessen, zumal in Anbetracht der Tatsache, daß zum Handsatz der über 1600 meist sehr komplizierten Formeln ein großer Arbeitsaufwand nötig war.

Mit der Herausgabe dieser Monographie hat der Akademie-Verlag ermöglicht, daß Professors RUSANOVs Oeuvre den Zugang auch zu demjenigen Leserkreis findet, welcher die russische Sprache nicht beherrscht. Diese Monographie sollte nicht in der Buchsammlung des Lehrers, Forschers oder Praktikers fehlen, der sich mit Mehrphasensystemen, sowie Kolloid- und Grenzflächenchemie beschäftigt.

E. WOLFRAM

Friedrich KLAGES: *Aufbau und Eigenschaften der Materie im Mikro- und Makrokosmos*

256 Seiten, Sammlung Göschen 2618, Walter de Gruyter, Berlin—New York, 1979

Das Buch ist nicht für Fachleute, sondern für einen weiteren Kreis naturwissenschaftlich interessierter Leser bestimmt, mit der Zielsetzung, ein zeitgemäßes Bild des Aufbaus unserer materiellen Umwelt zu vermitteln. Im besonderen ist der Verfasser bestrebt, zu zeigen, daß neben der unterschiedlichen chemischen Zusammensetzung das typische Erscheinungsbild der verschiedensten irdischen Materiearten nach dem heutzutage erreichten Stand unserer Kenntnisse auf verhältnißmäßig wenige, physikalisch genügend bekannte zwischenatomare Effekte zurückgeführt werden kann. Darüber hinaus wird auch angedeutet, wie diese unter den Bedingungen der Erdoberfläche "normal" wirkende Materie bei Änderung allein der physikalischen Umweltsbedingungen eine mehr oder weniger tiefgehende Umwandlung erfährt, so daß man in Extremfällen von einer "entarteten Materie" spricht.

Der obigen Zielsetzung entsprechend gliedert sich das Buch in drei Hauptteile:

I. Die Atome und die zwischen ihnen auftretenden Kräfte, worin der Aufbau der Atome aus Protonen, Neutronen und Elektronen, die zwischeatomaren Assoziationskräfte, das Zustandekommen der verschiedenen Arten der chemischen Bindung und schließlich der Zusammenschluß der Atome zu Molekülen und zusammenhängender Materie behandelt wird;

II. Die Materiearten der Erdoberfläche, mit Kapiteln über niedermolekulare Substanzen, Salze, Steine und Erden (mit Erörterung der verschiedenen Typen von Atomgittern), Eigenheiten der makromolekularen organischen Materie, Metalle;

III. Der Zusammenschluß der Materie zu unserer Umwelt, mit Kapiteln über die mineralische Umwelt (Land und Meer, chemische Umsetzungen im Mineralreich, Verwitterungserscheinungen), die lebende Materie (materieller Aufbau, Gerüstsubstanzen, Mannigfaltigkeit der Eiweißstoffe und Nucleinsäuren, Wasserstoffbrücken in der Biochemie) und schließlich physikalisch bedingte Umweltänderungen (Atmosphäre und Gravitation, Planetenatmosphären, Einfluß der Temperatur, extrem hohe Temperaturen, Aufbau der Erdkugel).

Die Kunst des Verfassers, ein so gewaltiges und verzweigtes Wissensmaterial in gut ausgewogener Menge und Verteilung auf knappem Seitenumfang auf angenehm lesbare und daher gut verständliche Weise darzustellen, ist recht bemerkenswert. Die unvermeidliche Notwendigkeit von Vereinfachungen und Beschränkung auf Knappheit führt jedoch bei derartigen Schriften fast immer dazu, daß hie und da Formulierungen unterlaufen, die nicht ganz stichhaltig sind oder vom Laienleser leicht mißverstanden werden können. Das vorliegende Buch weist erfreulich wenig derartige Mängel auf, ist aber doch nicht ganz frei von ihnen. So ist z. B. die Bemerkung auf S. 21, daß man im Elektronenmikroskop vom Wellencharakter der Elektronen Gebrauch macht, irreführend, da die Abbildung mit Hilfe von elektrischen und magnetischen "Linsen" die Tatsache ausnützt, daß die Elektronen geladene Teilchen sind, und nur die Möglichkeit der Erzeugung von Diffraktogrammen auf ihrer Wellennatur beruht. Man kann auch der Behauptung kaum zustimmen, daß das Wasser an dem eigentlichen biochemischen Geschehen nicht nennenswert beteiligt ist (S. 196), da ja bei der Assimilation der Kohlensäure, die für das Leben überhaupt von grundlegender Bedeutung ist, das Wasser

unter Freiwerden seines Sauerstoffs als Wasserstoffquelle dient, andererseits die Verbrennung zu Kohlensäure und Wasser im Stoffwechsel die zur Aufrechterhaltung des Lebens nötige Energie liefert. Die vom Verfasser vertretene Erweiterung des Molekülbegriffs, wonach z. B. Diamant, Quarz etc. und sogar Koks (S. 188) ohne Einschränkung schlechtwegs als makromolekulare Stoffe angesprochen werden, dürfte kaum die Zustimmung der Mehrheit der Fachleute finden.

Derartige vereinzelte Unzulänglichkeiten sind jedoch vom Gesichtspunkt des Leserkreises, für den das Buch bestimmt ist, von untergeordneter Bedeutung, das Wesentliche ist, daß ihm ein umfassendes und anschauliches naturwissenschaftliches Weltbild geboten wird, und diese Aufgabe wurde von Professor KLAGES meisterhaft erfüllt, so daß das Werk naturwissenschaftlich interessierten Lesern zur Weiterbildung wärmstens empfohlen werden kann.

G. SCHAY

Jürgen U. KELLER: *Technische Thermodynamik in Beispielen. Aufgaben, Rechenweg, Lösungen, Begriffssammlung. Teil* 1, *Grundlagen*

Walter de Gruyter, Berlin—New York, 1979. 307 Seiten

J. U. KELLERS Buch ist ein hervorragendes Hilfsmittel für das Studium. Dies was zu erwarten, da der Name des Verfassers durch sein früheres erfolgreiches Lehrbuch (Thermodynamik der irreversiblen Prozesse) bereits wohlbekannt war (auch dieses erschien in der Serie der de Gruyter Lehrbücher).

Im vorliegenden Buch führt der Verfasser die Anwendungsmöglichkeiten und Rechenwege an 70 Beispielen vor. Es sind recht gut gewählte praktische Aufgaben und die Art der Bearbeitung ist didaktisch sehr gut. Die Einteilung des ersten Teiles ist: Grundbegriffe der Thermodynamik und Maßeinheiten; der nullte Hauptsatz und die thermische Zustandsgleichung; der erste Hauptsatz der Thermodynamik; der zweite Hauptsatz der Thermodynamik und Mehrphasensysteme. Dieser erste Teil macht die Hälfte des Umfangs des Buches aus.

Der zweite Teil (und praktisch die zweite hälfte des Buches) ist eine recht gut zusammengestellte Begriffssammlung, welche die Deutung von 124 grundlegenden thermodynamischen Begriffen in kurzen, eindeutigen, definitionsmäßigen Formulierungen enhält. Der zweite Teil ist vielleicht noch nützlicher als der erste, insofern als er den Studierenden eine außerordentliche Hilfe bietet, der sich mit der — tatsächlich überhaupt nicht leichten — Thermodynamik befaßt und sie sich anzueignen bestrebt ist.

Im Buch werden ausschließlich das SI-Maßsystem und im wesentlichen das neue System der chemischen Bezeichnung und Definitionen angewendet. In letzterer Hinsicht habe ich jedoch gewisse Bedenken. So ist z. B. der Begriff Phase auf S. 250 nicht eindeutig, da z. B. Eis auch dann *eine* Phase darstellt, wenn bei 0 °C *mehrere* Eisstückchen im Wasser herumschwimmen. Ebenso halte ich es nicht für glücklich, den Ausdruck Molzahl anzuwenden. Es handelt sich hier offensichtlich einfach um die Stoffmenge, ausgedrückt in ihrer Einheit, dem Mol. Es gibt ja auch keine "Meterzahl", nur die in ihrer Einheit, dem Meter, ausgedrückte Länge.

Alldiese Dinge — deren Gebrauch auch sonst nicht ganz einheitlich ist — verringern jedoch die wahren Werte des Buches keineswegs. Auch drucktechnisch ist das Buch schön ausgestattet; in didaktischer Hinsicht ist es gut gegliedert und redigiert, und die Sprache ist klar.

Zusammenfassend ist J. U. KELLERS Buch ein sehr nützliches Werk, und es ist sicher ein Vergnügen, daraus zu lernen. So etwas wird eigentlich in Rezensionen selten geschrieben, es ist aber wahr.

E. BERECZ

LANDOLT-BÖRNSTEIN

Numerical Data and Functional Relationships in Science and Technology

New Series, Editor in Chief: K.-H. HELLWEGE
Group II: *Atomic and Molecular Physics*

Volume 9, *Magnetic Properties of Free Radicals*
Part c1, *Organic N-Centered Radicals and Nitroxide Radicals*
A. R. FORRESTER, F. A. NEUGEBAUER

Editors: H. FISCHER and K.-H. HELLWEGE
Springer-Verlag Berlin—Heidelberg—New York 1979, 1066 pp

This book is the third part of the supplement to the LANDOLT-BÖRNSTEIN New Series volume II/1 entitled "Magnetic Properties of Free Radicals" published in 1965. The complete supplement (volume II/9) will consist of the following parts:

a Atoms, Inorganic Radicals, and Radicals in Metal Complexes
b Organic C-Centered Radicals
*c*1 Organic N-Centered and NO Radicals
*c*2 Organic O-, P-, S-, Si-, Ge-, Sn-, Pb-, As-, Se-Centered Radicals
d Organic Radical Ions and Polyradicals, Spin Labelled Biomolecules

The scope of the compilation and the organization of the Tables have been described in a previous review [Acta Chim. Acad. Sci. Hung., **98**, 497 (1978)] The data are arranged in the following order:

— gross formula, name, structural formula
— description of the generation of the radical
— specification of the method used to determine g and a values
— absolute values of the g-tensor elements
— elements of the hyperfine coupling tensors a_λ
— references

The present book starts with the nitrogen-centered radicals of the basic structure $-\dot{N}-$, $-\dot{N}-N<$, $-\dot{N}-N=C<$, $-\dot{N}-O-$, $-\dot{N}-S-$, $>C=N-\dot{O}$, and $-N=N-\dot{O}$, both acyclic and cyclic. Then the nitroxide radicals follow constituting probably the largest chapter in the whole series. This is not surprising if considering the remarkable ease of production and stability of nitroxides and their special place, accordingly, in free radical chemistry. The number of source papers cited for nitroxide radicals only is around one thousand.

The literature was considered for the period from 1964 through 1975 with some references from 1976.

I. HARGITTAI

INDEX

PHYSICAL AND INORGANIC CHEMISTRY

ORGANIC CHEMISTRY

ANALYTICAL CHEMISTRY

CHEMICAL TECHNOLOGY

Printed in Hungary

A kiadásért felel az Akadémiai Kiadó igazgatója — Műszaki szerkesztő: Zacsik Annamária

A kézirat nyomdába érkezett: 1979. VII. 31. — Terjedelem: 9,8 (A/5) ív, 104 ábra

80.7378 Akadémiai Nyomda, Budapest — Felelős vezető: Bernát György

ACTA CHIMICA

ТОМ 103—ВЫП. 1

РЕЗЮМЕ

Влияние ртутных примесей на анодное поведение галлия

К. САБО и К. Г. ШОЙМОШ

Было исследовано влияние ртутных примесей на анодное рствореиие жидкого и твердого галлия в растворе 1 М HC[1]. Было установлено, что уже в количествах $9{,}7 \cdot 10^{-5}$ ат.% ртуть изменяет скорость анодного растворения твердого галлия, как на активно, так и на пассивном участках. В случае жидкого галлия, однако, скорость анодного растворения не изменяется значительно даже под влиянием трути в количестве $1{,}7 \cdot 10^{-2}$ ат.% В области низких концентраций ртути ($10^{-4} \div 10^{-3}$ ат.%) скорость анодного растворения твердого лаггия (*lgj*), как на активном, так и на пассивном участке, линейно возрастает с концентрацией ртути ($\lg C_{Hg}$). При более высоких концентрациях ртути повышение скорости растворимости с увеличением концентрации трути меньше (т. е. меньше $\partial \lg i / \partial \lg C_{Hg}$).

Наиболее вероятное объяснения влияния ртутных примесей заключается в следующем. Атомы ртути, адсорбированные на поверхности твердого галлия, ослабляютв своей окружности связи атомов галлия и тем самым разрывают слой окиси, предотвращающий растворение, который присутствует и на активном участке на твердом галлии. В результате этого повышается скорость анодного растворения.

Исследование гетероциклических соединений, содержащих связи S—Si—S, с помощью МС высокого разрешения

Т. МЮЛЛЕР, М. ЭЛЬ-КЁРШ, К. БЕКЕР-ПАЛОШИ и Й. БАЛЛА

Было проведено иследование масс-епектров некоторых новых синтезированных соединений дитиосилациклопентана. Были сняти спектры как низкого, так и высокого разрешения и наряду с молекулярными ионами были идентифицированы также наиболее характерные фрагментные ионы с помощью детектирования на фотопластинкее и измерениями массы с большой точностью. Предлагается механизм фрагментации. Были получены также некоторые информации относительно свойств связи S—Si—S и соответствующего гетероциклического кольца.

Исследование образования тройных ионов. Иодистый натрий в 1-октаноле при 25°C

П. БЕРОНИУС и Л. ПАТАКИ

Образование тройных ионов иодистого натрия в 1-октаноле при 25°C было исследовано методом электропроводимости в интервале концентраций от $0{,}5 \cdot 10^{-4}$ до $56 \cdot 10^{-4}$ *M*. Данные анализировали с помощью уравнения проводимости, включая эффекты ионной атмосферыи на подвижность ионов. Использованное уравнение включает предельную молярную проводимость тройных ионов Λ_{∞}^{T} и имплицитную константу ассоциации тройных ионов K_T, которые являются юстировочными параметрами. В расчетах полагалась равная вероятность образования двух различных типов тройных ионов Na_2I^+ и NaI_2^-. Образование тройных ионов оказалось незначительным при концентрациях меньших $3{,}6 \cdot 10^{-4}$ *M*, что находится в согласии с теорией. Наилучшее совпадение экспериментальных данных с уравнением проводимости было получено при $K_T = 97\ M^{-1}$ и $\Lambda_{\infty}^{T} = 0{,}48\ \Lambda_{\infty}$, где Λ_{∞} является предельной молярной проводимостью простых ионов.

Оксазепины и тиазепины, VII

Синтез и циркулярный дихроизм 2,3-дигидро-2,4-дифенил--1,5-бензотиазепин гликозидов

А. ЛЕВАИ, Р. БОГНАР и Й. КАЙТАР

Ацетаты 2,3-дилидро-2,4-дифенил-1,5-бензотиазепин глихозидов (**VII—X**) были синтезированы с помощью реакции 2-аминотиофенола с ацетатами халкон гликозидов (**III—VI**). При омылении первые дают соответствующие свободные гликозиды (**XI—XIV**). Были изучены также хироптические свойства этих соединений.

Гомогенное каталитическое гидрирование диолефинов и алкинов в присутствии комплексов палладия (II)

А. ШИШАК, И. ЯБЛОНКАИ и Ф. УНГВАРИ

Хлористый палладий(II) в диметилформамиде катализирует гидрирование сопряженных диолефинов и алкинов в гомогенной фазе. Селективно образуется моноолефин.

Применение постоянных Кун—Марк—Хаувинка в методе универсальной калибровки в гельпроницательной хроматографии

Г. ШАМАИ и Л. ФЮЗЕШ

Было исследовано влияние выбора постоянных Кун—Марк—Хаувинка из литературы на точность калибровочных кривых, полученных на основе универсальной калибрации в гельпроницательной хроматографии. Было найдено, что разница в калибрациях с использованием различных литературных постоянных Кун—Марк—Хаувинка мала, т. е. эффект выбора также мал. Для правильных расчетов универсальная калибрация должна быть сконструирована в интервале низкого молекулярного веса. Для калибраций материалов с низким молекулярным весом собственная вязкость может быть рассчитана из «тета данных» для постоянных Кун—Марк—Хаувинка.

Константы кислотности 1,2,3-циклогексантрион-диоксима-1,3 и 1,2,3-циклогексантриондиоксима

Й. ЖАКО, А. БЕНКЁ, Й. ХОРАКИ и Ч. ВАРХЕИ

Были синтезированы 1,2,3-циклогексантрион-диоксим-1,3 и 1,2,3-циклогексантриондиоксим. Их константы кислотности были определены как с помощью потенциометрического, так и с помощью спектрофотометрического методов при 20°С и с ионной силой $\mu = 0{,}1$ *М*. Приводятся спектры УФ видимого света. Обсуждается корреляция между кислотностью и молекулярной структурой.

Полуэмпирические квантово-химические расчеты конфигурации C_7 некоторых 7-замещенных 3-кето-4-ен стероидов

П. НАДЬ и ДЬ. БЕР

Нуклеофильное присоединение к 3-кето-4,6-диен стероидам приводит к 7-замещенным 3-кето-4-ен стероидам. Положение заместителя, зависящее от природы нуклеофильного реагента, обычно аксиальное (α). Расчеты PCILO подтверждают эти экспериментальные наблюдения. На основе исследования причин, приводящих к образованию данной конфигурации, было заключено, что образующаяся конфигурация, в первую очередь, определяется степенью стерического взаимодействия заместителя со стероидным скелетом.

Структурная теория для химической технологии

Т. БЛИКЛЕ и Г. ФАИ

Давая краткий исторический обзор исследований, касающихся работ по логической структуре систем химической технологии, проведенных в начале семидесятых годов в Венгрии, демонстрируется вероятный путь обработки логических отношений, характеризующих системы химической технологии с помощью точного алгебраического анализа (теория решеток). Приводится математические понятия *свойств, классов свойств* и общего нахождения этих свойств, одним словом, *возможности* систем химической технологии. Было доказано, что эти возможности образуют решетку (в алгебраическом смысле). Оценка этой решетки приводится согласно консервативному транспорту теоретических субстанций в системах химической технологии (масса, энергия, объем и т. д.). Таким образом, проблемы химической технологии могут быть исследованы с помощью теории решеток и эти исследования могут быть подвергнуты обработке на ЭВМ, особенно интерактивным, диалогическим путем.

Синтез некоторых 1,3,4-тиадиазолилмочевин и их производных, II

З. ДЬЁРФИ и ДЬ. ЧАВАШИ

Были исследованы синтез и некоторые химические свойства серии 1-(2-хлороэтил-, хлороацетил, дихлороацетил)-3-(5-алкил- или арил-1,3,4-тиадиазол-2-ил)мочевин, полученных присоединением 2-хлороэтил-, хлороацетил- или дихлороацетилизоцианатов к 2-амино-5-алкил- или арил-1,3,4-тиадиазолам. Некоторые из мочевин были затем превращены в соответствующие нитрозо и/или хидантоиновые производные.

Определение конфигурации и конформации двух диастереомеров 2,4; 3,5-ди-*O*-бензилиден-1,6-дибромо-1,6-дидекси-*D*-маннита с помощью ЯМР—H^1 и ЯМР—C^{13} спектроскопии

П. ШОХАР, Т. ХОРВАТ и Г. АБРАХАМ

Конфигурация и стабильная конформация двух диастереомеров 2,4; 3,5-ди-*O*-бензилиден-1,6-дибромо-1,6-дидеокси-*D*-маннита были определены с помощью ЯМР—H^1 и ЯМР—C^{13} спектроскопии.

Les Acta Chimica paraissent en français, allemand, anglais et russe et publient des mémoires du domaine des sciences chimiques.

Les Acta Chimica sont publiés sous forme de fascicules. Quatre fascicules seront réunis en un volume (3 volumes par an).

On est prié d'envoyer les manuscrits destinés à la rédaction à l'adresse suivante:

Acta Chimica
Budapest, P.O.B. 67, H-1450, Hongrie

Toute correspondance doit être envoyée à cette même adresse.

La rédaction ne rend pas de manuscript.

Le prix de l'abonnement: $ 36,00 par volume.

Abonnement en Hongrie à l'Akadémiai Kiadó (1363 Budapest, P. O. B. 24, C. C. B. 215 11488), à l'étranger à l'Entreprise du Commerce Extérieur « Kultura » (H-1389 Budapest 62, P. O. B. 149 Compte-courant No. 218 10990) ou chez représentants à l'étranger.

Die Acta Chimica veröffentlichen Abhandlungen aus dem Bereich der chemischen Wissenschaften in deutscher, englischer, französischer und russischer Sprache.

Die Acta Chimica erscheinen in Heften wechselnden Umfanges. Vier Hefte bilden einen Band. Jährlich erscheinen 3 Bände.

Die zur Veröffentlichung bestimmten Manuskripte sind an folgende Adresse zu senden

Acta Chimica
Budapest, Postfach 67, H-1450, Ungarn

An die gleiche Anschrift ist jede für die Redaktion bestimmte Korrespondenz zu richten.

Manuskripte werden nicht zurückerstattet.

Abonnementspreis pro Band: $ 36,00.

Bestellbar für das Inland bei Akadémiai Kiadó (1363 Budapest, Postfach 24, Bankkonto Nr. 215 11488), für das Ausland bei »Kultura« Außenhandelsunternehmen (H-1389 Budapest 62, P. O. B. 149. Bankkonto Nr. 218 10990) oder seinen Auslandsvertretungen.

«Acta Chimica» издают стихьи по лимии на русском, ангхийском, французском и немецком языкал.

«Acta Chimica» выподит отдехьными выпусками разного объемта, 4 выпуска составвхяют один том и за год выподят 3 тома.

Предназначенные дхя пубхикации рукописи сходует направвхять по адресу:

Acta Chimica
Budapest, P.O.B. 67, H-1450, ВНР

Всякую корреспонденцию в редакцию направвхяйте по этому же адресу.

Редакция рукописей не возвращает.

Подписная цена — $ 36,00 за том.

Отечественные подписчики направвхяйте свои заявки ;по адресу Издатехьства Академии Наук (1363 Budapest, P.O.B. 24. Текущий счет 215 11 188), а иностранные подписчики через организацию по внешней торговхе «Kultura» (H-1389 Budapest 62, P.O.B. 149. Текущий счет 218 10990) ихи через ее заграничные представитехьства и упохномеченныл.

Reviews of the Hungarian Academy of Sciences are obtainable at the following addresses:

AUSTRALIA
C.B.D. LIBRARY AND SUBSCRIPTION SERVICE, Box 4886, G.P.O., *Sydney N.S.W. 2001*
COSMOS BOOKSHOP, 145 Ackland Street, *St. Kilda (Melbourne), Victoria 3182*

AUSTRIA
GLOBUS, Höchstädtplatz 3, *1200 Wien XX*

BELGIUM
OFFICE INTERNATIONAL DE LIBRAIRIE, 30 Avenue Marnix, *1050 Bruxelles*
LIBRARIE DU MONDE ENTIER, 162 Rue du Midi, *1000 Bruxelles*

BULGARIA
HEMUS, Bulvar Ruski 6, *Sofia*

CANADA
PANNONIA BOOKS, P.O. Box 1017, Postal Station "B", *Toronto, Ontario M5T 2T8*

CHINA
CNPICOR, Periodical Department, P.O. Box 50, *Peking*

CZECHOSLOVAKIA
MAD'ARSKÁ KULTURA, Národní třida 22, *115 33 Praha*
PNS DOVOZ TISKU, Vinohradská 46, *Praha 2*
PNS DOVOZ TLAČE, *Bratislava 2*

DENMARK
EJNAR MUNKSGAARD, Norregade 6, *1165 Copenhagen*

FINLAND
AKATEEMINEN KIRJAKAUPPA, P.O. Box 128, *SF-00101 Helsinki 10*

FRANCE
EUROPERIODIQUES S.A., 31 Avenue de Versailles, *78170 La Celle St. Cloud*
LIBRARIE LAVOISIER, 11 rue Lavoisier, *75008 Paris*
OFFICE INTERNATIONAL DE DOCUMENTATION ET LIBRARIE, 48 rue Gay-Lussac, *75240 Paris Cedex 05*

GERMAN DEMOCRATIC REPUBLIC
HAUS DER UNGARISCHEN KULTUR, Karl-Liebknecht-Strasse 9, *DDR-102 Berlin*
DEUTSCHE POST ZEITUNGSVERTRIEBSAMT, Strasse der Pariser Kommüne 3—4, *DDR-104 Berlin*

GERMAN FEDERAL REPUBLIC
KUNST UND WISSEN ERICH BIEBER, Postfach 46, *7000 Stuttgart 1*

GREAT BRITAIN
BLACKWELL'S PERIODICALS DIVISION, Hythe Bridge Street, *Oxford OX1 2ET*
BUMPUS, HALDANE AND MAXWELL LTD., Cower Works, *Olney, Bucks MK46 4BN*
COLLET'S HOLDINGS LTD., Denington Estate, *Wellingborough, Northants NN8 2QT*
WM. DAWSON AND SONS LTD., Cannon House, *Folkestone, Kent CT19 5EE*
H. K. LEWIS AND CO., 136 Gower Street, *London WC1E 3BS*

GREECE
KOSTARAKIS BROTHERS, International Booksellers, 2 Hippokratous Street, *Athens-143*

HOLLAND
MEULENHOFF-BRUNA B.V., Beulingstraat 2, *Amsterdam*
MARTINUS NIJHOFF B.V., Lange Voorhout 9—11, *Den Haag*
SWETS SUBSCRIPTION SERVICE, 347b Heereweg, *Lisse*

INDIA
ALLIED PUBLISHING PRIVATE LTD., 13/14 Asaf Ali Road, *New Delhi 110001*
150 B-6 Mount Road, *Madras 600002*
INTERNATIONAL BOOK HOUSE PVT. LTD., Madame Cama Road, *Bombay 400069*
THE STATE TRADING CORPORATION OF INDIA LTD., Books Import Division, Chandralok, 36 Janpath, *New Delhi 110001*

ITALY
EUGENIO CARLUCCI, P.O. Box 252, *70100 Bari*
INTERSCIENTIA, Via Mazzé 28, *10149 Torino*
LIBERIA COMMISSIONARIA SANSONI, Via Lamarmora 45, *50121 Firenze*
SANTO VANASIA, Via M. Macchi 58, *20124 Milano*
D. E. A., Via Lima 28, *00198 Roma*

JAPAN
KINOKUNIYA BOOK-STORE CO. LTD., 17-7 Shinjuku-ku 3 chome, Shinjuku-ku, *Tokyo 160-91*
MARUZEN COMPANY LTD., Book Department, P.O. Box 5050 Tokyo International, *Tokyo 100-61*
NAUKA LTD. IMPORT DEPARTMENT, 2-40-19 Minami Ikebukuro, Toshima-ku, *Tokyo 171*

KOREA
CHULPANMUL, *Phenjan*

NORWAY
TANUM-CAMMERMEYER, Karl Johansgatan 41—43, *1000 Oslo*

POLAND
WĘGIERSKI INSTYTUT KULTURY, Marszałkowska 80, *Warszawa*
CKP I W ul. Towarowa 28 *00-958 Warszawa*

ROUMANIA
D. E. P., *Bucureşti*
ROMLIBRI, Str. Biserica Amzei 7, *Bucureşti*

SOVIET UNION
SOJUZPETCHATJ — IMPORT, *Moscow*
and the post offices in each town
MEZHDUNARODNAYA KNIGA, *Moscow G-200*

SPAIN
DIAZ DE SANTOS, Lagasca 95, *Madrid 6*

SWEDEN
ALMQVIST AND WIÓSELL, Gamla Brogatan 26, *101 20 Stockholm*
GUMPERTS UNIVERSITETSBOKHANDEL AB, Box 346, *401 25 Göteborg 1*

SWITZERLAND
KARGER LIBRI AG, Petersgraben 31, *4011 Basel*

USA
EBSCO SUBSCRIPTION SERVICES, P.O. Box 1943, *Birmingham, Alabama 35201*
F. W. FAXON COMPANY, INC., 15 Southwest Park, *Westwood, Mass, 02090*
THE MOORE-COTTRELL SUBSCRIPTION AGENCIES, *North Cohocton, N. Y. 14868*
READ-MORE PUBLICATIONS, INC., 140 Cedar Street, *New York, N. Y. 10006*
STECHERT-MACMILLAN, INC., 7250 Westfield Avenue, *Pennsauken N. J. 08110*

VIETNAM
XUNHASABA, 42, Hai Ba Trung, *Hanoi*

YUGOSLAVIA
JUGOSLAVENSKA KNJIGA, Terazije 27, *Beograd*
FORUM, Vojvode Mišića 1, *21000 Novi Sad*

26. III. 1980 HU ISSN 0001—5407 Index: 26.007

ACTA CHIMICA

ACADEMIAE SCIENTIARUM HUNGARICAE

TOMUS 103 FASCICULUS 2

AKADÉMIAI KIADÓ, BUDAPEST

1980

ACTA CHIM. ACAD. SCI. HUNG. ACASA2 103 (2) 111–224 (1980)

ACTA CHIMICA

A MAGYAR TUDOMÁNYOS AKADÉMIA KÉMIAI TUDOMÁNYOK OSZTÁLYÁNAK IDEGEN NYELVŰ KÖZLEMÉNYEI

Acta Chimica is a journal for the publication of papers on all aspects of chemistry in English, German, French and Russian.

Acta Chimica is published in 3 volumes per year. Each volume consists of 4 issues of varying size.

Manuscripts should be sent to

Acta Chimica
Budapest, P.O. Box 67, H-1450, Hungary

Correspondence with the editors should be sent to the same address. Manuscripts are not returned to the authors.

Subscription: $ 36.00 per volume.

Hungarian subscribers should order from Akadémiai Kiadó, 1363 Budapest, P.O. Box 24. Account No. 215 11488.

Orders from other countries are to be sent to "Kultura" Foreign Trading Company (H-1389 Budapest 62, P.O. Box 149. Account No. 218 10990) or its representatives abroad.

Acta Chimica Academiae Scientiarum Hungaricae, Tomus 103 (2), pp. 111—121 (1980)

PULSE MICROREACTOR PESTICIDES HYDRODECHLORINATION

A. H. WEISS and R. B. LAPIERRE*

(Department of Chemical Engineering Worcester Polytechnic Institute Worcester, Massachusetts)

Received December 8, 1978
Accepted for publication March 19, 1979

Catalytic hydrodechlorination of chlorinated pesticides and other environmentally undesirable chlorinated materials into lower chlorine content compounds has been studied in a pulse microreactor. Chlorine can be catalytically removed and replaced by hydrogen to produce partially chlorinated intermediates as well as completely dechlorinated hydrocarbons. Intermediates are equivalent to some of those obtained by natural degradation.

The pulse microreactor is a simple technique to predict both product composition and reaction severity required for laboratory scale preparation of such degradation products.

Introduction

Many of the widely used insecticides and other organic chemicals which have been found to persist in the environment and in the food chain are chlorinated compounds. These species are lost in nature mainly by chemical degradation and bacterial decomposition. However, little is known about the properties of the compounds formed by breakdown of organochlorine pesticides in soil, which are generally produced at very low concentrations. The differentiation between biological and non-biological degradation is difficult. Examples of the types of degradation that occur are included below for reference.

It was shown that ^{14}C DDT is hydrodechlorinated by microorganisms to DDD in anaerobic non-sterile soils [1]:

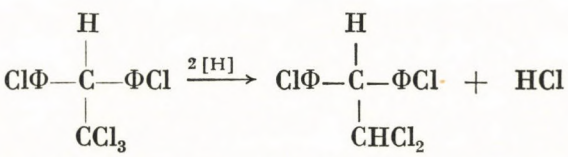

DDD also formed from DDT in alfalfa meal-muck mixtures. Conversion increases in the presence of lime and Fe^{2+} [2]. A relationship was obtained between the redox potential of iron and DDT degradation in the soils [3].

* Present address: Mobil Research Corp., Princeton, N. J.

With an *in vitro* Fe redox system, 20% of the original DDT undergoes an irreversible redox type of reaction. Aroclor 1221 was gradually decomposed to low molecular weight products by lake water bacteria during a 1-month incubation [4]. The degradation rates decrease in the order: biphenyl > 2-chlorobiphenyl > 4-chlorobiphenyl. In cultures containing glucose, dieldrin was degraded [5]. Toxaphene was rapidly degraded under anaerobic conditions especially where the soil was mixed with alfalfa meal [6]. G. C. analysis of toxaphene components was used to demonstrate the extent of degradation. The mechanism of toxaphene degradation in these systems is not known.

Mirex, $C_{10}Cl_{12}$, converts to kepone, $C_{10}Cl_{10}O$, in aerobic conditions [7]. However, in the presence of anaerobic microbes, hydrodechlorination of Mirex proceeds to yield $C_{10}HCl_{11}$ [8]. Mirex was also shown to undergo photolytic dechlorination to $C_{10}HCl_{11}$ and $C_{10}Cl_{10}O$ [9]. BROOKS [10] has shown that plants are also capable of reductive hydrodechlorination of DDT to DDD, nad KUHR [11] reviews insecticide metabolites in and on plants, showing examples of reductive dechlorination.

The studies mentioned so far show that hydrodechlorination, or replacement of some of the chlorine atoms in pesticides by hydrogen atoms (rather than hydroxyl), is an observed phenomenon (to some extent, at least) in the natural degradation of pesticides in the environment. However, it is also possible to proceed by a purely chemical route in the laboratory.

Catalytic hydrodechlorination can produce, in a short time, large quantities of dechlorinated products, some of which are the equivalent of those produced in the environment. DENNIS and COOPER studied the dechlorinaton of DDT, Heptachlor and Chlordane and Lindane [12] by the use of $NaBH_4$ as a reductant in the presence of catalytic nickel boride, Ni_2B. In this present paper, we present results obtained in a pulse microreactor on the Pd catalyzed hydrodechlorination of PCB, DDT, DDD, and Aldrin. These results were used as guidelines for batch and continuous laboratory scale studies on the hydrodechlorination of DDE, DDD, PCB, Aldrin, Dieldrin, and Toxaphene, the results of which are reported in a series of papers by LAPIERRE, *et al.* [13—16] as well as in the Final Report [17] and Executive Summary [18] of the EPA funded project.

The principal utility of the pulse microreactor, also described in [17], is for screening purposes — for rapid selection of useful catalyst types, for rough choice of pressure, temperature, and reaction time needed for a particular reaction. As set up for this work, the pulse microreactor is particularly useful for analysis of reaction products since it is a part of a gas chromatograph assembly and can be coupled to a mass spectrometer for product identification.

By definition, a pulse microreactor is a system where a pulse of reactant is adsorbed, reacted, and desorbed on a catalyst bed in a short period of time. The reactor used here was the glass liner of the injection port of a Perkin –

Elmer 900 gas chromatograph. The injector port aluminium block was heated from ambient to 400 °C. A precision ground glass liner slid into the heated block and was retained by a spring metal insert and septum cap. Carrier gas was introduced into the heated block and passed through an annulus into the 1mm channel in the glass liner. Temperature traverses along the length of the liner with He carrier gas flowing showed there was a zone 2 cm long where the temperature varied less than ± 1 °C.

Catalyst beds typically 2 to 10 mm long containing 2 to 10 mg of 1575—2362 holes/m (40—60 mesh) sieved ground catalysts were placed in the isothermal zone and sandwiched between plugs of pyrex wool. Catalysts were then pretreated at elevated temperature in flowing carrier gas, *e.g.*, the supported metal catalysts were reduced at 250 °C with 0.030 L/min STP H_2 for two hours and the reduction was monitored chromatographically. After the catalyst was pretreated, 0.5—2.0 μL samples of organochlorine compound in solvent were injected into the inlet, reacted, and passed directly to a 1.52 m OV-1 column for separation and analysis by the Perkin–Elmer 900 dual FID gas chromatograph interfaced to a DuPont 21—491 double focusing mass spectrometer.

Although the residence times, τ, calculated on the basis of carrier flow rate, were on the order of 10^{-2} s, reactants remained adsorbed on the bed for several minutes depending on temperature, catalyst surface area, and volatility of the reacting mixture. Thus the concept of rate must be carefully evaluated within these constraints. Large pore, low surface area catalysts were used in this study to minimize mass transfer effects.

Hydrodechlorination results

A. Aroclor 1248

Gas phase pulse microreactor experiments were made to determine the reactivity and selectivity of polychlorinated biphenyl (PCB) in catalytic hydrodechlorination. Aroclor 1248, a commercial PCB mixture produced by MONSANTO, was used as a model reaction mixture. Aroclor 1248 is a clear viscous oil containing 48% chlorine and having an average of 3.92 chlorine atoms per biphenyl molecule.

A series of experiments was carried out in the pulse microreactor at 220 $\pm$ 5 °C and 2.3 bar absolute pressure using a 0.7% solution of Aroclor 1248 in *n*-heptane over 5 mg of Pd on α-Al_2O_3 catalysts containing 0.00, 0.05, 0.10, and 0.35% Pd. The extent of reaction was measured by chlorine conversion X, defined as:

$$X = 1 - \frac{\sum_{i=0}^{n} i\,\Phi\Phi_i^t}{\sum_{i=0}^{n} i\,\Phi\Phi_i^\circ}$$

Table I

Pulse microreactor Aroclor 1248 hydrodechlorination

	$\Phi\Phi_i^\circ$				
Catalyst wt. (kg × 10⁶)		5.0	4.6	5.0	5.0
% Pd		0.00	0.05	0.10	0.35
$\Phi\Phi_0$	0.000		0.134	0.296	0.758
$\Phi\Phi_1$	0.001	0.003	0.058	0.068	0.043
$\Phi\Phi_2$	0.007	0.013	0.129	0.140	0.094
$\Phi\Phi_3$	0.259	0.305	0.337	0.279	0.078
$\Phi\Phi_4$	0.532	0.493	0.236	0.166	0.026
$\Phi\Phi_5$	0.201	0.189	0.091	0.046	—
X	0.000	0.013	0.304	0.469	0.855

where $\Phi\Phi_i^i$ is the % of biphenyl containing i chlorine atoms per molecule and $\Phi\Phi_i^\circ$ is the initial chlorine content. Results are summarized in Table I. While α-Al_2O_3 with no Pd had insignificant catalytic activity, Fig. 1 shows that products of any desired chlorine content could be produced by varying loading of the active component, Pd. A detailed kinetic analysis of these results and ones subsequently obtained in Ni catalyzed batch autoclave studies are

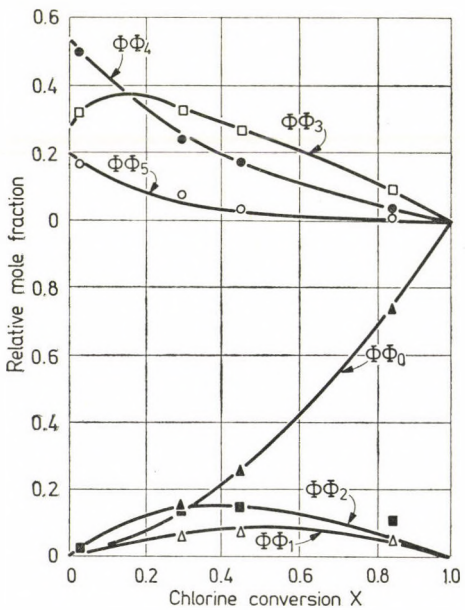

Fig. 1. Aroclor 1248 hydrodechlorination; 220 °C, 2.3 bar. Subscript indicates number of Cl atoms substituted on diphenyl molecule

found elsewhere [13]. It should also be noted that identical consecutive stepwise removal of chlorine and similar relative reactivities of individual isomeric species were observed in both pulse microreactor and in autoclave studies. These observations established the utility of the pulse microreactor technique in the study of hydrodechlorination of polychlorinated substances.

B. DDT, DDE and DDD

Experiments were performed to determine the extent of thermal decomposition of DDT in the pulse microreactor. Half microliter samples of 9.5% DDT in *p*-xylene were injected into the empty injector port. Helium carrier gas flow rate was fixed at 0.30 L/min while the temperature of the inlet was varied from 200 °C to 360 °C. DDE was identified as the major decomposition product by relative retention time.

In all cases the uncatalyzed reaction showed high selectivity to DDE by the following reaction.

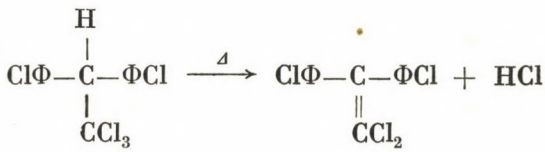

Decomposition was not significant at temperatures below 190 °C.

The same series of 0.00, 0.05, 0.10 and 0.35% Pd on α-Al_2O_3 catalysts used in the Aroclor experiments were used to investigate both DDT and DDD hydrodechlorination in the pulse microreactor at 220 °C, 2.3 bar H_2 and 0.01 s residence time.

Each set consisted of six experiments. The first two investigated thermal reactions in the empty reactor with helium or hydrogen as the carrier gas. The last four experiments in each set used hydrogen as a carrier gas and the series of Pd on α-Al_2O_3 catalysts containing 0.00, 0.05, 0.10 and 0.35% Pd.

Figures 2 and 3 show log response chromatograms of products obtained in the DDT and DDD experiments respectively. Identification of major species produced as determined by relative retention times is listed below and referenced numerically to Figures 2 and 3.

The DDT results, Fig. 2, show that thermaler action was minimal under these conditions and that α-Al_2O_3 alone catalyzed dehydrochlorination/hydrogenation reactions on the aliphatic portion of the molecule with DDE being the major product. In the presence of Pd, however, rapid reduction of DDT to 1,1-bis-*para*chlorophenyl ethane, followed by stepwise removal of aromatic chlorine, was observed.

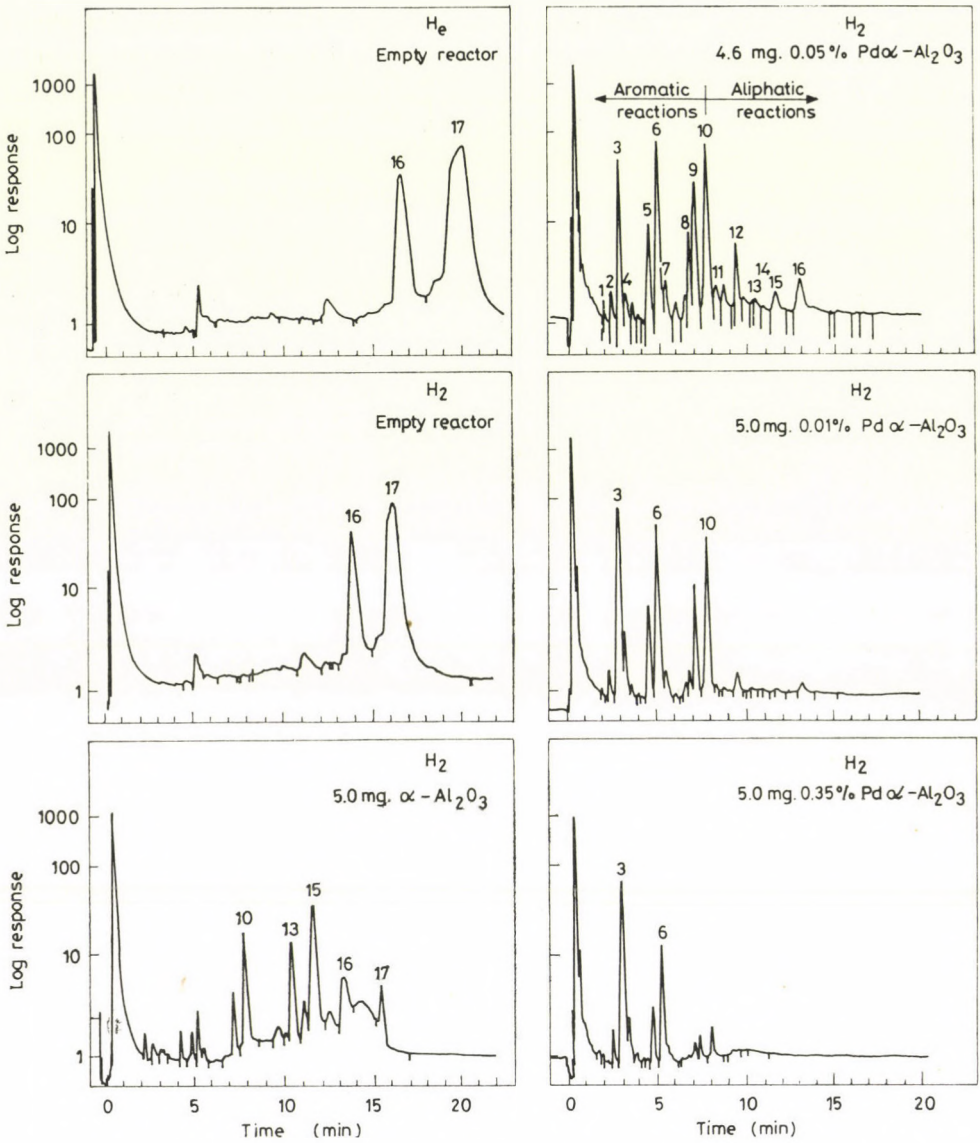

Fig. 2. DDT hydrodechlorination; 220° ± 10 °C, 2.3 bar

The DDD results, Fig. 3, show similar lack of thermal reaction; and dehydrochlorination by α-Al_2O_3 occured to a lesser extent. Product distributions were more complex indicating competitive rates of aromatic and aliphatic hydrodechlorination over Pd. DDD was generally less reactive than DDT at identical conditions.

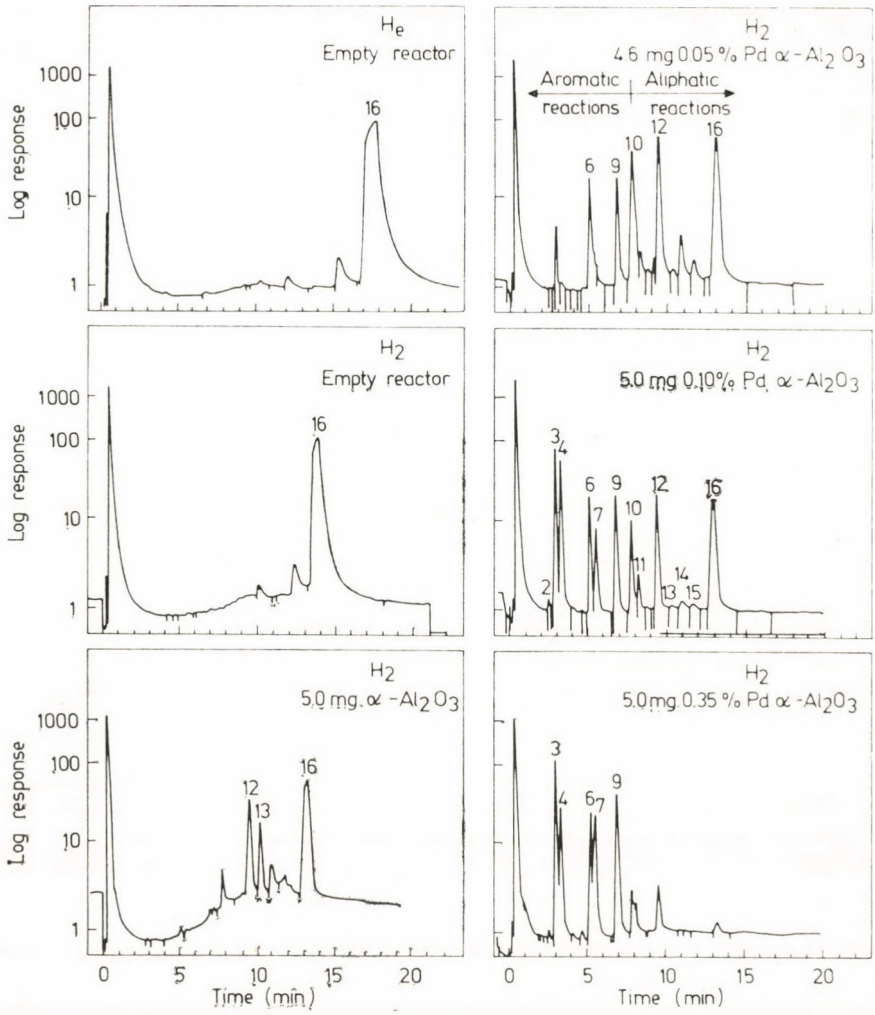

Fig. 3. **DDD hydrodechlorination; 225° ± 5 °C, 2.3 bar**

Identification of compounds

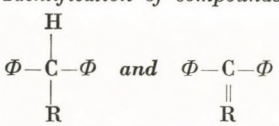

Annotated in Figures 2 and 3

R	Number of aromatic chlorines		
	0	1	2
$-CH_3$	3	6	10
$-CHCl_2$	9	12	16
$-CH_2Cl$	4	7	11
$-CCl_3$	—	—	17
$=CH_2$	—	—	15

Based on these encouraging results extensive studies were carried out in the gas phase in a continuous flow reactor [15] and in $C_2H_5OH-NaOH$ solutions in the batch mode [14]. Again, similar product distributions and relative reactivities were observed in both the pulse microreactor and continuous or batch experiments.

C. Aldrin

Reactions were carried out to determine the hydrodechlorination reactivity of Aldrin, which contains aliphatic and olefinic chlorine. The structure of Aldrin is as follows:

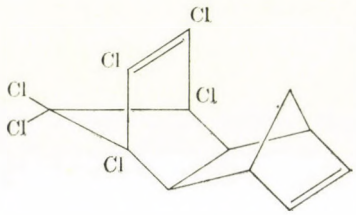

Analytical grade Aldrin obtained from Chem Service of West Chester, PA. was used for pulse microreactor screening.

Experiments were carried out in the pulse microreactor at 220 ± 8 °C and 2.3 bar absolute pressure using the same series of 0.00, 0.05, 0.10 and 0.35% Pd on α-Al_2O_3 catalysts used in the Aroclor and DDT, DDD screening experiments.

These experiments showed that no thermal hydrogenation/hydrodechlorination occured, but that α-Al_2O_3 alone converted 11% of the Aldrin to a product which later GC/MS studies on liquid phase products showed was Aldrin with one olefin hydrogenated. As Pd metal loading increased, hydrodechlorination to several partially dechlorinated products proceeded in parallel with olefin hydrogenation. Detailed analyses of the dechlorinated products were not obtained. These data are summarized in Table II and in the form

Table II

Pulse microreactor Aldrin hydrodechlorination

Carrier gas Catalyst (mg) % Pd	He 0	H_2 0	H_2 5.0 0.00	H_2 4.6 0.05	H_2 5.0 0.10	H_2 5.0 0.35
Product composition mole %						
Hydrodechlorination products	0.0	0.0	1.3	9.1	27.1	61.2
Aldrin	95.6	94.4	83.0	20.3	7.8	2.9
Aldrin + H_2	3.3	4.7	13.7	65.9	61.3	32.8
Other	1.1	0.9	2.0	4.7	3.8	3.1

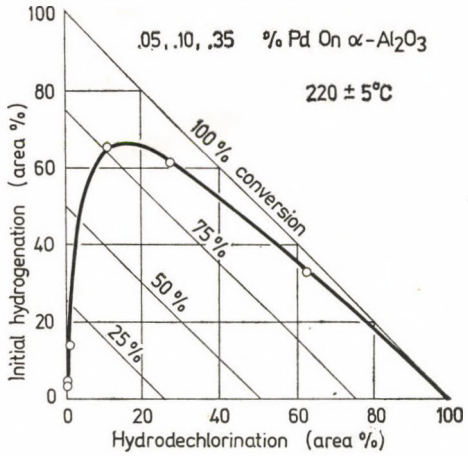

Fig. 4. Aldrin reaction path in H_2; 220° ± 5 °C; 2.3 bar

of a reaction path in Fig. 4. These data also indicate that Aldrin was the least reactive of all compounds studied in the pulse microreactor experiments.

Aldrin is a highly non planar molecule which may be adsorbed in such a configuration that hydrodechlorination reactions are not favored. Initial hydrogenation of an olefin may indicate that adsorption in the following configuration is favored.

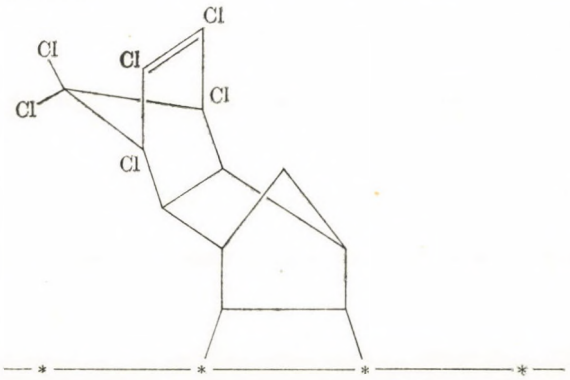

Conversely, hexachlorocyclopentadiene, which has a mix of aliphatic and olefinic chlorine similar to that of Aldrin can be adsorbed in a planar configuration *i.e.*

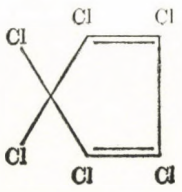

Pulse microreactor experiments showed that hexachlorocyclopentadiene was indeed much more reactive than Aldrin with concerted removal of all chlorine to a hydrocarbon species. This behavior supports the premise that Aldrin hydrodechlorination is sterically hindered.

In batch studies in the presence of Ni catalyst at 50 bar and 130 °C [16], Aldrin (initially hydrogenated) reacted to produce less chlorinated species *i.e.* $C_{12}H_8Cl_6 \rightarrow C_{12}H_{11}Cl_5 \rightarrow C_{12}H_{12}Cl_4 \rightarrow C_{12}H_{15}Cl_3 \rightarrow C_{12}H_{16}Cl_2$, and Dieldrin rapidly lost one chlorine, $C_{12}H_8Cl_6O \rightarrow C_{12}H_9Cl_5O$. Further reaction of Dieldrin to remove additional chlorine is difficult, although $C_{12}H_{10}Cl_4O$ forms [16]. As predicted by the pulse microreactor results, both Aldrin and Dieldrin reacted much more slowly than PCB or DDT.

Conclusions

Pulse microreactor studies on the hydrodechlorinations of pesticides and related substances not only show that products similar to some of those produced in the environment can be produced catalytically, but also indicate the relative severity required for laboratory scale preparation. Such product permit toxicity studies to be undertaken wich determine the level of degradation required to make the residues environmentally acceptable.

*

Financial support for this study was provided by the United States Environmental Protection Agency under EPA Contract R 802—857—01. The results presented here were used in partial fulfillment of the requirements for the Ph. D. degree at Worcester Polytechnic Institute for R. B. LaPierre. The authors wish to express their appreciation to Susan Valinski, who did much of the experimental work.

REFERENCES

[1] Guenzi, W. D., Beard, W. E.: Science, **156,** 1116 (1967)
[2] Parr, J. F., Smith, S.: Soil Sci., **118** (1), 45 (1974)
[3] Glass, B. L.: J. Agr. Food Chem., **20** (2), 324 (1972)
[4] Wong, P. T. S., Kaiser, K. L. E.: Bull. Environ. Contam. Toxicol., **13** (2), 249 (1975)
[5] Bixby, M. W., Boush, G. M., Matsumura, F.: *ibid.*, **6** (6) 491 (1971)
[6] Parr, J. F., Smith, S.: Soil Sci., **121** (1), 52 (1976)
[7] Carlson, D. A., Konyha, K. D., Wheeler, W. B., Marshall, G. P., Zaylskie, R. G.: Science, **194,** 939 (1976)
[8] Andrade, P. S. L., Wheeler, W. B., Carlson, D. A.: Bull. Environ. Contam. Toxicol., **14,** 473 (1975)
[9] Ivie, G. W., Dorough, H. W., Alley, E. G.: J. Agric. Food Chem., **22,** 933 (1974)
[10] Brooks, G. T.: Chlorinated Insecticides, CRC Press, Cleveland, Ohio 1974
[11] Kuhr, R.: Chemtech, 316—321, May 1976
[12] Dennis, W. H., Cooper, W. J.: Bull. Environ. Contam. Toxicol., **14** (6), 738 (1975); **16** (4), 425 (1976); **18** (1), 57 (1977)
[13] LaPierre, R. B., Guczi, L., Kranich, W. L., Weiss, A. H.: J. Catal., **52,** 230 (1978)
[14] *Ibid.*, **52,** 218 (1978)

[15] LaPierre, R. B., Wu, D., Kranich, W. L., Weiss, A. H.: *ibid.*, **52**, 59 (1978)
[16] Kranich, W. L., LaPierre, R. B., Guczi, L., Weiss, A. H.: Catalytic Hydrodechlorination of Polychlorinated Compounds, ACS Symposium Series No. 23, pp. 24—34, Disposol and Decontamination of Pesticides. Kennedy, M. V., (ed.) American Chemical Society, Washington, D. C. 1978
[17] LaPierre, R. B., Biron, E., Wu, D., Guczi, L., Kranich, W. L., Weiss, A. H.: Catalytic Conversion of Hazardous and Toxic Chemicals: Catalytic Hydrodechlorination of Polychlorinated Pesticides and Related Substances NTIS Document PB 262 804, January, 1977, National Technical Information Service, Springfield, VA. 22161
[18] Ebon Research Systems, Catalytic Hydrodechlorination of Polychlorinated Pesticides and Related Substances; An Executive Summary, EPA—600/888—013, September, 1977. National Technical Information Service, Springfield, VA. 22161

Alvin H. Weiss Department of Chemical Engineering Worcester Polytechnic Institute, Worcester, Massachusetts 01609 USA
Rene B. LaPierre Mobil Research Corp., Princeton, N. J.

Acta Chimica Academiae Scientiarum Hungaricae, Tomus 103 (2), pp. 123—133 (1980)

CONDENSED *AS*-TRIAZINES, VII*

A SIMPLIFIED METHOD FOR THE SYNTHESIS OF BENZO-*AS*-TRIAZINE DERIVATIVES

A. MESSMER,[1] GY. HAJÓS,[1] P. BENKÓ[2] and L. PALLOS[2]

([1]Central Research Institute for Chemistry, Hungarian Academy of Sciences, Budapest, and [2]EGYT Pharmaceutical Works, Budapest)

Received September 9, 1978

In revised form March 5, 1979

Accepted for publication March 21, 1979

A simplified ARNDT—ROSENAU synthesis has been elaborated which allows the preparation of differently substituted 3-mercapto- and 3-methylthio-benzo-*as*-triazines in high yields from *o*-nitroanilines in merely two steps. The syntheses of the more than 40 new benzo-*as*-triazine derivatives described here also include alkylation and nucleophilic replacement of the mercapto group. The ring closure of 5-chlorosubstituted *o*-nitroaniline showed an anomalous behaviour; this is explained by the influence of the nitro group exerting an electron withdrawing effect on the *para* position.

3-Mercaptobenzo-*as*-triazine-1-oxide (**4a**, Q=H), prepared by ARNDT—ROSENAU [1] ring closure reaction, seemed to be a convenient starting material for the synthesis of differently substituted benzo-*as*-triazine derivatives. However, the preparation of the starting compound of the above ring closure, *o*-nitrophenylthiourea (**3**), has been described in the literature [1, 2] as a two-step procedure of poor yield. In this study a simplified experimental method has been elaborated for the ARNDT—ROSENAU ring closure, making possible the synthesis of several new benzo-*as*-triazine derivatives.

This simplification is based on the evidence that the readily available crystalline 1-benzoyl-3-(*o*-nitrophenyl)thiourea (**2a**, Q=H) can be hydrolyzed by sodium hydroxide to the free thiourea (**3a**, Q=H), and simultaneous ring closure ensues to give 3-mercaptobenzo-*as*-triazine-1-oxide (**4a**, Q=H) (Chart 1).

First, benzoylthiourea derivatives (**2**) were prepared by the reactions of *o*-nitroanilines (**1**) with benzoylisothiocyanate [3]. Data of the products and reaction times are summarized in Table I.

A suspension of the benzoylthiourea derivative (**2**) in 10% sodium hydroxide solution gives, under reflux conditions, a deep red solution, and in 10 min. the desired mercaptobenzo-*as*-triazine derivative (**4**) can be isolated in crystalline form. As these mercapto compounds readily udergo oxidation in air, their purification is difficult; therefore the crude mercaptans were converted to the stable alkylthiobenzo-*as*-triazine derivatives (**5**) by alkylating

* Part VI: BENKÓ and L. PALLOS: Acta Chim. (Budapest) **91**, 327 (1976).

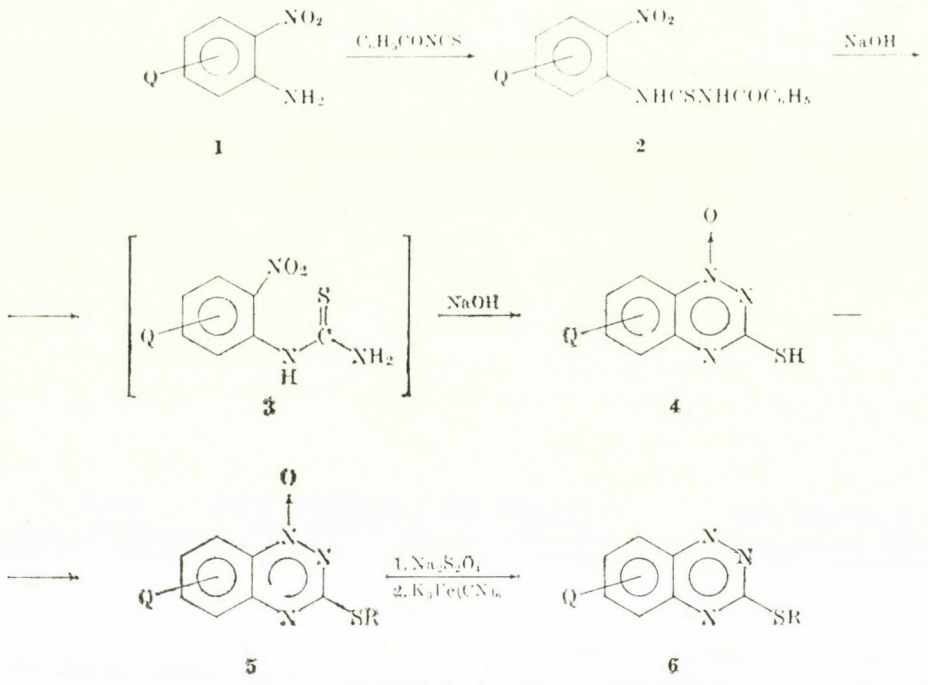

Chart 1

Table I

1-Benzoyl-3-o-nitrophenyl thioureas and reaction times of their preparation

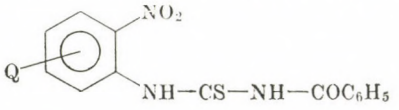

No.	Q	Reaction time, min	M.p., °C	Yield, %	Analysis					
					Caled.			Found		
					N	S	Cl	N	S	Cl
2a [3]	H	15	147—9	81	13.96	10.65	—	13.85	10.12	—
2b	4-Cl	120	164	74	—	9.55	10.56	—	9.42	10.35
2c	6-Cl	120	183—4	52	12.52	9.55	—	12.30	9.52	—
2d	5-Cl	60	203—4	75	—	9.55	—	—	9.80	—
2e	4-CH_3	15	177—8	71	13.32	10.16	—	13.26	10.04	—
2f	4-OCH_3	15	151—2	70	12.68	9.68	—	12.75	9.60	—

agents (*e.g.* dimethyl sulfate or methyl iodide). The methylated products (**5a**—**f**, R=CH_3) can also be prepared by direct methylation of the crude red reaction mixture.

Removal of the *N*-oxide function by the dithionite technique [10] affords the corresponding deoxy compounds (**6**) in good yields. Table II comprises data of the mercapto and methylthio derivatives.

Table II

3-Mercapto- and 3-methylthiobenzo-as-triazine derivatives

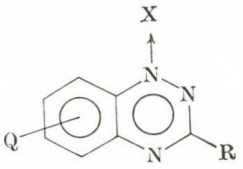

No.	Q	X	R	M.p., °C	Yield, %	Analysis	
						Calcd.	Found
4a[1]□	H	0	SH	—	77	—	—
4b□	7-Cl	0	SH	—	80	—	—
4c□	5-Cl	0	SH	—	72	—	—
4d□	6-SH	0	SH	—	40	—	—
4e□	7-CH_3	0	SH	—	72	—	—
4f□	7-OCH_3	0	SH	—	75	—	—
5a [1]	H	0	SCH_3	123—4	65	—	—
5b	7-Cl	0	SCH_3	144—6	50	S 14.08	S 14.30
5c	5-Cl	0	SCH_3	225	57	S 14.08 Cl 15.57	S 14.10 Cl 15.95
5d	6-SCH_3	0	SCH_3	150—2	34	S 26.79	S 26.41
5e	7-CH_3	0	SCH_3	168—70	58	N 20.27 S 15.47	S 15.39 N 20.42
5f	7-OCH_3	0	SCH_3	152—3	60	N 18.82 S 14.36	S 13.97 N 19.03
6a [1]	H	—	SCH_3	104	73	—	—
6b	7-Cl	—	SCH_3	102—4	72	S 15.14	S 15.00
6c	5-Cl	—	SCH_3	138—9	87	S 15.15 Cl 16.75	S 15.53 Cl 16.68
6d	6-SCH_3	—	SCH_3	124—5	75	S 28.71	S 28.42
6f	7-OCH_3	—	SCH_3	138—9	72	S 15.47	S 15.27

□ Isolated as a crude product, not suitable for analysis

This relatively convenient way to 3-mercaptobenzo-*as*-triazine-1-oxides (**4**) offered a possibility of synthesizing several new derivatives. Thus the reaction of the mercapto compounds with chloroacetic acid derivatives results in thioglycolic acids, whereas other alkylating agents give rise to alkylthio derivatives (**5g**—**5r** and **6g**—**6n**). These products are summarized in Table III.

Table III

Differently substituted C—3 sulfur-containing

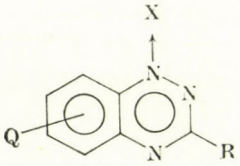

No.	Q	X	R	M.p., °C	Yield, %
5g	H	0	$SCH_2C_6N_5$	113	73
5h	H	0	$SCH_2CON(CH_2)_5$	154	58
5i	H	0	$SCH(CH_3)C_6H_5$	111	66
5j	H	0	$SCH_2COOC_2N_5$	91	83
5k	H	0	*S*-tetraacetyl-glucosyl	138—9	67
5l	7-Cl	0	$SCH_2C_6H_5$	118—9	53
5m	7-Cl	0	$SCH_2CON(CH_2)_5$	168	48
5n	7-Cl	0	$SCH_2CON(CH_2)_4O$	156—8	46
5o	7-Cl	0	$SCH_2COOC_2H_5$	108	45
5p	7-Cl	0	SCH_2COOH	157	48
5q	7-Cl	0	SCH_2CN	115	51
5r	7-Cl	0	*S*-tetraacetyl-glucosyl	191	49
6g	H	—	$SCH_2C_6H_5$	92	61
6h	H	—	$SCH_2CON(CH_2)_5$	98	58
6l	7-Cl	—	$SCH_2C_6H_5$	92—3	65
6m	7-Cl	—	$SCH_2CON(CH_2)_5$	139—40	45
6n	7-Cl	—	$SCH_2CON(CH_2)_4O$	191—3	69

The fact that the methylthio group in the 3-position of the benzo-*as*-triazine ring readily reacts with nucleophilic reagents also made possible the synthesis of amine derivatives. The aminobenzo-*as*-triazine derivatives (**7**) were obtained as crystalline compounds generally in good yields and were converted to the deoxy derivatives (**8**) by the dithionite method (Chart 2). These latter products can also be made by the reaction of 3-methylthiobenzo-*as*-triazines (**6**) with amines.

The reaction of 3-methylthiobenzo-*as*-triazine-1-oxides (**5**) with hydrazine hydrate also results, beside a substitution reaction, in reduction of the *N*-oxide function; the products are 3-hydrazinobenzo-*as*-triazines (**9**) (Chart 3). As these are key compounds for further ring closure reactions [11], this three-

benzo-as-triazine derivatives

Method of prepn.	Solvent for recryst.	Analysis	
		Calcd.	Found
A	EtAc	N 15.60 S 11.95	N 15.81 S 12.57
B	*i*PrOH	S 10.55	S 10.61
A	AcOH	N 14.83 S 11.39	N 15.03 S 11.62
C	MeOH	N 15.84 S 12.08	N 15.62 S 12.53
F	H_2O/EtOH	N 8.48 S 6.29	N 8.02 S 5.85
A	EtAc	N 13.88 S 10.55	N 13.51 S 10.40
B	*i*PrOH	S 9.45	S 9.56
B	BuOH	C 45.81 H 3.8 S 9.38	C 45.60 H 4.0 S 9.62
C	*i*PrOH	S 10.70	S 11.18
D	MeOH	C 39.78 H 2.2 S 11.80	C 40.10 H 2.5 S 11.96
E	*i*PrOH	Cl 14.03 S 12.69	Cl 13.70 S 13.00
F	H_2O/EtOH	S 5.89	S 6.00
G	CH	N 16.65 S 12.65	N 16.22 S 12.50
H	CH	S 11.10	S 10.80
G	CH	Cl 12.32 S 11.14	Cl 12.07 S 11.09
H	CCl_4/PE	N 17.36 S 9.93	N 17.02 S 10.10
H	AcN	N 17.24 S 9.84	N 17.08 S 10.21

Abbreviations: EtAc = ethyl acetate; *i*PrOH = isopropanol; AcOH = acetic acid; MeOH = methanol; EtOH = ethanol; BuOH = butanol; CH = cyclohexane, CCl_4 = carbon tetrachloride; AcN = acetonitrile

step synthesis, starting from *o*-nitroanilines, has considerable importance. Table IV contains the data of the amino and hydrazino compounds prepared.

Though this simplified procedure for the synthesis of benzo-*as*-triazine derivatives can be generalized for many compounds as shown in Tables I—IV, the ring closure reaction of 1-benzoyl-3-(2′-nitro-5′-chlorophenyl)thiourea (**2d**) showed some anomalies (Chart 4). To clarify the structures of the final reaction products in this case, intermediate **3d** was isolated in crystalline form, and treated with hot alkali solution. Although the product isolated by our general procedure contained a methylthio group in position 3, elementary analysis revealed the presence of another methylthio group instead of the chlorine

Table IV

Substituted 3-aminobenzo-as-

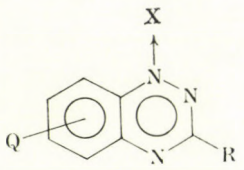

No.	Q	X	R	Reaction time, h	M.p., °C	Yield, %
7a [7]	H	0	Morpholino	6	173—5	62
7b	H	0	Di(hydroxyethyl)amino	3	114	40
7c [5]	7-Cl	0	Morpholino	6	175	60
7d	5-Cl	0	Morpholino	2	225	57
7e	6-SCH_3	0	Morpholino	6	156—7	68
8a	H	—	Morpholino	6	125	75
8b	H	—	Di(hydroxyethyl)amino	3	125	55
8c	7-Cl	—	Morpholino	4	168	68
8d	5-Cl	—	Morpholino	6	167—9	51
8e	6-SCH_3	—	Morpholino	5	132—4	70
8f	H	—	Piperidino	1	40	75
8g	H	—	*N*-methylpiperazino	**4**	72	70
8h	7-Cl	—	Piperidino	8	103	68
8i	7-Cl	—	*N*-methylpiperazino	4	98	58
9a [7]	H	—	Hydrazino	3	173—5	70
9b	7-Cl	—	Hydrazino	3	220—2	65
9c	7-CH_3	—	Hydrazino	3	109—10	65
9d	7-OCH_3	—	Hydrazino	3	231—2	72

For abbreviations, see Table III.

atom (**5d**). Another product, 2-nitro-5-chlorophenylcyanamide (**10**) was also isolated on acidification of the reaction mixture.

We suggest that this anomalous behaviour is due to the following structural pecularity: the chlorine atom in the starting material **2d** is in *para* position to the nitro group. The thiolate anion **3d** formed in the alkaline solution attacks therefore the chlorine atom of another, intact molecule; the attacking molecule is thus converted to the cyanamide (**10**) isolated from the reaction mixture, and the reactant is converted to 5-mercapto-2-nitrophenylthiourea which affords first a bis-(mercapto)-benzo-*as*-triazine derivative with sodium hydroxide, and gives finally the bis-(methylthio) compound (**5d**) on reaction with methyl iodide.

triazines

Method of prepn.	Recryst. from	Analysis	
		Calcd.	Found
I	AcOH	—	—
K	EtAc	C 52.79 H 5.2 N 22.38	C 52.51 H 4.8 N 22.40
I	EtAc	—	—
I	EtOH	N 22.35	N 22.43
I	AcOH	N 20.13 S 11.52	N 20.32 S 11.65
I, G	CH	N 25.91	N 26.00
K	EtAc	N 23.91	N 23.80
I	CH	Cl 14.15 H 22.35	Cl 14.05 N 21.96
I	EtOH	Cl 13.39 N 22.35	Cl 13.61 N 22.03
I	CH	N 21.36 S 12.22	N 21.50 S 12.55
I	$EtOH/H_2O$	N 26.15	N 26.62
I	CH	N 30.54	N 30.47
I	CH	Cl 14.25 N 22.52	Cl 13.90 N 22.61
I	CH	Cl 13.44 N 26.69	Cl 13.60 N 26.41
L	AcN	—	—
L	AcN	Cl 18.13 N 35.80	Cl 17.82 N 35.41
L	AcN	N 40.12	N 39.86
L	AcN	N 36.64	N 36.32

The structure of the new cyanamide (**10**) is supported by the IR band at 2250 cm^{-1} (cyano group). For further confirmation of the structure, compound **10** was converted to a crystalline carbodiimide derivative (**11**) by trityl chloride (Chart 5). Comparison of the wavenumbers of the cyano and carbodiimide IR bands in compounds **10** and **11** is in good agreement with this reaction.

Experimental

Infrared spectra were recorded with a Unicam SP 200 spectrophotometer. M.p.'s are uncorrected. 5-Chloro-2-nitroaniline [8], 6-chloro-2-nitroaniline [4], the chloroacetic acid derivatives [6] and iodoacetonitrile [9] were prepared according to standard procedures.

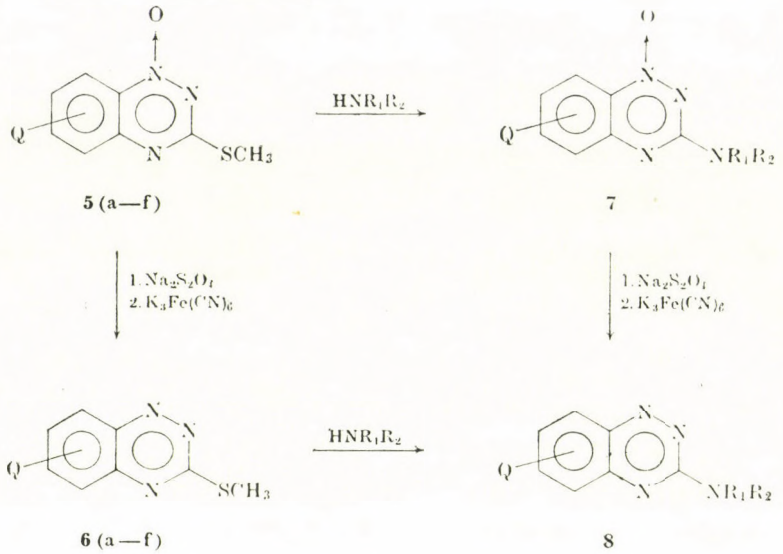

5 (a—f) **7**

6 (a—f) **8**

Chart 2

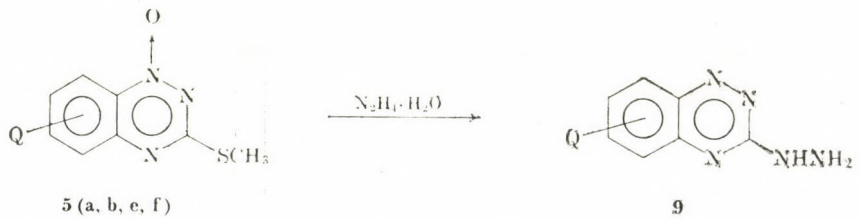

5 (a, b, e, f) **9**

Chart 3

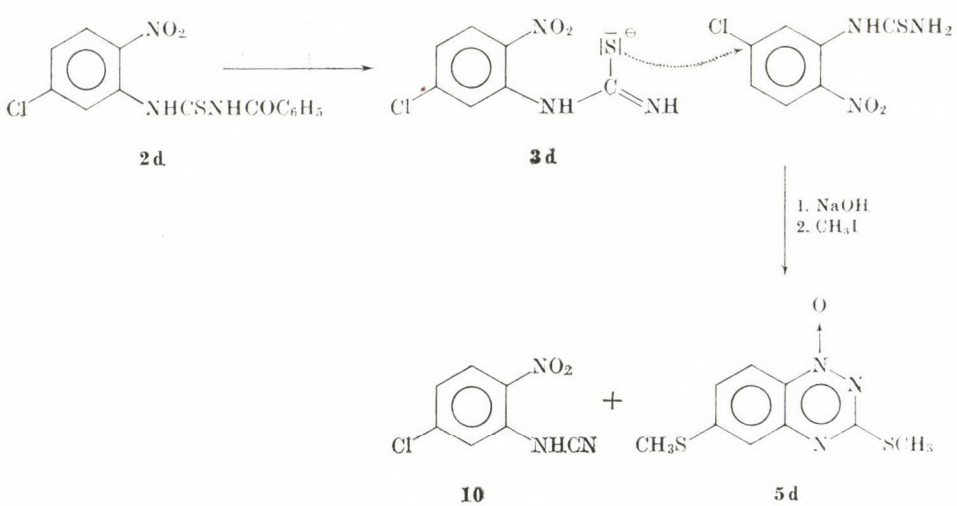

2d **3d**

10 **5d**

Chart 4

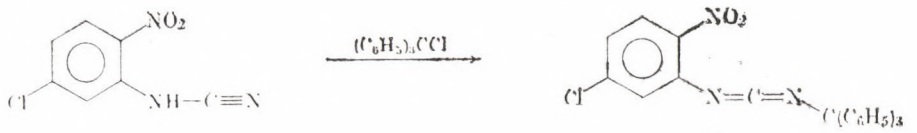

10 11

Chart 5

1-Benzoyl-3-(Q-2-nitrophenyl)thiourea (2)

Freshly distilled benzoyl chloride (0.2 mole) was added to a refluxing solution of ammonium rhodanide (0.2 mole) in acetone (200 ml). The mixture was stirred and refluxed for 10 min., then a solution of *o*-nitroaniline (0.2 mole) in acetone (200 ml) was added. After additional stirring and refluxing for the period given in Table I, the mixture was poured into water. The precipitate was filtered off, dried and recrystallized from benzene or dioxane. For data of the products, see Table I.

3-Mercapto- and 3-methylthio-Q-benzo-*as*-triazine-1-oxides (4, 5)

A mixture of 1-benzoyl-3-(Q-2-nitrophenyl)thiourea (**2**) (50 mmoles) and 240 ml of 10% sodium hydroxide solution was refluxed for 10 min. During this time the initial orange-coloured suspension turned to a deep red solution. After cooling, the reaction mixture was poured into a mixture of hydrochloric acid (80 ml) and ice (400 g), and after 15 min the red crystals which separated were filtered by suction.

The crude mercapto compound (**4**) (4.4 mmoles) was dissolved in hot 2% sodium hydroxide solution (150 ml) and the red solution was filtered. Dimethyl sulfate (7 ml; 9.1 g; 72 mmoles) was then added to the hot (70—80 °C) solution, whereupon an oil separated which soon solidified. The product was filtered off after 30 min, and recrystallized from an appropriate solvent (Table III).

The methylthio compounds (**5**) can also be prepared without isolation of the mercapto derivatives (**4**): the red alkaline reaction mixture obtained in the cyclization reaction described above was cooled, mixed with crushed ice (80 g), and a mixture of ethanol (20 ml) and methyl iodide (16 ml) was added to it by drops, with stirring. After 1 h, the resulting yellow precipitate was filtered off and recrystallized.

3-Mercapto- and 3-methylthio-Q-benzo-*as*-triazines (6)

The derivatives without *N*-oxide function (**6a**—**f**) were prepared by sodium dithionite reduction, according to method *G* (see below).

Further reactions of 3-mercapto- and 3-methylthio-benzo-*as*-triazine derivatives (5—9)

Alkylation of 3-mercaptobenzo-as-triazine derivatives

Method A: A mixture of the mercapto compound (**4**), ethanol (20 ml), alkyl chloride (5.2 mmoles) and a solution of sodium carbonate (1.0 g) in water (20 ml) was shaken for 3 h. A solid precipitated, which was filtered off and recrystallized from the appropriate solvent.

Method B: The requisite chloroacetic acid derivative (5.0 mmoles) was slowly added to a mixture of triethylamine (1 ml), the mercapto compound (**4**) (5.0 mmoles) and ethanol (20 ml). The mixture was stirred for 30 min. at 50 °C and for an additional 30 min at room temperature; it was then poured into water. The precipitate was filtered off and recrystallized.

Method C: To a mixture of the mercapto compound (**4**) (8.0 mmoles) and sodium ethoxide solution (prepared from 0.45 g of sodium and 30 ml of ethanol) there was added ethyl bromoacetate (10 mmoles), with stirring, at 5 °C. The mixture was then stirred for 30 min at 5 °C and 30 min. at room temperature. After filtration, the product was recrystallized from the given solvent.

Method D: To a solution of the mercapto compound (**4**) (3.0 mmoles) in pyridine (4 ml), iodoacetonitrile (3.0 mmoles) was added at room temperature during a period of 10 min. The product was recrystallized from ispropanol.

Method E: To a mixture of the mercapto compound (**4**) (3.0 mmoles) and sodium carbonate solution (2.0 g in 30 ml of water), bromoacetic acid (3.2 mmoles) was added, and the mixture was allowed to stand at room temperature for 30 min; the pH was then adjusted by hydrochloric acid to a value between 4 and 5, whereupon the product precipitated as yellow crystals.

Method F: To a solution of the mercapto compound (**4**) (30 mmoles) in dimethylformamide (220 ml), sodium ethoxide solution (prepared from 30 mmoles of sodium and 25 ml of ethanol) was added. Ethanol was then removed in vacuum on a rotatory evaporator at 50 °C (30 min). A solution of tetraacetylbromoglucose (30 mmoles in 20 ml of dimethylformamide) was then added to the above solution and the mixture was stirred at 50 °C for 30 min. It was poured into water, the precipitate was filtered off and recrystallized from aqueous ethanol.

Deoxygenation of benzo-as-triazine derivatives

Method G: To a solution of 3-methylthiobenzo-*as*-triazine (**5a—f**) (0.1 mole) in dimethylformamide (130 ml), a solution of 20% sodium dithionite solution (0.22 mole of $N_2S_2O_4$) was added. After stirring for 10 min, a colourless crystalline solid precipitated which was filtered off and, without purification, treated with a mixture of 20% potassium ferricyanide solution (0.25 mole) of $K_3[Fe(CN)_6]$ and *conc.* ammonium hydroxide solution (25 ml). After stirring for 30 min, the product was isolated either by filtration or by extraction with methylene chloride. Solvents for recrystallization are given in Table III.

Method H: To a suspension of the appropriate thioglycolic acid derivative (**5h, m, n**) (3.0 mmoles) in pyridine (10 ml), a solution of sodium dithionite (7.2 mmoles) in water (10 ml) was added. In a few minutes a colourless solution was obtained which was treated with 20% potassium ferricyanide solution (25 ml). The product was isolated from the bright yellow suspension by extraction with chloroform.

Nucleophilic substitution reactions

Method I: A mixture of the methylthio compound (**5a—f**; **6a—f**) (0.03 mole) and the amine (0.6 mole) was refluxed for the period given in Table IV. The reaction mixture was then poured into water. The crude product was filtered off and recrystallized from the given solvent.

Method K: A mixture of the methylthio compound (**5a—f**; **6a—f**) (5.0 mmoles) and diethanolamine (10 ml) was stirred at 125—130 °C for 3 h, and the reaction mixture was extracted continuously with ether for 6 h. After evaporation of the solvent, the residue was recrystallized from ethyl acetate.

Method L: A mixture of 3-methylthiobenzo-*as*-triazine-1-oxide (**5**), 100% hydrazine hydrate (3 ml) and butanol (3 ml) was refluxed for 3 h. During this time a deep yellow solution was formed and the evolution of methyl mercaptane was observed. On cooling the mixture, the product separated as needles; after filtration it was recrystallized from the solvent given in Table IV.

N-(5-chloro-2-nitrophenyl)thiourea (3d)

A mixture of 1-benzoyl-3-(3-chloro-6-nitrophenyl)thiourea (**2d**) and 2% sodium hydroxide solution (100 ml) was maintained at 70—80 °C until the starting materials had dissolved (2—3 min.). After cooling, the reaction mixture was acidified with acetic acid. The precipitated product was filtered off and recrystallized from dioxane to obtain 2.7 g (75%) of compound **3d**; m.p. 191—193 °C.

$C_7H_6ClN_3O_2S$ (231.67). Calcd. S 13.9. Found S 13.4%.

3,6-Bis-(methylthio)-benzo-*as*-triazine-1-oxide (5d) and 5-chloro-2-nitrophenylcyanamide (10)

A mixture of *N*-(3-chloro-6-nitrophenyl)thiourea (**3d**) (10.0 g; 46 mmoles) and 5% sodium hydroxide solution (100 ml) was boiled for 5 min. A deep red solution was obtained which, after cooling, was treated with a mixture of methyl iodide (10 ml) and ethanol (30 ml).

The reaction mixture was extracted with chloroform and the isolated product recrystallized from isopropanol to give 3.5 g (34%) of **5d** as yellow needles.

The aqueous phase remaining from the extraction was neutralized with acetic acid, whereupon a precipitate formed. It was filtered off and recrystallized from dioxane to give 3.4 g (40%) of 5-chloro-2-nitrophenylcyanamide, m.p. 165—167 °C.

$C_7H_4ClN_3O_2$ (197.59). Calcd. N 21.26; Cl 17.94. Found N 21.20; Cl 18.04 %

IR (KBr) 2250 cm^{-1} (C≡N).

1-(5-Chloro-2-nitrophenyl)-3-triphenylcarbodiimide (11)

A mixture of 5-chloro-2-nitrophenylcyanamide (**10**) (0.5 g; 2.5 mmoles), pyridine (5 ml) and trityl chloride (0.8 g; 2.8 mmoles) was refluxed for 30 min. The resulting yellow solution was evaporated and the residue triturated with acetone. A pale yellow solid was obtained, which was filtered off and recrystallized from acetonitrile to give 0.55 g (50%) of the carbodiimide **11**, m.p. 163—165 °C.

$C_{26}H_{18}ClN_3O_2$ (439.89). Calcd. Cl 8.06. Found Cl 8.47%.

IR ($CHCl_3$): 2000 cm^{-1}, intense band (—N=C=N—).

REFERENCES

[1] Arndt, F., Rosenau, B.: Ber., **50,** 1248 (1917)
[2] Elderfield, R. C., Short, F. W.: J. Org. Chem., **18,** 1092 (1951)
[3] Douglas, I. B., Dains, F. B.: J. Amer. Chem. Soc., **56,** 1408 (1934)
[4] Wolf, F. J., Pfister, K., Wilson, R. M., Robinson, C. A.: J. Amer. Chem. Soc,. **76,** 3551 (1954)
[5] Wolf, F. J., Wilson, R. M., Pfister, K., Tischler, M.: **J. Amer. Chem. Soc., 76,** 4611 (1954)
[6] Gandini, A., Schenone, P., Minardi, G.: Farmaco (Pavia), Ed. Sci., **18** (II), 828 (1963); C. A., **60,** 9313 (1964)
[7] Jiu, J., Müller, G. P.: J. Org. Chem., **24,** 813 (1959)
[8] Fuson, R. C.: J. Org. Chem., **12,** 799 (1974)
[9] Scholl: Ber., **29,** 2416 (1896)
[10] Katritzky, A. R., Lagowski, J. M. (Eds): Chemistry of the Heterocyclic N-oxides, Academic Press, London 1971 Vol. **9,** p. 209
[11] Messmer, A., Hajós, Gy., Benkó, P., Pallos, L.: Part VIII of this series (In press)

András Messmer
György Hajós } H-1525 Budapest, Pf. 17.

Pál Benkó
László Pallos } H-1106 Budapest, Pf. 100.

Acta Chimica Academiae Scientiarum Hungaricae, Tomus 103 (2), pp. 135—159 (1980)

ИЗУЧЕНИЕ ВЗАИМОДЕЙСТВИЯ НЕКОТОРЫХ ПОЛЯРНЫХ ВИНИЛМОНОМЕРОВ С $AlEt_3$ МЕТОДОМ ИНФРАКРАСНОЙ СПЕКТРОСКОПИИ

А. ДАНКОВИЧ,[1] Л. ЛЕНДВАИ,[2] Ю. В. КИССИН,[3] И. СЁЛЛЁШИ[2]

([1] Научно-исследовательский Институт Пластмассовой промышленности, Будапешт, [2]Политехнический Университет, Будапешт, [3] Институт Химической Физики АН СССР, Москва)

Поступила в редакцию 28 февраля 1978 г.

Принята к печати 29 марта 1979 г.

Процессы сополимеризации α-олефинов с такими полярными мономерами, как акрилонитрил, винилацетат, винилхлорид и т. п. в присутствии комплексных катализаторов Циглера—Натта, как правило, весьма затруднены вследствие того, что эти мономеры вступают в реакцию с одним или обоими компонентами каталитической системы. При этом активность последних значительно снижается или же полностью уничтожается [1—4].

Сейчас однако уже ясно, что при модифицировании системы этот недостаток предотвращается, и реакция успешно завершается. Модификация каталитической системы в основном может произойти двумя путями. Первый, это модификация каталитической системы с помощью комплексообразующих электродоноров, путем введения насыщенных соединений в реакционну зону [3, 4]. Второй путь, это образование комплекса между одним или обоими компонентами катализатора и полярным винилмономером перед реакцией сополимеризации [2—3], [5—7].

Комплексы, образующиеся при взаимодействии полярных винилмономеров и солей металла или металл-алкила, играют значительную роль в процессах полимеризации [8—11]. Скорость полимеризации комплексированнополярных винилмономеров (акрилонитрил, акрилаты, винилпиридин и т. д.) значительно повышается. При комплексообразовании мономера могут изменяться некоторые параметры реакции, как скорость инициирования, константа роста или обрыва цепи или же сам механизм реакции [1, 12, 13].

Комплексы, играющие большую роль в процессе полимеризации, были отделены и изучены методом ИКС или другими способами [2, 14—17]. По мнению авторов, такие мономеры как акрилонитрил, акриловая кислота, акрилаты, акриламид, т. е. вообще полярные ненасыщенные соединения, имеют два активных центра. Благодаря этому координация может происходить или с помощью полярной группы или же по двойной связи мономера [18].

Исследования по ИК, ЯМР и УФ спектроскопии доказывают, что комплексообразователь, находящийся во взаимодействии с мономером, нужно рас-

сматривать как новый заместитель в мономере, который повышает энергию сопряжения последнего и придает электронной оболочке молекулы дополнительную поляризацию [14, 16, 17]. До настоящего времени были изучены многочисленные комплексы различного строения, образующиеся при взаимодействии металл-алкила и полярного винилмономера. Ямамото [19] изучал комплекс акрилонитрила и никеля диэтилпиридила. По его мнению, атом никеля координируется через двойную связь мономера. Другой тип взаимодействия был обнаружен при реакции акрилонитрила с такими металлалкилами, как $AlEtCl_2$ [8, 20, 21], $AlEt_2Cl$ [22] и $Al(i\text{-}Bu)_2Cl$ [23]. При этом Al координируется с помощью группы нитрила [24]. При молярных соотношениях метилметакрилат-триэтилалюминий > 1, образуется комплекс, молярный состав которого 1 : 1. Алюминий координируется через карбонил [12, 13, 25, 26]. Акриловая кислота и ее гомологи образуют комплекс с металлалкилом, причем комплексованный мономер находится в виде соли [27]. Однако строение комплексов рассматривалось постоянным по всей продолжительности реакции полимеризации. Поэтому мы в настоящей работе с помощью ИКС стремились показать изменения, происходящие в строении комплекса за счет его старения. Мы предполагаем, что на основе этих данных (по изменению строения комплекса) можно дать ответ на некоторые аномалии, обнаруженные в процессе сополимеризации пропилена и полярного винилмономера [2, 3].

Экспериментальная часть

Толуол (растворитель) и мономеры были высушены молекулярным ситом (клиносорб-4), потом дистиллированы при атмосферном или пониженном давлении. Перегонка производилась в присутствии инертного газа.

Триэтилалюминий (производство E G A Chemie) был также перегнан в вакууме в присутствии инертного газа. В экспериментах был использован α-$TiCl_3$ (Stauffer AA).

Комплексообразование было проведено в специальном стеклянном сосуде емкостью 6 см³. Это стеклянное приспособление было снабжено зашлифованными пробками. Благодаря этому инертная атмосфера была обеспечена и во время отбора проб. Для приготовления комплекса необходимое количество $AlEt_3$ было добавлено к толуольному раствору мономера при 0 °C. После тщательного перемешивания раствор нагревался до комнатной температуры и потом, с помощью шприца, помещался в измерительную кювету для инфракрасного анализа. Молярные соотношения мономер $AlEt_3$ были следующие 1 : 1; 1 : 1,5; 1 : 2. Концентрация мономера в толуоле — 1 моль/л.

Исследования были проведены на двухлучевом спектрофотометре UR-10. Полосы поглощения толуола были скомпенсированы с помощью кюветы регулируемой толщины.

При отнесении полос инфракрасных спектров пользовались следующими символами:

ν — для частот валентных колебаний
δ — для частот деформационных колебаний (плоскостные)
γ — для частот деформационных колебаний (внеплоскостные: γ_ω — веерное (wagging), γ_t — крутильное (twisting) и γ_r — маятниковое (rocking).

Обсуждение результатов

Система акрилонитрил (AN)—$AlEt_3$

Ниже в таблице I перечислены положения некоторых полос в спектре акрилонитрила (AN) и его комплекса с $AlEt_3$. При сливании растворов AN и $AlEt_3$, между ними протекает быстрая реакция комплексообразования, сопровождающаяся смещением полосы валентных колебаний C ≡ N от 2235 до 2225 и 2275 $см^{-1}$ (рис. 1). Смещение в сторону более высоких частот полосы валентных колебаний C ≡ N свидетельствует о том, что комплекс образуется в случае реакции преимущественно благодаря донорно-акцепторному взаимодействию за счет неподеленной пары электронов атома азота [28, 29].

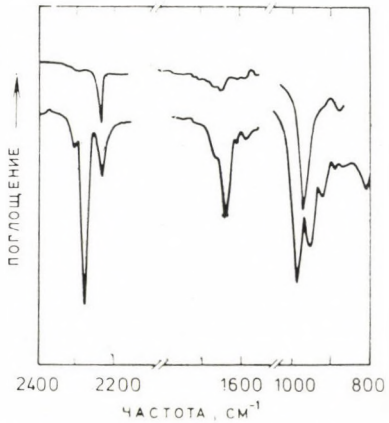

Рис. 1. Инфракрасный спектр акрилонитрила (верхний) и комплекса акрилонитрил-$AlEt_3$ (нижний)

Следовательно первый комплекс имеет строение $CH_2 = CH—C{\equiv}N : \cdot AlEt_3$ (комплекс **I**).

Комплекс **I** в отсутствии избыточного $AlEt_3$ при 20°C стабилен в течение нескольких часов, однако при небольшом избытке $AlEt_3$ он сравнительно быстро переходит в другой комплекс (комплекс **II**).

В ИК спектре нового комплекса, образующегося одновременно с разложением комплекса **I**, полоса валентных колебаний C≡N расположена при 2225 $см^{-1}$ (рис. 2). Как это доказывается, со старением комплекса интенсивность полосы при 2275 $см^{-1}$ уменьшается, а при 2225 $см^{-1}$ повышается. Скорость разложения комплекса **I** не является функцией молярного соотношения AN—$AlEt_3$. В то же время скорость образования комплекса **II** сильно зависит от молярного соотношения компонентов (рис. 3 и 4). Об этом подробно описано нами ранее [2, 3].

Надо сказать, что измерение оптической плотности полосы 2275 $см^{-1}$ при большой выдержке (длинное время старения) комплекса таит в себе некоторые трудности, так как к этому времени полоса частично перекрывается слабой полосой при 2288—2300 $см^{-1}$. Это последнее полгощение характеризует третий вид комплекса. Интенсивность полосы поглощения при 1640 $см^{-1}$ в спектре постоянна. В области 1000—900 $см^{-1}$ абсорбции довольно слабые и сильно перекрыты полосами поглощения металл-алкила.

При данных условиях частота полосы в области валентных колебаний C = C смещается мало. Полоса при 1650 $см^{-1}$ с образованием комплекса появляется при 1640 $см^{-1}$. В то же время полоса внеплоскостно-деформационных колебаний CH смещена от 970 $см^{-1}$ до 955 $см^{-1}$ [30]. Трудно решить вопрос, какому комплексу соответствует это небольшое смещение, так как в реакционной зоне одновременно существуют комплексы различного строения. Мы предполагаем, что донорноакцепторное взаимодействие (комплекс **I**) еще не влияет значительно на электронную оболочку связи C = C. В таком случае в этой области колебаний не ожидается изменения.

Таблица I

Акрилонитрил и его комплекс с $AlEt_3$

Акрилонитрил		Комплекс акрилонитрил-$AlEt_3$	
частота ($см^{-1}$)	отнесение полос AN-a	частота ($см^{-1}$)	отнесение полос AN-a
2235	ν (CN)	2300—2285 2275 2225	ν (CN)
		1640	ν (C = C)
1650	ν (C = C)		
970	$\gamma_\omega(CH_2)$	955	γ_ω (CH_2)

Слабое смещение в сторону низких частот (на 2225 $см^{-1}$) полосы валентного колебания C ≡ N в спектре комплекса **II** свидетельствует об отсутствии координации по атому N, а малые изменения в области валентных колебаний C = C указывают на отсутствие сильной π связи между двойной связью AN и атомом Al (в случае комплексов с сильной π связью между Ni нулевой валентности и акрилонитрилом полоса валентного колебания C = C смещается до 1446 $см^{-1}$. Полоса валентного колебания CN смещается до 2200—2145 $см^{-1}$, а полоса деформационного колебания C—H до 916 $см^{-1}$) [30].

Определенные соображения о структуре комплекса **II** высказать трудно, но судя по тому, что в его спектре полоса валентных колебаний CN смещается в область более низких частот по сравнению с комплексом **I**, можно предполагать, несмотря на малые изменения в области валентных колебаний

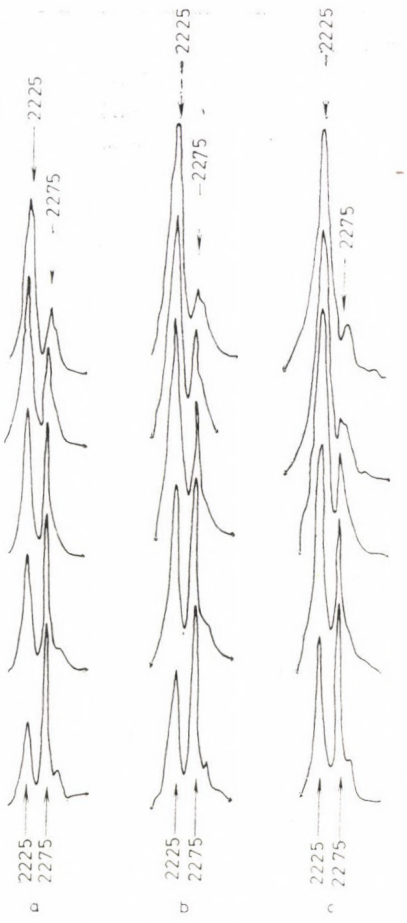

Рис. 2. Изменение интенсивностей полосы поглощения при 2225 и 2275 $см^{-1}$, молярное соотношение $AN—AlEt_3 = 1:1$ (a), 1 : 1,5 (b), 1 : 2 (c); время реакции (снизу вверх) в минутах: (a) — 15, 32, 50, 65, 78; (b) — 6, 21, 65, 101, 120; (c) — 5, 24, 65, 98, 130

C = C, что в комплексообразование здесь вовлечена и связь C = C, как это показано в работе [31].

С увеличением молярного соотношения $AN—AlEt_3$ и времени старения комплекса увеличивается вероятность образования комплекса **II** (рис. 2, 4, 5).

Кривые изменения оптических плотностей имеют максимум, то есть комплекс **II** также переходит за несколько часов в новый продукт, в спектре которого полоса валентных колебаний C ≡ N расположена уже в области 2288—2300 $см^{-1}$.

Кинетические характеристики перехода комплекса **I** в комплекс **II**, а также комплекса **II** в конечный продукт приведена в работах [2, 3].

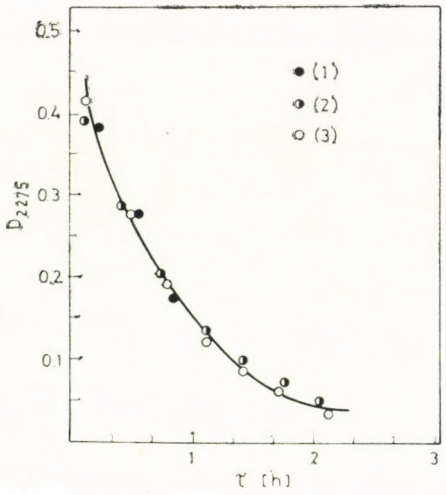

Рис. 3. Изменение оптической плотности полосы при 2275 $см^{-1}$; молярное соотношение $AN-AlEt_3 = 1:1$ (1); 1 : 1,5 (2); 1 : 2 (3); τ(h) — час

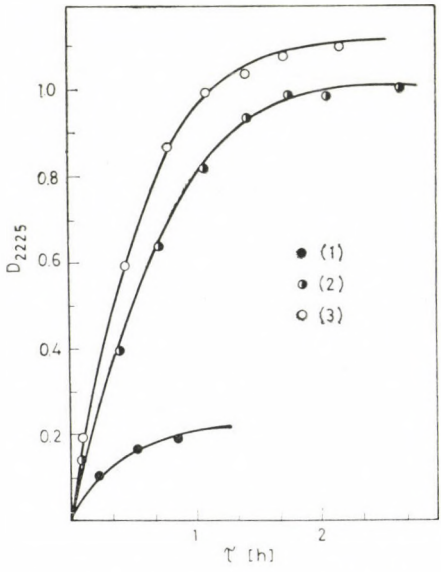

Рис. 4. Изменение оптической плотности полосы при 2225 $см^{-1}$; молярное соотношение $AN-AlEt_3 = 1:1$ (1); 1 : 1,5 (2); 1 : 2 (3)

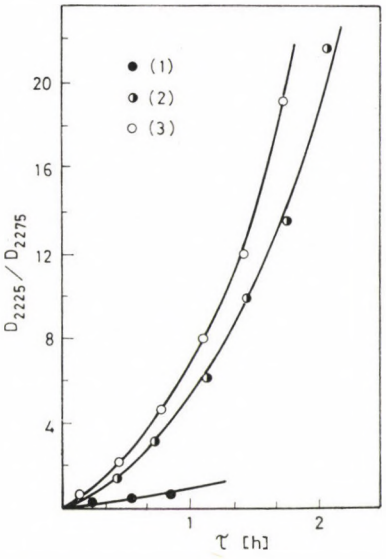

Рис. 5. Изменение значений D_{2225}/D_{2275} в зависимости от времени; молярное соотношение $AN-AlEt_3 = 1:1$ (1); 1 : 1,5 (2); 1 : 2 (3)

Система винилацетат (VAc) — $AlEt_3$

В соответствии с литературными данными при взаимодействии сложных эфиров с различными акцепторами электронов (например, $AlCl_3$, $AlMe_2Cl$, $AlMeCl_2$) образуются комплексы типа C = O . . . M, устойчивые при 20 °C [10, 15, 32—35]. Комплексообразование подобного типа сопровождается смещением полосы валентного колебания C = O эфира в область более низких частот, от 1740—1720 $см^{-1}$ на 50—130 $см^{-1}$, и смещением полосы валентного колебания C—O в 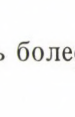 в область более высоких частот, от 1180—1250 $см^{-1}$ на 50—150 $см^{-1}$.

В то же время полоса валентного колебания C—O алкоксигруппы практически не смещается [10, 36]. Наблюдаемое смещение полосы валентных колебаний C = O в область более низких частот рассматривается как мера кислотности производных алюминия [35]. Аналогичная картина наблюдается и при взаимодействии VAc—$AlEt_3$.

В таблице II перечислены положения некоторых полос в спектре винилацетата (VAc) и его комплекса с $AlEt_3$.

На рис. 6 показан спектр винилацетата и его комплекса с $AlEt_3$. В образовании комплекса очень важную роль играет возникновение взаимодей-

Таблица II

Винилацетат и его комплекс с $AlEt_3$

Винилацетат		Комплекс винилацетат-$AlEt_3$	
частота ($см^{-1}$)	отнесение полос Vac-a	частота ($см^{-1}$)	отнесение полос VAc-a
1760	ν (C = O)	1679	ν (C = O)
1648	ν (C = C)	1640	ν (C = C)
1390	$\delta(CH_2)$, $\delta_a(CH_3)$	1390	$\delta(CH_2)$ и $\delta_a(CH_3)$
1375	$\delta_s(CH_3)$	1375	$\delta_s(CH_3)$
1220	ν (C—O—C)	1325—1290	ν (C—O—C)
1145	ν (C—O—C)	1155—1123	ν (C—O—C)

ствия карбонильной группы винилацетата и металл-алкила. В спектре комплекса полоса валентного колебания C = O смещается от 1760 $см^{-1}$ до 1679 $см^{-1}$ (рис. 6.) Сопоставление величины смещения полосы валентного колебания C = O в случае системы VAc—$AlEt_3$ ($\sim$82 $см^{-1}$) и приведенных в работе [35] данных для различных метильных производных алюминия показывает, что $AlEt_3$ приблизительно такая же по силе кислота, как и $AlMe_3$ (в спектре смеси $AlMe_3$—C_7H_{15}—COOEt сдвиг равен 79 $см^{-1}$).

Комплекс Vac—$AlEt_3$, описанный выше, нестабилен и при 20 °C быстро разлагается. Разрушение комплекса сопровождается выделением свободного

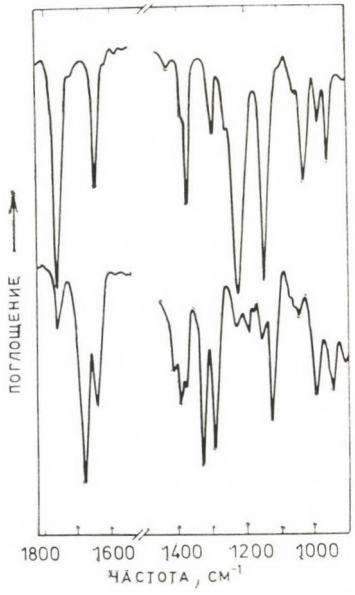

Рис. 6. Инфракрасный спектр винилацетата (верхний) и комплекса винилацетат-$AlEt_3$ (нижний)

VAc в количестве от 50% (при исходном соотношении $AlEt_3/VAc = 1:1{,}5$) до 20% (при соотношении $AlEt_3/VAc = 2$) от исходного. Разложение комплекса доказывается повторным появлением полосы поглощения карбонильной группы некомплексированного VAc при 1760 $см^{-1}$ (рис. 7). Интенсивность этой полосы с увеличением времени реакции увеличивается. Одновременно интенсивность полосы при 1679 $см^{-1}$ понижается. Однако надо сказать, что в спектрах разложений комплекса понижение интенсивности полосы комплексного карбонила (рис. 8) и одновременное повышение интенсивности абсорбции свободной карбонильной группы (рис. 7) носит в себе некоторые противоречия. Как видно, скорость разложения комплекса только при относительно

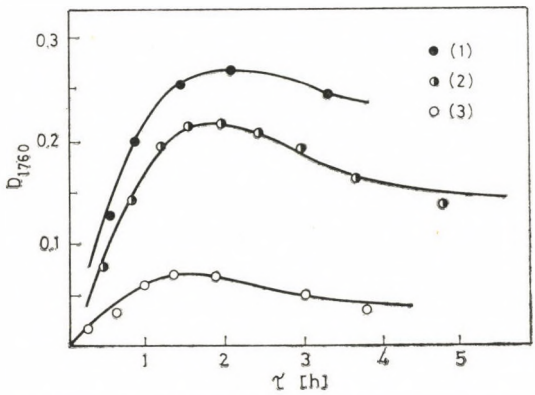

Рис. 7. Кинетика повторного появления полосы при 1760 $см^{-1}$, характеризующей группу C = O, молярное соотношение $VAc-AlEt_3 = 1:1$ (1); 1 : 1,5 (2); 1 : 2 (3)

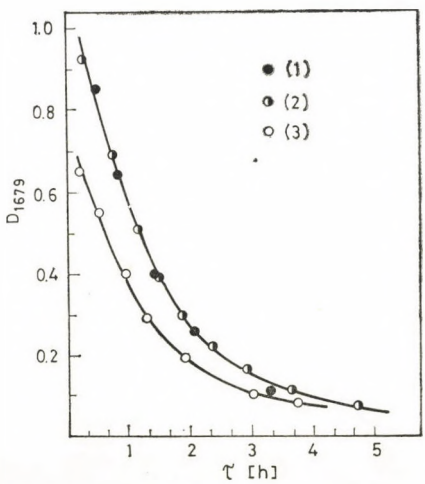

Рис. 8. Изменение оптической плотности полосы при 1679 $см^{-1}$; молярное соотношение $VAc-AlEt_3 = 1:1$ (1); 1 : 1,5 (2); 1 : 2 (3); τ(h) — час

небольшом избытке металлалкила зависит от молярного соотношения компонентов (рис. 8).

В то же время судя по повторному появлению полосы свободного карбонила, этот процесс во всех случаях является функцией молярных соотношений реагирующих веществ. Эти кривые имеют максимум (рис. 7).

Противоречие исключается, если предполагаем, что на составные части разлагается только некоторая часть первичного комплекса. Так как в спектрах смесей, записанных через несколько часов после начала взаимодействия, в области валентных колебаний C = O присутствует только полоса VAc, можно предположить, что рядом с полным разложением комплекса протекает и перегруппировка следующего типа:

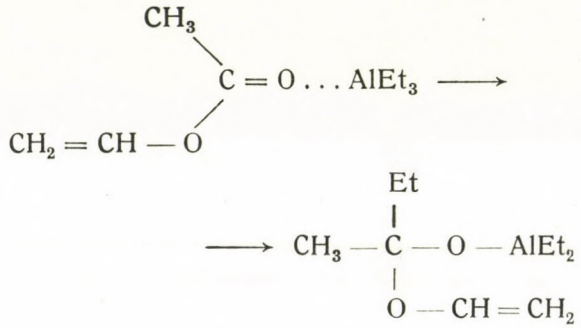

При этом эфирная группа C—O—R вытесняет винилацетат из комплекса, что и приводит к регенерации 50% исходного VAc:

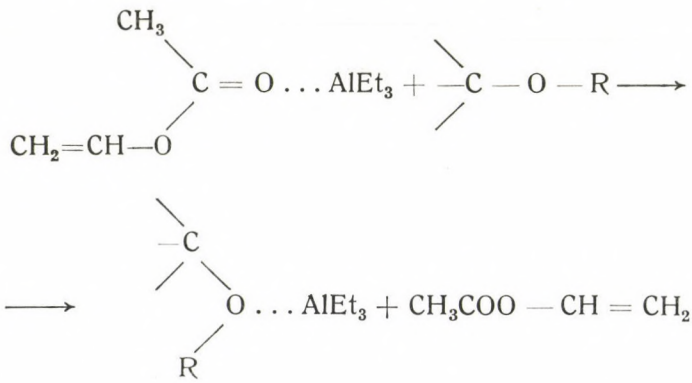

Естественно, что при избытке металл-алкила степень регенерации понижается (рис. 7).

Изменения, происходящие при образовании и разложении комплекса, равноценны изменениям, происходящим в интенсивностях полосы поглощения

карбонила. Комплексообразование приводит к смещению полосы ассиметричного валентного колебания С—О—С в сторону боле высоких частот (от 1220 $см^{-1}$ до 1290—1325 $см^{-1}$) вследствие индуктивного эффекта.

Разложение комплекса доказывается понижением интенсивности полосы поглощения С—О—С при 1325 $см^{-1}$ (рис. 9) и повторным появлением абсорбции при 1220 $см^{-1}$. Кинетическая кривая изменения интенсивностей полосы 1325 $см^{-1}$ имеет такой же вид, как и приведенные на рис. 8 данные для полосы 1679 $см^{-1}$.

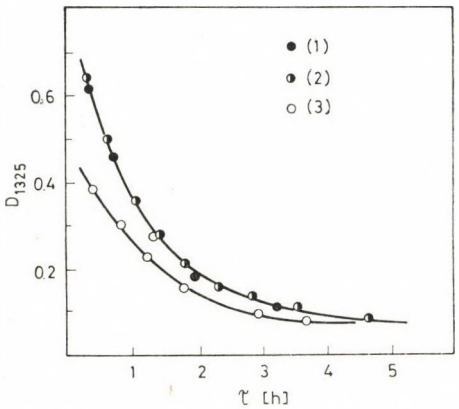

Рис. 9. Изменение оптических плотностей полосы при 1325 $см^{-1}$; молярное соотношение $VAc—AlEt_3$ 1 : 1 (1); 1 : 1,5 (2); 1 : 2 (3)

В области валентного колебания алкоксильной группы при комплексообразовании полоса поглощения в случае системы $VAc—AlEt_3$ смещается от 1145 $см^{-1}$ до 1123 и 1155 $см^{-1}$.

Изменение интенсивностей полос поглощения при 1325 (рис. 9) и 1123 — 1155 $см^{-1}$ (рис. 10) является функцией соотношения реагирующих веществ только при молярных соотношениях $VAc/AlEt_3 = 0{,}5$. При этом в дублете 1120—1155 $см^{-1}$ при $VAc/AlEt_3 = 1 : 1$ преобладает первая, а при $VAc/AlEt_3 = 1 : 2$ — последняя полоса.

Из экспериментальных данных следует, что период полураспада составляет примерно 60 минут, и к концу третьего часа комплекс данного строения почти полностью разлагается (рис. 10).

Полоса валентного колебания С = С в спектре комплекса при сравнительноя небольшом избытке алкила практически мало смещена по сравнению со спектром чистого винилацетата (от 1648 до 1640 $см^{-1}$). Однако ее полуширина значительно больше, повидимому, вследствие колебательного взаимодействия связей С = О и С = С.

Полоса валентного колебания при 1640 $см^{-1}$ в зависимости от молярного соотношения винилацетат-$AlEt_3$ в спектре комплекса появляется или в

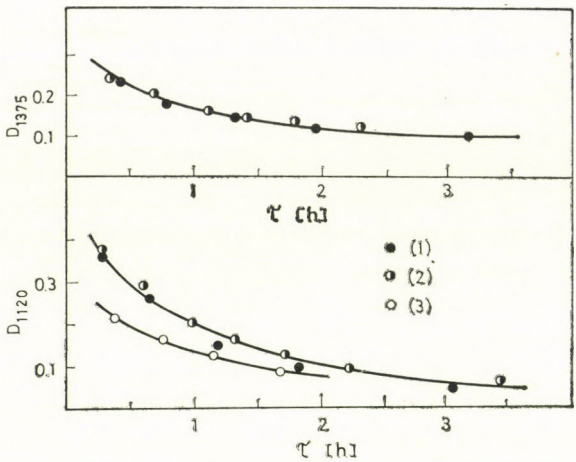

Рис. 10. Зависимость «оптическая плотность полос-время» (при 1375 и 1120 $см^{-1}$); молярное соотношение VAc—$AlEt_3$ = 1 : 1 (1); 1 : 1,5 (2); 1 : 2 (3)

виде плеча на полосе 1648 $см^{-1}$ или же как самостоятельная полоса средней интенсивности (при $VAc/AlEt_3 = 1 : 2$).

Дублет 1375—1390 $см^{-1}$ с образованием комплекса перегруппируется (рис. 10). Соответственно этому из двух полос преобладает последняя (1390 $см^{-1}$).

Область инфракрасного спектра 900—1000 $см^{-1}$ интерпретируется трудно, так как она сильно перекрыта полосами металл-алкила (как и в случае акрилонитрила).

Система метилметакрилат (MMA) — $AlEt_3$

Положение и отнесение некоторых полос в спектре метилметакрилата и его комплекса дано в таблице III. Кроме данных, приведенных в табл. III, в спектре находятся еще полосы поглощения с очень слабой интенсивностью

Таблица III

Метилметакрилат и его комплекс с $AlEt_3$

Метилметакрилат		Комплекс метилметакрилат-$AlEt_3$	
частота ($см^{-1}$)	отнесение полос ММА-а	частота ($см^{-1}$)	отнесение полос ММА-а
1725	ν (C = O)	1670	ν (C = O)
1640	ν (C = C)	1630	ν (C = C)
1445—1441	δ (CH_2)	1470—1455	δ(CH_2)
1328—1305	ν (C—O—C) ν_a (C—O—C)	1360—1340	ν (C—O—C) ν_a(C—O—C)
1203—1168	ν (C—O—C)	1245—1235 1190	ν (C—O—C)

при 990, 1380 и 1408 $см^{-1}$. Эти поглощения соответствуют деформационным колебаниям CH.

Полосы валентных колебаний C—C могут перегруппироваться в зависимости от соотношения компонентов.

ИК спектры метилметакрилата и его комплекса с $AlEt_3$ показан и на рис. 11.

С образованием комплекса метилметакрилат-$AlEt_3$ полоса валентного колебания C=O смещается от 1725 $см^{-1}$ в направлении более низких частот (1670 $см^{-1}$). В то же время полоса валентного колебания C—O смещается от 1168—1203 $см^{-1}$ в область более высоких частот (рис. 11). Картина совершенно аналогична комплексу винилацетат-$AlEt_3$. Все данные непременно означают, что при сливании растворов MMA и $AlEt_3$ быстро образуется комплекс, в котором металл-алкил координирован по карбонильной группе. Судя по величине смещения полосы валентного колебания C=O при комплексообразовании ($\sim$55 $см^{-1}$), кислотность $AlEt_3$ примерно такая, как у $AlMe_3$. Предполагаем, что основным продуктом взаимодействия MMA и $AlEt_3$ является комплекс, обладающий строением карбонил-металла следующего типа:

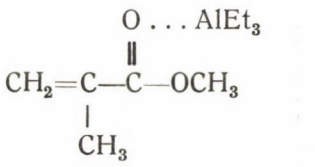

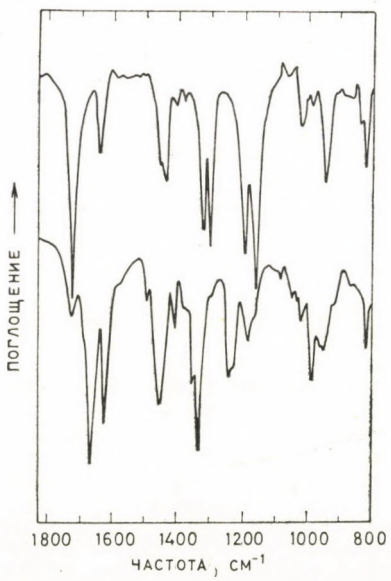

Рис. 11. Инфракрасный спектр метилметакрилата (верхний) и комплекса метилметакрилат-$AlEt_3$ (нижний)

Кинетические измерения показывают (рис. 12), что исходный комплекс нестабилен и медленно разлагается, хотя скорость его распада значительно меньше, чем в случае аналогичного комплекса $AlEt_3$—VAc. Со старением комплекса в спектре снова появляется полоса свободной карбонильной группы при 1725 $см^{-1}$. В то же время интенсивность полосы комплексного карбонила понижается (рис. 12). Устойчивость комплекса является функцией молярных соотношений ММА—$AlEt_3$. Стабильность увеличивается с понижением молярного соотношения ММА—$AlEt_3$.

Поскольку распад комплекса сопровождается с понижением интенсивности полосы валентного колебания C=C при 1630 $см^{-1}$ (рис. 13), можно предположить два пути разложения исходного комплекса (наряду с регенерацией некоторой части ММА).

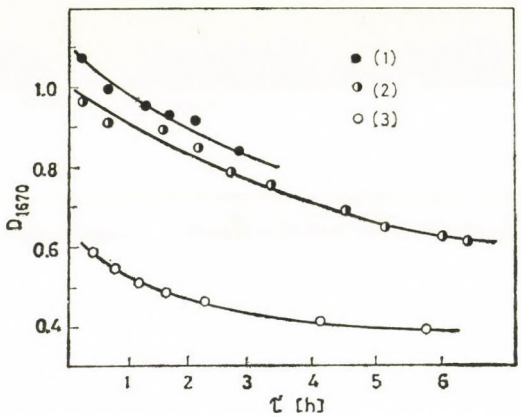

Рис. 12. Кинетика разложения комплекса по полосе поглощения при 1670 $см^{-1}$; молярное соотношение ММА—$AlEt_3$ = 1 : 1 (1); 1 : 1,5 (2); 1 : 2 (3); τ(h) — час

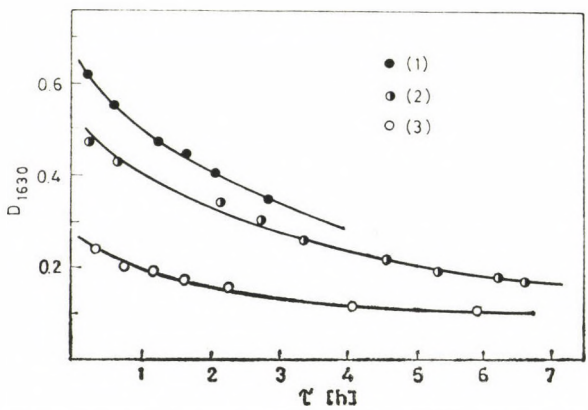

Рис. 13. Изменение оптической плотности полос при 1630 $см^{-1}$; молярное соотношение ММА—$AlEt_3$ = 1 : 1 (1); 1 : 1,5 (2); 1 : 2 (3)

1) Перегруппировка с разрывом C=O с образованием связи —O—Al (см. раздел «Система винилацетат-$AlEt_3$»). В пользу возможности такого процесса свидетельствует появление в спектре полосы 1055 $см^{-1}$ (рис. 14), которую можно отнести к колебанию группировки C—O—Al [37].

2) Полимеризация ММА или ее комплекса. В пользу возможности такого процесса свидетельствует появление новых полос поглощения в области 1700—1800 $см^{-1}$ (1705, 1740, 1770 $см^{-1}$) при длительной выдержке (21—26 часов) комплексов.

Изменения в интенсивностях валентных колебаний C=O соответствуют изменениям интенсивности полос C—O—C (рис. 14, 15). В то же время очень важно, что с образованием комплекса полоса группы C=O смеща-

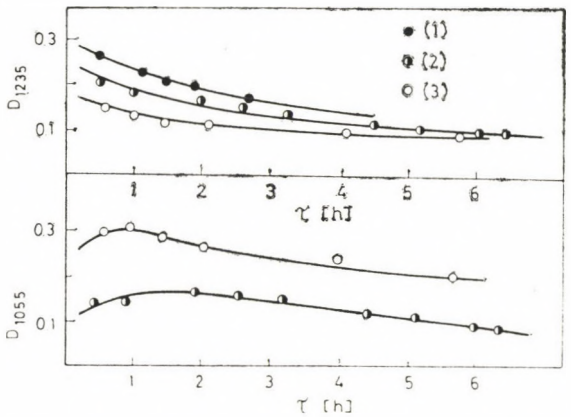

Рис. 14. Зависимость «оптические плотности полос-время» (при 1235 и 1055 $см^{-1}$), молярное соотношение ММА—$AlEt_3$ = 1 : 1 (1); 1 : 1,5 (2); 1 : 2 (3)

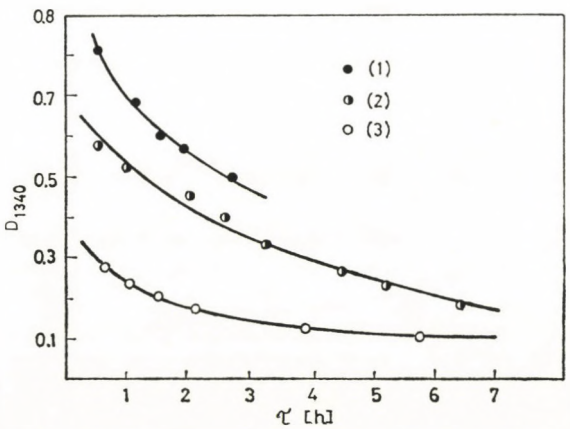

Рис. 15. Кинетика разложения комплекса по оптической плотности полосы при 1340 $см^{-1}$, молярное соотношение ММА—$AlEt_3$ = 1 : 1 (1); 1 : 1,5 (2); 1 : 2 (3)

ется в направлении более низких, а полоса группы C—O – в область более высоких частот (1190, 1235—45 и 1340—1360 $см^{-1}$). Можно утверждать, что скорость изменения интенсивности последних является функцией молярных соотношений исходных компонентов. Изменения особенно значительны в первые три часа реакции.

При молярных соотношениях компонентов ММА/$AlEt_3$ = 1 : 1 в дублете при 1235—1245 $см^{-1}$ преобладает последняя полоса. В случае избытка металл-алкила преобладает первая полоса. Контур дублета при 1340—60 $см^{-1}$ изменяется только при длительной выдержке комплекса.

Система акриловая кислота (АК)—$AlEt_3$

В таблице IV даны положения некоторых полос акриловой кислоты (АК) и ее комплекса с $AlEt_3$. Как видно, с образованием комплекса в инфракрасном спектре происходят значительные изменения (см. также рис. 16) Известно, что алюминийорганические соединения легко вступают в реакции взаимодействия с веществами, содержащими подвижные атомы водорода (вода, кислоты, спирты и т. д.). Эти реакции протекают с выделением углеводородов за счет расщепления связи Al—C [38]. В случае взаимодействия акриловой кислоты и $AlEt_3$ при молярном соотношении компонентов 1 : 1 можно ожидать протекания следующей реакции:

$$CH_2{=}CH{-}COOH + AlEt_3 \longrightarrow CH_2{=}CH{-}\overset{\overset{O}{\|}}{C}{-}O{-}AlEt_2 + C_2H_6$$

Анализ ИК-спектров подтверждает это предположение. При смешивании растворов акриловой кислоты и $AlEt_3$ из спектров исчезают полосы валентного колебания C=O кислоты в димерной форме при 1703 и 1720 $см^{-1}$, а также полосы валентного колебания C—O и деформационного колебания OH кислотной группы при 1300 и 1247 $см^{-1}$ [36]. Одновременно в спектре по-

Таблица IV

Акриловая кислота и ее комплекс с $AlEt_3$

Акриловая ;кислота		Комплекса акриловая кислота-$AlEt_3$	
частота ($см^{-1}$)	относение полос АК-ы	частота; ($см^{-1}$)	относение полос АК-ы
1720	ν (C = O)	1590—1568	$\nu_{as}(CO_2^-)$
1703	ν (C = O)		
1635	ν (C = C)	1645	ν(C = C)
1435	ν (C—O)	1470—1455	ν_s (CO_2^-)
1300—1247	ν (C—O) и δ (OH)		
1073 ⎫		1080 ⎫	
1050 ⎭	$\gamma_r(CH_2)$	1065 ⎭	$\gamma_r(CH_2)$

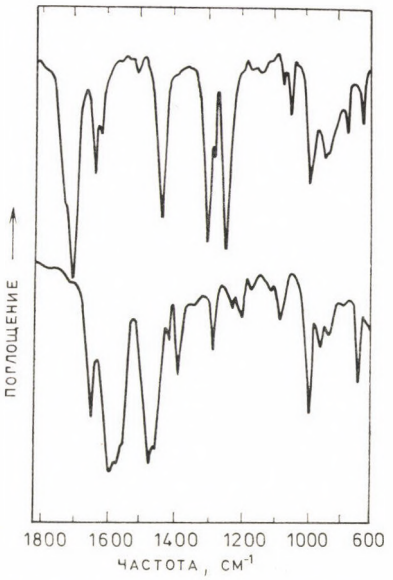

Рис. 16. Инфракрасный спектр акриловой кислоты (верхний) и комплекса акриловая кислота-$AlEt_3$ (нижний)

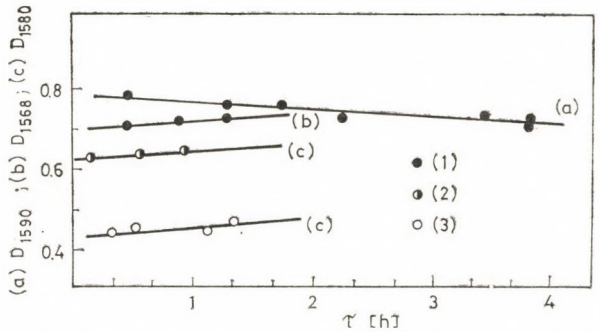

Рис. 17. Оптические плотности полос при 1590 $см^{-1}$ (a), 1568 (b) и 1580 $см^{-1}$ (c); τ(h) — час; молярное соотношение АК—$AlEt_3$ = 1 : 1 (1); 1 : 1,5 (2); 1 : 2 (3)

являются полосы колебаний иона: асимметричное валентное колебание COO^- при 1590—1568 $см^{-1}$ (рис. 17) и симметричное валентное колебание COO^- при 1470—1455 $см^{-1}$ [39, 40, 41] (см. рис. 16, 18). В то же время полосы колебаний двойной связи при переходе (практически) смещаются мало: для кислоты 1635 $см^{-1}$, для иона — 1645 $см^{-1}$ (рис. 16). Газохроматографические исследования также подтверждают вышесказанное предположение. При сливании растворов действительно было обнаружено выделение газа. С помощью газохроматографии было показано, что выделяющийся газ является этаном. В целом процесс взаимодействия и строение комплекса близки к

описанной в литературе системе $AlEt_2Cl$ — акриловая кислота [11, 41]. Интенсивность полосы поглощения при 1568—1590 $см^{-1}$ изменяется незначительно. В то же время интенсивность полос при 1470—1455, 1235, 1388 и 1645 $см^{-1}$ является функцией относительной концентрации мономера и металл-алкила. Последняя полоса (при 1645 $см^{-1}$) особенно сильна при молярном соотношении компонентов 1 : 1. Ее интенсивность при избытке металлалкила понижается.

При соотношении компонентов 1 : 1 продукт взаимодействия стабилен в течении более 4-х часов. За это время наблюдаются лишь слабые изменения в относительной интенсивности полос в области 1590—1560 $см^{-1}$: интенсивность полосы 1568 $см^{-1}$ незначительно возрастает (см. рис. 17), в то время, как двойная связь в продукте сохраняется.

В тех случаях, когда в смеси присутствует избыток металл-алкила (при соотношениях кислота: $AlEt_3$ = 1 : 1,5 и 1 : 2), в спектрах присутствуют интенсивные полосы при 1580 и 1470—55 $см^{-1}$, (рис. 16, 17, 18). Одновременно при 1415 $см^{-1}$ появляется новая полоса, интенсивность которой в случае $AK/AlEt_3 \geqslant 1$ значительна (рис. 18). Однако при этом резко понижается интенсивность полосы 1645 $см^{-1}$, что свидетельствует о протекании процессов с участием двойной связи. Низкая донорная активность связи $CH_2 = CH-$ делает маловероятной возможность образования стабильных комплексов типа $-CH = CH_2 \ldots Al$ [42]. Реакции алкилирования растворителя в данном случае также не протекают, так как в спектрах отсутствует полоса в области 800—820 $см^{-1}$, характерная для образующихся при алкилировании толуола пара-дизамещенных бензольных циклов [43].

Можно предположить, что исчезновение двойных связей при избытке $AlEt_3$ связано с реакцией полимеризации комплексированной акриловой кислоты (возможно, по анионному механизму). Интересно отметить, что при из-

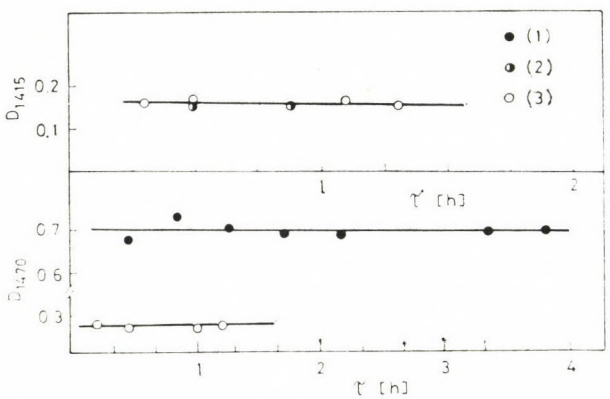

Рис. 18. Оптические плотности полос при 1415 и 1470 $см^{-1}$, молярное соотношение $AK-AlEt_3$ = 1 : 1 (1); 1 : 1,5 (2); 1 : 2 (3)

бытке алюминийорганического соединения в системе сохраняется часть исходных кислотных групп (около 10% от начальной концентрации кислоты), поглощающих при 1703 $см^{-1}$. В инфракрасном спектре акриловой кислоты полоса деформационного колебания CH находится при 1050 и 1073 $см^{-1}$.

С образованием комплекса (соотношение комплементов 1 : 1) появляется только единственная полоса при 1080 $см^{-1}$. Эта же полоса с увеличением относительной концентрации металл-алкила > 1 находится при 1065 $см^{-1}$.

Система акриламид (AA) — $AlEt_3$

Положения некоторых полос в спектре акриламида (AA) и его комплекса с $AlEt_3$ перечислены в таблице V. Исследование самого акриламида было проведено в твердом состоянии, так как мономер в толуоле не растворяется. При добавлении толуольного раствора металл-алкила к акриламиду, последний растворяется, и при этом происходят глубокие изменения и в спектре поглощения (рис. 19). Этот факт сам по себе говорит о комплексообразовании. Изменения в спектре намного значительнее того, чтобы объяснить это простым фазовым переходом. В спектре акриламида в области 1600—1700 $см^{-1}$ присутствуют две полосы большой интенсивности. Эти полосы сильно перекрыты другими поглощениями. Исходя из того положения, что во всех исследованных нами системах валентное колебание группы C = C находилось в области 1640—1670 $см^{-1}$, мы предполагаем, что и в случае системы акриламид-$AlEt_3$ поглощение непредельной связи C=C находится также в этой области. Это подтверждается и другим мнением [44]. Кроме того на примерах преды-

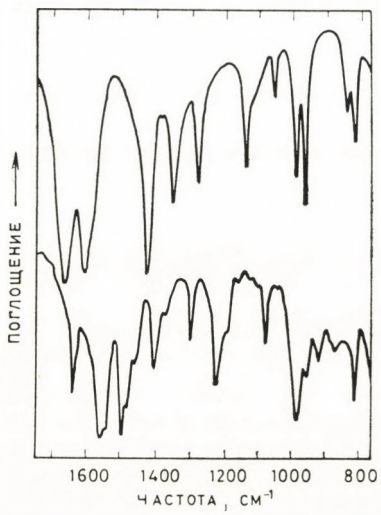

Рис. 19. Инфракрасный спектр акриламида (верхний) и комплекса акриламид-$AlEt_3$ (нижний)

дущих систем было показано, что при комплексообразовании полярных винилмономеров полосы, характеризующие полярные группы, сильно смещаются. В то же время полоса винильной связи смещается незначительно (8—10 $см^{-1}$). При комплексообразовании акриламид-$AlEt_3$ в области 1640—1670 $см^{-1}$ сложная полоса исчезает, и остается только одно самостоятельное поглощение средней интенсивности при 1650 $см^{-1}$. Исходя из этих соображений, можно предполагать, что в спектре комплексированного акриламида полоса при 1650 $см^{-1}$ характеризует группу C=C.

Таблица V

Акриламид и его комплекс с $AlEt_3$

Акриламид		Комплекс акриламид-$AlEt_3$	
частота ($см^{-1}$)	отнесение полос АА-а	частота ($см^{-1}$)	отнесение полос АА-а
1680—1670—1660	амид I и ν(C = C)	1650	ν(C = C)
1615—1608	амид II	1580—1565	амид I
1430 1356	амид III		
995 967	$\gamma_{\omega}(CH_2)$	1000 960	$\gamma_{\omega}(CH_2)$
		2305—2285 2275 2225	ν(CN)

Молекула акриламида как и молекула акриловой кислоты, содержит подвижный атом водорода. Значит в этом случае также наиболее вероятна реакция с разрывом связи Al—C.

В ИК спектре продукта взаимодействия при соотношении компонентов АА—$AlEt_3$ 1 : 1; 1 : 1,5; и 1 : 2 отсутствуют характерные для спектра кристаллического акриламида полосы амид I при 1670 $см^{-1}$ и амид II при 1615 $см^{-1}$. В то же время появляются интенсивные широкие полосы при 1580, 1505 и 1305 $см^{-1}$ (рис. 19), которые можно отнести к поглощению ациламидной группировки $CONH^- \ldots M^+$. Интенсивность последних полос поглощения меняется относительно незначительно (рис. 20—22).

Мера смещения полосы поглощения амид I при комплексообразовании является функцией молярных соотношений реагирующих компонентов. При небольшом избытке металл-алкила она смещается на 90 $см^{-1}$, а в случае $AA/AlEt_3 < 1$ на 105 $см^{-1}$.

При этом наблюдается значительное изменение и в интенсивностях.

Полосы колебаний винильной группы при взаимодействии акриламида и $AlEt_3$ смещаются мало: полоса валентного колебания C = C расположена

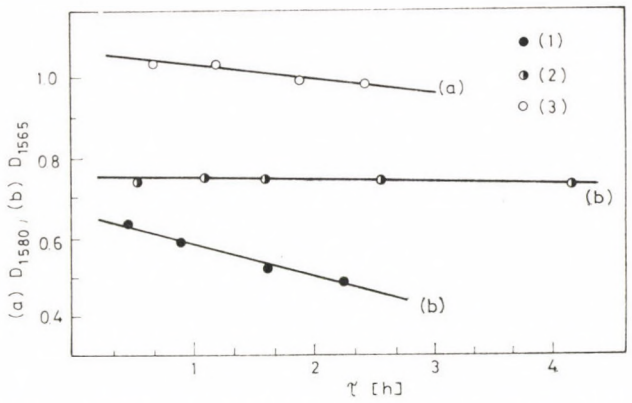

Рис. 20. Зависимость «оптическая плотность полос-время» (при 1565 и 1580 $см^{-1}$); молярное соотношение $AA-AlEt_3 = 1:1$ (3); 1 : 1,5 (2); 1 : 2 (1); τ(h) — час

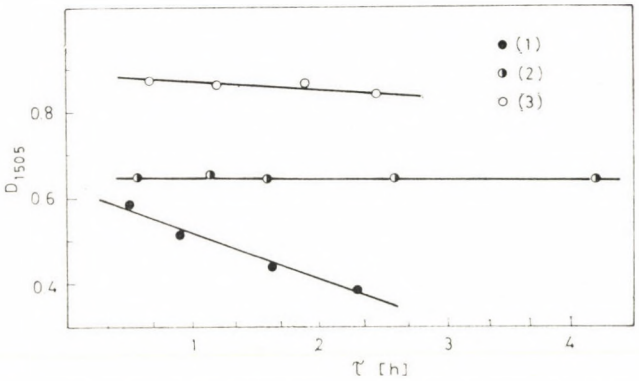

Рис. 21. «Оптическая плотность полосы при 1505 $см^{-1}$ — время»; молярное соотношение $AA-AlEt_3 = 1:1$ (3); 1 : 1,5 (2); 1 : 2 (2); τ(h) — час

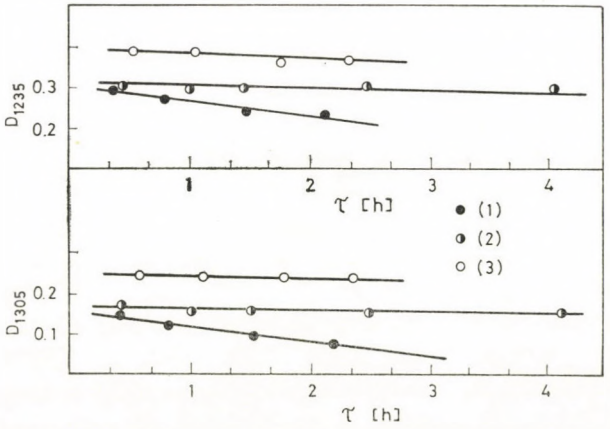

Рис. 22. «Оптическая плотность полос-время» (при 1235 и 1305 $см^{-1}$); молярное соотношение $AA-AlEt_3 = 1:1$ (3); 1 : 1,5 (2); 1 : 2 (1)

при 1650 $см^{-1}$ (в спектре акриламида 1660 $см^{-1}$), а полосы деформационных колебаний γ (CH) находятся в области 1000—960 $см^{-1}$ (в спектре акриламида 994 и 960 $см^{-1}$) [36].

Кроме того, газохроматографией было доказано, что при образовании комплекса выделяющийся газ является этаном. Эти данные позволяют предположить следующую реакцию в системе АА—$AlEt_3$ при соотношении компонентов 1 : 1:

$$CH_2{=}CHCO{-}NH_2 + AlEt_3 \longrightarrow CH_2{=}CHC(=O){-}H{-}AlEt_2 + C_2H_6$$

В соответствии с кинетическими измерениями в отсутствии избытка $AlEt_3$ продукт устойчив в течение нескольких часов.

При данных соотношениях (1 : 1) компонентов полоса колебания свободной амидной группы появляется снова в спектре только после 16—24 часов реакции. В небольшом избытке металл-алкила продукт также устойчив.

Интенсивности полос при 1507—1505 и 1305 $см^{-1}$, характеризующие группировки NH и CN, при образовании комплекса изменяются мало (рис. 21, 22).

В тех случаях, когда взаимодействие протекает в избытке $AlEt_3$, исходным продуктом являются также ациламидные соединения, однако полосы колебаний групп $CONH_2$ при этом смещаются дальше в направлении более высоких частот и расположены при 1565 и 1505 $см^{-1}$ (рис. 20, 21).

Скорость разложения комплекса увеличивается в присутствии значительного избытка металл-алкила. Так при молярном соотношении АА : $AlEt_3$ = 1 : 2 комплекс после 6 часов старения полностью разлагается (рис. 20—22).

Однако при этом в системе протекают дальнейшие химические превращения, сопровождающиеся частичным распадом ациламидной группы и образованием нитрильных групп, поглощающих при 2275, 2225 и 2300 $см^{-1}$ (рис. 23). Эти превращения не затрагивают винильной связи:

$$CH_2{=}CHCONH{-}AlEt_2 + AlEt_3 \longrightarrow$$

$$\longrightarrow CH_2{=}CH{-}C{\equiv}N \cdot AlEt_3 + Al \cdot \text{комплекс}$$

Поведение образующихся в этой реакции комплексов АА—$AlEt_3$ аналогично тому, которое наблюдается в системе AN—$AlEt_3$. В начале образуется комплекс, поглощающий при 2275 $см^{-1}$. Кривая оптических плотностей поглощений характеризуется максимумом, причем ход кривой не зависит от молярного соотношении компонентов. Предполагаем, что эта форма взаимодействия является донорно-акцепторной реакцией. Реакция осущест-

вляется благодаря свободной паре электронов атома азота (как и в случае акрилонитрила). Эта комплексная форма является нестабильной и одновременно переходит в комплекс, поглощающий при 2225 $см^{-1}$ (рис. 23).

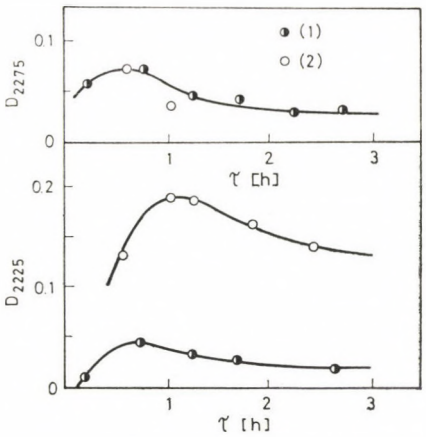

Рис. 23. Кинетика появления полосы поглощения при 2275 и 2225 $см^{-1}$; молярное соотношение АА—$AlEt_3$ = 1 : 1,5 (1); 1 : 2 (2)

При старении этот комплекс также разлагается и образовавшийся новый продукт поглощает при 2300 $см^{-1}$.

Обращает на себя внимание сходство взаимодействия АА—$AlEt_3$ и АК—$AlEt_3$. В реакцию вступают подвижные атомы водорода, входящие в состав групп COOH или NH_2.

Полосы деформационных колебаний CH расширяются, их интенсивность уменьшается. Полосы частично прекрыты полосами деформационных колебаний металл-алкила.

Выводы

Смещение полосы валентных колебаний C ≡ N в сторону более высоких частот при комплексообразовании акрилонитрила — $AlEt_3$ свидетельствует о том, что комплекс в первую очередь образуется за счет неподеленной пары электронов атома азота. Вероятность этого взаимодействия понижается при повышении реакционного времени и понижения молярного соотношения AN/$AlEt_3$. При увеличении времени реакции преобладает комплексообразование, в которое вовлечена и связь C = C.

В образовании комплекса винилацетат-$AlEt_3$ важную роль играет карбонильная группа. Определено, что стабильность взаимодействия является функцией молярного соотношения мономера и металл-алкила. С понижением концентрации металл-алкила стабильность комплекса повышается.

В случае образования комплекса метилметакрилат-$AlEt_3$ взаимодействие компонентов происходит через группы C = O метилметакрилата. При молярном соотношении $MMA/AlEt_3 \geqslant 1$ стабилность комплекса повышается. С увеличением времени реакции и концентрации металл-алкила могут происходить и реакции переалкилирования.

При взаимодействии акриловой кислоты и акриламида с $AlEt_3$ в реакцию вступают подвижные атомы H. С понижением молярного соотношения $АК/AlEt_3$ стабильность взаимодействия понижается. Стабильность комплекса АА—$AlEt_3$ понижается с увеличением концентрации металл-алкила. Появление абсорбции при 2225 и 2275 $см^{-1}$ в инфракрасном спектре при относительно большом избытке металл-алкила доказывает преобладание донорно-акцепторного взаимодействия между компонентами и реакции, происходящей с образованием нитрильной группы.

Из приведенных данных видно, что все исследованные виниловые мономеры вступают в энергичные реакции с $AlEt_3$. Первичные продукты этих взаимодействий стабильны в течении нескольких часов лишь при отсутствии избытка алюминийорганического соединения. Поскольку обычно реакция сополимеризации виниловых мономеров и олефинов проводится в условиях, когда концентрация винилового мономера ниже, чем концентрация $AlEt_3$ [1, 2], необходимо принимать во внимание также возможность дальнейших химических превращений в реакционной смеси, которые либо выводят часть винилового мономера из сферы реакции сополимеризации вследствие расхода двойных связей, либо приводят к образованию комплексов новых виниловых мономеров.

Summary

The formation of vinylmonomer — $AlEt_3$ complexes was investigated by IR Spectroscopy.

A shift in the position of the ν C ≡ N band due to the formation of acrylonitrile — $AlEt_3$ complexes proves the predominance of donor — acceptor interactions in this reaction. The contribution of this interaction, however, decreases with increasing $AN/AlEt_3$ ratio. If the reaction-time is longer, the C = C bonds also take part in the formation of complexes.

The carbonyl group plays an important role in the formation of vinyl acetate — $AlEt_3$ complexes. It was found that the stability of this interaction decreases as the molar ratio of the $AlEt_3$ increases.

In the case of methyl methacrylate — $AlEt_3$ complexes the C = O group of the MMA is responsible for the interaction. The complex showed greater stability when the $AlEt_3/MMA$ molar ratio was less than one. In the case of prolonged reaction-time or greater $AlEt_3$ concentrations an exchange of the alkyl groups might occur.

The analysis of the IR spectra of acrylic acid and $AlEt_3$ mixtures showed that the formation of complexes is due to the mobile H atoms. The stability of this interaction as well as that of the acryl amide — $AlEt_3$ complexes was higher at smaller $AlEt_3$ molar ratios.

The appearence of bands at 2225 and 2275 cm^{-1} (at relatively high $AlEt_3$ concentrations) proves the existence of the donor — acceptor interaction and the increased formation rate of nitrile groups.

Each vinyl monomer investigated was found to react readily with $AlEt_3$ and the primary products were stable for hours if no $AlEt_3$ surplus existed. As this latter condition is not fulfilled for most industrial processes, the possibility of secondary reactions should also be taken into consideration. In the course of these secondary reactions the vinyl groups for new types of complexes or have no contribution at all.

Литература

[1] Матковский, П. Е., Киссин, Ю. В., Чирков, Н. М., и др., Изв. Акад. Наук СССР, сер. хим., **6,** 1311 (1970)
[2] DANKOVICS, A., KISSIN, JU. V., SZÖLLŐSI, I.: J. Polym. Sci., Symp. No. **42,** 497 (1973)
[3] DANKOVICS, A., KISSIN, JU. V.: Acta Chim. Acad. Sci. Hung., **86,** 3, 307 (1975)
[4] DANKOVICS, A.: J. Polym. Sci., Symp. No. **42,** 487 (1973)
[5] TASUKA, S., TSUYI, K.: J. Phys. Chem., **71,** 2957 (1967)
[6] YAMAMOTO, S., ISHII, K.: J. Polym. Sci., A—1, **7,** 1577 (1969)
[7] GAYLORD, N. G., ANTROPIUSOVA, H.: J. Polym. Sci., B, **8,** 183 (1970)
[8] HIROOKA, M., YABUUCHI, H., MORILA, S.: J. Polym. Sci., B, **5,** 47 (1967)
[9] GAYLORD, N. G., TAKAHASHI, A.: J. Polym. Sci., B, **6,** 743 (1968)
[10] Куликова, В. П.: Высокомол. соед. А, **9,** 229 (1967)
[11] MATSUMURA, K., FUKUMOTO, O.: J. Polym. Sci., A—1, **9,** 471 (1971)
[12] ALLEN, P. E. N., CASEY, B. A.: Eur. Polym. J., **6,** 793 (1970)
[13] Лачинов, М. В., Зубов, В. П.: Высокомол. соед. Б. **12,** 4 (1970)
[14] KOMA, Y., KONDO, S., IIMURA, K.: J. Polym. Sci., Polym. Letter Ed., — в редакции
[15] Харламова, К. Н.: Ж. общей химии, **37,** 303 (1967)
[16] Голубов, В. Б., Зубов, В. П.: Высокомол. соед. А, **11,** 2689 (1969)
[17] TASUKO, S., OKAMURA, S.: J. Polym. Sci., B, **5,** 95 (1967)
[18] Кукушкин, Ю. Н.: Ж. неорг. хим., **12,** 1090 (1967)
[19] YAMAMOTO, A., IKEDA, S.: J. Am. Chem. Soc., **89,** 5989 (1967)
[20] KATO, A., ABE, I., KEII, T.: Nippon Kagaku Aishi, **1,** 893 (1973)
[21] KURAN, W., FASYNKIEWICH, S.: J. Organometal Chem., **23,** 343 (1970)
[22] NOVAKOVSKA, M.: Polymery, **9,** 516 (1964)
[23] Матковский, П. Е., Леонов, И. Д., Киссин, Ю. В., Чирков, Н. М.: Изв. Акад. Наук СССР, сер. хим., **4,** 930 (1968)
[24] HIROOKA, M., YABUUCHI, H., ISEKI, J., NAKAI, Y.: J. Polym. Sci., A—1, **6,** 1381 (1968)
[25] FURUKAWA, J., ISEDA, I., KOBAYASHI, E.: J. Polym. Sci., B, **8,** 631 (1970)
[26] FURUKAWA, J., ISEDA, I., KOBAYASHI, E.: Polym. J., **2,** 337 (1971)
[27] ALLEN, P. E. N., CASEY, B. A.: Eur. Polym. J., **2,** 9 (1966)
[28] Михайлов, М., Потапова, Т. В.: Изв. Акад. Наук СССР, сер. хим., **6,** 1153 (1968)
[29] IMOTO, M., OTSU, T.: Makromol. Chem., **65,** 194 (1964)
[30] FRITZ, H. P., SCHRAUZER, G. N.: Chem. Ber., **3,** 650 (1961)
[31] SCHRAUZER, G. N.: J. Am. Chem. Soc., **81,** 5310 (1959)
[32] Быстров, Д. Ц.: Ж. структурной хим., **4,** 548 (1963)
[33] Быстров, Д. Ц.: Ж. структурной хим., **4,** 691 (1963)
[34] Дембицкий, А. Д.: Опт. и спектр., **12,** 369 (1962)
[35] FASYNKIEWICH, S., STAROWIEYSKI, K.: Roczn. Chem., **41,** 1139 (1967)
[36] WALTON, W. L., HUGES, R. B.: J. Am. Chem. Soc., **79,** 3985 (1957)
[37] Сахаровская, Г. Б., Корнеев, Н. Н., и др.: Ж. общей хим., **39,** 788 (1969)
[38] Несмеянов, А. Н.: Методы элементоорганической химии, Наука, Москва (1964)
[39] Беллами, Л. А.: Инфракрасные спектры сложных молекул, Ин. Лит., Москва (1963)
[40] FLETT, M. S. C.: J. Chem. Soc. London, **1951,** 962
[41] NAKAMOTO, K.: Infrared Spectra of Inorganic and Coordination Compounds. Wiley, 1963
[42] ZIEGLER, K., KROLL, W. R.: Ann. Chem., **629,** 53 (1971)
[43] Сахаровская, Г. Б., Корнеев, Н. Н.: Промышленный синтез каучука, **11—12,** 6 (1969)
[44] HOLLY, S., SOHÁR, P.: Infravörös spektroszkópia. Műszaki Könyvkiadó, Budapest, 1968

Antal DANKOVICS H-1950 Budapest, Hungária krt. 114.
László LENDVAI H-1388 Budapest, P. O. B. 88. NIMDOK
Ю. В. Киссин Институт Химической Физики АН СССР, Москва, Б-334, Воробьевское Ш.
István SZŐLLŐSI H-1502 Budapest, P. O. B. 31.

Acta Chimica Academiae Scientiarum Hungaricae, Tomus 103 (2), pp. 161—170 (1980)

INFLUENCE OF PHOTOGRAPHIC AND PHOTOMETRIC EFFECTS ON SPECTROGRAPHIC EVALUATION, IV*

STUDY OF THE SHAPE OF THE BLACKENING CURVE, RELATION OF PHOTOGRAPHIC AND PHOTOMETRIC FACTORS IN DENSITOMETRY OF LINE SPECTRA

GY. HELTAI,[1] K. ZIMMER,[2] M. MATHERNY[3] and K. FLÓRIÁN[3]

([1] Department of Chemistry of the University of Agricultural Sciences, Gödöllő, [2] Institute for Inorganic and Analytical Chemistry of Eötvös L. University, Budapest, [3] Department of Chemistry of Metallurgical Faculty of Technical University, ČSSR, Košice)

Received december 27, 1978

Accepted for publication April 3, 1979

The shape of the blackening curve is highly influenced by the scattered light of the microdensitometer. Its interfering effect can be neglected in continuous spectra, while at line spectra increases with the enhancement of γ-value and decrease of line breadth, respectively. In consequence of this, the linear section of the blackening curve of line spectra always declines applying conventional microdensitometer, *e.g.* type Zeiss G II. The effect of scattered light is decreased by fog density. At the application of *l*-transformation, the fog density can be taken into account by adjusting $S_F = 0$.

Introduction

The first paper of our series [2] was dealing with the factors influencing the results of density measurement in details. Differences found between densities measured with different types of microdensitometers are due partly to the different geometric settling of the measuring systems [3], partly to the systematic errors (scattered light, linearity fault of the photometric system) [4—8] of density measurement. The effect of the above factors may differ under various photographic conditions. Therefore, from the point of view of spectrographic practice, it is not sufficient to compare the differences of the density values, but the shape of the blackening curve should be determined under various circumstances. Since the shape of the blackening curve is determined primarily by photographic factors, thus the observed differences give informations regarding the relationships existing between photographic and photometric factors. Taking into account the differences of the blackening curves determined from continuous and line spectra [9, 10] coming from photographic and photometric effects, respectively, firstly the blackening

* Previous paper: K. FLÓRIÁN, GY. HELTAI, K. ZIMMER: Acta Chim. Acad. Sci.Hung. [1] Papers of this series are simultaneously published in Magyar Kémiai Folyóirat in Hungarian language.

curves of line spectra are investigated and following it the relationships existing between blackening curves of line and continuous spectra are discussed. In the course of these experiments, the most important parameters of the blackening curve, the values of γ, S_L and S_{LL} have been determined graphically, while values γ and k with the help of a computer program described in the previous paper of this series [1]. Present paper gives first a short comparison of blackening curves determined from line and continuous spectra, respectively, then examinations of blackening curves of line spectra carried out with the conventional C. Zeiss G II microdensitometer are reported. Primarily, the length $\Delta S_L = S_{LL} - S_L$ of the straight section of the blackening curve measured in density has been studied in function of the γ-value. According to former examinations, the difference ΔS_L was found to be about 1.25 density unit in the case of different types of emulsion [11, 12]. In contradiction to this, when applying modern microdensitometers of wide measuring range, it could be stated that the straight section of the blackening curve is often continued even to density 4.0 towards high densities. Further on, the decline of the blackening curve experienced at previous measurements was found to be not a property of emulsion, but it is owed to the systematic error caused by the scattered light falling onto the detector of the microdensitometer [6—8, 13, 14]. As densities higher than S_{LL} can not be used reliably for analytical chemical purposes, from practical point of view it is of utmost importance to state the limits of validity of the above regularity.

Effect of the type of spectrum

It is known that the shapes of blackening curves determined by line and continuous spectra, respectively, are differing [8, 9, 16] due to photographic effects — mainly to EBERHARD-effect [15]. The γ-value determined from continuous spectrum is lower than that obtained from line spectrum [10, 11, 17]. The two cases are, however, differing also from the point of view of photometry. When measuring density of background-free spectral lines, the transparent surroundings of the spectral line does not impede the scattered light to reach the detector. On contrary in the case of continuous spectrum, the direct environment of the measured surface is acting like a filter, which weakens the scattered light proportionally to the transmittance measured and considerably decreases its interfering effect. In Table I. values γ, S_L, S_{LL} and ΔS_L determined at wave-length 300 nm on the basis of continuous spectra of a deuterium spectral lamp and of background-free iron spectra produced by d.c. arc excitation are shown. The spectra were recorded on the same spectral plate type Agfa-Gevaert 23 D 56 with the help of spectrograph Q 24. Photometric evaluation was performed both by the conventional Zeiss G II

and the modern G II—MFKI microdensitometers. In the table, values of γ and S_L were determined by a computer program [1] and S_{LL} was determined graphically.

Table I

Parameters of blackening curves of line and continuous spectra, respectively, on spectral plate Agfa-Gevaert 23 D 56, at wave-length 300 nm

Microdensitometer	Type of spectrum	γ	S_L	S_{LL}	ΔS_L
Zeiss G II	line	1.98	0.57	1.80	1.23
	continuous	1.60	0.49	>2.50	>2.01
G II-MFKI	line	2.19	0.61	2.20	1.59
	continuous	1.63	0.44	>2.80	>2.36

The data of the table well represent that in the case of line spectra decline of the blackening curve at high densities appears even if applying microdensitometer of wide measuring range. Opposite with this, decline of blackening curve has not been observed even at the upper limit of the measurable values (about density 2.5) when using microdensitometer Zeiss G II. Similarly in the case of microdensitometer type G II—MFKI having wide measuring range, the density values to be measured did not reach the upper limit of the linear section of blackening curve.*

These observations also prove that decline of the blackening curve at high densities — is not owed to the saturation exposure of photographic emulsion, but to the scattered light disturbing the density measurement of spectral lines [6—8, 13, 14]. Simultaneously, it has also been justified that if measuring continuous spectra, the interfering effect of scattered light is considerably lower, and using microdensitometer of good quality, it is not significant.

Finally, it can also be observed that the relation $\Delta S_L \simeq 1.25$ is valid only at line spectra, in the case of microdensitometer type Zeiss G II.

Examination of blackening curve of line spectra by means of microdensitometer of conventional type

Blackening curves of spectral plates types ORWO WU3 and Agfa-Gevaert 23 D 50 have been examined in a wave-length range of 230—380 nm. By means of d.c. arc excitation iron spectrogram series were made varying

* In this case the upper limit of the measurable density has not been reached, since the exposure time necessary to this would last for several hours with the given deuterium lamp. In the practice, there is no need for so long exposure and measuring so high background density.

the illumination intensity of a PGS-2 grating spectrograph, in 1st order, the slit width being 20 μm and using a three-step filter.

The ORWO WU3 plates by ORWO F43, while Agfa-Gevaert 23 D 50 plates were developed by Agfa 1 developer. In the above way practically background-free line spectra have been obtained in the examined range of wavelength excluding the glowing electrode tips during the illumination. The slit width of the microdensitometer was set to correspond to the 2/3 of the slit width of the spectrograph. Values S_L and S_{LL} determined at different wavelengths were plotted against their corresponding γ-values (Figs 1 and 2). It can be seen well in the figures, that at spectral plate type 23 D 50 the values of S_L and S_{LL} are increasing practically proportionally with the increase of γ-value, their average difference is $\Delta S_L \cong 1.20$. At plate type WU3, this is true only if $\gamma > 1.4$. If γ is lower than 1.4, S_{LL} and ΔS_L increase significantly. The difference can be understood when considering the fact that in the case of plate type 23 D 50 the γ-values are generally higher than 1.4, only the lowest value falls near to 1.4. Concluding the experimental results, it can be stated that rule $\Delta S_L \cong 1.25$ is valid even for line spectra, if the γ-value is higher

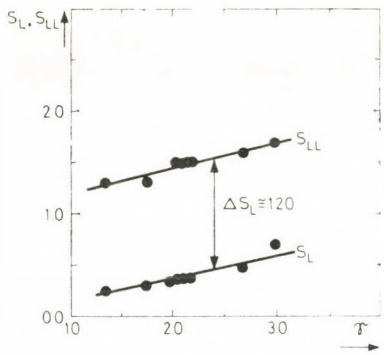

Fig. 1. Change of values S_L and S_{LL} in function γ-value on spectral plate type Agfa-Gevaert 23 D 50

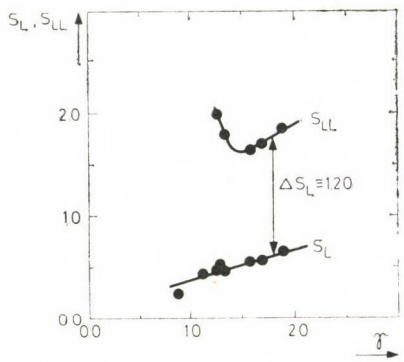

Fig. 2. Change of values S_L and S_{LL} in function of γ-value on spectral plate type ORWO WU3

than a certain limit (in present case this is 1.4) and if applying conventional microdensitometer type Zeiss G II. It is also reasonable that by further increasing the γ-value, above relation can hold only until the value of S_{LL} does not reach density 2.0, where the measurements are considerably interfered by the scattered light as proved by our examinations [2]. In the case of plate type Agfa-Gevaert 23 D 50 this upper limit of γ-value is about 3.0.

Generally in the basis of the above results it can be concluded that degree of interfering effect of the scattered light occurring in the microdensitometer is influenced by the γ-value. Therefore the decline of the blackening curve in function of γ-value begins at different densities. Consequently, because the γ-value is depending on the wave-length, thus S_{LL} is also changing with the wave-length.

Influence of the γ-value is probably caused by the connection between the line profile and γ-value. Increasing the γ-value the contour sharpness of the lines increases and the photographic width of the lines decreases. In this way, a higher quantity of scattered light may reach the detection system from the vicinity of the line, thus the blackening curve declines at lower density. This supposition provides an explanation for the decrease of S_{LL} values when increasing the γ-value, in the case of small γ-value (at $\gamma < 1.4$).

To support this idea, the density profile of an iron spectral line of wavelength 348 nm was determined by measuring the densities μm by μm both on an ORWO WU3 ($\gamma = 1.60$) and an Agfa-Gevaert 23 D 50 ($\gamma = 2.67$) spectral plate, respectively. The density value corresponding to the peak height of the line was found to be approximately similar in both cases, about 1.80 (Fig. 3).

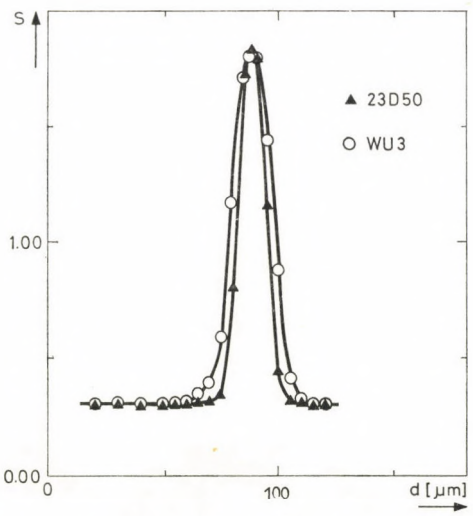

Fig. 3. Density profile of an iron spectral line of wave-length 348 nm, photographed on spectral plate type ORWO WU 3 and Agfa-Gevaert 23 D 50, respectively

However, if the γ-value is higher than 1.4, the value of S_{LL} starts to augment simultaneously with that of S_L. This fact can probably be explained so that the increase of the contour sharpness is counterbalanced by other photographic factors. Namely, the γ-value increases in function of wave-length especially above 300 nm. Whereas simultaneously with this, the absorptivity of silver halides decreases, so the photons of the illuminating light are able to enter even the deeper layers of the emulsion. In consequence of this, the density of spectral lines is formed in the more and more thick layers of the emulsion, and the photographic width of lines also increases in a small degree. Both phenomena reduce the quantity of the scattered light falling onto the detector, what explains the slow increase of S_{LL}.

Accordingly, the γ-value of the photographic emulsion influences the shape of the density profile, the photographic width and depth of the spectral line in the emulsion. At density measurement above factors influence the quantity of scattered light coming from the vicinity of the line and falling onto the detector and through this the value of density measured and the shape of blackening curve, too. If comparing Figures 1 and 2 it can also be assumed that the contour sharpness of the lines is the decisive factor. In the case of spectral plate type ORWO WU3 having averagely lower γ-value, the values of S_{LL} are always higher than at plate type Agfa-Gevaert 23 D 50 having relatively higher γ-value. The smaller is the γ-value, the less is the interfering effect of the scattered light. $\Delta S_L \cong 1.25$ is a rule which is valid only within certain limits of γ-value and is characteristic of the effect of the scattered light in the case of microdensitometer type Zeiss G II.

In the case of a given radiation source the shape and width of spectral lines are first of all determined by the way of light dispersion. It has also been shown, however, that the photographic shape is also dependent on the properties of emulsion. These factors influence the quantity of the scattered light reaching the detection system when measuring the density of the spectral lines. Beside this, one has to take into consideration the value of the slit width of the microdensitometer, too. These effects are represented by data of Table II. The table contains the results of evaluation of iron spectra obtained by various types of light dispersion (grating in 1st and 2nd order, and prism), measured with microdensitometer of different slit width at a wave-length of 300 nm. In addition to symbols already defined [1], d_{sp} means the slit width of the spectrograph, while d_m that of the microdensitometer. δS (2.0) denotes the deviation of the Churchill preliminary curve from the straight line of 45° representing the correct values, at an abscissa value of 2.0, in the direction of the ordinate [1].

This latter value demonstrates the interfering effect of the scattered light when using the same spectrograph and step filter. On the basis of the data of Table II it is clear that by increasing the slit width of the spectrograph and

Table II

Parameters of blackening curves of line spectra, determined under various conditions of recording at wave-length 300 nm

Spectral plate	Spectrograph (order of spectrum)	d_{sp}	d_m	γ	k	S_L	S_{LL}	ΔS_L	$\delta S(2.0)$
23 D 50	PGS—2 1st order	20 μm	2/3 d_{sp}	2.00	0.17	0.34	1.55	1.21	0.22
			1/3 d_{sp}	2.20	0.16	0.35	1.65	1.30	0.15
23 D 50	PGS—2 1st order	40 μm	2/3 d_{sp}	2.22	0.16	0.36	1.70	1.34	0.09
			1/3 d_{sp}	2.32	0.18	0.41	1.75	1.34	0.06
23 D 50	1st order PGS—2 2nd order	20 μm	2/3 d_{sp}	2.05	0.17	0.35	1.50	1.20	0.23
			2/3 d_{sp}	2.20	0.20	0.44	1.60	1.21	0.11
23 D 56	Q—24	20 μm	2/3 d_{sp}	1.97	0.29	0.57	1.80	1.23	0.07

reducing that of the microdensitometer, the effect of the scattered light can be decreased in a small degree. Similarly little change is caused by decreasing the slope of the line density contour according to data concerning the spectra of 1st and 2nd order. It is also observable that at light dispersion with prism the interfering effect of the scattered light is less than in the case of applying grating light dispersion operating with identical slit width of the spectrograph. Primarily this is due to the greater line width. In summary it can be established, too, that the effect of above factors can be detected, although it is not significant. Consequently rule $\Delta S_L \cong 1.25$ is valid within the limits of experimental errors, assuming if the γ-value falls into the range determined previously.

Examinations described so far related to spectra essentially without fog and background density. It can, however, be supposed that intensity of the scattered light is weakened by the fog or background density of the direct vicinity of the line and so its interfering effect is reduced. Naturally at the same time photographic effects also influence the shape of blackening curve. Further on, only the effect of fog density will be discussed. Impact of background density will be treated in a following publication.

Similarly to the first and second figures in Figure 4 values of S_L and S_{LL} are plotted against the γ-value, obtained on a spectral plate type Agfa-Gevaert 23 D 50 stored for a longer period of time, having fog density $S_F \cong 0.25$. The photometric evaluation was performed on two ways. Firstly, as in general the $S = 0$ density value was adjusted at the unexposed spot of the photographic emulsion, *i.e.* $S_F = 0$. Secondly, the emulsion was removed from

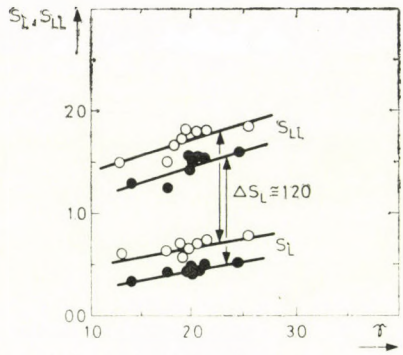

Fig. 4. Change of values S_L and S_{LL} in function of γ-value on spectral plate type Agfa-Gevaer 23 D 50 havig fog density $S_F \cong 0.25$; by adjusting the density zero point in two different ways

some mm² area of the plate and $S = 0$ value was adjusted on the clear glass plate. The figure unambiguously proves that the fog density reduces the amount of scattered light. By the usual way of photometry, curves practically similar to those seen in Fig. 1 are obtained. In the second case, however, values of S_L and S_{LL} equally moved into the direction of higher densities to an extent corresponding to S_F fog density. In this case, the upper limit of the reliably measured densities is greater with the value of fog density. At the same time, however, because of the similar increase of S_L values rule $\Delta S_L \cong 1.25$ held its validity.

According to earlier examinations, the *l*-transformation can be applied even at relatively high fog density, but in this case the range of density suitable for the analysis is more narrow [18]. From practical point of view it bears also importance that from among the two methods of adjusting the zero point which produces such density values for those the *l*-transformation is valid. It is well seen that the difference between density values measured on two different ways are equal to fog density S_F. Accordingly, the adjustment of zero point does not influence the γ-value, while it increases the k-value with $s_F = \dfrac{S_F}{\gamma}$ value corresponding to the reduced fog density. On the basis of the above and the definition of *l*-transformation [19] it may be proved that *l*-values calculated from densities measured on two ways can be identical only if $S_F = 0$. It is similarly conceivable that Δl-values belonging to given differences ΔY are equal only if $S_F = 0$. Thus *l*-transformation cannot produce correct results in both cases, when the fog density is not negligible. In Table III γ- and k-values determined with iteration accuracy of 0.001 from density values measured on two way, as well as standard deviation $s_{\Delta l}$ of Δl-values belonging to the two steps of the step filter are demonstrated. It can be seen that correct results can be obtained by *l*-transformation, if at density measurement density $S = 0$ is adjusted to fog density. When this can not be solved

Table III

Change of values γ, k and $s_{\Delta l}$ in function of wave-length, when density $S = 0$ was adjusted to fog density and glass plate, respectively, on spectral plate type Agfa-Gevaert 23 D 50

λ nm	$S = 0$ adjusting to fog			$S = 0$ adjusting to glass		
	γ	k	$s_{\Delta l}$	γ	k	$s_{\Delta l}$
235	1.30	0.25	0.0060	1.41	0.57	0.0241
240	1.77	0.24	0.0072	1.77	0.45	0.0260
250	2.08	0.21	0.0044	2.08	0.38	0.0197
270	2.02	0.21	—	1.93	0.37	0.0197
300	2.00	0.23	0.0070	1.93	0.44	0.0281
320	1.99	0.22	0.0067	1.96	0.41	0.0220
332	2.14	0.23	0.0068	2.15	0.51	0.0396
348	2.46	0.21	0.0177	2.55	0.47	0.0342

because of the too high fog density, value $S = 0$ can be adjusted also on the glass plate free of emulsion. In this case, however, l-transformation should not be performed with densities measured, but with that corrected by fog $S' = S - S_F$. Thus, definition of l-transformation is to be modified according to equation

$$l' = s' - (k - s')\, d'$$

where $s' = \dfrac{S'}{\gamma} = \dfrac{S}{\gamma} - \dfrac{S_F}{\gamma} = s - s_F$, and d' is the Gaussian difference logarithm belonging to s' [19]. Accordingly, reduced fog density s_F can be enrolled into among the constants of l-transformation

$$l' = s - s_F - (k - s + s_F)\,[s - s_F - \log (10^{s-s_F} - 1)]$$

Conclusions

The above results document that the scattered light occurring in the microdensitometer highly influences the shape of the blackening curve. The systematic error caused by the scattered light is significant mainly at photometric evaluation of line spectra, while at continuous spectra it can be neglected. In the case of measurement carried out by conventional Zeiss G II microdensitometer it was found that the straight section of the blackening curve of line spectra is always declining in the direction of high densities, while at continuous spectra this phenomenon cannot be observed at all up to the upper limit of measurable densities. In the latter case, namely, intensity of the scattered light is weakened by the light absorption of the vicinity of the surface measured.

The rule $\Delta S_L \cong 1.25$ related to the length of the straight section of the blackening curve is valid only within determined limits of γ-value, for blackening curves of line spectra obtained by means of microdensitometer type Zeiss G II. Influence of γ-value can be explained with the connection existing between the shape of the density line profile and γ-value. Every effect, decreasing the contour sharpness of spectral lines, or increasing the width of the line — reduces simultaneously the interfering effect of the scattered light, too. The interfering effect of the scattered light is similarly decreased by the fog- and backeground densities. In these cases, the amount of scattered light is reduced by he fog and background densities in the vicinity of the line. When fog density is occurring in a significant degree, it has to be taken into account also at employing the *l*-transformation. This can be solved either by adjusting density $S = 0$ to the fog, or if it is impossible (when the zero point was adjusted on a glass plate after removing the emulsion) the value of fog density should be subtracted from densities measured. In this last case, the reduced fog density s_F is counted to be also a transformation constant in addition to γ and k constants of *l*-transformation.

REFERENCES

[1] Flórián, K., Heltai, Gy., Zimmer, K.: Acta Chim. Acad. Sci. Hung. in press; Magy. Kém. Folyóirat, **85**, 271 (1979)
[2] Zimmer, K., Heltai, Gy.: Acta Chim. Acad. Sci. Hung. **100**, 319 (1979); Magyar. Kém. Folyóirat, **85**, 170 (1979)
[3] Callier, A.: Z. Wiss. Phot., **7**, 257 (1909)
[4] Schwarzschild, K., Viliger, W.: Astrophys. J., **23**, 284 (1906)
[5] Kántor, T., Erdey, L.: Acta Chim. Acad. Sci. Hung., **65**, 21 (1970)
[6] Török, T., Háfenscher, I.: Magy. Kém. Folyóirat, **84**, 183 (1978); Spectrochim. Acta, **33B**, 283 (1978)
[7] Heltai, Gy., Zimmer, K., Kozma, L.: Proc. XX. Annual Hung. Symp. on Spectral Analysis, Gyula, 1977, p. 19
[8] Zimmer, K., Heltai, Gy.: Spectrochim. Acta, **33B**, 417 (1978)
[9] Arrak, A.: Appl. Spectr., **16**, 124 (1962)
[10] Zimmer, K., Szabó, É.: Proc. 15th Coll. Spectrosc. Int., Madrid, 1969, Vol. IV. p. 55., Ibérica, Madrid, Tarragona (1970)
[11] Zimmer, K.: Dissertation D. Sc., Budapest, 1970
[12] Zimmer, K.: Proc. XI. Annual Hung. Symp. on Emission Spectral Analysis, Dunaújváros, 1968, p. 129
[13] Vecsernyés, L., Záray, Gy.: Proc. XV. Annual Hung. Symp. on Emission Spectral Analysis, Tatabánya, 1972, p. 155
[14] Vecsernyés, L., Záray, Gy.: Abstracts of Euroanalysis II. Budapest, 1975, 32
[15] Eberhard, G.: Physik. Z., **13**, 288 (1912)
[16] Strock, L. W.: J. Opt. Soc. Am., **32**, 103 (1942)
[17] Zimmer, K., Szabó, É.: Magy. Kém. Folyóirat, **77**, 198 (1971)
[18] Zimmer, K.: Bányászati és Kohászati Lapok — Kohászat, **104**, 445 (1971)
[19] Török, T., Zimmer, K.: Quantitative Evaluation of Spectrograms by Means of *l*-Transformation, ed. Akadémiai Kiadó, Budapest and Heyden and Sons London 1972

György Heltai H-2103, Gödöllő
Károly Zimmer H-1443 Budapest, P. O. B. 123.

Mikulaš Matherny
Karol Flórián } ČSSR-04385, Košice, Švermova 9.

Acta Chimica Academiae Scientiarum Hungaricae, Tomus 103 (2), pp. 171—179 (1980)

INFLUENCE OF PHOTOGRAPHIC AND PHOTOMETRIC EFFECTS ON SPECTROGRAPHIC EVALUATION, V*

INFLUENCE OF THE TYPE OF MICRODENSITOMETER ON THE SHAPE OF THE BLACKENING CURVE OF LINE SPECTRA AND ON THE EVALUATION PERFORMED BY *l*-TRANSFORMATION

GY. HELTAI[1] and K. ZIMMER[2]

([1] Department of Chemistry of the University of Agricultural Sciences, Gödöllő, [2] Institute for Inorganic and Analytical Chemistry of Eötvös L. University, Budapest)

Received December 27, 1978

Accepted for publication April 3, 1979

The shapes of blackening curves determined by microdensitometers of different type (modern and conventional, respectively) are different due to the scattered light having various intensity, and this difference rapidly increases in the function of density. Values γ, S_L and S_{LL} determined by instruments of different types are different. Using modern instruments containing little scattered light intensity, the upper limit S_{LL} of reliably measured densities is higher by density 0.5—1.5 than in the case of conventional instruments. Contrary to above differences, value k is independent on the type of instrument, and values Δl being equal to the logarithm of relative intensity values can be determined with the same accuracy, and even the l-values got by different instruments are approximately equal.

Introduction

Measuring with microdensitometers, the most significant source of systematic errors is the scattered light occurring in the instrument [2, 3]. Density is decreased by it, and also the highest value of measurable density is optically limited [2]. At the application of conventional microdensitometers the straight section of the blackening curve declines at high densities because of the interfering effect of the scattered light — the shape of the blackening curve becomes distorted [4—11]. Influence of the scattered light becomes significant, if its intensity is commensurable with the light intensity corresponding to the measurable density. However, its value is influenced also by the character of the measurable part of image and by the properties of photographic emulsion. It was shown that measuring continuous spectra, the error caused by scattered light can be neglected, while in the case of line spectra it has a significant effect [1, 10]. In the latter case, the upper limit of straight section

* Previous paper: GY. HELTAI, K. ZIMMER, M. MATHERNY, K. FLÓRIÁN, Acta Chim. Acad. Sci. Hung., **103,** 161 (1980).

Papers of this series are simultaneously published in Magyar Kémiai Folyóirat in Hungarian language.

of blackening curves determined by microdensitometer type Zeiss G II is in density range 1.5—2.0, and by increasing the γ-value, the interfering effect of scattered light increases, too. Owing to this fact, the earlier experienced regularity, according to which the length of the straight section of blackening curve measured in density is equal to $\Delta S_L = S_{LL} - S_L \cong 1.25$ [12, 13], is valid only within limited γ-values even if using the mentioned microdensitometer. The γ-value has, namely, an influence on the shape of the photographic line profil, and through this the quantity of scattered light getting to the detector [1].

According to former investigations [3, 7] intensity of scattered light getting onto the detector is different in various types of microdensitometers, thus its interfering effect is differing, too. As seen from above, these differences can be studied expediently by line spectra, and the influence of γ-value is also to be taken into account. In our present paper — considering above relationships — influence of the microdensitometer type upon the shape of the blackening curve, the length of the straight section and upon the shape of the *l*-transformed blackening curves are dealt with. From the point of view of spectrographic analysis these examinations bear of extreme importance in order to establish the upper limit of density — and corresponding of concentration range — reliably measured with the given type of microdensitometer. Further on, another important question is whether below these limits the systematic errors of density measurements have an influence on the analytical results or not, *i.e.* whether identical results are obtained by density transformation in the case of applying various types of microdensitometers.

Experimental

Background-free line spectra to these examinations have been produced as described in the previous paper of our series [1]: by d. c. arc excitation of iron electrodes, excluding the glowing electrode ends, varying the illumination intensity of a plane grating PGS 2 spectrograph of 20 μm slit width, applying a three-step filter. The series of spectrograms were recorded in first order on Agfa-Gevaert 23 D 50 and Agfa-Gevaert 34 B 50 spectral plates developed in developer Agfa 1. Spectrograms were evaluated at wave-length 300 nm by several microdensitometers of the same and different types. Thus, blackening curves determined under similar conditions could be compared beside γ-values $\gamma \cong 2.0$ (plate type 23 D 50) and $\gamma \cong 1.0$ (plate type 34 B 50). Measuring with conventional microdensitometer in the first case, the rule $\Delta S \cong 1.25$ was valid according to our experiences, while in the second case $\Delta S_L > 1.25$ [1].

Density of spectral lines falling into the wave-length range 300 ± 2 nm was measured on the filter steps of 100% and 50% transparency with the following eight microdensitometers: 3 Zeiss G II, 1 MF 2, 1 Joyce–Loebl MK III CS, 1 MF 2-MFKI (supplied with green glass pre-slit*), 1 MF 2-MFKI (with metal pre-slit*), 1 G II-MFKI (with metal pre-slit*). Taking into consideration the enlargement of instruments, the slit width was adjusted so, as to be equal to the 2/3 part of the slit-width of the spectrograph [15].

* The second paper of this series gives a picture on the modern photometric system and on the automated microdensitometer developed in the Research Institute of Technical Physics, Budapest [14]. Designation MFKI always indicates this kind of measuring system.

Results

From series of density value pairs measured by various microdensitometers firstly γ-value, S_L and S_{LL} densities belonging to the starting and finishing of the linear section of the blackening curve were determined by graphical preliminary curve method [16, 17]. Following this γ- and k-constants of l-transformation were determined by means of a computer program elaborated by us, with the help of value-pairs consisting of densities lower than the obtained density S_{LL} [18, 19], then value-pairs (l_a, l_b) belonging to density value pairs (S_a; S_b) their differences $\Delta l_{a,b}$, as well as the average $\overline{\Delta l}$ and standard deviation $s_{\overline{\Delta l}}$ of these latter values, have been calculated.

Experimental results are summarized in Tables I and II. In the tables values S_{LL} represent the results of the graphical determination.

On the basis of tables the following statements can be made:

a) The type of microdensitometer has considerable influence upon the shape of the blackening curve. Values of γ, S_L and S_{LL} parameters are different when using various types of microdensitometers. However, in the case of the three identical types Zeiss G II microdensitometers practically similar results were obtained. In agreement with earlier experiments of similar kind [4—7] it is well seen that — in the case of line spectra — the S_{LL} density the upper limit of the reliably measured densities is higher by 0.5—1.5 density unit at modern instruments of wide measuring range (Joyce-Loebl MK III CS, G II-MFKI) than at the conventional MF 2 and G II microdensitometers.

Table I

Parameters of blackening curves determined by means of various types of microdensitometers and the result of l-transformation, at wave-length 300 nm, using spectral plate type Agfa-Gevaert 23 D 50 ($\Delta Y_m = 0.289$)

Microdensitometer	γ	k	S_L	S_{LL}	ΔS_L	$\overline{\Delta l} \pm s_{\overline{\Delta l}}$
Zeiss G II 1.	2.12	0.18	0.39	1.55	1.16	0.290 ± 0.0076
2.	2.12	0.18	0.38	1.60	1.22	0.289 ± 0.0066
3.	2.02	0.17	0.34	1.55	1.21	0.289 ± 0.0090
MF 2	1.81	0.17	0.30	1.20	0.90	0.291 ± 0.0108
MF 2-MFKI green glass pre-slit	2.05	0.17	0.35	1.60	1.25	0.289 ± 0.0097
MF 2-MFKI metal pre-slit	2.37	0.18	0.42	1.90	1.48	0.288 ± 0.0098
G II-MFKI metal pre-slit	2.38	0.18	0.42	2.10	1.68	0.288 ± 0.0107
Joyce—Loebl MK III CS	2.19	0.20	0.43	2.10	1.67	0.291 ± 0.0190

Table II

Parameters of blackening curves determined by means of various types of microdensitometers and the result of l-transformation, at wave-length 300 nm, using spectral plate type Agfa-Gevaert 34 B 50 ($\Delta Y_m = 0.289$)

Microdensitometer	γ	k	S_L	S_{LL}	ΔS_L	$\bar{\Delta l} \pm s_{\bar{\Delta l}}$
Zeiss G II 1.	1.05	0.41	0.43	2.00	1.57	0.288 ± 0.0127
2.	1.07	0.41	0.43	2.00	1.57	0.289 ± 0.0137
3.	1.07	0.39	0.42	2.00	1.58	0.289 ± 0.0151
MF 2	0.94	0.38	0.36	1.70	1.34	0.287 ± 0.0172
MF 2-MFKI green glass pre-slit	1.10	0.41	0.45	2.00	1.55	0.289 ± 0.0144
MF 2-MFKI metal pre-slit	1.17	0.40	0.47	—	—	0.289 ± 0.0149
G II-MFKI metal pre-slit	1.17	0.41	0.48	3.00	2.52	0.291 ± 0.0175
Joyce—Loebl MK III CS	1.14	0.52	0.60	3.00	2.40	0.289 ± 0.0217

These differences can, first of all, be explained by the various amount of scattered light in different types of microdensitometers. In Fig. 1 S_{LL} values obtained by different kinds of microdensitometers are demonstrated. The left-side columns present S_{LL} values got on spectral plate type 23 D 50 ($\gamma \cong 2.0$), while the middle columns show those got on plate type 34 B 50 ($\gamma \cong 1.0$). In the right-side S_{max} values, characteristic of the amount of the scattered

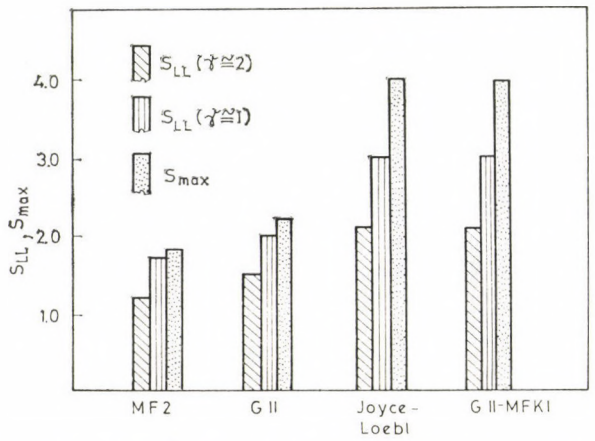

Fig. 1. S_{max} density values characteristic of the amount of scattered light and S_{LL} values obtained with microdensitometers of different types at different γ-values

light, are shown according to the results discussed in the first paper of our series [3]. One can well see, that the value of S_{LL} changes parallel with the amount of scattered light. It can also be observed that at each microdensitometer the density range measured without interference decreases when the γ-value is increased. The rule $\Delta S_L \simeq 1.25$ was found to be valid only in the case of microdensitometer type Zeiss G II within γ-values given earlier, in our case $\gamma \simeq 2.0$. At up-to-date instruments of wide measuring range the value of ΔS_L always exceeds 1.25.

b) The differences of γ-values can be explained by the differing amounts of scattered light. The differences of γ-values expressed in percent is practically the same in the case of both plates. Due to the differences of γ-values blackening curves obtained by various types of microdensitometers are divergent. When using microdensitometers types MF 2 and G II the γ-values are lower, and thus the blackening curves obtained by them lie below those got by instruments of wider measuring range (Joyce—Loebl MK III CS, G II-MFKI). These are represented in Figs 2a and b. In common ranges of reliably measurable densities by all microdensitometers determined by S_{LL}-value obtained with microdensitometer MF 2 of the narrowest measuring range, the average and standard deviation of densities measured by various microdensitometers, at the given spectral lines have been calculated. In the figures, standard deviation s_S of density values was plotted against the mean density $\bar{S}$. It is well seen that standard deviation of densities measured with various instruments rapidly increases in function of density, and in the vicinity of density 1.5—2.0 it even reaches the value ± 0.15. The deviations and accordingly the standard deviations, too, increase more rapidly in the case of plate of higher γ-value than lower γ-value.

c) In contradiction to above differences it is striking that the k-constant of l-transformation is practically equal at the various types of microdensitometers,* that is it does not depend on the type of instrument.

d) It was proved that l-transformation can be applied at each type of instruments separately with a suitable accuracy. The difference between filter constant ΔY_m and $\overline{\Delta l}$ average value is, in majority of the cases, equal to 0.001. Accordingly, a given logarithm intensity difference is corresponding to the same Δl-difference at each instrument.

e) The higher the γ-value, the more precise is the l-transformation. Namely, the standard deviation of measurement of a given density value with a microdensitometer can be regarded constant — disregarding the errors of

* One of the reasons for the difference experienced with the Joyce—Loebl microdensitometer is probably the uncertainty of the γ-determination. The automatic scanning provides no opportunity to correct the sharpness of the image. Eventual deterioration of sharpness leads in all cases to decreased γ-values, and gives rise to an increase in the standard deviation of the determination. The γ-value, being lower than the actual value, causes the value k to increase in accordance with the relationship $k = S_L/\gamma$.

development. Consequently, if γ-value is increased, the reduced density values and due to this the standard deviation of l-values decrease because of dividing by γ. In conformity with this, the average of standard deviations $s_{\overline{\Delta l}}$ obtained by different instruments on the spectral plate type 34 B 50 of lower γ-value, was found to be ± 0.0159, while on plate type 23 D 50 of higher γ-value ± 0.0104.

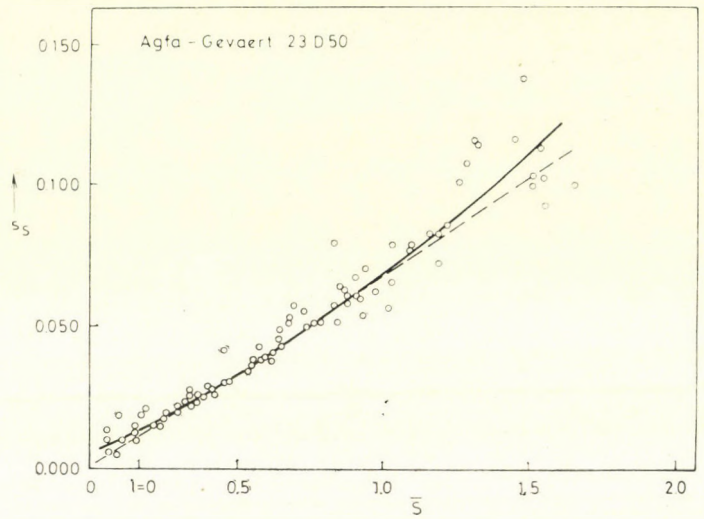

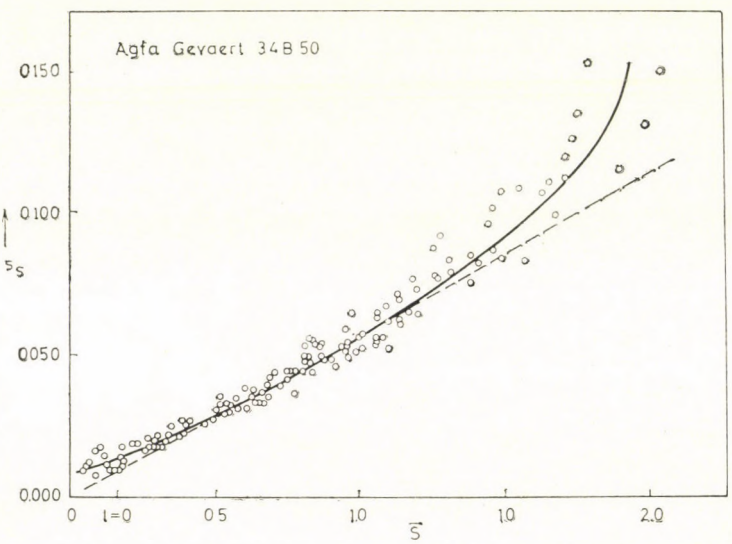

Fig2a and b. **Standard deviations s_S of densities measured by microdensitometers of different types in function of average density $\overline{S}$, in the case of spectral plates types Agfa-Gevaert 23 D 50 and 34 B 50, at wave-length 300 nm**

f) It was verified, too, that by applying l-transformation, not only the corresponding Δl-values are identical, but approximately identical l-values are obtained on the basis of densities measured with various microdensitometers. In Figures 3a and b standard deviation s_l of l-values determined with different types of microdensitometers at the single spectral lines, in function of $\bar{l}$ average value, was plotted. It can be seen that the standard

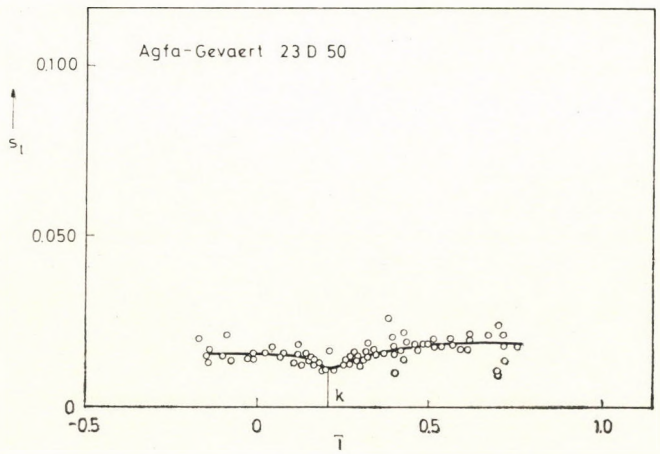

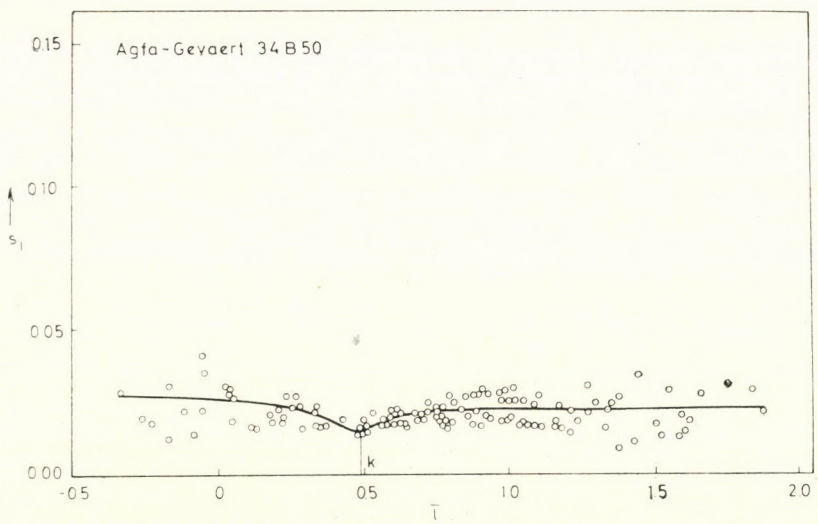

Fig. 3a and *b*. Standard deviation s_l of l-values determined by microdensitometers of different types in function of the average $\bar{l}$-value, in the case of spectral plates types Agfa-Gevaert 23 D 50 and 34 B 50, at wave-length 300 nm

deviation of l-values does not exceed: ± 0.030 in none of the cases, and in the vicinity of k-value, it is minimal. The standard deviations are lower in the case of higher γ-values. When using plate type 23 D 50, the standard deviation remains practically below ± 0.020, while at plate type 34 B 50 it falls between values ± 0.020 and 0.030.

Conclusions

The shape of blackening curve is influenced by the type of microdensitometer, too. In general, the density range reliably measured by the different types of microdensitometers is narrower than the total measuring range limited by the features of the instrument (stability, linearity, scattered light) [3]. The interfering effect of scattered light is minimal at continuous spectra [1], whereas in the case of line spectra it is increased by raising the γ-value. The differing intensity values of scattered light [3] result in different shapes of blackening curves in the case of various types of microdensitometers. The linear section of blackening curves determined by modern instruments containing little scattered light is considerably longer — by 0.5—1.5 unit — than in the case of conventional microdensitometer. The slope of the curves is also higher.

Limit value S_{LL} should always be given to the concrete experimental conditions in practical spectral analysis, since because of its dependence on γ-value, no data valid even for one instrument can be given. The maximal value of the concentration measurable with necessary accuracy is determined also by the value of S_{LL}. The value of S_{LL} can simply be determined by graphical preliminary curve method [16, 17, 18]. Although the blackening curves are divergent — as seen earlier — the l-transformation can be applied practically with similar accuracy in the same density range at each instrument. Using γ-values depending on the type of microdensitometer and k-values independent of this, not only the Δl-values corresponding to the given ΔY logarithm intensity difference, but also the l-values — *i.e.* the l-transformed blackening curves — determined by means of various microdensitometers are approximately identical. The higher are the γ-values and through it the accuracy of l-transformation, the less is the range of intensity measurable by photographic method and simultaneously the measurable concentration range.

In the case of density values lower than S_{LL}, when applying l-transformation and γ-values depending on the microdensitometer and k-values independent of it — analytical curves independent of the type of microdensitometer can be plotted. However, the upper limit of reliably measured densities is higher, and thus the measurable concentration range is wider in the case of up-to-date microdensitometers.

REFERENCES

[1] HELTAI, GY., ZIMMER, K., MATHERNY, M., FLÓRIÁN, K.: Acta Chim. Acad. Sci. Hung. **103,** 161 (1980) Magy. Kém. Folyóirat, **85,** 398 (1979)
[2] SCHWARZSCHILD, K., VILLIGER, W.: Astrophys. J., **23,** 284 (1906)
[3] ZIMMER, K., HELTAI, GY.: Acta Chim. Acad. Sci. Hung. **100,** 319 (1979); Magy. Kém. Folyóirat, **85,** 170 (1979)
[4] VECSERNYÉS, L., ZÁRAY, GY.: Proc. XV. Annual Hung. Symp. on Emission Spectral Analysis, Tatabánya, 1972, p. 155
[5] VECSERNYÉS, L., ZÁRAY, GY.: Abstracts of Euroanalysis II., Budapest, 1975, 32
[6] KÁNTOR, T., ERDEY, L.: Acta Chim. Acad. Sci. Hung., **65,** 21 (1970)
[7] TÖRÖK, T., HÁFENSCHER, I.: Spectrochim. Acta, **33B,** 283 (1978); Magy. Kém. Folyóirat, **84,** 183 (1978)
[8] HELTAI, GY., ZIMMER, K., KOZMA, L.: Proc. XX. Annual Hung. Symp. on Spectral Analysis, Gyula, 1977, p. 19
[9] HELTAI, GY., FLÓRIÁN, K., MATHERNY, M., ZIMMER, K.: Abstracts of 20th Coll. Spectrosc. Int., Prága, 1977, No 517
[10] ZIMMER, K., HELTAI, GY.: Spectrochim. Acta, **33B,** 417 (1978)
[11] HELTAI, GY., ZIMMER, K.: Proc. XXI. Annual Hung. Symp. on Spectral Analysis, Szeged, 1978, p. 51
[12] ZIMMER, K.: Dissertation D. Sc., Budapest, 1970
[13] ZIMMER, K.: Proc. XI. Annual Hung. Symp. on Emission Spectral Analysis, Dunaújváros, 1968. p. 129
[14] KOZMA, L.: Acta Chim. Acad. Sci. Hung., in press (IInd paper of this series)
[15] ZIMMER, K.: Proc. 14th Coll. Spectrosc. Int. Debrecen, 1967, Vol. I., 435. Hilger, London (1968)
[16] CHURCHILL, J. R.: Ind. Eng. Chem. Anal. Ed., **16,** 653 (1944)
[17] PLŠKO, E.: Chem. Zvesti, **23,** 150 (1969)
[18] TÖRÖK, T., ZIMMER, K.: Quantitative Evaluation of Spectrograms by Means of *l*-Transformation, ed. Akadémiai Kiadó, Budapest, and Heyden and Sons, London 1972
[19] FLÓRIÁN, K., HELTAI, GY., ZIMMER, K.: Acta Chim. Acad. Sci. Hung., in press (IIIrd paper of this series)

György HELTAI H-2103 Gödöllő.
Károly ZIMMER H-1443 Budapest, P. O. Box 123.

Acta Chimica Academiae Scientiarum Hungaricae, Tomus 103 (2), pp. 181—191 (1980)

STUDY OF THE GLYCOL—BORIC ACID COMPLEX FORMATION EQUILIBRIA IN AQUEOUS SOLUTION

T. L. PAÁL

(National Institute of Pharmacy, Budapest)

Received December 1, 1978

Accepted for publication April 6, 1979

The literature contains contradictory data on the formation and structure of neutral glycol—boric acid complexes. Liquid–liquid extraction is well suited for the investigation of these systems. The distribution of boric acid, further of electrolytes and neutral molecules in *n*-alcohol—water systems was investigated in detail, and from data measured in butanol—water system the stability constants of the boric acid complexes of D-sorbitol, D-mannitol, dulcitol and butane-1,3-diol were determined. The formation of the boric acid and borate complexes of butane-1,3-diol was investigated also by pH-metry. The formation of neutral boric acid complexes could not be detected in the case of ethylene glycol, propane-1,2-diol and glycerol. On the basis of the results, the formation equilibria of glycol—boric acid and —borate complexes are discussed.

It has been established a long time ago that the acidity of boric acid solution is increased by complex formation* with neutral di- and polyalcohols [1, 2]. However, even today there are many contradictions in the literature with respect to the reaction and the complexes formed. The most debated questions are the formation and the structure of 1,2- and 1,3-glycol—boric acids (Fig. 1) in aqueous solution, and the stability conditions of these and of the anion complexes.

Some authors presume also in aqueous solution the formation of glycol and bisglycol—boric acids, stronger acid than boric acid [7—13]. According to KALACHEVA *et al.* [10], the 1 : 1 complexes have a trigonal planar structure. ANTIKAINEN [11] assumed an equilibrium between the planar "pseudoacid" and the tetrahedral ion-pair, while others [12] for bisglycol—boric acids in chloroform the equilibrium among three complexes of different structure (Fig. 1). According to FISCHER and LOCHNER [13], in aqueous solution first planar, then by the uptake of one molecule of water tetrahedral glycol—boric

* Planar glycol—boric acids are called by several authors "esters", while glycol—borates of tetrahedral structure "complexes" [3—5]. Since boric acid is a Lewis acid, it is ionized by the uptake of hydroxide ion, but as up to pH 14 proton does not dissociate from its OH-groups (*i.e.* no $H_2BO_3^-$ is formed) [6], it can not be considered in aqueous solution as a H-acid, so that we think that this distinction is not necessary. Glycol—boric acids, which for that matter are formed and decomposed instantaneously, as contrary to esters, will be called in the following also complexes (*e.g.* [1,3-alkanediolato-hydroxo-borate(III)]).

acid is formed, and the proton dissociates subsequently. This were to explain according to the said authors that the borate complex of mannitol bound as 1,3-glycol has a higher stability than 1,2-diols, because the OC—CO bond angle of the latter is less than the bond angle of planar boric acid, and hereby the first step of complex formation is hindered.

DALE [3], on the other hand, thinks that the formation of 1,2-diol—boric acids in aqueous solution is impossible because of the different bond angles. These compounds can be prepared only in non-aqueous medium, and due to the strain of the ring, these acids will be actually stronger than boric acid [14].

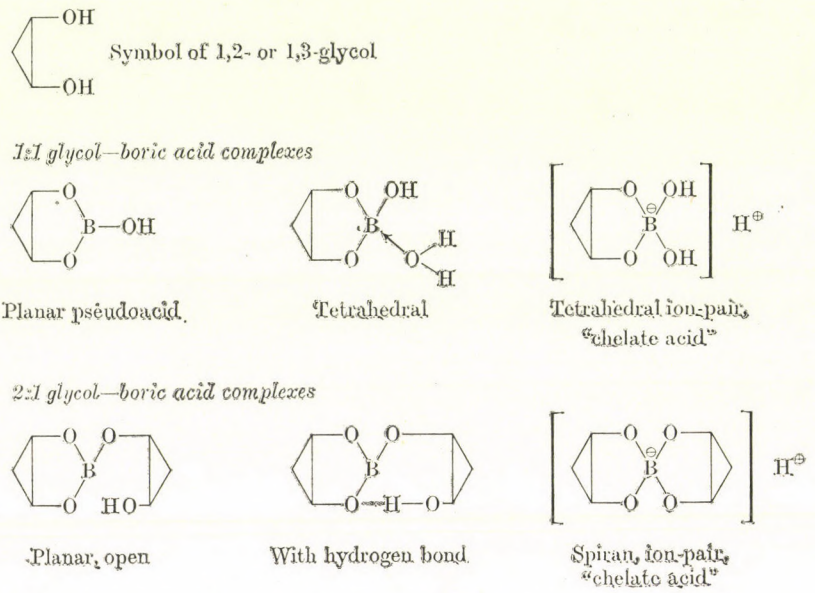

Fig. 1. Different representations of the structure of glycol—boric acid mononuclear complexes in the literature

The decrease in pH caused by 1,2-diols or polyalcohols in boric acid solution is explained also by other authors [15, 16] by the formation of tetrahedral glycol—borates, *i.e.* without the assumption of neutral complexes, by a shift of the dissociation equilibrium of boric acid. Moreover, certain authors [16] do not reckon with the formation of glycol—boric acid complex even in the case of 1,3-diols, featuring an OC—CO angle corresponding to that of planar boric acid.

CONNER and BULGRIN [16] are of the opinion that the borate complexes of 1,2-diols have a considerably higher stability than those of 1,3-diols because of a slighter decrease in rotational freedom. DALE [3] explains the same phenomenon by the action of the *axial* B—OH group present in 1,3-glycol—borate

of chair conformation, while according to others [17] the stabilities of 1,2- and 1,3-diol—borates are largely the same.

The question might be raised, whether the dispute on the structure of the complexes is of practical importance. Actually, from the aspect of the mathematical description of pH change caused in boric acid solutions by the addition of glycol, the formation of boric acid complexes or their absence is only of theoretical interest, because in the case of a larger glycol excess the systems behave as monobasic acids even if only the anion complexes are formed [18]. Measured data are described therefore by many authors with the aid of "apparent protonation constants" [9, 19, 20]. However, in the study of the reactions of boron complexes [21, 22] it is essential to know the bond angle of boron and the charge of the complex, particularly if a distribution between phases of the complex must also be reckoned with.

All this holds true also for the investigation of the boron complexes of drugs, and in general, for the *in vivo* behaviour of boric acid, as shown by the following two examples.

It has been described that the teratogenic and toxic effect of boric acid is based on its binding to riboflavin, borate ion attached to the ribityl side chain [27]. However, boric acid may also be attached to the ribityl group, and thus, the complex may loose its charge during absorption or excretion. This question has not been raised, though it might explain inconsistent experimental results concerning the pharmacological action of riboflavin—boric acid [24].

KRAL and STRAUSS found that the solubility of the borate complex of amphotericin B (an antibiotic containing 1,3-glycol groups both at its macrolid ring and the mycosamine part) is higher both in alkaline and acid solutions, than that of the antibiotic [25]. This has been attributed to the formation of the borate complex, stable also in a solution of pH 2.5. However, this observation indicates according to our opinion that the compound can form complexes with boric acid and borate ion alike.

However, in the study of the boron complexes of biologically active substances even working hypotheses can not be formulated until we have no general picture on the formation of 1,2- and 1,3-glycol—boric acid and —borate complexes and their stability.

In our earlier works [18, 26, 27] glycol—borate complex formation equilibria have been investigated in detail. It has been found [18] that only boric acid complexes of nearly identical stability as that of the anion complexes can be investigated by pH-metric method. PETTERSSON and ANDERSSON [28] studied the boric acid complex of mannitol by polarimetry. The extractive procedure has been utilized in the case of apolar 1,3-glycols and solvents also for analysis [5, 29, 30]. We wished to investigate the boric acid complexes of polar glycols, therefore, an organic solvent—water system had to be found,

in which boric acid has a readily measurable distribution. Various *n*-alcohols were compared from this point of view, to study then the formation of the boric acid complexes of butane-1,3-diol, D-mannitol, D-sorbitol, dulcitol, ethylene glycol, 1,2-propylene glycol and glycerol.

Experimental

Reagents, analytical methods

Boric acid recrystallized three times from hot water, the medium fraction of the distillate of butanol of analytical purity, and chemicals of analytical purity, checked for acid–base impurities were used.

Owing to the solidification point of laurol (25 °C), distribution was investigated at 27 ± 2 °C.

For the measurement of electromotive force and pH, Radiometer instrument pHm4 and Radiometer electrodes, for the potentiometric titrations Metrohm Potentiograph E536 and Dosimat E535 instruments were used. Infrared spectra were taken on a spectrophotometer UNICAM SP 1000 in butanol solutions of 0.1 mol/dm^3 concentration, at a layer thickness of 0.1 mm, against butanol.

In the investigations of distribution, the hydrogen bromide, perchloric acid and (after the addition of glycerol) the boric acid concentration of the samples taken from the phases was determined with suitably diluted sodium hydroxide standard solution in nitrogen atmosphere. Sodium bromide was determined potentiometrically with silver nitrate, and the concentration of compounds containing 1,2-glycol groups was measured by titration with periodic acid (in the case of samples taken from the alcohol phase, the solvent has been first removed in vacuum). The *n*-alcohol content of the aqueous phases was determined by acetylation [31], the water content of both phases by Karl Fischer's method, the sodium perchlorate content by drying at 130 °C to constant weight.

The butane-1,3-diol content in the butanol phase was measured by gas chromatography (Carlo Erba GD chromatograph, Chromosorb 102, carrier gas: hydrogen, 2.3 kp/cm^2, column temperature: 270 °C, FID). The butane-1,3-diol content of the aqueous phase was calculated in knowledge of the weight of the sample and the phase volumes after distribution.

The density of the solutions was measured by means of pycnometry.

Symbols

HB, B^-, BD^-, HBD, HBD_2 symbol of boric acid, borate ion, glycol—borate and —boric acid complexes [18]

D 1,2- or 1,3-diol or polyalcohol

C_B, C_D total concentration of boric acid and glycol, respectively, in the solution, mol dm^{-3}

( ), [ ] symbol of concentration (mol dm^{-3}) in the alcohol and the aqueous phase, respectively

[N] concentration of butanol in the aqueous phase

$\beta_N = [HBN]\,[HB]^{-1}\,[N]^{-1}$ stability constant of the butanol—boric acid complex [32]

β_{110} protonation constant of boric acid

$\beta_{011} = [BD^-]\,[B^-]^{-1}\,[D]^{-1}$ stability constant of the glycol—borate complex

$\beta_D^a = (HBD)\,(HB)^{-1}\,(D)^{-1}$ stability constant of the 1 : 1 glycol—boric acid complex formed in the alcohol phase

$K_D = [(HB)_2D]\,[HBD]^{-1}\,[D]^{-1}$ equilibrium constant of the reaction corresponding in the case of hexitols to the linkage of the second boric acid

$\beta_p = [HBD]\,[H^+]^{-1}\,[BD]^{-1}$ protonation constant of the glycol—boric acid complex in aqueous solution

d distribution coefficient measured experimentally, ratio of the total concentration of the substance tested (as indicated by the suffix) found in the alcohol and aqueous phases

I ionic strength

Elaboration of the measuring techniques

The distribution of boric acid, electrolytes and water has been investigated in various alcohol—water systems. In addition to the first *n*-alcohol only limitedly miscible with water (butanol) and to the last *n*-alcohol liquid at room temperature (laurol), octanol has been investigated. Water saturated with alcohol and alcohol saturated with water were used in the experiments.

Boric acid solution of 0.025 mol/dm^3 concentration and hydrogen bromide or sodium bromide solutions of 0.05 mol/dm^3 concentration were shaken with an identical volume of the alcohol tested. After 48 hours of standing and following centrifugation samples taken from the phases were analyzed. As seen from the results (Table I), the "alcohol" phase of the butanol—

Table I

Distribution data relevant to various n-alcohol—water equilibrium systems

	Butanol	Octanol	Laurol
Mole fraction of water in the alcohol phase	0.52 ± 0.02	0.28 ± 0.01	0.26 ± 0.01
Concentration of alcohol in the aqueous phase, mol/dm^3	0.79 ± 0.06	≤ 0.25	$\rightarrow 0$
d_{HB}	0.48 ± 0.08	0.24 ± 0.01	0.18 ± 0.01
d_{HBr}	0.33 ± 0.02	0.12 ± 0.02	0.12 ± 0.02
d_{NaBr}	0.049 ± 0.007	0.009 ± 0.002	$\rightarrow 0$

water equilibrium system is an almost stoichiometric butanol—water 1 : 1 mixture. With increasing length of carbon chain the sodium bromide content of the alcohol phase decreased to a greater extent than the ratio of the H-bond forming water or of hydrogen bromide. Of the compounds investigated the distribution coefficient of boric acid is the highest, and this indicates besides the formation of hydrogen bonds also other special solvatation. This might be the hydroxo—alkoxo ligand exchange, proceeding in the alcohol phase. In the infrared spectra of boric acid and boron trioxide dissolved in butanol νOH and δOH vibrations characteristic of "free" water actually appear (at about 3600 and 1650 cm^{-1}), while triethyl borate, investigated at the same time, exhibits also in butanol solution a spectrum identical to that published in the literature [33].

Next, the change in the distribution of the various compounds in the butanol—water system most favourable from the point of view of d_{HB} was investigated as a function of ionic strength. Experiments were carried out as described before. In the first experimental series the starting aqueous phase contained only various quantities of sodium perchlorate. In the further investigations, besides sodium perchlorate, used for the adjustment of ionic strength, 0.025 mol/dm^3 of boric acid or perchloric acid or 0.10 mol/dm^3 of D-mannitol was also dissolved in the solutions. Figure 2 shows the change of the distribution coefficients determined as a function of ionic strength. It can be seen that with increasing I the distribution coefficient of perchloric acid increases too, the proton readily solvatable in alcohol does not "compete" for the hydrate sheath. After initial increase, the d value of sodium perchlorate decreases parallel with that of water. The latter changes only slightly as a function of I, which proves the stability of the butanol—water associate in the alcohol phase. The distribution coefficients of mannitol and boric acid are similarly only slightly influenced by the ionic strength.

Since the alcohol phase contained a large quantity of water, it has been proved in a separate experiment that $B(OH)_4^-$ ions are not extracted. This was done by the determination of the protonation constant from extraction data, which ($\log \beta_{110} = 8.94 \pm 0.06$, $I = 0.50$, 27 °C) was in good agreement with the constant measured earlier pH-metrically (8.84, $I = 1.00$, 25 °C [18]). Presuming only the extraction of boric acid, the protonation constant was calculated on the basis of the pH dependence of d_{HB} in the usual way [34].

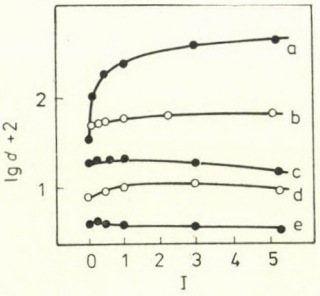

Fig. 2. Change of distribution coefficients in butanol—water system as a function of the ionic strength of the aqueous phase. *a* $HClO_4$, *b* $B(OH)_3$, *c* H_2O, *d* $NaClO_4$, *e* D-mannitol

An evaluation of our experiments showed that the system butanol—water is suitable for the study of boric acid complexes, if the ionic strength of the aqueous phase is high, and remains constant during the investigations.

In the investigation of boric acid—glycol complexes, perchloric acid, boric acid and sodium perchlorate were dissolved in the aqueous phase in quantities to give after the establishing of equilibrium pH 2.0, $C_B = 0.02$ and $I = 0.50$. The concentration of glycols varied between 0 and 0.6 mol/dm³ (that of dulcitol only up to 0.15 mol/dm³, because of its poor solubility). The solutions were shaken with an equal volume of butanol, and after 48 hours of standing the total boric acid content of both phases was measured. In the case of hexitols, experiments were carried out also in solutions of $C_B = 0.01$ boric acid concentration.

Calculation of the stability constants from extraction data

In absence of glycol, the experimentally measurable distribution coefficient of boric acid is:

$$d_{HB} = \frac{(HB)}{[HB] + [HBN]} = \frac{(HB)}{[HB]} \cdot \frac{1}{1 + \beta_N[N]} \tag{1}$$

The concentration of butanol transferred during extraction into the aqueous solution of 0.50 ionic strength was determined in a separate experiment. The stability constant of the butanol—boric acid complex formed in the aqueous phase, β_N, is 0.65 [32]. In the presence of glycol, when a 1 : 1 complex is formed in both phases:

$$d_{HB}^{\sim} = \frac{(HB) + (HBD)}{[HB] + [HBN] + [HBD]} = \frac{(HB)}{[HB]} \frac{1 + \beta_D^a d_D [D]}{1 + \beta_N[N] + \beta_D[D]} \tag{2}$$

Since the ratio (HB)/[HB] is the distribution coefficient of boric acid, (1) divided by (2)

$$\frac{d_{HB}}{d^D{}_{HB}} = \frac{1 + \beta_N[N] + \beta_D[D]}{(1 + \beta_N[N])\,(1 + \beta_D^a d_D [D])} \tag{3}$$

Owing to the large excess of the complex former: $[D] \approx C_D$. The stability constants can be calculated on the basis of (3) numerically, by curve fitting. This route was followed in the case of butane-1,3-diol, the distribution coefficient of which ($d_D = 0.57 \pm 0.07$) was determined in a separate experiment.

In the case of hexitols a straight line is obtained, when the ratio of the distribution coefficients is plotted as a function of glycol concentration (Fig. 3). This indicates that complex is formed only in the aqueous phase. Since [N] is constant during the investigation, in the case of $\beta_D^a = 0$ (3) is actually the equation of a straight line:

$$\frac{d_{HB}}{d^D{}_{HB}} = 1 + \frac{\beta_D}{1 + \beta_N[N]}\,[D]$$

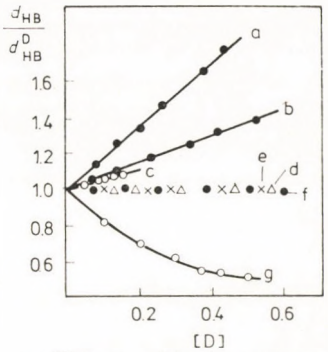

Fig. 3. Ratio of the distribution coefficients of boric acid, measured in the absence (d_{HB}) and in the presence (d^{D}_{HB}) of glycol, as a function of glycol concentration. *a* D-Sorbitol, *b* D-mannitol, *c* dulcitol, *d* ethylene glycol, *e* 1,2-propylene glycol, *f* glycerol, *g* butane-1,3-diol

The constant can be calculated on the basis of the slope. However, a second boric acid may also be attached to hexitols. If 1 : 1 and 1 : 2 glycol—boric acid complexes are formed in the aqueous phase, then:

$$\frac{d_{HB}}{d^{D}_{HB}} = 1 + \frac{\beta_D (1 + K_D[HB])}{1 + \beta_N [N]} [D]$$

Since experimental data measured in solutions of different boric acid concentrations were located along the same straight line, the formation of 1 : 2 complexes could be excluded

In the case of glycerol and 1,2- diols, the formation of glycol—boric acid complex could not be detected either in the aqueous or in the alcohol phase.

Table II

Stability constants of glycol—boric acid and —borate complexes
(reliability is expressed as the confidence interval belonging to the 95% level)

Glycol	Type of complex	Experimental conditions	Symbol	Numerical value of the constant
Ethylene glycol	BD⁻	*a*	β_{011}	1.83 ± 0.18
	HBD	*b*	not formed	
1,2-Propylene glycol	BD⁻	*a*	β_{011}	3.17 ± 0.20
	HBD	*b*	not formed	
Glycerol	BD⁻	*a*	β_{011}	23.6 ± 2.5
	HBD	*b*	not formed	
Butane-1,3-diol	BD⁻	*c*	β_{011}	1.38 ± 0.11
	HBD	*c*	β_D	0.54 ± 0.11
		b		0.42 ± 0.24
Dulcitol				0.91 ± 0.30
D-Mannitol	HBD	*b*	β_D	1.10 ± 0.37
D-Sorbitol				2.52 ± 0.48

a pH-metry, 25 °C, $I = 0.08$ [26];
b extraction, 27 °C, $I = 0.50$, present work;
c pH-metry, 25 °C, $I = 0.01$, present work

The stability constants of butane-1,3-diol complexes were determined also by pH-metry in solutions of pH 8—9 and of 0.01 ionic strength. Measuring techniques (cell without transference, method of "e.m.f. difference measurement") and mode of calculation were identical with those given earlier [26, 27]. According to the pH-metric investigations, butane-1,3-diol forms in weakly alkaline solution a 1 : 1 complex both with boric acid and the borate ion. Stability constants determined are contained in Table II.

Discussion

Stability of glycol—boric acid complexes

The agreement between the stability constants of mannitol—boric acid measured by us and published in the literature (0.72 ± 0.05, $I = 3.00$, 25 °C, polarimetry [28]) is acceptable. Data relevant to the 2,2-diphenylpropane-1,3-diol—boric acid complex ($\beta_D = 0.59 \pm 0.10$, $I = 0.5$ [5]) can also be well fitted to constants measured by us.

The stability behaviour of hexitol—boric acids can be interpreted on the basis of Fig. 4. The boric acid complex of the compound containing 1,3-*cis*-glycol group is cyclic, of chair conformation [3]. In the dulcitol complex one

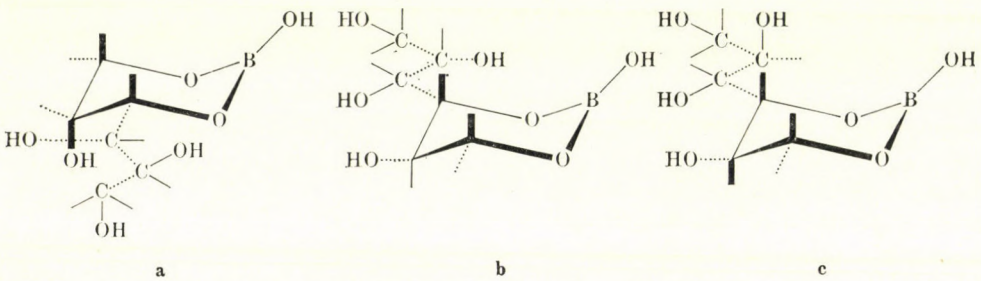

Fig. 4. The most probable structures of 1,3-glycol—boric acids on the basis of calotte models. *a* Dulcitol—, *b* D-mannitol—, *c* D-sorbitol—boric acid

of the alcoholic hydroxy groups gets into unfavurable *axial* position. On the large *equatorial* side chain of D-mannitol complex formed with the $C_1O—C_3O$ group, the steric position of the $C_5—OH$ group is more unfavourable than that of the $C_2—OH$ group in D-sorbitol—boric acid. In the latter case the side chain of the complex formed with the $C_4O—C_6O$ diol quasi turns away from the ring.

Results obtained show that the decrease in rotational freedom of the ligand plays a decisive role in the formation of glycol—boric acid complexes. In hexitols only the rotation of the terminal groups is possible, therefore, glycol groups of position 1,3 get easier into overlapping position, than in the case of butane-1,3-diol. The boric acid complex of this latter glycol is stabilized by the electron donor effect of the methyl group, however, the rotational freedom of the ligand decreases to a greater measure, than in hexitol complexes.

The C_2—OH group of glycerol diminishes electron density at the neighbouring carbon atoms, but does not substantially hinder at the same time the rotation of the terminal groups, this being the reason that no complex is formed.

It can be established that polar butanol is more suitable for the extractive investigation of low stability boric acid complexes, than the apolar solvents used earlier. This is supported besides the good agreement of the β_D values of butane-1,3-diol—boric acid measured by pH-metry and by extraction also by the fact that the extraction of the complex into butanol could also be followed. Using an apolar solvent, this complex could not be detected [5], though its formation has been described earlier [30].

General conclusions

Our measurements support DALE's conclusion [3], according to which 1,2-diol—boric acid complexes are not formed in aqueous solution because of ring strain. This excludes at the same time the formation of glycol—boric acids containing tetracoordinated boron (Fig. 1). Thus, the pH of the borate solution on addition of 1,2-diols decreases exclusively because of the formation of anion complexes.

Figure 5 summarizes those boric acid and borate complex formation equilibria, which could be proved experimentally.

1,3-Diols diminish the pH of the borate solution in a slighter measure than 1,2-diols, because boric acid complex is also formed besides borate complex. CONNER and BULGRIN did not take this into consideration, and thought therefore that the borate complexes of the latter are considerably more stable [16]. According to our investigations, the stability of the five- and six-membered cyclic borate complexes is almost equal, and this is consistent with findings based on ^{11}B-NMR measurements [17].

The fact that 1,3-diol—boric acid complexes have a lower stability than anion complexes may be caused by oxygens getting into overlapping position, which is only partly counterbalanced by the ceasing of axial B—OH in borate complexes.

The boric acid complexes of 1,3-diols are stronger acids than boric acid. It can be deduced that the ratio of their protonation constant and of that of boric acid

$$\frac{\beta_p}{\beta_{110}} = \frac{\beta_D}{\beta_{011}} \tag{4}$$

is for all the glycols investigated (Table II, [26]) smaller than 1.0. In the case of polyalcohols it is of an order of magnitude of 10^{-3}, because on taking up negative charge, the 1,3-diol bond reacts to form 1,2-diol complex, substantially more stable as an anion. Thus, the systems behave as acids stronger

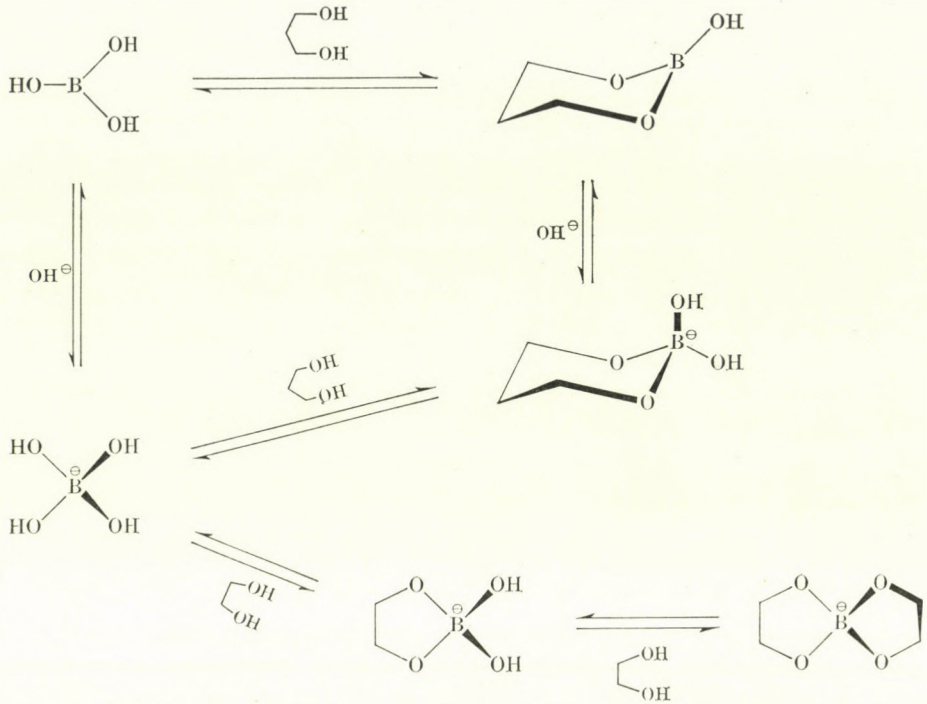

Fig. 5. Formation equilibria of the glycol complexes of boric acid and borate ion in aqueous solution

than boric acid, though the acceptor strength of boron, carrier the Lewis acid character, decreases by the coordination of the nucleophilic glycol.

Our results call the attention to the fact that in reactions where the formation of boron—glycol complexes is to be assumed, the formation of less studied glycol—boric acids must also be taken into consideration besides the formation of anion complexes.

*

The author thanks Professors L. BARCZA and J. LASZLOVSZKY for their comments and advices, to Dr. GY. MILCH for the recording of the IR spectra, Mrs. A. SZUCHOVSZKY for the performance of the gas chromatographic, and Mrs. E. BAGÓ for the periodic acid measurements.

REFERENCES

[1] MAGNANINI, G.: Z. phys. Chem., **11,** 284 (1893)
[2] HERMANS, P.: Z. anorg. Chem., **142,** 83 (1925)
[3] DALE, J.: J. Chem. Soc., **191,** 1961
[4] MAZUREK, M., PERLIN, A. S.: Can. J. Chem., **41,** 2403 (1963)
[5] EGNEUS, B., UPPSTRÖM, L.: Anal. Chim. Acta, **66,** 211 (1973)
[6] INGRI, N.: Svensk Kemisk Tidskrift, **75,** 4 (1963)
[7] SVARCS, E. M.: Boron Complexes of Polyoxycompounds. Zinatnie, Riga 1968 (In Russian)

[8] METHA, S. M., KVANTAK, K. V.: J. Amer. Chem. Soc., **74,** 3470 (1952)
[9] BELCHER, R., TULLY, G. W., SVEHLA, G.: Anal. Chim. Acta, **50,** 261 (1970)
[10] KALACHEVA, V. G., BEN'KOVSKII, V. G., SVARCS, E. M.: Latv. PSR Zinat., Akad. Vestis, Kim. Ser., **1969** (2), 149; **1968** (2), 152
[11] ANTIKAINEN, P. J.: Acta Chem. Scand., **13,** 312 (1959)
[12] FISCHER, F., LOCHNER, S.: Z. Chem., **4,** 301 (1964)
[13] FISCHER, F., LOCHNER, S.: J. prakt. Chem., **23,** 119 (1964)
[14] HUBERT, A. J., HARGITAY, B., DALE, J.: J. Chem. Soc., **192,** 1961
[15] SPRTA, F., BARTUSEK, M.: Scripta, **1973, 3,** Chemia (3) 91
[16] CONNER, J. M., BULGRIN, V. C.: J. Inorg. Nucl. Chem., **29,** 1953 (1967)
[17] HENDERSON, W. G., HOW, M. J., KENNEDY, G. R., MOONEY, E. F.: Carbohyd. Res., **28,** 1 (1973)
[18] PAÁL, T., BARCZA, L.: Acta Chim. (Budapest) **85,** 139 (1975)
[19] GRIPENBERG, S.: Soc. Sci. Fenn., Commentat Phys-Math., **32,** 38 (1966)
[20] NAZARENKO, V. A., ERMAK, L. D.: Zh. Neorg. Khim., **12,** 643, 2051 (1967)
[21] CAPON, B., GHOSH, B. CH.: Tetrahedron Lett., **25—26,** 1707 (1964)
[22] KENNEDY, G. R., HOW, M. J.: Carbohyd. Res., **28,** 13 (1973)
[23] ROE, D. A., MCCORMICK, D. B., REN-TSONG LIN: J. Pharm. Sci., **61,** 1081 (1972)
[24] FROST, D. V.: J. Biol. Chem., **145,** 693 (1942)
[25] KRAL, F., STRAUSS, G.: J. Antibiotics, **31,** 257 (1978)
[26] PAÁL, T.: Acta Chim. Acad. Sci. Hung., **95,** 31 (1977)
[27] PAÁL, T.: Acta Chim. (Budapest) **91,** 393 (1976)
[28] PETTERSSON, L., ANDERSSON, I.: Acta Chem. Scand., **27,** 1019 (1973)
[29] DRYSSEN, D. W., NOVIKOV, YU. P., UPPSTRÖM, L.: Anal. Chim. Acta, **60,** 139 (1972); AGAZZI, E. J.: Anal. Chem., **39,** 233 (1967); PUTNINS, A., SVARCS, E. M., BALODE, M.: Latv. PSR Zinat. Akad. Vestis, Kim. Ser., **1976** (5), 519
[30] IGNASS, R., SVARCS, E. M., ABELE, V., IEVINS, A.: Latv. PSR Zinat. Akad. Vestis, Kim. Ser., **1972** (2), 235
[31] SIGGIA, S.: Quantitative Organic Analysis via Functional Groups. Wiley, New York 1963
[32] PAÁL, T. L.: Acta Chim. Acad. Sci. Hung., **103,** 193 (1980)
[33] GRASSELLI, J. G. (Ed.): Atlas of Spectral Data and Physical Constants for Organic Compounds. Chem. Rubber Co. Press, Cleveland 1974
[34] ROSSOTTI, F. J. C., ROSSOTTI, H.: The Determination of Stability Constants. McGraw-Hill, London 1961

Tamás L. PAÁL H-1372 Budapest, P.O.B. 450.

Acta Chimica Academiae Scientiarum Hungaricae, Tomus 103 (2), pp. 193—198 (1980)

STUDY OF THE WEAK INTERACTIONS OPERATING BETWEEN BORIC ACID AND POLAR ORGANIC COMPOUNDS IN AQUEOUS SOLUTIONS

T. L. PAÁL

(National Institute of Pharmacy, Budapest)

Received December 1, 1978
Accepted for publication April 6, 1979

The increase in pH in boric acid—borate buffer on addition of polar organic compounds was attributed to the formation of 1 : 1 boric acid—Lewis base complexes. When the reagents were added instead of borate buffer to phosphate buffer of the same pH, only little changes in pH, caused by the medium effect of the polar organic compounds have been observed. Correcting with these pH changes data measured in boric acid—borate solutions, the stability constants of the boric acid complexes of dioxane, dimethyl formamide, dimethyl sulfoxide, acetone, butanol, propanol, methanol and acetonitrile have been determined.

It was concluded on the basis of the results that neither does the medium effect of glycols cause any considerable error in the pH-metric determination of the stability constants of glycol—borate complexes.

In the pH-metric determination of the stability constant of diol—borate complexes the concentration of total boron is generally kept at a low value (*max.* 0.025 mol/dm^3) in the solution [1, 2], to avoid the formation of polyborate ions [3]. Owing to the low stability of the complexes, the concentration of diol has to be thus increased during the investigation, sometimes up to 0.5—2.0 mol/dm^3. This raises the question, whether pH values measured in the concentrated solution of the organic reagent are actually characteristic of the diol—borate complex forming reaction, or are to be attributed to the general medium effect of the diol.

According to NAZARENKO and ERMAK [4], diols exert an important effect on the relative permittivity of the medium, therefore, the value of the measurable apparent stability constants will depend also on the prevailing glycol concentration. However, the substantial medium effect described by them could not be reproduced by other authors [1, 5]. In the determination of the stability of di- and polyalcohol—borate complexes, CONNER and BULGRIN used 2-methoxy ethanol for medium effect correction. Titrating with this compound dilute tetraborate solutions, they observed a slight increase in pH (as contrary to the slight decrease in pH, accompanying the formation of diol—borate complexes). They assumed that 2-methoxy ethanol does not interact with the borate ion or with boric acid, and used the pH changes obtained as a numerical measure of medium effect for the correction of the

pH values measured in the investigation of di- and polyalcohols [1]. EVANS *et al.* [5] adopted this method with the remark that it is questionable, within which limits this correction is valid.

It was found in our earlier work [6, 7] that on adding polar solvents (dimethyl formamide, dimethyl sulfoxide) to a borate buffer, a considerably larger increase in pH is obtained, than on adding the same reagents to other solutions of similar pH and buffer capacity (*e.g.* to glycine buffer). This finding was explained by the formation of boric acid—Lewis base complexes, the stability constants of which have been determined [6].

This paper reports on the investigation of the formation of boric acid complexes of further six polar organic compounds (dioxane, acetone, acetonitrile, methanol, propanol, butanol).

Experimental

Symbols

HB, B^-	boric acid, $B(OH)_3$, and the borate ion, $B(OH)_4^-$
N	the complex-forming polar organic compound (Lewis base)
HBN	symbol of the complex
$\beta_N = [HBN]\,[HB]^{-1}\,[N]^{-1}$	stability constant of the complex
β_{110}	according to the symbol used in an earlier communication [2], the protonation constant of boric acid
C_B	total concentration of the boron-containing particles in the solution
C_{Na}	concentration of sodium ions, equivalent to sodium hydroxide getting into the solution on partial neutralization of boric acid
s, *i*	as suffix to other symbols, they indicate values relevant to the starting solution (containing only borate buffer) and to other solutions titrated at the single measuring points (containing borate buffer and a given quantity of organic reagent), respectively
E	electromotive force
$\Delta E = E_s - E_i$	on titrating the buffer with the polar organic compound, the change in electromotive force, referred to the value before the beginning of titration
ΔE_b, ΔE_p	ΔE values measured in the borate and phosphate buffer, respectively
ΔE_{corr}	difference of the preceding two values, see expression (1)

Methods

Boric acid was recrystallized three times from hot water. The other reagents were of analytical purity, checked for acid and base impurities.

Electromotive force was measured in a vessel thermostated at 25 ± 0.2 °C, with a Radiometer pHm4 instrument and a Radiometer G200B glass electrode in the following cell:

glass electrode | test solution | 0.50 mol/dm³ $NaClO_4$ | 0.49 mol/dm³ $NaClO_4$, 0.01 mol/dm³ NaCl | Ag/AgCl

Stability constants were determined by the "e.m.f. difference method" [2]. Electromotive force (E_s) was measured in the test solution containing 0.020 mol/dm³ boric acid and the pH was adjusted with sodium hydroxide to about 8.0 then adding reagent to the solution, e.m.f. values (E_i) belonging to the given Lewis base concentration were noted down. During the experiments, the quantity of reagents in the solution increased up to 0.5 mol/dm³.

The change in e.m.f. (ΔE_b) belonging to a given Lewis base concentration may be caused besides the formation of the boric acid complex also by the medium effect of the reagents. To eliminate this latter non-specific interaction, the experiments were carried out under completely identical conditions instead of boric acid with another buffer. In the earlier experiments [6] glycine has been used, in the present work a phosphate buffer, containing similarly to borate a tetrahedral ion. According to our experiments ΔE values measured in glycine and

phosphate solutions were virtually the same very low values, not exceeding even at a reagent concentration of 0.50 mol/dm³ 1.5 mV. In absence of borate, the electromotive force increased on the addition of methanol, propanol and butanol, while it decreased in the case of the other reagents.

Standard deviation of E_s in parallel experiments was 1.2 mV, while ΔE could be reproduced very precisely, with a standard deviation of ± 0.3 mV.

Changes in e.m.f. measured in the borate buffer (ΔE_b) were corrected with the values obtained in the phosphate buffer (ΔE_p):

$$\Delta E_{corr} = \Delta E_b - \Delta E_p \tag{1}$$

Calculations of stability constants

On the basis of electroneutrality, during a titration, when the ions of sodium perchlorate are omitted:

$$C_{Na} + [H^+] = [B^-] + [OH^-] \tag{2}$$

Under the pH and concentration conditions used, the proton and hydroxide ion concentrations can also be omitted in (2). The boron concentration of the solution before the addition of the complex former can be described with Eq. (3) and during titration with Eq. (4):

$$C_{Bs} = [HB]_s + [B^-]_s \tag{3}$$

$$C_{Bi} = [HB]_i + [B^-]_i + [HBN]_i \tag{4}$$

Diluting the solution with the reagent, C_B and C_{Na} decrease in the same ratio, because the change in pH is small:

$$\frac{C_{Bs} - C_{Nas}}{C_{Nas}} = \frac{C_{Bi} - C_{Nai}}{C_{Nai}} \tag{5}$$

On the basis of Eqs (2)—(5)

$$\frac{[HB]_s}{[B^-]_s} = \frac{[HB]_i + [HBN]_i}{[B^-]_i},$$

substitution of the stability constants gives:

$$\beta_{110}\,[H^+]_s = \beta_{110}\,[H^+]_i + \beta_N\,\beta_{110}\,[H^+]_i\,[N]$$

and after reduction and rearrangement:

$$\frac{[H^+]_s}{[H^+]_i} = 1 + \beta_N\,[N]$$

$$pH_i - pH_s = \Delta pH = \lg\,(1 + \beta_N\,[N]) \tag{6}$$

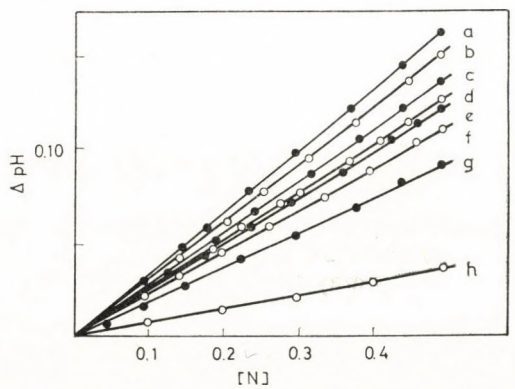

Fig. 1. Increase in pH (ΔpH) in borate solution on the addition of polar organic compounds, as a function of reagent concentration; *a* Dioxane, *b* dimethyl formamide, *c* dimethyl sulfoxide, *d* acetone, *e* butanol, *f* propanol, *g* acetonitrile, *h* methanol

ΔpH can be calculated from the value of ΔE_{corr}, while [N] can be considered as identical with the total concentration of the complex former, because of the large excess of the latter. The data of measurements are shown in Fig. 1.

All the data measured could be described on the basis of Eq. (6), the formation of the complexes $[B(OH)_3N_2]$ or $[B(OH)_2N](+)$ could be excluded [6]. Stability constants are given in Table I.

Table I

Stability constants of the complexes formed between boric acid and polar organic compounds in aqueous solution at 25 °C and 0.50 ionic strength. The errors of the constants are expressed by the confidence interval belonging to the 95% confidence level

Complex former	β_N
Dioxane	0.89 ± 0.15
Dimethyl formamide	0.81 ± 0.04 [6]
Dimethyl sulfoxide	0.75 ± 0.06 [6]
Acetone	0.68 ± 0.12
Butanol	0.65 ± 0.13
Propanol	0.61 ± 0.13
Acetonitrile	0.46 ± 0.16
Methanol	0.12 ± 0.11

Discussion

Interaction of boric acid with polar organic compounds in aqueous solution

The interaction of methanol, propanol, butanol and boric acid can be probably attributed to the formation of [alkoxo-dihydroxo-borate(III)] via the ligand exchange

$$B(OH)_3 + ROH \rightleftharpoons B(OR)(OH)_2 + H_2O.$$

This is supported by the finding that the infrared spectrum of boric acid dissolved in butanol indicates besides the appearance of water formed in the reaction the presence of tri-coordinated boron [8]. Owing to the coordination of the alkoxy group, electron density is increased at the boron, its acceptor strength is reduced, which represses the coordination of the hydroxide ion. In aqueous solution the reaction proceeds in a just detectable measure.

Aprotic, polar molecules may form with boric acid Lewis-type acid–base adducts:

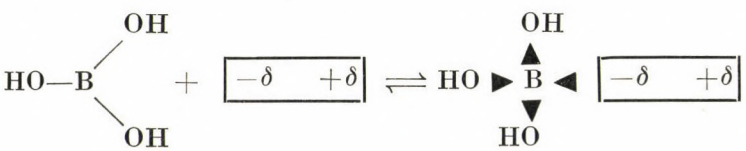

This is supported also by observations reported in the literature, according to which the ionization rate of boric acid decreases in dimethyl sulfoxide—water mixture, as compared to that in aqueous solution [9], and boric acid is present also in acetone—dimethyl sulfoxide mixtures in the monomeric form [10]. The stability constants of these complexes (Table I) reflect in aqueous medium the Lewis base strength of the polar compound with respect to boric acid, and can be compared only partly with other expressions of the donor strength, because the Lewis acid—base interaction is accompanied by other processes (change in symmetry about boron, a decrease on B—O bond order [11]). It can be established, however, that the order of the β_N values in the series dimethyl formamide — acetone — acetonitrile follows that of the donacity [12], while the complex of dimethyl formamide even in the case of boron trihalides is more stable than the complex of dimethyl sulfoxide [13]. In addition to the magnitude of the $(\delta-)$-charge of Lewis bases, the hard-soft character also asserts itself, and this may explain the fact that the boric acid complex of the least polarizable dioxane has a somewhat higher stability, than the complexes of the more basic solvents.

It is noteworthy that the stability of the Lewis acid—base adducts approaches that of the cyclic diol—boric acid complexes.

Correction of the medium effect of polar compounds in the determination of the stability constants of boric acid and borate complexes by electromotive force measurement

The order of magnitude of E_p values measured in phosphate buffer is in good agreement with recently published similar data, measured by KAKABADSE *et al.* [14] for the system acidic methanol—water with a glass electrode. It is noteworthy that alcohols, stronger proton donors than water, and Lewis bases acceptors at the H-bond, caused pH changes of opposite direction. It seems an acceptable approximation to characterize the medium effect of the compounds with these data, though it was found by the authors mentioned [14] that in methanol—water mixtures of the same composition the change in e.m.f. depends also on the kind of glass electrode used. Thus, an increase in the concentration of the polar compounds does not exert its influence on the value of the electromotive force measurable in the solution through the changing of the ionic activities alone.

In the determination of the stability constants of glycol—borate complexes, "medium effect correction" with 2-methoxy ethanol, as reported earlier in the literature [1, 5], gives erroneous results. Calculations on the basis of "pH corrections" published [1, 5] show that this compound forms a boric acid complex of $\beta_N \approx 0.2$ stability. CONNER and BULGRIN did not take this into consideration, and this is the reason why they published higher values

for the stability constants of diol—borates, particularly of 2 : 1 complexes, than other authors. (They found *e.g.* for the lg β_1 and lg β_2 constants of ethylene glycol—borate 0.33 and 0.06 [1], as contrary to the values 0.27 and −1.00 of other authors [15] and to our results of 0.23 and −0.85 [2].)

We investigated how far the earlier published stability constants of glycol—borate complexes calculated on the basis of uncorrected e.m.f. values are modified by the medium effect correction used by us.

With ΔE_p data obtained in the titration of phosphate buffer with ethylene glycol (in the case of 1.0 mol/dm^3 glycol concentration an e.m.f. increase of 2.51 mV) the medium effect correction has been carried out for our measurements [2] relevant to the ethylene glycol—borate system. The logarithm of the stability constant of the 1 : 1 complex was reduced thereby from 0.23 to 0.18, that of the 2 : 1 ethylene glycol—borate complex from −0.85 to −1.10.

It can be seen from this that the medium effect of glycols is actually manifested in concentrated solutions during pH measurement, but results only small pH-shifts, which do scarcely affect the value of the stability constants, and do not alter the general view on the glycol—borate complexes [2, 8].

REFERENCES

[1] Conner, J. M., Bulgrin, V. C.: Inorg. Nucl. Chem., **29,** 1953 (1967)
[2] Paál, T.: Acta Chim. (Budapest) **91,** 393 (1976); **95,** 31 (1977)
[3] Ingri, N.: Svensk Kemisk Tidskrift, **75,** 4 (1963)
[4] Nazarenko, V. A., Ermak, L. D.: Zh. Anal. Khim., **12,** 643, 2051 (1967)
[5] Evans, W. J., Frampton, V. L., French, A. D.: J. Phys. Chem., **81,** 1810 (1977)
[6] Paál, T.: Magy. Kém. Folyóirat, **83,** 527 (1977)
[7] Paál, T.: Magy. Kém. Folyóirat, **84,** 547 (1978)
[8] Paál, T.: Acta Chim. Acad. Sci. Hung. **103,** 181 (1980)
[9] Fiordiponti, P., Rallo, F.: J. Chim. Phys. Physicochim. Biol., **69,** 805 (1972)
[10] Shcherbakov, V. A., Kamars, A., Svarcs, E. M.: Latv. PSR Zinat. Akad. Vestis, Kim. Ser., **1977** (1), 115
[11] Dale, J.: J. Chem. Soc., **191** (1961)
[12] Gutmann, V.: Coordination Chemistry in Non-Aqueous Solutions. Springer, New York 1968
[13] Jatsimirskii, K. B. (Ed.): Recent Results in Chemistry of Coordination Compounds. Naukova Dumka, Kiev 1975 (in Russian)
[14] Kakabadse, G. J., Maleila, H. A., Khayat, M. N., Tassopoulos, G., Vahdati, A.: Analyst, **103,** 1046 (1978)
[15] Roy, L. G., Laferriére, A. L., Edwards, J. O.: J. Inorg. Nucl. Chem., **4,** 106 (1957)

Tamás L. Paál H-1372 Budapest P.O.Box 450.

Acta Chimica Academiae Scientiarum Hungaricae, Tomus 103 (2), pp. 199—215 (1980)

INVESTIGATION OF BINARY SURFACTANT SYSTEMS, I

STUDIES OF AQUEOUS SODIUM-OCTANOATE SOLUTIONS BY ACTIVITY MEASUREMENTS

Zs. Bedő and E. Berecz

(Department of General and Physical Chemistry Technical University for Heavy Industry Miskolc, Hungary)

Received January 26, 1979

Accepted for publication April 6, 1979

The activities of surfactant ions and counterions were directly obtained by EMF measurements in aqueous solutions of sodium-octanoate depending on the concentration and the temperature. The mean activity coefficient were also calculated. From these data, together with the temperature and concentration dependence of the surface tension the CMC and its dependence on the temperature were determined.

The mean activity coefficient at the CMC was found to be considerably smaller then that calculated by the Debye—Hückel equation, which can be explained by the premicelle formation.

The amount of adsorption and the heat of adsorption were calculated using the Gibbs adsorption isotherm for the adsorption of sodium-octanoate.

On the basis of the temperature dependence of the $\Delta G°$, $\Delta H°$ and $\Delta S°$ for the micelle formation it can be concluded that the entropy is the most important factor in stabilizing the hydrophobic bonds of the micelle formation, due to changes in the water structure.

The charged phase separation model was verified as the mechanism of the micelle formation, and the degree of counterion attachment was calculated to be 0.665.

Introduction

On the basis of experimental results [1, 2, 3, 4] it can be concluded that short chain alkyl carboxylates form polynuclear aggregates (micelles). These aggregation processes can be explained in terms of the structure-stabilizing effect of hydrocarbon chains on water on the one hand, and of the increased torsional vibrations of hydrocarbon chains as they aggregate on the other [5].

The study of the activity of the aqueous surfactant solutions is important as a bassis for interpreting the properties of these systems. However, there have been few such reports [6—9] because of the difficulty of measurement at low concentrations where surfactants are generally used and of the inevitable error involved in the methods of measurement. The activity measurement of the ionic surfactants requires those of both the surfactant ion and the counter ion.

Among the various methods the measurement of the electromotive force of a concentration cell containing an ion-exchange membrane semipermeable

to a surfactant anion, and the pNa measurements for the counterion have proved to be the most effective [10, 11].

The determination of the activity and surface tension for the aqueous solutions of surfactants allows to draw conclusions in the temperature interval examined for the mechanism of the micelle formation, the structure of the micelles and the degree of counterion attachment, as well as the applicability of the Gibbs' adsorption isotherm and the Debye—Hückel equation.

1. Experimental

To achieve the goals set in the introduction, the EMF of aqueous sodium-octanoate solutions (NaC_8) in cells assembled to the purpose, and the surface tension of the solutions and their dependence on temperature and concentration were determined.

The activity of sodium ions (a_{Na}) was measured by using an OP—Na 711 type Radelkis sodium responsive glass electrode.

pNa electrode	NaC_8 a_{Na}	1 *M* NH_4NO_3 4% agar bridge	KCl sat.	calomel electrode saturated	(1)

A sodium chloride of known activity was used to control the cell for the Nernstian response.

For the measurement of the *activity of octanoate ions* (a_{Oct}) a concentration cell of the following type was used:

calomel el. sat.	KCl sat.	1 *M* NH_4NO_3 4% agar bridge	NaC_8 a_{Oct}	NaC_8 a^*_{Oct}	KCl sat.	1 *M* NH_4NO_3 4% agar bridge	calomel el. sat.	(2)

The sample solutions (a_{Oct}) and the standard solutions (a^*_{Oct}) were kept apart by a [MA—40 type anion-exchange membrane (USSR)]. The reference (standard) solution was 0.20 mol/dm^3 NaC_8.

Four percent agar in 1.0 mol/dm^3 NH_4NO_3 solution was used to prepare the bridges. The membrane was stored in an aqueous 0.50 mol/dm^3 NaCl solution, and prior to use it has been soaked in the 0.20 mol/dm^3 NaC_8 reference solution for two or three days, and then rinsed with deionized water. When not in use, both parts of the cell were filled with the standard solution.

The EMF was measured by using an OP 205 type Radelkis "Precision pH Meter" with a sensitivity of 0.10 MV. Steady EMF value (E'_{MF}) was usually obtained after 30—60 min, and the equilibrium value (E_{MF}) was calculated by taking into account the asymmetry potential (E_{as}):

$$E_{MF} = E'_{MF} - E_{as} \tag{3}$$

The asymmetry potential was measured by filling both sides of the membrane with the reference solution.

The *surface tension* was measured using a K 8600 type du Noüy-tensiometer. Steady values were obtained after 30 min and adopted as equilibrium values.

The EMF and surface tension measurements were carried out at 20, 30, 40, 50° ($\pm$0.1 °C)

The salt *sodium-octanoate* used was an analytically pure product of Merck. It was dried under vacuum at 120 °C for 48 h to purify it from traces of water.

The *water* used was ion-exchanged distilled water.

2. Results and Discussion

2.1. *Calculation of the activity and activity coefficients*

The activity of sodium ions (a_{Na}) was calculated from

$$\log a_{Na} = \frac{0.4343\,F}{RT}(E_{MF,Na} - E_{Na,O}) \tag{4}$$

where $E_{MF,Na}$ EMF of cell (1),
F Faraday constant (C mol^{-1}),
T absolute temperature (K),
$E_{Na,O}$ a constant depending on the calomel and glass electrodes (V),
R gas constant.

The $E_{Na,O}$ values were determined by extrapolating an extrapolation function [12]:

$$\Delta_{Na} = \frac{0.4343F}{RT} E_{MF,Na} - \log c \tag{5}$$

$$E_{Na,O} = \frac{RT}{0.4343F} \lim_{c \to 0} \Delta_{Na} \tag{6}$$

where: c: the concentration of the sodium-octanoate solutions.

The activity of octanoate ions (a_{Oct}) was calculated on the basis of EMF in the (2) concentration cell ($E_{MF,Oct}$):

$$E_{MF,Oct} = \frac{\Delta u RT}{0.4343F} \log \frac{a_{Oct}}{a^*_{Oct}} \tag{7}$$

where $\Delta u = u_{Oct} - u_{Na}$; u_{Oct} and u_{Na} are the transport numbers of the octanoate and sodium ions in the membrane.
a_{Oct} and a^*_{Oct}, the activities of the octanoate ion in the sample and the standard solutions, respectively.

The value of Δu of is close to unity and constant [13], that is the differentiation of Eq. (7) with respect to log c gives:

$$\mathrm{d}\, E_{MF,Oct}/\mathrm{d} \log c = (\Delta u\ 2.303\ RT/F)\ (\mathrm{d} \log a_{Oct}/\mathrm{d} \log c) \tag{8}$$

Since d $E_{MF,\,Oct}$/d log c is found to be nearly equal to 2.303. RT/F in the concentration range from $5.0 \cdot 10^{-4}$ to $1.0 \cdot 10^{-1}$ mol/dm^3 Eq. (8) gives:

$$\Delta u\ (\mathrm{d} \log a_{Oct}/\mathrm{d} \log c) \cong 1 \tag{9}$$

Since d log a_{Oct}/d log c is not greater than unity for such dilute solutions as in the present experiment, Δu is expected to be nearly equal to unity.

Thus, Eq. (7) can be reduced, and the unknown activity of the octanoate ions is given by

$$\log a_{\mathrm{Oct}} = \frac{0.4343F}{RT} E_{\mathrm{MF,Oct}} - \log a^{*}_{\mathrm{Oct}} \tag{10}$$

The activity of the octanoate ions in the reference solutions was also determined by extrapolating an extrapolation function [12]:

$$\Delta_{\mathrm{Oct}} = \frac{0.4343F}{RT} E_{\mathrm{MF,Oct}} - \log c \tag{11}$$

and

$$\log a^{*}_{\mathrm{Oct}} = - \lim_{c \to 0} \Delta_{\mathrm{Oct}} \tag{12}$$

On the basis of the ionactivities (a_{Na}, a_{Oct}) calculated according to Eqs (4) and (10) the mean activity ($a_{\pm}$) of NaC_8, the individual (γ_{Na}, γ_{Oct}) and mean activity coefficients ($\gamma_{\pm}$) can be determined:

$$a_{\pm} = (a_{\mathrm{Na}}\, a_{\mathrm{Oct}})^{1/2}$$

$$\gamma_{\pm} = (\gamma_{\mathrm{Na}}\, \gamma_{\mathrm{Oct}})^{1/2} \tag{13}$$

The individual ionactivities and activity coefficients, as well as the mean activities and activity coefficients and their dependence on the concentration and temperature are shown in Tables I—IV and in Figs 1—4.

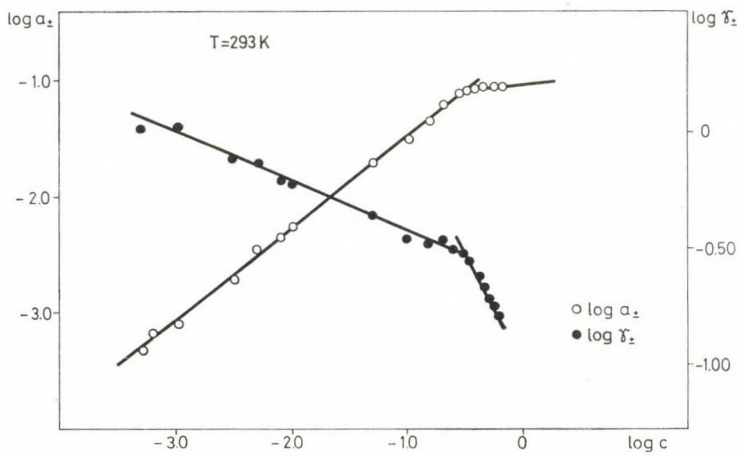

Fig. 1. The mean activity and activity coefficient of the surfactant in the aqueous sodium-octanoate solutions depending on the concentration at 293 K

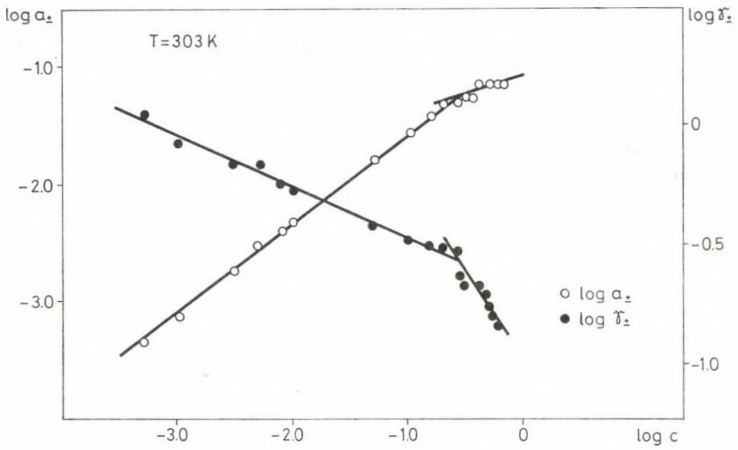

Fig. 2. The mean activity and activity coefficient of the surfactant in the aqueous sodium-octanoate solutions depending on the concentration at 303 K

From Figs 1—4 the CMC values were derived; these data and the corresponding densities of the solutions are given in Table V.

The CMC is affected by many variables, the most important of which are temperature and pressure. Surfactants usually show a shallow minimum in the CMC as a function of temperature [14, 15]. In the case of ionic detergents the minimum can be explained by the difference in temperature dependences of the head-group and hydrocarbon chain interactions [16]. As is shown in Fig. 5, the CMC of the aqueous sodium octanoate depending on the temperature has a minimum at 313 K.

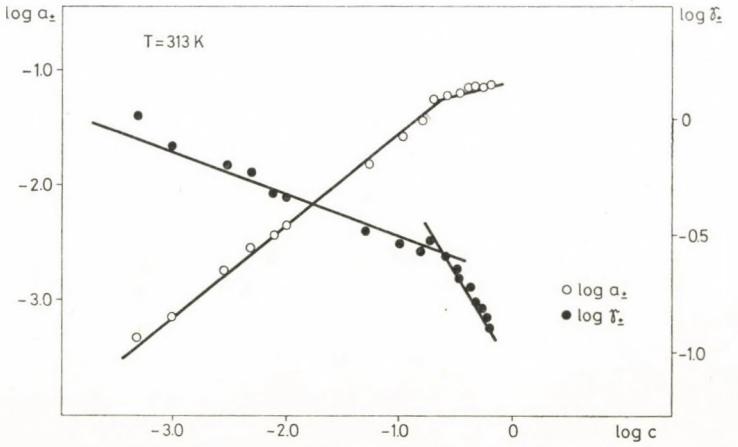

Fig. 3. The mean activity and activity coefficient of the surfactant in the aqueous sodium-octanoate solutions depending on the concentration at 313 K

Table I

The activity of the surfactant in the aqueous sodium-octanoate solutions depending on the concentration at 293 K

c/mol · dm^{-3}	Δ_{Na}	Δ_{Oct}	$-\log a_{Na}$	$-\log a_{oct}$	$-\log a_{\pm}$	$-\log \gamma_{\pm}$
$5.0 \cdot 10^{-4}$	3.73	1.42	3.3011	3.3046	3.3033	0.0022
$1.0 \cdot 10^{-3}$	3.69	1.33	3.0430	3.0899	3.0688	0.0688
$3.0 \cdot 10^{-3}$	3.65	1.25	2.6126	2.7108	2.6614	0.1393
$5.0 \cdot 10^{-3}$	3.64	1.21	2.3975	2.5129	2.4548	0.1522
$8.0 \cdot 10^{-3}$	3.58		2.3598	2.3838	2.3227	0.2225
$1.0 \cdot 10^{-2}$	3.56	1.13	2.1737	2.2891	2.2321	0.2331
$5.0 \cdot 10^{-2}$			1.5369	1.8244	1.6809	0.3796
$1.0 \cdot 10^{-1}$			1.2787	1.6351	1.4577	0.4610
$1.5 \cdot 10^{-1}$			1.1410	1.4802	1.3122	0.4880
$2.0 \cdot 10^{-1}$			0.9345	1.4200	1.1780	0.4788
$2.5 \cdot 10^{-1}$			0.9008	1.3167	1.1095	0.5109
$3.0 \cdot 10^{-1}$			0.8484	1.2651	1.0570	0.5362
$3.2 \cdot 10^{-1}$			0.8484	1.2651	1.0570	0.5630
$4.0 \cdot 10^{-1}$			0.8226	1.2478	1.0369	0.6369
$4.5 \cdot 10^{-1}$			0.7968	1.2651	1.0325	0.6882
$5.0 \cdot 10^{-1}$			0.7709	1.2823	1.0291	0.7341
$5.5 \cdot 10^{-1}$			0.7431	1.3015	1.0223	0.7637
$6.0 \cdot 10^{-1}$			0.7172	1.3192	1.0184	0.7959

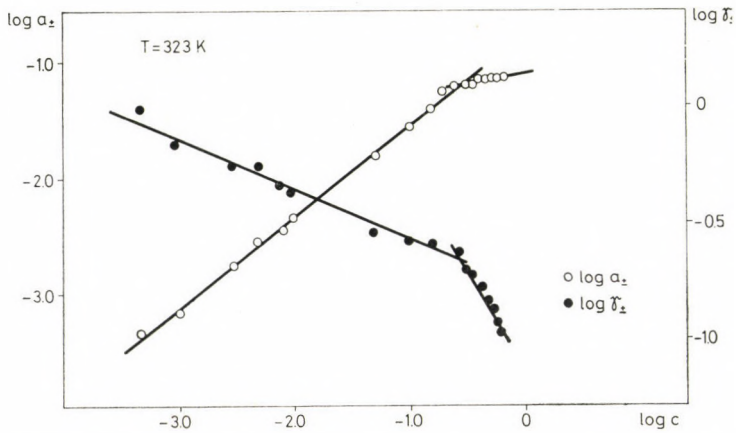

Fig. 4. The mean activity and activity coefficient of the surfactant in the aqueous sodium-octanoate solutions depending on the concentration at 323 K

Table II

The activity of the surfactant in the aqueous sodium-octanoate solutions depending on the concentration at 303 K

c/mol · dm^{-3}	Δ_{Na}	Δ_{Oct}	$-\log a_{Na}$	$-\log a_{oct}$	$-\log a_{\pm}$	$-\log \gamma_{\pm}$
$5.0 \cdot 10^{-4}$	3.76	1.38	3.3370	3.3370	3.3364	0.0362
$1.0 \cdot 10^{-3}$	3.71	1.28	3.0926	3.1343	3.1211	0.1141
$3.0 \cdot 10^{-3}$	3.65	1.18	2.6682	2.7598	2.7145	0.1926
$5.0 \cdot 10^{-3}$	3.64	1.16	2.4602	2.5600	2.5114	0.2104
$8.0 \cdot 10^{-3}$	3.57	1.09	2.3270	2.4269	2.3789	0.2785
$1.0 \cdot 10^{-2}$	3.55	1.07	2.2438	2.3520	2.2986	0.3003
$5.0 \cdot 10^{-2}$	3.48		1.6197	2.8777	1.7496	0.4518
$1.0 \cdot 10^{-1}$			1.3617	1.6613	1.5129	0.5119
$1.5 \cdot 10^{-1}$			1.2202	1.5115	1.3677	0.5484
$2.0 \cdot 10^{-1}$			1.0871	1.4200	1.2551	0.5541
$2.5 \cdot 10^{-1}$			0.9872	1.3451	1.2360	0.5659
$3.0 \cdot 10^{-1}$			0.9789	1.2868	1.2001	0.6709
$3.2 \cdot 10^{-1}$			0.9788	1.2868	1.2001	0.7110
$4.0 \cdot 10^{-1}$			0.8957	1.3055	1.1009	0.7077
$4.5 \cdot 10^{-1}$			0.8790	1.3201	1.1009	0.7479
$5.0 \cdot 10^{-1}$			0.8541	1.3367	1.0960	0.7991
$5.5 \cdot 10^{-1}$			0.8262	1.3489	1.0880	0.8326
$6.0 \cdot 10^{-1}$			0.8020	1.3693	1.0856	0.8698

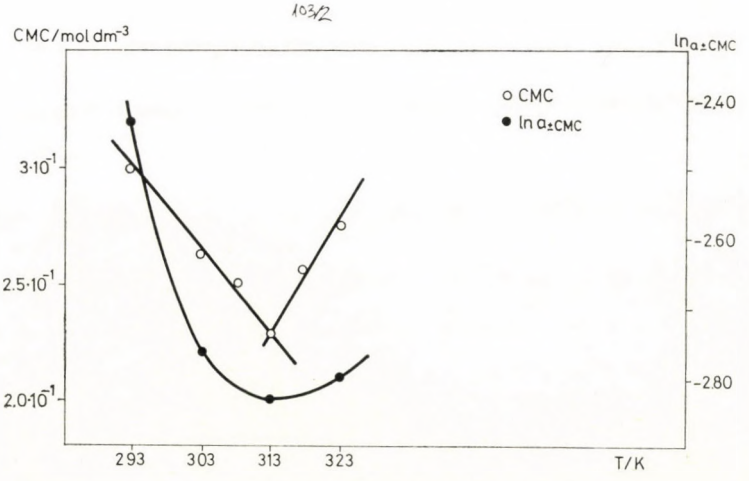

Fig. 5. The CMC and the mean activity at the CMC depending on the temperature

Table III

The activity of the surfactant in the aqueous sodium-octanoate solutions depending on the concentration at 313 K

c/mol · dm^{-3}	Δ_{Na}	Δ_{Oct}	$-\log a_{Na}$	$-\log a_{oct}$	$-\log a_{\pm}$	$-\log \gamma_{\pm}$
$5.0 \cdot 10^{-4}$	3.79	1.35	3.3383	3.3495	3.3441	0.0434
$1.0 \cdot 10^{-3}$	3.71	1.25	3.1208	3.1481	3.1347	0.1339
$3.0 \cdot 10^{-3}$	3.65	1.15	2.7019	2.7775	2.7393	0.2161
$5.0 \cdot 10^{-3}$	3.63	1.13	2.5006	2.5761	2.5387	0.2381
$8.0 \cdot 10^{-3}$	3.56	1.03	2.3668	2.4634	2.4151	1.3170
$1.0 \cdot 10^{-2}$	3.54	1.02	2.2911	2.3748	2.3329	0.3335
$5.0 \cdot 10^{-2}$	3.46		1.6708	2.8995	1.7857	0.4842
$1.0 \cdot 10^{-1}$			1.4211	1.6578	1.5396	0.5388
$1.5 \cdot 10^{-1}$			1.2680	1.5289	1.3983	0.5712
$2.0 \cdot 10^{-1}$			1.0747	1.4000	1.2376	0.5378
$2.5 \cdot 10^{-1}$			1.0457	1.3517	1.1989	0.5941
$3.0 \cdot 10^{-1}$			1.0747	1.2872	1.1812	0.6611
$3.2 \cdot 10^{-1}$			1.0747	1.2872	1.1812	0.6903
$4.0 \cdot 10^{-1}$			0.9538	1.3275	1.1410	0.7367
$4.5 \cdot 10^{-1}$			0.9377	1.3436	1.1418	0.7925
$5.0 \cdot 10^{-1}$			0.9135	1.3678	1.1407	0.8326
$5.5 \cdot 10^{-1}$			0.8907	1.3740	1.1334	0.8674
$6.0 \cdot 10^{-1}$			0.8643	1.3807	1.1228	0.8964

Regressional analysis on the basis of Figs 1—4 shows that

$$\begin{aligned} \log \gamma_{\pm}^{293} &= -(0.21 \log c + 0.646) \\ \log \gamma_{\pm}^{303} &= -(0.21 \log c + 0.747) \\ \log \gamma_{\pm}^{313} &= -(0.18 \log c + 0.698) \\ \log \gamma_{\pm}^{323} &= -(0.22 \log c + 0.780) \end{aligned} \qquad (14)$$

hold for the concentration region from $5.0 \cdot 10^{-4}$ mol/dm^3 up to the CMC.

The mean activity coefficient for the CMC depending on the temperature was found to be $\gamma_{\pm} = 0.22 - 0.29$. This is considerably smaller than the value $\gamma_{\pm} = 0.73$, calculated by the Debye—Hückel equation [17] which takes into account the molecular size (ionic diameter). The low $\gamma_{\pm}$ values can be explained by the dimerization or premicelle formation of surfactant molecules [26] due to the effect of long hydrophobic chains in the molecule. A similar

Table IV

The activity of the surfactant in the aqueous sodium-octanoate solutions depending on the concentration at 323 K

c/mol · dm^{-3}	Δ_{Na}	Δ_{oct}	$-\log a_{Na}$	$-\log a_{oct}$	$-\log a_{\pm}$	$-\log \gamma_{\pm}$
$5.0 \cdot 10^{-4}$	3.80	1.34	3.3396	3.3594	3.3495	0.0507
$1.0 \cdot 10^{-3}$	3.70	1.24	3.1367	3.1643	3.1507	0.1505
$3.0 \cdot 10^{-3}$	3.64	1.12	2.7229	2.8052	2.7639	0.2423
$5.0 \cdot 10^{-3}$	3.61	1.10	2.5277	2.6022	2.5648	0.2650
$8.0 \cdot 10^{-3}$	3.55	1.02	2.3872	2.3773	2.4325	0.3345
$1.0 \cdot 10^{-2}$	3.51	0.99	2.3092	2.4070	2.3580	0.3593
$5.0 \cdot 10^{-2}$	3.42		1.7159	1.9308	1.8243	0.5292
$1.0 \cdot 10^{-1}$			1.4739	1.6810	1.5779	0.5730
$1.5 \cdot 10^{-1}$			0.3099	0.5561	1.5330	0.6013
$2.0 \cdot 10^{-1}$			1.1382	1.4000	1.2691	0.5712
$2.5 \cdot 10^{-1}$			0.0992	1.3766	1.2381	0.6321
$3.0 \cdot 10^{-1}$			1.1538	1.2985	1.2262	0.7038
$3.2 \cdot 10^{-1}$			1.1538	1.2985	1.2262	0.7266
$4.0 \cdot 10^{-1}$			1.0055	1.3609	1.1831	0.7802
$4.5 \cdot 10^{-1}$			0.9899	1.3766	1.1842	0.8419
$5.0 \cdot 10^{-1}$			0.9664	1.3844	1.1755	0.8771
$5.5 \cdot 10^{-1}$			0.9498	1.3905	1.1709	0.9267
$6.0 \cdot 10^{-1}$			0.9274	1.4125	1.1702	0.9602

difference has been observed for other surfactants too [10, 13, 18] from which the conclusion has been drawn that molecular interactions exist which are neglected in the Debye—Hückel equation [19].

2.2. *The surface tension of the aqueous sodium-octanoate solutions*

The surface tension (σ) of the different aqueous sodium-octanoate solutions as a function of the concentration for various temperatures are presented in Figs 6—9. The values of CMC derived from these curves show a good agreement with the CMC obtained on the basis of Figs 1—4.

2.3. *The adsorption isotherm and the determination of the adsorption heat*

Gibbs' adsorption isotherm is written in its general from for 1—1 electrolytes as:

$$\Gamma = \frac{-\mathrm{d}\,\sigma}{2RT\,\mathrm{d}\ln a_{\pm}} = \frac{-\mathrm{d}\,\sigma}{2RT\,\mathrm{d}\ln \gamma_{\pm} c} \qquad (15)$$

Table V

The CMC and density values as functions of the temperature

Nr.	T/K	CMC/mol dm^{-3}	X_{CMC}	ϱ/g cm^{-3}
1	293	$3.00 \cdot 10^{-1}$	$5.597 \cdot 10^{-3}$	1.0092
2	303	$2.63 \cdot 10^{-1}$	$4.910 \cdot 10^{-3}$	1.0041
3*	308	$2.50 \cdot 10^{-1}$		
4	313	$2.29 \cdot 10^{-1}$	$4.278 \cdot 10^{-3}$	0.9986
5*	318	$2.56 \cdot 10^{-1}$		
6	323	$2.75 \cdot 10^{-1}$	$5.193 \cdot 10^{-3}$	0.9949

(The values marked with an asterisk were obtained by extrapolation)

where: σ surface tension of the solution (Jm^{-2}),
Γ amount of adsorption for the solute component,
$a_{\pm}$ mean activity of the solute component,
$\gamma_{\pm}$ mean activity coefficient of the solute component.

In a number of studies reported earlier, the mean activity coefficient of Eq. (15) was calculated either by using the Debye—Hückel equation, or it was assumed to be unity [17, 20, 21]. Our method enables to determine by direct measurement, the mean activity and activity coefficients, and the amount of adsorption too.

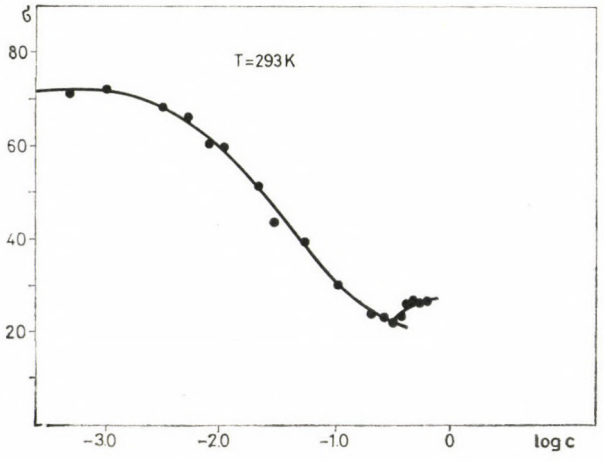

Fig. 6. The surface tension of the aqueous sodium-octanoate solutions depending on the concentration at 293 K

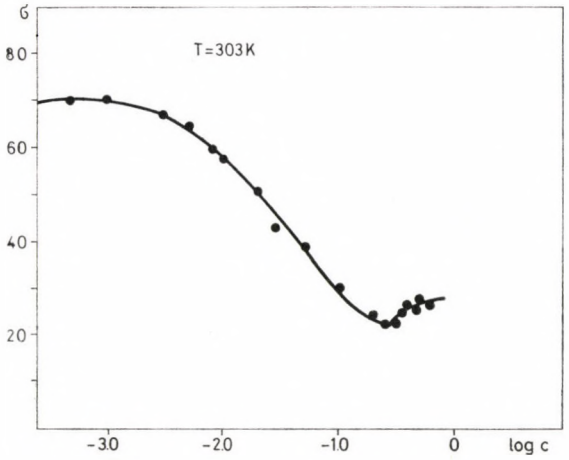

Fig. 7. The surface tension of the aqueous sodium-octanoate solutions depending on the concentration at 303 K

Equation (15) is rewritten for the aqueous solution of sodium-octanoate as

$$\Gamma = \frac{-0.4343\ \mathrm{d}\sigma/\mathrm{d}\log c}{RT\ \mathrm{d}\log a_{\mathrm{Na}}/\mathrm{d}\log c + \mathrm{d}\log a_{\mathrm{Oct}}/\mathrm{d}\log c} \qquad (16)$$

According to Eq. (16), the amount of adsorption as a function of the concentration at different temperature can be calculated from $\mathrm{d}\,\sigma/\mathrm{d}\log c$, which is obtained from the slope of the curves in Figs 6—9, and $\mathrm{d}\log a_{\mathrm{Na}}/\mathrm{d}\log c$ and $\mathrm{d}\log a_{\mathrm{Oct}}/\mathrm{d}\log c$ which are obtained on the basis of Tables I—IV.

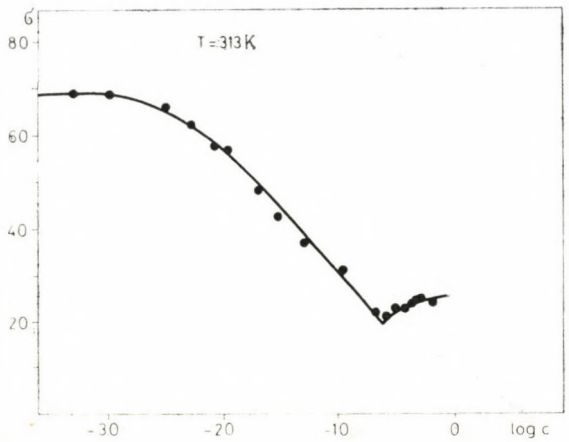

Fig. 8. The surface tension of the aqueous sodium-octanoate solutions depending on the concentration at 313 K

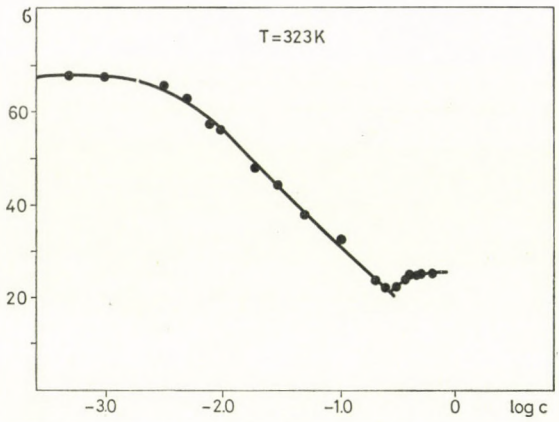

Fig. 9. The surface tension of the aqueous sodium-octanoate solutions depending on the concentration at 323 K

The adsorption isotherms calculated for 293 K and 303 K are given in Fig. 10 and the maximum amount of adsorption as a function of temperature in Table VI.

The differential adsorption enthalpy (ΔH_{ads}) can be calculated with a good approximation by the Rehbinder equation [22] from the temperature dependence of adsorption:

$$\Delta H_{ads} = RT^2 \left(\frac{\mathrm{d} \ln \Gamma}{\mathrm{d} T} \right)_c \tag{17}$$

The adsorption enthalpy values determined for various temperatures in the saturated range of the adsorption isotherm (10^{-2}—10^{-1} mol/dm^3) are also summarized in Table VI.

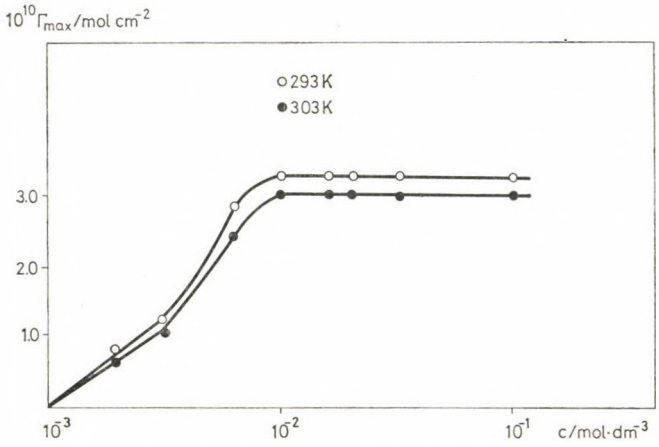

Fig. 10. The adsorption isotherm of the aqueous sodium-octanoate solution at 293 K and 303 K

Table VI

The maximum amount of adsorption and the adsorption heat as functions of the temperature

T/K	$10^{10}\,\Gamma_{max}$/mol cm^{-2}	$-\Delta H_{ads}$/kJ mol^{-1}
293	3.37	7.4908
303	3.07	8.0108
313	2.69	8.5483
323	2.51	9.1032

The sign of the adsorption enthalpy is negative, which corresponds to the tendency of the solute molecules in the aqueous solutions of the surfactants for spontaneous adsorption or orientation on the surface resulting a decrease in the free energy of the system.

2.4. *Thermodynamics of micellization*

For the thermodynamics of micelle formation two models have been used to interpret the behaviour of micelles. The first approach to be developed was the mass-action model [24], the second one introduced later was the phase-separation model [23, 25]. According to the phase-separation model the micelles of an ionic detergent, together with their bound counterions, are considered as a separate phase. From the phase rule it follows, that monomers and micelles are in equilibrium for only one monomer concentration, the CMC. Thus, monomer activity above the CMC should remain constant.

The equations derived for the standard free energy (ΔG°) and enthalpy (ΔH°) of the micelle formation are similar in form and are deduced from both models [27, 26]:

$$\Delta G^\circ = 2RT \ln a_{\pm CMC} \tag{18}$$

$$\Delta H^\circ = -2RT^2\, \partial \ln a_{\pm CMC}/\partial T \tag{19}$$

where $a_{\pm CMC}$: is the mean activity of surfactant at the CMC, and

$$a_{\pm CMC} = \gamma_{\pm}\, x_{CMC}$$

The numerical values of ΔG° and ΔH° calculated from the two models differ because the mole fractions (x_{CMC}) are calculated in different ways [26]. In the phase separation approach the total number of moles is equal to those of the water plus monomer. In the massaction approach micelles and free

Table VII

The $\Delta G°$, $\Delta H°$ and $\Delta S°$ of the micellization depending on the temperature

T/K	$a_{\pm CMC}$	$\Delta G°$/kJ mol^{-1}	$\Delta H°$/kJ mol^{-1}	$T\Delta S°$/kJ mol^{-1}
293	0.0877	−11.852	46.971	58.823
303	0.0631	−13.915	10.513	24.428
313	0.0589	−14.732	0	14.732
323	0.0605	−15.059	−4.647	10.412

counter ions are also included. (Our calculations were done by the phase-separation model.)

The values of $\Delta G°$, $\Delta H°$ and $T\,\Delta S°$ determined from Eqs. (18) and (19) as function of the temperature are presented in Table VII and in Fig. 11.

The enthalpy of micellization can be explained as the heat effect of the micelle stabilization by hydrophobic interactions [28].

The sign of $\Delta H°$ is determined by the strength of the hydrophobic interactions which increases with the rise in temperature up to a certain temper-

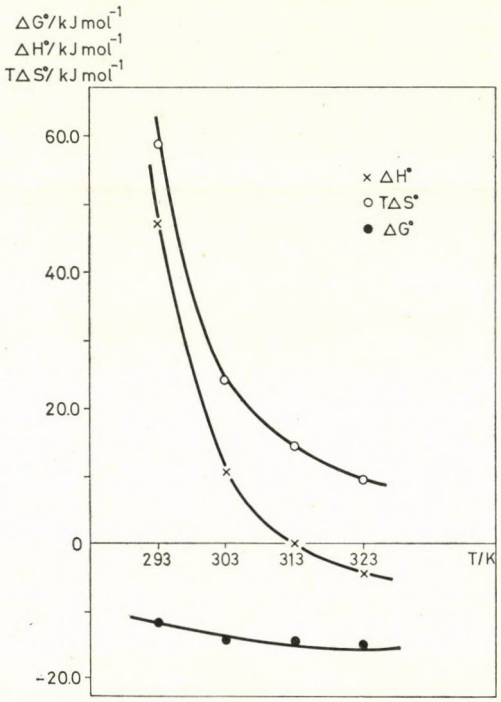

Fig. 11. The $\Delta G°$, $\Delta H°$ and $\Delta S°$ of the micellization depending on the temperature

ature and decreases at higher temperatures [28, 29]. On the basis of the results in Table VII and Fig. 11 it can be concluded that the standard enthalpy of the aqueous sodium-octanoate solutions decreases with the rise in temperature, and at the temperature related to the minimal CMC $\Delta H^\circ = 0$ [23, 28]. Consequently the temperature range under consideration the strength of hydrophobic interactions increases with increasing temperature. The change in the sign of ΔH° is due to the temperature variation of the CMC's (Fig. 5), becoming more and more negative as the temperature increases [28, 30].

Considering the sign of the thermodynamic functions of micelle formation in aqueous solutions of sodium-octanoate ($\Delta G^\circ < 0$, $\Delta S^\circ > 0$, $\Delta H^\circ > 0$) we can conclude that the entropy is the most important factor in stabilizing the hydrophobic bounds of the micellization and it is due to changes in the water structure [29]. During the micelle formation the stability of the system increases ($G^\circ < 0$) and in the temperature range examined the standard free energy decreases as the temperature rises.

2.5. *Micelle formation and counterion attachment*

The degree of counterion attachment, r, of an ionic micelle is described in different ways by the models of micelle formation proposed in [25, 31, 32] Various methods have been employed to estimate r [10, 33—35]; the values are spread over a wide range depending on the experimental methods.

In this study, the activity measurements allow the interpretation of the micellization's mechanism, and the dgree of counterion attachment. We shall now survey the main points of the two models in the respect mentioned above. According to the mass-action law, the micelle formation of sodium-octanoate is expressed in terms of homogeneous equilibrium as

$$p\ \mathrm{Oct}^- + q\ \mathrm{Na}^+ + (\mathrm{Na}_q\ \mathrm{Oct}_p)^{-(p-q)}$$

and the condition of the equilibrium by

$$[a_\mathrm{M}/a_\mathrm{Oct}^p \cdot a_\mathrm{Na}^q = \mathrm{constant}]_{p,T} \tag{20}$$

where a_M is the activity of the micelles, and p and q are the numbers of Oct^- and Na^+ ions, respectively. According to the phase-separation theory the micelles are considered as a separate microphase or pseudophase [31, 32] and the micelle formation is expressed as follows:

a) in the case of an uncharged phase separation by

$$p\ \mathrm{Oct}^- + p\ \mathrm{Na}^+ \rightleftharpoons \mathrm{Na}_p\ \mathrm{Oct}_p$$

and the equilibrium condition by

$$[a_{Na} \cdot a_{Oct} = \text{constant}]_{p,T} \tag{21}$$

b) in the case of charged phase-separation by

$$p\ Oct^- + q\ Na^+ \rightleftharpoons (Na_q\ Oct_p)^{-(p-q)}$$

and the equilibrium condition by

$$[a_{Na}^q \cdot a_{Oct}^p = \text{constant}]_{p,T} \tag{22}$$

Eqs (20—22) may be summarized to give, since $r = q/p$,

$$\log a_{Oct} + r \log a_{Na} \neq \text{constant} \tag{23/a}$$

for the mass action model, and

$$\log a_{Oct} + r \log a_{Na} = \text{constant} \tag{23/b}$$

for the phase separation model, when

$r = 1$ for the uncharged phase-separation model,

$r \neq 1$ for the charged phase-separation model.

On the basis of our experimental results Fig. 12 shows $\log a_{Oct}$ plotted against $\log a_{Na}$ for the temperature range examined, giving parallel straight lines expressed by

$$\log a_{Oct} + r \log a_{Na} = \text{constant} \tag{24}$$

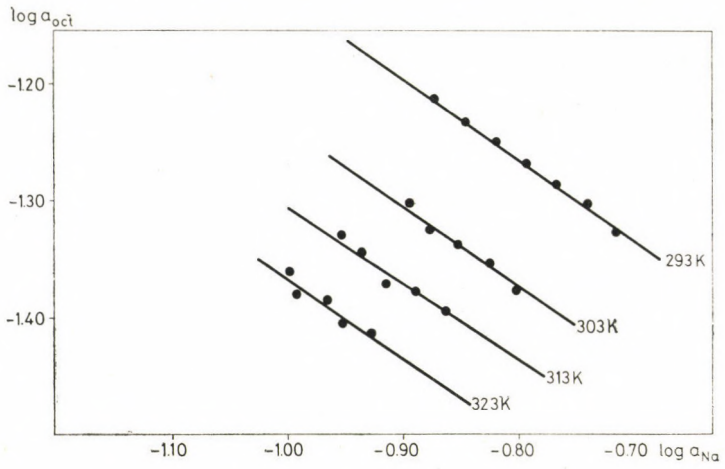

Fig. 12. $\log a_{Oct}$ *vs.* a_{Na} above CMC

with $r = 0.665$ and the values of constant depending on the temperature investigated are: -1.795, -1.902, -1.965 and -2.029. According to Eqs (23/b) and (24) the charged phase-separation is the most probable mechanism of the micelle formation in the aqueous solution of sodium-octanoate; the charged micelles with the degree of counterion attachment of 0.665 are considered as being formed in the concentration range from CMC to $6.0 \cdot 10^{-1}$ mol/dm^3.

The charged phase-separation model accounts for the slow increase of the mean activity ($a_{\pm}$) above the CMC [9, 36], which is shown in Figs 1—4 presenting our experimental results.

REFERENCES

[1] Danielsson, I.: Finska Kemistsamfundets Medd., **75,** 65 (1966)
[2] Stenius, P.: Proc. Int. Congr. Surface Active Subst., 5th, **3,** 1023 (1969)
[3] Danielsson, I., Stenius, P.: J. Colloid Interface Sci., **37,** 264 (1971)
[4] Ödberg, L., Svens, B., Danielsson, I.: J. Colloid Interface Sci., **41,** 298 (1972)
[5] Svens, B., Rosenholm, B.: J. Colloid Interface Sci., **44,** 495 (1973)
[6] Botre, C., Hall, G., Scowen, R. V.: Kolloid-Z. U. Z. Polym., **250,** 900 (1972)
[7] Botre, C., Matiis, De., Solinas, M.: J. Phys. Chem., **68,** 3624 (1964)
[8] Gavach, C.: Proc. 5th Int. Congr. Sard. Act. Sub., **2,** 859 (1969)
[9] Ekwall, P., Eiken, H., Stenius, P.: Acta Chem. Scand., **21,** 1639 (1967)
[10] Sasaki, T., Hattori, M., Sasaki, J., Nukina, K.: Bull. Chem. Soc. Japan, **48,** 1397 (1975)
[11] Satake, J., Tahara, T., Matuura, R.: Bull. Chem. Soc. Japan, **42,** 319 (1969)
[12] Robinson, R. A., Stokes, R. H.: "Electrolyte Solutions" 2nd, ed., Butterworths Scientific Pub., London 1959, p. 190
[13] Koshinuma, M., Sasaki, T.: Bull. Chem. Soc. Japan, **48,** 2755 (1975)
[14] Kishimoto, H., Sumida, K.: Chem. and Pharm. Bull. Japan, **22,** 1108 (1974)
[15] Crook, E. H., Trebbi, G. F., Fordycem, D. B.: J. Phys. Chem., **68,** 3592 (1964)
[16] Tanford, G.: "The Hydrophobic Effect", John Wiley and Sons, New York 1973
[17] Kielland, J.: J. Amer., Chem. Soc., **59,** 1675 (1937)
[18] Rusanov, A. J., Krotov, V. V.: Proc. 6th Int. Congr. Surface Active Substances, 2. Part **2,** 794 (1975)
[19] Mukerjee, P., Mysels, K. J., Dulin, C. J.: J. Phys. Chem., **62,** 1390 (1958)
[20] Flenges, S. N., Rideal, E.: Trans. Faraday Soc., **55,** 339 (1959)
[21] Güntenberg, E.: Z. Phys. Chem., **123,** 199 (1926)
[22] Rehbinder: Zhurn. Prikl. Fiz., **1,** 151 (1924)
[23] Shinoda, K., Nakagava, T., Tamamushi, B., Isemura, T.: Colloidal Surfactants, Acad. Pr. New York 1963
[24] Jones, E. R., Bury, C. R.: Phil. Mag., **4,** 481 (1927)
[25] Shinoda, K., Hutchinson, E.: J. Phys. Chem., **66,** 577 (1962)
[26] Fischer, L. R., Oakenfull, D. G.: Chem. Soc. Reviews, **6,** 25 (1977)
[27] Corkill, J. M., Goodman, J. F., Harold, S. P., Tate, J. R.: Trans. Faraday Soc., **62,** 994 (1966)
[28] Ray, A., Némethy, G.: J. Phys. Chem., **75,** 804 (1971)
[29] Némethy, G., Scheraga, H. A.: J. Phys. Chem., **66,** 1773 (1962)
[30] Corkill, J. M., Goodman, J. F., Harrold, S. P., Trans. Faraday Soc., **60,** 202 (1964)
[31] Stainsby, G., Alexander, A. E.: Trans. Faraday Soc., **46,** 527 (1960)
[32] Shinoda, K.: Bull. Chem. Soc. Japan, **26,** 101 (1953)
[33] Phillips, J. N.: Trans. Faraday Soc., **51,** 561 (1955)
[34] Feinstein, M. E., Rosano, H. L.: J. Colloid Interfac. Sci., **24,** 73 (1967)
[35] Fishman, M. L., Eirich, E. R.: J. Phys. Chem., **75,** 3135 (1971)
[36] Mysels, K. J., Mukerjee, P., Abu-Hamdiyyah: J. Phys. Chem., **67,** 1943 (1963)

Zsuzsa Bedő
Endre Berecz
} H-3515 Miskolc, Egyetemváros

Acta Chimica Academiae Scientiarum Hungaricae, Tomus 103 (2), pp. 217—224 (1980)

INVESTIGATION OF BINARY SURFACTANT SYSTEMS, II

STUDIES OF SODIUM-OCTANOATE–HEAVY WATER SOLUTIONS BY ACTIVITY MEASUREMENTS

Zs. Bedő and E. Berecz

(Department of General and Physical Chemistry Technical University for Heavy Industry Miskolc, Hungary)

Received February 10, 1979

Accepted for publication April 6, 1979

The ion activities, and the mean activities and activity coefficients of the surfactant in the sodium-octanoate — heavy water system depending on the temperature and concentration were determined on the basis of EMF measurements. From these data the CMC and its dependence on the temperature were given.

The influence of the solvent's quality on the CMC of the surfactant solutions, on the mean activity and the activity coefficient of the surfactant for the CMC, and on the stability of the micellar solution examined were studied.

On the basis of the temperature dependence of $\Delta G°$, $\Delta H°$ and $\Delta S°$ for the micelles in the NaC_8-D_2O system is smaller than that in the NaC_8-H_2O system, which can be interpreted by the decrease of the strength of hydrophobic bonds in heavy water.

The stability of the micelles formed in the aqueous solutions of the surface-active agents is affected mainly by the nature of the hydrophobic bonds* developed. The strength of these hydrophobic bonds may be different depending on the quality of the solvent and solute [1].

In this paper, to study the influence of the solvent's quality on the conditions of the stability, we will compare the critical micelle concentrations (CMC), the mean activities and mean activity coefficients at the CMC, and the thermodynamical functions of micelle formation in the sodium-octanoate — water and sodium-octanoate — heavy water binary micellar system. The knowledge of these characteristic quantities gives possibility to draw conclusions on the basis of our experimental results for the effect determining the stability and micelle formation in the two systems examined.

1. Experimental

To achieve the goals mentioned above, the ion activities and their dependence on the concentration and temperature were determined on the basis of the EMF measured in the sodium-octanoate (NaC_8) — heavy water system.

* The formation of a hydrophobic bond can be considered as a dimerization or trimerization reaction of two or more hydrophobic chains surrounded by water, when the total number of water molecules in contact with them and the translational and rotational entropy are decreasing [5].

The experimental method, and the preparative procedure have been described elsewhere [2].

Deuterium oxide (99.7% D) was obtained from the Central Research Institute for Physics.

2. Results and Discussion

The method of the calculation of the activity of sodium and octanoate ions (a_{Na}, a_{oct}) the mean activity ($a_{\pm}$) and the mean activity coefficient ($\gamma_{\pm}$) are described also elsewhere [2].

The individual ion activities and activity coefficients, as well as the mean activities and activity coefficients and their dependence on the concentration and temperature are shown in Tables I—IV and in Figs 1—2.

The critical micelle concentration derived from the break-points of the figures, and the values of the mean activities and activity coefficients at the CMC depending on the temperature are given in Table V.

On the basis of our experimental investigation of the temperature dependence of CMC — corresponding with many publications [1, 3, 4] — a shallow minimum of these functions can be concluded. As shown in Fig. 3 the CMC of the sodium-octanoate — heavy water solutions depending on the temperature — similarly to the aqueous solutions — has a minimum at 313 K.

Table I

The activity of the surfactant in the NaC_8—D_2O system depending on the concentration at 293 K

c/mol dm^{-3}	Δ_{Na}	Δ_{oct}	$-\lg a_{Na}$	$-\lg a_{oct}$	$-\lg a_{\pm}$	$-\lg \gamma_{\pm}$
$1.0 \cdot 10^{-3}$	3.921	1.160	3.0192	3.0588	3.0389	0.0388
$3.0 \cdot 10^{-3}$	3.899	1.120	2.5631	2.6027	2.5826	0.0597
$5.0 \cdot 10^{-3}$	3.850	1.040	2.3909	2.4564	2.4235	0.1223
$8.0 \cdot 10^{-3}$	3.826	1.020	2.2102	2.2843	2.2472	0.1501
$1.0 \cdot 10^{-2}$	3.815	0.976	2.1242	2.2155	2.1699	0.1697
$5.0 \cdot 10^{-2}$	3.788		1.4529	1.7077	1.5805	0.2792
$1.0 \cdot 10^{-1}$			1.1861	1.4926	1.3392	0.3390
$1.5 \cdot 10^{-1}$			0.9968	1.3205	1.1589	0.3348
$2.0 \cdot 10^{-1}$			0.8503	1.2000	1.0253	0.3260
$2.5 \cdot 10^{-1}$			0.8244	1.1693	0.9970	0.3948
$3.0 \cdot 10^{-1}$			0.7556	1.1398	0.9476	0.4246
$4.0 \cdot 10^{-1}$			0.7384	1.0805	0.9093	0.5111
$5.0 \cdot 10^{-1}$			0.7040	1.0681	0.8860	0.5849
$6.0 \cdot 10^{-1}$			0.6420	1.0189	0.8303	0.6082

Table II

The activity of the surfactant in the NaC_8-D_2O system depending on the concentration at 303 K

c/mol dm^{-3}	Δ_{Na}	Δ_{oct}	$-\lg a_{Na}$	$-\lg a_{oct}$	$-\lg a_{\pm}$	$-\lg \gamma_{\pm}$
$1.0 \cdot 10^{-3}$	3.924	1.128	3.0463	3.0324	3.0394	0.0392
$3.0 \cdot 10^{-3}$	3.896	1.092	2.5960	2.5913	2.5940	0.0709
$5.0 \cdot 10^{-3}$	3.849	1.011	2.4216	2.4499	2.4360	0.1346
$8.0 \cdot 10^{-3}$	3.811	0.982	2.2552	2.2751	2.2651	0.1680
$1.0 \cdot 10^{-2}$	3.797	0.960	2.1720	2.2000	2.1861	0.1860
$5.0 \cdot 10^{-2}$	2.773		1.4979	1.7001	1.5995	0.2983
$1.0 \cdot 10^{-1}$			1.2483	1.4762	1.3623	0.3620
$1.5 \cdot 10^{-1}$			1.0402	1.3098	1.1751	0.3509
$2.0 \cdot 10^{-1}$			0.8821	1.1600	1.0211	0.3219
$2.5 \cdot 10^{-1}$			0.8738	1.1384	1.0122	0.4039
$3.0 \cdot 10^{-1}$			0.8155	1.1184	0.9669	0.4439
$4.0 \cdot 10^{-1}$			0.7906	1.0685	0.9294	0.5314
$5.0 \cdot 10^{-1}$			0.7573	1.0601	0.9086	0.5794
$6.0 \cdot 10^{-1}$			0.6612	1.0500	0.8555	0.6335

Table III

The activity of the surfactant in the NaC_8-D_2O system depending on the concentration at 313 K

c/mol dm^{-3}	Δ_{Na}	Δ_{oct}	$-\lg a_{Na}$	$-\lg a_{oct}$	$-\lg a_{\pm}$	$-\lg \gamma_{\pm}$
$1.0 \cdot 10^{-3}$	3.926	1.123	3.0636	3.0170	3.0403	0.0401
$3.0 \cdot 10^{-3}$	3.909	1.073	2.6278	2.5900	2.6089	0.0859
$5.0 \cdot 10^{-3}$	3.864	0.988	2.4506	2.4531	2.4518	0.1507
$8.0 \cdot 10^{-3}$	3.821	0.961	2.2975	2.2759	2.2867	0.1896
$1.0 \cdot 10^{-2}$	3.805	0.945	2.2170	2.1953	1.9643	0.2060
$5.0 \cdot 10^{-2}$	3.823		1.5403	1.7120	1.5052	0.3250
$1.0 \cdot 10^{-1}$			1.2986	1.4703	1.3039	0.3842
$1.5 \cdot 10^{-1}$			1.0730	1.3092	1.1066	0.3669
$2.0 \cdot 10^{-1}$			0.9522	1.1400	1.0390	0.3471
$2.5 \cdot 10^{-1}$			0.9280	1.1255	0.9897	0.4245
$3.0 \cdot 10^{-1}$			0.8636	1.0514	0.9695	0.4345
$4.0 \cdot 10^{-1}$			0.8394	1.0756	0.9534	0.5594
$5.0 \cdot 10^{-1}$			0.8072	1.0675	0.9373	0.6360
$6.0 \cdot 10^{-1}$			0.7105	1.0594	0.8849	0.6628

Table IV

The activity of the surfactant in the NaC_8—D_2O system depending on the concentration at 323 K

c/mol dm^{-3}	Δ_{Na}	Δ_{oct}	$-\lg a_{Na}$	$-\lg a_{oct}$	$-\lg a_{\pm}$	$-\lg \gamma_{\pm}$
$1.0 \cdot 10^{-3}$	3.913	1.126	3.0274	3.0436	3.0355	0.0394
$3.0 \cdot 10^{-3}$	3.866	1.063	2.5980	2.6298	2.6639	0.0909
$5.0 \cdot 10^{-3}$	3.816	0.974	2.4263	2.4971	2.4617	0.1606
$8.0 \cdot 10^{-3}$	3.768	0.950	2.2701	2.3176	2.2939	0.1967
$1.0 \cdot 10^{-2}$	3.749	0.938	2.1921	2.2317	2.2118	0.2117
$5.0 \cdot 10^{-2}$	3.745		1.4973	1.7711	1.6342	0.3331
$1.0 \cdot 10^{-1}$			1.2865	1.5213	1.4039	0.4037
$1.5 \cdot 10^{-1}$			1.0523	1.3574	1.2049	0.3807
$2.0 \cdot 10^{-1}$			0.9508	1.1700	1.0605	0.3613
$2.5 \cdot 10^{-1}$			0.9118	1.1622	1.0341	0.4348
$3.0 \cdot 10^{-1}$			0.8493	1.0997	0.9744	0.4515
$4.0 \cdot 10^{-1}$			0.8260	1.1232	0.9745	0.5763
$5.0 \cdot 10^{-1}$			0.7947	1.1154	0.9550	0.7099
$6.0 \cdot 10^{-1}$			0.6932	1.1075	0.9003	0.6782

We can explain the observed behaviour only partly in terms of hydrophobic bonds or different temperature dependence of their interactions. In case of ionic detergents the stability of the micelles is affected by the macroscopic dielectric properties of the medium as well [1]; lowering the relative

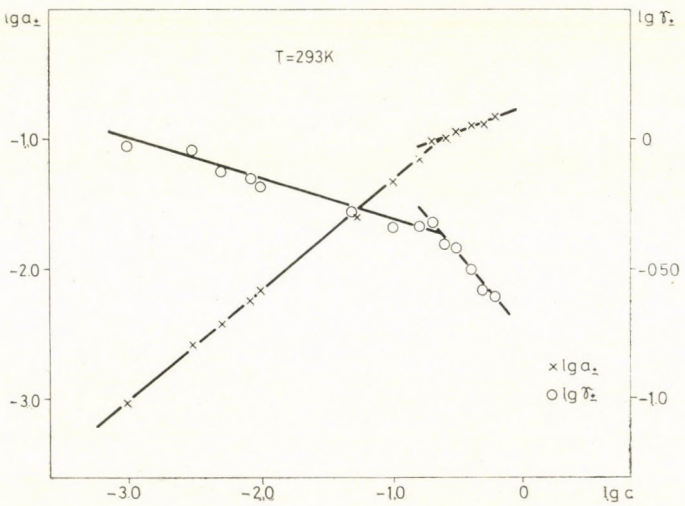

Fig. 1. The mean activity and activity coefficient of the surfactant in the NaC_8—D_2O system depending on the concentration at 293 K

Table V

The CMC in the NaC_8—D_2O system, and the surfactant's mean activity and mean activity coefficient at the CMC as a function of the temperature

T, K	CMC/mol dm^{-3}	$-\ln a_{\pm CMC}$	$-\ln \gamma_{\pm CMC}$
293	$2.345 \cdot 10^{-1}$	2.3025	0.8524
303	$1.995 \cdot 10^{-1}$	2.4864	0.8744
308*	$1.880 \cdot 10^{-1}$		
313	$1.698 \cdot 10^{-1}$	2.5558	0.7826
318*	$1.920 \cdot 10^{-1}$		
323	$2.188 \cdot 10^{-1}$	2.5094	0.9899

(The values marked with an asterisk were obtained by extrapolation)

permittivity of the medium (by increasing the temperature) should tend to break up the micelles, *i.e.*, to raise the CMC by increasing the repulsive force between the ionic heads of the detergent molecules.

There are thus two opposing effects to consider: at low temperatures the hydrophobic effect predominates over the dielectric effect, and at high temperature the opposite tendency is realized. Thus, the observed maximum in the stability can be explained sufficiently.

The change of the CMC's values, affected by the quality of the solvent, can be interpreted by taking into account the dielectrical properties of the medium and the standard free energy change of formation of the hydrophobic

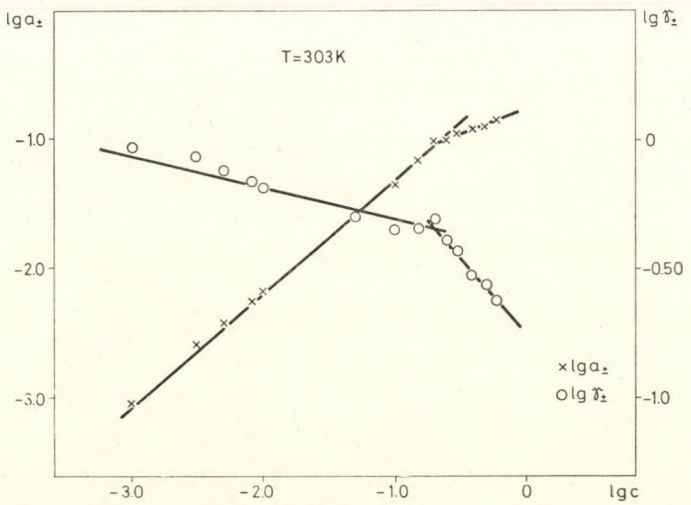

Fig. 2. The mean activity and activity coefficient of the surfactant in the NaC_8—D_2O system depending on the concentration at 303 K

bond [1]. The total standard free energy change of formation of the hydrophobic bond can be written as [5]:

$$\Delta G^\circ_H = \Delta G^\circ_W + \Delta G^\circ_S$$

where ΔG°_W the standard free energy change derived from the change of the water structure,

ΔG°_S the standard free energy change derived from the change in the states of the side chains.

Since the relative permittivity of D_2O is only very slightly lower than that of H_2O over the wide temperature range, the electrical contribution makes the micelle only negligibly less stable in D_2O at any particular temperature than in H_2O.

Discussion of the free energy change of the hydrophobic bonds is considerably more equivocal. The influence of the solutes on water structure is complicated, a definite prediction is impossible.

Since the heavy water has a higher energy density than the H_2O, insertion of the hydrocarbon chains, having much smaller energy density, into the heavy water is more unfavourable (from the point of view of free energy) than in case of H_2O. The changes in the structure of water surrounding the hydrocarbon chains play an important role in the formation of hydrophobic bonds and in the determination of the free energy change for the process [5]. The effect of the dissolved hydrocarbon molecules on the water structure has

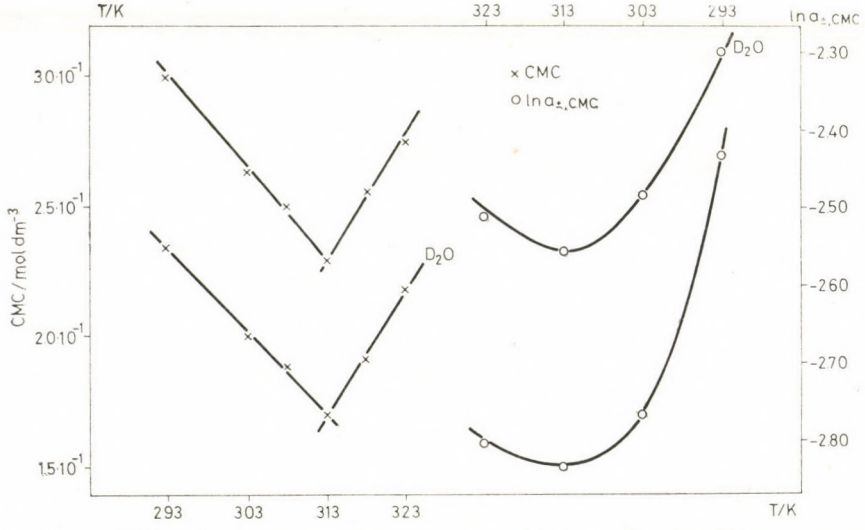

Fig. 3. The CMC and the mean activity at the CMC depending on the temperature

been discussed by FRANK and EVANS [6], who introduced the concept of "iceberg", *i.e.* an increased ordering of water around the hydrocarbon chains, accompanied by an increase in the degree of hydrogen bonding. Since D_2O is the more structured solvent, the formation of icebergs in heavy water has a larger thermodynamical probability than in case of H_2O.

However, the two processes affecting the values of CMC — the dielectrical and hydrophobic interactions — (especially the latter) as a function of the temperature and the quality of the solvent and the solute are various for every concrete systems, therefore the methods of the accurate prediction can not be treated yet.

In the system of sodium-octanoate — heavy water the values of CMC are smaller, the mean activities and the mean activity coefficients at the CMC are larger than those of sodium-octanoate — water solutions. On the basis of the knowledge of these data further thermodynamic properties of the examined micellar solutions can be compared.

To explain the influence of the quality of the solvent on the thermodynamic characteristics of the micellar system, the standard free energy change (ΔG°), the enthalpy change (ΔH°) and the entropy change (ΔS°) for the micelle formation in the sodium-octanoate — heavy water system were determined on the basis of the required theoretical consideration [2].

The values of ΔG°, ΔH° and $T\Delta S^\circ$ as a function of the temperature concerning the two systems examined, are presented in Table VI and in Fig. 4.

According to the values of the mean activity at the CMC in the systems of the sodium-octanoate — water and sodium-octanoate — heavy water, and on the basis of the thermodynamic functions of micellization for the two solutions ($\Delta G^\circ_{H_2O} < \Delta G^\circ_{D_2O}$; $T\Delta S^\circ_{H_2O} > T\Delta S^\circ_{D_2O}$) as well, we can draw the conclusion that the stability of the micelles of sodium-octanoate in D_2O is smaller than in H_2O, which can be interpreted by a decrease in the hydrophobic bond strength.

The mean activity coefficient for the CMC depending on the temperature was found to be $\gamma_\pm = 0.37 - 0.43$, which — similarly to the aqueous solutions

Table VI

The ΔG°, ΔH° and ΔS° of the micellization depending on the temperature

T, K	$-\Delta G^\circ$/kJ mol^{-1}	ΔH°/kJ mol^{-1}	$T\Delta S^\circ$/kJ mol^{-1}
293	11.212	26.239	37.451
303	12.521	10.589	23.110
313	13.295	0	13.295
323	13.471	— 8.046	5.425

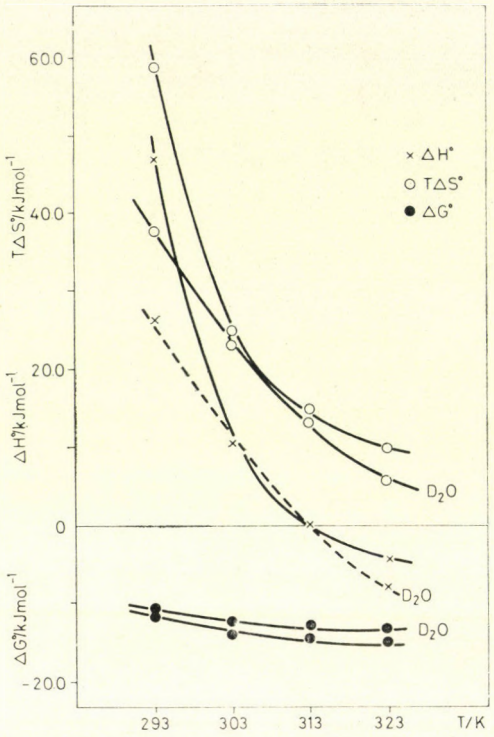

Fig. 4. The ΔG°, ΔH° and ΔS° of the micellization depending on the temperature

of the sodium-octanoate — are smaller than the value calculated by the Debye—Hückel equation [2]. This difference can be explained by the "pre-micelle" formation [7], that kind of molecular interactions are neglected in the Debye—Hückel equation [8, 9, 10].

REFERENCES

[1] EMERSON, M. F., HOLTZER, A.: J. Phys. Chem., **71,** 10 (1967)
[2] BEDŐ, Zs., BERECZ, E.: Magyar Kém. Folyóirat (to be published)
[3] KISHIMOTO, H., SUMIDA, K.: Chem. and Pharm Bull. Japan, **22,** 1108 (1974)
[4] CROOK, E. H., TREBBI, G. F., FORDYCEM, D. B.: J. Phys. Chem., **68,** 3592 (1964)
[5] NÉMETHY, G., SCHERAGA, H. A.: Phys. Chem., **66,** 1773 (1962)
[6] FRANK, H. S., EVANS, M. W.: J. Chem. Phys., **13,** 507 (1945)
[7] FISCHER, L. R., OAKENFULL, D. G.: Chem. Soc. Rev., **6,** 25 (1977)
[8] SASAKI, T., HATTORI, M., SASAKI, J., NUKINA, K.: Bull. Chem. Soc. Japan, **48,** 1397 (1975)
[9] KOSHINUMA, M., SASAKI, T.: Bull. Chem. Soc. Japan, **48,** 2755 (1975)
[10] RUSANOV, A. J., KROTOV, V. V.: Proc. 6th Int. Congr. Surface Active Substances, 2. Part **2**, 794 (1975)

Zsuzsa BEDŐ
Endre BERECZ
H-3515 Miskolc, Egyetemváros

INDEX

PHYSICAL AND INORGANIC CHEMISTRY

ORGANIC CHEMISTRY

ANALYTICAL CHEMISTRY

CHEMICAL TECHNOLOGY

Printed in Hungary

A kiadásért felel az Akadémiai Kiadó igazgatója. Műszaki szerkesztő: Zacsik Annamária

A kézirat nyomdába érkezett: 1979. VIII. 7. — Terjedelem: 10,15 (A/5) ív, 70 ábra

80.7396 Akadémiai Nyomda, Budapest — Felelős vezető: Bernát György

ACTA CHIMICA

ТОМ 103—ВЫП. 2

РЕЗЮМЕ

Гидродехлорирование пестицидов в импульсном реакторе

А. Х. ВЕЙС и Р. Б. ЛАПЬЕР

Каталитическое гидродехлорирование хлористых пестицидов и других хлорированных материалов, не желаемых с точки зрения охраны природы, в соединения с более низким содержанием хлора было исследовано в импульсном реакторе. Хлор может быть каталитически удален и замещен водородом, давая как частично хлорированные промежуточные продукты, так и полностью дехлорированные углеводороды. Промежуточные продукты эквивалентны некоторым продуктам, полученным природной деградацией.

Импульсный реактор представляет собой простую технику, позволяющую предсказывать как состав продуктов, так и условия реакции, требуемые для получения таких еградированных продуктов в лабораторных масштабах.

Конденсированные асим-триазины, VII

Упрощенный метод синтеза производных бензо-асим-триазина

А. МЕССМЕР, ДЬ. ХАЙОШ, П. БЕНКО и Л. ПАЛЛОШ

Был разработан упрощенный синтез типа Арндт—Розенау, приводящий к образованию 3-меркапто-бензо-*асим*-триазинам. С помощью данного синтеза 3-меркапто- и 3-метилтио-бензо-*асим*-триазины могут быть получены из *орто*-нитроанилинов на двух ступенях и с высоким выходом. Синтезы более чем 40 новых производных бензо-*асим*-триазина, описанные здесь, включают в себя алкилирование и нуклеофильное замещение меркапто-группы. Циклизация 5-хлорозамещенного *о*-нитроанилина протекает аномально; это объяснялось электроноакцепторным эффектом нитрогруппы на *пара*-положение.

Изучение взаимодействия некоторых полярных винилмономеров с $AlEt_3$ методом инфракрасной спектроскопии

А. ДАНКОВИЧ, Л. ЛЕНДВАИ, Ю. В. КИССИН и И. СЁЛЛЁШИ

Смещение полосы валентных колебаний C≡N при комплексообразовании акрилонитрила — $AlEt_3$ в сторону более высоких частот свидетельствует о том, что комплекс в первую очередь образуется за счет неподеленной пары электронов атома азота. Вероятность этого взаимодействия понижается при повышении реакционного времени и понижении молярного соотношения $AN/AlEt_3$. При увеличении времени реакции преобладает комплексообразование, в которое вовлечена и связь C = C.

В образовании комплекса винилацетат-$AlEt_3$ важную роль играет карбонильная группа. Определено, что стабильность взаимодействия является функцией молярного соотношения мономера и металл-алкила. С повышением концентрации металл-алкила стабильность комплекса повышается.

В случае образования комплекса метилметакрилат — $AlEt_3$ взаимодействие компонентов происходит через группы C = O метилметакрилата. При молярном соотношении $MMA/AlEt_3 < 1$ стабильность комплекса повышается. С увеличением времени реакции и концентрации металл-алкила могут производить и реакции переалкилирования.

При взаимодействии акриловой кислоты и акриламида с $AlEt_3$ в реакцию вступают подвижные атомы Н. С понижением молярного соотношения АК/$AlEt_3$ стабильность взаимодействия понижается.

Стабильность комплекса АА—$AlEt_3$ понижается с увеличением концентрации металл-алкила.

Появление абсорбции при 2225 и 2275 $см^{-1}$ в инфракрасном спектре при относительно большом избытке металл-алкила доказывает преобладание донорно-акцепторного взаимодействия между компонентами и реакции, происходящей с образованием нитрильной группы.

Из приведенных данных видно, что все исследованные виниловые мономеры вступают в энергичные реакции с $AlEt_3$. Первичные продукты этих взаимодействий стабильны в течении нескольких часов лишь при отсутствии избытка алюминийорганического соединения. Поскольку обычно реакция сополимеризации виниловых мономеров и олефинов проводится в условиях, когда концентрация винилового мономера ниже, чем концентрация $AlEt_3$ (1, 2), необходимо принимать во внимание также и возможность дальнейших пимических превращений в реакционной смеси, которые либо выводят часть винилового мономера из сферы реакции сополимеризации вследствие расхода двойных связей, либо приводят к образованию комплексов новых виниловых мономеров.

Влияние фотографических и фотометрических параметров на спектрографическую оценку, IV

Исследование кривой почернения. Зависимости фотографических и фотометрических параметров при фотометрии полосовых спектров

ДЬ. ХЕЛТАИ, К. ЦИММЕР, М. МАТЕРНИ и К. ФЛОРИАН

Рассеянный свет, попадающий в фотометр полосовых спектров в значительной мере влияет на вид кривой почернения. В случае непрерывного спектра этим мешающим действием можно пренебречь, однако, при измерении полосовых спектров с увеличением величины γ это действие возрастает с уменьшением ширины полосы. В результате этого, линейный участок кривой почернения полосовых спектров, при использовании обычного фотометра полосовых спектров Zeiss GII, всегда загибается. Поэтому правило для длины ΔS_L, измеренной при почернении на линейном участке кривой почернения, согласно которому $\Delta S_L \simeq 1{,}25$, справедливо лишь в определенном интервале величин γ. Вуальное почернение также понижает влияние рассеянного света.

Влияние фотографических и фотометрических параметров на спектрографическую оценку, V

Влияние типа фотометра полосовых спектров на вид кривой почернения полосовых спектров и на оценку с помощью *l*-трансформации

ДЬ. ХЕЛТАИ и К. ЦИММЕР

Сравнивая контуры кривых почернения, полученных с помощью фотометров полосовых спектров различного типа (обычных и современных) было установлено, что формы кривых различаются вследствие различной интенсивности рассеянного света и эти отклонения, в зависимости от почернения, быстро увеличиваются. Величины γ, S_L и S_{LL}, определенные на различных приборах, различаются. В современных приборах с небольшим рассеянным светом, высшее — надежно измеряемое — предельное значение почернения S_{LL} больше на 0,5—1,5 почернения, нежели в случае обычных приборов. Однако, величины k, в противоположность этому, не зависит от типа прибора и величины Δl, равные логарифму величины относительной интенсивности, могут быть определены с помощью *l*-трансформации с одинаковой точностью, к тому же значения l, полученные на различных установках, приблизительно одинаковы.

Исследование равновесий комплексообразования между гликолями и борной кислотой в водных растворах

Т. Л. ПААЛ

В литературе встречаемся с противоречивыми представлениями относительно строения и образования нейтральных комплексов гликолей с борной кислотой. Для исследования таких систем с успехом может быть применим метод экстракции жидкость — жидкость. Подробно было изучено распределение борной кислоты, а также электролитов и нейтральных молекул в системе *н*-спирт — вода, а затем из данных измерений в системе бутанол — вода, были определены константы равновесия комплексов D-сорбита, D-маннита, дульцита и бутан-1,3-диола с борной кислотой. Образование комплексов бутан-1,3-диол с борной кислотой и боратами было исследовано pH-метрически. В случае этиленгликоля, пропан-1,2-диола и глицерина не удалось обнаружить образования нейтральных комплексов с борной кислотой. На основе полученных результатов обсуждаются равновесия комплексообразования между гликолями и борной кислотой, а также боратами.

Исследование слабых взаимодействий в водных растворах между борной кислотой и полярными органическими соединениями

Т. Л. ПААЛ

Повышение pH, наблюдаемое при добавлении полярных органических соединений к буферным растворам борная кислота — борат, объясняется на основе образования комплексов борная кислота — основание Льюиса с составом 1 : 1. При добавлении тех же самых реагентов к буферным растворам с тем же pH, в которых вместо бората присутствует фосфат, наблюдалось лишь минимальное изменение pH, вызванное влиянием среды полярных органических соединений. Внося поправку на это, были рассчитаны константы равновесия комплексов диоксана, диметилформамида, диметилсульфоксида, ацетона, бутанола, пропанола, метанола и ацетонитрила с борной кислотой.

На основе полученных результатов было заключено, что влияние среды гликолей не оказывает какого-либо эффекта на постоянные величины констант равновесия комплексов гликолей с боратами, определенных pH-метрически.

Исследование бинарных систем с поверхностно-активным веществом, I

Исследование водных растворов октаноата натрия с помощью изменения активности

Ж. БЕДЁ и Э. БЕРЕЦ

Активности ионов поверхностно-активных веществ и противоионов были непосредственно получены ие ЭДС измерений в водных растворах октаноата натрия в зависимости от концентрации и температуры. Был рассчитан также средний коэффициент активности. Из этих данных, а также из температурной и концентрационной зависимости поверхностного натяжения были определены ККМ и их зависимости от температуры.

Было найдено, что средний коэффициент активности при ККМ значительно ниже, чем рассчитанный с помощью уравнения Дэбая—Хюккеля, что может быть объяснено премицеллярным образованием.

Количество адсорбции и теплота адсорбции были рассчитаны, используя изотерму адсорбции Гиббса для адсорбции октаноата натрия.

На основе температурной зависимости $\Delta G°$, $\Delta H°$ и $\Delta S°$ для образования мицелл было заключено, что наиболее важным фактором в стабилизации гидрофобных связей при образовании мицелл является энтропия, вследствие изменений в структуре воды.

Модель заряженного разделения фаз изменялось с механзмом образования мицелл; рассчитанная отсюда степень присоединения противоионов равна 0,665.

Исследование бинарных систем с поверхностно-активным веществом, II

Исследование растворов октаноата натрия в тяжелой воде с помощью измерения активности

Ж. БЭДЁ и Э. БЕРЕЦ

На основе ЭДС измерений были определены активности ионов, средние активности и коэффициенты активности поверхностно-активного вещества (ПАВ) в системе октаноат натрия — тяжелая вода в зависимости от температуры и концентрации. Исходя из этих данных приводятся ККМ и ее температурная зависимость.

Было исследовано влияние качества растворителя на ККМ растворов ПАВ, на среднюю активность и коэффициент активности ПАВ для ККМ, а также на стабильность мицеллярных растворов.

На основе температурной зависимости $\Delta G°$, $\Delta H°$ и $\Delta S°$ при образовании мицелл было заключено, что стабильность мицелл в системе $NaC_8—D_2O$ меньше, чем в системе $NaC_8—H_2O$, что объясняется уменьшением силы гидрофобных связей в тяжелой воде.

Les Acta Chimica paraissent en français, allemand, anglais et russe et publient des mémoires du domaine des sciences chimiques.

Les Acta Chimica sont publiés sous forme de fascicules. Quatre fascicules seront réunis en un volume (3 volumes par an).

On est prié d'envoyer les manuscrits destinés à la rédaction à l'adresse suivante:

Acta Chimica
Budapest, P.O.B. 67, H-1450, Hongrie

Toute correspondance doit être envoyée à cette même adresse.

La rédaction ne rend pas de manuscript.

Le prix de l'abonnement: $ 36,00 par volume.

Abonnement en Hongrie à l'Akadémiai Kiadó (1363 Budapest, P. O. B. 24, C. C. B. 215 11488), à l'étranger à l'Entreprise du Commerce Extérieur « Kultura » (H-1389 Budapest 62, P. O. B. 149 Compte-courant No. 218 10990) ou chez représentants à l'étranger.

Die Acta Chimica veröffentlichen Abhandlungen aus dem Bereich der chemischen Wissenschaften in deutscher, englischer, französischer und russischer Sprache.

Die Acta Chimica erscheinen in Heften wechselnden Umfanges. Vier Hefte bilden einen Band. Jährlich erscheinen 3 Bände.

Die zur Veröffentlichung bestimmten Manuskripte sind an folgende Adresse zu senden

Acta Chimica
Budapest, Postfach 67, H-1450, Ungarn

An die gleiche Anschrift ist jede für die Redaktion bestimmte Korrespondenz zu richten.

Manuskripte werden nicht zurückerstattet.

Abonnementspreis pro Band: $ 36,00.

Bestellbar für das Inland bei Akadémiai Kiadó (1363 Budapest, Postfach 24, Bankkonto Nr. 215 11488), für das Ausland bei »Kultura« Außenhandelsunternehmen (H-1389 Budapest 62, P. O. B. 149. Bankkonto Nr. 218 10990) oder seinen Auslandsvertretungen.

«Acta Chimica» издают стихьи по лимии на русском, ангхийском, французском и немецком языкал.

«Acta Chimica» выподит отдехьными выпусками разного объемта, 4 выпуска составхяют один том и за год выподят 3 тома.

Предназначенные дхя пубхикации рукописи сходует направхять по адресу:

Acta Chimica
Budapest, P.O.B. 67, H-1450, BHP

Всякую корреспонденцию в редакцию направхяйте по этому же адресу.

Редакция рукописей не возвращает.

Подписная цена — $ 36,00 за том.

Отечественные подписчики направхяйте свои заявки ;по адресу Издатехьства Академии Наук (1363 Budapest, P.O.B. 24. Текущий счет 215 11 188), а иностранные подписчики через организацию по внешней торговхе «Kultura» (H-1389 Budapest 62, P.O.B. 149. Текущий счет 218 10990) ихи через ее заграничные представитехьства и упохномеченныл.

Reviews of the Hungarian Academy of Sciences are obtainable at the following addresses:

AUSTRALIA
C.B.D. LIBRARY AND SUBSCRIPTION SERVICE, Box 4886, G.P.O., *Sydney N.S.W. 2001*
COSMOS BOOKSHOP, 145 Ackland Street, *St. Kilda (Melbourne), Victoria 3182*

AUSTRIA
GLOBUS, Höchstädtplatz 3, *1200 Wien XX*

BELGIUM
OFFICE INTERNATIONAL DE LIBRAIRIE, 30 Avenue Marnix, *1050 Bruxelles*
LIBRARIE DU MONDE ENTIER, 162 Rue du Midi, *1000 Bruxelles*

BULGARIA
HEMUS, Bulvar Ruski 6, *Sofia*

CANADA
PANNONIA BOOKS, P.O. Box 1017, Postal Station "B", *Toronto, Ontario M5T 2T8*

CHINA
CNPICOR, Periodical Department, P.O. Box 50, *Peking*

CZECHOSLOVAKIA
MAD'ARSKÁ KULTURA, Národní třída 22, *115 33 Praha*
PNS DOVOZ TISKU, Vinohradská 46, *Praha 2*
PNS DOVOZ TLAČE, *Bratislava 2*

DENMARK
EJNAR MUNKSGAARD, Norregade 6, *1165 Copenhagen*

FINLAND
AKATEEMINEN KIRJAKAUPPA, P.O. Box 128, *SF-00101 Helsinki 10*

FRANCE
EUROPERIODIQUES S.A., 31 Avenue de Versailles, *78170 La Celle St. Cloud*
LIBRAIRIE LAVOISIER, 11 rue Lavoisier, *75008 Paris*
OFFICE INTERNATIONAL DE DOCUMENTATION ET LIBRAIRIE, 48 rue Gay-Lussac, *75240 Paris Cedex 05*

GERMAN DEMOCRATIC REPUBLIC
HAUS DER UNGARISCHEN KULTUR, Karl-Liebknecht-Strasse 9, *DDR-102 Berlin*
DEUTSCHE POST ZEITUNGSVERTRIEBSAMT, Strasse der Pariser Kommüne 3—4, *DDR-104 Berlin*

GERMAN FEDERAL REPUBLIC
KUNST UND WISSEN ERICH BIEBER, Postfach 46, *7000 Stuttgart 1*

GREAT BRITAIN
BLACKWELL'S PERIODICALS DIVISION, Hythe Bridge Street, *Oxford OX1 2ET*
BUMPUS, HALDANE AND MAXWELL LTD., Cower Works, *Olney, Bucks MK46 4BN*
COLLET'S HOLDINGS LTD., Denington Estate, *Wellingborough, Northants NN8 2QT*
WM. DAWSON AND SONS LTD., Cannon House, *Folkestone, Kent CT19 5EE*
H. K. LEWIS AND CO., 136 Gower Street, *London WC1E 3BS*

GREECE
KOSTARAKIS BROTHERS, International Booksellers, 2 Hippokratous Street, *Athens-143*

HOLLAND
MEULENHOFF-BRUNA B.V., Beulingstraat 2, *Amsterdam*
MARTINUS NIJHOFF B.V., Lange Voorhout 9—11, *Den Haag*
SWETS SUBSCRIPTION SERVICE 347b Heereweg, *Lisse*

INDIA
ALLIED PUBLISHING PRIVATE LTD., 13/14 Asaf Ali Road, *New Delhi 110001*
150 B-6 Mount Road, *Madras 600002*
INTERNATIONAL BOOK HOUSE PVT. LTD., Madame Cama Road, *Bombay 400069*
THE STATE TRADING CORPORATION OF INDIA LTD., Books Import Division, Chandralok, 36 Janpath, *New Delhi 110001*

ITALY
EUGENIO CARLUCCI, P.O. Box 252, *70100 Bari*
INTERSCIENTIA, Via Mazzé 28, *10149 Torino*
LIBERIA COMMISSIONARIA SANSONI, Via Lamarmora 45, *50121 Firenze*
SANTO VANASIA, Via M. Macchi 58, *20124 Milano*
D. E. A., Via Lima 28, *00198 Roma*

JAPAN
KINOKUNIYA BOOK-STORE CO. LTD., 17-7 Shinjuku-ku 3 chome, Shinjuku-ku, *Tokyo 160-91*
MARUZEN COMPANY LTD, Book Department, P.O. Box 5050 Tokyo International, *Tokyo 100-61*
NAUKA LTD. IMPORT DEPARTMENT, 2-40-19 Minami Ikebukuro, Toshima-ku, *Tokyo 171*

KOREA
CHULPANMUL, *Phenjan*

NORWAY
TANUM-CAMMERMEYER, Karl Johansgatan 41—43, *1000 Oslo*

POLAND
WĘGIERSKI INSTYTUT KULTURY, Marszałkowska 80, *Warszawa*
CKP I W ul. Towarowa 28 *00-958 Warszawa*

ROUMANIA
D. E. P., *Bucureşti*
ROMLIBRI, Str. Biserica Amzei 7, *Bucureşti*

SOVIET UNION
SOJUZPETCHATJ — IMPORT, *Moscow*
and the post offices in each town
MEZHDUNARODNAYA KNIGA, *Moscow G-200*

SPAIN
DIAZ DE SANTOS, Lagasca 95, *Madrid 6*

SWEDEN
ALMQVIST AND WIÓSELL, Gamla Brogatan 26, *101 20 Stockholm*
GUMPERTS UNIVERSITETSBOKHANDEL AB, Box 346, *401 25 Göteborg 1*

SWITZERLAND
KARGER LIBRI AG, Petersgraben 31, *4011 Basel*

USA
EBSCO SUBSCRIPTION SERVICES, P.O. Box 1943, *Birmingham, Alabama 35201*
F. W. FAXON COMPANY, INC., 15 Southwest Park, *Westwood, Mass, 02090*
THE MOORE-COTTRELL SUBSCRIPTION AGENCIES, *North Cohocton, N. Y. 14868*
READ-MORE PUBLICATIONS, INC., 140 Cedar Street, *New York, N. Y. 10006*
STECHERT-MACMILLAN, INC., 7250 Westfield Avenue, *Pennsauken N. J. 08110*

VIETNAM
XUNHASABA, 42, Hai Ba Trung, *Hanoi*

YUGOSLAVIA
JUGOSLAVENSKA KNJIGA, Terazije 27, *Beograd*
FORUM, Vojvode Mišića 1, *21000 Novi Sad*

28. III. 1980 HU ISSN 0001—5407 Index: 26.007

ACTA CHIMICA

ACADEMIAE SCIENTIARUM HUNGARICAE

TOMUS 103 FASCICULUS 3

AKADÉMIAI KIADÓ, BUDAPEST

1980

ACTA CHIM. ACAD. SCI. HUNG. ACASA2 103 (3) 225–327 (1980)

ACTA CHIMICA

A MAGYAR TUDOMÁNYOS AKADÉMIA KÉMIAI TUDOMÁNYOK OSZTÁLYÁNAK IDEGEN NYELVŰ KÖZLEMÉNYEI

Acta Chimica is a journal for the publication of papers on all aspects of chemistry in English, German, French and Russian.

Acta Chimica is published in 3 volumes per year. Each volume consists of 4 issues of varying size.

Manuscripts should be sent to

Acta Chimica
Budapest, P.O. Box 67, H-1450, Hungary

Correspondence with the editors should be sent to the same address. Manuscripts are not returned to the authors.

Subscription: $36.00 per volume.

Hungarian subscribers should order from Akadémiai Kiadó, 1363 Budapest, P.O. Box 24. Account No. 215 11488.

Orders from other countries are to be sent to "Kultura" Foreign Trading Company (H-1389 Budapest 62, P.O. Box 149. Account No. 218 10990) or its representatives abroad.

Acta Chimica Academiae Scientiarum Hungaricae, Tomus 103 (3), pp. 225—230 (1980)

A NOVEL METHOD FOR DETERMINATION OF ENZYME ACTIVITIES

E. NOSZTICZIUS,[1] D. KALMÁR[2] and Z. NOSZTICZIUS[3]

([1]Department of Physical Chemistry, Technical University, Budapest, [2]Reanal Fine Chemicals Factory, Budapest and [3]Institute of Physics, Technical University, Budapest)

Received January 11, 1979
Accepted for publication April 6, 1979

In this report we describe the application of the flame ionization detector (FID) for the measurement of urease activity as an example. The method is uniquely suited to the study of rates of enzymatic reactions accompanied by CO_2 evolution. The CO_2 is stripped with H_2 from the reaction mixture and then methanized in a catalytic reactor. The concentration of methane produced is measured by FID. In steady state, the measured ionization current is strictly proportional to the reaction rate.

The method described here was originally developed in our laboratory to monitor oscillating CO_2 and CO evolution in the Belousov—Zhabotinskii reaction [1]. Many enzymatic reactions are also followed by CO_2 evolution and this fact is the basis of the well known manometric methods [2]. Our aim was to replace the manometric Warburg apparatus with a rapid and sensitive analytical system. To this end, the instrument shown in Fig. 1 was designed

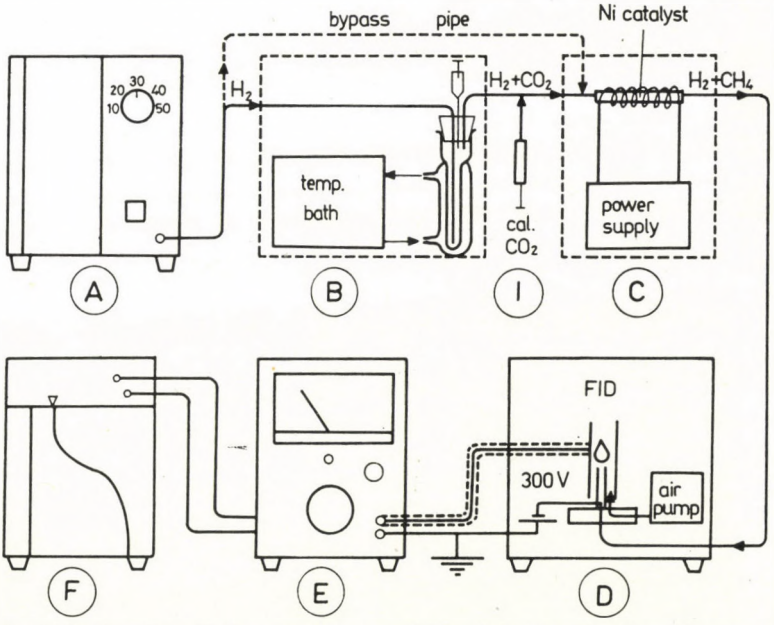

Fig. 1. Schematic drawing of the apparatus used for the determination of urease activity. See text for description of the various components

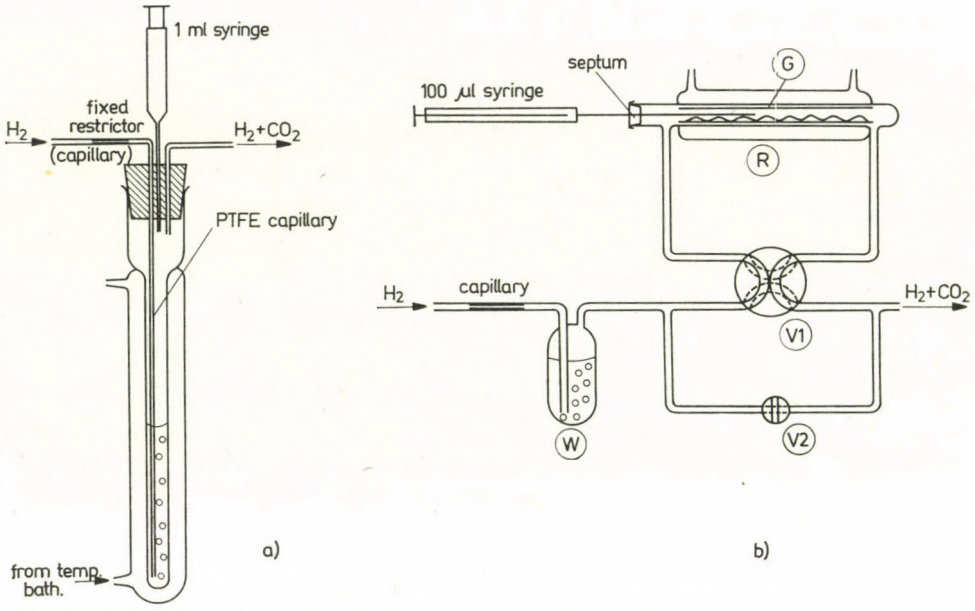

Fig. 2. Two types of the applied enzyme reactors for continuous (a) and integrating (b) measurements

and built. The instrument can be operated in two modes; in a direct and in an integrating way applying two kinds of enzyme reactors, as can be seen in Fig. 2.

The system can be used whenever a biochemical or chemical reaction produces CO_2. We discuss the urea-urease reaction as an example.

Materials and Methods

Urea, urease and other reagent grade chemicals were supplied by Reanal Fine Chemical Factory Budapest. The enzyme and substrate solutions were prepared according to the literature [3].

The incorporation of the FID in the instrument used for the determination of urease activity is illustrated in Fig. 1. The instrument consists of the following main components:

(A) Electrolytic H_2 generator producing an electronically controlled, constant molar flow-rate of H_2.

(B) Thermostated enzyme reactor, Fig. 2 (a) or (b).

(C) Catalytic converter containing Ni as catalyst, heated electrically to 300 °C.

(D) FID unit: Here a pump producing a constant flow of clean air and a stabilized high voltage source (300 V) was also incorporated.

(E) The current of the FID was measured by a Keithley 610-B electrometer.

(F) The measured current was recorded by a Radelkis OH-814/1 potentiometric recorder.

(I) An injection port for calibration by CO_2 could be inserted between (B) and (C).

Method *a*

The procedure to measure the urease activity with the enzyme reactor depicted in Fig. 2 (a) was as follows. An aliquot of enzyme solution was introduced into the reactor. Typically 1 cm^3 aliquots were used. The whole system was flushed by allowing the H_2 to bubble at a con-

stant flow rate (30 cm^3/min) through the reactor and to flow through the other components. After that the flame was ignited. It is important to apply a fixed restrictor *(e.g.* a narrow glass capillary) just before the enzyme reactor to achieve a high "bubbling frequency" and not to disturb the flame. When the system stabilized and the background current dropped below 40 pA (about 5 min), 1 cm^3 substrate solution was introduced from a syringe mounted to the top of the reactor. The waiting time can be reduced if the catalytic reactor is maintained in H_2 atmosphere during the filling procedure of the enzyme reactor: a bypass pipe can be inserted for this purpose.

After the addition of the substrate solution to the enzyme reactor, the decomposition of the urea begins and the evolving CO_2 is continuously stripped by the H_2 flow. If the rate of the reaction is constant, a steady state will be achieved after a transient period. In the steady state the amount of CO_2 produced in the reaction is equal to the amount stripped from the reaction mixture, thus F_{CO_2}, the molar flow rate of CO_2 in H_2, is a quantitative measure of the reaction rate. In the catalytic converter, the CO_2 is methanized and the burning of methane causes an ionic current in the FID. A graph produced in this way is depicted in Fig. 3a.

The electric current (I) produced by the FID can be described by the equation

$$I = I_0 + k_{Me} F_{Me} \tag{1}$$

where I_0 is the background current, usually 10–20 pA, F_{Me} is the methane flow rate in mol/s, k_{Me} is a factor of proportionality showing the ionization efficiency, C/mol. In practice $F_{Me} = F_{CO_2}$ thus the expression

$$\frac{I_s - I_0}{k_{Me}} = F_{CO_2} \tag{2}$$

gives the evolution rate of carbon dioxide in the steady state. I_5 is the ionic current corresponding to the steady state.

The enzyme activity can be calculated on the basis that 1 enzyme unit produces 0.5 μmol CO_2/min. (This is a consequence of the international convention according to which 1 enzyme unit produces 1 μmol NH_3 in 1 minute.)

Determination of k_{Me} and substrate concentrations

Introducing a known amount of CO_2 (n_{CO_2}) into the system, k_{Me} can be determined. By definition

$$n_{CO_2} \equiv \int_{t_i}^{\infty} F_{CO_2} \, dt \tag{3}$$

thus, based on Eq. (2)

$$k_{Me} = \frac{\int_{t_i}^{\infty} (I - I_0) \, dt}{n_{CO_2}} \tag{4}$$

Where t_i is the time of introduction of CO_2. In practice, it is easy to find a Δt time interval for which the approximation

$$\int_{t_i}^{\infty} (I - I_0) \, dt \approx \int_{t_i}^{t_i + \Delta t} (I - I_0) \, dt \tag{5}$$

holds within the experimental error. The system can be calibrated with gaseous CO_2 or with a chemical or biochemical reaction producing a known amount of CO_2.

Conversely, an unknown amount of a substrate can be determined measuring n_{CO_2} produced from the substrate during the enzyme reaction

$$n_{CO_2} = \frac{1}{k_{Me}} \int_{t_i}^{t_i + \Delta t} (I - I_0) \, dt \tag{6}$$

Method *b*

This procedure differs from the previous one mainly in the applied enzyme reactor. The schematic diagram of this system is given in Fig. 2b. Here a filter paper is wetted by an aliquot of the enzyme substrate mixture (usually 0.1 cm^3). Thus the time constant of the system

is reduced due to the smaller volume and larger specific surface of the reaction mixture [4]. The filter paper is placed into a glass tube G which can be changed easily.

Valve V1 has two positions: an "open" position when the H_2 saturated in water-filled saturator W flows through enzyme reactor R, and a closed position when the H_2 is stagnating

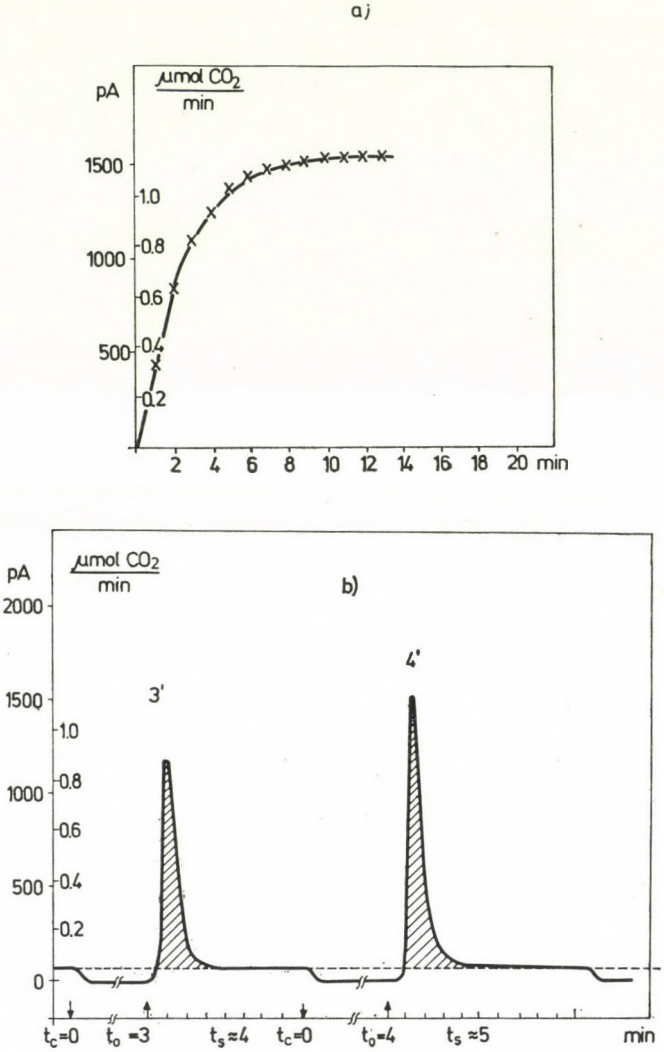

Fig. 3. Ionization current *vs.* time curves measured by the continuous (a) and the integrating method (b)

in the reactor thus allowing the CO_2 evolving from the reaction mixture to accumulate in the closed volume. After an accumulation period of some minutes (V1 is closed), a shorter purging period follows (V1 is open). Stopcock V2 is open only during the short time when valve V1 changes position to prevent the flame to go out. The CO_2 collected in this way was methanized again and appeaed in the FID liker a chromatographic peak. The area under this peak divided by the time elapsed in the closed position gives the evolution rate of carbon dioxide that is the

reaction rate

$$F_{CO_2} = \frac{1}{k_{Me}} \frac{\int_{t_c}^{t_s} (I - I_s)\, dt}{t_0 - t_c} \tag{7}$$

where t_c is the moment when V1 was closed to concentrate the evolving CO_2, t_0 is the moment when V1 was opened to flush CO_2 toward the detector, and t_s the moment when the system reached the steady state within the experimental error. Alternately F_{CO_2} can be calculated using the *It* value and expression (2) again, however, applying reasonable conditions, Eq. (7) gives a more accurate result. A graph of an experiment according to procedure *b* is shown in Fig. 3b.

Comparison of methods *a* and *b*

Method *a* is well suited to substrate determinations because the enzyme and the substrate solution can be mixed in the reactor. When it is used to determine enzyme activities, it takes to change the whole reactor and to reach the steady state.

Method *b* is well suited to activity determinations. The samples can be changed rapidly and the steady state is reached quickly. As the mixing of the solutions on the filter paper is difficult, it is not convenient to measure substrate concentrations in this way.

Results

The sensitivity of FID was $k_{Me} = 79.7 \pm 0.4 \frac{mC}{mol\ CO_2}$ measured in March 1977. k_{Me} was measured again in October and it was found to be $79.8 \pm \pm 0.4 \frac{mC}{mol\ CO_2}$. According to this, a CO_2 flow rate of 1 μmol/min causes an ionization current of 1328 ± 6 pA. Calibration with gaseous CO_2 (calculated to normal state) and with CO_2 produced from a known amount of urea by urease gave the same results within the experimental error of 0.5%. Thus the method is suitable to measure unknown concentrations of urea as well.

Method a

The result of an experiment by method *a* can be seen in Fig. 3a. 1 cm^3 enzyme solution (concentration 0.11 mg/1 cm^3 0.02 *M* pH 7.0 phosphate buffer) was pipetted into the enzyme reactor and 1 cm^3 substrate solution (concentration: 30 mg urea/1 cm^3 0.75 *M*, pH 7.0 phosphate buffer) was added with from a syringe. The steady state ionization current was 1540 ± 20 pA, thus the measured activity was 2.32 ± 0.03 U. The specific activity was calculated to be 21.1 ± 0.3 U/mg. Application of albumine or more concentrated enzyme solutions makes the mixture foamy and thus produces a noisy signal.

Method b

Two curves produced by method *b* are depicted in Fig. 3 b. The two peaks differ only in the time of gas collection: 3 minutes for the first one and 4 minutes for the second one. The procedure was as follows. A 100 μl aliquot

of enzyme substrate mixture was injected onto a piece of folded filter paper (size 6 cm $\times$ 1.5 cm).

The integrals of the dashed areas were 222 pA min and 305 pA min, respectively. The recorded curves were integrated numerically applying Simpson's rule. The calculated steady state currents were 74.0 pA and 76.3 pA. The specific activity based on five experiments was found to be 20.6 $\pm$ 0.4 U/mg.

To check methods *a b*, the specific activity of urease was determined according to the literature [3] by titration of the ammonium produced from urea, and it was found to be 22 $\pm$ 1 U/mg. Thus the results measured by the classical and the new methods agree within the experimental error.

Discussion

The advantages of the method reported here may be summarized as follows:

1. It is an absolute method in the sense that the whole amount of CO_2 produced in a reaction is measured and the calibration does not depend of the origin of the carbon dioxide.

2. The method is especially suitable for kinetic measurements because the signal is directly proportional to the rate of the reaction.

3. The flame ionization detector applied here has some well known advantages: a high sensitivity, a wide linear dynamic range and a good stability. Experiments are in progress to apply the method for other enzymatic reactions coupled with CO_2 producing steps to measure enzyme activities, kinetic parameters and substrate concentrations as well.

*

This research was partly supported by the Medicor Works Budapest. We wish to thank Dr. György Székely for helpful discussions and Zsuzsa Nagy for valuable technical assistance.

REFERENCES

[1] Noszticzius, Z.: J. Phys. Chem., **81**, 185 (1977)
[2] Bergmeyer, H. U.: Methods of Enzymatic Analysis, pp. 29—42. Academic Press, New York 1963
[3] Worthington Enzyme Manual, Worthington Biochem. Co., Reehold, New Yersey, USA 1972
[4] Danckwerts, P. V.: Gas–Liquid Reactions. pp. 264—267, 1970

Eszter Noszticzius H-1521 Budapest, Budafoki út 8.
Dezső Kalmár H-1441 Budapest, P.O. Box 54.
Zoltán Noszticzius H-1521 Budapest, Budafoki út 8.

Acta Chimica Academiae Scientiarum Hungaricae, Tomus 103 (3), pp. 231—240 (1980)

FLUORINATED STEROIDS, I
3-FLUORO-5,6-UNSATURATED DERIVATIVES

Á. NÉDER, A. USKERT**, É. NAGY,
Zs. MÉHESFALVI and J. KUSZMANN*

(Institute for Drug Research, Budapest)

Recieved February 26, 1979
Accepted for publication April 9, 1979

The hydroxyl–fluorine exchange reaction of 3-hydroxypregn-5-en-20-one (**13**) with FAR (**4**) was investigated in detail. Besides the 3β-fluoro derivative **18** the ester **15**, the 3,3'-ether **17**, the 3α,5-cyclo-6α-methoxy compound **20**, as well as the corresponding 6α-hydroxy derivative **21** were isolated as by-products. The solvent dependence of the product distribution is explained by the proposed mechanism of the reaction. Among the solvents tried, chloroform was found to give the highest yields of the fluorinated steroids. Four further 3β-fluoro-5-ene steroid derivatives **23**, **25**, **27** and **29** were also synthesized. All structures were unambiguously established by PMR spectroscopy.

The interesting biological properties [1] of fluorinated steroids prompted the synthesis of 3-fluoro-5,6-dihalogeno derivatives. Such compounds can be obtained, in principle, starting from 3-hydroxy-5-ene steroids **1**, replacing first the hydroxyl group by fluorine (**2**) and then saturating the double bond with halogen (**3**). Accordigly, the influence of the different reaction conditions on the OH–F exchange reaction of 3-hydroxy-5,6-unsaturated steroids was investigated in detail.

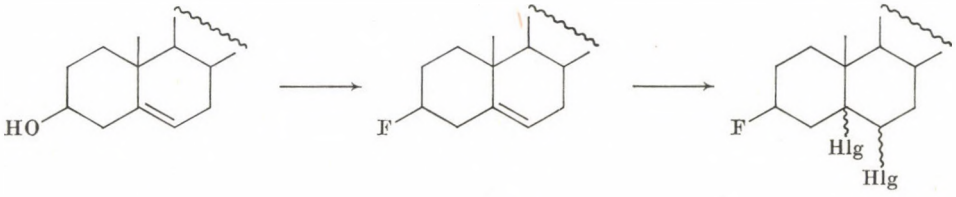

1 **2** **3**

Fig. 1

The method introduced by OLAH *et al.* [2], applying a 9 : 1 HF–pyridine complex for the replacement of secondary and tertiary hydroxyl groups by fluorine, was found unsuccessful in our case. Another method [3] recommending 100% HF for the same reaction gave the fluorinated compounds in very low yield, consequently it is not suitable for large-scale synthesis.

* To whom correspondence should be addressed.
** Present address: Institute of Agricultural Chemical Technology, University of Technical Sciences, Budapest.

In 1950 PRUETT *et al.* [4] described the synthesis of 2-chloro-1,1,2-trifluorotriethylamine **4** which was successfully applied by YAROVENKO and RAKSHA [5] for the replacement of hydroxyl groups by fluorine. This reagent was introduced for the synthesis of fluorinated steroid derivatives simultaneously by AYER [6] as well as by KNOX *et al.* [7] in 1962. Two years later a detailed study was published [8] about the fluorination of 3-hydroxysteroids by means of **4**. In all these papers, among other steroids, the reactions of

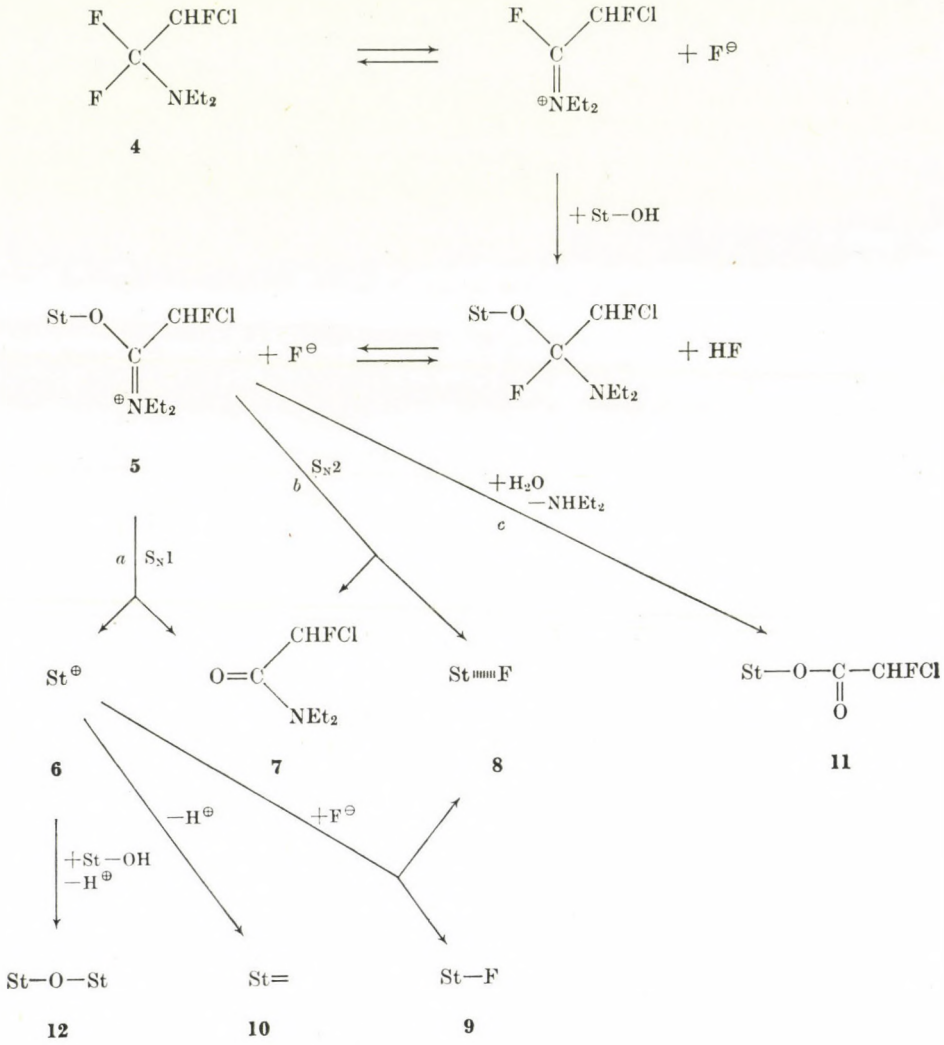

St = steroid

Scheme 1

3β-hydroxyandrost-5-ene and -pregn-5-ene derivatives with **4** were also described, but Ayer isolated only the corresponding 3β-fluoro derivatives in excellent yields, whereas KNOX *et al.* mentioned that in the case of 3β-hydroxyandrost-5-en-17-one the expected 3β-fluoro isomer could only be isolated in a yield of 58%, and the corresponding 3β,3'β-ether was obtained as a by-product [8]. From their detailed investigation of saturated 3-hydroxysteroids it became obvious, that the OH–F exchange reaction proceeds *via* an active "ester-amide" **5** intermediate, which is formed from **4** and the corresponding hydroxysteroid by elimination of HF [6—9] (Scheme 1). The intermediate **5** can undergo three types of reaction: it can decompose to the acetamide **7** yielding simultaneously the steroid cation **6** *(a)*; it can be transformed by a direct S_N2 mechanism into the fluorinated steroid **8** *(b)* and, in the presence of moisture, it can yield the steroid ester **11** *via* elimination of diethylamine *(c)*. The steroid cation **6** formed by route *(a)* might be stabilized by deprotonation yielding an unsaturated derivative **10**, or addition of fluorine takes place. In the latter case, depending on the feature of the cation **6** at least two diastereomers **8** and **9** can be expected theoretically, or if **6** is stabilized by delocalization, other isomers can also form. In the case of saturated hydroxysteroids inversion of configuration was observed*, showing that the exchange reaction may take place *via* route *(b)*. When the cation **6** is stabilized by delocalization, it can be attacked not only by fluoride, which is a rather weak nucleophile, but also by the hydroxyl group of the unreacted hydroxysteroid, leading to the formation of the corresponding ether **12**.

KNOX *et al.* [8] investigated the influence of different solvents and that of the temperature on the reaction of **4** with 3β-hydroxyandrostan-17-one and isolated only three products, the unsaturated steroid **10**, the 3α-fluoro isomer **8**, and the ester **11**, in different amounts.

In our experiments first the reaction of **4** with 3β-hydroxypregn-5-en-20-one (**13**) was studied, choosing tetrahydrofuran, methylene chloride, acetonitrile and chloroform, respectively, as solvents. In contradiction to the literature [6, 8] five products could be isolated instead of three (Scheme 2). In addition to the known 3β-fluoride **18**, the ether **17** (analogous to **12**), the 3β-ester **15** (analogous to **11**), and two 3α,5-cyclo derivatives, containing a methoxyl (**20**) or a hydroxyl group (**21**) at position 6 were separated (Table I). The ester **15** is formed on hydrolysis [8] of the active ester-amide **14**, which is the first intermediate of the reaction. Its structure could be proved by spectroscopy. The ester carbonyl band appeared in its IR spectra at 1750 and 1770 cm^{-1}, besides the carbonyl absorption of the 20-keto group at 1705 cm^{-1}. In its PMR spectrum the CHFCl group gave a characteristic doublet at 5.8 and

* The statement of AYER [6] that "the replacement of hydroxyl by fluorine proceeds with essentially complete inversion of configuration" cannot be generalized and is even contradicted by his own findings, discussed at the beginning of Ayer's paper.

Table I

Solvent-dependent product distribution (yields in %) of the reaction of* **13** *with* **4**

Solvent	ester **15**	ether **17**	3β-fluoride **18**	6α-methoxy **20**	6α-hydroxy **21**
THF	9.4	1.6	19.7	32.6	<1.0
CH_2Cl_2	<1.0	<1.0	87.0	<1.0	<1.0
CH_3CN	<1.0	10.5	30.4	3.7	14.8
$CHCl_3$	<1.0	<1.0	90.4	1.5	1.5

* Reaction conditions: **4** was applied in a three-fold molar ratio. The reaction temperature was in the case of THF 0 °C, 2 h and then 25 °C, 2 h; in all other cases 0 °C, 1 h, then 25 °C, 3 h

6.65 ppm, respectively (J_{HF} 50 Hz). All the other compounds can originate from the non-classical homoallylic cation [8] **16**. Theoretically any nucleophile can attack at either of the "terminal" atoms, C-3 and C-6. Owing to steric factors, the more stable 3β-substituted 5-ene derivatives **17** and **18** will be formed preferably in a thermodynamically controlled reaction [10, 11]. The strong solvent dependence of the ratio of the isolated products, however, suggested that significant amounts of a less stable [12], 3α,5-cyclo-6-fluoro intermediate **19** can also be formed in a kinetically controlled reaction; this is then decomposed during the work-up of the reaction mixture to give the corresponding 6α-methoxy (**20**) and 6α-hydroxy (**21**) derivatives. In contradiction to the literature [13, 14] which assigned 6β-configuration to these derivatives, PMR proved their 6α structure. The problem of the steric arrangement of the substituent at C-6 in 3α,5-cyclosteroids was discussed in 1952 independently by two research groups [15, 16] in detail, but with contradictory results, suggesting *e.g.* the 6β [15] and 6α configuration [16], respectively, for the same 3α,5-cyclocholestan-6-ol. This problem is still unsolved, and the different authors refer to one or the other alternative making the situation even more confused.

The above mentioned stereochemical problem can be solved unambiguously by NMR spectroscopy, taking into consideration the conformation of the molecules. In **20** the 4,4'-protons of the strained cyclopropyl ring appeared as a double of doublets at 0.4 and 0.55 ppm (J 2.5 Hz), and the signal of 6-H, the proton geminal to the methoxyl group, gave a triplet at 2.75 ppm with a coupling constant of J 3 Hz, proving its *equatorial* arrangement*. In steroids with A/B-*trans*-fused rings this would mean a 6α proton, according to the chair conformation of ring B. In the 3α,5-cyclo derivatives, however, ring A resembles an A-nor-5β-substituted steroid, consequently the steric arrangement of the A/B rings is rather like an A/B *cis* fused system, due to

* *Lit.* [13] data: t at 2.77 ppm, (J 2.5 Hz).

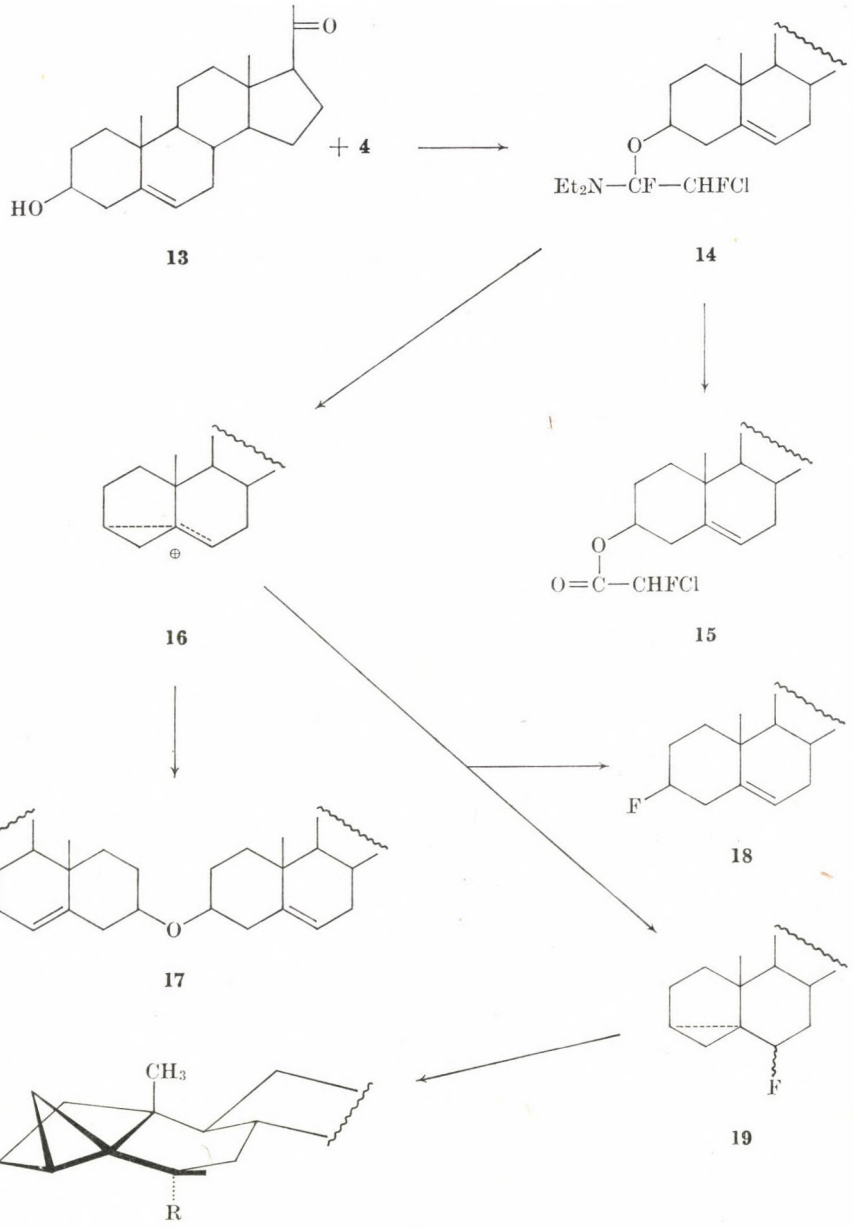

13 **14** **16** **15** **18** **17** **19**

20 R = OMe
21 R = OH

Scheme 2

Table II

IR and PMR data of compounds* **15, 18, 20, 21, 23, 25, 27** *and* **29**

Compound	IR ($\nu_{C=O}$ cm^{-1})	H—3	H—6	CH_3—18	CH_3—19	CH_3—21	Other signals
15	1705, 1750, 1770	4.8 (28)	5.35	0.65	1.05	2.15	5.8; 6.65 (J_{HF} = 50 Hz) CHFCl
17	1700	3.3 (25)	5.35	0.65	1.00	2.10	
18	1700	3.95; 4.80 (30)	5.45 (10)	0.65	1.05	2.15	J_{HF} = 52 Hz
20	1705		2.75 (*d*, J = 3 Hz)	0.66	1.05	2.10	0.40; 0.55 (*dd*, J = 2.5 Hz) H-4,4'; 3.32 CH_3O
21	1690		3.35 (*d*, J = 3 Hz)	0.70	1.10	2.15	0.30; 0.45 (*dd*, J = 3 Hz) H-4,4'
23	—	3.85; 4.70 (26)	5.35 (10)	0.70	1.05	—	J_{HF} = 52 Hz
25	1770	3.85; 4.65 (30)	5.35 (10)	0.95	1.05	—	J_{HF} = 52 Hz
27	1640	3.90; 4.75 (30)	5.45 (8)	0.95	1.08	2.27	6.72 (*t*, J = 3 Hz) H-16; J_{HF} = 51 Hz
29	1682	3.90; 4.85 (26)	5.40 (10)	0.65	1.03	2.15	3.20 CH_3O; 4.35 H-16; J_{HF} = 57 Hz

* δ-scale, half band width in Hz is given in brackets

which ring B has to adopt a boat conformation, and the *equatorial* proton in position 6 is β-oriented, indicating the α-arrangement of the geminal substituent. The same holds for the 6-hydroxy derivative **21,** where the signal of the cyclopropyl protons appear at 0.3 and 0.45 ppm as a double of doublets (J 3 Hz), and the 6-H gives a triplet at 3.35 ppm, the coupling constant being J 3 (Table II).

It is worth mentioning that the ether **17** is formed preferentially in acetonitrile. In this solvent the reaction is very slow and about 10% of unchanged starting material can be recovered. On the other hand, the known weak nucleophilicity of the fluoride ion is further decreased by the solvent which, due to its strong donor capacity, forms a very stable solvated complex with anions. The relative high concentration of the unreacted starting material facilitates ether formation.

To investigate the structure–activity relationship, the synthesis of several other 3β-fluorosteroids was also accomplished. As according to our investigations the maximum yield (90%) of the 3β-fluoro derivative **18** could be attained in chloroform solution, the corresponding 3-hydroxy-5-ene derivatives were allowed to react with **4** in this solvent.

3β-Hydroxyandrost-5-ene (**22**) gave the expected 3β-fluoride **23** in an excellent yield. When the 3β-hydroxy-17-lactone (**24**) was treated with **4**, the corresponding 3β-fluoride **25** was obtained in a moderate yield only, probably as a consequence of the different work-up of the reaction mixture. As the solubility of compound **25** in the by-product 7 of the reaction is much higher than

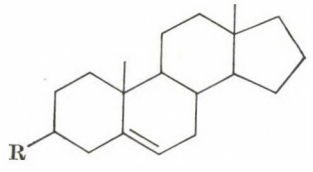

22 R = OH
23 R = F

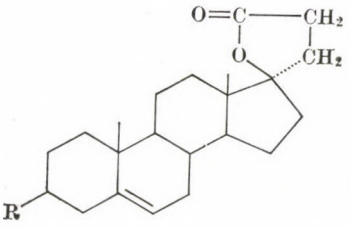

24 R = OH
25 R = F

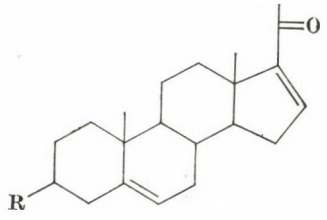

26 R = OH
27 R = F

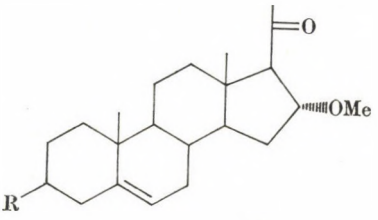

28 R = OH
29 R = F

Fig. 2

that of the aforementioned fluorinated steroids, two subsequent chromatographic steps had to be applied for their complete separation.

Reaction of the 5,16-dien **26**, as well as the 16α-methoxy derivative **28**, which was obtained from the former by treatment with methanol in the presence of K_2CO_3 as a by-product, gave the expected 3β-fluoro derivatives **27** and **29**, respectively, in fairly good yields.

All 3β-fluorosteroids had characteristic PMR spectra, proving not only the presence of a proton geminal to the fluorine atom (J_{HF} 50—55 Hz), but also the β-position of the fluorine, as the half band width of the corresponding geminal proton varied between 26—30 Hz, in accordance with its *axial* (α) arrangement [8] (Table II).

Experimental

M.p.'s were determined with a Boetius apparatus and are uncorrected. TLC was effected on Kieselgel HF_{254} with benzene–tetrahydrofuran 40 : 3 (*A*). For detection a 20% solution of $SbCl_5$ in chloroform was used with subsequent heating at 110 °C. Column chromatography was

carried out on Woelm Silica Gel (63—200 μm) using beneze (*B*), benzene–tetrahydrofuran 25 : 1 (*C*) and acetonitrile saturated with cyclohexane (*D*) for elution. The PMR spectra were recorded at 60 MHz with a JEOL-60-HL spectrometer in deuterochloroform, using tetramethylsilane as internal standard. IR spectra were recorded in KBr pellets with a Perkin—Elmer 577 spectrometer. Mass spectra were obtained with a Varian MAT SM-1 instrument.

All evaporations were performed in a rotary evaporator under diminished pressure after having dried the organic solutions over sodium sulfate. The reactions with 2-chloro-1,1,2-trifluorotriethylamine [17] (FAR, **4**) were carried out in glassware previously dried at 110 °C. Optical rotations were determined in chloroform ($c = 1$).

The reactions of 3β-hydroxypregn-5-en-20-one (13) with FAR (4)

Method (a), using tetrahydrofuran as solvent

To a stirred solution of **13** (5 g; 15.8 mmoles) in dried tetrahydrofuran (80 ml) FAR (**4**, 8 ml; 53.5 mmoles) was added dropwise at 0 °C. The reaction mixture was stirred at 0 °C for 2 h and then at room temperature for 2 h. Sodium fluoride (8 g; 190 mmoles) was then added to bind the hydrogen fluoride. After 1 h the reaction mixture was cooled to 0 °C and the excess of **4** was decomposed by the addition of dry methanol (8 ml). The precipitated inorganic salts were filtered off and the residue of the evaporated filtrate was separated by column chromatography, using solvent *C* for elution.

The fractions having R_f 0.76 (*A*) were re-chromatographed using solvent (*B*) for elution. The residue obtained after evaporation was recrystallized from ethanol to yield 3β-fluoropregn-5-en-20-one (**18**, 0.99 g; 19.7%), m.p. 166.5—168 °C, $[\alpha]_D^{20}$ +12°; *lit.* [18] m.p. 164—165 °C, $[\alpha]_D^{20}$ +14°.

The fractions having R_f 0.70 (*A*) were re-chromatographed using solvent (*B*) for elution. On evaporation and recrystallization of the residue from ethanol, 3β-(chlorofluoroacetoxy)-pregn-5-en-20-one (**15**, 0.61 g; 9.4%) was obtained, m.p. 138—139 °C, $[\alpha]_D^{20}$ +7.5°.

$C_{23}H_{32}O_3ClF$ (410.95). Calcd. C 67.1; H 7.83; Cl 8.62; F 4.62. Found C 66.98; H 7.74; Cl 8.50; F 4.87%.

The fractions having R_f 0.60 (*A*) gave on evaporation and recrystallization of the residue from ethanol 3α,5-cyclo-6α-methoxy-5α-pregnan-20-one (**20**, 1.70 g; 32.6%), m.p. 122—124 °C, $[\alpha]_D$ +117°; *lit.* [19] m.p. 114 °C, $[\alpha]_D^{20}$ +121°.

The fractions of R_f 0.55 (*A*) gave on evaporation and recrystallization of the residue from ethanol di-(pregn-5-en-20-one)-3β-yl ether (**17**, 0.16 g; 1.6%), m.p. 225—228 °C, $[\alpha]_D^{20}$ +23°.

MS: peaks at *m/e* 614 [(M^+), 19.2%], 314 (65), 300 (68), 299 (100), 298 (65), 281 (21), 161 (26) and 149 (20).

$C_{42}H_{62}O_3$ (614.92). Calcd. C 8202; H 10.16; O 7.8. Found C 82.15; H 9.93; O 8.11%.

The fractions having R_f 0.40 (*A*) gave on evaporation and recrystallization of the residue from ethanol traces of 3α,5-cyclo-6α-hydroxy-5α-pregnan-20-one (**21**), m.p. 181—182 °C, $[\alpha]_D$ +119°; *lit.* [14] m.p. 180—181 °C, $[\alpha]_D$ +123° ($c = 0.663$).

Method (b), using dichloromethane as solvent

To a stirred solution of **13** (5 g; 15.8 mmoles) in dry dichloromethane (150 ml) compound **4** (8 ml; 53.5 mmoles) was added dropwise at 0 °C. Stirring was continued at 0 °C for 1 h and then at room temperature for 3 h. The reaction mixture was then poured into ice. The organic solution was separated and washed with a saturated aqueous solution of sodium carbonate (3 × 50 ml) and then with water. The dried solution was evaporated and the residue recrystallized from methanol to give a first crop of the mixture containing the different components. The mother liquor was evaporated, then decaline (10 ml) was added to, and evaporated from, the residue at 0.05 mm Hg to remove the bulk of the contaminating acetamide **7**. The residue gave a second crop of the isomeric mixture which was separated together with the first crop by column chromatography (solvent *C*) yielding besides the 3β-fluoro derivative **18** (4.39 g; 87%) the other components **15**, **17**, **20** and **21** only in yields <1%, all of them being indentical with those obtained according to method (*a*).

Method (c), using acetonitrile as solvent

To a stirred slurry of **13** (6.4 g; 20.2 mmoles) in dry acetonirtile (175 ml) compound **4** (10.5 ml; 70 mmoles) was given dropwise at 0 °C. The resulting clear solution was processed as described in method (*b*). The following compounds were isolated: **18** (1.96 g; 30.4%) **15** (below 1%); **20** (0.25 g; 3.75%), **17** (1.30 g; 10.55%) and **21** (0.82 g; 14.8%).

Method (d), using chloroform as solvent

To a stirred solution of **13** (5.0 g; 15.8 mmoles) in dry chloroform (150 ml) compound **4** (7 ml; 46.8 mmoles) was given dropwise at 0 °C. The reaction mixture was processed as described in method (*b*). The following compounds were isolated: **18** (4.55 g; 90.4%), **20** (0.1 g; 1.5%) and **21** (0.08 g; 1.5%).

3β-Fluoro-androst-5-ene (23)

To a stirred slurry of 3β-hydroxyandrost-5-ene [20] (**22**; 6.5 g; 23.8 mmoles) in dry chloform (60 ml) compound **4** (7.5 ml; 50 mmoles) was added dropwise at 0 °C. Complete solution was obtained after 5 ml of the reagent had been added. The reaction mixture was stirred for 2 h at 0 °C and then for 2 h at room temperature. After work-up according to method (*b*), compound **23** (5.79 g; 89%) was obtained, m.p. 95—97 °C, R_f 0.82 (*A*), $[\alpha]_D^{20}$ —94°.

$C_{19}H_{29}F$ (276.42). Calcd. F 6.87. Found F 6.85%.

3'(3β-Fluoro-17β-hydroxyandrost-5-en-17-α-yl)propanoic acid lactone (25)

A stirred solution of compound **24** [21] (3 g; 8.75 mmoles) in dry chloroform (30 ml) was treated with compound **4** (3 ml; 20 mmoles) at 0 °C. Stirring was continued at 0 °C for 1 h and then at room temperature for 3 h. Sodium fluoride (2 g) was then added to the reaction mixture and, after cooling to 0 °C, methanol (2 ml) was added dropwise. The precipitated salts were filtered off after 1 h of stirring and the filtrate was evaporated. The residue was separated from the amide **7** by column chromatography using solvent *D* for elution. The residue of the evaporated eluate was re-chromatographed using solvent *C* for elution. The fractions having R_f 0.74 (*A*) were evaporated to yield, after recrystallization from methanol, compound **25** (1.98 g; 66%), m.p. 115—117 °C, $[\alpha]_D^{20}$ —96.5°.

$C_{22}H_{31}O_2F$ (346.49). Calcd. F 5.50. Found F 5.30%.

3β-Fluoropregna-5,16-dien-20-one (27)

A solution of compound **26** (5 g; 16 mmoles) in dry chloroform (50 ml) was treated with compound **4** (5 ml; 33.3 mmoles) as described in method *(b)*. After column chromatography, the fractions having R_f 0.80 (*A*) were evaporated and the residue recrystallized from methanol to give compound **27** (3.71 g; 73.5%), m.p. 187—193 °C (subl.) $[\alpha]_D^{20}$ —40°.

$C_{21}H_{29}OF$ (316.49). Calcd. F 6.0. Found F 6.35%.

3β-Fluoro-16α-methoxypregn-5-en-20-one (29)

A solution of compound **28** (10.0 g; 29 mmoles) in dry chloroform (80 ml) was treated with compound **4** (10.5 ml, 70 mmoles) as described in method (*b*). After column chromatography, the fractions having R_f 0.55 (*A*) were evaporated to give, on recrystallization from methanol, compound **29** (7.15 g; 71.3%), m.p. 102—104 °C, $[\alpha]_D^{20}$ —37°.

$C_{22}H_{33}O_2F$ (348.46). Calcd. F 5.48. Found F 5.75%.

*

The authors are indebted to Gy. HORVÁTH for recording and evaluating the mass spectra.

REFERENCES

[1] Ciba Foundation Symposium: Carbon-Fluorine Compounds, Ass. Sci. Publ., Amsterdam—London—New York 1972
[2] OLAH, G. A., NOJIMA, M., KEREKES, J.: Synthesis, **1973,** 786
[3] BOWERS, A., HOLTON, P. G., DENOT, E., LOZA, M. C., URQUIZA, E.: J. Am. Chem. Soc. **84,** 1050 (1962)
[4] PRUETT, R. L., BARR, J. Ta., RAPP, K. E., BAHNER, C. T., GIBSON, J. D., LAFFERTY, Jr., R. H.: J. Am. Chem. Soc. **72,** 3646 (1950)
[5] YAROVENKO, N. N., RAKSHA, M. A.: Zh. Obshch. Khim., **29,** 2159 (1959)
[6] AYER, D. E.: Tetrahedron Lett., **1962,** 1065
[7] KNOX, L. H., VELARDE, E., BERGER, S., CUADRIELLO, D., CROSS, A. D.: Tetrahedron Lett., **1962,** 1249

[8] KNOX, L. H., VELARDE, E., BERGER, S., CUADRIELLO, D., CROSS, A. D.: J. Org. Chem., **29,** 2187 (1964)
[9] MOUSSERON-CANET, M., LANET, J. C.: Bull. Soc. Chim. France, **1969,** 1745
[10] SHOPPEE, C. W., SUMMERS, G. H. R.: J. Chem. Soc., **1957,** 4813
[11] MOUSSERON-CANET, M., BRIAL, J. C.: Bull. Soc. Chim. France, **1966,** 3867
[12] KOSOWER, E. M., WINSTEIN, S.: J. Am. Chem. Soc., **78,** 4354 (1956)
[13] NARWID, T. A., COONEY, K. E., USKOKOVIČ, M. R.: Helv. Chim. Acta, **57,** 771 (1974)
[14] PATEL, D. K., PETROW, V., STUART-WEBB, I. A.: J. Chem. Soc., **1957,** 665
[15] WAGNER, A. F., WOLFF, N. E., WALLIS, E. S.: J. Org. Chem., **17,** 529 (1952)
[16] SHOPPE, C. W., SUMMERS, G. H. R.: J. Chem. Soc., **1952,** 3361
[17] USKERT, A., NÉDER, Á.: 6th European Symp. on Fluorine Chemistry, Abstracts 0—18, Dortmund, 1977
[18] JACOBSEN, T. N., JENSEN, V.: Chem. and Ind., **1957,** 172
[19] HUTCHINS, R. R. N., THOMPSOM, M. J., SVOBODA, J. A.: Steroids, **15,** 113 (1970)
[20] SHOPPEE, C. W., KRUEGER, G.: J. Chem. Soc., **1961,** 3641
[21] CELLA, J. A., BROWN, E. A., BURTNER, R. R.: J. Org. Chem., **24,** 743 (1959)

Ágnes NÉDER
Éva NAGY
Zsuzsanna MÉHESFALVI
János KUSZMANN

H-1045 Budapest, Szabadságharcosok útja 47—49.

Andor USKERT

H-1111 Budapest, Gellért tér 4.

Acta Chimica Academiae Scientiarum Hungaricae, Tomus 103 (3), pp. 241—258 (1980)

A STUDY ON THE KINETICS OF THE SELECTIVE HYDROGENATION OF PHENOL

T. MÁTHÉ, J. PETRÓ, A. TUNGLER, Z. CSŰRÖS and K. LUGOSI

(Research Group for Organic Chemical Technology, Hungarian Academy of Sciences, Budapest)

Received October 12, 1978
In revised form March 28, 1979
Accepted for publication April 13, 1979

Selective hydrogenation of phenol to cyclohexanone using a palladium catalyst on a molecular sieve support was studied in the temperature range of 145 to 175 °C. The kinetic equation yielding the best fitting to integral conversion data was determined by computerized non-linear parameter estimation. The kinetic equation allows to presume that the introductory step of selective hydrogenation takes place between atomically adsorbed hydrogen and gaseous phenol (Rideal—Eley type mechanism), while adsorbed atoms and molecules participate in the further steps (Langmuir—Hinshelwood mechanism).

Introduction

JORIS and VITRONE [1] were the first to hydrogenate phenol selectively, in the liquid phase and at atmospheric pressure, utilizing a palladium catalys on active carbon support. They later modified the procedure but continued to use palladium as catalyst on various supports.

According to thermodynamic calculations [2], selective hydrogenation is practically irreversible below 200 °C, *i.e.* the equilibrium of the reaction

$$C_6H_5OH + 2H_2 \rightarrow C_6H_{10} \qquad (1)$$

is essentially shifted in the direction of the product cyclohexanone.

Only two papers concerning the kinetics of the above process could be found in the literature. STRELETS and coworkers [3] determined the rate of the reaction in a circulation reactor, in the temperature range of 110—150 °C. A palladium catalyst on alumina support was used [4]. Already at 110 °C, a side reaction took place in which cyclohexanol was formed. The results were evaluated by computer using the gradient method. The conclusion was made that hydrogen is adsorbed atomically and on different active centers than phenol; cyclohexanol is probably formed from cyclohexanone slowly being desorbed from the catalyst surface.

HANCIL and coworkers [5] studied the hydrogenation of phenol to cyclohexanone and the hydrogenation of cyclohexanone to cyclohexanol, using a

platinum catalyst. They calculated the parameters of the kinetic equation using linear and non-linear least squares methods. The better solution was obtained with the non-linear method. Even mathematical statistical considerations did not allow to establish essential differences between three kinetic equations. The authors consider the kinetic equation the most likely, according to which the surface reaction between phenol and two adsorbed hydrogen molecules is the rate-controlling step.

As may be seen, the authors of the cited two papers hold rather different opinions as to what mechanism is likely in the selective hydrogenation of phenol.

The objective of our experiments was to determine the most likely reaction mechanism, based on detailed kinetic studies and computerized evaluation of the results. These studies were made possible by the high activity and selectivity, remaining unchanged for several hundred hours, of the catalyst utilized in our process [6] for cyclohexanone production.

Experimental

1. *Apparatus*

Selective hydrogenation was investigated in an isothermal integral flow reactor. Hydrogen and argon (used as diluting gas) were introduced into the preheater of the reactor through flow control, stabilized and measuring units and gas purifying equipment (deoxygenation and drying). Molten phenol was also introduced into the preheater at a constant rate, using a high precision dosing device. The granular glass packing similar in grain size to the catalyst and accommodated above the catalyst bed ensured that the characteristic flow conditions of the reaction mixture should be established already before it reaches the catalyst bed. The temperature of the catalyst bed was measured with an iron-constantan thermocouple and kept at constant temperature within ± 1 °C by means of suitably controlled electric heating. The mixture leaving the reactor was cooled and passed through a gas-liquid separator. The analysis of the products was performed with a Chrom-III gas chromatograph. Argon carrier gas and flame ionization detection was used. Quantitative evaluation was performed with an electronic integrator. The accuracy of the analysis was $\pm 0.5\%$.

2. *Characteristics of the catalyst*

The catalyst support was a natural molecular sieve occurring in Hungary and containing about 70 vol.% clinoptilite. The support was impregnated with a palladium chlorid solution, treated with 0.1 *N* NaOH and finally reduced in the reactor in hydrogen stream at 200 °C. At this temperature, the catalyst reaches maximum activity and selectivity after 1 hr of activation. We wish to note that with the catalyst containing 0.4—0.5 wt% Pd (this was found to be the best), at a conversion of 90%, the cyclohexanol content of the reaction mixture is less than 1 mol%, and does not exceed 3 mol% even at conversions of 99%. In our kinetic measurements the maximum conversion was 50%, *i.e.* the reaction proceeded unequivocally according to Eq. (1) and no by-product formation (above all that of cyclohexanol) had to be taken into account. The activity and loadability of the catalyst is characterized by the following: 5 to 8 mol phenol *per* 1 g of palladium can be converted per hour to cyclohexanone. The activity and selectivity of the catalyst did not decrease in the course of continuous operation for more than 500 hours.

3. *Kinetic measurements*

The reaction described by Eq. (1) is exothermic and accompanied by a change in the number of molecules, *i.e.* by volume change. Therefore we used argon as diluting gas in the kinetic studies. The amounts of diluting gas and catalyst were chosen so as to ensure that the

volume change of the reaction mixture due to conversion should not exceed 3%. Mass transport by longitudinal diffusion did not exceed 5% of the total mass flow, *i.e.* the reactor was close to the operation of the ideal tube reactor. The change in the particle size of the support between 0.6 and 2.5 mm did not affect the activity of the catalyst, demonstrating that pore

Table I

Conversion of reaction (1);
total pressure 1 atm; initial hydrogen to phenol mole ratio: $n^{\circ}_{H}/n^{\circ}_{Ph} = 6 : 1$; initial partial pressure of phenol $p^{\circ}_{Ph} = 0.0552$ atm

s^{-1} ($g_{Pd}g_{mix}s$)	$Conv_{Ph}$ (mol %)	$n_{Ph} \times 10^3$ ($mol_{Ph}g^{-1}_{mix}$)	p_{Ph} (atm)	p_H (atm)	p_{ON} (atm)
0	0	1.8181	0.0552	0.3312	0
		Temperature 145 °C			
1.173	12.48	1.5912	0.0490	0.3219	0.0070
1.374	14.83	1.5485	0.0478	0.3202	0.0083
1.686	17.62	1.4978	0.0464	0.3179	0.0099
2.347	23.12	1.3978	0.0436	0.3138	0.0131
3.198	30.06	1.2715	0.0399	0.3082	0.0172
4.463	35.51	1.1725	0.0370	0.3039	0.0204
		Temperature 155 °C			
1.173	15.22	1.5413	0.0476	0.3199	0.0085
1.374	17.55	1.4990	0.0464	0.3181	0.0098
1.686	20.52	1.4450	0.0449	0.3157	0.0115
2.347	27.90	1.3422	0.0411	0.3100	0.0156
3.198	32.47	1.2278	0.0387	0.3063	0.0183
4.463	39.02	1.1087	0.0351	0.3010	0.0225
		Temperature 165 °C			
1.173	17.58	1.4985	0.0464	0.3180	0.0099
1.374	20.27	1.4495	0.0450	0.3160	0.0114
1.686	23.96	1.3825	0.0431	0.3130	0.0136
2.347	31.16	1.2515	0.0394	0.3075	0.0178
3.198	38.26	1.1225	0.0356	0.3017	0.0221
4.463	46.42	0.9742	0.0311	0.2950	0.0270
		Temperature 175 °C			
1.173	24.36	1.3752	0.0429	0.3128	0.0138
1.374	27.70	1.3145	0.0412	0.3102	0.0158
1.686	31.61	1.2434	0.0391	0.3070	0.0181
2.347	39.58	1.0985	0.0349	0.3007	0.0229
3.198	48.86	0.9298	0.0296	0.2931	0.0285
4.463	56.08	0.7985	0.0258	0.2870	0.0329

diffusional inhibition is negligible. This was to be expected since phenol cannot penetrate into the pores of the catalyst and diffusion control is improbable with hydrogen. Our experiments also convinced us that diffusion control across the gas film can also be disregarded.

Kinetic measurements were performed with 4.75 g catalyst on 1—1.4 mm particle size support. This catalyst amount allows to neglect all interfering effects of the above factors.

Table II

Conversion of reaction (1);
total pressure 1 atm; $n^{\circ}_{H}/n^{\circ}_{Ph} = 8 : 1$; $n^{\circ}_{Ph} = 0.0552$ atm

S^{-1} ($g_{Pd}\ g_{mix}^{s}$)	$Conv_{Ph}$ (mol %)	$n_{Ph} \times 10^{3}$ ($mol_{Ph} g_{mix}^{-1}$)	p_{Ph} (atm)	p_{H} (atm)	p_{ON} (atm)
0	0	2.1087	0.0552	0.4416	
		Temperature 145 °C			
1.361	15.58	1.7802	0.0474	0.4319	0.0088
1.594	17.75	1.7344	0.0463	0.4306	0.0100
1.944	22.30	1.6285	0.0440	0.4275	0.0126
2.723	29.51	1.4864	0.0402	0.4229	0.0168
3.718	34.83	1.3742	0.0374	0.4193	0.0200
5.182	41.61	1.2313	0.0337	0.4141	0.0240
		Temperature 155 °C			
1.361	17.97	1.7298	0.0462	0.4304	0.0100
1.594	21.16	1.6625	0.0446	0.4284	0.0118
1.944	24.51	1.5919	0.0428	0.4261	0.0137
2.723	30.89	1.4573	0.0359	0.4220	0.0174
3.718	38.35	1.3000	0.0355	0.4169	0.0216
5.182	46.46	1.1290	0.0311	0.4108	0.0270
		Temperature 165 °C			
1.361	20.80	1.6700	0.0448	0.4286	0.0118
1.594	23.58	1.6115	0.0433	0.4268	0.0134
1.944	27.99	1.5185	0.0410	0.4238	0.0159
2.723	35.86	1.3525	0.0369	0.4187	0.0206
3.718	43.45	1.1925	0.0328	0.4153	0.0252
5.182	52.70	0.9975	0.0277	0.4065	0.0308
		Temperature 175 °C			
1.361	28.78	1.5018	0.0406	0.4234	0.0164
1.594	31.56	1.4432	0.0392	0.4216	0.0181
1.944	36.40	1.3411	0.0366	0.4181	0.0209
2.723	46.62	1.1256	0.0311	0.4114	0.0271
3.718	54.42	0.9611	0.0268	0.4059	0.0320
5.182	61.90	0.8035	0.0225	0.4000	0.0366

Table III

Conversion of reaction (1);
total pressure 1 atm; $n^{\circ}_{H}/n^{\circ}_{Ph} = 10 : 1$; $p^{\circ}_{Ph} = 0.0552$ atm

S^{-1} ($g_{Pd}\, g_{mix}^{-1}$ s)	$Conv_{Ph}$ (mol %)	$n_{Ph} \times 10^3$ ($mol_{Ph}\, g_{mix}^{-1}$)	P_{Ph} atm	P_H (atm)	P_{ON} (atm)
0	0	2.5098	0.0552	0.5521	0
		Temperature 145 °C			
1.080	12.76	2.1895	0.0489	0.5457	0.0071
1.621	18.28	2.0510	0.0461	0.5429	0.0103
1.898	21.13	1.9795	0.0446	0.5415	0.0119
2.314	24.60	1.8925	0.0428	0.5395	0.0140
3.239	32.56	1.6926	0.0386	0.5354	0.0186
4.416	39.34	1.5224	0.0350	0.5317	0.0218
		Temperature 155 °C			
1.080	15.15	2.1300	0.0476	0.5445	0.0084
1.621	21.17	1.9785	0.0446	0.5414	0.0118
1.898	24.40	1.8974	0.0429	0.5398	0.0137
2.314	28.54	1.7935	0.0407	0.5374	0.0160
3.239	35.04	1.6304	0.0373	0.5341	0.0197
4.416	43.25	1.4243	0.0329	0.5295	0.0245
		Temperature 165 °C			
1.080	16.39	2.0985	0.0470	0.5439	0.0092
1.621	23.80	1.9125	0.0432	0.5401	0.0135
1.898	26.64	1.8413	0.0417	0.5386	0.0152
2.314	31.38	1.7223	0.0392	0.5359	0.0179
3.239	36.69	1.5137	0.0348	0.5316	0.0229
4.416	48.13	1.3018	0.0302	0.5269	0.0281
6.165	54.95	1.1307	0.0264	0.5223	0.0322
		Temperature 175 °C			
1.080	22.18	1.9531	0.0440	0.5409	0.0126
1.621	31.01	1.7315	0.0394	0.5363	0.0177
1.898	34.14	1.6350	0.0378	0.5346	0.0196
2.314	39.39	1.5212	0.0350	0.5316	0.0227
3.239	50.06	1.2534	0.0292	0.5259	0.0293
4.416	58.46	1.0426	0.0245	0.5211	0.0345
6.165	64.49	0.8912	0.0211	0.5169	0.0383

Table IV

Conversion of reaction (1);
total pressure 1 atm; temperature 165 °C

S^{-1} ($g_{Pd}\,g_{mix}^{-1}\,s$)	$Conv_{Ph}$ (mol %)	$n_{Ph}\times10^3$ ($mol_{Ph}\,g_{mix}^{-1}$)	p_{Ph} (atm)	p_H (atm)	p_{ON} (atm)
$n_H^\circ/n_{Ph}^\circ = 4:1$; $p_{Ph}^\circ = 0.0552$ atm					
0.000	0.00	1.5976	0.0552	0.2208	0.0000
1.031	15.41	1.3513	0.0475	0.2074	0.0087
1.208	17.21	1.3226	0.0466	0.2058	0.0097
1.473	21.01	1.2618	0.0446	0.2023	0.0119
2.063	27.24	1.1623	0.0414	0.1967	0.0155
2.810	33.65	1.0600	0.0380	0.1907	0.0193
3.929	42.30	0.9217	0.0334	0.1824	0.0245
$n_H^\circ/n_{Ph}^\circ = 6:1$; $p_{Ph}^\circ = 0.1104$ atm					
0.000	0.00	5.3120	0.1104	0.6624	0.0000
1.714	18.55	4.3252	0.0935	0.6482	0.0214
2.007	21.02	4.1941	0.0915	0.6462	0.0243
2.447	23.83	4.0453	0.0888	0.6437	0.0278
3.428	27.97	3.8250	0.0848	0.6404	0.0329
4.671	31.95	3.6132	0.0808	0.6368	0.0380
$n_H^\circ/n_{Ph}^\circ = 6:1$; $p_{Ph}^\circ = 0.0276$ atm					
0.000	0.00	0.7856	0.0276	0.1656	0.0000
1.014	10.83	0.7002	0.0248	0.1606	0.0030
1.187	12.74	0.6853	0.0242	0.1594	0.0035
1.448	14.40	0.6712	0.0238	0.1589	0.0040
2.027	17.08	0.6514	0.0231	0.1577	0.0048
2.762	19.75	0.6300	0.0224	0.1563	0.0055
3.863	22.55	0.6080	0.0212	0.1548	0.0063

Conversion was determined at 165 °C, at four different hydrogen/phenol mole ratios and 6 different feed rate of phenol. In one series of experiments the initial partial pressure of phenol was kept constant, while in another series the hydrogen/phenol mole ratio was constant and the initial partial pressure of phenol was varied. At 145, 155 and 175 °C, the experiments were carried out at three different hydrogen/phenol mole ratios. The activity of the catalyst did not change in the course of the experiments; this was established from the identical conversions measured under similar conditions in the initial and final stage of each series.

Conversions measured under controlled steady state conditions, and partial pressures of the reactants calculated from the conversion values are listed in Tables I, II, III and IV. From these data, integral conversion curves were plotted (Fig. 1), representing the amount of unconverted phenol *vs.* reciprocal flow rate. The derivative of these integral conversion curves directly furnishes the rate of reaction, expressed in $mol_{Ph}g_{Pd}^{-1}s^{-1}$ units (the dimension of conversion is $mol_{ph}g_{mixture}^{-1}$, and the reciprocal flow rate is expressed in $g_{Pd}g_{mixtures}^{-1}$).

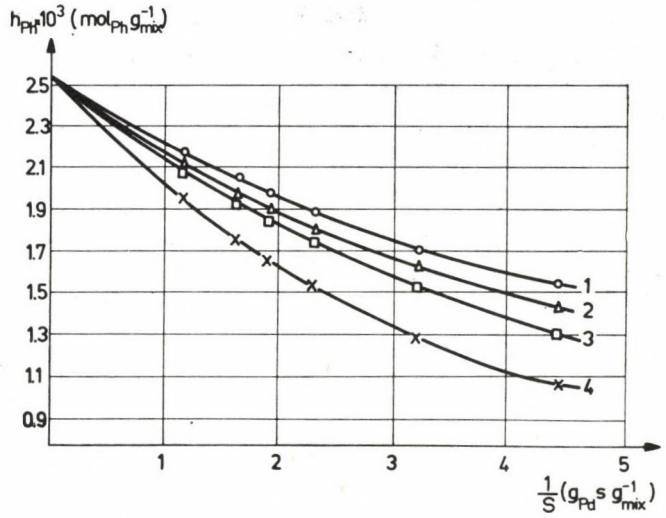

Fig. 1. Conversion curves of reaction (1); total pressure 1 atm; hydrogen to phenol mole ratio in the feed 10 : 1; initial partial pressure of phenol 0.0552 atm; temperature 145 °C (1), 155 °C (2), 165 °C (3), and 175 °C (4)

We also studied the effect of cyclohexanone partial pressure on the rate of reaction. Phenol and cyclohexanone were fed together onto the catalyst. We found that a change in the partial pressure of cyclohexanone does not affect the rate of reaction or the selectivity. In the mixture leaving the reactor, no cyclohexanol could be detected, *i.e.* the rate of further hydrogenation of cyclohexanone is substantially lower than that of phenol hydrogenation to cyclohexanone.

Results

1. *Kinetic equations and computerized data processing*

The catalytic conversion proceeding under the participation of phenol and two molecules of hydrogen can be divided into elementary steps on the basis of two presumed mechanisms:

(i) Langmuir—Hinshelwood mechanism, *i.e.* the surface reaction proceeds between sorbed phenol and hydrogen,

(ii) Rideal—Eley mechanism, *i.e.* only one reactant is sorbed, and reacts with the gasous reactant in the surface reaction.

In both mechanisms, we reckoned with the possibilities of molecular and atomic adsorption of hydrogen. In mechanism (i), we took into consideration the possibilities of concurrent and non-concurrent adsorption. For these cases, we set up the corresponding kinetic equations, using known methods [7], by assuming one particular step as rate controlling. The equations are presented in Table V and VI.

These equations are non-linear with respect to the parameters. HOUGEN and WATSON [7] linearized the equations and selected the kinetic equation

Table V

Kinetic equations based on Langmuir—Hinshelwood mechanisms

No.	Rate-controlling step	Kinetic equation
101		$W = k \frac{p_{Ph}}{1 + K_H p_H + K_{ON} p_{ON}}$
102		$W = k \frac{p_H}{1 + K_{Ph} p_{Ph} + K_{ON} p_{ON}}$
103		$W = k \frac{K_{Ph} K_H p_{Ph} p_H}{(1 + K_{Ph} p_{Ph} + K_H p_H + K_{ON} p_{ON})^2}$
104	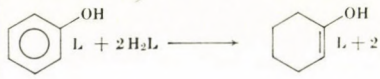	$W = k \frac{K_{Ph} K_H^2 p_{Ph} p_H^2}{(1 + K_{Ph} p_{Ph} + K_H p_H + K_{ON} p_{ON})^3}$
105		$W = k$
106		$W = k$
107		$W = k \frac{p_{Ph}}{1 + (K_H p_H)^{1/2} + K_{ON} p_{ON}}$
108		$W = k \frac{p_{Ph}}{(1 + K_{Ph} p_{Ph} + K_{ON} p_{ON})^2}$
109	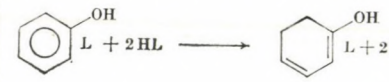	$W = k \frac{K_{Ph} K_H p_{Ph} p_H}{(1 + K_{Ph} p_{Ph} + (K_H p_H)^{1/2} + K_{ON} p_{ON})^3}$
110	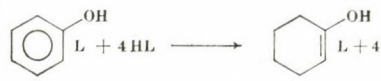	$W = k \frac{K_{Ph} K_H^2 p_{Ph} p_H^2}{(1 + K_{Ph} p_{Ph} + (K_H p_H)^{1/2} + K_{ON} p_{NO})^5}$
111	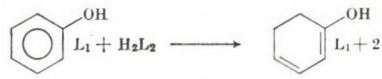	$W = k \frac{K_{Ph} K_H p_{Ph} p_H}{(1 + K_{Ph} p_{Ph} + K_{ON} p_{ON})(1 + K_H p_H)}$
112	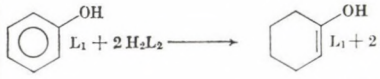	$W = k \frac{K_{Ph} K_H^2 p_{Ph} p_H^2}{(1 + K_{Ph} p_{Ph} + K_{ON} p_{ON})(1 + K_H p_H)^2}$
113	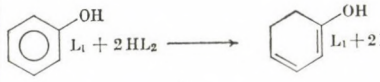	$W = k \frac{K_{Ph} K_H p_{Ph} p_H}{(1 + K_{Ph} p_{Ph} + K_{ON} p_{ON})(1 + (K_H p_H)^{1/2})^2}$
114		$W = k \frac{K_{Ph} K_H^2 p_{Ph} p_H^2}{(1 + K_{Ph} p_{Ph} + K_{ON} p_{ON})(1 + (K_H p_H)^{1/2})^4}$

* For the meaning of symbols, see footnote to Table VI

Table VI

Kinetic equations based on Rideal—Eley mechanisms

No.	Rate-controlling step	Kinetic equation
215	$H_2 + L \longrightarrow H_2L$	$W = k \frac{p_H}{1 + K_{ON} p_{ON}}$
216		$W = k \frac{K_H p_{Ph} p_H}{1 + K_H p_H + K_{ON} p_{ON}}$
217	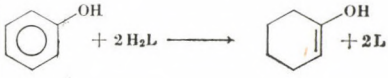	$W = k \frac{K_H^2 p_{PH} p_H^2}{(1 + K_H p_H + K_{ON} p_{\Theta N})^2}$
218	$H_2 + 2L \longrightarrow 2HL$	$W = k \frac{p_H}{(1 + K_{ON} p_{ON})^2}$
219		$W = k \frac{K_H p_{Ph} p_H}{(1 + (K_H p_H)^{1/2} + K_{ON} p_{ON})^2}$
220		$W = k \frac{K_H^2 p_{Ph} p_H^2}{(1 + (K_H p_H)^{1/2} + K_{ON} p_{ON})^4}$
221		$W = k \frac{p_{Ph}}{1 + K_{ON} p_{ON}}$
222		$W = k \frac{K_{Ph} p_{Ph} p_H}{1 + K_{Ph} p_{Ph} + K_{ON} p_{ON}}$

L is the active site of the catalyst
W is the reaction rate (mol g sec^{-1})
k is the rate constant (mol g sec^{-1} atm^{-1}) (or without atm)
K is the adsorption equilibrium constant (atm^{-1})
p is the partial pressure (atm); and subscripts Ph, H, and ON refer to phenol, hydrogen, cyclohexanone, respectively

best fitting the experimental data by the least squares method. Later several objections were raised against this treatment. BARD and LAPIDUS [8] demonstrated that the kinetic equations can formally be linearized, but in this case partial pressures will appear on both sides of the equation, *i.e.* as both dependent and independent variables. Consequently, the error of a quite different equation will be minimized, and its is improbable that the minima of the error functions of the two equations should occur at identical values of the parameters.

On top of the above counter-arguments, we considered the Hougen—Watson method unsatisfactory, because calculation of the parameters of the

linearized equations would have involved the use of graphical derivatives of the integral conversion curves, and would thereby have introduced a further significant error. We therefore decided to attempt a solution of the problem by computer calculation allowing to obtain parameters of the non-linearized equations.

In order to calculate the parameters of the kinetic equations, the difference between experimental and calculated values should be minimized, i.e.

$$\sum_{i=1}^{M} (n_{\mathrm{Ph},k}^{\mathrm{exp}} - n_{\mathrm{Ph},i}^{\mathrm{calc}})^2 \Rightarrow \text{minimum} \tag{2}$$

where M is the number of measurements, n_{Ph} is the amount of phenol in mol *per* gram of mixture, and $n_{\mathrm{Ph}}^{\mathrm{exp}}$ and $n_{\mathrm{Ph}}^{\mathrm{calc}}$ are experimental and calculated values, respectively belonging to one and the same flow rate.

The values of $n_{\mathrm{Ph}}^{\mathrm{calc}}$ were calculated as follows:

$$n_{\mathrm{Ph}}^{\mathrm{calc}} = \int_{0}^{S-1} \mathrm{f}(X)\ \mathrm{d}(1/S) \tag{3}$$

where S is the mass flow rate relative to unit mass of catalyst: $g_{\mathrm{mixture}}\ g_{\mathrm{Pd}}^{-1}\ s^{-1}$, and $\mathrm{f}(X)$ is one of the kinetic equations in Tables V and VI.

Numerical integration can be performed using the trapezium method or the Simpson formula. Both gave closely similar fitting.

Numerous minimum searching procedures have been described in the literature [8, 9]. We chose the method of HOOKE and JEEVES [10], this being a direct search method, *i.e.* it does not require the calculation of derivatives. The computer program was checked by means of the function described by ROSENBROCK [11]:

$$\mathrm{f}(x_1, x_2) = 100(x_2 - x_1^2)^2 + (1 - x_1)^2 \tag{4}$$

which, in effect, corresponds to a steep-wall parabolic valley. We found that in its original form, the Hooke—Jeeves method is not quite efficient and yields erroneous results in some cases. We therefore modified the procedure so as to allow a rapid change of the search direction.

2. *Selection of the most probable kinetic equation*

A CDC 3300 computer was used for calculations. We first evaluated data measured at 165 °C with all kinetic equations. We have shown that with all equations containing the parameter K_{Ph} (equations No. 102—104 and 108—

114 in Table V, and equation No. 222 in Table VI), the value of K_{Ph} is negative in the minimum of the error function (2), and hence these equations can be excluded since they do not satisfy theoretical requirements.

Table VIIa

Values of n_{Ph}^{calc} calculated with equations No. 216, 217, 219 and 220; temperature 145 °C

$n_{Ph}^{exp} \times 10^3$ ($mol_{Ph}\ g_{mix}^{-1}$)	$n_{Ph}^{calc} \times 10^3$ ($mol_{Ph}\ g_{mix}^{-1}$)			
No.	216	217	219	220
$n_H^\circ/n_{Ph}^\circ = 6:1$				
1.8181	1.8181	1.8181	1.8181	1.8181
1.5912	1.6081	1.5930	1.5918	1.5938
1.5485	1.5735	1.5577	1.5562	1.5586
1.4978	1.5261	1.5049	1.5030	1.5059
1.3978	1.4273	1.3987	1.3958	1.3999
1.2715	1.3112	1.2736	1.2693	1.2749
$n_H^\circ/n_{Ph}^\circ = 8:1$				
2.1087	2.1087	2.1087	2.1087	2.1087
1.7802	1.7879	1.7812	1.7838	1.7836
1.7344	1.7384	1.7305	1.7335	1.7333
1.6385	1.6673	1.6575	1.6611	1.6608
1.4864	1.5207	1.5070	1.5118	1.5114
1.3742	1.3499	1.3311	1.3373	1.3359
$n_H^\circ/n_{Ph}^\circ = 10:1$				
2.5098	2.5098	2.5098	2.5098	2.5098
2.1895	2.1854	2.1998	2.1985	2.1987
2.0510	2.0386	2.0592	2.0573	2.0576
1.9795	1.9669	1.9904	1.9883	1.9886
1.8925	1.8637	1.8913	1.8889	1.8892
1.6926	1.6510	1.6865	1.6836	1.6840

The best fit was obtained with equations Nos 216, 217, 219 and 220. Thus the number of probable equations could be reduced to four. Since these kinetic equation describe a similar mechanism, we evaluated the data measured at 145, 155, 165 and 175 °C with all four equations. Values calculated for

n_{Ph}^{calc} with different equations are listed in Tables VIIa, b, c and d. For comparison, experimental values n_{Ph}^{exp} are also presented. Sums of squared deviations at the different temperatures, obtained with the four equations, are

Table VIIb

Values of n_{Ph}^{calc} calculated with equations No. 216, 217, 219 and 220; temperature 155 °C

$n_{Ph}^{exp} \times 10^3$ ($mol_{Ph}\, gm_{fx}^{-1}$)	$n_{Ph}^{calc} \times 10^3$ ($mol_{Ph}\, gm_{fx}^{-1}$)			
No.	216	217	219	220
$n_H^\circ/n_{Ph}^\circ = 6:1$				
1.8181	1.8181	1.8181	1.8181	1.8181
1.5413	1.5810	1.5622	1.5612	1.5612
1.4990	1.5446	1.5228	1.5216	1.5217
1.4450	1.4903	1.4640	1.4624	1.4625
1.3109	1.3830	1.3477	1.3451	1.3455
1.2278	1.2567	1.2106	1.2067	1.2074
$n_H^\circ/n_{Ph}^\circ = 8:1$				
2.1087	2.1087	2.1087	2.1087	2.1087
1.7298	1.7454	1.7376	1.7405	1.7395
1.6625	1.6906	1.6814	1.6847	1.6836
1.5919	1.6118	1.6006	1.6045	1.6032
1.4573	1.4479	1.4319	1.4372	1.4354
1.3000	1.2592	1.2372	1.2441	1.2417
$n_H^\circ/n_{Ph}^\circ = 10:1$				
2.5098	2.5098	2.5098	2.5098	2.5098
2.1300	2.1425	2.1603	2.1584	2.1597
1.9785	1.9794	2.0046	2.0019	2.0038
1.8974	1.9002	1.9289	1.9259	1.9280
1.7935	1.7873	1.8208	1.8174	1.8198
1.6304	1.5541	1.5971	1.5929	1.5959

given in Table VIII. By means of the F-test well known in mathematical statistics [12], equation No. 216 can unequivocally be excluded. The ratios of the sums of squared deviations calculated by means of equations No. 217, 219 and 220 do not exceed the critical values of F distribution. On the basis

that the sum of squared deviations obtained with equation No. 219 is smallest at all temperatures, this kinetic equation may be considered as the most probable, that is, the best kinetic equation of the selective hydrogenation of phenol in the temperature range of 145 to 175 °C is

$$W = k \frac{K_H p_{Ph} p_H}{[1 + (K_H p_H)^{1/2}]^2} \tag{5}$$

Table VIIc

Values of n_{Ph}^{calc} calculated with equations No. 216, 217, 219 and 220; temperature 165 °C

$n_{Ph}^{exp} \times 10^3$ ($mol_{Ph}\, g_{mix}^{-1}$)	$n_{Ph}^{calc} \times 10^3$ ($mol_{Ph}\, g_{mix}^{-1}$)			
No.	216	217	219	220
		$n_H^\circ/n_{Ph}^\circ = 6:1$		
1.8181	1.8181	1.8181	1.8181	1.8181
1.4985	1.5468	1.5150	1.5142	1.5149
1.4495	1.5061	1.4693	1.4682	1.4690
1.3825	1.4457	1.4013	1.3998	1.4009
1.2515	1.3273	1.2676	1.2653	1.2669
1.1225	1.1912	1.1135	1.1097	1.1120
		$n_H^\circ/n_{Ph}^\circ = 8:1$		
2.1087	2.1087	2.1087	2.1087	2.1087
1.6700	1.6937	1.6831	1.6860	1.6851
1.6115	1.6322	1.6197	1.6231	1.6220
1.5185	1.5445	1.5290	1.5330	1.5317
1.3525	1.3657	1.3434	1.3488	1.3471
1.1925	1.1638	1.1330	1.1399	1.1377
		$n_H^\circ/n_{Ph}^\circ = 10:1$		
2.5098	2.5098	2.5098	2.5098	2.5098
2.0985	2.0863	2.1143	2.1123	2.1126
1.9125	1.9015	1.9409	1.9381	1.9385
1.8413	1.8126	1.8572	1.8541	1.8546
1.7223	1.6862	1.7381	1.7346	1.7350
1.5137	1.4304	1.4963	1.4921	1.4926

Table VIId

Values of n_{Ph}^{calc} calculated with equations No. 216, 217, 219 and 220; temperature 175 °C

$n_{Ph}^{exp} \times 10^3$ ($mol_{Ph}\, g_{mix}^{-1}$)	$n_{Ph}^{calc} \times 10^3$ ($mol_{Ph}\, g_{mix}^{-1}$)			
No.	216	217	219	220
	$n_H^\circ/n_{Ph}^\circ = 6:1$			
1.8181	1.8181	1.8181	1.8181	1.8181
1.3752	1.4574	1.4069	1.4059	1.4089
1.3145	1.4063	1.3481	1.3468	1.3502
1.2434	1.3315	1.2617	1.2598	1.2640
1.0985	1.1873	1.0946	1.0914	1.0972
0.9298	1.0291	0.9101	0.9051	0.9128
	$n_H^\circ/n_{Ph}^\circ = 8:1$			
2.1087	2.1087	2.1087	2.1087	2.1087
1.5018	1.5601	1.5449	1.5485	1.5485
1.4432	1.4839	1.4657	1.4699	1.4699
1.3411	1.3760	1.3553	1.3583	1.3584
1.1256	1.1639	1.1313	1.1378	1.1380
0.9611	0.9355	0.8909	0.8991	0.8995
	$n_H^\circ/n_{Ph}^\circ = 10:1$			
2.5098	2.5098	2.5098	2.5098	2.5098
1.9531	1.9414	1.9848	1.9824	1.9825
1.7315	1.7060	1.7658	1.7627	1.7627
1.6530	1.5948	1.6620	1.6585	1.6586
1.5212	1.4384	1.5126	1.5117	1.5118
1.2534	1.1337	1.2294	1.2250	1.2250

Table VIII

Sums of squared deviations calculated with equations No. 216, 217, 219 and 220

Temp (°C)	$\sum_{i=1}^{M=15}{}' (n_{Ph,i}^{calc} - n_{Ph,i}^{exp})^2 \times 10^9$ ($\bar{n}ol_{Ph}\, g_{mix}^{-1}$)^2			
No.	216	217	219	220
145	9.815	3.133	2.916	3.011
155	20.939	12.542	11.261	11.709
165	32.002	7.187	6.255	6.528
175	74.441	13.215	12.863	13.038

3. *Temperature dependence of the kinetic constants*

The values of the adsorption equilibrium constants and rate constants at different temperatures are summarized in Table IX. Their logarithms *vs.* $1/T$, *i.e.* the Arrhenius relationships are represented in Figs 2 and 3. From

Table IX

Rate constants (k) and adsorption equilibrium constants of hydrogen for Eq. (5)

Temp (°C)	$k \times 10^2$ ($mol_{Ph}\, g_{Pd}^{-1}\, s^{-1}\, atm^{-1}$)	K_H (atm^{-1})
145	2.67	0.665
155	3.06	0.694
165	3.71	0.887
175	5.03	1.005

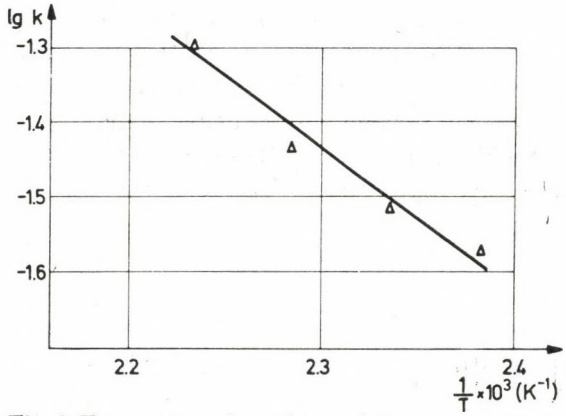

Fig. 2. Temperature dependence of the rate constants

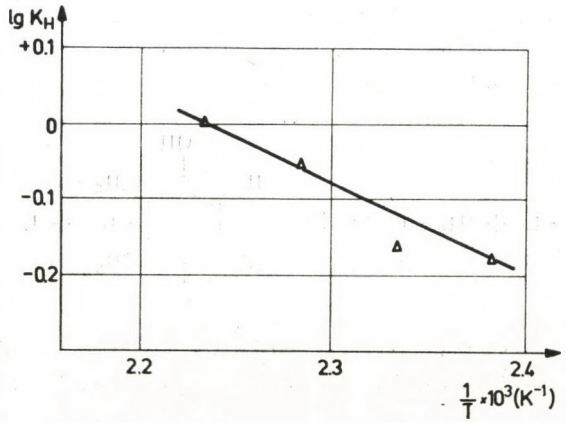

Fig. 3. Temperature dependence of the adsorption equilibrium constants of hydrogen

the slope of the straight line in Fig. 2, the activation energy of the rate-controlling surface reaction is 7.3 kcal/mol.

From the temperature dependence of the equilibrium constant of hydrogen adsorption (Fig. 3), it follows that dissociative adsorption is endothermic and its energy requirement is 5 kcal/mol.

Discussion

Equation (5), yielding the best fit, describes a reaction that starts with dissociative adsorption of hydrogen, followed by the reaction of gas-phase phenol with two adsorbed hydrogen atoms in an irreversible rate-controlling step. The subsequent uptake of two hydrogen atoms and the tautomeric rearrangement of cyclohexenol into cyclohexanone is a fast process and proceeds presumably on the surface between sorbed intermediates. However, based on chemical considerations, this mechanism appears improbable, since it involves a ternary collision in the rate-controlling step. This would involve strict geometrical requirements for the adsorbed hydrogen and colliding phenol, which would again reduce the probability of the mechanism. Another mechanism, also consistent with the most probable kinetic equation can, however, also be conceived: atomically adsorbed hydrogen reacts with gas-phase phenol in a reversible step:

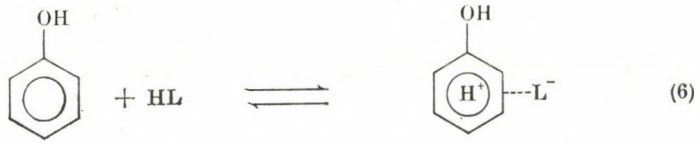

(6)

In the intermediate of the above reaction, the electronic system of the aromatic ring is not yet broken down, but only polarized in part. When the following hydrogen atom is added, the aromatic ring ceases to exist, and hence this is the rate-controlling and irreversible step:

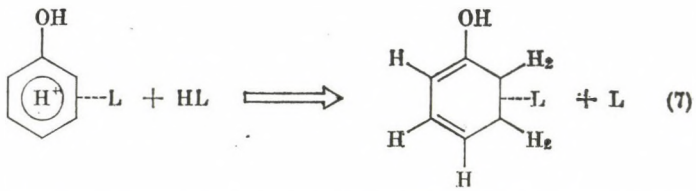

(7)

If the surface concentration of adsorbed hydrogen atoms is higher by several orders of magnitude than that of the intermediate formed in (6), *i.e.*

$$[\mathrm{HPhL}]_{\mathrm{ads}} \ll [\mathrm{HL}]_{\mathrm{ads}} ,$$

the mechanism described by Eqs (6) and (7) will result in a kinetic equation identical with Eq. (5). In this mechanism, no ternary collision is involved and no geometrical requirements concerning adsorbed hydrogen and colliding phenol arise.

Cyclohexadienol formed in reaction (7) adds two further hydrogen atoms in a fast reaction:

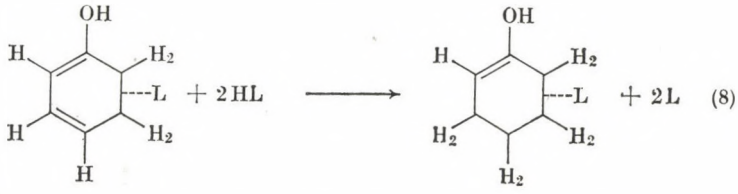

and subsequently cyclohexenol is rearranged into cyclohexanone and desorbed:

Thus the introductory step of the process, namely reaction (6), proceeds according to the Rideal—Eley mechanism between an adsorbed hydrogen atom and a colliding phenol molecule from the gas phase, whereas the further steps proceed according to the Langmuir—Hinshelwood mechanism between adsorbed atoms and molecules.

The above discussion exemplifies how, on the basis of the most probable kinetic equation found by computerized parameter estimation, chemical considerations will help derive a more probable reaction mechanism whose kinetic equation will agree with the equation found to fit best to experimental data.

*

The authors wish to thank Prof. Dr. F. NAGY and Prof. Dr. P. FEJES for helpful discussions.

REFERENCES

[1] JORIS, G. G., VITRONE, J.: US Patent 2 829 156 (1958)
[2] BAKOS, M.: Unpublished results
[3] STRELETS, M. M., SNAGOVSKY, Y. S., BORISOV, V. V., LYUBARSKY, G. D.: Khim. Prom., **44**, 567 (1968)
[4] LYUBARSKY, G. D., STRELETS, M. M.: Khim. Prom., **43**, 481 (1967)
[5] HANCIL, V., MITSCHKA, P., BERANEK, L.: J. Catal., **13**, 435 (1969)

[6] CSŰRÖS, Z., PETRÓ, J., MÁTHÉ, T., TUNGLER, A., BAKOS, M.: Hungarian Patent 159 608 (1969)
[7] HOUGEN, O. A., WATSON, K. M.: Chemical Process Principles, Vol. **3**, p. 902. John Wiley, New York 1954
[8] BARD, Y., LAPIDUS, L.: Cat. Rev., **2**, 67 (1968)
[9] BOX, M. J.: Computer J., **9**, 61 (1966)
[10] HOOKE, R., JEEVES, T. A.: J. Ass. Comp. Mach., **8**, 212 (1961)
[11] ROSENBROCK, H. H.: Computer J., **3**, 175 (1960)
[12] DAVIES, O. L.: Statistical Methods in Research and Production, p. 66. Oliver and Boyd, London 1957

Tibor MÁTHÉ
József PETRÓ
Antal TUNGLER
Zoltán CSŰRÖS
Károly LUGOSI

H-1521 Budapest, Műegyetem rkp. 3.

Acta Chimica Academiae Scientiarum Hungaricae, Tomus 103 (3), pp. 259—269 (1980)

ELECTRON DEFICIENT HETEROAROMATIC AMMONIOAMIDATES, XVIII*

THE SYNTHESIS AND PHOTOCHEMISTRY OF SOME *N*-ISOQUINOLINIO(THIOAMIDATES)

M. LEMPERT-SRÉTER,[1] K. LEMPERT,[2] J. TAMÁS[3] and K. VÉKEY[3]

(*[1]Department of Organic Chemistry, Eötvös Loránd University, Budapest, [2] Department of Organic Chemistry, Technical University, Budapest, [3] Central Research Institute for Chemistry of the Hungarian Academy of Sciences, Budapest*)

Received February 16, 1979
Accepted for publication April 26, 1979

Thioacylation of isoquinolinioamide furnished the *N*-isoquinolinio(thioamidates) 2a—2c. Depending on the solvent, 2c exists either as a mixture with its tricyclic tautomer 5, or exlusively as the latter. The NMR and mass spectra, and the photochemistry of compounds 2a—2c are discussed. The photoproducts obtained include 3,4-dimethoxybenzonitrile, 3,4-dimethoxy(thiobenzamide), *O*-ethyl thiocarbamate, 1(2*H*)-isoquinolinethione (7a), 1(2*H*)-isoquinolinone (7b) and [1,3,4]thiadiazolo[2,3-*a*]isoquinolin-4-ium-2--olate (8a). Differences between the fragmentation upon electron impact and the photochemistry of the thioamidates of Types 1 and 2, as well as between the photochemistry of the thioamidates 2 and their amidate counterparts of Type 3 are discussed. Potassium permanganate oxidation of [1,3,4]thiadiazolo[2,3-*a*]isoquinolin-4-ium-2-thiolate (8b furnishes the olate 8a and 1-isoquinolyl thiocyanate (12).

While the chemistry [1], including the photochemistry [2], of electron deficient heteroaromatic ammonioamidates has been extensively studied, little is known about the related thioamidates. The only known members of the latter class of compounds were some thiosemicarbazide derivatives of Type **1** [3—5] (with isoquinoline [6], acridine [7] and pyrazine rings [8] replacing the pyridine ring in some cases); and only the thioamidates **1** (R=Me, R'=H) and **1** (R=Ph, R'=Me) have been subjected to irradiation to yield the parent pyridine, sulfur and an *N*-cyanoamine by photofragmentation [4]. The fragmentation of the latter compounds in the mass spectrometer was identical with their photofragmentation [4].

We wish to report here on the synthesis of the *N*-isoquinolinio(thioamidates) **2a—2c**, their fragmentation upon electron impact and their photochemistry. Some differences between the photochemistry of these thioamidates and their amidate counterparts of Type **3** will also be pointed out.

The thioamidates **2a—2c** were obtained by allowing to react 2-aminoisoquinolinium chloride (**4**) [6] in the presence of base with *S*-[3,4-dimethoxy-(thiobenzoyl)]thioacetic acid [10], *O*-ethyl *S*-methyl dithiocarbonate [11] and

* For Part XVII, see BARTA-SZALAI, G., FETTER, J., LEMPERT, K., MØLLER, J.: Acta Chem. Scand. B, **33**, 79 (1979)

methyl dithiopivalate [12], respectively.* Acylation of **4** with 3,4-dimethoxybenzoyl chloride in the presence of base similarly furnished compound **3a**.

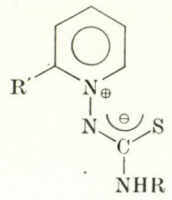

1

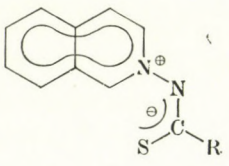

2

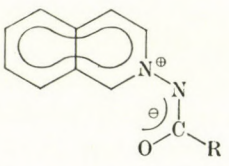

3

2, 3

a: R = 3,4-$(MeO)_2C_6H_3$
b: R = EtO
c: R = *t*-Bu

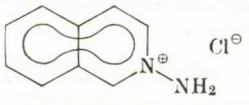

4

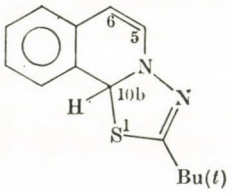

5

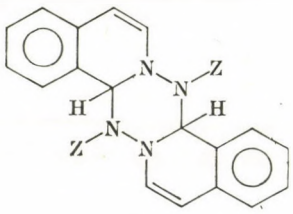

6

a: Z = *t*-Bu—CS—
b: Z = *t*-Bu—CO—
c: Z = H

The thiopivalamidate **2c** and/or its tautomer **5** (see below) are rather unstable: they decompose, as shown by TLC and changes of the ^1H NMR spectra (of which the appearance of additional *t*-butyl signals is the most conspicuous), in CH_2Cl_2 and $CDCl_3$ solutions rapidly at room temperature in the dark, more slowly in ethanol solution (decomposition starts in CH_2Cl_2 solution within 15 min, and within 2 h in ethanol) and even in the crystalline state. **2c** ≒ **5** is even less stable at elevated temperatures. As a result, recovery after recrystallization is low, and the recrystallized product is less pure than the crude material (^1H NMR); moreover, the mass spectrum is time dependent. Solutions of the thioamidates **2a** and **2b** are more stable at room temperature but they, too, decompose at elevated temperatures. Their recovery on recrystallization is therefore low. Although the m.p.'s of the crude products

* With *O,O'*-diphenyl thiocarbonate as the acylating agent compound **2** (R=PhO) has recently been obtained by R. HUISGEN and M. BEHRENS [13].

were slightly raised upon recrystallization, the crude products were already essentially pure (TLC, ^{1}H NMR). All reactions of the thioamidates were therefore carried out with the crude products.

^{1}H NMR spectra and tautomerism of the thioamidates

The most characteristic features of the ^{1}H NMR spectra ($CDCl_3$) of the thioamidates **2a** and **2b** are the low-field one-proton signals at δ 8.85 and 9.3 ppm, respectively, of the C(1)-protons which are diagnostic for the isoquinolinio(thioamidate) structure. These signals are considerably shifted upfield as compared with the corresponding signals of the related amidates **3a** and **3b** [6], which appear at 9.86 and 10.02 ppm [6], respectively.

There is no corresponding low-field signal in the ^{1}H NMR spectrum (measured in $CDCl_3$) of the thiopivalamidate **2c**, and the intensity of the low-field signal at δ 8.80 ppm in the spectrum of this compound measured in CD_3OD is about 0.65 H. Addition of TFA to the $CDCl_3$ solution of **2c** results in the appearance of a signal at δ 9.35 ppm (intensity about 0.8 H). These observations are rationalized by the assumption of an equilibrium between the thioamidate form **2c** and a cyclic form, probably **5**, which is practically completely shifted towards the cyclic form in $CDCl_3$ solution, while in the more polar solvent CD_3OD the ratio of the dipolar ionic (**2c**) and the non-ionic forms (**5**) is about 2 : 1. As TFA protonates the acyclic nitrogen atom of **2c**, the equilibrium is shifted towards **2c** · $H^{\oplus}$.* Structure **5** is substantiated by the presence of two one-proton doublets at δ 6.35 and 7.25 ppm (corresponding to 6-H and 5-H, respectively, of the cyclic form) in the $CDCl_3$ spectrum. Analogous changes could be expected if it were the dimeric form **6a**, which is in equilibrium with the thioamidate form **2c**. However, structure **6a** is less likely than structure **5** for the non-ionic form, since there is no indication of the presence even of traces of the related dimer **6b** in the ^{1}H NMR spectrum of the pivalamidate **3c** (measured in $CDCl_3$). The ready formation of **5**, while no analogous tricyclic tautomer is formed from the pivalamidate, may, on the other hand, be easily explained in terms of the well-known differences in the nucleophilicities of sulfur and oxygen.

No tricyclic tautomers are formed from the thioamidates **2a** and **2b**. This is readily explained by noting that, while the $+I$-effect of the *t*-butyl group tends to destabilize the thioamidate moiety of **2c**, the $-I$-effect of the 3,4-dimethoxyphenyl and the ethoxy groups in **2a** and **2b**, respectively, has the opposite effect.

* That the intensity of the δ 9.35 ppm signal is less than 1 H, probably reflects partial decomposition of **2c** $\rightleftarrows$ **5** *before* the addition of TFA.

Mass spectra

The mass spectra of all three thioamidates **2a—2c** exhibit molecular ions and $(M-H)^+$ ions of variable abundances, as had been observed earlier for the related *N*-isoquinolinioamidates [14, 15]. Interestingly, these two peaks are the most abundant in the spectrum of the (thermally) least stable compound **2c**. The structures **a** may be assigned to the $(M-H)^+$ ions by analogy [14, 16]. Elimination of RCN from the molecular ions of **2a—2c** furnishes the *m/z* 161 ion which may be formulated either as **b′** or as **b″**. (For the latter, *cf.* the formulation of the corresponding oxygen-containing ion in the spectra of some *N*-isoquinolinioamidates **3** in Ref. [14].) In the case of compound **2a** the same fragmentation of the molecular ion, but with retention of the positive charge on the complementary part, leads to the formation of the *m/z* 163 ion $(RC\overset{+\cdot}{N})$ containing a stable conjugated aromatic skeleton *(cf.* Ref. [14]), and subsequent consecutive elimination of $\cdot CH_3$ and CO from the latter to the formation of the *m/z* 148 and 120 ions. The insignificant abundance of the $[M-RCN]^{+\cdot}$ ions and the comparatively low intensity of $RCN^{+\cdot}$ in the case of *N*-isoquinoliniobenzamidate [14] as compared with that of **2a** indicate that the above-mentioned rearrangement (heteroatom migration) is favoured in the Type **2** sulfur compounds rather than in their Type **3** oxygen analogues.

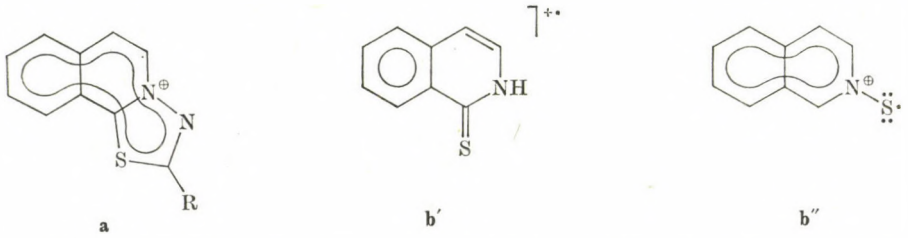

a **b′** **b″**

The base peak in all three spectra is the *m/z* 129 peak corresponding to the molecular ion of isoquinoline, the parent heterocycle. This ion could, in principle, be formed either directly from $M^{+\cdot}$ by cleavage of the N—N bond, or by elimination of sulfur from the *m/z* 161 ion. In the absence of appropriate metastables it was not possible to establish whether one or the other (or both) of these pathways operate. The molecular ions of the parent heterocycles (pyridine and isoquinoline, respectively) have also been observed in the mass spectra of compounds **1** and **3**. However, in the former case they are formed exclusively by consecutive loss of sulfur and a cyanoamine [4] (whereas no fragments due to elimination of sulfur were observed in the present case); and in the case of the compounds **3** the molecular ion of isoquinoline is formed either by cleavage of the N—N bond of the amidate or by consecutive loss of R· and ·NCO [14, 15]. Elimination of the group R (with retention of the positive charge either on the $M-R$ (187) or the R (57) fragment has been observed

among the compounds **2** only in the case of **2c**⇌**5**. The loss of $\cdot SC_2H_5$ from the molecular ion of **2b** to yield the *m/z* 171 fragment, rather than that of $\cdot OC_2H_5$ to furnish the *m/z* 187 fragment, is interesting because it indicates (partial and probably thermal) isomerization *(cf.* Ref's [17—19]) of the molecular ions prior to fragmentation to a large extent; this may be responsible for the almost complete lack of RCN elimination in this case. The comparative weakness of the $O-C_2H_5$ bond in the molecular ion of **2b** is shown also by the formation of the low-intensity *M*—Et *(m/z* 203) peak.

Elimination of HCN from *m/z* 129 gives rise to the formation of the *m/z* 102 fragments in all three spectra. Additional peaks are found at *m/z* 229, 210 and 134 in the spectrum of **2c**⇌**5**; the former two arise from elimination of $\cdot CH_3$ and H_2S, respectively, from $M^{+\cdot}$, while the *m/z* 134 peak is, as shown by the appropriate metastable, the result of HCN elimination from *m/z* 161. Interestingly, the *m/z* 134 peak is practically absent from the mass spectra of compounds **2a** and **2b**.

Photochemistry

Irradiation of compounds **2a**—**2c** in ethanolic solution with a high-pressure mercury immersion lamp through Pyrex under nitrogen furnished the following products:

from **2a**: 3,4-dimethoxybenzonitrile [20] (36%), 1(2*H*)-isoquinolinethione (**7a**) [21] (41%), and 3,4-dimethoxy(thiobenzamide) [22] (8%);

from **2b**: isoquinoline (55%), *O*-ethyl thiocarbamate [23] (41%), and [1,3,4]thiadiazolo[2,3-*a*]isoquinolin-4-ium-2-olate (**8a**) (9.3%);

from **2c**⇌**5** : 1(2*H*)-isoquinolinethione (**7a**) [21] (36%) and 1(2*H*)-isoquinolinone (**7b**) [24] (1.5%).

In all three cases considerable amounts of highly insoluble, high-melting products, probably polymers (whose structures were not elucidated) were also formed.

The structures of the photoproducts were derived from their mass and IR and/or NMR spectra, and those of the known compounds were substantiated by comparison with authentic samples. For the proof of structure of compound **8a** (whose mass spectrum is very similar to that of the known compound **8b** [25] and which may be rationalized by assuming structure **9** for the molecular ion, *cf.* Ref. [26]) see below.

The photochemistry of compounds **2a**—**2c** thus considerably differs from that of both their *N*-pyridinio(thiocarbamoylamide) (**1**) [4] and *N*-isoquinolinioamidate (**3**) counterparts [6, 9, 27]. Although the parent heterocycle and nitriles, corresponding to cleavage of the N—N bond of the thioamidate and elimination of S from the side chain, have been obtained both from compounds **1** and **2**, important differences exist between the two cases. With compounds **1**

photofragmentation starts with the elimination of sulfur (recovered as elemental sulfur) and not with rupture of the N—N bond which should lead *via* a thiocarbamoylnitrene $\left(R—NH—C\begin{matrix}S\\ \\ N:\end{matrix}\right)$ to hydrogen abstraction and/or insertion products of the latter. Such products have, however, as explicitly stated in Ref. [4], not been observed. In contrast, 3,4-dimethoxy(thiobenzamide) and *O*-ethyl thiocarbamate, isolated from the photolysis mixtures of compounds **2a** and **2b**, respectively, are obviously formed *via* the corresponding thiocarbamoyl nitrenes. On the other hand, formation of thioxo derivatives structurally related to 1(2*H*)-isoquinolinethione (**7a**) has not been observed on photolysis of Type **1** compounds.

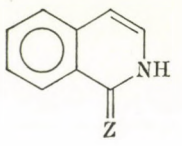

7a: Z = S
7b: Z = O

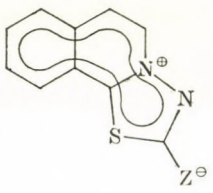

8a: Z = O
8b: Z = S

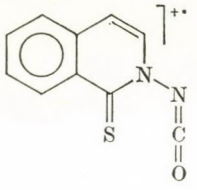

9

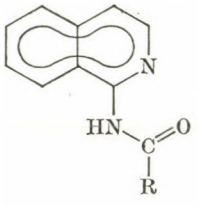

10

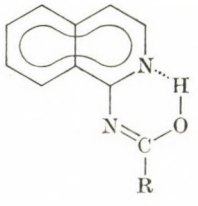

11

[**11a**: R = 3,4-$(MeO)_2C_6H_3$]

The mesoionic compound **8a**, too, is a novel type photoproduct, analogs of which have never been observed in the photolysis mixtures of Type **1** or **3** compounds. The photochemical formation of a mesoionic compound is in itself unique; the details of the process leading from **2b** to **8a** and involving (formal) loss of one molecule of ethane are not known.

Irradiation of *N*-isoquinolinioamidates has always been found to result in photoisomerisation to the corresponding *N*-(1-isoquinolyl)amides (**10**) [6, 9, 27] which, depending on the nature of R, may exist as the corresponding imidic acid tautomers **11** [15], and in no case in photofragmentation.* Compound **3a**

* Photofragmentation to yield the parent heterocycle has been observed in the case of other electron deficient heteroaromatic ammonioamidates [2].

has now been found to yield, in addition to the imidic acid **11a**, the fragmentation product 3,4-dimethoxybenzamide in 28% yield on photolysis.

The structure of compound **8a** was established by oxidation of the known **8b** [25] with potassium permanganate in acetone and by dipolar cycloaddition of carbonyl sulfide to the known [5] isoquinolinioamide. From the oxidation mixture of **8b** a second compound (containing one sulfur atom less than **8a**) was isolated in addition to **8a**. Its mass and IR spectra suggested the structure of 1-isoquinolyl thiocyanate (**12**) for this compound, and this structure was proven by comparison with an authentic sample obtained by allowing to react 1(2*H*)-isoquinolinethione (**7a**) with cyanogen bromide in the presence of alkali.

Experimental

Mass spectra were obtained at 70 eV with an AEI MS-902 using direct sample insertion, ^{1}H-NMR spectra at 60 MHz with Perkin—Elmer R 12 and Varian A60D spectrometers using, except where noted, TMS as the internal reference. The FT ^{1}H NMR spectrum of compound **8a** was obtained on a Varian XL spectrometer. UV spectra were recorded with Specord UV VIS (Carl Zeiss, Jena, GDR) and IR spectra with Spektromom 2000 (Hungarian Optical Works, Budapest) and Specord IR 75 (Carl Zeiss) spectrometers, respectively.

N-Isoquinolinio-3,4-dimethoxy(thiobenzamidate) (2a)

2*N* aqueous NaOH (1.8 ml) was added by drops to a mixture of 2-aminoisoquinolinium chloride (**4**) [6] (0.25 g; 1.35 mmoles), *S*-[3,4-dimethoxy(thiobenzoyl)]thioacetic acid [10] (0.4 g; 1.4 mmoles) and water (4 ml) to obtain 0.34 g (74%) of the title compound as an insoluble product, m.p. 134—137 °C which, according to TLC, proved homogeneous. Attempted recrystallization from benzene, chlorobenzene or butanol led to partial decomposition. An analytically pure sample was therefore obtained by stirring the product with 1000 parts of EtOH at room temperature and isolating the insoluble material (about 30%) which had m.p. 144—146 °C.

$C_{18}H_{16}N_2O_2S$ (324.4). Calcd. C 66.64; H 4.97; N 8.64. Found C 66.55; H 5.23; N 9.05%.

UV (EtOH): 224 (4.57), 260 (4.28), 289 (4.29). UV (EtOH—*N*/10 HCl, 1 : 1): 225 (4.54); 259 (4.28); 284 (4.29).

^{1}H NMR ($CDCl_3$): δ 3.9 s + 3.95 s, $(MeO)_2$; 6.85 d, J = 9 Hz, 1 H 5-H of dimethoxyphenyl group; 7.55—8.15 m, 8 H, 3-H — 8-H of isoquinoline ring, +2-H and 6-H of dimethoxyphenyl group; 8.85 s, 1 H, 1-H of isoquinoline ring. After addition of TFA: δ 3.95 s, 6 H, $(MeO)_2$; 6.95 d, J = 9 Hz, 1 H, 5-H of dimethoxyphenyl group; 7.6—7.85 m + 8.1—8.45 m, total intensity 8 H, 3-H — 8-H of isoquinoline ring, +2-H and 6-H of dimethoxyphenyl group; 9.55 s, 1 H, 1-H, isoquinoline ring. The spectra did not change on prolonged standing.

MS (150 °C), *m/z* (rel.int.): 324 (2.2, *M*); 323 (2.5, *M*—H); 164 (5.5); 163 (72, $[MeO]_2C_6H_3CN^{+\cdot}$); 161 (13, *M*-163); 149 (2.4); 148 (28, 163 $\overset{*}{-}$ Me); 130 (8.3); 129 (**100**, $C_9H_7N^{+\cdot}$); 128 (19); 120 (10, 148-CO); 117 (4); 103 (5.5); 102 (30, 129 $\overset{*}{-}$ HCN); 101 (4.5); 92 (9.4); 77 (17).

By concentrating in vacuum the ethanolic filtrate of the pure product, a further, less pure crop, 50%, m.p. 138—140 °C, was obtained.

N-Isoquinolinio[ethoxy(thioformamidate)] (2b)

A solution of 2-aminoisoquinolinium chloride (**4**) [6] (1.8 g; 10 mmoles) in water (4 ml) and subsequently 2*N* aqueous NaOH (18 ml) were added to a solution of *O*-ethyl *S*-methyl dithiocarbonate [11] (2.0 g; 14.5 mmoles) in dry ethanol (25 ml). The mixture was stirred for 1 h at room temperature. Water (10 ml) was added and the mixture kept for 1 h in a refrigerator to yield 1.7 g (73.5%) of the title compound, m.p. 124—125 °C.

$C_{12}H_{12}N_2OS$ (232.3). Calcd. C 62.04; H 5.21; N 12.06; S 13.80. Found C 62.33; H 5.34; N 11.80; S 14.44%.

UV (EtOH): 226 (4.54); 248 (4.45); 277 (3.98); 327 (3.62); 354 (3.35), sh.

^{1}H NMR ($CDCl_3$): δ 1.4 t, 3 H, +4.55 qu, 2 H, $J = 7$ Hz, OEt; 7.7—8.05 m, 5 H, 4-H — 8-H; 8.4 dd, $J = 7.5$ and 1.5 Hz, 3-H; 9.3 d, $J = 1.5$ Hz, 1 H, 1-H.

MS (110 °C), *m/z* (rel.int.): 233 (1.7); 232 (8.9, *M*); 231 (2.4, *M*—H); 203 (1.1, *M*—Et); 171 (7.8, *M*—SEt); 161 (1.2, *M*—EtOCN); 160 (1.0); 130 (11); 129 (*100*, $C_9H_7N^{+\cdot}$); 128 (19); 103 (6); 102 (22, 129 ± HCN); 101 (5); 64 (8.5); 51 (8).

N-Isoquinolinio(thiopivalamidate) (2c)

The mixture of an ethanolic (40 ml) solution of methyl dithiopivaloate [12] (1.7 g; 10 mmoles) and an aqueous (5 ml) solution of 2-aminoisoquinolinium chloride (**4**) [6] (1.6 g; 9 mmoles) was treated with 2*N* aqueous NaOH (14 ml), allowed to stand for 1 h at room temperature and evaporated to dryness in vacuum. The residue was taken up in water to obtain 1.9 g (86%) of the yellow crystals of the title compound, m.p. 78—81 °C. The crude product was dissolved in 9 ml of hot EtOH to yield 0.68 g (36% recovery) of recrystallized material, m.p. 83—85 °C, which, according to its ^{1}H NMR spectrum was less pure than the crude product.

$C_{14}H_{16}N_2S$ (244.36). Calcd. N 11.47; S 13.12. Found N 11.53; S 12.72%.

UV (EtOH): 221 (4.46); 259 (4.05); 285 (3.89); 325 (3.62), sh; 354 (4.42), sh.

^{1}H NMR ($CDCl_3$; *freshly* prepared solution of *crude* product): δ 1.37 s, 9 H, *t*—Bu; 6.35 d + 7.25 d, 1 H, each, $J = 8$ Hz, 6-H and 5-H of the cyclic form **5**; 7.35—7.7 m, 5 H 7-H — 10b-H of **5**. Decomposition on standing is indicated by the appearance of signals at δ 1.43 and 1.54 in addition to the main *t*—Bu signal at 1.37 ppm. The spectrum of the *recrystallized* product is essentially identical, but weak signals at δ 1.4 (as a shoulder on the main *t*—Bu signal at 1.37 ppm) and 1.5 were already present in the spectrum of the fresh solution.

^{1}H NMR, *crude* product ($CDCl_3$ + TFA, added after about 1/2 h): δ 1.4 weak s + 1.5 s + + 1.65 weak s, total intensity 9 H, *t*—Bu; 7.95—8.5 m, about 6.2 H, 3-H — 8-H of protonated form, + olefinic and aromatic H's of decomposition products; 9.35 broad s, about 0.8 H, 1-H of protonated form. The spectrum remained essentially unchanged after the solution was allowed to stand for 4 days at room temperature.

^{1}H NMR (*recrystallized* product, *freshly* prepared solution; CD_3OD, CHD_2OD = 3.35): δ 1.40 weak s + 1.46 s + 1.71 weak s, total 9 H, *t*—Bu; 7.0—8.5 m, about 6.35 H, 3-H — 8-H of thioamidate form, + olefinic and aromatic H's of cyclic form and of decomposition products; 8.80 s, 0.65 H, 1-H of thioamidate form. The intensity of the latter signal slightly decreased after the solution had been kept for 24 h at room temperature in the dark.

The MS (130 °C) is time-dependent, indicating decomposition and/or isomerization in the mass spectrometer. Initial spectrum (130 °C), *m/z* (rel.int.): 246 (2.6); 245 (8.8); 244 (38, *M*); 243 (30, *M*—H); 229 (1.1, *M*—Me); 211 (1.5); 210 (9.4, *M*—H_2S); 203 (2.8); 188 (3.8); 187 (38, *M* — *t*=Bu); 162 (4.4); 161 (43, *M* — *t*=BuCN); 160 (11); 145 (14); 134 (9.0, 161 ± HCN); 131 (6.6); 130 (23); 129 (*100*, $C_9H_7N^{+\cdot}$); 128 (33); 118 (2.5); 117 (5.6); 116 (4.7); 102, (18, 129 ± HCN); 101 (9.4); 90 (7.5); 89 (11); 57 (36); 51 (11).

The filtrate of the recrystallized product was evaporated to dryness in vacuum and the residue was taken up in CH_2Cl_2 to obtain 0.3 g of a crystalline product, m.p. 223—227 °C, of unknown structure.

N-Isoquinolinio-3,4-dimethoxybenzamidate (3a)

2-Aminoisoquinolinium chloride (**4**) [6] (0.9 g; 5 mmoles) was heated with 3,4-dimethoxybenzoyl chloride (3.0 g; 15 mmoles) for 2 h at 105—110 °C. The mixture was allowed to cool, taken up in CH_2Cl_2 and shaken with dil. aqueous NaOH until the aqueous phase remained distinctly alkaline. Routine work-up of the CH_2Cl_2 solution and recrystallization from benzene furnished 0.76 g (49.5%) of the title compound, m.p. 132—134 °C.

$C_{18}H_{16}N_2O_3$ (308.3). Calcd. C 70.12; H 5.23; O 15.57. Found C 70.16; H 5.39; O 15.33%.

^{1}H NMR ($CDCl_3$): δ 3.95 s and 3.97 s, $(MeO)_2$; 6.9 d, $J = 8$ Hz, 1 H, 5-H of dimethoxyphenyl group; 7.7—8.15 m, total intensity 7 H, 4-H — 8-H of isoquinoline ring, +2-H and 6-H of dimethoxyphenyl group; 8.45 dd, $J = 7$ and 1.5 Hz, 1 H, 3-H of isoquinoline ring; 9.86 s, 1 H, 1-H of isoquinoline ring.

IR (KBr): *no* amide I band; hydrochloride: 1700 cm^{-1}.

N-Isoquinoliniopivalamidate (3c)

This compound was obtained as described in Ref. [9].

^{1}H NMR ($CDCl_3$): δ 1.32 s, 9 H, *t*—Bu; 7.7—8.1 m, 5 H, 4-H — 8-H; 8.26 dd, J = 7 and 1.5 Hz, 1 H, 3-H; 9.65 s, 1 H, 1-H.

Irradiation of compounds 2a, 2b, 2c ⇌ 5 and 3a

Nitrogen-flushed ethanolic solutions of the title compounds were irradiated with a high-pressure mercury immersion lamp (HPK-125, Philips) trough Pyrex with continuous stirring and ice-cooling until, according to TLC, the starting compounds were completely used up. The solvent was evaporated in vacuum and the residues were worked up by conventional procedures.

(a) Compound **2a** (1.0 g; 3.1 mmoles) was irradiated for 8 h in ethanol (300 ml). The dry residue was taken up in CH_2Cl_2, the insoluble material (**A**; 0.03 g) filtered off and the filtrate worked up by preparative TLC (Kieselgel $PF_{254+366}$, Merck; benzene-$CHCl_3$-EtOH, 8 : 1 : 1) to obtain, in descending order of their R_f values, 0.18 g (36%) of 3,4-dimethoxybenzonitrile, m.p. 66—67 °C (MeOH), *lit.* [20] m.p. 67—68 °C, IR (KBr): 2230 cm^{-1}; 0.2 g (41%) of 1(2*H*)-isoquinolinethione (**7a**), m.p. 168—169 °C (EtOH), *lit.* [21] m.p. 171 °C; 0.05 g (8%) of 3,4-dimethoxy(thiobenzamide), m.p. 187—189 °C (dec,; aqueous EtOH), *lit.* [22] m.p. 193—194 dec.); and another 0.17 g of fraction **A**, probably polymeric material whose structure was not elucidated.

Mass spectra, *m/z* (rel. intensity). **3,4-Dimethoxybenzonitrile** (150 °C): 164 (11); 163 (*100*, *M*); 148 (22, *M* ± Me); 120 (11, 148 ± CO); 102 (5.4); 92 (8.8); 17 (13); **(2*H*)-isoquinolinethione** (150 °C): 163 (5.4); 162 (10); 161 (*100*, *M*); 134 (11, *M* — HCN); 128 (35, *M* — SH); 101 (5, *M* — HCN — SH); 80.5 (8, M^{++}); 67 (9, 134^{++}): **3,4-dimethoxy(thiobenzamide)** (180 °C): 199 (6.1); 198 (11); 197 (**100**, *M*); 182 (6); 181 (7); 264 (68, *M* — SH); 163 (13); 148 (8).

(b) Compound **2b** (0.6 g; 2.6 mmoles) was irradiated for 14 h in ethanol (250 ml). Steam distillation of the dry residue furnished 0.17 g (55%) of isoquinoline (isolated by extraction with ether from the distillate after saturation with NaCl). The non-volatile material was extracted with $CHCl_3$, and the combined organic phases were dried and evaporated to dryness. The residue was triturated with methanol to obtain 0.1 g of a highly insoluble, high-melting and probably polymeric substance which was discarded. The methanolic filtrate of this product was worked up by preparative TLC (Kieselgel $PF_{254+366}$; benzene-$CHCl_3$-EtOH, 1 : 1 : 1) to obtain 0.11 g (41%) of *O*-ethyl thiocarbamate,* identified by comparison (IR, NMR, TLC) with an authentic sample [23], and 0.05 g (9.3%) of compound **8a**, m.p. 234—235 °C, identified by comparison with an authentic sample obtained as described below.

NMR ($CDCl_3$): δ 1.23 t, 3 H, +4.52 qu, 2 H, J = 7.1 Hz, OEt; 6.4 very bs, 2 H, NH_2.

(c) Compound **2c** ⇌ **5** (1.2 g; 5 mmoles) was irradiated for 1.5 h in ethanol (1000 ml). The dry residue was worked up as described under *(a)* to obtain, in addition to a considerable amount of a high-melting, highly insoluble polymeric material, 0.28 g (36%) of 1(2*H*)-isoquinolinethione (**7a**), identical (m.p., IR, TLC) with an authentic sample [21], and 0.01 g (15%) of 1(2*H*)-isoquinolinone (**7b**), m.p. 201—202 °C (MeOH), *lit.* [24] m.p. 207—208 °C.

1(2*H*)-Isoquinolinone. Mass spectrum (120 °C), *m/z* (rel.int.): 146 (8.2); 145 (*100*, *M*); 131 (1.5); 118 (25, *M*—HCN); 117 (8.1); 90 (20, $C_7H_6^{+\cdot}$); 89 (40%); 58.5 (8.4; 117^{++}).

(d) Compound **3a** (0.61 g; 2 mmoles) was irradiated for 6 h in ethanol (500 ml). The dry residue was recrystallized from methanol to obtain 0.35 g (57%) of 1-[(α-hydroxy-3,4-dimethoxybenzylidene)amino]isoquinoline (**11a**), m.p. 158—160 °C.

$C_{18}H_{16}N_2O_3$ (308.3). Calcd. C 70.12; H 5.23; N 9.04. Found C 69.68; H 5.63; N 9.01%.

IR (KBr): *no* amide I band.

MS (140 °C), *m/z* (rel. int.): 310 (2.5); 309 (24); 309 (*100*, *M*); 307 (60, *M* — H); 293 (6); 292 (12, *M* — NH_2); 280 (15, *M* — CO); 279 (16, *M* — HCO); 171 (45, *M* — dimethoxyphenyl); 166 (6.2); 165 (50, dimethoxybenzoyl$^+$), 128 (25, 171 — HNCO).

The methanolic filtrate of compound **11a** was worked up by preparative TLC (Kieselgel $PF_{254+366}$; benzene-chloroform-ethyl acetate, 1 : 1 : 1) to obtain 1.0 g (28.5%) of 3,4-dimethoxybenzamide, m.p. 162—163 °C (MeOH), *lit.* m.p. 164 °C [28].

IR (KBr): 3370, 3290 sh, 3175, 3080 sh, 1650 cm^{-1}, identical with the spectrum of an authentic sample.

* Distillation even in vacuum causes considerable decomposition of this compound.

Hydrolysis of compound 11a:

The above product (0.44 g; 1.45 mmole) was refluxed for 4 h with 20% aqueous HCl and the mixture evaporated to dryness. The residue was triturated with 2*N* NaOH to obtain an insoluble product (0.18 g; 87%) which proved identical (IR) with an authentic sample of 1-aminoisoquinoline. The alkaline filtrate of this product was acidified to yield 0.16 g (61%) of 3,4-dimethoxybenzoic acid.

[1,3,4] Thiadiazolo[2,3-*a*]isoquinolin-4-ium-2-thiolate (8b)

A mixture of the dimer (**6c**) [5] (1.0 g; 3.5 mmoles) of isoquinolinioamide, ethanol (5 ml) and CS_2 (1 ml) was stirred for 2 h, and allowed to stand overnight to yield 0.65 g (46%) of the title compound, m.p. 265—267 °C (AcOH), *lit.* [13] m.p. 263 °C (dec.), which was washed with AcOH and EtOH; according to TLC, it proved homogeneous before recrystallization.

The UV spectrum was identical with that reported in literature [13, 25].

MS (150 °C) *m/z* (rel.int.): 220 (6.3); 219 (8.4); 218 (69, *M*); 186 (1.8 *M*—S); 174 (1.7, *M*—CS); 161 (3); 160 (16, *M* ± NCS); 159 (6); 154 (11, *M*—2 S); 134 (3); 133 (11, 160 ± HCN); 129 (15); 128 (*100*, $C_9H_6N^+$); 127 (3); 116 (12, 160 ± CS); 109 (M^{++}); 102 (7); 101 (12, 128 ± HCN); 89 (21); 75 (8).

[1,3,4]Thiadiazolo[2,3-*a*]isoquinolin-4-ium-2-olate (8a)

(a) Finely pulverized $KMnO_4$ was added in small portions to a refluxing suspension of compound **8b** (0.5 g, 2.5 mmoles) in a mixture of acetone (50 ml) and water (1 ml) until the violet colour was persistent. The MnO_2 was filtered off, washed with acetone, and the combined filtrates were evaporated to dryness. The residue was taken up in chloroform. The insoluble impurities were filtered off, and the filtrate was evaporated to dryness to obtain 0.25 g of a mixture which was worked up by preparative TLC (Kieselgel $PF_{254+366}$; benzene-$CHCl_3$-EtOAc, 1 : 1 : 1). The following two compounds were obtained in descending order of their R_f values:

1-isoquinolyl thiocyanate, **12**, 0.1 g (21%), identical (m.p., IR, R_f) with an authentic sample, obtained as described below;

compound **8a**, 0.07 g (15%), m.p. 234—235 °C (methanol).

IR (KBr): *no* bands in the cumulative double bond region.

^{1}H NMR ($CDCl_3$): δ 7.65 d, J = 7.7 Hz, 1 H, 6-H; 7.75—8.1 m, 4 H, [7-H — 10-H; 8.4 d, J = 7.7 Hz, 1 H, 5-H.

MS (150 °C), *m/z* (rel.int.): 204 (5.2); 203 (12); 202 (*100*, *M*); 174 (1.4, *M*—CO); 161 (1.1); 160 (12, *M*—NCO); 159 (2.4); 147 (2.2); 146 (18 ± N_2CO); 145 (10, 146 ± H); 142 (0.9); 133 (3, 160 ± HCN); 129 (4.2); 128 (31, $C_9H_9N^+$); 116 (160-CS); 102 (18, 146 ± CS and 128 ± ± C_2H_2); 101 (4.4, M^{++}); 89 (6.6); 75 (4); 51 (4).

(b) The dimer (**6c**) [5] (0.25 g; 0.87 mmole) of isoquinolinioamide was stirred at room temperature for 3 days with a solution of carbonyl sulfide [29] (1.7 g; 28 mmoles) in ethanol (60 ml). The mixture was evaporated to dryness, the residue taken up in $CHCl_3$ and worked up by preparative TLC Kieselgel $PF_{254+366}$; EtOAc—EtOH, 4 : 1) to obtain 0.15 g (46%) of compound **8a**, identical (m.p., IR, TLC) with the product prepared according to *(a)*.

1-Isoquinolyl thiocyanate (12)

A solution of KCN (0.3 g; 4.6 mmoles) in water (1.7 ml) was added by drops, with stirring and ice-cooling, to Br_2 (0.2 ml; 3.9 mmoles) covered by water (1 ml), until the colour of bromine just disappeared. The resulting aqueous suspension of BrCN was treated at 0 °C with continuous stirring with the solutions of 1(2*H*)-isoquinolinethione (**7a**) [21] (0.32 g; 2 mmoles) in acetone (5 ml) and NaOH (0.08 g; 2 mmoles) in water (5 ml). The mixture was kept for 1 h at 0 °C and allowed to stand overnight at room temperature to obtain 0.18 g (50%) of the title compound, m.p. 65—66 °C.

$C_{10}H_6N_2S$ (186.2). Calcd. N 15.05. Found N 14.60, 15.15%.

IR (KBr): 2165 cm^{-1}.

MS (130 °C), *m/z* (rel.int.): 188 (4); 187 (8); 186 (68, *M*); 160 (1.8, *M*—CN); 159 (1.5, *M*—HCN); 129 (10); 128 (*100*, *M*—SCN); 101 (12, 128 ± HCN); 93 (4, M^{++}); 89 (3.5); 77 (5.5); 75 (7.0).

Attempted recrystallization of compound **12** from benzene resulted in the formation of a new compound, m.p. 126—130 °C, which, according to its MS, has a mol. wt. of 288 and contains two isoquinoline rings and one S atom.

*

The authors are grateful to Mrs. H. MEDZIHRADSZKY-SCHWEIGER and Mrs. I. BALOGH-BATTA and staffs for the microanalyses, to Dr. L. RADICS for the FT ^{1}H NMR spectrum of compound **8a**, to Dr. P. KOLONITS and Mr. I. KÖVESDI for the other ^{1}H NMR spectra and to Dr. F. RUFF for the IR and UV spectra.

REFERENCES

[1] TIMPE, H. J.: in Adv. Heterocyclic Chem., Vol. **17** (Edited by A. R. KATRITZKY and A. J. BOULTON), p. 213. Academic Press, New York, San Francisco, London 1974; MCKILLIP, W. J., SEDOR, E. A., CULBERTSON, B. M., WAWZONEK, S.: Chem. Revs., **73,** 255 (1973)
[2] For a short rewiew, see FETTER, J., LEMPERT, K., BARTA-SZALAI, G., MOLLER, J., PÁRKÁNYI, L.: Acta Chim. (Budapest), **94,** 233 (1977)
[3] BEYER, H., LEVERENZ, K., SCHILLING, H.: Angew. Chem., **73,** 272 (1961)
[4] POTTS, K. T., DUGAS, R.: Chem. Commun. **1970,** 732
[5] KRISCHKE, R., GRASHEY, R., HUISGEN, R.: Liebigs Ann. Chem., **1977,** 498
[6] ÁGAI, B., LEMPERT, K.: Tetrahedron, **28,** 2069 (1972)
[7] ÁGAI, B., LEMPERT, K.: Acta Chim. (Budapest), **88,** 75 (1976)
[8] ÁGAI, B., LEMPERT, K.: Acta Chim. (Budapest), **86,** 203 (1975)
[9] BECHER, J., LOHSE, C.: Acta Chem. Scand., **26,** 4041 (1972)
[10] LEMPERT-SRÉTER, M., LEMPERT, K., BRUCK, P., TÓTH, G.: Acta Chim. (Budapest), **94,** 391 (1977)
[11] SOLOMON, F.: J. prakt. Chem., [2] **8,** 116 (1874)
[12] JENSEN, K. A., PEDERSEN, Ch.: Acta Chem. Scand., **15,** 1087 (1961)
[13] HUISGEN, R.: Private communication of September 21, 1978
[14] IKEDA, M., TSUJIMOTO, N., TAMURA, Y.: Org. Mass Spectrom., **5,** 61 (1971)
[15] MØLLER, J., BECHER, J., LOHSE, C., LEMPERT, K., ÁGAI, B.: Acta Chem. Scand., **27,** 3647 (1973)
[16] FETTER, J., LEMPERT, K., MØLLER, J.: Tetrahedron, **31,** 2559 (1975)
[17] SCHÖNBERG, A., VARGHA, L. v.: Ber., **63,** 178 (1930); SCHÖNBERG, A., VARGHA, L. v., PAUL, V.: Liebigs Ann. Chem., **483,** 107 (1930)
[18] KARJALA, S. A., MCELVAIN, S. M.: J. Am. Chem. Soc., **55,** 2966 (1933)
[19] SMITH, S. G.: J. Am. Chem. Soc., **83,** 4285 (1961)
[20] GARELLI, F.: Gazz. chim. ital., **20,** 700 (1890)
[21] ALBERT, A., BARLIN, G. B.: J. Chem. Soc., **1959,** 2384
[22] KORNFELD, E. C.: J. Org. Chem., **16,** 131 (1951)
[23] DEBUS, H.: Liebigs Ann. Chem., **75,** 128 (1850)
[24] ALBERT, A., PHILLIPS, J. N.: J. Chem. Soc., **1956,** 1303
[25] TALUKDAR, P. B., SENGUPTA, S. K., DATTA, A. K.: Indian J. Chem., Sect. B, **14B,** 176 (1976)
[26] OLLIS, W. D., RAMSDEN, Ch. A.: in Adv. Heterocyclic Chem., Vol. **19** (Edited by A. R. KATRIZKY and A. J. BOULTON), p. 88. Academic Press, New York, San Francisco, London, 1976, and references cited therein
[27] TAMURA, Y., TSUJIMOTO, N., ISHIBASHI, H., IKEDA, M.: Chem. Pharm. Bull., **19,** 1285 (1971)
[28] MEYER, H.: Monatsh., **22,** 429 (1901)
[29] KLASON, P.: J. prakt. Chem., [2] **36,** 69 (1887)

Magda LEMPERT-SRÉTER — H-1088 Budapest, Múzeum krt. 4/b.
Károly LEMPERT — H-1521 Budapest, Gellért tér 4.
József TAMÁS, Károly VÉKEY — H-1025 Budapest, Pusztaszeri út 59—67.

Acta Chimica Academiae Scientiarum Hungaricae, Tomus 103 (3), pp. 271—279 (1980)

RING TRANSFORMATION OF CHROMONES INTO 4-HYDROXYCOUMARINS

V. SZABÓ, J. BORDA and E. THEISZ

(Institute of Applied Chemistry, Kossuth Lajos University, Debrecen, Hungary)

Received March 2, 1979
Accepted for publication April 26, 1979

The reaction of chromone and its C-3 substituted analogues with hydroxylamine in aqueous solution resulted in isoxazoles **II** *via* a monooxime intermediate (**VI**). Under alkaline conditions both **VI** and **II** transformed into the nitrile **III** which is in a ring–chain tautomeric equilibrium with coumarin imine **IV**, dependent on the substitution conditions and hydroxyl ion concentration. Compounds **IV** could be converted into 4-hydroxycoumarins (**V**) which reaction offers a generalizable ring transformation of C-2 unsubstituted chromones into 4-hydroxycoumarin derivatives.

In previous papers [1—3] we have described that hydroxylamine attacks chromone (**Ia**) and isoflavone (**Ic**) at position C-2. As a result of this attack, the γ-pyrone ring is cleaved and a phenyl (**IIa**) or diphenylisoxazole derivative (**IIc**) is formed *via* a monooxime intermediate (**VIa, c**). The structures of the prepared isoxazole derivatives, unsubstituted at C-3, were proved by cleavage of the isoxazole ring under alkaline conditions to obtaine 4-hydroxycoumarin derivatives. This latter reaction unequivocally supports both the structure of the isoxazole derivative and the place of attack of hydroxylamine. This reaction is generalizable for certain chromone derivatives as it has been pointed out in our previous paper [4]. The present work deals with the details and conditions of this ring transformation reaction.

Results and Discussion

It has been reported that both chromone [3] and isoflavone [1, 2] transform into isoxazole **II** on treatment with hydroxylamine in aqueous ethanol of different pH, *via* an aldoxime intermediate **VI**, and the two compounds showed different reactivities. The difference appeared both in the rate of the nucleophilic substitution (the rate of conversion of **Ia** was lower than that of **Ic**) and also in the direction of the reaction. Namely, in alkaline solution (pH = 8—12) chromone (**Ia**) transformed into a mixture of the aldoxime **VIa** and the dioxime **VIIa**, whereas from isoflavone (**Ic**) the isoxazole derivative **IIc** was obtained in a good yield. Compound **VIa** could be readily separated from **VIIa** and cyclized into **IIa** under mild acidic conditions.

Table I

The conditions of reactions **I** → **II** *and the physical data of the 4.5-diphenylisoxazoles formed*

Compound	Reaction time, h	Yield, %	M.p., °C	Analysis	UV-spectrum		IR-spectrum (cm^{-1})			NMR-spectrum (ppm*)		
				N%	λ_{max} (nm)	lg ε	OH	C=N	N—O	C_5—H	OH	OCH_3
IIc	3.0	92.8	163—164	C: 5.90 F: 5.84	228 263	4.28 4.03	3420	1620	970	9.05	10.10	—
d	4.0	82.0	155—157	C: 5.24 F: 5.20	236 279	4.16 3.96	3170	1600	975	8.60	9.75	3.65
e	8.0	75.1	165—166	C: 5.24 F: 5.35	233 276	4.17 3.90	3150	1615	975	8.67	9.70	3.80
f	0.5	87.2	331—332	C: 9.39 F: 9.20	275	4.04	3150	1620	980	8.80	9.62	—

C = calculated
F = found
* The NMR spectra were recorded in DMSO-d_6 solutions

formaldoxime **VIb** to give the corresponding nitrile **IIIb**, which then undergoes immediate ring closure.

Naturally, the isoxazole ring of **IIb** can also be cleaved it the alkali concentration is as high as that used for the splitting of **Ib**, yet the ring cleavage in this case is somewhat slower. It was surprising that **IIIb** could not be detected as an intermediate even in 4*M* sodium hydroxide solution. Acidification of the reaction mixture gave **IVb** in a good yield.

The dehydration process **VIa** → **IIIa** was also observed with chromone (**Ia**), nevertheless the route **I** → **VI** → **III** → **IV** is not proposed for the synthesis of **IVa**, because compound **IIIa** is stable under alkaline conditions, it also reacts with hydroxylamine, and the formation of a hitherto unidentified by-product makes the separation difficult.

The isoflavones **Ic—f** gave the corresponding isoxazoles (**IIc—f**), *via* the monooxime intermediates, in excellent yields even under alkaline conditions. The isoxazoles could be converted into the nitriles (**IIIc—f**) in reasonable yields in 1.0—1.25*M* sodium hydroxide solutions (Table II). These nitriles are less stable in the crystalline state than **IIIa** and cyclize to give the coumarin imines **IVc—f** on the effect of light or moderate heating. The ring closure was found to be very rapid under both acidic or mild alkaline conditions.

Acid hydrolysis of compounds **IVa—f** resulted in 4-hydroxycoumarins **Va—f** [6, 8—10].

4-Hydroxycoumarin imines are stable neither in acidic nor in alkaline conditions. With the exception of **IVb**, all the imines undergo ring cleavage to yield the corresponding β-ketonitriles (**III**) in 1—4*M* sodium hydroxide solution, at a rate dependent both on the alkali concentration and the substitution

Table II

Physical characteristics of 2-hydroxy-α-nitrilodeoxybenzoins

Compound	Yield*, %	M.p., °C	Analysis	UV-spectrum		IR-spectrum (cm^{-1})		
			N%	λ_{max} (nm)	lg ε	C=O	C≡N	OH
IIIc	78.0	97—99	C: 5.90 F: 5.84	285	4.00	1640	2250	3150**
d	66.5	98—100	C: 5.24 F: 5.13	282	3.97	1645	2260	3150**
e**	55	81—83	C: 5.94 F: 5.19	286	3.98	1625	2240	3150
f	76.5	105—107	C: 9.39 F: 9.19	288	4.06	1620	2230	3260 3580

C = calculated
F = found

* The yields are calculated for the nitriles prepared by method (*a*).

** NMR ($CDCl_3$, δ ppm): **IIIc:** 11.75 (s, 1 H, OH broad, disappearing on treatment with D_2O)
IIId: 11.40 (s, 1 H, OH broad, disappearing on treatment with D_2O)

*** The isolation of compound **IIIe** was difficult

pattern. At the same time, **III** is converted into **IV** at a rate increasing with the decrease of the alkali concentration. This observation supports our earlier experience [2] that **III** and **IV** are related as ring-chain tautomers, their ratio being dependent, apart from the substituent effect, on the hydroxyl ion concentration.

As the simplest kinetic parameters, the values of the decomposition times of the investigated isoxazoles, determined under analogous conditions, support the mechanism proposed in our earlier papers [1*, 2] (Table III).

Table III

Reaction times of the conversion **II** → **III** → **IV**

Compound	IIa	b	c	d	e	f
Reaction time, h	>36	>36	3	5	4.5	1

The reactions were made with a 0.66% solution of **II** in 0.75*M* aqueous ethanolic sodium hydroxide (ethanol 25%). The reactions were monitored by TLC, and the given reaction times mean the period necessary for the disappearence of the spot of the starting material.

Table IV

The conditions of the thermal reaction **II** → **IV** *and the physical data of the 4-hydroxycoumarin imines prepared*

Compound	Reaction		Yield, %	M.p., °C	*Lit.* M.p., °C	UV-spectrum		IR-spectrum, (cm^{-1})	
	temperature °C	time min.				λ_{max} (nm)	lg ε	C=N	NH
IVa	190	120	96.2	272—273	272—275 [6]	290	4.06	1640	3250 NH, OH, broad
c	160	15	94.1	225—226	219—220 [8]	262 302	3.88 4.06	1645	3380
d	180	15	88.0	224—225	214—215.5 [9]	257 307	3.97 3.95	1630	3370
e	190	15	85.4	240—241	232—232.5 [8]	253 305	4.20 4.14	1635	3370
f	240	10	90.2	329—330	—	248 306	4.17 4.14	1625	3360

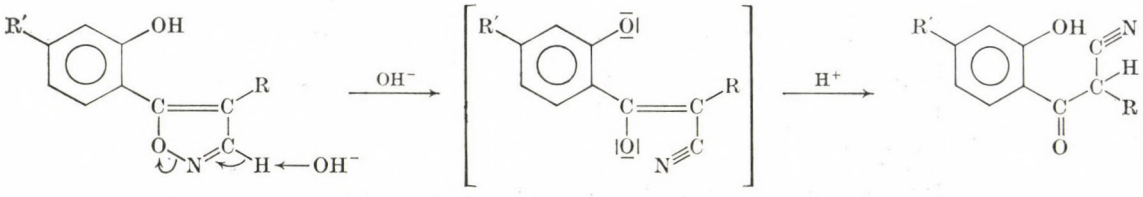

II *Scheme 2* **III**

* Simultaneously with our communication, Italian authors [5] also suggested this reaction mechanism

Diphenylisoxazoles are more sensitive to bases than phenylisoxazoles. Furthermore, electron-donor substituents and electron-withdrawing substituents (in both aromatic rings) lower or accelerate, respectively, the rate of the reaction. Thus, the mechanism of nitrile formation probably includes initial deprotonation followed by rupture of the N—O bond of the resulting intermediary anion.

The investigated isoxazoles transform into coumarin imines *via* the corresponding β-ketonitriles on the effect of heat. Under controlled conditions, good yields have been obtained. The greater reactivity of diphenylisoxazoles is evident also in this reaction (Table IV).

Experimental

UV spectra were obtained in ethanol solutions with a UNICAM SP-800 instrument. IR spectra were recorded in KBr pellets with a Spektromom 2000 instrument. The NMR spectra were obtained with a Jeol MH-100 (100 MHz) spectrometer. The reactions were monitored on DC-Alurolle Kieselgel 254 F (Merck) layer using 9 : 1 benzene–ethanol as the solvent system. M.p.'s are uncorrected.

2-Hydroxy-ω-formylacetophenone aldoxime (VIa)

To a solution of chromone (**Ia**) (0.438 g; 3.0 mmoles) in ethanol (6 ml) a solution of 0.84 g (12 mmoles) of hydroxylamine hydrochloride in Britton—Robinson buffer (pH $\sim$ 12) (6 ml) was added. The pH of the mixture was then adjusted with 2*M* sodium hydroxide solution to 12 and the mixture was kept at room temperature for 35 min. The colourless product which precipitated on acidification with acetic acid, was filtered off, washed with water and recrystallized from aqueous ethanol to obtain pure **VIa** (0.22 g; 40.9%), m.p. 126—127 °C. As a by-product the dioxime **VIIa** was isolated.

$C_9H_9NO_3$ (179.17). Calcd. N 7.82. Found N 7.67%.

UV, λ_{max} (nm): 243 (lg ε: 4.20); 299 (lg ε: 4.02).

IR, ν(cm^{-1}): 920 (N—O); 1640 (C=N, C=O); 2850 (CH_2); 2900—3400 (N—OH, OH).

NMR(DMSO-d_6; δ ppm): 3.92—3.98 (d, 2 H, CH_2); 6.68—7.60 (m, 4 H, aromatic); 8.30 (s, 1 H, C_3—H); 10.50 (s, 2 H, N—OH and OH, broad, disappearing on the addition of D_2O).

5-(2-Hydroxyphenyl)isoxazole (IIa)

A solution of **VIa** (1.79 g; 10 mmoles) in ethanol (30 ml) and *conc.* hydrochloric acid (1 ml) were boiled for 1—2 min. The mixture was cooled, diluted with water and evaporated until a colourless solid precipitated. It was washed with water until neutral and crystallized from aqueous ethanol to give **IIa** (1.50 g; 93.1%), m.p. 185—185.5 °C.

$C_9H_7NO_2$ (161.16). Calcd. N 8.69. Found N 8.68%.

UV, λ_{max} (nm): 261 (lg ε: 4.26); 272 (lg ε: 4.14); 306 (lg ε: 4.02).

IR, ν (cm^{-1}): 940 (N—O); 1615 (C=N); 3080 (CH); 3400 (OH, broad).

NMR (DMSO-d_6, δ ppm): 6.70—7.25 (m, 4 H, aromatic); 7.65—7.70 (d, 1 H, C_4—H); 8.35—8.37 (d, 1 H, C_2—H); 10.25 (s, 1 H, OH, disappearing on the addition of D_2O).

4-Methyl-5-(2-hydroxyphenyl)isoxazole (IIb)

A mixture of 3-methylchromone (**Ib**) (0.48 g; 3. O mmoles) and hydroxylamine hydrochloride (0.84 g; 12 mmoles) in 80% aqueous ethanol (15 ml) was boiled for 8 h. The conversion was found to be *cca.* 35%, and the product was separated from the unchanged **Ib** by preparative

layer chromatography, using benzene as the eluant. The product was eluted from the adsorbent to yield 0.17 g (32.2%) of **IIb**, m.p. 119—120 °C.

$C_{10}H_9NO_2$ (175.18). Calcd. N 8.00. Found N 7.83%.

UV, λ_{max}(nm): 252 (lg ε: 4.02); 293 (lg ε: 3.73).

IR, ν (cm^{-1}): 940 (N—O); 1600 (C=C); 1640 (C=N); 2920 (CH_3); 2950—3300 (CH, OH).

General procedure for the preparation of 4,5-diphenylisoxazoles (IIc—f)

A solution of hydroxylamine hydrochloride (2.0 g; 30 mmoles) and crystalline sodium acetate (3.92 g; 30 mmoles) in 80% aqueous ethanol was added to the isoflavone (**Ic—f**) (10 mmoles). The pH of the mixture was then adjusted to 8 with 2*M* sodium hydroxide solution and it was boiled until the spot of the starting **II** had disappeared on the thin-layer chromatogram. Concentration of the reaction mixture resulted in the precipitation of the product, which was filtered off, washed with water and crystallized from 80% aqueous ethanol. The conditions of the reactions and the physical parameters of the products are summarized in Table I.

2-Hydroxy-ω-nitriloacetophenone (IIIa)

(a) A solution of **IIa** (0.8 g; 5 mmoles) in a mixture of ethanol (10 ml) and 4 *M* sodium hydroxide (40 ml) was kept at room temperature for 1 day. It was then cooled to 0 °C and acidified with acetic acid. The colourless crystals which separated were quickly filtered off and washed with water until neutral to yield 0.45 g (56.2%) of **IIIa**, m.p. 113—114 °C.

From the mother liquor of **IIIa** 4-hydroxycoumarin imine (**IVa**) was isolated (0.19 g; 23.7%), m.p. 266—267 °C.

(b) Compound **IVa** (4.83 g; 30 mmoles) was dissolved in 4 *M* sodium hydroxide and the solution was kept at room temperature for 1 day. Working up the reaction mixture as described in method *(a)* gave 3.70 g (76.6%) of **IIIa**, m.p. 113—113.5 °C. *(Lit.* [6, 7] m.p. 108—110 °C.) The mixed m.p. of the samples prepared by methods *(a)* and *(b)* did not show depression.

UV, λ_{max} (nm): 253 (lg ε: 3.94); 327 (lg ε: 3.66).

IR, ν (cm^{-1}): 1620 (C=O); 2220 (C≡N); 3350 (OH).

NMR (DMSO-d_6, δ ppm): 4.60 (s, 2 H, CH_2); 6.70—7.60 (m, 4 H, aromatic); 10.83 (s, 1 H, OH, disappearing on treatment with D_2O).

General procedure for the preparation of 2-hydroxy-α-nitrilodeoxybenzoins (IIIc—f)

(a) From isoxazoles (**II → III**)

The 4,5-diphenylisoxazole derivative (**IIc—f**) was dissolved in a mixture of ethanol (10 ml) and 2.5*M* sodium hydroxide solution (10 ml). The homogeneous yellow (in the case of **IIf**: brown) solution was kept at room temperature for about 1 h and then worked up as described for the preparation of **IIIa** [method *(a)*].

The preponderant amount of the by-product (**IVc—f**) remained in the acidic aqueous phase; the product was purified by quick recrystallization from 80% aqueous ethanol.

(b) From coumarin imines (**IV → III**)

The 4-hydroxycoumarin imine (**IVc—f**; mmole) was dissolved in a 1 : 1 mixture of ethanol and 4*M* sodium hydroxide solution (6 ml) and the solution was kept at room temperature for 30—60 min. Work-up followed the procedure described above for the preparation of **IIIa** [method *(a)*].

The physical data of the prepared compounds (**IIIc—f**) are summarized in Table II.

3-Methyl-4-hydroxycoumarin imine (IVb)

Compound **Ib** (0.32 g; 2 mmoles) was dissolved in ethanol (6 ml) and treated with a solution of hydroxylamine hydrochloride (0.56 g; 8 mmoles) in pH = 12 Britton—Robinson buffer (6 ml). The pH of the mixture was adjusted to 12 with aqueous sodium hydroxide and it was kept at room temperature for 2 h. It was then acidified with hydrochloric acid to pH = 2 and a part of the ethanol was evaporated. The precipitated colourless product was filtered off, washed with water and crystallized from ethanol to give 0.15 g (46.8%) of **IVb**, m.p. 240—241 °C. *(Lit.* [6] m.p. 238—241 °C.)

UV, λ_{max} (nm): 307 (lg ε: 4.07).

IR, ν (cm^{-1}): 1600 (C=C); 1640 (C=N); 2920 (CH_3); 3080 (CH); 3240 (OH, NH, broad).

Preparation of 4-hydroxycoumarin imines (IVa, c—f) from the corresponding isoxazoles in a thermal reaction (II → IV)

1 Millimole of the 5-phenyl-(**IIa**) or 4,5-diphenylisoxazole (**IIc—f**) derivative was maintained in a closed capillary tube at a temperature higher than the m.p. for 10—60 min. After cooling, the product was crystallized from ethanol.

The conditions of the reactions and the physical data of the products are summarized in Table IV.

Preparation of 3-(*p*-nitrophenyl)-4,7-dihydroxycoumarin (Vf) from the corresponding imine (IVf)

1 Millimole of the imine **IVf** was dissolved in 2*M* hydrochloric acid (5 ml) and the solution was refluxed for 1 h. The precipitated yellow substance was filtered off and washed with water until neutral to obtain pure **Vf** (0.26 g; 86.9%), m.p. 314—315 °C.

$C_{15}H_9NO_6$ (299.24). Calcd. N 4.68. Found N 4.60%.

UV, λ_{max}(nm): 247 (lg ε: 4.23); 307 (lg ε: 4.17).

IR, ν (cm^{-1}): 1670 (C=O); 3250 (OH).

REFERENCES

[1] SZABÓ, V., BORDA, J., LOSONCZI, L.: Magyar Kém. Folyóirat, **83,** 278 (1977)
[2] SZABÓ, V., BORDA, J., LOSONCZI, L.: Acta Chim. Acad. Sci. Hung., **97,** 69 (1978)
[3] SZABÓ, V., BORDA, J., THEISZ, E.: Magyar Kém. Folyóirat, **84,** 134 (1978)
[4] SZABÓ, V., BORDA, J.: Acta Chim. Acad. Sci. Hung., **95,** 333 (1977)
[5] DE MUNNO, A., BERTINI, V., LUCCHESINI, F.: J. Chem. Soc. Perkin Trans. II., **1977,** 1121
[6] KAWASE, Y., SAKASHITA, K.: Bull. Chem. Soc. Japan, **35,** 1869 (1962)
[7] CECCHI, S., VETTORI, L. P.: Gazz. Chim. Ital., **96,** 874 (1966)
[8] KAWASE, Y.: Bull. Chem. Soc. Japan, **31,** 440 (1958)
[9] KAWASE, Y.: Bull. Chem. Soc. Japan, **32,** 9 (1959)
[10] MENTZER, C., VERCIER, P.: Monatsch., **88,** 264 (1957)

Vince SZABÓ
Jenő BORDA
Edit THEISZ
H-4010 Debrecen 10.

Acta Chimica Academiae Scientiarum Hungaricae, Tomus 103 (3), pp. 281—287 (1980)

ON FINITE AMPLITUDE WAVES IN A CHEMICALLY REACTING GAS MIXTURE

V. D. SHARMA and RADHESHYAM

(Applied Mathematics Section Institute of Technology Banaras Hindu University, Varanasi-5, India)

Received March 6, 1979
Accepted for publication May 11, 1979

The propagation of a finite amplitude gas dynamic disturbance headed by a wave front of an arbitrary shape through a chemically reacting gas mixture is studied. The influence of the thermodynamic properties on the wave propagation when the medium ahead of the wave is in a state of chemical equilibrium or disequilibrium is discussed. The effects of the wave front curvature on the growth and decay behaviour of these waves are also investigated.

1. Introduction

CLARKE [1] analysed the one-dimensional unsteady motion of a reacting gas in the presence of plane waves only. Since CLARKE [1] considered only plane waves, he did not determine the effects of wave front curvature on the growth and decay properties of the waves. This paper, which presents in a generalized form the results of [1], deals with the three-dimensional unsteady motion of a reacting gas mixture in the presence of a finite amplitude gas dynamic disturbance headed by a wave front of an arbitrary shape. The thermodynamic properties of the medium are assumed to be the same as was the case of [1].

The basic equations governing the unsteady motion of a reacting gas mixture, neglecting the various transport effects, are [1]

$$\frac{\partial \varrho}{\partial t} + u_i \varrho_{,i} + \varrho u_{i,i} = 0, \tag{1}$$

$$\varrho \frac{\partial u_i}{\partial t} + \varrho u_j u_{i,j} + p_{,i} = 0 \tag{2}$$

$$\frac{\partial p}{\partial t} + u_i p_{,i} + \varrho a_f^2 u_{i,i} = \varrho(\gamma - 1) Q W n \omega, \tag{3}$$

$$\frac{\partial c}{\partial t} + u_i c_{,i} = -W n \omega, \tag{4}$$

where u_i are the gas velocity components, p is the pressure, ϱ is the density, c is the mass fraction of the reactant species X, which takes part in the simple

reversible reaction $n\ \mathrm{X} \rightleftharpoons \mathrm{Y}$ (Y is the product species which can dissociate to produce n molecules of X), W is the molecular weight of X, γ is the frozen specific heat ratio, a_f, given by $a_f^2 = \gamma p/\varrho$ is the frozen sound velocity, Q is the energy of formation per unit mass of X, and ω is the reaction rate given by

$$\omega = \tau^{-1}\{c^n - (1 - c)\,\delta\}$$

where the quantities τ and δ are, respectively, the forward reaction time and the equilibrium constant given by

$$\tau^{-1} = F \exp(-E_x \varrho/p)$$

and

$$\delta = z \exp(-nQ\varrho/p)$$

where E_x is the activation energy, and F and z are constants which depend on the physical properties of the gas only. In Eqs (1—4), the summation convention on repeated indices is employed, and a comma followed by an index denotes partial differentiation with respect to a space variable. The range of the indices i, j is taken to be 1, 2, 3.

2. Wave as a singular surface

Let $f(x_i, t) = 0$ or, for brevity $\Sigma(t)$, denote the weak discontinuity surface. Let us denote by $n_i = \dfrac{f_{,i}}{|\mathrm{grad}\ f|}$ the components of the unit normal to $\Sigma(t)$ and by $G_1 = -\dfrac{\partial f/\partial t}{|\mathrm{grad}\ f|}$ the normal speed of propagation to $\Sigma(t)$. Here we shall restrict our attention to singular surfaces $\Sigma(t)$ across which the flow variables u_i, p, ϱ and c are essentially continuous but discontinuities in their derivatives are permitted. We infer that the quantities a_f and ω will behave similarity and that they will have subscript "0" values at the wave front. A subscript "0" indicates a value in the medium just ahead of the wave front. The unperturbed field ahead of the wave, whose behaviour is to be investigated, is assumed to be spatially uniform, and, therefore, Eqs (1)—(4) yield

$$\varrho_0 = \text{constant},\quad u_0 = 0,\quad \left(\frac{\partial p}{\partial t}\right)_0 = \varrho_0(\gamma - 1)\,QWn\omega_0 \text{ and } \left(\frac{\partial c}{\partial t}\right)_0 = -Wn\omega_0 \qquad (5,\ 6,\ 7,\ 8)$$

The reaction rate ω_0 will be zero if the chemical time τ becomes infinite or, more practically, of the state ahead of the wave is one of chemical equilibrium.

For the present case, the geometrical and kinematic conditions of first and second order deduced by THOMAS [2] reduce to

$$[Z_{,i}] = B\,n_i; \quad \left[\frac{\partial Z}{\partial t}\right] = -GB \tag{9}$$

$$\left.\begin{aligned} [Z_{,ij}] &= \bar{B}\,n_i n_j + g^{\alpha\beta}\,B_{,\alpha}(n_i\,x_{j,\beta} + n_j\,x_{i,\beta}) - Bg^{\alpha\beta}\,g^{\sigma\delta}\,b_{\alpha\sigma}\,x_{i,\beta}\,x_{j,\delta} \\ \left[\frac{\partial^2 Z}{\partial x_i\,\partial t}\right] &= \left(-G\bar{B} + \frac{\delta B}{\delta t}\right) n_i - Gg^{\alpha\beta}\,B_{,\alpha}\,x_{i,\beta} \end{aligned}\right\} \tag{10}$$

where the quantity Z may represent any of the flow variables u_i, p, ϱ and c. The square brackets stand for the value of the quantity enclosed immediately behind the wave surface minus its value just ahead of the wave surface. The quantities $B = [Z_{,i}]n_i$ and $\bar{B} = [Z_{,ij}]\,n_i n_j$ are defined on the singular surface $\Sigma(t)$. The operator $\delta/\delta t = \partial/\partial t + Gn_i\,\partial/\partial x_i$ denotes the time derivative along an orthogonal trajectory of $\Sigma(t)$. A comma followed by a Greek index (α) denotes partial differentiation with respect to the surface coordinate y^α. The range of the Greek indices is taken to be 1, 2. The first and second fundamental forms of $\Sigma(t)$ are denoted by $g^{\alpha\beta}$ and $b_{\alpha\beta}$, respectively. We also recall the following relations which we shall be using in our subsequent analysis

$$n_{i,\alpha} = -g^{\beta\delta}\,b_{\beta\alpha}\,x_{i,\delta}; \quad 2\Omega = g^{\alpha\beta}\,b_{\alpha\beta} \tag{11}$$

where Ω is the mean curvature of $\Sigma(t)$.

Taking jumps, across $\Sigma(t)$, in Eqs (1—4) and making use of (6) and (9) we have,

$$G\zeta = \varrho_0\,\lambda_i\,n_i, \quad \varrho_0\,G\lambda_i = \xi n_i, \quad G\xi = \varrho_0 a_{f_0}^2\,\lambda_i\,n_i, \quad G\eta = 0 \qquad (12,\ 13,\ 14,\ 15)$$

where $\lambda_i = [u_{i,j}]n_j$, $\xi = [p_{,i}]n_i$, $\zeta = [\varrho_{,i}]n_i$ and $\eta = [c_{,i}]n_i$ are the quantities defined on the wave front $\Sigma(t)$.

Now if $G \neq 0$, then $\eta = 0$ and it follows from Eqs (13) and (14) that

$$\varrho_0\lambda(G^2 - a_{f_0}^2) = 0 \tag{16}$$

where $\lambda = \lambda_i n_i$ is the amplitude of the discontinuity.

Equation (16) suggests that either $G = \pm a_{f_0}$ or $\lambda = 0$. Since λ cannot vanish, for if it does, then it follows from (12, 13, 14) that $\lambda = \xi = \zeta = 0$, which violates the basic assumption about $\Sigma(t)$. Hence, for an advancing wave, we shall take

$$G = a_{f_0} \tag{17}$$

We thus note that the discontinuity surface $\Sigma(t)$ propagates through the medium with the frozen sound velocity and the relations (12, 13) become

$$\lambda = \xi/\varrho_0 G = G\zeta/\varrho_0 \tag{18}$$

3. Behaviour at the wave front

Differentiating Eqs (2) and (3) with respect to x_k and taking jumps across $\Sigma(t)$, we find on using (6), (9), (10), (11), (17) and (18) that

$$\varrho_0 \frac{\delta\lambda}{\delta t} + (\bar{\xi} - \varrho_0 a_{f_0} \bar{\lambda}_i n_i) = 0 \tag{19}$$

$$\frac{\delta\xi}{\delta t} - a_{f_0}(\bar{\xi} - \varrho_0 a_{f_0} \bar{\lambda}_i n_i) - 2(\Lambda_1 + \Lambda_2 + a_{f_0}\Omega)\xi + (\gamma+1)\varrho_0 a_{f_0} \lambda^2 = 0 \tag{20}$$

where

$$\bar{\lambda}_i = [u_{i,jk}] n_j n_k, \quad \bar{\xi} = [p_{j,i}] n_i n_j ,$$

$$\Lambda_1 = \frac{1}{2}\frac{(\gamma-1)^2}{\gamma}\frac{Q E_x Wn}{(p_0/\varrho_0)^2}\left\{\omega_0 - (1-c_0) n \frac{\delta_0}{\tau_0}\frac{Q}{E_x}\right\} \tag{21}$$

and

$$\Lambda_2 = \frac{1}{2}\frac{\gamma-1}{\gamma}\frac{Q Wn\omega_0}{(p_0/\varrho_0)} \tag{22}$$

Eliminating the term $(\bar{\xi} - \varrho_0 a_{f_0}\bar{\lambda}_i n_i)$ between (19) and (20) and using (17) and (18), we get

$$\frac{\delta}{\delta t}\log\{(\varrho_0 a_{f_0})^{\frac{1}{2}}\lambda\} + \frac{(\gamma+1)}{2}\lambda - (\Lambda + a_{f_0}\Omega) = 0 \tag{23}$$

where

$$\Lambda = \Lambda_1 + \Lambda_2 .$$

Integrating (23) between t_i (where $\lambda = \lambda_i$) and t, we obtain

$$\lambda = \frac{\lambda_i (a_{f_{0i}}/a_{f_0})^{\frac{1}{2}} \exp\left\{\int_{t_i}^{t}(\Lambda + a_{f_0}\Omega)\,\mathrm{d}t\right\}}{1 + \frac{(\gamma+1)}{2}\lambda_i \int_{t_i}^{t}(a_{f_{0i}}/a_{f_0})^{\frac{1}{2}} \exp\left\{\int_{t_i}^{t}(\Lambda + a_{f_0}\Omega)\,\mathrm{d}t\right\}\mathrm{d}t} \tag{24}$$

Equation (24) gives the variation of discontinuity λ associated with $\Sigma(t)$ as it moves into a reacting gas mixture. It is evident from (24) that the temporal

behaviour of the velocity gradient at the wave head will depend critically on the sign of Λ.

Equation (24) can be specialized to waves with plane ($\Omega = 0$), cylindrical ($\Omega = -1/2R$) and spherical ($\Omega = -1/R$) geometry where $R(t)$ is the radius of the wave front at any time t.

4. Discussion

Case (*i*). If ω_0 is zero, so that the medium ahead of the wave is one of uniform equilibrium, (21) and (22) show that $\Lambda = \Lambda_1 = -\frac{1}{2}\frac{(\gamma-1)}{\gamma}\frac{Q^2 W n^2}{(p_0/\varrho_0)^2}$ $(1 - c_0)\frac{\delta_0}{\tau_0} < 0$. Also, the mean curvature $\Omega(t)$ at any point of the wave surface $\Sigma(t)$ is given by [3]

$$\Omega(t) = \frac{\Omega_0 - K_0 a_{f_0} t}{1 - 2\Omega_0 a_{f_0} t + K a_{f_0}^2 t^2}$$

where Ω_0 and K_0 are, respectively, the mean and Gaussian curvatures of $\Sigma(t)$ at $t = 0$. Here t_i has been set equal to zero for convenience. Then Eq. (24) becomes

$$\lambda = \frac{\lambda_i (1 - 2\Omega_0 a_{f_0} t + K_0 a_{f_0}^2 t^2)^{-\frac{1}{2}} \exp(-|\Lambda| t)}{1 + \frac{(\gamma+1)}{2}\lambda_i \int_0^t \{(1 - 2\Omega_0 a_{f_0} t + K_0 a_{f_0}^2 t^2)^{-\frac{1}{2}} \exp(-|\Lambda| t)\}\, dt} \tag{25}$$

which can be specialized to waves of plane, cylindrical and spherical geometry.

Equation (25) shows that if $\lambda_i > 0$ (*i.e.* an expansion wave front) then $\lambda \to 0$ as $t \to \infty$, *i.e.* the wave decays and damps out ultimately. Also if $\lambda_i < 0$ (*i.e.* a compression wave front) and $|\lambda_i| < \lambda_c$, where λ_c is a positive quantity given by

$$\lambda_c = \begin{cases} 2|\Lambda|/(\gamma+1) & \text{for a plane wave} \\ 2\left(\frac{|\Lambda| a_{f_0}}{\pi R_0}\right)^{\frac{1}{2}} \frac{\exp(-|\Lambda| R_0/a_{f_0})}{(\gamma+1)\, erfc\,(|\Lambda| R_0/a_{f_0})^{\frac{1}{2}}} & \text{for a cylindrical wave} \\ \frac{2 a_{f_0} \exp(-|\Lambda| R_0/a_{f_0})}{(\gamma+1) R_0 E_i(|\Lambda| R_0/a_{f_0})} & \text{for a spherical wave} \end{cases}$$

where $erfc\,(x) = 2/\sqrt{\pi}\int_x^\infty e^{-t^2}\, dt$, $E_i(x) = \int_x^\infty t^{-1} e^{-t}\, dt$ and R_0 is the value of R at $t = 0$, then $\lambda \to 0$ as $t \to \infty$, the wave damps out ultimately. But, if $\lambda_i < 0$

and $|\lambda_i| > \lambda_c$, then there exists a finite time t_s given by

$$t_s = \frac{1}{|\Lambda|} \log \left\{1 - \frac{2|\Lambda|}{|\lambda_i|(\gamma+1)}\right\}^{-1} \quad \text{for a plane wave}$$

$$\int_0^{t_s} (R_0/R)^{\frac{1}{2}} \exp(-|\Lambda|\hat{t})\, \mathrm{d}\hat{t} = \frac{2}{|\lambda_i|(\gamma+1)} \quad \text{for a cylindrical wave}$$

$$\int_0^{t_s} (R_0/R) \exp(-|\Lambda|\hat{t})\, \mathrm{d}\hat{t} = \frac{2}{|\lambda_i|(\gamma+1)} \quad \text{for a spherical wave}$$

such that $|\lambda| \to \infty$ as $t \to t_s$, *i.e.* the wave terminates into a shock at an instant t_s. Thus we find that a compression wave steepens up into shock after a finite time only if the initial discontinuity associated with the wave is sufficiently strong. From the above expressions of λ_c, one can see that $\lambda_c/\partial|\Lambda| > 0$ which means that the chemical reactions in the flow have a stabilizing effect on the tendency of the wave surface to grow into a shock in the sense that an increase in $|\Lambda|$ will cause λ_c to increase. Also, $\partial\lambda_c/\partial R_0 < 0$, which implies that the curvature has a stabilizing effect in that an increase in the initial curvature causes an increase in λ_c.

Case (*ii*). If the medium ahead is in a state of disequilibrium, *i.e.* $\omega_0 \neq 0$, and one considers only a short interval of time, so that the quantities a_{f_0} and Λ do not change appreciably between t_i and t, it is evident that (24) can be written in the approximate form

$$\lambda \simeq \frac{\lambda_i \exp\left(\int_0^t \bar{a}_{f_0} \Omega\, \mathrm{d}t\right) \exp(\bar{\Lambda} t)}{1 + \frac{(\gamma+1)}{2} \lambda_i \int_0^t \left\{\exp\left(\int_0^t \bar{a}_{f_0} \Omega\, \mathrm{d}t\right) \exp(\bar{\Lambda}\hat{t})\right\} \mathrm{d}\hat{t}} \tag{26}$$

where $\bar{a}_{f_0}$ and $\bar{\Lambda}$ indicate suitable mean values over the interval t_i to t, and t_i has been set equal to zero for convenience.

An examination of (26) leads to the conclusion that if $\lambda_i < 0$ and $\bar{\Lambda} > 0$, then there exists a finite time t_s^* given by

$$t_s^* = \frac{1}{|\bar{\Lambda}|} \log \left\{1 + \frac{2\bar{\Lambda}}{|\lambda_i|(\gamma+1)}\right\} \quad \text{for a plane wave}$$

$$\int_0^{t_s^*} [R_0/(R_0 + \bar{a}_{f_0} t)]^{\frac{1}{2}} \exp(\bar{\Lambda} t)\, \mathrm{d}t = \frac{2}{|\lambda_i|(\gamma+1)} \quad \text{for a cylindrical wave}$$

$$\int_0^{t_s^*} [R_0/(R_0 + \bar{a}_{f_0} t)] \exp(\bar{\Lambda} t)\, \mathrm{d}t = \frac{2}{|\lambda_i|(\gamma+1)} \quad \text{for a spherical wave}$$

such that $|\lambda| \to \infty$ as $t \to t_s^*$, provided (26) remains valid over the requisite period. Thus, we find that in a state of disequilibrium, a discontinuity associated with a compression wave, no matter how small, always steepens up into a shock after a finite time and the stabilizing influence of the wave front curvature is unable to overcome the tendency of the wave surface to grow into a shock. On the other hand if $\lambda_l > 0$ and $\bar{\Lambda} > 0$, then, using l'Hospital's rule, it follows from (26) that for a plane, cylindrical or a spherical wave, $\lambda \to 2\bar{\Lambda}/(\gamma + 1)$ as $t \to \infty$. Thus, when the medium ahead of the wave is in a state of disequilibrium, it is interesting to note that a discontinuity associated with an expansion wave tends towards a fixed value which is independent of its initial value.

REFERENCES

[1] CLARKE, J. F.: J. Fluid Mech., **81**, 257 (1977)
[2] THOMAS, T. Y.: Int. J. Engng. Sci., **4**, 207 (1966)
[3] LANE, E. P.: Metric Differential Geometry of Curves and Surfaces Univ. Chicago Press, Chicago 1940

V. D. SHARMA
RADHE SHYAM
Applied Mathematics Section, Institute of Technology
B.H.U., Varanasi 221005, India.

Acta Chimica Academiae Scientiarum Hungaricae, Tomus 103 (3), pp. 289—299 (1980)

INFLUENCE OF PHOTOGRAPHIC AND PHOTOMETRIC EFFECTS ON SPECTROGRAPHIC EVALUATION, VI*

INVESTIGATION OF BLACKENING CURVES OF LINE AND CONTINUOUS SPECTRA. EFFECT OF BACKGROUND DENSITY UPON THE SHAPE OF BLACKENING CURVE OF LINE SPECTRA

K. ZIMMER* and Gy. HELTAI[1]

(Institute for Inorganic and Analytical Chemistry of L. Eötvös University, Budapest, [1] Department of Chemistry of the University of Agricultural Sciences, Gödöllő)

Received December 27, 1978
Accepted for publication May 21, 1979

In this paper the effect of background density upon the γ-value of the line spectrum has been investigated, comparing the differences of the shape of blackening curves determined on the basis of line and continuous spectra, respectively.

The ratio γ_L/γ_U does not depend on the wavelength, however, it is definitely dependent on the type and condition of emulsion. With increasing the background density the value γ_{L+U} of the line spectrum decreases as a saturation function. On the basis of the mathematical description of experimental data an equation has been deduced which is suitable for the simple calculation of γ_{L+U} from values γ_L and γ_U. The equation includes only one parameter depending on the experimental conditions.

Introduction

In our earlier publications it has been shown in accordance with literature data that the shapes of blackening curves determined on the basis of line and continuous spectra are differing, and this difference is to be taken into consideration in practical spectral analysis when applying background correction in order to increase the length of the linear portion of the analytical curve and the accuracy [2—8]. These differences are due partly to photometric [3, 4], partly to photographic effects [6, 7, 9, 10]. According to our examinations, in the above two cases the photometric interfering effect of scattered light appears in different degrees in the microdensitometer: for continuous spectra it is almost negligible, however, for line spectra it is quite significant [1, 4].

As it has already been pointed out the interfering effect of the scattered light appearing in the microdensitometer always reduces the γ-value of line spectra, therefore it can not be at all the cause of the fact that γ_L-value re-

* Previous Paper: Gy. HELTAI, K. ZIMMER: Acta Chim. Acad. Sci. Hung., (In the press)
Papers of this series are simultaneously published in Magyar Kémiai Folyóirat in Hungarian language.

lating to line spectrum is always higher than γ_U of the continuous spectrum [2]. Accordingly, this difference is primarily of photographic origin, and is mainly the consequence of the EBERHARD effect [9, 10].

In practical spectral analysis the spectrograms are generally formed by the simultaneous effect of th eline spectrum containing the useful information and background of continuous spectrum. That is, in general, line spectra of various background densities are obtained. It is supposed that for these spectra, blackening curves neither of the continuous, nor of the background-free line spectrum do not hold, and γ_{L+U} value determined by means of these spectra falls between γ_L and γ_U values. While the difference between γ_U and γ_L is caused, first of all, by developing [9], in the difference between γ_{L+U} and γ_L the illumination may also play a role. Namely, upon the effect of complementary illumination the steepness of blackening curve is decreasing [3, 11] and its influence is the strongest if it is simultaneous with the main illumination [12]. The background radiance can be regarded essentially as a complementary illumination affecting simultaneously with the line spectra of the main illumination.

According to the above mentioned, to perform a background correction the appropriate blackening curves are to be taken into consideration. In favourable cases, it is enough to calculate the line intensity on the basis of blackening curves of line spectra and the background intensity on those of continuous spectra [2, 8]. This method can, however, be applied only at such relatively low background density, at which the shape of blackening curve of the line spectrum is not significantly changed by the background. The aim of our investigations was to study the relation existing among the blackening curves of line and continuous spectra. First of all, the effect of background density upon the shape of the blackening curve of line spectrum was examined. Earlier these kinds of experiments were hindered by the quite narrow measuring range of the conventional microdensitometers, while with the help of the up-to-date microdensitometer type G II-MFKI [13] a sufficiently wide range of density can be measured [1, 3].

Experimental

Instruments and method

Our experiments have been carried out by means of spectrograph type Q 24. A deuterium spectral lamp served to produce continuous spectra. Thus, continuous spectra in the wave length range of 230—360 nm could be studied. Background-free line spectrum was produced — as described in our earlier papers [1, 4] — by d.c. arc excitation of iron electrodes excluding the glowing electrode-ends. Series of spectrograms necessary to plot the blackening curves were prepared by varying the exposure time applying a selective, two-step, γ-compensation light filter type NAGY [14]. The slit width of the spectrograph was 20 μm. Densities were measured with microdensitometer type G II-MFKI, its slit width was mostly adjusted so as to correspond to the 2/3 of the spectral line breadth. Parameters of blackening curve and

l-transformation [15], as well have been determined, as described earlier, graphically with preliminary curve [16, 17] and with computer program, respectively [18].

Line spectra of different background densities were modelled by the successive exposure of the two types of spectra. During a preliminary experiment the effect of the sequence of the two different types of illumination on the shape of the blackening curve was investigated. Line spectra of different background densities were exposed on the same Agfa-Gevaert 23 D 56 type spectral plate by previous and subsequent illumination with deuterium spectral lamp. For the sake of comparison, also background-free line spectra were recorded on the plate. γ_{L+U} and k_{L+U} values determined at wave length 300 nm are presented in Table I. It is clear that the sequence of the two kinds of illumination has no influence upon the results. In the

Table I

The γ_{L+U} and k_{L+U} values determined at 300 nm wave length on the basis of successive exposed line and continuous spectra, in various sequence, to spectral plate type Agfa-Gevaert 23 D 56 at two background levels

Sequence of exposure	S_U	γ_{L+U}	k_{L+U}
1. Deuterium spectral lamp, 2. DC iron arc	0.15	1.94	0.33
	0.39	1.76	0.36
1. DC iron arc, 2. Deuterium spectral lamp	0.15	1.87	0.33
	0.39	1.77	0.35
DC iron arc	0.00	2.02	0.31

course of our further experiments, the exposure of continuous spectra always preceded that of line spectra.

Our examinations were performed with various kinds of spectral plates produced by Agfa-Gevaert, emulsion type 23 D 56 was mainly used, in which case the difference among the blackening curves of the two kinds of spectra can be well studied.

Results

1. Comparison of the blackening curves of the two kinds of spectra

a) *Influence of the wave length*

Background-free line and continuous spectra were recorded on the same spectral plate type Agfa-Gevaert 23 D 56. In the wave length range of 240—360 nm values γ_L and γ_U belonging to the two kinds of spectra (Fig. 1), their difference and ratio (Fig. 2) and the k-values were determined (Fig. 3). It can be seen that the difference of the two kinds of γ-values increases as the wave length does, while their ratio remains approximately constant. Mean value of the differences $\gamma_L - \gamma_U$ is 0.48, their standard deviation is ± 0.19, while in the case of the ratio γ_L/γ_U the above factors are 1.26 ± 0.07. In contrast

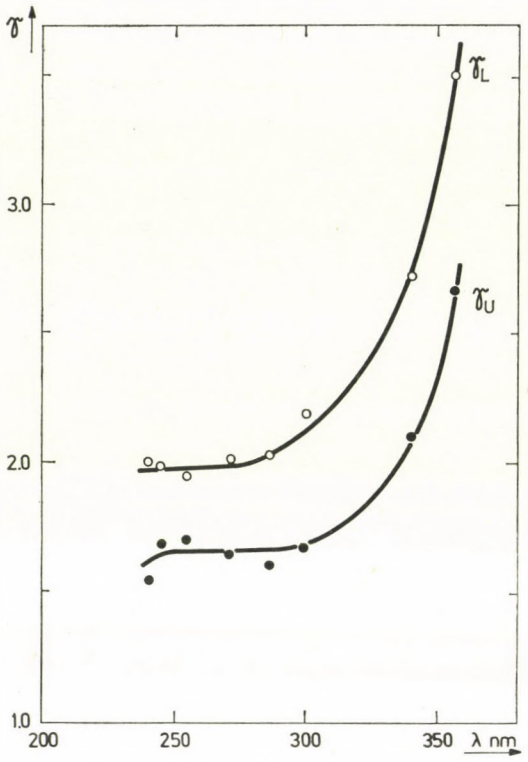

Fig. 1. Variation of γ_L and γ_U values determined by line and continuous spectra in function of wave length in the case of emulsion type Agfa-Gevaert 23 D 56

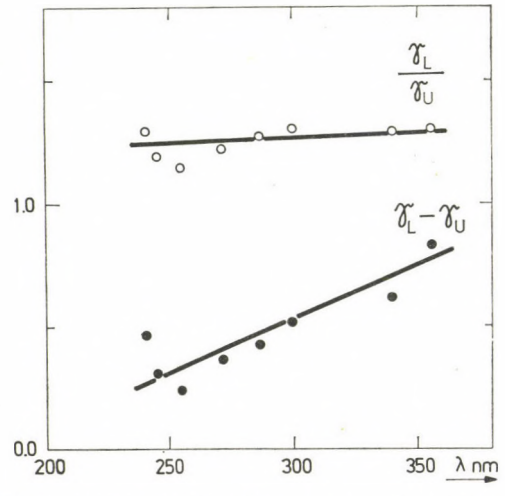

Fig. 2. Variation of the difference and ratio of γ_L and γ_U values in fuction of wave length in the case of emulsion type Agfa-Gevaert 23 D 56

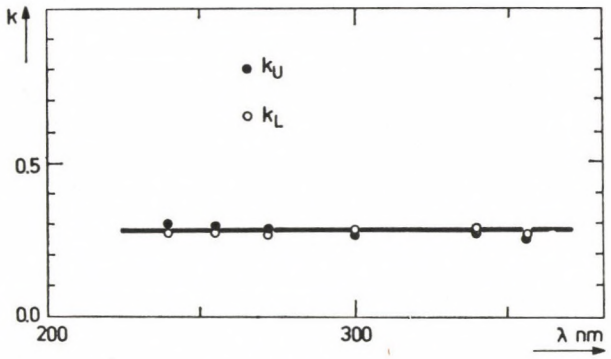

Fig. 3. Variation of k_L and k_U values determined by line and continuous spectra in function of wave length in the case of emulsion type Agfa-Gevaert 23 D 56

to the difference in γ-values, the k-values belonging to the two different types of spectra are practically identical and independent on the wavelength, *i.e.* $k_L = k_U$.

b) *Influence of the type of the spectral plate*

Agfa-Gevaert spectral plates of various types have been compared at a chosen (300 nm) wavelength. Experimental results are to be seen in Table II. In addition to the symbols already defined in the table the following symbols are used: fog density S_F, d_L slit width of the spectrograph and d_m of the corresponding microdensitometer slit width. It is clear that both the ratio and

Table II

γ_L and γ_U values determined on spectral plates of different types at wavelength 300 nm on the basis of line and continuous spectra

Meaning of denotations: S_F fog density: d_m: slit width of microdensitometer; d_L slit width of spectrograph

Plate	$\gamma_L \pm s_{\gamma L}$	$\gamma_U \pm s_{\gamma U}$	$\gamma_L - \gamma_U$	$\frac{\gamma_L}{\gamma_U}$
23 D 56	2.190 ±0.151	1.664 ±0.089	0.526	1.315
$S_F \cong 0.2$ 34 B 50	1.148 ±0.079	1.008 ±0.126	0.140	1.139
$S_F \cong 0.5$	1.097 ±0.049	1.050 ±0.071	0.047	1.044
$d_m = 2/3\ d_L$ 23 D 50	1.472 ±0.091	1.377 ±0.066	0.095	1.070
$d_m = 1/3\ d_L$	1.535 ±0.120	1.364 ±0.095	0.171	1.124

difference of the two kinds of γ-values depend on the type and conditions of plate too. In general it can be established that the higher are the γ-values the greater is their difference. This is the explanation of the effect of fog density at the emulsion type 34 B 50. Namely, at any wavelength the γ-value of each plate decreases during storage owing to the increase of fog density. When applying old pates or milder developer the difference of lower γ-values is also smaller.

In the above comparison the relation d_m/d_L of the slit widths of the spectrograph and the microdensitometer should also be taken into consideration. If the slit width of the microdensitometer is reduced, the γ_L-value determined on line spectrum increases, while γ_U-value of continuous spectrum remains unchanged, therefore their difference increases. This is represented by data given for emulsion type 23 D 50.

2. Influence of background density upon the shape of blackening curves of line spectra

These investigations were carried out with spectral plates types Agfa-Gevaert 23 D 56 and 23 D 50 by successive exposure of continuous and line spectra as described above. To investigate a sufficient wide range of background density more spectral plates were required and therefore both line-free continuous and background-free line spectra were exposed on every plate for comparison. Emulsion type 23 D 56 at wave lengths 300 and 340 nm was evaluated, while emulsion type 23 D 50 at 300 nm was evaluated with microdensitometer having

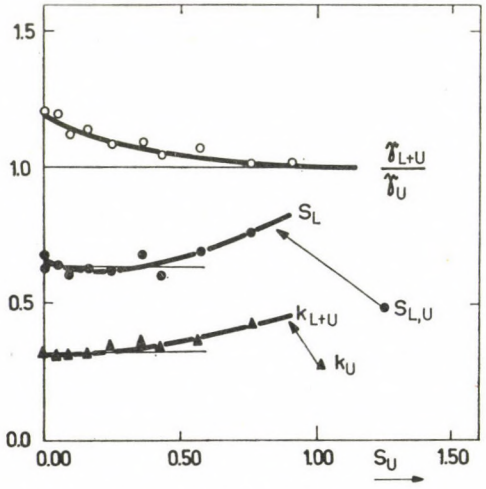

Fig. 4. Variation of γ_{L+U}, k_{L+U} and S_L values in function of background density S_U in the case of emulsion type Agfa-Gevaert 23 D 56 at wave length 300 nm. $S_{L,U}$, means the S_L-value determined on the basis of continuous spectra

a slit width d_m corresponding to 2/3 and 1/3, respectively, of the d_L slit width of the spectrograph. The appropriate γ_{L+U} and k_{L+U} values were determined on the basis of at least 30 data pairs at each of the background values. From the γ_{L+U}- and k_{L+U}-values the S_L density values also were calculated. Our measuring results are shown on Figs 4, 5 and 6. For comparison the k_U- and

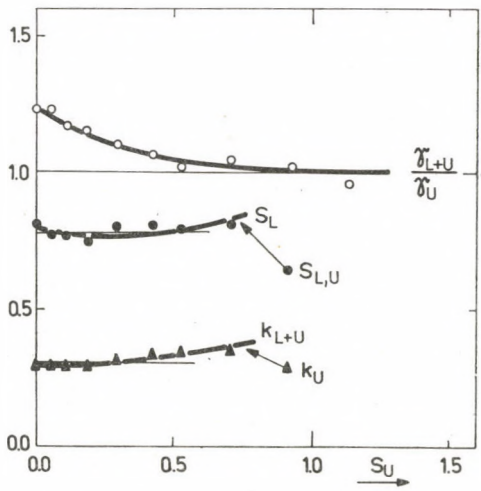

Fig. 5. Variation of γ_{L+U}, k_{L+U} and S_L values in function of background density S_U in the case of emulsion type Agfa-Gevaert 23 D 56 at wave length 340 nm. $S_{L,U}$ means the S_L-value determined on the basis of continuous spectra

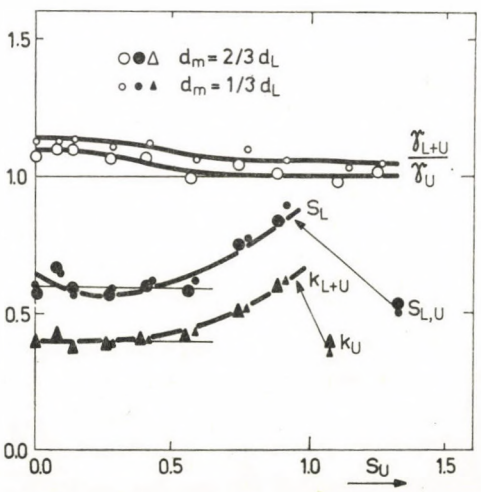

Fig. 6. Variation of γ_{L+U} value determined by two different d_m slit widths of microdensitometer and of k_{L+U} and S_L values in function of background density S_U using emulsion type Agfa-Gevaert 23 D 50, at wave length 300 nm. $S_{L,U}$ means the S_L-value determined on the basis of continuous spectra

$S_{L,U}$-values determined on continuous spectra are also shown in the Figures. Naturally these do not belong to a fixed abscissa value.

On the basis of the results the following statements can be made:

a) The γ_{L+U}-value of line spectra decreases by enhancing the background density in every case and after reaching a special limit it becomes practically equal to the γ_U-value of the continuous spectrum. In the case of emulsion type 23 D 50 it can be observed, that the γ_{L+U}-value is influenced by the microdensitometer slit width, too. The γ-value of background-free line spectra is higher than γ_U primarily because of the EBERHARD effect [9]. The developing agents can diffuse to the surface of the emulsion at the spectral lines from the solution not only at right, but at other angles and within the emulsion layer from the vicinity of the line. In the case of continuous spectra [8], however, development on a large surface decreases the concentration of developing agents, and thereby the rate of the development, too, which finally results in a low γ_U-value. With line spectra by enhancing the background density the possibility of diffusion change within the emulsion layer gradually decreases and the developer solution in the vicinity of the lines is exhausted more and more. So the difference in the rate of development of line and background, respectively, gradually decreases and after exceeding a certain limit it becomes practically negligible, and so the γ-values of two kinds become practically equal. This limiting background density is approximately equal to S_L in the cases studied.

b) The k-constant of l-transformation by enhancing the background density practically does not change, as the horizontal lines show in Figs 4, 5, 6. The value k shows a small increase only with background densities approaching the value of S_L. In these extreme cases, which practically do not occur in the course of analyses (so the horizontal lines at these are not continued) the underexposed part of the blackening curve is shortened to such an extent, that the determination of k_{L+U}-value becomes unreliable. If the S_U reaches or exceeds the value of S_L, the determination of k_{L+U} is pointless also theoretically. Considering the above it can be established, that the value of k_{L+U} that can be determined reliably does not depend on background density. Previously it was proved that $k_U = k_L$ (Fig. 3), so the lower limit of the linear part of the blackening curve, the S_L density is reached at the same exposure in the case of either line or continuous spectra or their simultaneous effect; *i.e.* $Y_L = k_L = k_U = k_{L+U}$.

Numerous functions of different kinds seem to be suitable to describe the correlation existing between γ_{L+U}-value and background density S_U if considering the graphical plotting. Based on this, the mathematical description of the correlation was approximated with the following functions:

$$y = ax + b \tag{1}$$

$$y = \frac{1}{ax + b} \tag{2}$$

$$y = \sqrt{ax + b} \tag{3}$$

$$y = \frac{1}{\sqrt{ax + b}} \tag{4}$$

$$y = \ln(ax + b) \tag{5}$$

$$y = be^{ax} \tag{6}$$

$$y = \frac{a}{1 + bc^x} \tag{7}$$

$$y = a(1 - bc^x) \tag{8}$$

Above equations contain background density S_U or the corresponding l_U values as independent variables. The dependent variable was in each case γ_{L+U}/γ_U. In every case examined the correlation coefficient was higher than 0.8. From this the conclusion can be drawn that a number of functions can be fitted to the relatively few measuring points beside considerable standard deviation. At each data rank, however, in the case of saturation functions (7) and (8) correlation coefficients generally much higher than in other cases, $r \cong 0.950$, have been obtained. Equation (7) always produced an r value higher by 0.001—0.002 than (8).

Interpretation of constants in Eq. (7) is represented by data obtained by emulsion 23 D 56 at wavelength 300 nm. The regression equation is as follows:

$$y = \frac{a}{1 + bc^x} \quad x = S_U \quad y = \frac{\gamma_{L+U}}{\gamma_U}$$

$$\frac{\gamma_{L+U}}{\gamma_U} = \frac{1.015}{1 - 0.159 \cdot 0.054\, S_U}$$

$$r = -0.951$$

In the equation parameter "a" represents the saturation value. The theoretical value of this is the unit, the value determined from experimental data is 1.015, which is a quite good agreement. Considering this, the value of parameter b can also be interpreted, namely if $S_U = 0$, $\gamma_{L+U} = \gamma_L$ and $c^{S_U} = c0 = 1$, then

$$\frac{\gamma_L}{\gamma_U} = \frac{1}{1 + b} \qquad b = \frac{\gamma_U}{\gamma_L} - 1$$

In this case $\gamma_L = 2.095$, $\gamma_U = 1.740$ and from it follows that $b = -0.170$. This value shows a good agreement with -0.159, calculated on the basis of experimental data. Earlier it has been proved that in the case of a given spectral plate the value γ_U/γ_L is independent on the wavelength, and consequently so is b.

Taking into consideration the above mentioned the value γ_{L+U} can be expressed from the regression equation as follows:

$$\gamma_{L+U} = \frac{\gamma_L \cdot \gamma_U}{\gamma_L(1 - c^{S_U}) + \gamma_U c^{S_U}}$$

The equation is made more representative by a simple transformation

$$\frac{1}{\gamma_{L+U}} = \frac{1 - c^{S_U}}{\gamma_U} + \frac{c^{S_U}}{\gamma_L}$$

Thus, it is clear that c^{S_U} value has a decisive role in the addition of the γ-values of the two different kinds of spectra. It is also understandable that c^{S_U} value can not exceed 1, so $c \leq 1$. As the above examinations show, the value of factor c is depending on the type and state of emulsion, on the conditions of development and other experimental circumstances, too. Accordingly, the theoretical calculation of factor c can not be solved on a simple way, however its value can be calculated on the basis of a single γ_{L+U} determination, in the knowledge of γ_L and γ_U.

Conclusions

On the basis of the experimental results, in agreement with earlier ones [2—10] it can be established that the shapes of blackening curves of line and continuous spectra are differing. The γ-values are different due to photographic effects, while the k-values are identical. Difference of γ_L and γ_U depends, the ratio of γ_L and γ_U, however, does not depend upon the wavelength, only on the type and condition of plate and on other experimental conditions. As a general rule, it can be stated that the deviation increases with increasing the γ-values. At lower, 1.0—1.5 γ-values, the deviations can frequently be neglected from the point of view of background correction. At higher γ-values this negligence is not permitted. In this case, however, one has to take into consideration that the value of γ_{L+U} of the line spectrum is decreasing with the increasing of S_U background density according to the saturation function. The k-value proved to be independent on the background density, so its value determined at lower background density can also be applied. If the γ_L-value of the background-free line spectrum, and γ_U of continuous spectrum are

known, the value of constant only necessary to the description of their relation can also be determined, by measuring the γ_{L+U} value at a given background density S_U. Following this, value γ_{L+U} can be calculated even by an arbitrary background value and it can be utilized for the calculation of line intensities. It is, however, more frequently the case that γ_{L+U} can be measured by a given background density S_U, and γ_U value is to be determined to the background correction without measuring. Based on the above equations the value γ_U can theoretically be calculated by measuring the γ_{L+U} value belonging to three different background values.

REFERENCES

[1] HELTAI, Gy., ZIMMER, K.: Acta Chim. Acad. Sci. Hung. (in press); Magy. Kém. Folyóirat **85**, 403 (1979)
[2] ZIMMER, K., SZABÓ, É.: Magy. Kém. Folyóirat, **77**, 198 (1971)
[3] ZIMMER, K., HELTAI, Gy.: Acta Chim. Acad. Sci. Hung. **100**, 319 (1979); Magy. Kém. Folyóirat, **85**, 170 (1979)
[4] HELTAI, Gy., ZIMMER, K., MATHERNY, M., FLÓRIÁN, K.: Acta Chim. Acad. Sci. Hung. (in press); Magy. Kém. Folyóirat **85**, 398 (1979)
[5] ARRAK, A.: Appl. Spectr., **16**, 124 (1962)
[6] STROCK, L. W.: J. Opt. Soc. Am., **32**, 103 (1942)
[7] SLAVIN, M.: Appl. Spectr., **16**, 173 (1962)
[8] ZIMMER, K., SZABÓ, É.: Proc. 15th Coll. Spectrosc. Int., Madrid 1969, Vol. **IV.**, p. 55, Ibérica, Madrid, Tarragona (1970)
[9] EBERHARD, G.: Physik. Z., **13**, 288 (1912)
[10] TÖRÖK, T.: Tagungsband Optik und Spektroskopie aller Wellenlängen, Akademie-Verlag, Berlin, 1962, 573
[11] INTONTI, R., TADDEUCCI, A.: Spectrochim. Acta, **18**, 379 (1962)
[12] DENISOFF, A.: Z. Wiss. Phot., **27**, 128 (1929)
[13] KOZMA, L.: Acta Chim. Acad. Sci. Hung. (in press); Magy. Kém. Folyóirat **85**, 266 (1979)
[14] NAGY, Z.: Magy. Kém. Folyóirat, **73**, 104 (1967)
[15] TÖRÖK, T., ZIMMER, K.: Quantitative Evaluation of Spectrograms by Means of *l*-Transformation, ed. Akadémiai Kiadó, Budapest and Heyden and Sons, London 1972
[16] CHURCHILL, J. R.: Ind. Eng. Chem. Anal. Ed., **16**, 653 (1944)
[17] PLŠKO, E.: Chem. Zvesti, **23**, 150 (1969)
[18] FLÓRIÁN, K., HELTAI, Gy., ZIMMER, K.: Acta Chim. Acad. Sci. Hung. (in press); Magy. Kém. Folyóirat **85**, 271 (1979)

Károly ZIMMER H-1443 Budapest, P.O. Box 123.
György HELTAI H-2103 Gödöllő

Acta Chimica Academiae Scientiarum Hungaricae, Tomus 103 (3), pp. 301–322 (1980)

INFLUENCE OF PHOTOGRAPHIC AND PHOTOMETRIC EFFECTS ON SPECTROGRAPHIC EVALUATION, VII*

MULTI-ELEMENT SPECTROCHEMICAL METHOD FOR POLLUTION CONTROL — A BASIS FOR OPTIMATION OF SPECTROGRAPHIC EVALUATION

K. FLÓRIÁN* and N. PLIEŠOVSKÁ

(Department of Chemistry, Metallurgical Faculty of Technical University, Košice, Czechoslovakia)

Received December 27, 1978
Accepted for publication May 21, 1979

A spectrographic method developed for pollution control is described and evaluated on the basis of chosen parameters. The method may serve as a basic method for demonstration of the optimated evaluation application which has been dealt with in earlier works. All disadvantages were pointed out which can be avoided by using the optimalized evaluation. The results thus obtained will be discussed in a separate paper.

1. Introduction

Previous papers of this series have given a detailed survey on the factors influencing the spectrographic evaluation and on the possibility of their optimation. Following theoretical experiments, the optimation possibilities were studied in concrete analytical tasks. For the demonstration of the results achieved a task especially important in environmental analytical chemistry has been chosen: the determination of trace elements in aerial dust deposits.

Present paper gives a description about the spectrographic method based on conventional evaluation, which is the control of our results achieved in optimation of evaluation.

Application of physico-chemical micromethods in environmental analytical chemistry

Recently several analytical chemical methods suitable for the determination of the gaseous contaminants present in air have been elaborated, however, the methods for the investigation of dust developed much slower. The reason for this is primarily that this task is much more complicated, the solution of which can be performed only with the help of the most modern

* Previous paper: K. ZIMMER, Gy. HELTAI: Acta Chim. Acad. Sci. Hung., **103,** 289 (1980)
Papers of this series are simultaneously published in Magyar Kémiai Folyóirat in Hungarian language.

(and no widely spread) analytical chemical methods. This analytical chemical task has been characterized by MALISSA and GRASSERBAUER [1] as follows:

a) large-scale analysis of powder samples for all the assumed elements,

b) characterization of individual components of the samples,

c) study of size and morphology of sample particles.

According to experiences obtained on such samples by the above authors, only those methods can be considered which are:

a) micromethods,

b) methods with high power of detection,

c) selective and specific for elements as much as possible,

d) make possible the simultaneous determination of all these elements rather wide concentration ranges,

e) rapid and simple,

f) suitably precise and reliable under the given circumstances,

g) methods not requiring the digestion of samples.

The above described conditions are well met also by emission spectral analysis, but because of its great standard deviation (10—100 in relative %) this method has been listed only among the semiquantitative analytical methods [2].

2. Elaboration of emission spectral analytical method

Prior to the elaboration of the method, the composition of samples to be analysed was examined in order to be able to establish the experimental conditions to be applied on the basis of the occurrence of elements.

Characterization of aerial dust deposit samples and choosing of elements to be determined

The drawback of the widespread BEIGERHOFF method [3] employed for the sampling of dust deposits is that the powder sample should be separated from rain water by evaporation during which gases soluble in water can react with the powder and consequently the chemical composition of the sample may change [1]. Some samples obtained by this method have been used as starting material for the elaboration of the method. The samples were evaporated in Pt-dish on a water bath, then dried at 105 °C. According to the place of sampling powder samples weighing between 3.7 and 224 mg were obtained. By elaboration of the method one has to consider the fact that in extreme cases only a very little amount of sample can be available.

When choosing the elements to be determined we started first of all from 83 literature data reported between 1970 and 1975, and established which elements present in dust samples had been examined by spectrochemical

methods. Corresponding to our aims, only such methods were considered which offered the simultaneous determination of at least 5 elements. Naturally, requirements of pollution control and toxicology were taken also into consideration [4] (see Table I). The determination of the following elements were required: Ag, As, B, Ba, Bi, Cd, Cr, Co, Cu, Fe, Hg, Mn, Mo, Ni, Pb, Sb, Sn, Sr, Ti, V and Zn. Al, Ca, Mg and Si were considered as main components.

Table I

Systematization of elements from the point of view of pollution control and toxicology [4]

Group	Toxicological characterization	Necessity of examination	Elements
A I	strongly toxic	absolutely necessary	Ba, Cd, Co, Cr, Cu, Mn, Ni, Pb
A II	toxic	absolutely necessary	As, Ca, Fe, Hg, K, Mo, Sn, V, Zn
B	toxic	necessary	Ag, Al, Au, B, Mg
C I	toxic	suggested	Be, Bi, Ge, Sb
C II	toxic	suggested	Ga, In, Nb, Os, Pd, Pt, Ta, Te, Tl, Zn, W
D	—	according to conditions	Li, Si, Ti, lanthanides

Naturally, the determination of some of the above listed 21 elements (As, Hg) by emission spectral analysis involves difficulties, further it is well-known that some elements have analysis line only in the visible range (*e.g.* Ba, Sr and partly Cr, Pb, too), while others have it in the far ultra-violet range (*e.g.* Ba, As, Cd). This is why the determination of all elements in one single step can hardly be realized, although there exists such a wavelength range in which majority of them can be determined on a single spectrum. Such a wavelength range is *e.g.* between 270 and 350 nm, where with the exceptions of As, B, Ba, Cd, Hg and Sr the remaining 15 elements can be determined.

Choice of the composition of the matrix

For the determination of dust deposits there are no natural reference samples of known composition available, and even not such quantity of sample, from which the composition of standard samples by means of other analytical chemical method could be determined. Therefore, only synthetic standard samples can be applied, but in this case the essential problem is to choose an appropriate matrix. For this, the necessary informations were provided partly by literature data (Table II), partly by analytical data on the Ca- and Mg-contents of some samples (Table III). Considering the data of the tables and

Table II

Percental composition of the main components of powder samples based on literature data

Main component	Composition in %				
	[5]	[6]	[7]	[8]	[9]
SiO_2	$s \times 10$	20.0	28.0	60.0	32.0
Fe_2O_3	s			20.0	8.0
MgO	s	50.0		2.0	5.0—6.0
CaO	$s \times 10$	25.0		6.0	20.0
Na_2O				3.0	
K_2O				1.0	
Al_2O_3	s	5.0			6.0
MnO_2					0.2

Note: s = some

Table III

Ca and Mg content of some dust deposit samples

Sample (place of sampling	Ca (%)	Mg (%)
Košice 25	22.0	22.3
Humenné	6.0	0.7
Košice 41	20.0	35.6
Košice 38	29.0	37.0
Rožnava	15.0	0.7
Košice 26	69.0	19.0
Košice 39	62.0	12.0

peculiarities of the sampling area (Košice and vicinity) the following matrix composition was chosen:

40% SiO_2, 40% CaO, 15% MgO, 5% Al_2O_3.

The appropriate matrix was prepared by mixing spectral pure metal oxides (Johnson—Matthey).

Determination of the optimal ratio of mixing the samples, and experiments aimed to decrease the matrix effect

On the basis of the literature data (Table II) and experimental results (Table III) it is assumed that the concentration of the main components of the samples examined can vary within wide limits. Therefore, the standard

and experimental samples should be mixed with the additives in such a ratio that the matrix effect [10, 11] be reduced as much as possible. By neglecting this fact a systematic error can be introduced [12].

For the investigation of similar samples, AgCl [5, 13], LiCl [7], and NaCl or NaF, Na_2CO_3 [8] additives have been used most frequently, either in itself or mixed with graphite powder. In our case also silver was determined, and NaF and LiCl were not available in spectroscopical purity. Based on our favourable results obtained earlier [14, 15], Na_2CO_3 and Li_2CO_3 additives were employed in the following ratio: 1 part of sample — 1 part of additive (Na_2CO_3 and Li_2CO_3, resp.) — 2 parts of carbon. The trace elements to be determined and the appropriate reference elements were introduced into the powder mixture by adding them to carbon.

Degree of reducing the matrix effect was investigated on the shape of the analytical curve of some elements applying synthetic samples prepared partly from the matrix chosen, partly from its additives (CaO, MgO, SiO_2, Al_2O_3) and partly from pure carbon. Namely, if the shapes of analytical curves in the different kind of samples are identical then it is assumed that in concrete cases the great variation of the concentration of the main components will not produce significant matrix effect. The matrix effect used to manifest itself by parallel shifting of analytical curves or by the change of their slope.

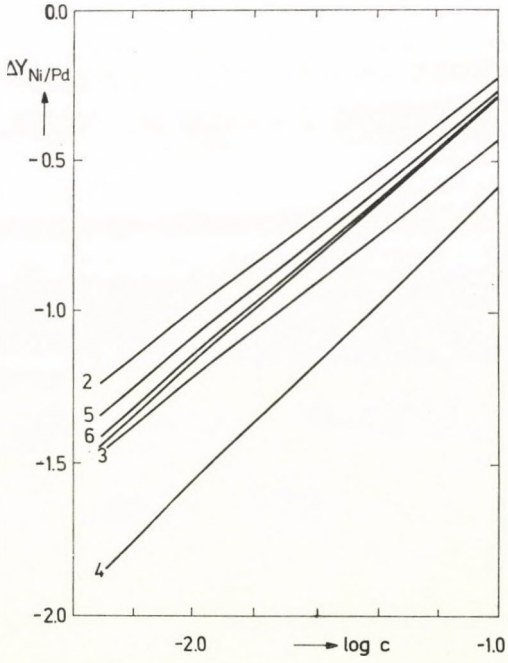

Fig. 1. Shape of the analytical curves of line pair Ni/Pd in various matrices, adding Na_2CO_3. 1: matrix, 2: CaO, 3: MgO, 4: SiO_2, 5: C, 6: Al_2O_3

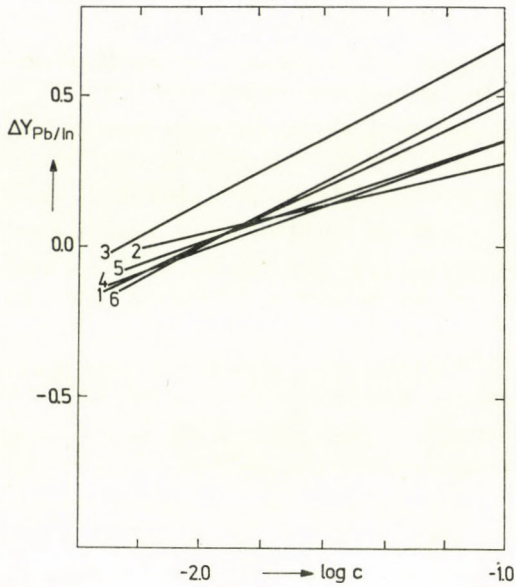

Fig. 2. Shape of the analytical curves of line pair Pb/In, in various matrices, adding Na_2CO_3
1: matrix, 2: CaO, 3: MgO, 4: SiO_2, 5: C, 6: Al_2O_3

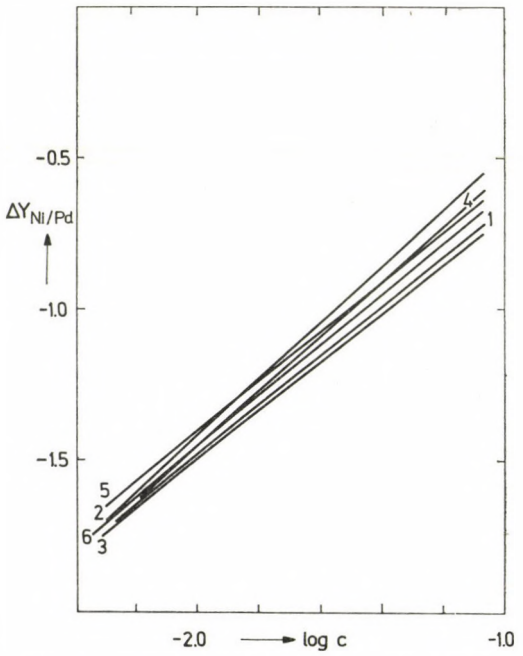

Fig. 3. Shape of the analytical curves of line pair Ni/Pd in various matrices, adding Li_2CO_3.
1: matrix, 2: CaO, 3: MgO, 4: SiO_2, 5: C, 6: Al_2O_3

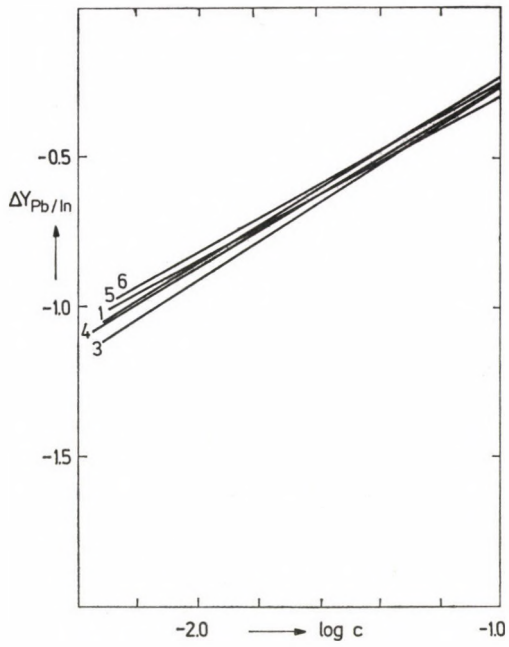

Fig. 4. Shape of the analytical curves of line pair Pb/In in various matrices, adding Li_2CO_3. 1: matrix, 2: CaO, 3: MgO, 4: SiO_2, 5: C, 6: Al_2O_3

Results achieved in some typical cases with Na_2CO_3 additive, are shown in Figs 1 and 2, while with Li_2CO_3 additive in Figs 3 and 4. Based on these, it can be pointed out that in the case of Na_2CO_3 additive some matric effect can still be observed, but with Li_2CO_3 additive this effect does not occur any more. The analytical curves are practically of identical shape as it is proved also by the statistical comparison [16] of constants $A_{X,R}$ and B_X defining the curves. This result is not surprising at all, if it is considered that 1 part of Li_2CO_3 contains spectrochemically effective cations half as much again as 1 part of Na_2CO_3.

According to above results, further Li_2CO_3 additive was employed in a mixing ratio given earlier.

Choosing of experimental conditions

The detection power of spectrochemical methods for trace analysis can be regarded to be optimal according to KAISER [17] if:

a) line/background intensity ratio is maximum,

b) the resolving power and the reciprocal dispersion are chosen correctly,

c) such experimental conditions are applied with which the average background density is about 0.2.

In order to improve the detection power of spectrographic methods, questions of resolving power [18, 19, 20] and role of suitable photographic emulsion [20, 21, 22] have been treated by several authors. Influence of resolving power and reciprocal dispersion of grating spectrographs upon the efficiency of the method was thoroughly studied [23, 24]. A theoretical re-

Table IV

Experimental conditions

Spectrograph	PGS-2 grating spectrograph, $m = 2$
dispersion	0.363 nm · mm^{-1}
blaze wave length	280 nm
Wave length range	270—350 nm
Focussing	Zeiss-type 3-lens system
Aperture of intermediate diaphragm	3.2 mm
Slit width	20 μm
Electrodes	Product of Elektrokarbon n.p. Topolčany carbon (SW-), or graphite (SU-), resp.
carrier electrode	type — 302
counter electrode	type — 201
Emulsion	ORWO, WU-3
Development	10 min at 20 °C in developer type ORWO F-43
Excitation	total burning d.c. arc
Generator	UBI-1
Effective current intensity	7.5 A
Exposure time	82 s (using time-switch of the UBI generator)

solving power $R = 100\,000$ was found to be optimal when using grating spectrograph type PGS-2, which is corresponding to the second order spectrum of a grating of grating pitch 651 lines/mm. At the application of various grating types and single or double radiation path, respectively [24], it has been established that to choose an optimal slit width and intermediate diaphragm is also very important. However, these are to be chosen for each task separately so, as the line/background intensity ratio reach the highest value.

Series of spectrograms were produced under the experimental conditions summarized in Table IV. The slit width, the intermediate diaphragm and the exposure time were gradually changed. On spectra obtained in this way, some spectral lines and the adjacent background density were measured, these values were converted into intensity values by *l*-transformation, then line/background intensity ratios were formed. The obtained I_L/I_U values were plotted against the parameters chosen. Some characteristic data are represented in Figs 5, 6 and 7. Based on these, the following can be established:

a) Change of I_L/I_U ratio upon the slit width is highly dependent on the type of the given element and on the type and position in the spectrum of

the chosen spectral line, in generally, however, the 20 μm wide slit was found to be the most convenient.

b) The line/background intensity ratio unambiguously varies in function of the intermediate diaphragm with the only exception of Bi, the most favourable diaphragm is of 3.2 mm. With regard to the applied excitation method and the relatively small electrode gap-length this is quite comprehensible.

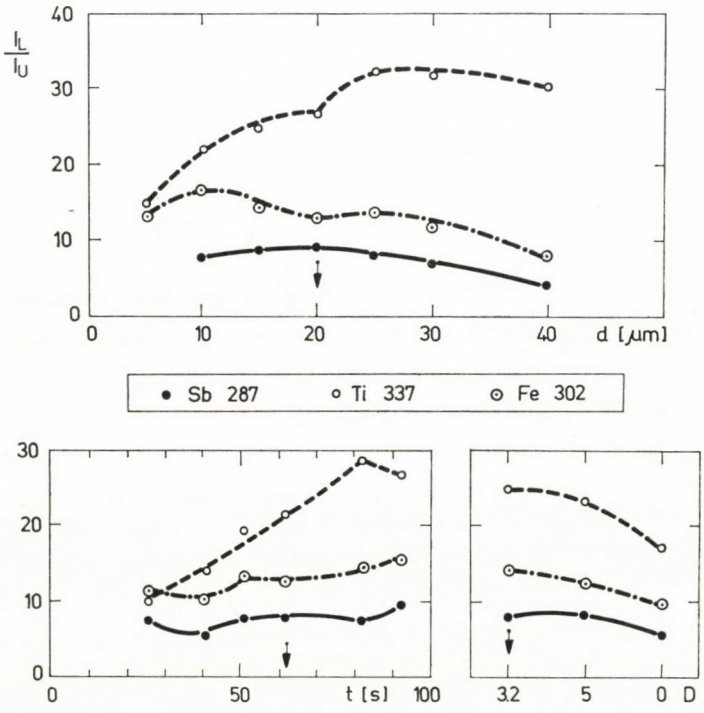

Fig. 5. Influence of slit width and aperture of intermediate diaphragm and the exposure time upon the I_L/I_U ratio, in the case of spectral lines of Sb, Ti and Fe

c) The most complicated task of all is the determination of the optimal exposure time, since in this case we have to manipulate with the mixture of easily, averagely and hardly evaporating elements. In the first group (*e.g.* Bi and Pb) the maximum line intensity is reached after about 40 s arcing time and following this only the background intensity is increasing. In contrast with this, in the second and mainly in the third groups (*e.g.* Ni, Ti and Mo) line intensity becomes maximum value only just prior to the total evaporation. In this case the required safety is provided by total evaporation, however, even then exposure time 82 s should not be exceeded.

Acta Chim. Acad. Sci. Hung. 103, 1980

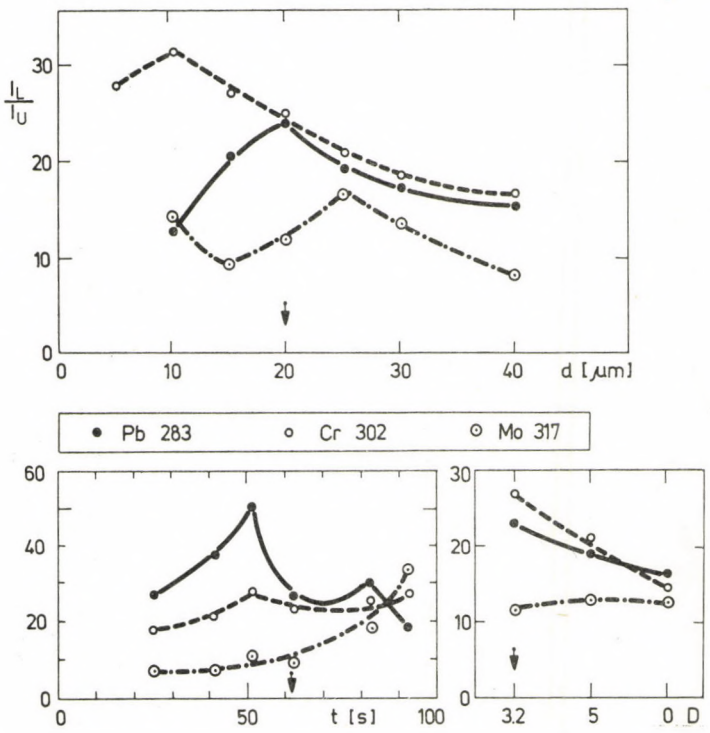

Fig. 7. Influence of slit width and aperture of intermediate diaphragm and the exposure time upon the I_L/I_U ratio, in the case of spectral lines of Pb, Cr and Mo

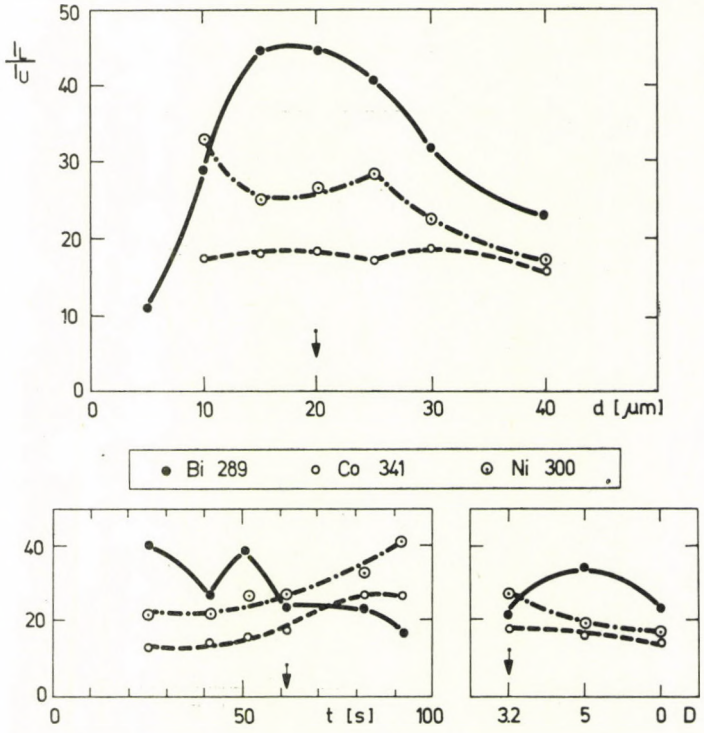

Fig. 6. Influence of slit width and aperture of intermediate diaphragm and the exposure time upon the I_L/I_U ratio, in the case of spectral lines of Bi, Co and Ni

Choosing of the suitable reference element and electrode type

Although by the application of d.c. excitation and total evaporation the selective effects of the evaporation process are roughly eliminated [26], from the point of view of the suitable reference element the evaporation processes are expediently to be taken into consideration. It is important chiefly for the fact, because, although theoretically it would be advisable to apply to each element the characteristically most similar reference element, in the practice, however, generally at most two reference elements are employed [27].

In emission spectral analysis the evaporation processes are studied with the help of time-resolved spectra and evaporation or so-called relative in-

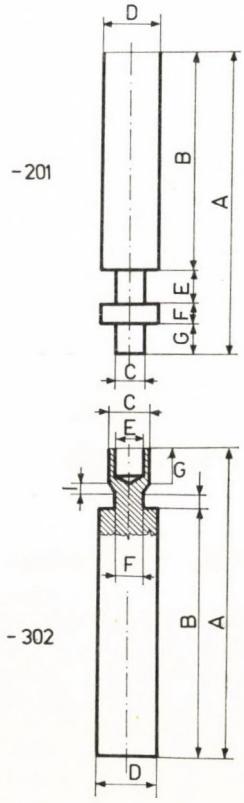

	A	B	C	D	E	F	G
mm	30	22	3	6	3	2	3

	A	B	C	D	E	F	G	H	I
mm	30	24	4	6	3	2.5	3.5	1.5	1

Electrode type	Specific electrical resistance [$\mu\Omega$. cm]	Specific thermal conductivity [W/m . K]
SU -	1000	140
SW -	6000	20

Fig. 8. Electrodes applied and their main features

Table V

Spectral lines used and their main features [38, 39]

Element	Wavelength	Excitation energy, eV	Intensity in Cu-arc
Mn I	279.48	4.44	800
Cu I	282.44	5.78	50
Pb I	283.31	4.37	950
Sn I	286.33	4.32	1000
Sb I	287.79	5.36	140
Ni I	300.24	4.16	320
Fe I	302.11	4.16	300
Cr I	302.16	5.13	360
Pd I	302.79	5.05	130
In I	303.94	4.08	800
Bi I	306.77	4.04	3600
Mo I	313.26	3.96	1800
V I	318.34	3.91	420
Pd I	325.16	5.06	300
In I	325.86	4.08	300
Cu I	327.40	3.78	2500
Ti II	336.12	3.71	600
Ag I	338.29	3.66	2800
Zn I	330.26	7.78	90
Co I	345.35	4.02	1300

tegrated evaporation curves, respectively [28]. For this purpose the series of spectrograms is made by cassette moving method, or by gradually changing S- [29] or *T*- [30] diaphragms of the spectrograph. In order to gain more data to plotting curves $I = f(t)$, spectra were recorded by moving continuously with a rate of about 1 mm/s the cassette of the spectrograph PGS-2 in the full height of the plate, what corresponded to exposure time 76 s. The spectra were evaluated photometrically each by 2 mm, at small slit height, obtaining the density data in intervals of 2 s and from these by means of the *l*-transformation the suitable intensity values, respectively. Evaporation processes were studied by graphite (SU) and carbon (SW) carrier electrodes, the main characteristics of electrodes in Fig. 8, the used spectral lines and their chief features on Table V are shown. Partly based on literature data [6, 8, 13], partly on our own experiences [14, 15] as reference element Pd (to elements evaporating hardly and in average measure) and In (to easily evaporating elements) were used.

Shape of volatilization curves proves that the evaporation of Pb, Bi and In are similar (Fig. 9); the same is holding for Cu, Sb and Zn, though evaporation of In is the fastest among the elements listed. The course of evaporation of the Sn, Mo, Fe and Pd is similar (Figs 10 and 11), the same is the situation with Co, Ni and Ti. With good approximation V and Pd (Fig. 10) were found to volatilize similarly, just as in the case of Ag and Cr. A fully different situ-

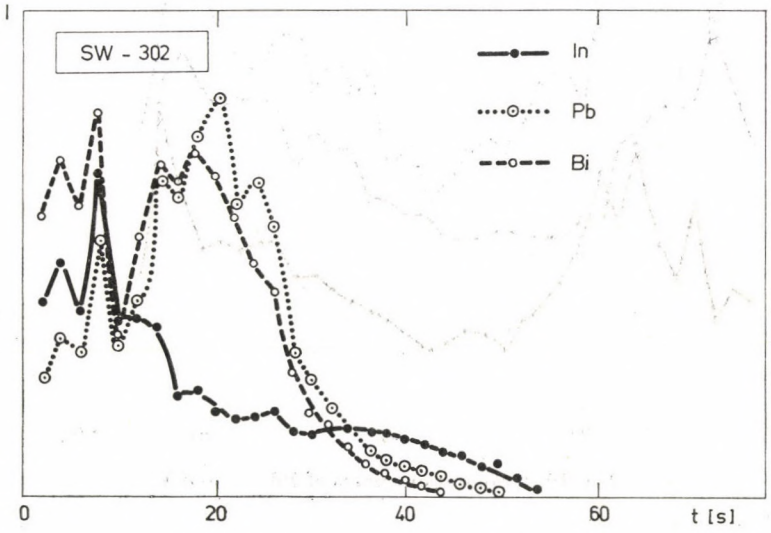

Fig. 9. Evaporation curves of In, Pb and Bi

ation is offered by the comparison of the volatilization of Mn and Pd, Mn and In, respectively (Fig. 12). Volatilization of Mn does not resemble neither to that of Pd, nor of In. This is also justified by Fig. 13 representing a correlation of intensities changing in time of the analysis and reference elements on the basis of correlation coefficients r. It can be observed that Pd is a favourable reference element to some elements (Co, Fe, Mo, Ni), while to others (Cr, V, Ti) the correlation can be still accepted in the period of exposure during which In is volatilizing. In the case of Mn a suitable correlation is got only with background intensity I_U measured beside the line. Correlation of intensity values was investigated also by electrodes made of other materials (graphite — SU) (Fig. 14). However, out of 10 cases in 7, the application of carbon (SW) electrodes is more favourable. A further experimental experience is that in the case of carbon electrode the arc is burning much more quietly and evenly during the whole exposure time. The appropriate reference elements and electrode types have been chosen on the basis of above results.

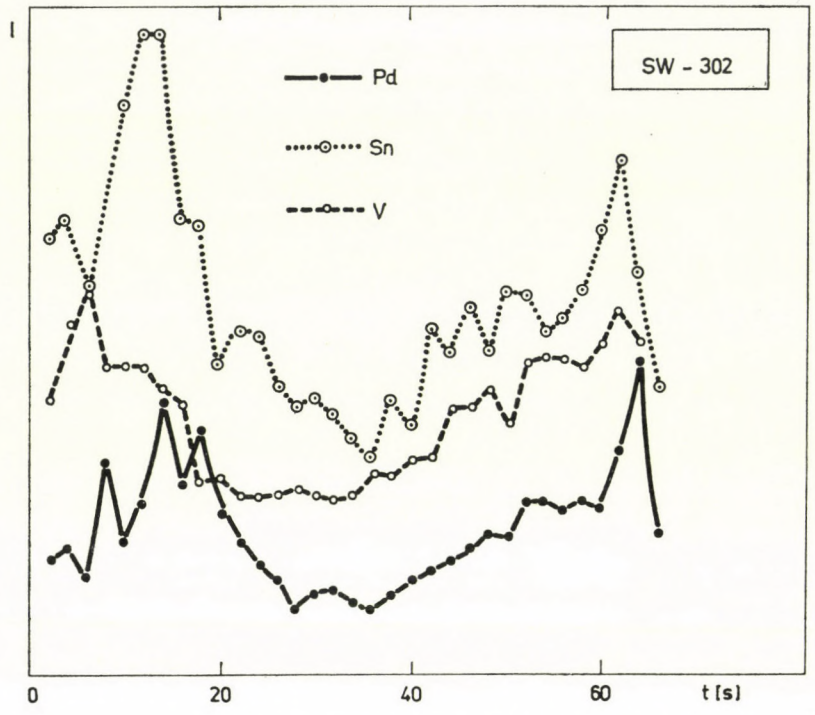

Fig. 10. Evaporation curves of Pd, Sn and V

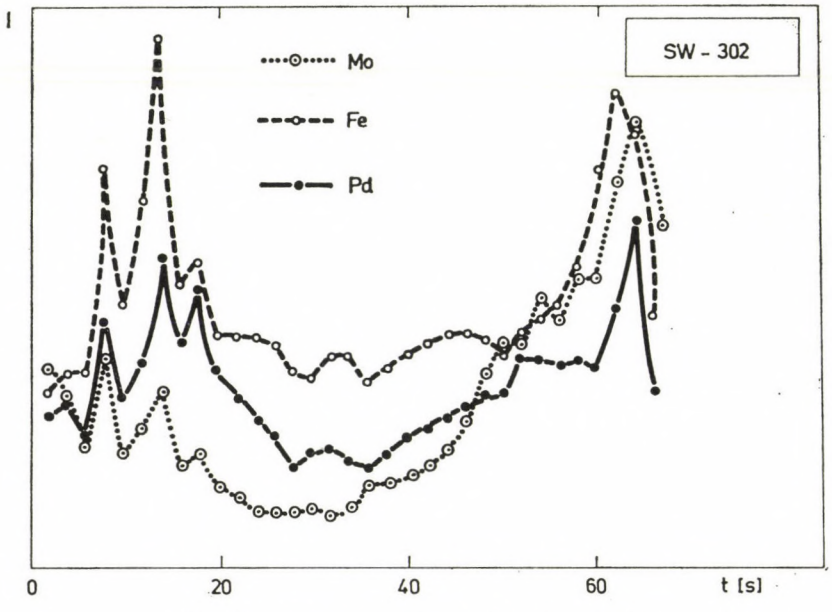

Fig. 11. Evaporation curves of Mo, Fe and Pd

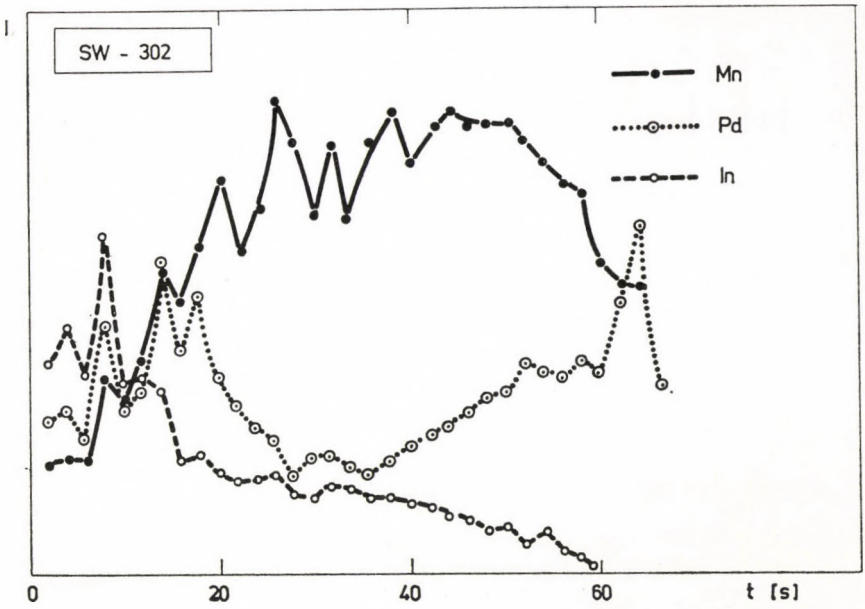

Fig. 12. Comparison of the evaporation curve of Mn with those of Pd and In, respectively

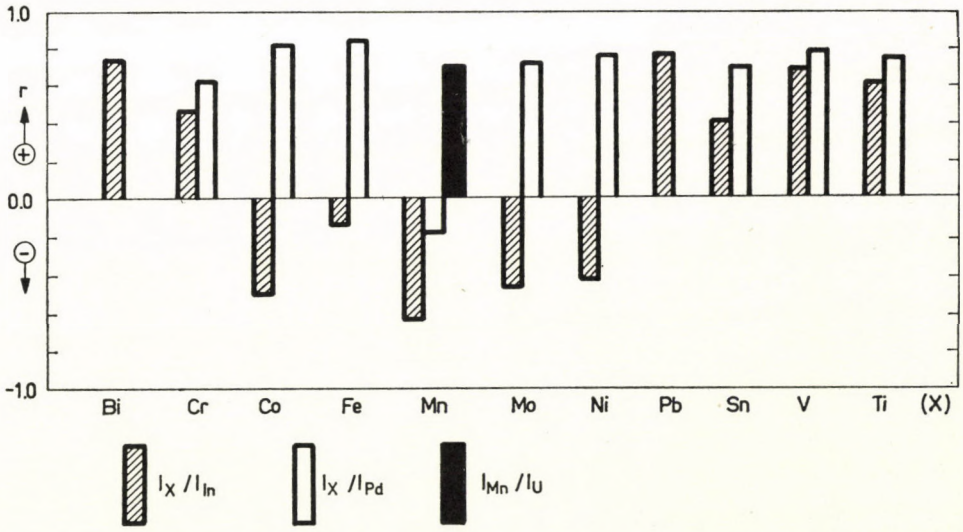

Fig. 13. Correlation coefficients characterizing the correlation between intensities of analysis and reference elements

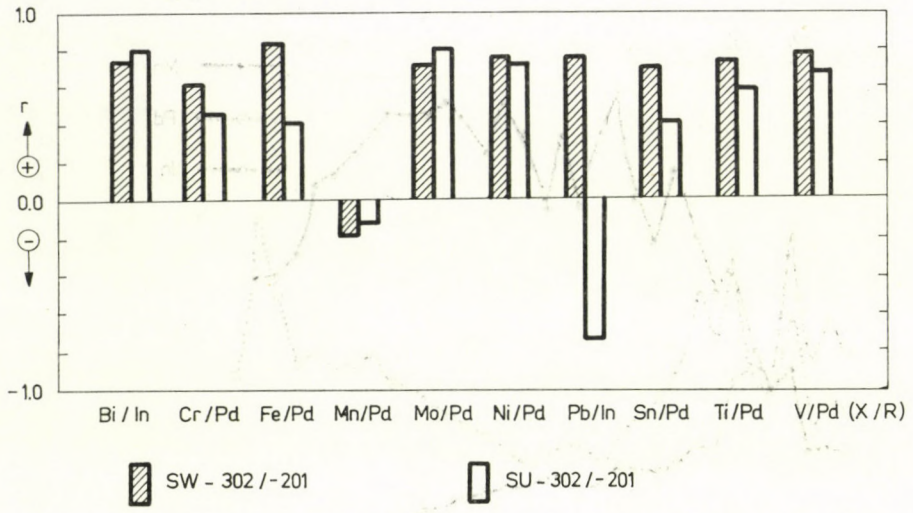

Fig. 14. Correlation coefficients characterizing the correlation between intensities of analysis and reference elements when applying 2 different types of electrodes

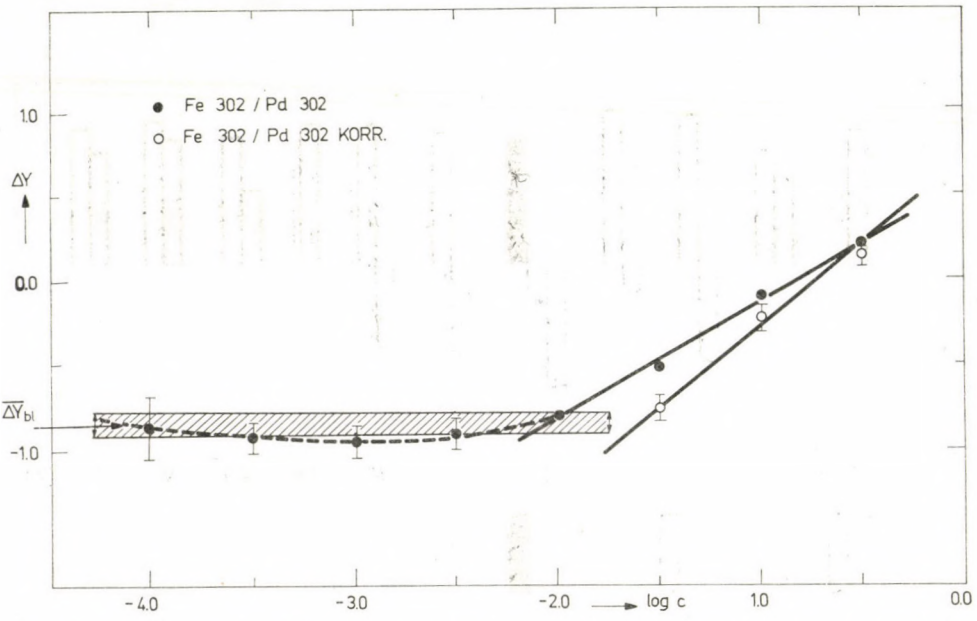

Fig. 15. Shape of analytical curves of line pair Fe/Pd using blank correction (KORR)

3. Evaluation of the method elaborated

Prior to discussion of the concrete results a short survey is given on the methods of evaluation, and the chosen evaluating parameters are defined which play an important role in the discussion of results achieved by optimated evaluation.

Course of evaluation

The first step of the evaluating process is the density transformation. The *l*-transformation [25] was applied, the gradation γ of the spectral plates and transformation constant k were determined with the help of a computer, as reported earlier [31].

For quantitative analysis the analytical curves were applied in the following form:

$$\Delta Y = A_{X,R} + B_X \log c_X \tag{1}$$

9 standard samples — prepared on the way described earlier — served to their plotting. These standard samples contained the elements to be determined in 1.0—0.316—0.1—0.0316—0.01—0.00316—0.001—0.000316—0.0001%. Five parallel spectrograms were made on each sample, the constants and the other important parameters of linear part of the analytical curves were calculated by means of a computer [32].

The value of detection limit [33] essential in trace analysis was determined on the basis of the mean value of background intensity near the given spectral line and its standard deviation, respectively, on the spectrum of the sample of lowest concentration — as suggested by MATHERNY [34].

In the lack of suitable reference samples of natural origin, accuracy of the method elaborated was investigated by 2 synthetic control samples containing the elements to be determined in 0.0658 and 0.00658%, respectively. By samples 3 parallel spectra were recorded. Concentration values were calculated by using suitable computer program. Some dust deposit samples being at our disposal were similarly analysed.

Evaluating parameters of efficiency

For the comparison of various spectrographic methods and for the evaluation of their efficiency the following parameters are suggested [23]:

a) the *relative sensitivity* of the method which is expressed by the slope B_X of the analytical curve [35], optimally $B_X = 1$,

b) standard deviation characteristic of the *relative precision* of the method [36]

$$s_c/c(\%) = \frac{2.3\, s_{\Delta Y}}{B_X} \cdot \sqrt{\frac{1}{N} + \frac{1}{K}} \tag{2}$$

where N is the number of calibration concentrations and K is the number of parallel measurements performed by concentrations,

c) Detection power of the method can be characterized by the values of *detection limits* of the single elements.

In addition to these the statistical test of linearity [32] is also important, this serves to decide whether the experimental points surely lie on a straight line or not. The test is destined for to compare the standard deviation of points determined experimentally related to the theoretical regression line with the sum of standard deviations of the repeated measurements.

From the point of view of the actual task a further important factor is the concentration range which can be covered by linear analytical function, *i.e.* well applicable for the analysis. Namely, determination of such a concentration is not advisable by the given method, which lies considerably out of the range limited by values $c_{max} - c_{min}$.

As it is commonly known the exactness of the analytical method is determined by its precision and accuracy [37]. Precision of the method is given either by s_c/c value or on the basis of repeated analysis of the samples to be analysed:

$$s_c^*/c(\%) = \frac{s_c}{\bar{c}} \cdot 100 \tag{3}$$

where s_c is the standard deviation of the repeated determinations. Accuracy of the method is checked by the analysis of control samples (in optimal case etalons). In our case the following parameter was used for this purpose:

$$\Delta c(\%) = \frac{|c_{calculated} - \bar{c}_{measured}|}{c_{calculated}} \cdot 100 \tag{4}$$

Discussion

The evaluating parameters and data are summarized in Table VI. It can be seen that out of 16 line pairs used (at Cu, 2 line pairs were applied: the spectral line of Cu at 282 nm at higher, while that of Cu at 327 nm at lower concentration ranges) only in 4 cases was the *upper limit* (c_{max}) *of the concentration range* of linear part of analytical curve equal with that of the concentration range examined (1.0%). This is partly caused by the bending of calibration curves due to self-absorption (it is valid, however, only for 4 cases) on the other hand, the high density values are measured inaccurately (the traditional microdensitometer type G II is able to reliably measure density only as high as 1.7). In this respect necessarily an improvement is expected by applying the optimated evaluation.

Table VI

Values of evaluating parameters

Line pair	Ag 328 / Pd 325	Bi 306 / In 303	Co 345 / Pd 325	Cr 302 / Pd 302	Cu 282 / In 303	Cu 327 / In 325	Fe 302 / Pd 302	Fe 302* / Pd 302	Mn 279 / Pd 302
c_{max} (%)	0.01	0.1	0.316	0.1	1.0	0.0316	0.316	0.316	0.0316
c_{min} (%)	0.000316	0.00316	0.00316	0.001	0.1	0.000316	0.01!	0.0316	0.001
B_X	0.738	0.884	0.841	0.973	0.644	0.803	0.675	0.930	0.805
s_c/c (%)	14.4	12.0	14.1	5.8	17.5	16.3	6.6	10.7	6.3
$\underline{c}$ (ppm)	0.3	13	46	7.6	110	1.1	(1.8)	—	4.0
Δc (%) I.	—	12.8	29.1	13.9	—	—	6.6	20.4	—
II.	9.8	21.2	21.4	8.1	—	89.9!	—	—	14.4

Line pair	Mo 313 / Pd 325	Ni 300 / Pd 302	Pb 283 / In 303	Sb 287 / In 303	Sn 286 / Pd 302	Ti 336 / Pd 325	V 318 / Pd 325	Zn 330 / In 325	
c_{max} (%)	0.0316	0.316	0.1	1.0	1.0	0.316	0.1	1.0	
c_{min} (%)	0.001	0.00316	0.001	0.1	0.00316	0.01	0.00316	0.1	
B_X	0.904	0.790	0.643	0.787	0.919	1.044	0.960	0.720	
s_c/c (%)	9.8	14.1	13.7	11.0	6.4	8.4	5.0	13.6	
$\underline{c}$ (ppm)	3.6	8.4	5.4	102	16	26	10	1400	
Δc (%) I.	—	6.5	—	—	6.0	22.4	1.4	—	
II.	2.3	25.5	11.1	—	7.1	16.5	8.1	—	

* Data obtained with blank correction

The lower limit of the concentration range examined (0.0001%), however, is corresponding to the range of determined detection limit values. The $\underline{c}$ value calculated was found to be less than this value only in a single case (Ag), and in another case (Cu) it approaches this value. At all of the other elements the *lower limit of the concentration range* (c_{min}) covered by a linear analytical curve is higher than this value by one (Cr, Mn, Mo, Pb), one and a half (Bi, Co, Ni, Sn, V) and even more orders of magnitude. Especially unfavourable values have been obtained for Sb and Zn, and the appropriate $\underline{c}$ values were similar, too.

A special case is presented by the analytical curve of Fe/Pd line pair (Fig. 15), which is deviating from linear line under concentration 0.01% due to the blank value, and is practically horizontal. It is presumably caused by the iron contamination of the "spectroscopically pure" compounds and auxiliary electrodes, respectively. These establishments are supported by the shape of the calibration curve calculated by blank correction (Fig. 15), and the values of their parameters, respectively. However, from the point of view of the method elaborated the above circumstance does not cause a drawback, since in the given samples the expected Fe-content falls mostly into the range of higher concentrations. This fact is also referred to by literature data indicating Fe as main component [5, 8, 9].

The *relative sensitivity* of the method scarcely reaches the optimal $B_X = 1$ value (Cr, V and Ti), in some cases it is considerably smaller than 1 (Ag, Cu, Mn, Ni, Pb, Sb and Zn). By the application of the optimated evaluation improvement can be expected also in this field, as the photometric error caused by scattered light occurring at higher densities is not negligible.

The *relative precision* (s_c/c) obtained for the analytical curves of the individual line pairs is lower than $\pm 15\%$ except one case (Cu) and in 7 cases than $\pm 10\%$. The s_c^*/c values (Table VII) calculated on the basis of the results

Table VII

Relative precision of analyses

Element	Ag	Bi	Cr	Cu	Mn	Mo	Pb	Sn	Ti	V
s_c^*/c (%)	14.0	12.9	10.1	9.2	13.1	7.1	21.0	9.1	12.4	8.8

of concrete analyses are somewhat higher, but even they remain below $\pm 15\%$, with the exception of Pb. The results achieved can be qualified as satisfactory, and by all means much better than those given for this method in the literature of environmental pollution control [1, 2].

Δc values characterizing the *accuracy of method* are similarly acceptable. The only exception is repeatedly the Cu. Both evaluating parameters can be

improved to a certain extent when introducing the optimated evaluation, owing to photometric evaluation resulting in more correct values.

Values of *detection limits* do not exceed 10 ppm in the half part of the elements examined. Further optimation of the values obtained can be achieved by using a more sensitive and contrasty emulsion. Because of the enlarged measuring range ($S = 4.0$) no objections can be made against these kinds

Table VIII

Characterization of the method elaborated

Element	The determined concentration values in x cases from 15 are			
	$X < \underline{c}$	$\underline{c} < X < c_{min}$	$c_{min} < X < c_{max}$	$X > c_{max}$
Ag	7	4	4	—
Bi	—	6	4	5
Cr	—	—	10	5
Cu	—	—	11	4
Fe	—	—	—	15
Mn	—	—	1	14
Mo	15	—	—	—
Ni	15	—	—	—
Pb	—	—	15	—
Sb	15	—	—	—
Sn	—	4	11	—
Ti	—	—	12	—
V	—	1	14	—
Zn	15	—	—	—

of emulsions (owing to the considerably higher γ-values the concentration range to be examined decreases).

Our method elaborated has been applied for the analysis of 15 dust deposit samples being at our disposal. Data summarized in Table VIII. also serve the characterization of the method. These data grouping the experimental results show that in the case of some elements (Fe, Mn, partly Bi, Cr and Cu) the upper limit of the presently examinable concentration range, while in other cases (Mo, Ni, Sb and Zn) the detection power of the method should be improved. Question of detection power can not be discussed from the point of view of detection limits to be achieved, since no data — defining the minimal trace element concentrations in aerial dust deposits — are available, as it is in the case of drinking water.

*

The authors are indebted to Prof. K. ZIMMER, D. Sc., for his valuable comments.

REFERENCES

[1] MALISSA, H., GRASSERBAUER, M.: Mikrochim. Acta, **1975 II,** 325
[2] SACKS, R. D., BREWER, S. W.: Appl. Spectrosc. Rev., **6,** 313 (1973)
[3] HARTKAMP, H.: Staub-Reinhalt. Luft, **34,** 12 (1974)
[4] ZADUBAN, M.: unpublished data
[5] ALEXANDROV, N. N., GUNIYA, G. S., GUNTSHENKO, A. I., TURKIN, Yu. I.: Trudy GGO, **314,** 104 (1974)
[6] AUGUSTIN, J.: Diploma Work, Košice, 1976
[7] PÉTER, F., JENEY, E., NAGY, Z.: Egészségtudomány, **7,** 52 (1963)
[8] SUGIMAE, A.: Anal. Chem., **46,** 1123 (1974)
[9] GEGUS, E.: private communication
[10] MATHERNY, M.: Chem. Analityczna, **21,** 339 (1976)
[11] FLÓRIÁN, K.: Kémiai Közl., **48,** 347 (1977)
[12] MATHERNY, M.: Chem. Analityczna, **21,** 1053 (1976)
[13] SUGIMAE, A.: Appl. Spectrosc., **28,** 458 (1974)
[14] FLÓRIÁN, K., PLIEŠOVSKÁ, N.: Zborník vedeckých prác VŠT v Košiciach (in press)
[15] FLÓRIÁN, K., ZIMMER, K.: Proc. XXI. Annual Hung. Symp. on Spectral Analysis, Szeged, 1978, p. 59
[16] FLÓRIÁN, K., PLIEŠOVSKÁ, N.: Chem. Analityczna, **23,** 575 (1978)
[17] KAISER, H.: Spectrochim. Acta, **3,** 40 (1947)
[18] LAQUA, K.: Z. anal. Chem., **221,** 44 (1966)
[19] EHRLICH, G.: Proc. XIV. Coll. Spectrosc. Internat., Debrecen, 1967, 237
[20] ZILBERSHTEIN, Kh. I.: Spektralniy analiz chistih vesshestv, Khimiya, Leningrad, 1971, 70
[21] GERBATSCH, R.: C. Sc. Thesis, GEOCHI, 1967
[22] GERBATSCH, R., KRASNOBAEVA, N.: Izv. IONCH, **5,** 13 (1967)
[23] FLÓRIÁN, K., FLÓRIÁNOVÁ, K., MATHERNY, M.: Acta Chim. Acad. Sci. Hung., **82,** 403 (1974)
[24] FLÓRIÁN, K., MATHERNY, M.: Acta Chim. (Budapest), **94,** 183 (1977)
[25] TÖRÖK, T., ZIMMER, K.: Quantitative Evaluation of Spectrograms by Means of *l*-Transformation, Heyden, London and Akadémiai Kiadó, Budapest 1972
[26] TÖRÖK, T., MIKA, J., GEGUS, E.: Emission Spectrochemical Analysis, Adam Hilger Ltd., Bristol and Akadémiai Kiadó Budapest 1978, 114
[27] *ibid.*, 254
[28] PLŠKO, E.: Chem. Zvesti, **18,** 830 (1964)
[29] PLŠKO, E., KUBOVÁ, J.: Chem. Zvesti, **27,** 781 (1973)
[30] FLÓRIÁN, K.: Chem. Zvesti, **28,** 306 (1974)
[31] FLÓRIÁN, K., HELTAI, Gy., ZIMMER, K.: Magy. Kém. Foly. **85,** 266 (1979)
[32] FLÓRIÁN, K., LAVRIN, A., MATHERNY, M.: Chem. Zvesti **27,** 623 (1973)
[33] ZIMMER, K.: Proc. XX. Coll. Spectrosc. Internat., Praha, 1977, Invited lectures II., 17
[34] MATHERNY, M.: Z. anal. Chem., **271,** 101 (1974)
[35] de GALAN, L.: Spectrosc. Lett., **3,** 123 (1970)
[36] LAVRIN, A.: C. Sc. Thesis, VŠB Ostrava, 1975
[37] ECKSCHLAGER, K.: Chem. Listy, **67,** 19 (1973)
[38] ZAYDEL, A. N., PROKOF'EV, V. K., RAYSKIY, S. M., SLAVNIY, V. A., SHREYDER, E. J.: Tablitsi spektralnih liniy, Nauka, Moscow, 1969
[39] ADDINK, N. W. H.: D. C. Arc Analysis, Philips Technical Library, 1971

K. FLÓRIÁN
N. PLIEŠOVSKÁ
Katedra chémie HF-VŠT, CS-04385 Košice, Švermová 9

RECENSIONES

E. H. ANDREWS, P. E. REED, J. G. WILLIAMS and C. B. BUCKNALL

Advances in Polymer Science, Vol. 27
Failure in Polymers, Molecular and Phenomenological Aspects

Springer Verlag, Berlin, Heidelberg, New York, 1978
153 pages, 97 figures, 2 tables, 216 references

This volume consists of three separate chapters, covering three distinct but complementary aspects of the fracture of polymers.

The first chapter: "*Molecular Fracture in Polymers*" by E. H. ANDREWS and P. E. REED starts with a very brief summary of the different theories of fracture and their development. The authors then review the experimental methods of the detection of structural changes in materials under stress. Special emphasis is laid on electron spin resonance, as it gives direct information about the rupture of the polymer chain, but other methods such as infrared spectroscopy, low angle X-ray scattering *etc.* are also mentioned. This chapter gives a clear qualitative picture about the role of molecular fracture in the failure of polymeric solids.

The second chapter, "*Applications of Linear Fracture Mechanics*" was written by J. G. WILLIAMS. The reader is step by step introduced to fracture mechanics of perfectly elastic materials. The modifications necessary to apply the results of the above theory to the brittle fracture of polymers are discussed in detail and some examples of application are shown. The author deals with the time dependence of crack growth, temperature and environmental effects, fatigue and impact testing. For the reader who is not familiar with general fracture mechanics it may be advantageous to read this chapter first.

The third chapter "*Fracture and Failure of Multiphase Polymers and Polymer Composites*" was written by C. B. BUCKNALL. In this chapter the special problems of fracture of filled polymers are shown. Plastics filled with rigid particles, rubbers and voids *(i.e.*, polymeric foams) are treated but fibers are excluded. The mechanism and kinetics of yielding is discussed in detail and the applicability of linear elastic fracture mechanics and ductile fracture mechanics is investigated. The author also emphasizes that several basic questions of this field have to be answered in the future.

This book does not cover all aspects of failure of polymers, but all three chapters on their own are good reviews of their field. The book is valuable not only for polymer scientists but also for engineers who meet the everyday problems of polymer application.

T. T. NAGY

M. W. RANNEY: *Fuel Additives for Internal Combustion Engines Recent developments*

Chemical Technology Review No. 112.
Energy Technology Review No. 30.
Noyes Data Corp.,
Park Ridge, N.J. U.S.A. (1978)

This recent book of the Noyes Data Corporation presents the review of the latest developments on the field of fuel additives, based — similarly to the earlier publications of the series — on the more than 200 U.S. patents issued between January 1975 and February 1978 in this field.

Fuel additives as chemical compounds are chemically very diverse. Thus the author also follows the usual way, arranging and describing the various types of fuel additives according to their functions. In this way, one chapter is devoted to each of the following groups:

— detergents and anti-icing additives
— flow improvers and pour depressants
— oxidation and corrosion inhibitors
— octane improvers and anti-knock compounds
— antistats, biocides, dyes and other special additives.

Combustion aids and fuel compositions are dealt with in a separate chapter.

In the introduction of each chapter a short description is given on those combustion or other engine problems which necessitate the use of additives with the given function. This introduction is followed by the review of the separate patents, arranged into groups on the basis of types of chemical compounds. Patent examples and experimental data showing the effectiveness of the given additives are also frequently included in the review.

As it is declared in the foreword of the book, there has been no bias in the selection of patents for inclusion, practically all patents issued on the subject in the United States during the period mentioned above are reviewed and included. In accordance with the purpose of the book no comparative evaluations of the additives or fuel compositions are given by the author, but only descriptive informations are offered. At the same time, by indicating all the information that is significant and eliminating legal jargon and juristic phraseology, the descriptions together with the included data make possible for the reader to make comparisons and evaluations in many cases.

This publication of the Noyes Data Corporation presents a valuable review of a very diverse research and development field, describing its latest results in well arranged, easy to handle form. For experts dealing with fuel additives — and with additives for the petroleum industry in general — the book can be used as a handbook, saving a lot of time and energy for it's user. On the other hand it is a very useful book for the expert who is just interested as it provides a comprehensive picture of the research and technological developments on the field of fuel additives.

The book contains 300 pages, 5 figures and several tables in the text. Indexes of the reviewed patents by company, inventor and patent number help in providing easy access to the information contained.

I. SZEBÉNYI

Advances in Polymer Science, Vol. 29

Structure and Properties of Polymers
(Springer Verlag, Berlin—Heidelberg—New York, 1978)

This volume of the series contains three treatises. The first is about photoconductive polymers, the second discusses the characterization of graft polymers and the third deals with the preparation and study of block copolymers with ordered structures.

These topics are rather divergent, thus are better studied one by one.

1. *Polymers with Photoconductive Properties.* Milan STOLKA and Damodar M. PAI (Xerox Corporation, Rochester), 46 pages, 159 references.

A survey of the photoconductivity of organic polymers is given. Photoconductivity is the increase of conductance in consequence of the irradiation of a solid phase. This phenomenon is composite and its occurence requires the simultaneous realization of several processes, *viz.* the formation of charge carriers and the migration of charges due to an external field. Following the elucidation of fundamental principles and the description of the experimental techniques suitable for the measuring of this phenomenon, the mechanism of the formation of these charge carrier particles is explained, poly *N*-vinylcarbazole PNVC and a 1 : 1 mixture of PNVC with 2,4,7-trinitro-9-fluorenone TNF serving as examples. The migration of charged particles in an electrostatic field depends on the chemical composition of the polymer film.

Photoconductive polymers can be classified as follows.

a) Polymers highly conjugated in their principal chain. These can be used in visible light and in the near-infrared region of the spectrum.

b) Polymers with a condensed aromatic group within the principal chain or bound to it. Generally, these polymers are photoconductors only in the ultraviolet region below 400 μm

since it is radiation in this region which these substances absorb; in other ranges they are charge carriers only.

c) Various compounds which contain substituted aromatic amino groups. These too are photoactive in the region below 400 μm and include the majority of substances used in electrophotography.

A wide range of industrial applications is open to these photoconductive organic polymer systems though the fundamental theoretical information concerning them is far from complete as yet.

2. *Characterization of Graft Copolymers.* Y. IKADA, 46 pages, 36 references.

In the case of graft copolymerization, the product is a mixture of homopolymer A, homopolymer B and graft copolymer AB. The effective means of how to separate the graft copolymer and how to determine its purity, are described. Also the determination of the number of branchings and of the lengths of lateral chains in the graft copolymer, as well as the characterization of the skeleton polymer are discussed.

Frequently, characterization by means of statistical computation is much more simple than by means of experimental work. Such a description of the product is successful provided that reliable data concerning the probability of the grafting of the monomer onto the polymer skeleton are known.

Selective precipitation and extraction can be used for the separation of the graft copolymer. According to experiments, selective precipitation is a suitable technique when it effects the precipitation of poly-A and poly AB, *i.e.* the graft copolymer, and leaves poly-B dissolved. If a theta solvent is found whose theta temperatures for the two homopolymers are widely different, precipitation can be effected by changing the temperature of the solution.

Extraction with the help of selective solvents seems to be simpler, though this technique is timeconsuming. In practice, the graft copolymer may dissolve, owing to the formation of micelles, also in a solvent that dissolves but one of the homopolymers. When separating the homopolymer from the graft copolymer, the microstructure of the product must be taken into account.

There are but few methods suitable for the determination of the purity of a graft copolymer after its separation, such as density gradient ultracentrifuging and thin-layer chromatography (TLC). Turbidimetry, ultraviolet, infrared and NMR spectroscopy cannot be said to be reliable in this application. TLC is easier to carry out than ultracentrifuging, consequently, this method is more general.

The most important data concerning the chemical structure of a separated and purified graft copolymer reveal the number of branchings and the molecular masses of the skeleton and of the lateral chains, respectively. Generally, one has to be content with average figures since the recording of distributions is a very complicated job and very often cannot be carried out at all. The determination of these figures is illustrated by means of three examples: redox graft copolymerization, irradiation graft copolymerization, and the case of a graft copolymer prepared *via* the coupling reaction of prepolymers.

Surface grafting belongs into a separate group: here grafting occurs on the surfaces of films, fibres, or plastics bodies, and the usual methods cannot be applied or only with modifications.

In the case of graft copolymers where biologically active substances, *e.g.* proteins, hormones or polysaccharides become bound to natural or synthetic polymers, also the nature of the chemical bond between the two polymers of different kind must be defined; further, the configuration of the graft biopolymer and its denaturation should also be known. A noteworthy instance of such copolymerization is the fixation of enzymes: the industrial utilization of this is highly important.

3. *Preparation and Study of Block Copolymers with Ordered Structures.* R. BERNARD and M. GALLOT, 129 pages, 285 references.

One of the main endeavours of polymer chemists is the synthesis of novel substances which are eminently applicable for given specific purposes. The use of novel monomers, each for a separate instance of application, is not feasible, thus mixtures of polymers have been resorted to in the last twenty years. However, polymer mixtures which would possess all the required qualities cannot be produced because the incompatibility of the components. This difficulty can be surmounted by creating covalent bonds between them and thus producing block or graft polymers. In these, the incompatibility of the polymer chains is turned to advantage: separation by phases in the blocks produces the micro-domains which are responsible for the specific properties of these block polymers. For instance: a combination of rubber-elastic and thermoplastic blocks produces a polymer which is rubber-elastic at room temperature but is a melt at elevated temperatures and can be worked like a thermoplastic polymer.

The review discusses only properties of block polymers which are relevant to this micro-domain structure.

Syntheses of copolymers are feasible either by making homopolymer A react with monomer B, or by making homopolymers A and B react with each other. The techniques themselves are manyfold; the majority of block polymers are made by anionic polymerization.

The structure of a block polymer is studied mostly by X-ray diffraction or electron microscopy. The micro-domains or regions have the form of platelets, rods or globules, depending on the per cent composition of the copolymer. As far as their sizes are considered, the micro-regions are surprisingly regular: electron microscopy shows this clearly.

The copolymers which contain only amorphous blocks can be divided into three principal groupes, *viz.* block copolymers with polybutadiene, those with polyisoprene, and those with no polydiene content.

A separate group among copolymers with amorphous and crystallizable blocks is that of multiblock and multiphase polymers with polyurethane segments: in these, hard segments alternate with soft ones and thus various mechanical properties can be realized. However, polyurethane block copolymers do not posses a regular periodic structure, thus are not dealt with in any detail in this discussion.

Other copolymers composed of amorphous and of crystallizable blocks have well ordered periodic structures. In this group belong polystyrene-poly(ethylene oxide) (SEO), polybutadiene-poly(ethylene oxide) (BEO) and similar block copolymers. The phase diagrams of these always show two phases: at temperatures higher than the melting point of the crystallizable chains they show either a hexagonal or a lamellar structure, at temperature lower than the melting point, they crystallize via folding of the crystallizable chains. The crystal structure that emerges depends also on the solvent, *i.e.* whether the solvent of the crystallizable or that of the amorphous phase is used. The periods of chain folding can be substantially affected by the choice of conditions.

The copolymer which contains polyvinyl blocks and hydrophobic polypeptide blocks, and that which contains saccharide and polypeptide blocks and has been prepared by the team working with the author, may become quite important from the view point of biology.

This volume informs about three new fields in which progress is quite rapid. The summaries prepared by leading authorities greatly facilitate orientation for readers interested in these topics.

G. BODOR

Ch. S. SODANO: *Vitamins, Synthesis, Production and Use. Advances since 1970*

Chemical Technological Review No. 119. 305 pages
Noyes Data Corporation, Park Ridge, New Yorsey, USA 1978

The series published by the Noyes Data Corporation including the present volume, a technological summary dealing with vitamins, is based essentially on USA patents and has a double purpose: it gives detailed information for both the industry (including research institutes) and commerce, not only on the newest procedures patented, but also about the methods and possibilities of use. The subject-matter has remained, to a large extent, un-published in periodicals, thus the book supplies a want in the modern process of the development of industry, although the rather long period of patenting is certainly a hidrance to rapid practical application. On the other hand, the Noyes Company reduced the time required for publishing the book by the use of a novel printing technique to allow quick applicability of the procedures.

The book dealing with nearly 270 patents actually consists of two main parts: in the first part the knowledge patented since 1970 regarding the most important prosthetic and inductive vitamins is summarized in such a way that, beyond the synthesis of a given vitamine, the preparation of its isomeric and other derivatives, the relevant problems in medical, nutritional and veterinary hygienic sciences, industrial formulation methods and stabilization possibilities are also treated. Thus information is offered for the solution of many problems which may appear as a faraway research project to some research institutes. Special attention should be paid to the results obtained in enriching food, nutriments, baby food and fodder with vitamins, and in maintaining the quality of the enriched food, which can lead to reductions in the development costs in some important economic sections. The text is free from special legal terms it can easily be understood; of course, detailed information cannot be always given,

but the descriptions are suitable for calling attention to many facts and serve well as a guide how to look for some actual answer.

The second part of the book deals with combinations of vitamins and offers a very interesting picture of the broad field where vitamins can successfully applied today. This field is very heterogeneous, as illustrated by a few examples. Thus, vitamin combinations have been developed for the rapid curing of *Herpes simplex*, for reducing or stopping the smoking or drinking habit, *etc.* Several combinations have been patented for increasing the deliciousness of food stuffs, mainly sweets, *e.g.*, of breakfast cereals, jellies, soft drinks, and for preventing fat-containing products from becoming rancid, *etc.* In this part the packing and marketing methods of vitamin mixtures is also discussed often representing very practical solutions for a given application *e.g.*, patents are reviewed dealing with the novel preparation of injections, or with the dispersion of an inductive (fat-soluble) vitamin mixture in a simpler way than before. Other patents are concerned with the reduction of the smell of vitamin combinations, with the controlling of their absorption and of the time required for it, and with the elimination of some defects of pills containing vitamins.

The examples mentioned seem to be enough to indicate the richness and variousness characteristic of the review. It must be emphasized again, however, that the value of the book is the richness of topics; the possibility of actual realization must be determined by the virtual user in the knowledge of his own aims. In view of all these, the book is a useful help for experts dealing with vitamins. The book contains a very good table of contents, an author index, patent index and a list of the patentee companies. The book, with its fine getting up, is a good supplement to the recently rather scarce literature of vitamin technology and application.

É. BERNDORFER-KRASZNER

INDEX

PHYSICAL AND INORGANIC CHEMISTRY

ORGANIC CHEMISTRY

ANALYTICAL CHEMISTRY

Printed in Hungary

A kiadásért felel az Akadémiai Kiadó igazgatója — Műszaki szerkesztő: Zacsik Annamária

A kézirat nyomdába érkezett: 1979. IX. 19. — Terjedelem: 10,15 (A/5) ív, 62 ábra

80.7513 Akadémiai Nyomda, Budapest — Felelős vezető: Bernát György

M. Nógrádi

STEREOCHEMISTRY: BASIC PRINCIPLES AND APPLICATIONS

Going well beyond the level of introductory textbooks, but not burdening the reader with details required only by the specialist, this book has been designed for those who wish to widen their knowledge of stereochemistry and bring it to an up-to-date level. The subject matter includes a modern summary of the fundamentals, static stereochemistry, a description of methods determining the configuration, resolution and dynamic stereochemistry, a thorough treatment of the main types of conformational motions. Great attention is paid to problems of stereoselectivity and its role in concerted reactions and also in enzymic reactions. A brief treatment of the stereochemistry of polymers and inorganic complexes completes this concise and modern book.

In English – Approx. 270 pages – 17×25 cm – Cloth
ISBN 963 05 2022 2

AKADÉMIAI KIADÓ, Budapest **PERGAMON PRESS, Oxford**

B. Beke

The Process of Fine Grinding

Manuals of mineral dressing generally say little or nothing about the processes taking place in the material to be comminuted although the purpose of the operation is to enhance wanted or avoid unwanted changes in the material. The object of this monograph is to supply this information. The sequence of ideas is applicable to the grinding of all brittle materials. This book should thus be of interest to the plant- and research workers of many industries, covering e.g. cement, ceramics, ore and coal dressing, chemistry, colours, pharmaceuticals, etc. The problems of cement grinding and those of ball milling are explained in more detail. The main chapters are: granulometry, grinding kinetics, energetics, grindability, classification, perspectives. The problems of energy consumption, relative investment costs and availability are discussed for all sorts of equipment.

In English – Approx. 120 pages – 88 figures – 17×25 cm – Cloth

ISBN 963 05 2071 0

AKADÉMIAI KIADÓ,
Publishing House of the Hungarian Academy of Sciences
Budapest

ACTA CHIMICA

ТОМ 103—ВЫП 3

РЕЗЮМЕ

Новый метод определения активности ферментов

Э. НОСТИЦИУС, Д. КАЛЬМАР и З. НОСТИЦИУС

Описывается применение детектора ионизации пламени (ДИП) для измерения активности на примере уреазы. Метод уникально применим для исследования скоростей ферментативных реакций, сопровождаемых выделением CO_2. Двуокись углерода вытесняется из реакционной смеси с помощью H_2 и метанизируется в каталитическом реакторе. Концентрация образующегося метана измеряется с помощью ДИП. В стационарном состоянии измеряемый ток ионизации строго пропорционален скорости реакции.

Фторированные стероиды, I
3-Фтор-5,6-ненасыщенные производные

А. НЕДЕР, А. УШКЕРТ, Е. НАДЬ, Ж. МЕХЕШФАЛВИ и Й. КУСМАНН

Детально была изучена реакция обмена OH—F 3-гидрокси-прегн-5-ен-20-она **(13)** с FAR (4). Наряду с 3 β-фторопроизводными **18**, эфир **15**, 3,3'-эфир **17**, 3 α, 5-цикло-6α-метоксисоединение **20**, были изолированы в качестве побочных продуктов соответствующие 6α-гидроксипроизводные **21**. Распределение продуктов в зависимости от растворителя может быть объяснено на основе предположенного механизма реакций. Среди растворителей хлороформ дает наиболее высокие выходы фторированных стероидов. Были синтезированы также дальнейшие 4 производные 3β-фторо-5-ен-стероида **23**, **25**, **27** и **29**. Структура полученных соединений была определена с помощью ЯМР—H^1 спектроскопии.

Исследование кинетики селективного гидрирования фенола

Т. МАТЭ, Й. ПЕТРО, А. ТУНГЛЕР, З. ЧЮРЁШ и К. ЛУГОШИ

Селективное гидрирование фенола до циклогексанона на палладиевом катализаторе, нанесенном на молекулярные сита,;было исследовано в интервале температур 145—175°С. Кинетическое уравнение, дающее наилучшее совпадение с данными интегральной конверсии, было получено методом нелинейного определения параметров на ЭВМ. На основе кинетического уравнения можно полагать, что на вводной ступени селективного гидрирования происходит взаимодействие водорода, адсорбированного атомно, с фенолом в газовой фазе (механизм типа Ридиля-Или), а затем адсорбированные атомы и молекулы взаимодействуют на следующих ступенях (механизм Лангмюра—Хиншельвуда).

Электроно-обедненные гетероароматические аммониоамидаты, XVIII
Синтез и фотохимия некоторых *N*-изохинолинио тиоамидатов

М. ЛЕМПЕРТ-ШРЕТЕР, К. ЛЕМПЕРТ, Й. ТАМАШ и К. ВЕКЕИ

Тиоацилирование изохинолиниоамида дает *N*-изохинолинио(тиоамидаты) **2a**—**2c**. В зависимости от растворителя, **2c** существует либо в смеси с его трициклическим таутомером **5**, либо исключительно как последний. Обсуждаются спектры ЯМР и МС, а также фотохимия соединений **2a**—**2c**. Среди фотохимических продуктов были найдены 3,7-ди-

метоксибензонитрил, 3,4-диметокси(тиобензамид), *О*-этил тиокарбамат, 1(2*H*)-изохинолинтион (**7a**), 1(2*H*)-изохинолинон (**7c**) и [1, 3, 4] тиадиазоло [2, 3-*a*] изохинилин-4-ий-2-олат (**8a**). Обсуждаются различия между фрагментацией под действием электронного удара и между фотохимией тиоамидатов типа **1** и **2**, а также между фотохимией тиоамидатов **2** и их амидатных дубликатов типа **3**. Окисление [1, 3, 4] тиадиазоло [2, 3-*a*] изохинолин - 4-ий-2-тиолата (**8b**) с помощью перманганата калия дает олат **8a** и 1-изохинолил тиоцианат (**12**).

Циклические превращения хромонов до 4-гидроксикумаринов

В. САБО, Е. БОРДА и Э. ТЭЙС

Хромон и его C_3-замещенные производные (**I**) в водноспиртовой среде с гидроксиламином дают изоксазоли **II** через монооксимы **VI**. Соединения **VI** и **II** в щелочной среде также превращаются в нитрилы **III**, которые в зависимости от замещения и концентрации гидроксидного иона, находятся в таутомерии цикл-цепь с кумаринимином **IV**. Соединение **VI** в кислой среде превращается в 4-гидроксикумарин (**V**). Таким образом удалось осуществить циклическое превращение хромон → 4-гидроксикумарин, являющееся всегда справедливым для хромонов, не замещенных в положении 2.

О волнах с конечной амплитудой в химически реагирующей газовой смеси

В. Д. ШАРМА и РАДЕШЬЯМ

Был исследован рост газово-динамических возмущений конечной амплитуды, встречающихся с волновым фронтом произвольной формы, через химически реагирующую газовую смесь. Обсуждается влияние термодинамических свойств на рост волны, когда среда, находящаяся перед волной, находится в состоянии химического равновесия или неравновесия. Были исследованы также эффекты искривления фронта волны на возрастание и затухание этих волн.

Влияние фотогафических и фотометрических эффектов на спектрографическую оценку, VI

К. ЦИММЕР и Г. ХЕЛЬТАИ

В настоящем сообщении обсуждается эффект плотности фона на величину γ полосатых спектров, сравнивая различные формы кривых почернения, определенных из полосатых и непрерывных спектров, соответственно.

Отношение γ_L/γ_U не зависит от длины волны, но определенно зависит от типа и условий эмульсии. С увеличением плотности фона величина γ_{L+U} полосатого спектра уменьшается подобно функции насыщеня. На основе математического описания экспериментальных данных было выведено уравнение для простого расчета γ_{L+U} из величин γ_L и γ_U. Это уравнение содержит лишь один параметр, зависящий от экспериментальных условий.

Влияние фотографических и фотометрических эффектов на спектрографическую оценку, VII

Мультиэлементарный спектрохимический метод контроля загрязнений — основа для оптимальности спектрографической оценки

К. ФЛОРИАН и Н. ПЛИШОВСКА

Описан спектрографический метод для оценки загрязнений, разработанный на основе выбранных параметров. Метод может служить для демонстрации применения оптимальной оценки, что уже рассматривалось в более ранней работе. Были отмечены все помехи, которые могут быть устранены, используя оптимализированную оценку. Полученные результаты будут обсуждены в другой статье.

Les Acta Chimica paraissent en français, allemand, anglais et russe et publient des mémoires du domaine des sciences chimiques.

Les Acta Chimica sont publiés sous forme de fascicules. Quatre fascicules seront réunis en un volume (3 volumes par an).

On est prié d'envoyer les manuscrits destinés à la rédaction à l'adresse suivante:

Acta Chimica
Budapest, P.O. Box 67, H-1450, Hongrie

Toute correspondance doit être envoyée à cette même adresse.

La rédaction ne rend pas de manuscript.

Le prix de l'abonnement: $36,00 par volume.

Abonnement en Hongrie à l'Akadémiai Kiadó (1363 Budapest, P. O. B. 24, C. C. B. 215 11488), à l'étranger à l'Entreprise du Commerce Extérieur « Kultura » (H-1389 Budapest 62, P. O. B. 149 Compte-courant No. 218 10990) ou chez représentants à l'étranger.

Die Acta Chimica veröffentlichen Abhandlungen aus dem Bereich der chemischen Wissenschaften in deutscher, englischer, französischer und russischer Sprache.

Die Acta Chimica erscheinen in Heften wechselnden Umfanges. Vier Hefte bilden einen Band. Jährlich erscheinen 3 Bände.

Die zur Veröffentlichung bestimmten Manuskripte sind an folgende Adresse zu senden

Acta Chimica
Budapest, Postfach 67, H-1450, Ungarn

An die gleiche Anschrift ist jede für die Redaktion bestimmte Korrespondenz zu richten.

Manuskripte werden nicht zurückerstattet.

Abonnementspreis pro Band: $36,00.

Bestellbar für das Inland bei Akadémiai Kiadó (1363 Budapest, Postfach 24, Bankkonto Nr. 215 11488), für das Ausland bei »Kultura« Außenhandelsunternehmen (H-1389 Budapest 62, P. O. B. 149. Bankkonto Nr. 218 10990) oder seinen Auslandsvertretungen.

«Acta Chimica» издают статьи по химии на русском, английском, французском и немецком языках.

«Acta Chimica» выходит отдельными выпусками разного объема, 4 выпуска составляют один том и за год выходят 3 тома.

Предназначенные для публикации рукописи следует направлять по адресу:

Acta Chimica
Budapest, P.O. Box 67, H-1450, ВНР

Всякую корреспонденцию в редакцию направляйте по этому же адресу.

Редакция рукописей не возвращает.

Подписная цена — $36,00 за том.

Отечественные подписчики направляйте свои заявки по адресу Издательства Академии Наук (1363 Budapest, P.O.B. 24, Текущий счет 215 11488), а иностранные подписчики через организацию по внешней торговле «Kultura» (H-1389 Budapest 62, P.O.B. 149. Текущий счет 218 10990) или через ее заграничные представительства и уполномоченных.

Reviews of the Hungarian Academy of Sciences are obtainable at the following addresses:

AUSTRALIA
C.B.D. LIBRARY AND SUBSCRIPTION SERVICE, Box 4886, G.P.O., *Sydney N.S.W. 2001*
COSMOS BOOKSHOP, 145 Ackland Street, *St. Kilda (Melbourne), Aictoria 3182*

AUSTRIA
GLOBUS, Höchstädtplatz 4, *1200 Wien XX*

BELGIUM
OFFICE INTERNATIONAL DE LIBRAIRIE, 30 Avenue Marnix, *1050 Bruxelles*
LIBRAIRIE DU MONDE ENTIER, 162 Rue du Midi, *1000 Bruxelles*

BULGARIA
HEMUS, Bulvar Ruszki 6, *Sofia*

CANADA
PANNONIA BOOKS, P.O. Box 1017, Postal Station "B", *Toronto, Ontario M5T 2T8*

CHINA
CNPICOR, Periodical Department, P.O. Box 50, *Peking*

CZECHOSLOVAKIA
MAD'ARSKÁ KULTURA, Národní třida 22, *115 66 Praha*
PNS DOVOZ TISKU, Vinohradská 46, *Praha 2*
PNS DOVOZ TLACE, *Bratislava 2*

DENMARK
EJNAR MUNKSGAARD, Norregade 6, *1165 Copenhagen*

FINLAND
AKATEEMINEN KIRJAKAUPPA, P.O. Box 128, *SF-00101 Helsinki 10*

FRANCE
EUROPERIODIQUES S. A., 31 Avenue de Versailles, *78170 La Celle St. Cloud*
LIBRAIRIE LAVOISIER, 11 rue Lavoisier, *75008 Paris*
OFFICE INTERNATIONAL DE DOCUMENTATION ET LIBRAIRIE, 48 rue Gay-Lussac, *75240 Paris Cedex 05*

GERMAN DEMOCRATIC REPUBLIC
HAUS DER UNGARISCHEN KULTUR, Karl-Liebknecht-Strasse 9, *DDR-102 Berlin*
DEUTSCHE POST ZEITUNGSVERTRIEBSAMT, Strasse der Pariser Kommüne 3—4, *DDR-104 Berlin*

GERMAN FEDERAL REPUBLIC
KUNST UND WISSEN ERICH BIEBER, Postfach 46, *7000 Stuttgart 1*

GREAT BRITAIN
BLACKWELL'S PERIODICALS DIVISION, Hythe Bridge Street, *Oxford OX1 2ET*
BUMPUS, HALDANE AND MAXWELL LTD., Cowper Works, *Olney, Bucks MK46 4BN*
COLLET'S HOLDINGS LTD., Denington Estate, *Wellingborough, Northants NN8 2QT*
WM. DAWSON AND SONS LTD., Cannon House, *Folkestone, Kent CT19 5EE*
H. K. LEWIS AND CO., 136 Gower Street, *London WC1E 6BS*

GREECE
KOSTARAKIS BROTHERS, International Booksellers, 2 Hippokratour Street, *Athens-143*

HOLLAND
MEULENHOFF-BRUNA B.V., Beulingstraat 2, *Amsterdam*
MARTINUS NIJHOFF B.V., Lange Voorhout 9—11, *Den Haag*
SWETS SUBSCRIPTION SERVICE, 374b Heereweg, *Lisse*

INDIA
ALLIED PUBLISHING PRIVATE LTD., 13/14 Asat Ali Road, *New Delhi 110001*
150 B-6 Mount Road, *Madras 600002*
INTERNATIONAL BOOK HOUSE PVT. LTD., Madame Cama Road, *Bombay 400039*
THE STATE TRADING CORPORATION OF INDIA LTD., Books Import Division, Chandralok, 36 Janpath, *New Delhi 110001*

ITALY
EUGENIO CARLUCCI, P.O. Box 252, *70100 Bari*
INTERSCIENTIA, Via Mazzé 28, *10149 Torino*
LIBRERIA COMMISSIONARIA SANSONI, Via Lamarmora 45, *50121 Firenze*
SANTO VANASIA, Via M. Macchi 58, *20124 Milano*
D. E. A., Via Lima 28, *00198 Roma*

JAPAN
KINOKUNIYA BOOK-STORE CO. LTD., 17-7, Shinjuku-ku 3 chome, Shinjuku-ku, *Tokyo 160-91*
MARUZEN COMPANY LTD., Book Department P.O. Box 5056 Tokyo International, *Tokyo 100-31*
NAUKA LTD., IMPORT DEPARTMENT, 2-30-19 Minami Ikebukuro, Toshima-ku, *Tokyo 171*

KOREA
CHULPANMUL, *Phenjan*

NORWAY
TANUM-CAMMERMEYER, Karl Johansgatan 41—43, *1000 Oslo*

POLAND
WĘGIERSKI INSTYTUT KULTURY, Marszałkowska 80, *Warszawa*
CKP I W ul. Towarowa 28 *00-958 Warsaw*

ROUMANIA
D. E. P., *Bucureşti*
ROMLIBRI, Str. Biserica Amzei 7, *Bucureşti*

SOVIET UNION
SOJUZPETCHATJ — IMPORT, *Moscow*
and the post offices in each town
MEZHDUNARODNAYA KNIGA, *Moscow G-200*

SPAIN
DIAZ DE SANTOS, Lagasca 95, *Madrid 6*

SWEDEN
ALMQVIST AND WIKSELL, Gamla Brogatan 26, *101 20 Stockholm*
GUMPERTS UNIVERSITETSBOKHANDEL AB, Box 346, *401 25 Göteborg 1*

SWITZERLAND
KARGER LIBRI AG, Petersgraben 31, *4011 Basel*

USA
EBSCO SUBSCRIPTION SERVICES, P.O. Box 1943, *Birmingham, Alabama 35201*
F. W. FAXON COMPANY, INC., 15 Southwest Park, *Westwood, Mass, 02090*
THE MOORE-COTTRELL SUBSCRIPTION AGENCIES, *North Cohocton, N. Y. 14868*
READ-MORE PUBLICATIONS, INC., 140 Cedar Street, *New York, N. Y. 10003*
STECHERT-MACMILLAN, INC., 7250 Westfield Avenue, *Pennsauken* N. J. 08110

VIETNAM
XUNHASABA, 32, Hai Ba Trung, *Hanoi*

YUGOSLAVIA
JUGOSLAVENSKA KNJIGA, Terazije 27, *Beograd*
FORUM, Vojvode Mišića 1, *21000 Novi Sad*

14. V. 1980 HU ISSN 0001—5407 Index: 26.007

ACTA CHIMICA

ACADEMIAE SCIENTIARUM HUNGARICAE

TOMUS 103 FASCICULUS 4

AKADÉMIAI KIADÓ, BUDAPEST

1980

ACTA CHIM. ACAD. SCI. HUNG. ACASA2 103 (3) 329–420 (1980)

ACTA CHIMICA

A MAGYAR TUDOMÁNYOS AKADÉMIA KÉMIAI TUDOMÁNYOK OSZTÁLYÁNAK IDEGEN NYELVŰ KÖZLEMÉNYEI

Acta Chimica is a journal for the publication of papers on all aspects of chemistry in English, German, French and Russian.

Acta Chimica is published in 3 volumes per year. Each volume consists of 4 issues of varying size.

Manuscripts should be sent to

Acta Chimica
Budapest, P.O. Box 67, H-1450, Hungary

Correspondence with the editors should be sent to the same address. Manuscripts are not returned to the authors.

Hungarian subscribers should order from Akadémiai Kiadó, 1363 Budapest, P.O. Box 24. Account No. 215 11488.

Orders from other countries are to be sent to "Kultura" Foreign Trading Company (H-1389 Budapest 62, P.O. Box 149. Account No. 218 10990) or its representatives abroad.

Acta Chimica Academiae Scientiarum Hungaricae, Tomus 103 (4), pp. 329—332 (1980)

BAEYER—VILLIGER OXIDATION OF 3-β-CHLOROCHOLEST-5-EN-7-ONE

SHAFIULLAH and E. A. KHAN

(Department of Chemistry, Aligarh Muslim University, Aligarh, India)

Received March 8, 1979
Accepted for publication April 9, 1979

Oxidation of 3β-chlorocholest-5-en-7-one (**1**) with perbenzoic acid (1 or 2 mole equivalents) in the presence of *p*-toluenesulfonic acid monohydrate as catalyst afforded 3β-chloro-5,6-α-oxido-5α-cholestan-7-one (**2**), 3β-chloro-7a-oxa-B-homocholest-5-en-7-one (**3**), 3β-chloro-5-formyl-6-oxa-5α-cholestan-7-one (**4**) and 3β-chloro-5-oxo-5,7-*seco*-6-norcholestan-7-oic acid (**5**). With 3 mole equivalents, **1** provided, in addition to **2–5**, 5-oxo-5,7-*seco*-6-norcholest-3-en-7-oic acid (**6**). The *seco*-acids **5** and **6** were converted to the methyl esters (**7**) and (**8**). The structures of the compounds have been established on the basis of their spectral properties, chemical transformations and comparison with authentic samples.

Baeyer—Villiger oxidation of conjugated steroidal enones is noted for the multiplicity of the products it furnishes. Past efforts, principally with 4-en-3-one systems, have enlightened the mechanistic and stereochemical aspects of rearrangement phenomena [1, 2]. In comparison, little has been done on the peracid oxidation of 5-en-7-ones. We illustrate here our extension of the above work employing 3β-chlorocholest-5-en-7-one (**1**).

The title compound **1** was submitted to perbenzoic acid oxidation at different concentrations using *p*-toluenesulfonic acid monohydrate as catalyst. Reaction of **1** with 1 or 2 mole equivalent of peracid gave 3β-chloro-5,6α-oxido-5α-cholestan-7-one (**2**), 3β-chloro-7a-oxa-B-homocholest-5-en-7-one (**3**), 3β-chloro-5-formyl-6-oxa-5α-cholestan-7-one (**4**) and 3β-chloro-5-oxo-5,7-*seco*-6-norcholestan-7-oic acid (**5**). Treatment of **1** with 3 mole equivalents of peracid gave, along with **2–5**, 5-oxo-5,7-*seco*-6-norcholest-3-en-7-oic acid (**6**).

The identity of **2** was partly established from its IR spectrum showing saturated carbonyl at 1700 cm^{-1} (also evidenced by a transparent UV spectrum) and epoxy grouping at 910 cm^{-1} [3]. The PMR spectrum gave a broad multiplet at δ 3.88 ppm for the C-3 proton. The half-band width (20 Hz) of this signal was a clear indication of its *axial* (α) nature and a *trans* A/B ring junction [4], providing the α-position of the epoxide in **2**. The C-6 proton appeared as a singlet at δ 2.91 ppm.

Support for the α, β-unsaturated lactones structure **3** came from the UV spectrum (δ_{max} 238 nm) and the IR band at 1685 cm^{-1} for conjugated carbonyl. In the PMR spectrum, the vinylic proton was seen at δ 5.75 ppm and the diagnostic C-8 methine proton was observed as a broad unresolved signal centred at δ 4.1 ppm, with its end merging with the multiplet centred at δ 3.8 ppm for

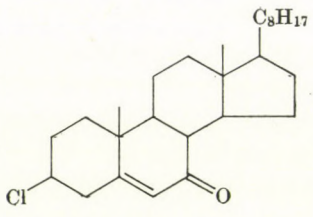

1

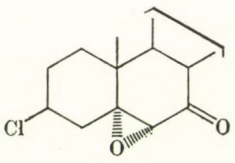

2

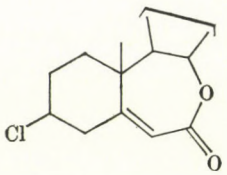

3

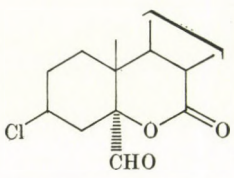

4

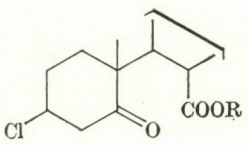

5 R = H
7 R = CH_3

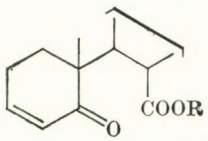

6 R = H
8 R = CH_3

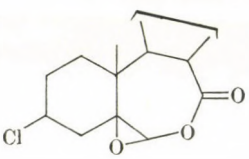

9

the C-3 proton. The oxygen insertion between C-7 and C-8 in **3** rather than C-6 and C-7 demonstrated that the migratory tendency of a more substituted carbon like C-8 almost parallels that of C-6, a vinylic proton.

The presence of a formyl group and lactone ring in **4** was established by the IR bands at 1750 cm^{-1} (δ-lactone) and 1720 cm^{-1} (formyl) [5] and was upheld by the PMR signal for an aldehydic proton at δ 9.56 ppm (singlet). The configuration (α or β) of the C-5 formyl function was decided on the basis of the C-3 proton multiplet at δ 4.23 ppm having a half-band width of 17 Hz. Evidently, this proton is *axial* (α) and the A/B ring junction is *trans* [4], rendering the formyl group to assume an α-orientation. A positive Fehling's test chemically ascertained the presence of aldehyde.

The IR spectrum of the keto *seco*-acid **5** exhibited a broad flattened band at about 3200 cm^{-1} for acid hydroxy, and bands at 1720 and 1710 cm^{-1} for the acid and ring carbonyls. Besides the acid proton signal at δ 8.15 ppm the PMR spectrum had other signals of interest at δ 4.66 m ppm (C3-αH; $W^1/_2$ 12 Hz) and a multiplet-like signal spread between δ 3.86 and 3.13 ppm (C-4-H_2). The acid **5** was converted into the ester **7** by diazomethane.

The unsaturated keto seco-acid **6** derived from **5** upon elimination of HCl, was identified by its spectral features, m.p. and transformation to the ester **8**. Both **6** and **8** were identified by means of authentic samples [5, 6].

The experiments have proved that the formyl derivative and seco-acid arise by acid-catalyzed rearrangements of the epoxy enol lactone intermediate and that β-epoxy enol lactones lead to 5α-formyl derivatives and *vice versa* [1]. Thus **9** may be taken as the intermediate in the conversion of **1** into **4** and **5**. Loss of HCl from **5** afforded **6**.

Experimental

All m.p's are uncorrected. UV spectra were determined in ethanol and IR spectra were measured in KBr on a Perkin—Elmer 621 Granting Infrared Spectrophotometer. PMR spectra were run in $CDCl_3$ on a Varian A60 instrument with $SiMe_4$ as the internal standard. TLC plates were coated with silica gel and sprayed with a 20% solution of perchloric acid. Light petroleum refers to a fraction of b.p. 60—80 °C. The compounds **2**—**5** and **7** gave a positive Beilstein test for halogen. (PMR: s, singlet; d, doublet; m, multiplet; br, broad).

Perbenzoic acid oxidation of 1
(a) With 1 or 2 mole equivalents of perbenzoic acid

To a solution of **1** (m.p. [7] 144—145 °C; 3 g) in chloroform (20 ml) there were added a freshly prepared chloroform solution of perbenzoic acid (1 mole equivalent) and a few crystals of *p*-toluenesulfonic acid monohydrate, and the reaction mixture was allowed to stand at room temperature for 140 h. The solvent was then removed under reduced pressure. The residue was extracted with ether and the ethereal solution washed with water, sodium bicarbonate solution (5%) and water, and dried over anhydrous sodium sulfate. On removal of the solvent, the crude product (*ca.* 2.9 g) was chromatographed over silica gel (70 g). (Fractions of 30 ml each were taken.) Elution with a mixture of light petroleum and ether (20 : 1) gave **2** which was recrystallized from light petroleum to obtain the product (100 mg), m.p. 106 °C.

$C_{27}H_{43}O_2Cl$. Calcd. C 74.65; H 9.90. Found C 74.53; H 9.81%.

IR: ν max 1700 (C=O), 910 (epoxy), 705 cm^{-1} (C—Cl).

PMR: δ 3.88 br,m (C-3-α H; $W1/2$ 20 Hz), 2.91s (C-6-β H), 1.03s (C10–CH_3), 0.63s (C13-CH_3), 0.90, 0.80 (remaining methyls).

Light petroleum ether (19 : 1) eluted the unchanged **1**; recrystallized from light petroleum (200 mg), m.p. and m.m.p. 145 °C.

Elutes from light petroleum ether (10 : 1) furnished **4**, which was recrystallized from light petroleum to give 200 mg of the product, m.p. 113 °C.

$C_{27}H_{43}O_3Cl$. Calcd. C 72.0; H 9.55. Found C 71.98; H 9.45%.

IR: ν max 1750 (δ-lactone), 1720 (formyl), 755 cm^{-1} (C—Cl).

PMR: δ 9.56s (HC=O), 4.23 br,m (C-3α H; $W1/2$ 17 Hz), 1.31s (C10–CH_3), 0.60s (C13–CH_3), 0.9, 0.8 (remaining methyls).

Elution with light petroleum ether (5 : 1) gave **3**, (100 mg) recrystallized from light petroleum, m.p. 140 °C.

$C_{27}H_{43}O_2Cl$. Calcd. C 74.65; H 9.90. Found C 74.55; H 9.85%.

UV: λ max 238 nm (ε 6,820).

IR: ν max 1685 (C=O), 1625 (C=C), 830 cm^{-1} (C—Cl).

PMR: δ 5.75s (C-6-H), 4.1br (C-8-β H), 3.8br,m (C-3-α H), 1.29s (C10–CH_3), 0.65 (C13–CH_3), 0.9, 0.8 (remaining methyls).

Light petroleum ether (3 : 1) furnished the seco-acid **5** (240 mg); recrystallized from light petroleum ether, m.p. 170 °C.

$C_{26}H_{43}O_3Cl$. Calcd. C 71.23; H 9.81. Found C 71.25; H 9.89%.

IR: ν max 3200br (acid-OH), 1720, 1710 (acid CO and C=O unassigned), 720 cm^{-1} (C—Cl).

PMR: δ 8.15 (acid-OH; exchangeable with deuterium), 4.66m (C-3-α H; $W1/2$ 12 Hz), 3.86—3.13m (C-4-H_2), 2.75m (C-8-β H), 1.1s (C10–CH_3), 0.7s (C13–CH_3), 0.9, 0.8 (remaining methyls).

Methyl 3h-chloro-5-oxo-5,7-*seco*-6-norcholestan-7-oate (7)

An ethereal solution of **5** (150 mg) was treated with an excess of an ethereal solution of diazomethane in the cold and, after 10 min. the reaction mixture was worked up in the usual manner. Removal of the solvent gave **7** which was crystallized from light petroleum to give the product (100 mg), m.p. 77 °C.

$C_{27}H_{45}O_3Cl$. Calcd. C 71.68; H 9.95. Found C 71.60; H 9.95%.

IR: ν max 1730 (ester CO), 1710 (C=O), 1170, 1080 (C—O), 730 cm^{-1} (C—Cl).

NMR: δ 4.74m (C3-α $\underline{H}$; $W1/2$ 10 Hz), 3.48s ($COOCH_3$; the signal for C4-H_2 was around and beneath this signal), 2.56m (C8-β $\underline{H}$), 1.0s (C10-$C\underline{H}_3$), 0.75s (C13-$C\underline{H}_3$), 0.91, 0.83 (remaining methyls).

(b) Reaction of (**1**) with 2 mole equivalents of perbenzoic acid in a similar manner also provided products **2**—**5**.

(c) With 3 mole equivalents of perbenzoic acid

The ketone **1** (13 g) on treatment with 3 mole equivalents of perbenzoic acid in the manner described above produced, in addition to **2**—**5** obtained as above, compound **6** which was recrystallized from light petroleum to obtain the pure seco-acid (130 mg), m.p. and m.m.p. 180—181 °C [5, 6].

PMR: δ 6.81m (C3–H; *major* J = 10 Hz), 5.91d (C4–H; J = 10 Hz), 1.1s (C10-$C\underline{H}_3$), 0.65s (C13-$C\underline{H}_3$), 0.9, 0.8 (remaining methyls).

The acid **6** was identical with an authentic sample [5].

Methyl 5-oxo-5,7-*seco*-6-norcholest-3-en-7-oate (8)

The seco-acid **6** (100 mg) was methylated with diazomethane in the manner described above to afford the ester **8** (80 mg) as a non-crystallizable oil, which was in all respects identical with an authentic sample [6].

The authors thank Prof. W. RAHMAN, Head, Department of Chemistry, for facilities, Prof. M. S. AHMAD for a helpful discussion and CSIR (New Delhi) for financial assistance to one of us (EAK).

REFERENCES

[1] PINHEY, J. T., SCHAFFNER, K.: Aust. J. Chem., **21**, 1873 (1968)
[2] AHMAD, M. S., SHAFIULLAH, MUSHFIQ, M.: Aust. J. Chem., **27**, 2693 (1974)
[3] BELLAMY, L. J.: "The Infrared Spectra of Complex Molecules", 2nd ed., John Wiley, New York 1958
[4] BHACCA, N. S. WILLIAMS, D. H.: "Applications of NMR Spectroscopy in Organic Chemistry". Holden-Day, San Francisco 1964
[5] KUTNEY, J. P., JOHNSON, R. A., VLATTAS, I.: Can. J. Chem., **41**, 613 (1963)
[6] JACOBS, T. L., BROWNFIELD, R. B.: J. Amer. Chem. Soc., **82**, 4033 (1960)
[7] MILBURN, A. H., TRUTER, E. V.: J. Chem. Soc., **1956**, 1736

SHAFIULLAH, EJAZ AHMAD KHAN } Department of Chemistry, Aligarh Muslim University, Aligarh-202001, India

Acta Chimica Academiae Scientiarum Hungaricae, Tomus 103 (4), pp. 333—337 (1980)

RING A-FUSED STEROIDAL TETRAZOLES

SHAFIULLAH and M. A. GHAFFARI

(Department of Chemistry, Aligarh Muslim University, Aligarh, India)

Received December 12, 1978
In revised form April 18, 1979
Accepted for publication May 8, 1979

Reaction of 4-methylcholest-4-en-3-one (**1**) with excess hydrazoic acid (BF_3-etherate catalyst) provided 3-aza-A-homo-4a-methylcholest-4a-en-4-one (**2**) and 3-aza-A-homo-4a-methylcholest-4a-eno[3,4-*d*]tetrazole (**3**). Under similar reaction conditions, 4,4-dimethylcholest-5-en-3-one (**4**) gave 4,4-dimethyl-5α-cholestan-3,6-dione (**5**) and 4-aza-A-homo-4a,4b-dimethylcholest-5-eno[4,3-*d*]tetrazole (**6**). Reaction of the 4-monoethyl analogue (**7**) of (**1**) afforded 3-aza-A-homo-4a-ethylcholest-4a-eno[3,4-*d*] tetrazole (**8**) and its 4-aza isomer (**8a**), whereas the 4,4-diethylcholest-5-en-3-one (9) analogue of (**4**) furnished 4,4-diethyl-3,4-*seco*-4β-azidocholest-5-en-3-nitrile (**10**) and 4-aza-A-homo-4a,4b-diethylcholest-5-eno[4,3-*d*]tetrazole (**11**). The structures of these compounds were established on the basis of their spectral properties. A mechanism of the abnormal transformation is suggested.

Steroidal tetrazoles have become of interest in recent years on account of their pharmacological potentialities [1, 2]. For this reason we started a program of synthesizing steroidal tetrazoles from sterically hindered ketones, such as 4-methylcholest-4-en-3-one (**1**) and 4,4-dimethylcholest-5-en-3-one (**4**) and their ethyl analogues **7** and **9**, respectively.

The reaction of (**1**) [3] with an excess of hydrazoic acid, in the presence of BF_3 catalyst, furnished 3-aza-A-homo-4a-methylcholest-4a-en-4-one (**2**) as an oil and 3-aza-A-homo-4a-methylcholest-4a-eno[3,4-*d*]tetrazole (**3**).

The oily compound **2** analyzed for $C_{28}H_{47}NO$ indicating the insertion of only one nitrogen atom, which was confirmed by the IR and NMR spectra. The 3-aza structure of the lactam **2** was conclusively shown by the broad signal at δ 3.6 in its NMR spectrum, which can be ascribed to the C2-H_2 protons in the vicinity of the nitrogen atom. The 3-aza formulation of the lactam was chemically supported by treating the ketone **1** with one mole equivalent of sodium azide in sulfuric acid; the compound isolated was similar to **2** in all respects.

Compound **3** had correct analysis for $C_{28}H_{46}N_4$ showing the presence of a tetrazole moiety in the molecule. Choice between structures **3** and its isomer **3a** was possible on the basis of the NMR spectrum. A multiplet at δ 4.35 for two protons supported the presence of the methylene group directly attached to the ring nitrogen atom [4].

Similar treatment of **4** [3] afforded **5** and **6**. Compound **5** analysed correctly for $C_{29}H_{48}O_2$, thus addition of one oxygen atom to the substrate is indicated. The IR spectrum of compound **5** had a strong band at 1700 cm^{-1}

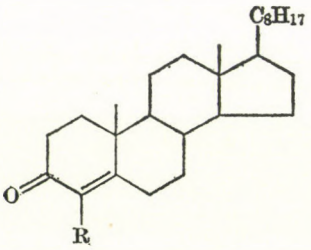

	R
1	$-CH_3$
7	$-CH_2-CH_3$

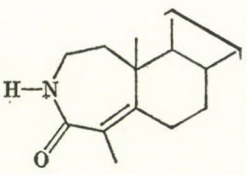

2

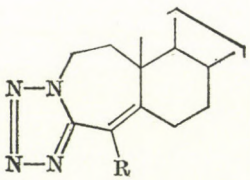

	R
3	$-CH_3$
8	$-CH_2-CH_3$

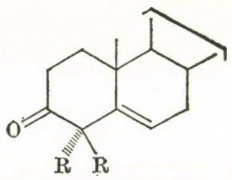

	R
4	$-CH_3$
9	$-CH_2-CH_3$

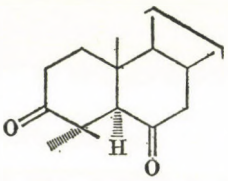

5

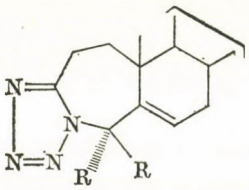

	R
6	$-CH_3$
11	$-CH_2-CH_3$

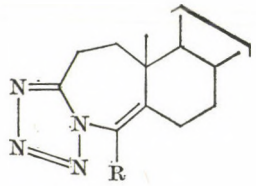

	R
3a	$-CH_3$
8a	$-CH_2-CH_3$

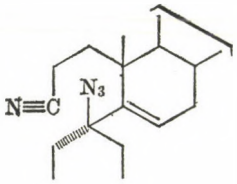

10

($>C=O$) (negative tetranitromethane). Structure **5** was also supported by the NMR spectrum which was clean in the downfield region and did not show any signal for vinylic protons. To account for the formation of the diketone **5**, the following mechanism is proposed.

Compound **6** had correct analysis for $C_{28}H_{48}N_4$, which is clear evidence for the presence of the tetrazole moiety in the compound. The 4-aza structure

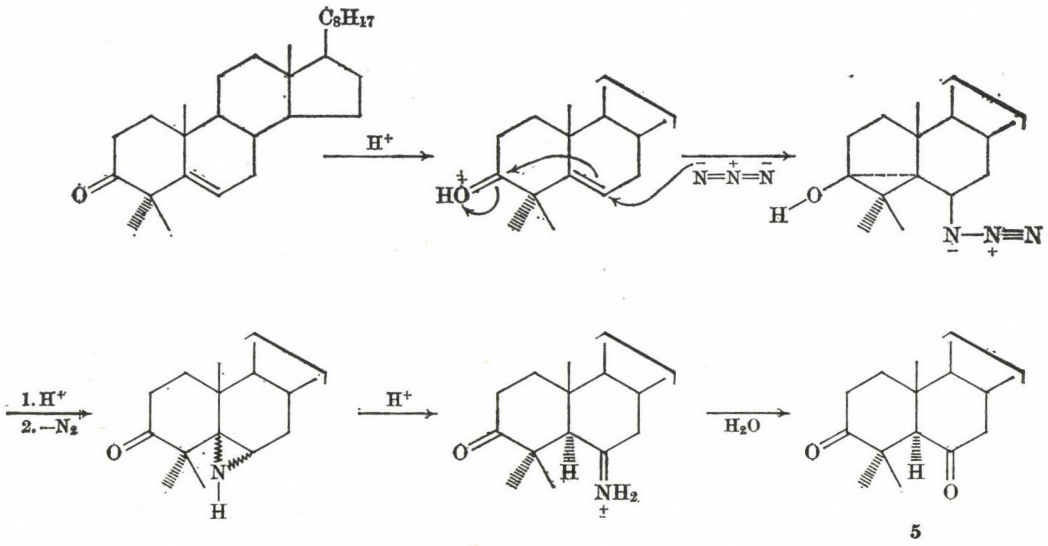

of compound **6** is supported by the NMR spectrum which displayed a multiplet centred at δ 3.16 (—N=C—C2—$\underline{H}_2$) [4]. The insertion of nitrogen between C3 and C4 causes considerable downfield shift of the C4a-dimethyl protons.

Compound **7** [3] when subjected to similar reaction conditions gave the isomeric tetrazoles **8** and **8a**, whereas the ketone **9** [3] afforded the nitrile **10** and the tetrazole **11**. The formation of a nitrile such as **10** has been reported earlier [5]. The structures of these compounds are compatible with their spectral data shown in Table I.

Table I

Compound	IR (ν max; cm^{-1})	NMR* δ
2	3400(N$\underline{H}$), 1650(CONH) 1635 (>C=C<)	δ 3.6br (C2—$\underline{H}_2$), 6.27s (N$\underline{H}$, exchangeable by D_2O), 2.25s (C4a—C$\underline{H}_3$), 0.91 and 0.81 (remaining methyls).
3	1600 (>C=C<), 1510, 1450, 1375 (C=N, N=N)	δ 4.35mc (2C—$\underline{H}_2$), 2.31s (C4a—C$\underline{H}_3$), 0.98 and 0.88 (remaining methyls)
5	1700 (>C=O)	δ 2.2 mc (methylene protons), 0.95 and 0.85 (remaining methyls)
6	1640 (>C=C<), 1510, 1460, 1375 (C=N, N=N)	δ 6.17 (C6—$\underline{H}$), 3.16 mc (C2—$\underline{H}_2$), 1.94 and 1.82 (C4a—β—C$\underline{H}_3$), 0.9 and 0.8 (remaining methyls)
8	1600 (>C=C<), 1510, 1450, 1380 (C=N, N=N)	4.39 mc (C2—$\underline{H}_2$), 0.95 and 0.85 (remaining methyls)
8a	1630 (>C=C<), 1530, 1450, 1370 (C=N, N=N)	2.89 mc (C2—$\underline{H}_2$), 0.9 and 0.8 (remaining methyls)
10	2240 (—C≡N), 2100 ($-N_3$), 1630 (>C=C<)	5.28 mc (C6—$\underline{H}$), 0.9 and 0.8 (remaining methyls)
11	1635 (>C=C<), 1510, 1450, 1380 (C=N, N=N)	5.89 mc (C6—$\underline{H}$), 2.96 mc (C2—$\underline{H}_2$), 0.83 and 0.8 (remaining methyls)

* C10β and C13β-methyls appeared between δ 1.22 and 0.67

Experimental

All m.p.'s are uncorrected. IR spectra were determined in Nujol with a Perkin—Elmer 237 spectrophotometer. NMR spectra were run in $CDCl_3$ on a Varian A60 instrument with Me_4Si as the internal standard. UV spectra were obtained in methanol with a Beckmann DK2 spectrophotometer. TLC plates were coated with silica gel. A 20% aqueous solution of perchloric acid was used as the spraying agent. Light petroleum refers to a fraction of b.p. 60—80 °C. Anhydrous sodium sulfate was used as drying agent. NMR values are given in ppm (s = singlet, d = doublet, t = triplet, br = broad, mc = multiplet centred at).

Reaction of (1) with hydrazoic acid-BF_3 etherate

(*A*) A solution of **1** (2.0 g) in benzene (25 ml) was added during 5 h to a mixture of hydrazoic acid [6] in benzene and borontrifluoride etherate (2 ml) (freshly distilled) maintained at 0 °C. After having complete addition, the reaction mixture was allowed to stand at room temperature for 3 days. Thereafter it was washed with sodium bicarbonate solution (5%) and water and dried. Removal of the solvent yielded an oily residue (1.7 g), which was chromatographed on a column of silica gel (40.0 g). Elution with light petroleum ether (9 : 1) gave an oil **2** (0.53 g).

$C_{28}H_{47}NO$. Calcd. C 81.35; H 11.38; N 3.38. Found C 81.40; H 11.32; N 3.29%.

Further elution with light petroleum benzene (3 : 4) furnished a solid **3** which was recrystallized from ethyl alcohol (0.78 g), m.p. 141 °C.

$C_{28}H_{46}N_4$. Calcd. C 76.71; H 10.50; N 12.78. Found C 76.30; H 10.56; N 12.85%.

Reaction of (4) with hydrazoic acid-BF_3 etherate

B) A solution of the ketone **4** (2.0 g) in benzene (25 ml) was treated with hydrazoic acid–boron trifluoride as above. After the usual work-up, the residue (1.8 g) obtained was chromatographed on silica gel (40.0 g). Elution with light petroleum ether (16 : 1) gave the diketone **5** which was recrystallized from petrol (0.40 g); m.p. 168 °C (*lit.* [3] m.p. 140—146 °C).

$C_{29}H_{48}O_2$. Calcd. C 81.30; H 11.21. Found C 81.28; H 10.98%.

Further elution with light petroleum ether (14 : 1) gave compound **6** as a solid which was recrystallized from ethyl alcohol (0.83 g), m.p. 132 °C.

$C_{29}H_{48}N_4$. Calcd. C 76.99; H 10.61; N 12.38. Found C 76.40; H 10.72; N 12.47%.

Reaction of (7) with hydrazoic acid-BF_3 etherate

(*A*) The ketone **7** (2.0 g) was treated as above and chromatographed. Elution with petroleum ether–ether (7 : 1) gave a solid **8**, which was recrystallized from petroleum ether (0.43 g), m.p. 96 °C.

$C_{29}H_{48}N_4$. Calcd. C 76.99; H 10.62; N 12.39. Found C 77.0; H 10.59; N 12.35%.

Further elution with petroleum ether–ether (6 : 1) gave another solid **8a** which was recrystallized from petroleum ether (0.39 g), m.p. 72 °C.

$C_{29}H_{48}N_4$. Calcd. C 76.99; H 10.62; N 12.39. Found C 77.12; H 10.58; N 12.36%.

Reaction of (9) with hydrazoic acid-BF_3 etherate

(*B*) The ketone **9** (2.0 g) was subjected to the same reaction conditions and chromatography. Elution with petroleum ether–ether (19 : 1) gave **10** as a pure oil (0.23 g).

$C_{31}H_{52}N_4$. Calcd. C 77.5; H 10.83; N 11.66. Found C 77.5; H 10.83; N 11.66%.

Further elution with petroleum ether–ether (2 : 1) gave **11** as a solid, which was recrystallized from ethyl alcohol (0.69 g), m.p. 135 °C.

$C_{31}H_{52}N_4$. Calcd. C 77.5; H 10.83; N 11.66. Found C 77.66; H 10.80; N 11.63%.

*

The authors are grateful to Prof. W. RAHMAN, Head, Department of Chemistry, for providing necessary facilities, to Prof. M. S. AHMAD for encouragement, and to CSIR (New Delhi) for financial assistance to one of us (M.A.G.).

REFERENCES

[1] SHROFF, A. P.: J. Med. Chem., **16,** 113 (1973) and references cited therein
[2] MECHOULAM, R.: Isr. J. Chem., **6,** 909 (1968)
[3] JUST, G., RICHARDSON, KEITH, St. C.: Canad. J. Chem., **42,** 464 (1964)
[4] DIMAIO, G., PERMUTTI, V.: Tetrahedron, **22,** 2063 (1965)
[5] SINGH, H., MALHOTRA, R. K., PARASHAR, V. V.: Tetrahedron Letters, **1973,** 2583
[6] MOURAL, J., SYHORA, K.: Coll. Czechoslov. Chem. Commun., **35,** 3018 (1970)

SHAFIULLAH
MOHAMED ABUZAR GHAFFARI } Department of Chemistry, Aligarh Muslim University, Aligarh-202001, India

Acta Chimica Academiae Scientiarum Hungaricae, Tomus 103 (4), pp. 339–341 (1980)

ELIMINATION OF PHENOLIC HYDROXYL GROUP: CONVERSION OF (—)-α-NARCOTOLINE INTO (—)-β-HYDRASTINE

P. KEREKES, GY. GAÁL and R. BOGNÁR

(Institute of Organic Chemistry, Kossuth Lajos University, Debrecen, Hungary)

Received February 5, 1979
Accepted for publication May 8, 1979

Natural (—)-α-narcotoline was converted into narcotoline-8-(1-phenyl-1*H*-5-tetrazolyl) ether which yielded (—)-β-hydrastine on catalytic hydrogenation.

In an earlier paper [1] the elimination of the C-3 phenolic hydroxyl group of morphine was reported. Of the methods known for the elimination of phenolic hydroxyl groups [1], the hydrogenolysis of the phenyltetrazolyl ether was employed.

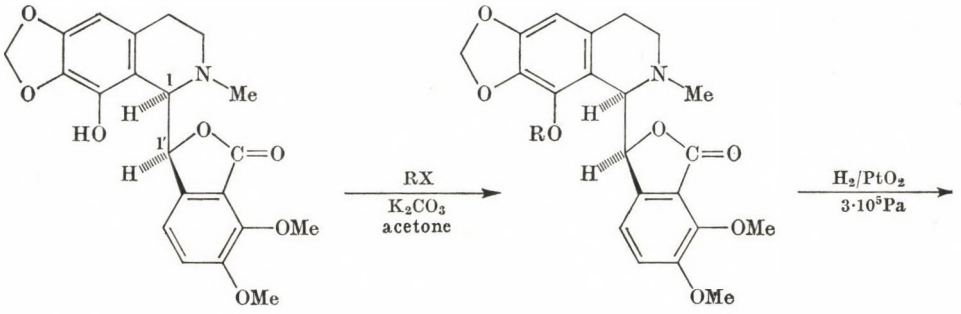

(—)-α-Narcotoline (1*R*:1′*S*)

1 **2**

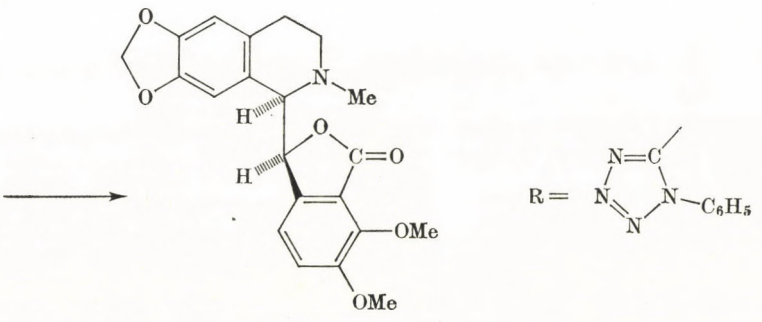

(—)-β-Hydrastine (1*R*: 1′*S*)

3

In the present paper the conversion of natural (—)-α-narcotoline (**1**) into (—)-β-hydrastine (**3**) is discussed.

Earlier, TEITEL and O'BRIEN [2] effected similar conversions in phthalide-isoquinoline alkaloids. In their method, the methylenedioxy group of (—)-β-hydrastine was cleaved by means of boron trichloride, and the product containing two phenolic hydroxyl groups was converted into the bis-phenyl-tetrazolyl ether, which was then subjected to catalytic hydrogenation. On the basis of the NMR, ORD and CD spectra of the product it was stated that no racemization had occurred during the hydrogenolysis, and the absolute configuration of the product (1*R*, 1'*S*) was identical with that of the starting material.

In the course of our studies, (—)-α-narcotoline (**1**) was allowed to react with 5-chloro-1-phenyl-1*H*-tetrazole under the usual conditions, and the desired phenyl-tetrazolyl ether (**2**) was obtained in a satisfactory yield. Hydrogenolysis of the ether at an initial pressure of $3 \cdot 10^5$ Pa yielded (—)-β-hydrastine (**3**). On the basis of physical data (rotation and R_f value) IR and PMR spectra of the product, it proved to be identical with natural (—)-β-hydrastine; its melting point was higher by 10 °C than the value reported in the literature [3]. No racemization was observed during the reaction.

Experimental

M.p.'s are uncorrected. The IR spectra were recorded with a Perkin—Elmer 283 spectrophotometer in KBr pellets, the PMR spectra were obtained with a Jeol Minimar 100 MHz instrument in deuterochloroform. Chemical shifts are given in ppm (δ) values, using TMS internal standard. The rotation values were measured with a Bendix NPL 143 D and with a Perkin—Elmer 241 polarimeter.

Narcotoline-8-(1-phenyl-1*H*-5-tetrazolyl) ether (2)

A mixture of (—)-α-narcotoline (4.0 g; 10 mmoles), 5-chloro-1-phenyl-1*H*-tetrazole (1.8 g; 10 mmoles) and K_2CO_3 (2.8 g; 20 mmoles) in anhydrous acetone (150 ml) was refluxed for 24 h; the reaction mixture was poured into water (150 ml) then extracted with $CHCl_3$ (1×50, 2×30 ml). The chloroform solution was washed with 10% NaOH (3×20 ml), with water (2×30 ml), dried ($MgSO_4$) and evaporated to dryness.

The solid crude product (5.4 g) was twice recrystallized from ethanol; the yield was 4.4 g (81%), m. p. 209—210 °C (d.).

$C_{28}H_{25}N_5O_7$ (543.52). Calcd. C 61.87; H 4.64; N 12.89. Found C 62.14; H 4.78; N 12.52%.

$[\alpha]_D^{25} - 112°$ ($c = 1.0$; $CHCl_3$).

IR: ν C = O 1760 cm^{-1}.

PMR: 2.52 (3 H, s, NCH_3), 3.84 and 4.02 (6 H, 2s, $2 \times OMe$), 4.21 (1 H, d, $J = 4$ Hz, C-1 H), 5.38 (1 H, d, $J = 4$ Hz, C-1' H), 5.96 (2 H, s, OCH_2O), 6.53 (1 H, d, $J = 8$ Hz, C-7' H), 6.99 (1 H, d, $J = 8$ Hz, C-6' H), 6.61 (1 H, s, C-5 H), 7.5—7.9 (5 H, m, aromatic protons).

(—)-β-Hydrastine (3)

A solution of the phenyltetrazolyl ether (**2**) (8.18 g; 15 mmoles) in anhydrous ethanol (500 ml) was hydrogenated in the presence of 10% Pd/C (1.6 g) at an initial pressure of $3 \cdot 10^5$ Pa at 80 °C for 9 h. After the absorption of hydrogen had ceased, the catalyst was filtered off

and the solvent evaporated in vacuum. The residue was dissolved in chloroform (200 ml), washed with 10% NaOH (3×75 ml) and water (2×50 ml), dried ($MgSO_4$) and evaporated to dryness. A yellow oil (6.05 g) was obtained, which solidified on rubbing with anhydrous ether (25 ml) to give 4.1 g of the crude product, m. p. 140—142 °C. This was recrystallized from ethanol (19 ml) (3.8 g; 66%), m.p. 141—143 °C.

$C_{21}H_{21}NO_6$ (383.39). Calcd. C 65.78; H 5.52; N 3.65. Found C 66.00; H 5.57; N 3.78%.

$[\alpha]_D^{25}$ — 59.9° (c = 1.0; $CHCl_3$); *lit.* [4] $[\alpha]_D^{25}$ —61° (c = 0.8; $CHCl_3$).

IR: ν C = O 1760 cm^{-1}.

PMR: 2.52 (3 H, s, NCH_3), 3.84 and 4.04 (6 H, 2s, 2×OCH_3), 5.86 (2 H, s, OCH_2O), 3.95 (1 H, d, J = 4 Hz, C-1 H), 5.42 (1 H, d, J = 4 Hz, C-1' H), 6.48 (1 H, d, J = 8 Hz, C-7' H), 7.04 (1 H, d, J = 8 Hz, C-6' H), 6.36 and 6.52 (2 H, 2s, C-8 and C-5 protons).

*

The authors' thanks are due to the Alkaloida Chemical Works (Tiszavasvári, Hungary) and to the Hungarian Academy of Sciences for supporting this research. Technical assistance by Miss E. Jeszenszki is gratefully acknowledged.

REFERENCES

[1] Bognár, R., Gaál, Gy., Kerekes, P., Horváth, G., Kovács, M. T.: Org. Prep. Proced. Int., **6**, 305 (1974) and references cited therein; Magyar Kém. Foly., **81**, 51 (1975)
[2] Teitel, S., O'Brien, J. P.: J. Org. Chem., **41**, 1657 (1976)
[3] Stanek, J., Manske, R. H. F.: in The Alkaloids, (edited by Manske, R. H. F. and Holmes, H. L.) Vol. **IV**: p. 186. Acad. Press, New York, 1954
[4] Snatzke, G., Wollenberg, G., Hrbek, Jr. J., Šantavý, F., Bláha, K., Klyne, W., Swan, R. J.: Tetrahedron, **25**, 5059 (1969)

Péter Kerekes
György Gaál
Rezső Bognár
H-4010 Debrecen, P. O. B. 20.

Acta Chimica Academiae Scientiarum Hungaricae, Tomus 103 (4), pp. 343–353 (1980)

REACTIONS OF NARCOTINE ISOMERS WITH CYANOGEN BROMIDE

P. KEREKES and Gy. GAÁL

(Institute of Organic Chemistry, Kossuth Lajos University, Debrecen, Hungary)

Received February 5, 1979
Accepted for publication May 8, 1979

(−)-α-Narcotine (1*R*, 1'*S*) (**1**) and (+)-β-narcotine (1*S*, 1'*S*) (**4**) were allowed to react with cyanogen bromide in tetrahydrofuran–water or ethanol–chloroform solvent mixture in the presence of magnesium oxide. The reactions of both narcotine isomers in tetrahydrofuran–water solvent mixture yielded the same product, (−)-*N*-cyano-1(*S*)-hydroxy-1,2-*seco*-1'(*S*)-narcotine (**5a**). When ethanol–chloroform solvent mixture was used, compounds, **1** and **4** gave again the same product, which was (−)-*N*-cyano-1(*S*)-ethoxy-1,2-*seco*-1'(*S*)-narcotine (**5b**). The corresponding enantiomeric narcotine isomers, namely, (+)-α-narcotine (1*S*, 1'*R*) (**2**) and (−)-β-narcotine (1*R*, 1'*R*) (**3**), yielded the enantiomeric seco compounds (**6a** and **6b**) under identical reaction conditions. Refluxing of the seco compounds in dilute hydrochloric acid resulted in cyclization, thus **5a**–**5b** and **6a**–**6b** were converted into (+)-β-narcotine and (−)-β-narcotine, respectively, as the main product.

The absolute configuration of the seco compounds was determined and an interpretation of the stereochemical course of the ring cleavage and ring closure reactions is suggested.

In an earlier paper [1] we reported on the reaction of (—)-α-narcotine (**1**) with cyanogen bromide. The conversion was effected in one of the solvents generally used in the von Braun reaction [2], benzene. The "cyanamide" formed on cleavage of the tetrahydroisoquinoline ring could not be isolated from the reaction mixture as a uniform, well-defined substance. Refluxing of the crude product with dilute hydrochloric acid resulted in cyclization, and (+)-β-narcotine (**4**) was isolated as the main product. The reaction of (—)-β-narcotine (**3**) and (+)-β-narcotine (**4**) under identical conditions led to the starting narcotine isomers. On the basis of the experiments carried out up to that time, the β-isomers seemed to fail in reacting with cyanogen bromide.

American researchers [3] were the first to report the reaction of tertiary amines with cyanogen bromide under solvolytic conditions. The solvents participating in the von Braun reaction were water and ethanol. In the case of the reactions carried out with yohimbine and pseudoyohimbine, ring cleavage was observed and the seco compounds, obtained in high yields, contained a hydroxyl or ethoxyl group attached to the benzyl carbon atom, while the hydrogen bromide formed in the reaction was bound by the alkaloid used in 1 mole excess.

The reactions with yohimbine yielded one single epimeric seco compound and, on the basis of the structure of the products, the authors concluded that the *N*-cyano quaternary salt intermediate was subjected to nucleophilic attack by water or ethanol, and the inversion of configuration took place in an S_N2

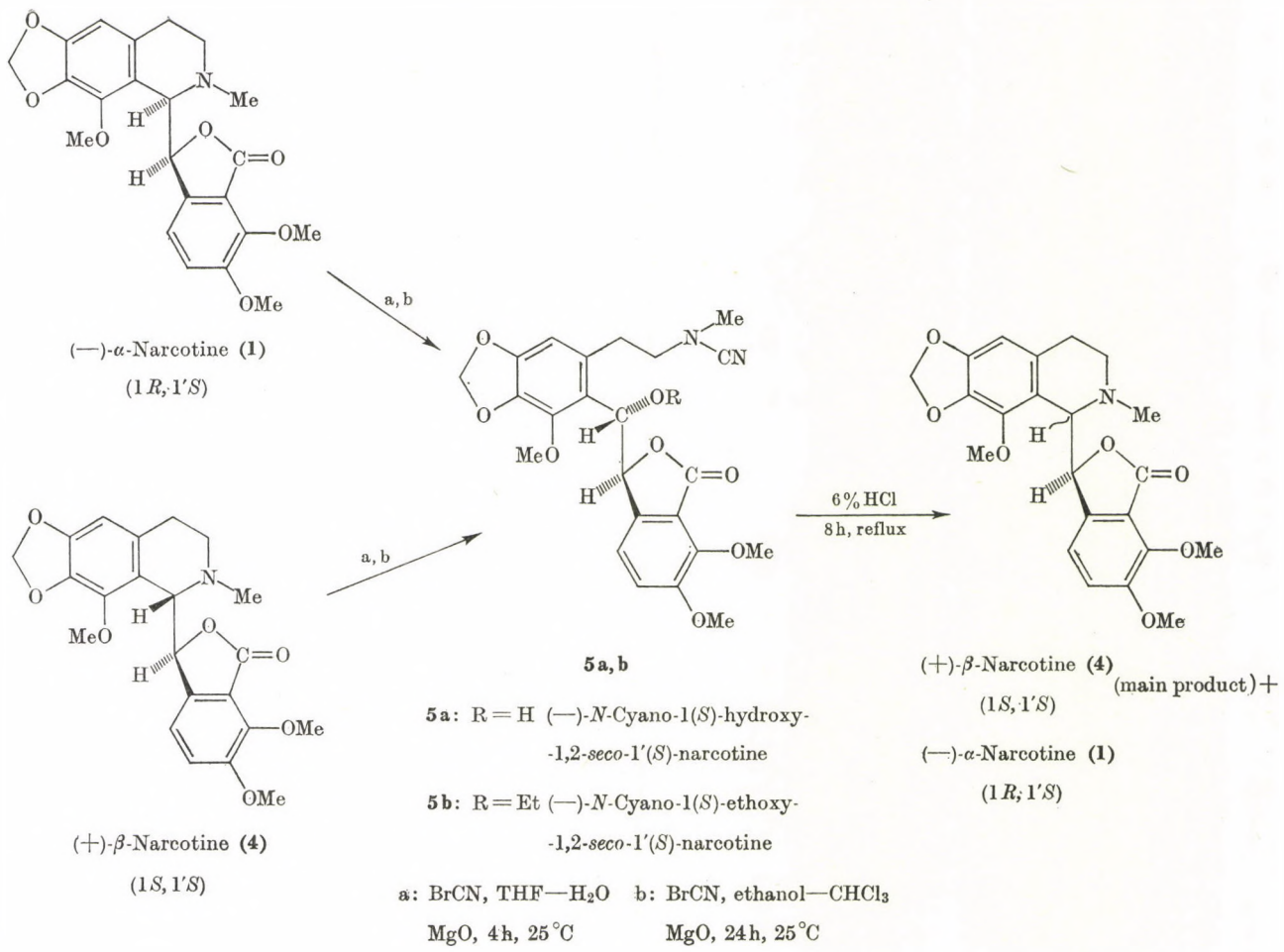
(—)-α-Narcotine (1)
(1R,1'S)
a, b
(+)-β-Narcotine (4)
(1S,1'S)
a, b
5a, b
5a: R = H (—)-N-Cyano-1(S)-hydroxy--1,2-seco-1'(S)-narcotine
5b: R = Et (—)-N-Cyano-1(S)-ethoxy--1,2-seco-1'(S)-narcotine
a: BrCN, THF—H2O MgO, 4h, 25 °C
b: BrCN, ethanol—CHCl3 MgO, 24h, 25 °C
6% HCl
8h, reflux
(+)-β-Narcotine (4)
(1S,1'S)
(main product)+
(—)-α-Narcotine (1)
(1R,1'S)

reaction. In the case of pseudoyohimbine, a mixture of epimeric seco compounds was isolated and the formation of epimers was explained by simultaneous S_N1 and S_N2 reactions.

The von Braun reaction effected under solvolytic conditions was examined further by RÖNSCH [4]. Inorganic bases were tried for binding the hydrogen bromide formed in the reaction; of these, magnesium oxide proved to be the most suitable. The author used only racemic alkaloids in the reactions, thus stereochemical changes were not discussed by him.

In view of these recent results, we re-examined the reaction of the four possible narcotine isomers with cyanogen bromide.

The reactions of (—)-α-narcotine (1*R*, 1'*S*) (**1**) and (+)-β-narcotine (1*S*, 1'*S*) (**4**) with cyanogen bromide in tetrahydrofuran–water solvent mixture in the presence of magnesium oxide yielded the same seco compound, (—)-*N*-cyano-1(*S*)-hydroxy-1,2-*seco*-1'(*S*)-narcotine (**5a**) in high yields, in the form of a homogeneous substance. Formation of the C-1 isomeric compound could not be detected.

The reaction effected in the chloroform–ethanol solvent mixture yielded an analogous result. Both isomers (**1** and **4**) were converted into the same seco compound, which was (—)-*N*-cyano-1(*S*)-ethoxy-1,2-*seco*-1'(*S*)-narcotine (**5b**), in 60% yield. The formation of an isomeric compound was not observed in this reaction either.

Refluxing of the seco compounds **5a** and **5b** in dilute hydrochloric acid resulted in ring closure. The main product isolated from the reaction mixture was (+)-β-narcotine (**4**) in about 50% yield. On the addition of (+)-α-narcotine (**2**), the mother liquor of crystallization yielded the very scarcely soluble (±)-α-narcotine (α-gnoscopine). The amount of this compound indicated that (—)-α-narcotine (**1**) had also been formed during the ring closure step in 10% yield.

As expected, the other two narcotine isomers (+)-α-narcotine (1*S*, 1'*R*) (**2**) and (—)-β-narcotine (1*R*, 1'*R*) (**3**) gave the products being in enantiomeric relationship with the former (**5a** and **5b**) seco compounds, *i.e.* (+)-*N*-cyano-1(*R*)-hydroxy-1,2-*seco*-1'(*R*)-narcotine (**6a**) and (+)-*N*-cyano-1(*R*)-ethoxy-1,2-*seco*-1'(*R*)-narcotine (**6b**), respectively, was isolated from the solvent mixtures used in the reaction.

In this case, the main product of ring closure occurring on refluxing in dilute acid was (—)-β-narcotine (**3**), and on the addition of (—)-α-narcotine the mother liquor yielded α-gnoscopine, thus (+)-α-narcotine (**2**) had also been formed in the reaction.

In the seco compounds **5a** and **6a**, the relative configuration of the C-1 atom related to the C-1' chiral centre, as well as its absolute configuration (since this centre remains unchanged during the reaction, therefore its absolute configuration is known), were determined on the basis of the PMR spectra.

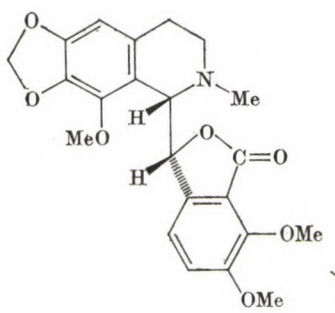

(+)-α-Narcotine **(2)**

(1*S*, 1′*R*)

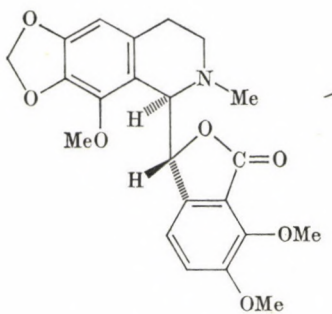

(−)-β-Narcotine **(3)**

(1*R*, 1′*R*)

a, b

a, b

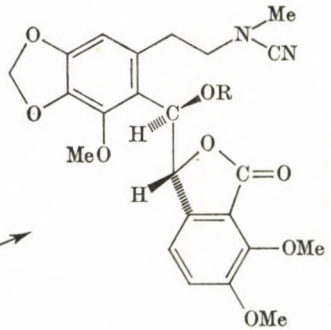

6a, b

6%HCl
8h, reflux

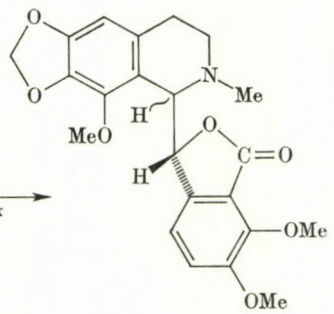

(−)-β-Narcotine **(3)** (main product) +

(1*R*, 1′*R*)

(+)-α-Narcotine **(2)**

(1*S*, 1′*R*)

6a: R = H (+)-*N*-Cyano-1(*R*)-hydroxy--1,2-*seco*-1′(*R*)-narcotine

6b: R = Et (+)-*N*-Cyano-1(*R*)-ethoxy--1,2-*seco*-narcotine

a: BrCN, THF—H_2O MgO, 4h, 25°C

b: BrCN, ethanol—$CHCl_3$ MgO, 24h, 25°C

In the PMR spectrum of (—)-α-narcotine (**1**) the coupling constant of the H-1 and H-1' protons is low ($J_{1,1'} = 4$ Hz), and the chemical shifts of the H-6' and H-7' aromatic protons (6.99 and 6.09 ppm) indicate that the H-7' aromatic proton in ring D falls into the shielding region of ring A; on the basis of these considerations, the most probable configuration of the compound is the following [5, 6]:

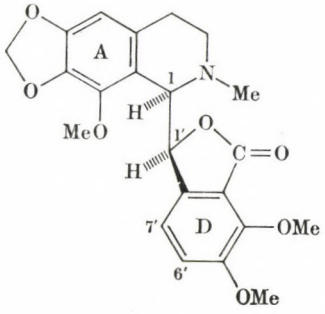

(1)

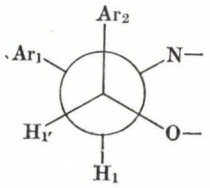

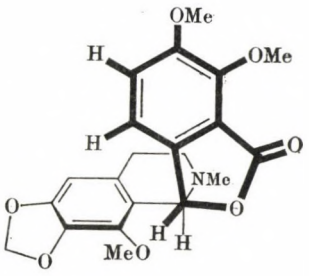

(1)

In the PMR spectrum of the seco compound **5a**, the coupling constant of the H-1 and H-1' protons is $J_{1,1'} = 8$ Hz, indicating the presence of protons of antiperiplanar position; the chemical shifts of the H-6' and H-7' protons (7.02 and 6.20 ppm) also show that H-7' of ring D is within the shielding region of ring A. Of the six possible staggered conformations of the seco compounds that can be derived from (—)-α-narcotine by retention or inversion of the configuration of the C-1 carbon atom, these spectral data are only in accordance with the B1 conformation, thus this seems to be the most populated one.

In view of these facts it can be stated that during the ring cleavage of the α-isomers inversion of the configuration at C-1 takes place.

The staggered conformations of the seco compound **5a** in the case of retention are as follows:

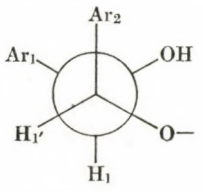

A 1

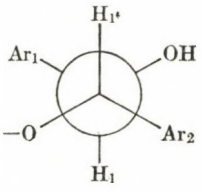

A 2

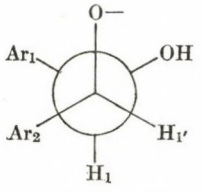

A 3

The staggered conformations of the seco compound **5a** in the case of inversion are:

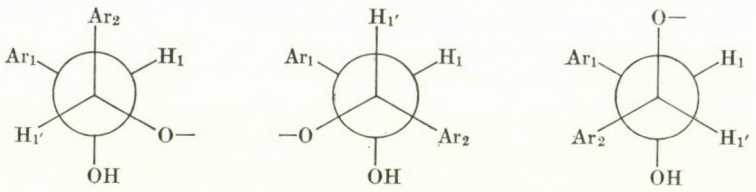

B 1 B 2 B 3

The spectroscopic determination of the configuration of (—)-*N*-cyano-1(*S*)-hydroxy-1,2-*seco*-1'(*S*)-narcotine, prepared from (—)-α-narcotine, is also supported by the X-ray diffraction analysis of the compound [7].

Similar considerations hold for the confirmation of the configuration of the seco compound **6a**.

According to the PMR spectral data of (—)-β-narcotine, the H-1 and H-1' protons are in the same position as in (—)-α-narcotine ($J_{1,1'} = 4$ Hz), yet the resonance signals of the H-6' and H-7' protons appear at nearly identical field strengths (6.96 and 7.18 ppm), as in this case the protons of ring D are outside the shielding region of ring A. The most probable configuration of (—)-β-narcotine (**3**) is the following:

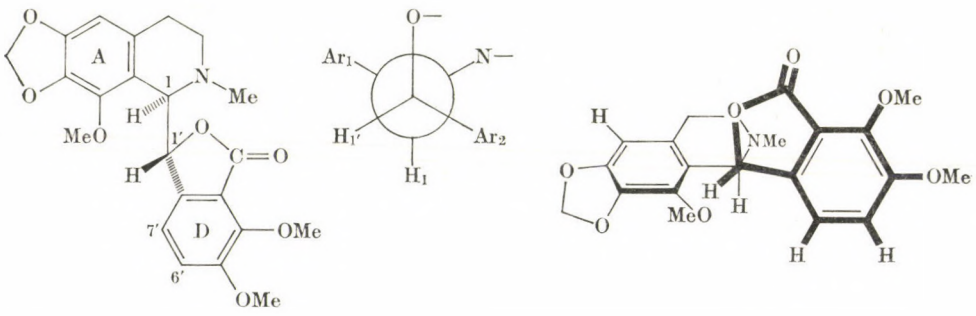

(3) (3)

The PMR spectrum of the seco compound **6a** is entirely identical with the spectrum of compound **5a** ($J_{1,1'} = 8$ Hz; H-6' 7.02; H-7' 6.2 ppm), thus A2 is the most probable one of the six possible staggered conformations of the seco compounds that can be derived from (—)-β-narcotine through retention or inversion.

Consequently, the ring cleavage of the β-isomers involves the retention of the C-1 configuration.

The staggered conformations of the seco compound **6a** in the case of retention are the following:

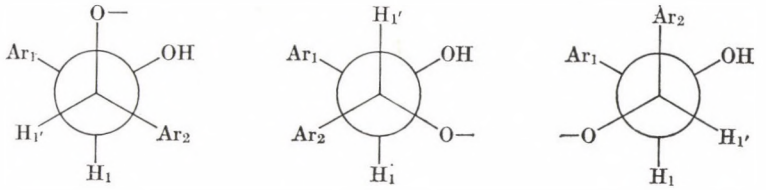

A 1 A 2 A 3

The staggered conformations of the seco compound **6a** in the case of inversion are:

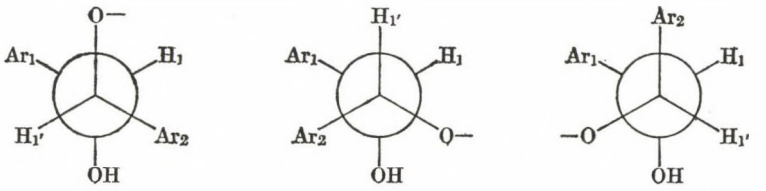

B 1 B 2 B 3

The above conclusions are in accordance with the experimental observation that (—)-α- and (+)-β-narcotine, as well as (—)-β- and (+)-α-narcotine yield enantiomeric seco compounds (**5a** and **6a**, respectively).

In the knowledge of the absolute configuration of the seco compounds, the following statements can be made as regards the stereochemical course of the reaction.

In the case of α-narcotine (*erythro*) isomers, the *N*-cyanoammonium salt [8] formed primarily is attacked by the nucleophilic water or alcohol on the side opposite to the C-1-N bond, and an S_N2 reaction occurs with the inversion of configuration.

In the case of β-narcotine (*threo*) isomers, a reaction of S_N1 type is assumed, which results in retention, instead of racemization, because the carbenium cation formed on fission, of the C-1-N bond is probably shielded by the oxygen atom of the lactone ring from the side opposite to the attack of the nucleophilic agent.

The critical importance of the presence of the lactone ring is also supported by the experimental observation that the ring cleavage of 1(*R*)-(—)-laudanosine and 1(*S*)-(+)-laudanosine [9] with cyanogen bromide in tetrahydrofuran–water solvent mixture was accompanied by complete racemization. The product obtained from both isomers was identical with the seco compound prepared from (±)-laudanosine by RÖNSCH [4].

During the ring closure step, it is probably the non-protonated form of the secondary amine, formed on acid hydrolysis that effects an internal nucleophilic attack (S_Ni) on the C-1 carbon atom of benzyl type, which is supposedly also affected by a complex neighbouring group participation (chiral centre, electronic interaction), and the reaction at the C-1 carbon atom takes place mainly with retention of the configuration (formation of β-isomers of *threo* relative configuration), and inversion occurs to a limited extent only (formation of α-isomers of *erythro* relative configuration).

Experimental

M.p.'s are uncorrected. The IR spectra were recorded with a Unicam SP 200 instrument in KBr pellets, the PMR spectra were obtained with a Jeol Minimar 100 MHz apparatus in deuterochloroform. The chemical shifts are given in ppm (δ) related to TMS internal standard. The rotation values were measured with a Bendix NPL 143 D polarimeter.

(—)-*N*-Cyano-1(*S*)-hydroxy-1,2-*seco*-1'(*S*)-narcotine

(*a*) *From* (−)-α-*narcotine*

(−)-α-Narcotine (**1**) (20.65 g; 50 mmoles) was dissolved in a mixture of THF (215 ml) and water (85 ml), then MgO (2.5 g), and cyanogen bromide (6.3 g; 60 mmoles) were added. The reaction mixture was allowed to stand at room temperature for 4 h with occasional shaking. The inorganic substance was then filtered off, washed with some water, and THF was removed in vacuum. The oily product solidified on standing; it was filtered off, washed with water and dried. The crude product (22.3 g) was crystallized from ethanol (180 ml) to yield 20.15 g (88%) of **5a**, m. p. 154—156 °C.

$C_{23}H_{24}N_2O_8$ (456.44). Calcd. C 60.52; H 5.30; N 6.14. Found C 61.04; H 5.35; N 6.26%.

$[\alpha]_D^{25}$ −56° (c = 0.5; $CHCl_3$).

IR: ν C≡N 2220, ν OH 3380 cm^{-1}.

PMR: 2.76 (3 H, s, NCH_3), 3.85, 4.01 and 4.07 (9 H, 3s, 3×OCH_3), 4.92 (1 H, d, J = 8 Hz, C-1 H), 5.86 (1 H, d, J = 8 Hz, C-1' H), 5.98 (2 H, s, OCH_2O), 6.20 (1 H, d, J = 8 Hz, C-7' H), 7.02 (1 H, d, J = 8 Hz, C-6' H), 6.47 (1 H, s, C-5 H).

(*b*) *From* (+)-β-*narcotine*

A solution of (+)-β-narcotine (**4**) (4.13 g; 10 mmoles) in a mixture of THF (43 ml) and water (17 ml) was allowed to react with cyanogen bromide (1.26 g; 12 mmoles) in the presence of MgO (0.5 g) as described above.

The crude product (4.3 g) was crystallized from ethanol (35 ml) to yield 3.75 g (82%) of the product, m. p. 154—156 °C; no m.p. depression was observed in admixture with the seco compound prepared from (−)-α-narcotine.

$[\alpha]_D^{25}$ − 53° (c = 0,5; $CHCl_3$).

IR: ν C≡N 2222, ν OH 3381 cm^{-1}.

(+)-*N*-Cyano-1(*R*)-hydroxy-1,2-*seco*-1'(*R*)-narcotine

(*a*) *From* (+)-α-*narcotine*

A solution of (+)-α-narcotine (**2**) (1.03 g; 2.5 mmoles) in a mixture of THF (11 ml) and water (4 ml) was allowed to react with cyanogen bromide (0.32 g; 3 mmoles) in the presence of MgO (0.12 g) at room temperature for 4 h.

The crude product (1.05 g) was crystallized from ethanol (9 ml) to yield 0.9 g (79%) of **6a**, m.p. 157—158 °C.

$C_{23}H_{24}N_2O_8$ (456.44). Calcd. C 60.52; H 5.30; N 6.14. Found C 60.37; H 5.34; N 6.15%.

$[\alpha]_D^{25}$ + 52° (c = 0.5; $CHCl_3$).

IR: ν C≡N 2220, ν OH 3378 cm^{-1}.

The PMR spectral data were completely identical with those of **5a**.

(*b*) *From* (−)-*β-narcotine*

(−)-*β*-narcotine (**3**) [10] (4.13 g; 10 mmoles) was allowed to react as described above. The crude product (4.05 g) was crystallized from ethanol (35 ml) to obtain 3.65 g (80%) of the product, m.p. 156−157 °C; no mixed melting point depression was observed with the seco compound prepared from (+)-α-narcotine.

$[\alpha]_D^{25}$ + 56° (*c* = 0.5; $CHCl_3$).

IR: *ν* C≡N 2222, *ν* OH 3380 cm^{-1}.

Cyclization of the 5a seco compound [(+)-β- and (—)-α-narcotine]

A mixture of **5a** (2.3 g; 5 mmoles) and 6% hydrochloric acid (70 ml) was refluxed for 8 h. After cooling, the mixture was made alkaline with conc. NH_4OH, the precipitate was filtered off, washed with water and dried.

The crude product (1.9 g) was recrystallized three times from ethanol to obtain 1.0 g (48%) of (+)-*β*-narcotine, m. p. 176−177 °C; $[\alpha]_D^{26}$ + 92° (*c* = 0.5; $CHCl_3$).

The alcoholic mother liquors were evaporated to about 12 ml, then a solution of (+)-α-narcotine (0.5 g) dissolved in hot ethanol (11 ml) was added. White needles separated (0.6 g, m.p. 220−223 °C). The product was crystallized from a mixture of chloroform (4 ml) and ethanol (20 ml) to yield 0.48 g, m. p. 228−229 °C of (±)-α-narcotine (α-gnoscopine). No m. p. depression was observed with authentic α-gnoscopine. The quantity of the product corresponds to 11.5% of (−)-α-narcotine.

Cyclization of the 6a seco compound [(—)-β- and (+)-α-narcotine]

Compound **6a** (2.3 g; 5 mmoles) and 6% hydrochloric acid (70 ml) were refluxed for 8 h. The crude product (1.95 g) obtained from the reaction mixture was recrystallized three times from ethanol to obtain 1.05 g (51%) of (−)-*β*-narcotine, m. p. 176−177 °C; $[\alpha]_D^{26}$ − 82° (*c* = 0.5; $CHCl_3$).

The alcoholic mother liquors were treated as described above; thus (±)-α-narcotine (m.p. 230−231 °C) was isolated on the addition of (−)-α-narcotine (0.5 g). The yield (0.4 g) corresponds to 10% of (+)-α-narcotine.

(—)-*N*-Cyano-1(*S*)-ethoxy-1,2-*seco*-1'(*S*)-narcotine (5b)

(*a*) *From* (−)-*α-narcotine*

(−)-α-narcotine (**1**) (4.13 g; 10 mmoles) was disolved in a mixture of anhydrous ethanol (10 ml) and dry chloroform (30 ml), then MgO (0.5 g) and cyanogen bromide (1.26 g; 12 mmoles) were added to the solution. The reaction mixture was allowed to stand at room temperature for 24 h, with occasional shaking. The inorganic material was removed by filtration and the solvent evaporated in vacuum. The residue was twice recrystallized from methanol, to give 3.05 g (63%) of **5b**, m. p. 129−132 °C.

$C_{25}H_{28}N_2O_8$ (484.49). Calcd. C 61.97; H 5.82; N 5.78. Found C 62.31; H 5.80; N 5.95%.

$[\alpha]_D^{26}$ − 40° (*c* = 1.0; $CHCl_3$).

IR: *ν* C≡N 2219 cm^{-1}.

PMR: 1.16 (3 H, t, $\underline{CH_3}-CH_2-O$), 3.55 (2 H, q, $CH_3-\underline{CH_2}-O$), 2.80 (3 H, s, NCH_3), 3.78, 3.88 and 4.07 (9 H, 3s, $3\times OCH_3$), 4.76 (1 H, d, *J* = 8 Hz, C-1 H), 5.81 (1 H, d, *J* = 8 Hz, C-1' H), 6.02 (2 H, s, OCH_2O), 6.13 (1 H, d, *J* = 8 Hz, C-7' H), 7.08 (1 H, d, *J* = 8 Hz, C-6' H), 6.47 (1 H, s, C-5 H).

(*b*) *From* (+)-*β-narcotine*

(+)-*β*-narcotine (**4**) (2.06 g; 5 mmoles) was allowed to react in the above manner; the crude product was twice recrystallized from methanol to yield 1.3 g (54%) of the product, m. p. 128−131°C; no m. p. depression was observed in admixture with the seco compound prepared from (−)-α-narcotine.

$[\alpha]_D^{26}$ − 40° (*c* = 1.0; $CHCl_3$).

IR: *ν* C≡N 2220 cm^{-1}.

(+)-*N*-Cyano-1(*R*)-ethoxy-1,2-*seco*-1'(*R*)-narcotine (6b)

(*a*) *From* (+)-α-*narcotine*

(+)-α-narcotine (**2**) (0.82 g; 2 mmoles) was allowed to react in the above manner, and the crude product was twice recrystallized from methanol to obtain 0.56 g (58%) of **6b**, m. p. 129—131 °C.

$C_{25}H_{28}N_2O_8$ (484.49). Calcd. C 61.97; H 5.82; N 5.78. Found C 62.00; H 5.84; N 5.88%.

$[\alpha]_D^{26}$ + 39.5° (c = 1.0; $CHCl_3$).

IR: ν C≡N 2220 cm^{-1}.

(*b*) *From* (−)-β-*narcotine*

The product obtained from (−)-β-narcotine (**3**) (2.06 g; 5 mmoles) was twice recrystallized from methanol. Yield 1.41 g (59%), m. p. 129—132 °C, no mixed melting point depression was observed with the seco compound prepared from (+)-α-narcotine.

$[\alpha]_D^{26}$ + 38.5° (c = 1.0; $CHCl_3$).

IR: ν C≡N 2203 cm^{-1}.

Cyclization of the seco compound 5b [(+)-β-narcotine]

A mixture of **5b** (4.84 g; 10 mmoles) and 6% hydrochloric acid (145 ml) was refluxed for 8 h. The product obtained on processing the reaction mixture was recrystallized from ethanol three times, to yield 2.05 g (50%) of (+)-β-narcotine, m. p. 175—176 °C; no m. p. depression was observed with an authentic sample.

Cyclization of the seco compound 6b [(—)-β-narcotine]

A mixture of **6b** (2.42 g; 5 mmoles) and 6% hydrochloric acid (70 ml) was refluxed for 8 h. The product obtained on processing the reaction mixture was recrystallized from ethanol three times. The yield was 0.95 g (46%), m. p. 174—175 °C; no mixed melting point depression was observed with (−)-β-narcotine.

The alcoholic mother liquor was concentrated to about 10 ml, then a solution of (−)-α-narcotine (0.5 g) in hot ethanol (10 ml) was added to it. The crystalline substance which separated was recrystallized from a mixture of chloroform and ethanol to obtain 0.4 g of (±)-α-narcotine, m. p. 228—229 °C. The yield corresponds to 10% of (+)-α-narcotine.

(±)-*N*-Cyano-1-hydroxy-1,2-*seco*-laudanosine

(*a*) A solution of 1(*R*)-(−)-laudanosine [9] (0.9 g; 2.5 mmoles) in a mixture of THF (50 ml) and water (20 ml) was mixed with cyanogen bromide (0.32 g) in the presence of MgO (0.12 g), and stirred for 1.5 h. The crude product (0.88 g, m. p. 108—110 °C) was crystallized from a mixture of THF and ether, to obtain 0.6 g of the product, m. p. 109—111 °C, which gave no melting point depression in admixture with the seco compound prepared from (±)-laudanosine [4].

(*b*) The data of the product obtained from 1(*S*)-(+)-laudanosine (0.9 g; 2.5 mmoles) after purification were: 0.6 g, m. p. 109—111 °C.

*

The authors thank the Alkaloida Chemical Works (Tiszavasvári, Hungary) and the Hungarian Academy of Sciences for supporting this research.

Thanks are due to Prof. G. Casinovi (Istituto Superiore di Sanità, Rome, Italy) and to Mr. L. Szilágyi for recording of the PMR spectra and discussions, and to Miss E. Jeszenszki for technical assistance.

REFERENCES

[1] Gaál, Gy., Kerekes, P., Bognár, R.: J. prakt. Chem., **313**, 935 (1971); Magyar Kém. Folyóirat, **77**, 533 (1971)

[2] Hageman, H. A.: Org. Reactions, **7**, 198 (1953)

[3] ALBRIGHT, J. D., GOLDMAN, L.: J. Amer. Chem. Soc., **91,** 4317 (1969)
[4] RÖNSCH, H.: J. prakt. Chem., **314,** 382 (1972)
[5] SAFE, R., MOIR, R. Y.: Can. J. Chem., **42,** 160 (1964)
[6] BATTERSBY, A. R., SPENCER, H.: J. Chem. Soc., **1965,** 1087
[7] SASVÁRI, K., PÁRKÁNYI, L., KEREKES, P., BOGNÁR, R.: Acta Crystallogr., Sect. B, **35,** 986 (1979)
[8] FODOR, G., ABIDI, S., CARPENTER, T. C.: J. Org. Chem., **39,** 1507 (1974)
[9] CAVA, M. P., AFZALI, A.: J. Org. Chem., **40,** 1553 (1975)
[10] MARSHALL, M. A., PYMAN, F. L., ROBINSON, R.: J. Chem. Soc., **1934,** 1315

Péter KEREKES
György GAÁL
H-4010 Debrecen, P.O.B. 20.

Acta Chimica Academiae Scientiarum Hungaricae, Tomus 103 (4), pp. 355—363 (1980)

COMPUTERIZED CALCULATIONS OF COMPLEX EQUILIBRIA, I

A GENERAL PROGRAM FOR THE EVALUATION OF SPECTROPHOTOMETRIC EQUILIBRIUM MEASUREMENTS

F. GAIZER and M. MÁTÉ

(College of Food Technology, Department of Chemistry, Hódmezővásárhely, Hungary)

Received October 27, 1978
Accepted for publication May 21, 1979

A computer program, SPEF-3, of low memory requirements and of short running time, has been elaborated for the evaluation of equilibria of the type: $q\,M + p\,L + r\,H^+ \rightleftharpoons M_qL_p(H^+)_r$ from spectrophotometric measurements (r and/or q may be equal to zero). The program calculates the optimal values and probable errors of formation constants and molar extinction coefficients of the species giving the best fit with the measured absorbancies. The calculation of the values of the parameters is made according to the GAUSS method by a least squares procedure from the experimental data: T_M, T_L, $[H^+]$ and A. The best convergence was found by numerical differentiation with respect to the $\log \beta$ values.

The program, written in ASA FORTRAN language, may be used in the case of the formation of as many as 9 complex species, for the simultaneous treatment of measurements made at a maximum of 3 wavelengths and for the refinement of 2—5 parameters in one refining cycle. The program can easily be extended and portions can be used for the evaluation of other types of complex equilibria.

Spectrophotometry is a method frequently used for the study of complex equilibria. For the calculation of the formation constants and molar extinction coefficients, and sometimes also the compositions of the species formed in a studied system, many numerical and graphical methods [1, 2] have been elaborated. However, these methods make possible only the evaluation of simpler systems, which restricts the applicability of this experimental method. For the evaluation of more complicated systems containing several mono- and polynuclear, as well as mixed ligand complexes, only computerized procedures are applicable. Most of the computer programs published up to this time [3—12] can be used only for the calculation of simpler systems, but some of them can be used in the case of the formation of more than two complexes, either after improvement [8, 9] or if the experimental conditions are favorable [11]. The most effective programs so far are the LETAGROP-SPEFO [13, 14], its improved version [15], and the SQUAD program [16], which is based on the principle of the SCOGS program [17].

The present paper deals with the SPEF-3* program and reports on the results of our experiments to study its applicability and operating features.

* The program, with the necessary information, is available upon request.

This program is an improved version of the previously published [18] and successfully employed [19—21] SPEFCA program, which can also be used in cases of several mono- and polynuclear species.

Problems to be evaluated and the principle of evaluation

In the case of spectrophotometric measurements, 3 types of problems occur most often:

1. The protonation ($+r$) or deprotonation ($-r$) of the ligand(s):

$$r\,H^+ + p\,L \rightleftharpoons (H^+)_r L_p \tag{1}$$

2. Only the metal ions and ligands form complexes:

$$q\,M + p\,L \rightleftharpoons M_q L_p \tag{2}$$

3. Protonated (deprotonated) metal complexes are formed:

$$q\,M + p\,L + r\,H^+ \rightleftharpoons M_q L_p (H^+)_r \quad (\equiv c_j) \tag{3}$$

The equilibrium constant of this last process is as follows:

$$\beta_{rqp} = \frac{[M_q L_p (H^+)_r]}{[M]^q [L]^p [H^+]^r} \tag{4}$$

With omission of the reactants absent from the process, Eq. (4) is valid for all the three processes and is used in the program.

Assuming the validity of Beer's law, for the absorbancy reduced to 1 cm layer thickness of an equilibrium system containing N complex species we may write:

$$A_m = \varepsilon_M[M] + \varepsilon_L[L] + \sum_{j=1}^{j=N} \varepsilon_j c_j = \varepsilon_M[M] + \varepsilon_L[L] + \sum_{j=1}^{j=N} (\beta_j \varepsilon_j [M]^q [L]^p [H^+]^r)_j \tag{5}$$

In spectrophotometric measurements the following experimental data are available: the total ligand and the total metal ion concentrations (T_L and T_M), the measured absorbancies (A_m) of the reactions mixtures, and, if the chemical process is pH-dependent, the free hydrogen ion concentrations. The aim of the calculations is to obtain from these data the value of the formation constant and molar extinction coefficient of each complex formed and, if the compositions of the complexes are unknown, these too. With the SPEF-3

program the optimal values of the parameters can be calculated that give the smallest deviation between the measured (A_m) and calculated (A_{calc}) absorbancies in the least squares sense:

$$U = \sum^{expts} (A_{m,i} - A_{calc,i})^2. \tag{6}$$

Instead of U it is more advantageous to calculate and use for the measure of the fit the standard deviation, $\sigma(A)$, because this quantity has to be as large as the errors estimated after the experimental conditions and the reproducibility of measurements.

The course of the calculation in the program is as follows: first, the number of complexes (N) and their compositions (rqp combinations), as well as their β- and ε-values, are assumed. Then correction values are calculated for the parameters β and ε, and the initial values are corrected. Finally, the extent of the fit is checked and, if it is not satisfactory or appears to be improvable, the refinement cycle is repeated, taking the corrected parameter values as initial ones. This process can be repeated several times until there is no further significant change in the parameter values in the course of subsequent refinements.

Calculation of the optimal values of parameters

In a mathematical sense the problem to be solved is the calculation of the parameters of the function of type $y_i = f(\gamma_1, \gamma_2, \ldots \gamma_m; x_i)$, which give the minimum error square sum (U) of the measured (y_i) and calculated ($y_{calc,i}$) intensities. For the minimization of such a function the GAUSS method [22, 23] is followed. By this method the elements of the vector $\mathbf{h}$ correcting the initial values of parameters can be calculated by the following equation:

$$\overset{\downarrow}{\mathbf{h}} = (\mathbf{G}^T \mathbf{W}\mathbf{G})^{-1} \mathbf{G}^T \mathbf{W}\overset{\downarrow}{\mathbf{d}} \tag{7}$$

In Eq. (7) $\mathbf{W}$ is the weighting matrix, $\mathbf{W} = \text{diag}\ (w_1, w_2, w_3, \ldots w_n)$, $\mathbf{d}$ is the deviation vector the elements of which are the differences between the measured intensities (y_i) and those calculated (y_i°) from the initial values of the parameters. The matrix $\mathbf{G}$ consists of the elements $g_{ij} = \partial f_i / \partial \gamma_j$. The errors in the parameters $[\sigma(\gamma_j)]$ can be calculated from the diagonal elements (g_{jj}^{inv}) of $(\mathbf{G}^T\mathbf{G})^{-1}$ as follows:

$$\sigma(\gamma_j) = \sqrt{|g_{jj}^{inv}| \frac{U}{n - P - 1}} \tag{8}$$

(n and P are the number of experimental points and parameters, respectively).

It can be seen that for the calculation of the correction vector according to Eq. (7), only the calculation of the elements of **d** and **G** is necessary. The elements of the matrix **G** can be obtained by numerical or analytical differentiation. The simplest formula for the former is $g_{ij} = (y_i^\circ - y'_{ij})/\Delta t_j$, where y'_{ij} means the intensity calculated by increasing the j-th parameter by the increment Δt_j. For spectrophotometric measurements the function is of the type $A_i = f(\vec{\beta}, \vec{\epsilon}, T_M, T_L, [H^+])$ and the analytical differentiation of Eq. (5) with respect to the β's yields:

$$g_{ij} = \frac{\partial A_i}{\partial \beta_j} = \frac{\varepsilon_j c_{ij}}{\beta_j} \tag{9a}$$

On the other hand, making the differentiation with respect to the ε's, one gets:

$$g_{ij} = \frac{\partial A_i}{\partial \varepsilon_j} = c_{ij} \tag{9b}$$

It can be seen that if the concentrations of the species are calculated, then the matrix **G** can easily be built up. A further important feature of formula (9b) is that it is valid for the free species [M] and [L] too, and if they are taken as the $(N+1)$-th and $(N+2)$-th species, their molar extinction coefficients will also be refinable parameters.

Description of the program

The SPEF-3 program can be used in its present form if a maximum of nine complexes are formed, and for simultaneous calculation of three wavelength data reduced to 1 cm layer thickness. The experimental points are not weighted. The program calculates the values of formation constants and molar extinction coefficients of the species, as well as the errors in these parameters. In the program the molar extinction coefficients of the reactants are dealt with as unknown parameters.

The main part of the program written for the refinement of parameters (Fig. 1) has been constructed as a unit which can be used for the calculation of the correction vector elements and of the error in each parameter, independently of the experimental origin of the elements of **d** and **G**. In the present form of the program, of the (in principle) unlimited number of parameters, a maximum of five can be refined simultaneously, with the inputting of their serial numbers.

In the program a possibility is also given for the "search" of the initial values of parameters, either within a given interval or around their assumed values. This part of the program can also be used to find the value of a param-

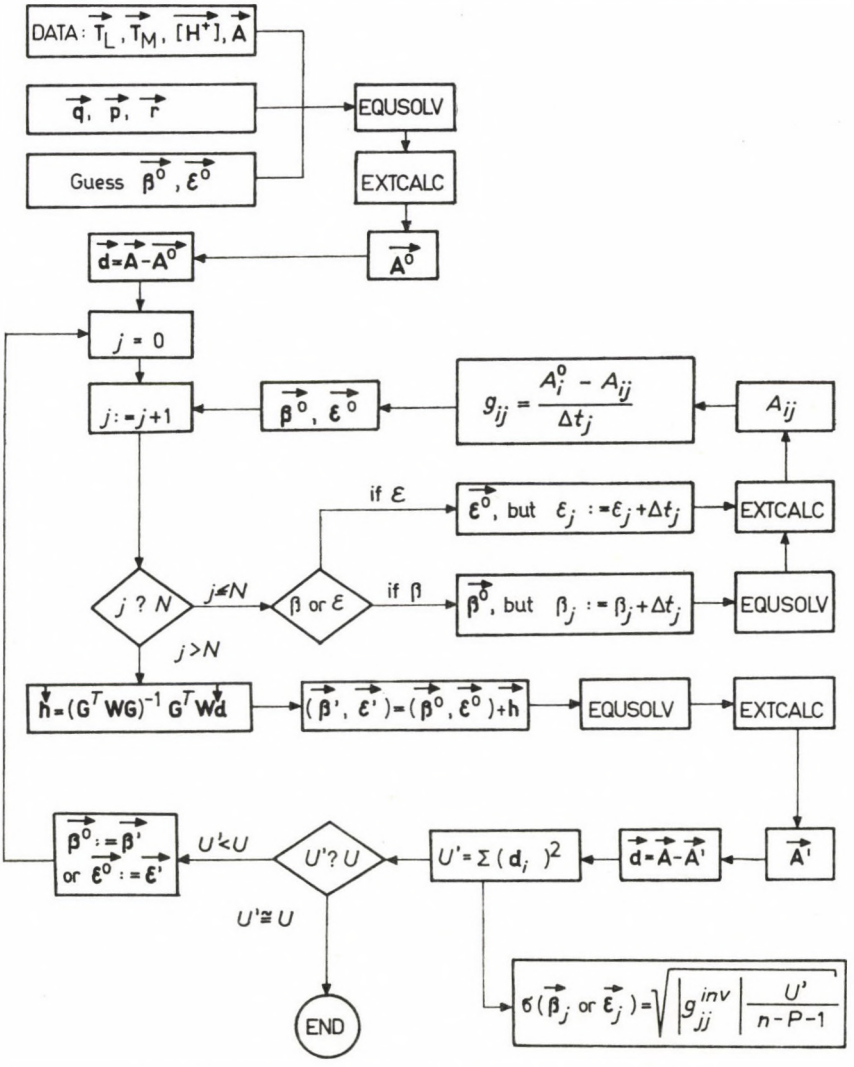

Fig. 1. The flow chart of the refinement of parameters

eter when the contribution of its complex to the measured absorbancy is small, *e.g.* owing to its relatively low concentration in the measured range. In such cases it often occurs that the parameters can not be refined at all.

The EQUSOLV subroutine is written for the solution of mass balance equations and for the calculation of the concentrations of species for a given set of β's. The mass balance equations to be solved are as follows:

$$T_M = [M] + \sum_{j=1}^{j=N} (q\beta_{rqp}[H^+]^r [M]^q [L]^p)_j \qquad (10)$$

$$T_L = [L] + \sum_{j=1}^{j=N} (p\beta_{rqp}[H^+]^r [M]^q [L]^p)_j \qquad (11)$$

The equations have two unknowns, [M] and [L], since $[H^+]$ is a measured quantity. The only exception is when the protonation (deprotonation) of a species takes place and therefore only Eq. (11) with one unknown is to be solved.

For the solution of the mass balance equations two iterative procedures are used in the program. The first is the Newton — Raphson method, which has the shortest conceivable running time, but with poor initial values or with equations containing terms of higher degrees it can diverge. In our experience, if convergence occurs, the third or fourth iteration cycle yields satisfactory or exact solutions, but if the fourth cycle does not give a solution either, it usually indicates divergence. In such a case the program automatically turn to the other method [24, 18], which modifies the starting values taken for the unknowns [M] and [L] by systematically alternating increments until the differences between the experimental and calculated total concentrations are less than the desired value. This method gives a satisfactory solution in every case, but only after 80—150 iteration cycles.

The EXTCALC subroutine of the program calculates the absorbances with the concentrations of the species calculated by the EQUSOLV subroutine and with their molar extinction coefficients. This subroutine also contains the calculation of the sum of squares.

Discussion

By the development of SPEF-3, a simple computer program of low memory requirements and of short running time has been constructed for the evaluation of equilibria of type (1)—(3). In constructing the program we took care with regard to easy extension and also to the possibility of using parts of the program for other problems without any alterations. By insertion or substitution of certain statements, the program can be extended to deal with any number of complexes, to carry out calculations with any layer thickness, and to the weighting of experimental points.

In spite of its simplicity, the GAUSS method used in the program for the refinement of parameters has proved to be a good and reliable procedure, if not more than four parameters are simultaneously refined. Although five or more parameters can be refined, divergence can easily occur. In this case trouble mainly arises from the parameters not substantially determined by the experimental data, *i.e.* if their complexes are formed only in small concentrations relative to others. However, the applicability of the program is not restricted by this, because the parameters can always be refined by dividing them into groups of 2 or 3.

To calculate the elements of matrix **G**, the applicability of both numerical and analytical derivation has been examined. The analytical one requires less running time, because it needs activization of the EQUSOLV subroutine only twice, *viz.* at the beginning of the refinement and after the correction of the values of the parameters. However, with this method several difficulties arise. The most serious is the slow convergence, and sometimes divergence. These originate from the fact that the analytical differentiation can be carried out only with respect to the β-values. This results in a difference of as much as 6—8 orders of magnitude between the determining values of matrix **G**; the difference appears as one of 12—16 orders of magnitude between the elements of matrix $(\mathbf{G}^T\mathbf{G})$. This might be the most reasonable explanation of the wrong correction values. Although there are suitable mathematical methods to solve this problem [25], our aim was to find the conditions that guarantee reliable convergence while maintaining simple mathematics and small program size.

A further difficulty occurring in the analytical differentiation is the treatment of nonabsorbing complexes, because their differentiation with respect to the ε-values results in columns of infinite value in the matrix **G**.

By using numerical differentiation with respect to the $\log \beta$ values to calculate the elements of matrix **G**, a very good convergence was found in all cases. In this case the columns of **G** are of nearly the same order of magnitude and the calculated correction values of the parameters are realistic. Further advantages are that it is possible to refine simultaneously the $\log \beta$ values and the molar extinction coefficients, while the formation constants do not become negative, but rather their values will decrease to a large extent. Therefore overall, numerical differentiation is used in the program, although this increases the running time of the program to some extent, for the EQUSOLV procedure must be run as many times as there are β's to be refined. However, this surplus time is recovered by faster and more reliable convergence.

Our experiments to find the optimal values of the increments of parameters (Δt) by numerical differentiation have led to the conclusion that their effects on the effectivity of convergence is less than one would expect. It has been found that if the formation of a species is not too small, the following values are optimum: if $\log \beta < 10$, then $\Delta t = 0.03-0.04$; if $10 < \log \beta < 20$, then $\Delta t = 0.04-0.05$, *etc.* For the increments of molar extinction coefficients, the best values are 1—5% of their total value.

By the usage of the refinement process several possibilities have been observed that stopped the running of the program. Most of these have been eliminated by suitable statements. This part of the program now works in a reliable way, except in the case of error in input or bad guesses.

For the calculation of the errors of parameters according to (8), individually calculated error square sums (U') are used in the program, employing only those experimental points where the formation of a species relating to a

parameter is significant. In this way, *i.e.* leaving out experimental points that give no information about a parameter refined, the errors and the reliabilities of the obtained parameter values can be judged better; *e.g.* whether their error originates from inaccurate measurements (if so $\sigma(A)$ is large) or the experimental method is not sensitive to detect some species, *etc.* Further, the number of experimental points (relative to the total) that give useful information for a parameter can also be seen. If it is too small, for example, the value of such a parameter is not well defined and can not be used.

An important preliminary requirement of the refinement process is the approximate knowledge of the values of the parameters to be optimized. Although there are methods for the calculation of the molar extinction coefficients of complexes formed [1], these methods can be used only for the formation of not more than two complexes. If there are three or more complexes in the system studied, only rough estimates can be obtained for the ε's. On the other hand, for the values of formation constants, only the often laborious numerical or graphical methods can give results, if there are no available data from the literature. However, as our experience has proved, it is not necessary to take trouble with these difficulties, because it is possible to find satisfactory initial values for the formation constants even if only rough estimates of molar extinction coefficients are available. Therefore, we can suggest initiating the calculation with the "sought" values of parameters, and to use other methods only if this is unsuccessful or the results of refinement seem to be checked.

The running time of the SPEF-3 program is very favorable in spite of the numerical differentiation used. The matrix operations of the refinement process require only seconds. The time-determining operations are the solution of the mass balance equations, *i.e.* the running time of the EQUSOLV subroutine. This subroutine is constructed in such a way that after the first run the roots found in the previous one are taken as starting iteration values. By this means, generally one or two Newton—Raphson cycles are successful for each experimental point.

Finally, it must be emphasized that the chemical usefulness of this program is only to find the best fit of the experimental data with one or several model(s). However, reliable conclusions can not be drawn from the results of such calculations without a critical check of the calculated parameter values from a chemical point of view, and in the acceptance of one of the formally possible models the chemical evidence must be decisive even if the accepted model gives a less favorable fit than another.

REFERENCES

[1] Beck, M. T.: Chemistry of Complex Equilibria, Akadémiai Kiadó, Budapest 1970
[2] Rossotti, F. J. C., Rossotti, H. S.: The Determination of Stability Constants, McGraw Hill, New York 1961
[3] Rabideau, S. W., Kleine, R. J.: J. Phys. Chem., **64**, 690 (1960)

[4] CONROW, K., JOHNSON, G. D., BOWEN, R. E.: J. Amer. Chem. Soc., **86,** 1025 (1964)
[5] ROTH, B., BUNNETT, J. F.: J. Amer. Chem. Soc., **87,** 334 (1965)
[6] ROPARS, C., VIOVY, R.: Bull. Soc. Chim. France, **1966,** 3637
[7] NAGANO, K., METZLER, D. E.: J. Amer. Chem. Soc., **89,** 2891 (1967)
[8] WENTWORTH, W. E., HIRSCH, W., CHEN, E.: J. Phys. Chem., **71,** 218 (1967)
[9] ROSSEINSKY, D. R., KELLAWI, H.: J. Chem. Soc. (A), **1969,** 1207
[10] LINGANE, P. J., HUGUS, Z. Z., Jr.: Inorg. Chem., **9,** 757 (1970)
[11] HAVEL, J., KUBAN, V.: Scripta Fac. Sci. Natur. Univ. Purkynianae Brun., **1,** 87 (1971)
[12] LIKUSSAR, W.: Anal. Chem., **45,** 1926 (1973)
[13] SILLÉN, L. G., WARNQVIST, B.: Acta Chem. Scand., **22,** 3032 (1968)
[14] SILLÉN, L. G., WARNQVIST, B.: Arkiv Kémi., **31,** 377 (1969)
[15] LYHAMN, L.: Chem. Scripta, **10,** 49 (1976)
[16] LEGGETT, D. J., MCBRYDE, W. A. E.: Anal. Chem., **47,** 1065 (1975)
[17] SAYCE, I. G.: Talanta, **15,** 1397 (1968)
[18] GAIZER, F.: Magy. Kém. Folyóirat, **83,** 250 (1977)
[19] GAIZER, F., BUXBAUM, P., PAPP-MOLNÁR, E., BURGER, K.: J. Inorg. Nucl. Chem., **36,** 859 (1974)
[20] BURGER, K., GAIZER, F., PAPP-MOLNÁR, E., TRAN THI BINH: J. Inorg. Nucl. Chem., **36,** 863 (1974)
[21] GAIZER, F., TRAN THI BINH, BURGER, K.: J. Inorg. Nucl. Chem., **36,** 1601 (1974)
[22] GAUSS, C. F.: Theoriae Combinationis Observationum Errobus Minimis Obnoxiae, 1821. In Gauss' Werk, Bd. IV. Göttingen (1873)
[23] KIM, H.: J. Chem. Educ., **47,** 120 (1970)
[24] INGRI, N., SILLÉN, L. G.: Acta Chem. Scand., **16,** 173 (1962)
[25] GANS, P.: Coord. Chem. Rev., **19,** 99 (1976)

Ferenc GAIZER
Maria MÁTÉ
H-6801 Hódmezővásárhely, IV., Lenin u. 15.

Acta Chimica Academiae Scientiarum Hungaricae, Tomus 103 (4), pp. 365—369 (1980)

CONVERSIONS OF TOSYL AND MESYL DERIVATIVES OF THE MORPHINE GROUP XXII*

SOME NUCLEOPHILIC SUBSTITUTION REACTIONS OF 6-*O*-MESYLNEOPINE**

S. BERÉNYI, S. MAKLEIT***, R. BOGNÁR and A. TEGDES

(Institute of Organic Chemistry, Kossuth Lajos University, Debrecen, Hungary)

Received March 2, 1979
Accepted for publication May 21, 1979

6-*O*-Mesylneopine, a compound not yet reported in the literature, has been prepared and some of its nucleophilic substitution reactions have been examined. As a result of the reactions, the 6β-chloro-, 6β-bromo- and 6β-azido derivatives, unknown up to now, have been obtained, furthermore, 6-demethoxythebaine, described so far only as an assumed intermediate has been prepared simply and in a satisfactory yield. This product offers several interesting possibilities for further conversions following from its structure. An S_N2 + E mechanism is suggested in the formation of 6-demethoxythebaine. The structures of the new compounds are substantiated by the elemental analyses IR, PMR and ^{13}C-NMR spectra and by chemical conversions.

In an earlier paper [1] a new, efficient and convenient procedure was described for the preparation of neopine from thebaine. In the meantime the isolation of natural neopine was also achieved without interference with the technology of processing poppy-head by the Kabay method [2].

Of the morphine group, neopine is one of the least examined compounds [3]. In connection with our investigations, only the work of RAPOPORT *et al.* [4] should be mentioned here. They prepared Δ^8-desoxycodeine from 6-*O*-tosylneopine with lithium tetrahydridoaluminate(III).

In the present work, the starting material was 6-*O*-mesylneopine, which can be prepared more easily [1] and, instead of the hydride anion, F^-, Cl^-, Br^-, I^- or N_3^- anions were employed as the nucleophilic partners.

Compound **1** did not yield the expected 6β-fluoro derivative with tetrabutylammonium fluoride in acetonitrile, but 6-demethoxythebaine (**2**) was obtained instead, in a high yield.

On the effect of lithium chloride in dimethylformamide, the 6β-chloro derivative (**3**) was formed; however, **2** could also be isolated from this reaction. The two products were formed in 6 : 4 ratio.

When lithium bromide was used in dimethylformamide, the 6β-bromo derivative (**4**) was obtained together with **2**, their ratio being 7 : 3.

* Part XXI: G. SOMOGYI, S. MAKLEIT, R. BOGNÁR: Acta Chim. Acad. Sci. Hung., **97**, 339 (1978); G. SOMOGYI, S. MAKLEIT, R. BOGNÁR: Magyar Kémiai Folyóirat, **83**, 327 (1977)
** 3-Methoxy-4,5-α-epoxy-6α-methanesulfonyloxy-8,14-didehydro-17-methylmorphinan
*** To whom correspondence should be addressed

The reaction with sodium iodide in dimethylformamide gave only **2**, and no product containing halogen could be isolated.

In connection with the formation of the above compounds it was assumed that the first step of the reaction is an S_N2 type reaction of the nucleophilic agent yielding the 6β-halogen derivative and these are converted into 6-demethoxythebaine in an elimination step.

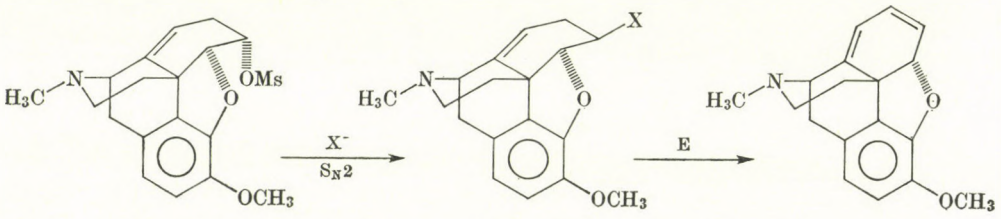

1 **3**: X = Cl **2**

4: X = Br

5: X = N_3

6: X = NH_2

The S_N2 character of the first step could be inferred from the conditions of the reaction and from the structure of the halogen derivatives formed. In compounds 3 and 4 the 6β position of the halogen atom was confirmed unambiguously by the $J_{5,6}$ value characteristic of the so-called iso derivatives: the actual value was 9.5—10 Hz for both **3** and **4** [5].

In order to confirm the above statements, **1** was allowed to react with sodium azide in dimethylformamide to obtain the 6β-azido derivative (**5**) ($J_{5,6}$ 10 Hz); this was then converted into the 6β-amino compound (**6**) with lithium tetrahydridoaluminate(III). The latter was further reduced in the presence of platinum dioxide into the 6β-aminodihydrocodeine derivative (3-methoxy-4,5α-epoxy-6-β-amino-17-methylmorphinan) (**7**), which had been prepared by us earlier and its steric structure had also been established [6].

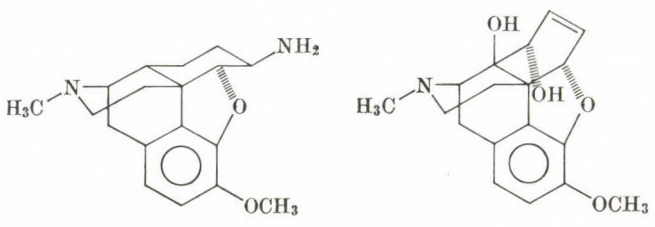

7 **8**

The extent of the elimination is a function of the reaction conditions. It was a surprising experience that under the conditions mentioned the 6β-fluoro derivative was not formed even in traces; this can be explained in view

of the statement in the literature that tetraalkylammonium salts are very suitable for effecting elimination reactions [7].

When examining the effect of this reagent on the halogen derivatives of neopine, in the case of compounds **3** and **4** its was observed that under identical reaction conditions in acetonitrile medium the extent of elimination was 50% from **3**, whereas **4** was quantitatively converted into **2**.

The ratio of the halogen derivatives (**3** or **4**) to **2** can be reliably determined by the PMR method.

The structure of **2** was verified, beyond the IR, PMR and ^{13}C-NMR spectra, by tis conversion with hydrogen peroxide in formic acid into the known compound [8], 14-hydroxy-*allo*pseudocodeine (**8**).

Of the new compounds prepared, compound **2** has been mentioned in the literature as a probable intermediate [9] in connection with the hydroboration of thebaine. This compound has now been obtained very conveniently and in a satisfactory yield. A consideration of its structure suggests several important possibilities for further conversions.

Experimental

Homogeneity of the substances was checked in each case by TLC using chloroform: acetone : diethylamine (5 : 4 : 2) developing mixture on Silica gel G layer. The detecting agent was Dragendorff reagent. M.p.'s are uncorrected; they were measured on a Koffler hot-stage. With all substances the IR (Unicam SP 200G and PE 283) and PMR (Jeol 100 MHz) spectra were recorded; the ^{13}C-NMR spectrum of **2** was also obtained (Varian XL 100 MHz).

6-*O*-Mesylneopine (1)

Neopine (10.0 g; 33.41 mmoles) was dissolved in anhydrous pyridine (40 ml), cooled to 0 °C, and a solution of methanesulfonyl chloride (3.32 ml; 4.9 g; 42.7 mmoles) in anhydrous pyridine (40 ml) was added dropwise. The solution was stirred at this temperature for 2 h then allowed to stand at room temperature for 24 h. It was then poured into water (1000 ml) saturated with sodium carbonate and extracted with chloroform (3 × 100 ml). The chloroform solution was washed with water, dried and evaporated to dryness. The residue was rubbed with anhydrous ether whereupon it crystallized rapidly to give 11.3 g (89.6%) of **1**. It was recrystallized from methanol; m.p. 177—178 °C.

$C_{19}H_{23}N_5OS$ (377.47). Calcd. N 3.7; S 8.47. Found N 3.19; S 8.41%.

$[\alpha]_D$ + 14° (c = 0.5, chloroform).

6-Demethoxythebaine (2)

(*a*) 6-*O*-Mesylneopine (**1**) (6.6 g; 17.48 mmoles) was dissolved in anhydrous acetonitrile (400 ml) and tetrabutylammonium fluoride (21.58 g; 87.4 mmoles) was added; the solution was then refluxed for 2.5 h. It was then poured into water (3000 ml) and extracted with chloroform (5 × 150 ml.) The chloroform solution was washed with water, dried and evaporated to dryness. The sticky residue crystallized on standing to give 3.81 g (77.7%) of **2**, m.p. 68—70 °C.

$C_{18}H_{19}O_2N$ (280.35). Calcd. N 4.99. Found N 4.75%.

$[\alpha]_D$ — 194° (c = 0.5, chloroform).

(*b*) 6-*O*-Mesylneopine (5.0 g; 13.24 mmoles) was dissolved in anhydrous dimethylformamide (250 ml), sodium iodide (19.78 g; 132 mmoles) was added, and the solution was refluxed at 120 °C for 30 h. It was then poured into water (500 ml) and extracted with ether

(4 × 100 ml). The ethereal solution was washed with water, dried and evaporated to dryness to leave 0.8 g (21.6%) of **2**. The reaction mixture was extracted with chloroform; in this way **1** (2.0 g; 36%) could be recovered.

(*c*) The bromo derivative (**4**) (0.5 g; 1.38 mmoles) was dissolved in anhydrous acetonitrile (30 ml) and after the addition of tetrabutylammonium fluoride (1.63 g) the solution was refluxed for 4 h. The mixture was processed as described under (*a*) to obtain **2** (0.28 g; 72%).

(*d*) The chloro derivative (**3**) (0.25 g; 0.786 mmoles) was dissolved in anhydrous acetonitrile (15 ml) and the solution was refluxed in the presence of tetrabutylammonium fluoride for 4 h; processing of the mixture as under (*a*) gave a 1 : 1 mixture of **2** and **3** (0.2 g).

6β-Chloro derivative (3)

6-*O*-Mesylneopine (5.0 g; 13.25 mmoles) was dissolved in anhydrous dimethylformamide (150 ml). Lithium chloride (5.59 g; 132 mmoles) was added to the solution and it was refluxed at 120 °C for 6 h. The solution was then poured into water (500 ml) and extracted with benzene (3 × 100 ml). The benzene solution was washed with water, dried and evaporated to dryness to leave a solid residue (2.9 g), which was recrystallized from methanol to yield 1.6 g (38.2%) of **3**, m.p. 145 °C.

$C_{18}H_{20}O_2NCl$ (317.81). Calcd. N 4.4; Cl 11.1. Found N 4.2; Cl 10.82%.

$[\alpha]_D$ — 121° (*c* = 0.5, chloroform).

The mother liquor of the crystallization from methanol was processed and 6-demethoxythebaine (**2**) (1.2 g), very slightly contaminated with **3**, was isolated.

6β-Bromo derivative (4)

6-*O*-Mesylneopine (3.0 g; 11.32 mmoles) was dissolved in anhydrous dimethylformamide (120) ml) and lithium bromide (9.8 g; 113 mmoles) was added. The solution was then refluxed at 120 °C for 11 h. The reaction mixture was processed as described for the preparation of **3** to obtain a solid residue (1.64 g), which was recrystallized from methanol to give 0.94 g (32.6%) of **4**, m.p. 149—151 °C.

$C_{18}H_{20}O_2NBr$ (362.28). Calcd. N 3.86; Br 22.05. Found N 3.97; Br 22.05%.

$[\alpha]_D$ — 132° (*c* = 0.5, chloroform).

From the mother liquor 0.7 g of a product could be isolated; this contained **2** and **4** in 3 : 1 ratio.

6β-Azido derivative (5)

6-*O*-Mesylneopine (10.0 g; 26.5 mmoles) was dissolved in anhydrous dimethylformamide (300 ml). Sodium azide (17.22 g; 265 mmoles) was added to the solution, and it was refluxed at 100 °C for 24 h. It was then poured into water (1000 ml) and extracted with ether (4 × 100 ml). The ethereal solution was washed with water, dried and evalporated to dryness. The residue was a crystalline substance (4.8 g; 55.8%); after recrystallization from ether–petroleum ether it had m.p. 112—115 °C.

$C_{18}H_{20}O_2N_4$ (324.37). Calcd. N 17.27. Found N 17.05%.

$[\alpha]_D$ — 76° (*c* = 0.5, chloroform).

IR: N_3 2100 cm^{-1}.

6β-Amino derivative (6)

A solution of **5** (1.0 g) in dry ether was added dropwise to a suspension of lithium tetrahydridoaluminate(III) in dry ether (100 ml), with cooling and stirring; the mixture was then refluxed for 1 h. The excess reagent was decomposed with ether saturated with water or water saturated with ether. The aqueous phase was extracted with ether. The ethereal solutions were combined, dried and evaporated to dryness to leave a crystalline product (0.3 g; 32.9%), m.p. 128—130 °C.

$C_{18}H_{22}O_2N_2$ (298.4). Calcd. N 9.38. Found N 9.73%.

6β-Amino-dihydro derivative (7)

Compound **6** (0.2 g) was dissolved in 50% acetic acid (10 ml) and hydrogenated in the presence of platinum dioxide (0.05 g) catalyst. The catalyst was removed by filtration, the solution was evaporated to dryness, the residue was dissolved in water, made alkaline with 10% sodium hydroxide and extracted with chloroform. After washing and drying the solution was evaporated to dryness, the residue was rubbed with ether and a crystalline product was obtained (0.12 g). Its physical data were identical with those given in the literature [6].

14-Hydroxy-allopseudocodeine (8)

6-Demethoxythebaine (1.0 g) was dissolved in 85% formic acid (4 ml) and 30% hydrogen peroxide (0.5 ml) was added. The mixture was then stirred at 40 °C for 2 h, poured into ice-water and made alkaline with ammonium hydroxide. After standing for 2 h, the mixture was extracted with chloroform, washed with water, dried and evaporated to dryness. The white crystalline residue was crystallized from a mixture of chloroform and petroleum ether to obtain 0.8 g (71.2%), of a product which was in every respect identical with **8** described in the literature [8]. (Compound **8** was also prepared according to Ref. [8] from **6**-*O*-tosyl-14-hydroxycodeine by solvolysis.) M.p. 135—137 °C.

$[\alpha]_D$ — 270° (c = 0.5, chloroform).

*

The authors' thanks are due to the Alkaloida Chemical Works, Tiszavasvári, Hungary for supporting this research, and to the analytical and spectroscopical laboratories of the Institute for the analyses and for the recording and evaulation of the IR and PMR spectra. Recording of the ^{13}C-NMR spectrum is gratefully acknowledged to Dr. L. RADICS.

REFERENCES

[1] MAKLEIT, S., BERÉNYI, S., BOGNÁR, R.: Acta Chim. (Budapest) **94,** 165 (1977); MAKLEIT, S., BERÉNYI, S., BOGNÁR, R.: Magyar Kém. Folyóirat, **83,** 478 (1977)
[2] MAKLEIT, S., BERÉNYI, S., BOGNÁR, R., DOBÁNY, ZS., PALINCZA, J., TAR, I., GULYÁS, S.: Hungarian Patent (pending)
[3] BENTLEY, K. W.: The Chemistry of the Morphine Alkaloids, p. 124. Oxford, Clarendon Press 1954; MANSKE, R. H. F.: The Alkaloids, Chemistry and Physiology. Vol. **XIII,** p. 8, 23, 59. New York, London, Academic Press 1971
[4] RAPOPORT, H., BONNER, R. M.: J. Amer. Chem. Soc., **73,** 2872 (1951)
[5] BATTERHAM, T. J., BELL, K. H., WEISS, U.: Aust. J. Chem., **18,** 1799 (1965)
[6] MAKLEIT, S., BOGNÁR, R.: Kémiai Közl., **30,** 289 (1968); BOGNÁR, R., MAKLEIT, S.: Acta Chim. Acad. Sci. Hung., **58,** 203 (1968); BOGNÁR, R., MAKLEIT, S.: Magyar Kém. Folyóirat, **74,** 523 (1968); BOGNÁR, R., MAKLEIT, S.: Acta Chim. Acad. Sci. Hung., **59,** 373 (1969)
[7] CLARK, J. H.: J. C. S. Chem. Commun., **1978,** 789
[8] CURRIE, A. C., GILLON, J., NEWBOLD, G. T., SPRING, F. S.: J. Chem. Soc., **1960,** 773
[9] TAKEDA, M., INOUE, H., KUGITA, A.: Tetrahedron, **25,** 1839 (1969)

Sándor BERÉNYI
Sándor MAKLEIT
Rezső BOGNÁR
Anikó TEGDES

H-4010 Debrecen, P.O.Box 20.

Acta Chimica Academiae Scientiarum Hungaricae, Tomus 103 (4), pp. 371—375 (1980)

N-DEMETHYLATION OF MORPHINE ALKALOIDS. PREPARATION OF NORNEOPINE

S. HOSZTAFI, S. MAKLEIT* and R. BOGNÁR

(Institute of Organic Chemistry, Kossuth Lajos University, Debrecen, Hungary)

Received March 9, 1979
Accepted for publication May 21, 1979

On the basis of an analysis of the methods reported for the *N*-demethylation of morphine alkaloids, two reaction paths have been elaborated for the preparation of norneopine, a compound unknown up to now; the starting material was neopine of allylamine structure.

N-Nitroso-norneopine, also unknown in the literature, has been prepared, which yields norneopine on hydrolysis with dilute hydrochloric acid. In connection with this, the *N*-demethylation of codeine and dihydrocodeine described in a similar manner was re-examined.

The reaction of neopine and azodicarboxylic acid dimethyl ester was found even more suitable for the preparation of norneopine. The reaction of thebaine and azodicarboxylic acid dimethyl ester reported in the literature was also studied, and modified conditions leading to the preparation of northebaine free from thebaine are described.

N-Demethylation of morphine alkaloids can be achieved in several ways.

The von Braun reaction [1], using cyanogen bromide, is one of the oldest and most frequently employed methods.

Azodicarboxylic acid esters [2] have also been used for long for the demethylation of codeine, however, norcodeine is obtained in this way in a very low yield (16%) only.

Another possibility is offered by the method of SPEYER and WALTHER [3], where the *N*-methyl group is converted into the *N*-nitroso derivative with nitrous acid, and the nor compound is then obtained by treatment with dilute hydrochloric acid.

In connection with this method it may be noted that only a few examples are known for the nitrosation of tertiary amines and the yields are low [4].

Lately, several papers have dealt with the examination of *N*-demethylation reactions by means of alkyl chloroformates [5], which can also be used in this field and the application of 2,2,2-trichloroethyl chloroformate [6] can be regarded as particularly favourable, since the conversion of the urethane derivative into the nor compound can be effected under very mild conditions.

Special methods have also been described for the conversion of codeine into norcodeine, such as the oxidation of codeine-*N*-oxide with potassium chromate [7] or the photo-oxidation of codeine [8].

* To whom correspondence should be addressed

The von Braun method is practicable for the preparation of the nor derivatives of most morphine alkaloids, although the yields vary. However, the reaction of thebaine (**1**) with cyanogen bromide does not yield the desired product; instead, a so-called cyano-normethine (**2**) is isolated [9, 10, 11], as a result of cleavage of the nitrogen-containing ring.

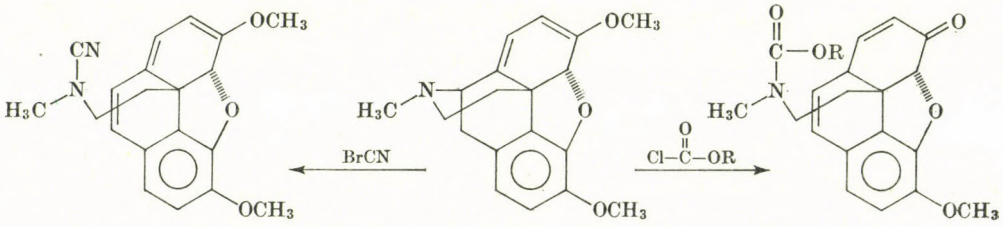

2 **1** **3**

When alkyl chloroformates were allowed to react with thebaine (**1**), again the nitrogen-containing ring was split and the product was acyl-normethine-codeinone (**3**) [12].

Northebaine was first synthesized by BARTELS-KEITH [13] from dihydronorcodeinone, and later RAPOPORT *et al.* [14] also prepared it in a similar manner. In 1966 a Dutch patent [15] described the preparation of northebaine from thebaine by the use of azodicarboxylic esters, in 50% yield. The unstable addition product (**4**) can be decomposed with saturated ammonium chloride solution or pyridine hydrochloride.

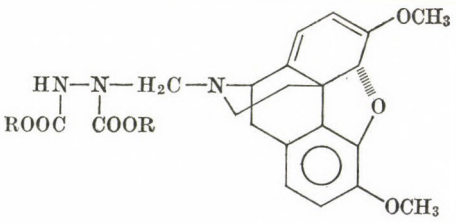

4

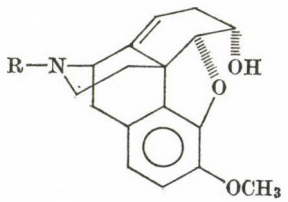

5a: R = CH_3

5b: R = H

The disadvantage of the method is that thebaine acting as a philodiene partner will also enter a Diels—Alder reaction with compounds of the ROOC—N=N—COOR type [16].

Morphine alkaloids which contain 8,14-double bond and thus have an allylamine structure, react with cyanogen bromide like thebaine does. This was observed with Δ^8-desoxycodeine (= desoxyneopine) and neopine (**5a**) [17].

Recently, azodicarboxylic esters have been increasingly employed for *N*-demethylation: in the case of the so-called BENTLEY compounds [18, 19], benzomorphanes [20] and also of 5β-methyldihydromorphinone (Metopon) [21], although the yields are lower than 50%.

In continuation of the work done by us lately on neopine [22, 23, 24], we wished to prepare the nor derivative (**5b**) (3-methoxy-4,5α-epoxy-8,14-didehydromorphinan) from neopine of allylamine structure (**5a**), taking into consideration all the experiences reported by users of the above methods.

Neopine is much less sensitive to acids than thebaine; therefore the demethylation method utilizing the *N*-nitroso derivative suggested by SPEYER and WALTHER [3] was tried first with codeine and dihydrocodeine, since for these compounds the authors [3] stated yields identical with those obtainable by von Braun's method, but did not publish the actual data.

When starting from codeine, the above method yielded the *N*-nitroso derivative in 50% yield; its hydrolysis occurred in 86% yield, and the preparation of the base from the hydrochloride was achieved in 80% yield; thus norcodeine was obtained in 30% overall yield (by the von Braun method, codeine and 6-*O*-acetylcodeine can be converted into norcodeine in 38 and 70% yield, respectively).

When dihydrocodeine was treated according to Ref. [3], the yields were even lower: 33% for nitrosation, 79% for hydrolysis, and 64% in the conversion of the hydrochloride to the base, the overall yield thus being 16.6%. (No literature data are available for the yield of the von Braun reaction.)

According to our investigations, the preparation of norneopine (**5b**) can be achieved in the manner given for dihydrocodeine, although in a low yield. The *N*-nitroso derivative was obtained in 25% yield, its hydrolysis into norneopine without the isolation of the chlorohydrate could be achieved in 73% yield, thus the overall yield was 18.2%.

The most promising method was, in our opinion, *N*-demethylation by means of azodicarboxylic ester. However, the conditions of the Dutch patent [15] of preparing northebaine were first examined and modified. We found that when a 1.1-fold excess of azodicarboxylic acid dimethyl ester (ADDE) is used, a significant amount of thebaine remains unchanged and thebaine hydrochloride cannot be separated from northebaine hydrochloride by crystallization from water. The amount of unchanged thebaine can, however, be reduced by the use of a 1.5-fold excess os ADDE. In this case the Diels—Alder adduct also appears among the products, but the latter can be separated from northebaine without difficulty, since the adduct is well soluble in hot ethanol, while northebaine hydrochloride is insoluble. In this reaction pure northebaine hydrochloride can be obtained in 30% yield.

When using a twofold excess of ADDE, neopine gives the norneopine base in 35% yield. It is advisable, however, to isolate the adduct (of type **4**)

and carry out the hydrolysis with aqueous ammonium chloride; the hydrochloride cannot be isolated, as it is well soluble in both water and ethanol. The solubility of also the norneopine base in water is significant.

It is to be mentioned that, according to our observations, both thebaine and neopine react with ADDE much slower than codeine does (codeine was completely converted in 3 h with ADDE). The adduct of type **4** is very unstable (hydrazo ester) and the presence of the nor derivative can be detected in threaction mixture before hydrolysis. The compound to be demethylated is allowed to react preferably in benzene: the use of alcohols as solvent is unfavourable because of interaction of the solvent and ADDE [25].

Experimental

Homogeneity of the compounds was checked in each case by TLC using chloroform: : diethylamine : acetone (5 : 2 : 4) developing mixture on Silica gel G layer; Dragendorff reagent was used for detection. M.p.'s are uncorrected; they were measured on a Koffler hot-stage. IR (Unicam SP 200 G and PE 203) and PMR (Jeol 100 MHz) spectra of the compounds were recorded.

N-Nitroso-norneopine

Neopine (1.5 g) and sodium nitrite (7.5 g) were dissolved in water (45 ml) and 2*N* sulfuric acid was added dropwise at 90 °C, with stirring, at a rate of using 35—40 ml of sulfuric acid during 1.5 h. After some time a crystalline substance precipitated, which was filtered off after cooling. The filtrate was extracted with chloroform (3×20 ml), the combined organic phase was washed with 10% hydrochloric acid (3×10 ml), then with water, dried and the solvent evaporated. The residue was combined with the crystalline substance which had been filtered off previously, and recrystallized from some water to obtain 400 mg of the product, m.p. 180—182 °C.

$C_{17}H_{18}N_2O_4$ (314). Calcd. N 8.92. Found N 9.15%.

Norneopine (5b)

(*a*) *N*-Nitroso-norneopine (300 mg) was refluxed in ethanol saturated with hydrochloric acid (10 ml) for 1 h, then the solution was evaporated to dryness. The residue was dissolved in water and made alkaline with 25% ammonium hydroxide solution, then extracted with chloroform (3×10 ml). The combined organic phase was washed with water, dried and evaporated to dryness. The residue was crystallized from ethyl ecetate to obtain. 190 mg (73%) of **5b**, m.p. 185—187 °C. It was in all respects (TLC, IR, PMR) identical with the product prepared according to (*b*) (see below).

(*b*) Neopine (1.5 g; 5 mmoles) and azodicarboxylic acid dimethyl ester (1.5 ml; 10 mmoles) were refluxed in dry benzene (10 ml) for 4.5 h. The solution was evaporated to dryness and the residue rubbed with ether. The solid was filtered off, dissolved in 96% ethanol (50 ml), an aqueous solution (10 ml) of ammonium chloride (4 g) was added, and the mixture was refluxed for 5 h. Afterwards, 1*N* HCl (20 ml) was added and the ethanol evaporated in vacuum. The residual solution was extracted with chloroform (3×20 ml), the cold aqueous phase was made alkaline with 10% sodium carbonate and extracted with chloroform (4×20 ml). The combined organic phase was washed with water saturated with sodium chloride and dried. Amorphous norneopine (1.15 g) was obtained on evaporation (35%); this was crystallized from ethyl acetate, m.p. 184—187 °C; after repeated recrystallizations, m.p. 189—191 °C.

$[\alpha]_D$ — 44° (*c* = 0.5, chloroform).

$C_{17}H_{19}NO_3$ (285). Calcd. C 4.92. Found N 4.94%. The structure was confirmed by the IR and PMR spectra.

*

The authors' thanks are due to the Alkaloida Chemical Works, Tiszavasvári, Hungary, for supporting this research, and to the analytical and spectroscopical laboratories of the Institute for the analyses and recording and evaluating the IR and PMR spectra.

REFERENCES

[1] HAGEMAN, H. A.: Org. Reactions, Vol. **7**, p. 221—222
[2] DIELS, O., FISCHER, E.: Ber., **47**, 2043 (1914)
[3] SPEYER, E., WALTHER, L.: Ber., **63**, 852 (1930)
[4] HEIM, G. E.: J. Chem. Educ., **40**, 181 (1963)
[5] BRINE, G. A., BOLDT, K. G., HART, C. K., CAROLL, F. I.: Org. Prep. Poc. Int., **8**, 103 (1976)
[6] BOROWITZ, I. J., DIAKIW, V.: J. Heterocycl. Chem., **12**, 1123 (1975)
[7] DIELS, O., FISCHER, E.: Ber., **49**, 1721 (1916)
[8] LINDNER, J. H. E., KUHN, H. J., GOLLNICK, K.: Tetrahedron Lett., **1972**, 1705
[9] von BRAUN, J.: Ber., **47**, 2312 (1914)
[10] SPEYER, E., ROSENFELD, H.: Ber., **58**, 1125 (1925)
[11] BERTGEN, C., FLEISCHHACKER, W., VIELBÖCK, F.: Ber., **100**, 2992 (1967)
[12] BERTGEN, C., FLEISCHHACKER, W., VIELBÖCK, F.: Ber., **100**, 3002 (1967)
[13] BARTELS-KEITH, J. R.: J. Chem. Soc. (C), **1966**, 617
[14] RAPOPORT, H., LOVELL, C. H., REIST, H. R., WARREN JR., M. E.: J. Amer. Chem. Soc., **89**, 1942 (1967)
[15] Neth. Pat. 6515815; C. A., **65**, P 15441 (1966)
[16] MERZ, H., POOK, K. H.: Tetrahedron, **26**, 1727 (1970)
[17] RAPOPORT, A., BONNER, R. M.: J. Amer. Chem. Soc., **73**, 2872 (1951)
[18] BENTLEY, K. W., HARDY, D. G.: J. Amer. Chem. Soc., **98**, 3281 (1967)
[19] BENTLEY, K. W., BOWER, J. D., LEWIS, J. W., READHEAD, M. J., SMITH, A. C. B., YOUNG, G. R.: J. Chem. Soc. (C), **1969**, 2237
[20] KANEMATSU, K., TAKEDA, M., JACOBSON, A. E., MAY, E. L.: J. Med. Chem., **12**, 405 (1969)
[21] SARGENT, L. J., MAY, E. L.: J. Med. Chem., **13**, 1061 (1970)
[22] MAKLEIT, S., BERÉNYI, S., BOGNÁR, R.: Acta Chim. (Budapest) **94**, 165 (1977)
[23] MAKLEIT, S., BERÉNYI, S., BOGNÁR, R.: Magyar Kém. Folyóirat, **83**, 478 (1977)
[24] BERÉNYI, S., MAKLEIT, S., BOGNÁR, R., TEGDES, A.: Acta Chim. Acad. Sci. Hung. **103**, 365 (1980) and Magyar Kém. Folyóirat **85**, 499 (1979)
[25] JONEDA, F., SUZUKI, K., NITTA, I.: J. Amer. Chem. Soc., **88**, 2328 (1966)

Sándor HOSZTAFI
Sándor MAKLEIT
Rezső BOGNÁR
H-4010 Debrecen, P.O.Box 20.

Acta Chimica Academiae Scientiarum Hungaricae, Tomus 103 (4), pp. 377–386 (1980)

STEUERUNG METALLKATALYSIERTER REAKTIONEN, VIII*

DIE LIGANDKONZENTRATIONS-STEUERUNGSKARTE DES SYSTEMS NICKEL/BUTADIEN/DIPHENYLPHENOXIPHOSPHAN

A. SISAK[1], H. SCHENKLUHN[1,2] und P. HEIMBACH[1,2]

([1] Max-Planck-Institut für Kohlenforschung, Mülheim/Ruhr, BRD, [2] Universität Essen — GHS, Fb 8 Organische Chemie I, BRD)

Eingegangen am 6. April 1979
Zur Veröffentlichung angenommen am 25. Mai 1979

Durch Variation des Diphenylphenoxiphosphan-Nickel-Molverhältnisses ($[L]_0/[M]_0$) in einem Intervall von sieben Zehnerpotenzen wurde die Selektivität der homogenen katalytischen Butadien-Cyclooligomerisation untersucht. Die Auftragung der Produktverteilung als Funktion von lg ($[L]_0/[M]_0$) (Ligandkonzentrations-Steuerungskarte) ermöglicht die Erkennung von Ligandassoziationsphänomenen bei den verschiedenen Komplexen der katalytischen Cyclen und von Kopplungen der einzelnen Teilcyclen.

Einführung

Die Cyclooligomerisation von 1,3-Butadien führt in Gegenwart von N- bzw. P-modifizierten Nickel-(0)-Katalysatoren zu Gemischen von Cyclodimeren und -trimeren [2, 3]. Es wurde bei neueren Untersuchungen darauf hingewiesen, daß diese Reaktion ein ausgezeichnetes Modell ist, den Effekt einer Ligandkonzentrationsvariation auf die Produktselektivität zu studieren [4].

Ergebnisse

Wir untersuchten die Cyclooligomerisation von Butadien in Gegenwart des katalytischen Systems [Bis-(*cis, cis*-Cycloocta-1,5-dien) Nickel (0)]/Diphenylphenoxiphosphan. Das Molverhältnis Ligand/Metall wurde im Intervall 10^{-5} bis 10^{2} variiert. Wir fanden, daß der Prozeß — ähnlich wie früher publiziert [2, 3, 4] — zu Produktgemischen von fast ausschließlich Cyclotrimeren und -dimeren führt (Tabelle I).

* Steuerung metallkatalysierter Reaktionen: VII. Mitteilung (siehe [1])

Tabelle I

Versuchsdaten zur Ligandkonzentrations-Steuerungskarte des Systems Nickel/Butadien/Diphenylphenoxyphosphan. Reaktionsbedingungen:
$T = 60\,°C$, $t = 15$ h, $Ni_0 = 40$ mMol l^{-1}, Ni/Butadien = 1 : 160

Nr.	$\lg([L]_0/[Ni]_0)$	Oligomere (Mol-%, bezogen auf Umsatz = 100%)						Umsatz Butadien (Gew.-%)
		VCH	COD	*n*-OT	*ttt*-CDT	*ttc*-CDT	*tcc*-CDT	
1	$-\infty$	4,3	4,6	1,4	73,1	5,7	10,9	98,5
2	$-\infty$	3,7	4,2	0,9	75,0	5,5	10,7	98,9
3	−5,00	3,8	4,5	1,4	74,1	5,6	10,6	98,9
4	−4,51	3,9	4,5	1,4	73,7	5,9	10,6	97,4
5	−3,90	4,1	4,6	1,3	73,4	5,6	11,0	98,4
6	−3,47	4,0	5,4	1,1	73,4	5,6	10,6	97,9
7	−3,30	3,9	5,8	1,0	72,8	5,6	10,9	96,8
8	−3,23	3,7	4,5	1,0	73,3	5,8	11,7	97,9
9	−2,95	3,9	6,8	1,2	74,0	5,7	8,4	98,1
10	−2,79	3,9	7,7	1,3	73,9	5,7	7,5	96,5
11	−2,65	3,6	6,8	1,4	74,2	5,7	8,2	98,6
12	−2,51	4,6	11,9	1,6	71,3	5,2	5,4	99,0
13	−2,46	4,0	11,3	1,9	73,4	5,3	4,1	97,4
14	−2,43	4,1	11,2	2,2	72,6	5,4	4,5	97,6
15	−2,34	4,3	13,9	2,2	72,1	5,2	2,3	99,1
16	−2,15	4,4	14,7	1,2	73,0	5,4	1,3	98,8
17	−1,86	5,3	17,6	0,9	69,7	5,1	1,4	98,5
18	−1,75	6,5	22,7	0,9	64,8	4,7	0,4	99,7
19	−1,51	8,5	29,7	0,7	56,9	3,9	0,3	99,0
20	−1,26	8,5	30,7	0,4	55,9	4,0	0,5	99,8
21	−1,15	11,7	41,7	0,7	42,5	3,1	0,3	100,0
22	−1,15	10,7	37,4	0,8	47,6	3,2	0,3	99,6
23	−0,72	15,4	52,8	—	29,9	1,9	—	99,7
24	−0,53	17,0	56,3	—	25,2	1,5	—	99,3
25	−0,34	17,9	57,1	—	23,6	1,4	—	99,8
26	−0,07	20,5	62,2	0,5	15,7	1,0	0,1	99,4
27	0,21	28,4	69,8	0,4	1,3	0,1	—	99,8
28	0,25	28,8	68,4	0,2	2,4	0,2	—	99,7
29	0,41	35,7	63,8	0,1	0,3	0,1	—	99,6
30	0,58	42,5	55,7	1,8	—	—	—	97,7
31	0,58	42,4	55,8	1,8	—	—	—	98,3
32	0,78	42,9	51,6	5,5	—	—	—	98,3
33	0,93	50,8	46,1	3,0	0,1	—	—	95,1
34	0,93	51,0	45,2	3,6	0,2	—	—	95,0
35	1,29	66,9	28,9	4,0	0,2	—	—	58,5
36	1,49	73,6	19,0	7,1	0,3	—	—	34,1
37	1,77	77,2	12,6	8,9	1,3	—	—	8,0
38	1,77	77,8	12,1	9,0	1,1	—	—	5,5

Bei den angewandten Reaktionsbedingungen bildeten sich drei Isomere des 1, 5, 9-Cyclododecatriens (CDT) (**1a—c**).

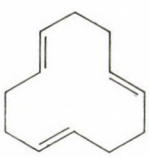

ttt-CDT
(1a)

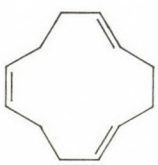

ttc-CDT
(1b)

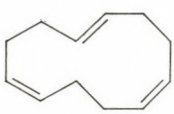

tcc-CDT
(1c)

sowie 4-Vinyl-1-cyclohexen (VCH) (2), *cis, cis*-Cycloocta-1,5-dien (COD) (3) und *cis*-1,2-Divinyl-cyclobutan (DVCB) (4)*

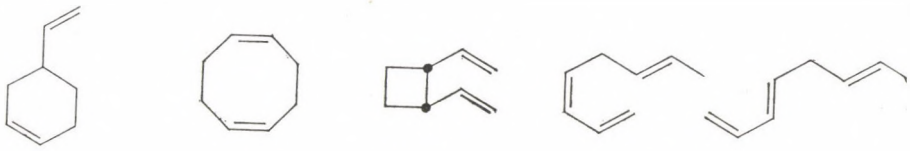

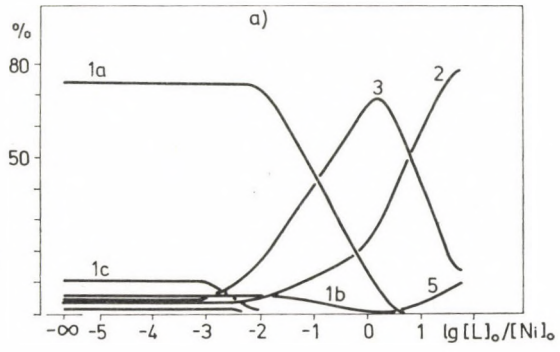

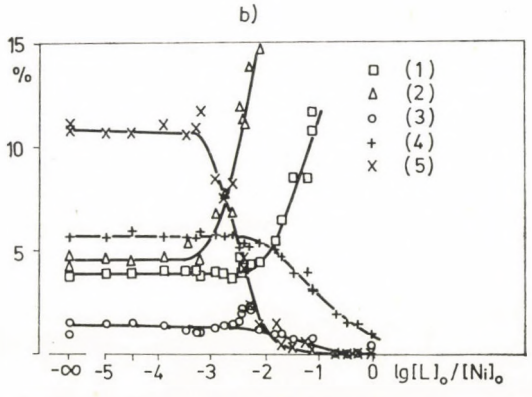

Abb. 1a. Ligandkonzentrations-Steuerungskarte für das katalytische System Nickel/Butadien/Diphenylphenoxiphosphan (Produktverteilung in Mol-% bezogen auf umgesetztes Butadien). Reaktionsbedingungen: $T = 60°$ C, Ni = 40 mMol l^{-1}; $t = 15$ h, Ni/Butadien = 1 : 160, Lösungsmittel: Toluol

Abb. 1b. Teilvergrößerung der Abb. 1a (Symbole: (1) VCH, (2) COD, (3) *n*-OT, (4) *ttc*-CDT, (5) *tcc*-CDT)

* Bei einem Butadien-Umsatz kleiner 85% kann im Produktspektrum auch *cis*-1,2-Divinyl-cyclobutan (4) nachgewiesen werden. Wegen der von uns gewählten langen Reaktionszeit (15 h) lagerte sich (4) vollständig in (2) und (3) um [2].

neben geringen Mengen von offenkettigen Dimeren [vor allem Octatrienisomeren (*n*-OT) (**5a, b**)].

Zur Bestimmung der Zusammenhänge zwischen der Ligandkonzentration und der Produktverteilung erwies sich eine halblogarithmische Auftragung, die wir Ligandkonzentrations-Steuerungskarte [4] nennen, als zweckmäßig. Die Summe aller Oligomeren wurde gleich 100 Prozent gesetzt und die einzelnen Produkte (in Mol-%) als Funktion des logarithmischen Molverhältnisses Ligand zu Metall ($\lg [L]_0/[M]_0$) aufgetragen (Abb. 1a). Einen Teilausschnitt

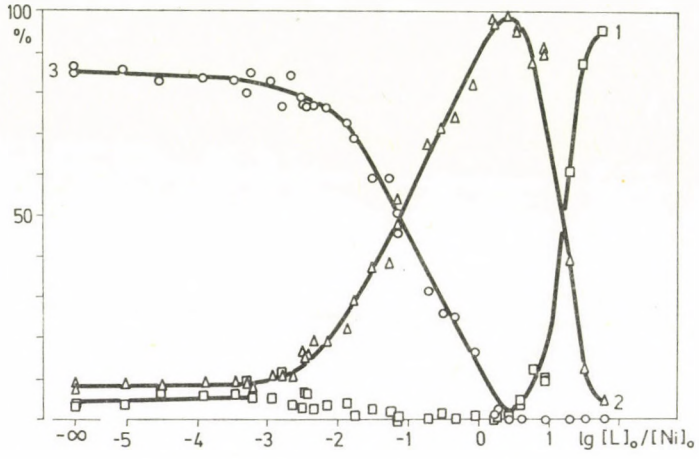

Abb. 2. Teilsteuerungskarte für die Oligomerenverteilung (Mol% bezogen auf eingesetztes Butadien). Symbole: (1) Monomere, (2) Dimere, (3) Trimere

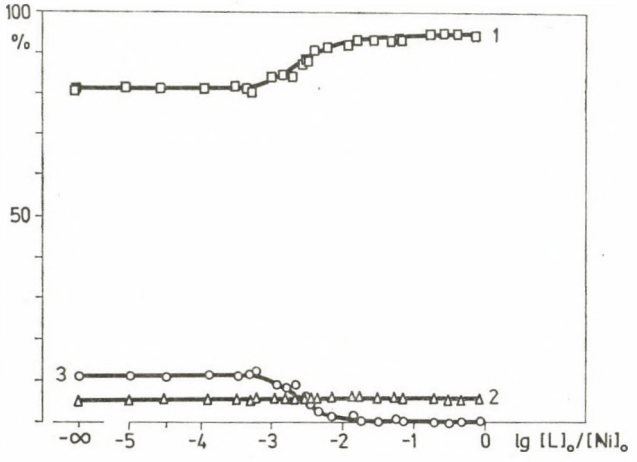

Abb. 3. Teilsteuerungskarte für die Trimerenverteilung (Summe der Trimeren gleich 100% gesetzt). Symbole: (1) *ttt*-CDT, (2) *ttc*-CDT, (3) *tcc*-CDT

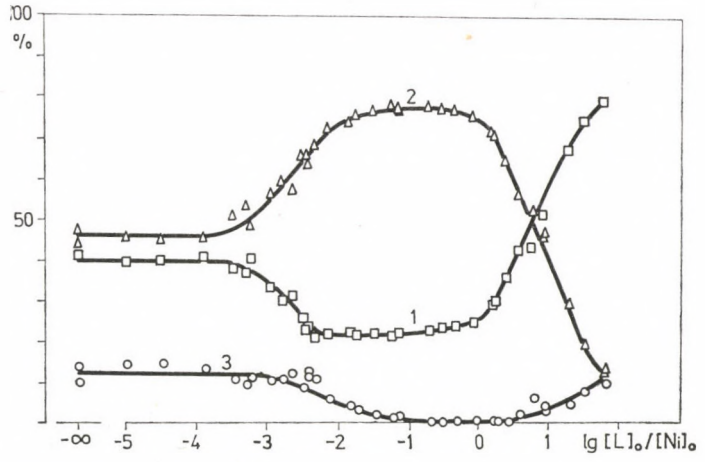

Abb. 4. Teilsteuerungskarte für die Dimerenverteilung (Summe der Dimeren gleich 100% gesetzt). Symbole: (1) VCH, (2) COD, (3) *n*-OT

zeigt die Abbildung 1b. Diese Darstellung ist jedoch für eine Interpretation zu kompliziert. Deshalb wurde die Steuerungskarte in drei Teilkarten zerlegt. In Abb. 2 sind die Produkte nach dem Oligomerisationsgrad zusammengefaßt, in Abb. 3 und 4 jeweils die isomeren Trimeren bzw. Dimeren gesondert dargestellt.

Die Produktverteilung ist vom jeweiligen Ligand/Nickel-Verhältnis abhängig. Es ergeben sich typische "Titrationskurven" mit Umschaltbereichen von *ca.* zwei Zehnerpotenzen im Ligand/Nickel-Verhältnis.

Abweichend von Erfahrungen mit Pyridin als Ligand [4] ergeben sich bei Phosphanen weitere Produktumsteuerungen [5, 6]. Diese Erscheinungen sind durch weitere Ligandassoziationsprozesse der stärker assoziierenden Liganden mit Phosphor als Zentralatom erklärbar.

Diskussion

Die im untersuchten System auftretenden Ligandassoziationsphänomene sind in drei Grundformen (Abb. 5) einzuordnen.

Wenn irgend eine Spezies M (z. B. ein Zwischenkomplex eines katalytischen Cyclus) einem zweistufigen Assoziationsprozeß eines Liganden L unterliegt, so ergibt sich für die Molenbrüche* von M, ML und ML_2 in halblogarith-

* Der Molenbruch ist hier auf $[M]_0$ bezogen und damit eigentlich ein (Lewis-) "Säurebruch" [7]; dementsprechend sind in unseren Ligandkonzentrations-Steuerungskarten die Konzentrationen der Produkte den "Metallbrüchen" (z. B. $X_M = [M]/[M]_0$) proportional, d. h. den Molenbrüchen der Zwischenprodukte, bezogen auf die Gesamtmenge des zugegebenen katalytischen Ausgangskomplexes M.

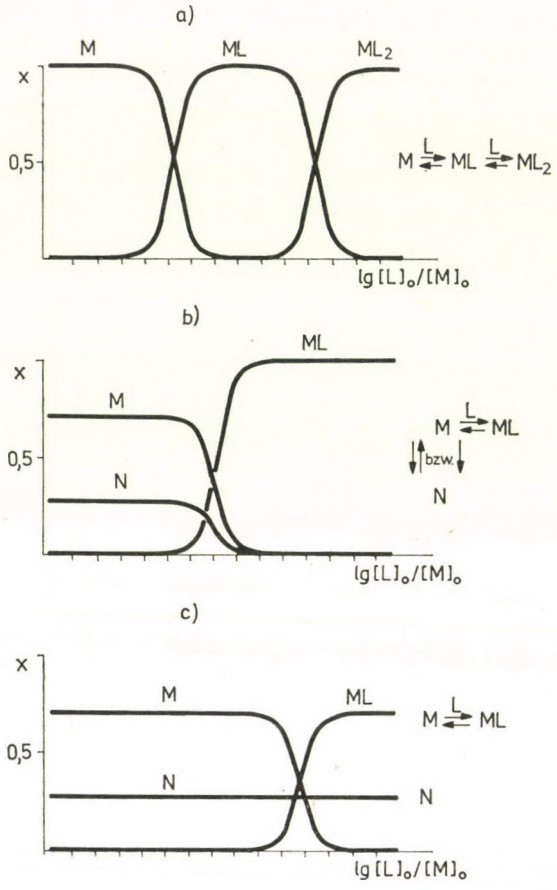

Abb. 5. Typische Titrationskurven: (a) für eine stufenweise Mehrfachassoziation eines Liganden L an einen Metallkomplex M; für eine Ligandassoziation an einen mit einer anderen Spezies N (b) gekoppelten bzw. (c) davon isolierten Metallkomplex M

mischer Darstellung das in Abb. 5 a dargestellte Bild. Alle Assoziationsstufen sind durch typische Titrationskurven erkennbar.

Wenn mehrere isomere Zwischenprodukte der gleichen Assoziationsstufe existieren, ergibt sich ein Bild entsprechend Abb. 5b bzw. Abb. 5c, je nachdem, ob die Spezies mit gleicher Assoziationsstufe (M und N) miteinander gekoppelt sind oder nicht.

Die jeweiligen Gleichgewichtskonstanten beeinflussen natürlich die Lage der Umschaltungen. Ebenso wird sie auch dadurch beeinflußt, daß das Metall nicht auf alle katalytischen Teilcyclen gleichmäßig verteilt ist. Ist z. B. nur 1% der zugegebenen Menge des Metalls im Komplex des produktbestimmenden Elementarschrittes eines Teilcyclus vorhanden, so verschiebt sich die Umschal-

tung für diesen um zwei Zehnerpotenzen zu kleineren Werten. Die Formfaktoren der auftretenden An-, Ab- und Umschaltkurven sollen im Rahmen dieser Publikation nicht diskutiert werden.

In einem homogen metallkatalysierten Prozeß werden im allgemeinen nicht alle Koordinationsstellen der aktiven Metallspezies durch das Substrat belegt, so daß sich je nach Art und Konzentration zugesetzter Lewissäuren und -basen weitere Assoziationsprozesse entsprechend folgendem Prinzipschema ergeben (L = Ligand, P = Produkt, S = Substrat, m = Metallrumpfkomplex).

$$\begin{array}{ccccc} S_1 + S_2 + m & \rightleftharpoons & S_1\text{-m-}S_2 & \longrightarrow & P + m \\ & & \textbf{(6)} & & \\ \Big\downarrow\!\uparrow L & & L\Big\downarrow\!\uparrow & & \\ S_1 + S_2 + mL & \rightleftharpoons & S_1\text{-m-}S_2 & \longrightarrow & P' + mL \\ & & \Big\downarrow\!\uparrow L & & \\ & & \textbf{(7)} & & \end{array}$$

Die Produktselektivität [P/(P+P')] ist abhängig

a) von den sich einstellenden Gleichgewichten ("thermodynamische Selektivität") und

b) von der Lebensdauer der entsprechenden Komplexe (**6**) bzw. (**7**) ("kinetische Selektivität").

Jede Assoziation beeinflußt Orientierungsfaktoren der Zwischenkomplexe (Änderung von Konformation und Konfiguration der organischen Liganden sowie der gesamten Struktur der Komplexe), beeinflußt somit das Produktspektrum und eröffnet vielfältige Steuerungsmöglichkeiten.

Da die Bildung der jeweiligen Produkte den entsprechenden aktuellen Zwischenkomplexkonzentrationen proportional ist, sollten sich in katalytischen Systemen bei Variation der Konzentration der Liganden im Prinzip ähnliche Zusammenhänge wie in Abb. 5a—c zeigen. Die evtl. verschiedenen Abreaktionsgeschwindigkeiten sollten zusätzlich die Lage der Umschaltungen in der Konzentrations-Steuerungskarte verschieben, bei Aktivierung zu niedrigeren und bei Hemmung zu höheren $[L]_0/[Ni]_0$-Verhältnissen.

Die Ligandkonzentrations-Steuerungskarte Abb. 1a zeigt ein zu kompliziertes Steuerungsverhalten, um sie direkt anhand der Prinzipbilder Abb. 5 interpretieren zu können. Dagegen ist die Teilsteuerungskarte des Oligomerisationsgrades Abb. 2 dem Assoziationsschema Abb. 5a sehr verwandt.

Danach ergibt sich folgendes Assoziationsschema für die in dieser Teilsteuerungskarte sichtbaren Zwischenkomplexe [L = $P(OC_6H_5)(C_6H_5)_2$]:

$$\{DIM_S\} \underset{②}{\overset{L}{\rightleftharpoons}} \{DIM_L\} \underset{③}{\overset{L}{\rightleftharpoons}} \{STOP\}^*$$

$$①\downarrow \text{ bzw. } \uparrow\!\downarrow \boxed{1a}$$

$$\{TRIM\}$$

Durch die Abreaktion (1) (kinetische Kopplung) bzw. das Gleichgewicht **1a** (thermodynamische Kopplung) ist die Trimerenbildung bevorteilt (beim ligandfreien Katalysator liegt der relative Anteil der Dimeren bei *ca.* 10%); die Ligandassoziation (2) führt zur ausschließlichen Dimerenbildung (vgl. Abb. 5b, wenn N und ML das gleiche Produkt liefern); die nächste Ligand-Assoziation (3) ergibt dann den katalytisch inaktiven "Stopkomplex".

Die Teilsteuerungskarte der Trimeren (Abb. 3) ähnelt der entsprechenden Pyridin-Konzentrations-Steuerungskarte [4]. Auch hier ist der Abschaltprozeß in der Bildung von *tcc*-CDT (**1c**) bei einem erstaunlich niedrigen Ligand/Metall-Verhältnis von $10^{-3,5}$ bis 10^{-2}. Die steady-state-Konzentration der entsprechenden Zwischenkomplexe sollte also sehr niedrig sein *(ca.* 1% des zugegebenen Metalls).

Anders als bei der Pyridin-Steuerung erfolgt die Abschaltung von (**1c**) nicht zugunsten des Trimeren (**1a**), sondern des Dimeren COD (**3**), wie ein Blick auf den Teilausschnitt der Gesamtsteuerungskarte Abb. 1b deutlich zeigt. Die Teilsteuerungskarte der Trimeren täuscht dies nur aufgrund der andersartigen Normierung (Summe aller Trimeren gleich 100% gesetzt) vor.

In der Teilsteuerungskarte der Dimeren (Abb. 4) findet sich der oben erwähnte Umschaltprozeß von (1c) in (**3**) in dem Anstieg des COD bei vergleichbarem $[L]_0/[Ni]_0$-Verhältnis wieder. VCH und *n*-OT täuschen wegen der Normierung (Summe aller Dimeren gleich 100% gesetzt) den entsprechenden Gegenprozeß vor. Der Anstieg der Dimeren COD und VCH im Bereich $[L]_0/[Ni]_0$ von 10^{-2} bis $10^{-0,3}$ erfolgt proportional (vgl. Abb. 1a); dem entsprechend sind die Kurvenzüge beider Produkte in der Teilsteuerungskarte Abb. 4 parallel. Daß nicht jeweils alle drei Isomeren (**2**, **3**, **5**) an gleicher Stelle der Dimeren-Teilsteuerungskarte umgesteuert werden, deutet auf eine kinetische Separation

* Die geschweiften Klammern symbolisieren jeweils einen Zwischenkomplex aus dem katalytischen Teilcyclus, der durch das in Klammern in Abkürzung angegebene Produkt gekennzeichnet ist; {DIM} bzw. {TRIM} symbolisiert also einen Zwischenkomplex des Teilcyclus, aus dem heraus *Dim*ere bzw. *Trim*ere des Butadiens gebildet werden; {STOP} stellt einen *Stop*komplexldar, der nicht mehr katalytisch aktiv ist. Die mit den Gleichgewichtspfeilen symbolisierten Ligandassoziationen (z. B. $\underset{③}{\overset{L}{\rightleftharpoons}}$) implizieren nicht ein direktes Assoziationsgleichgewicht der entsprechenden Zwischenkomplexe (z. B. $\{DIM_L\} \underset{③}{\overset{L}{\rightleftharpoons}} \{STOP\}$), sondern eine thermodynamische Kopplung der jeweiligen Teilcyclen. Welche Zwischenkomplexe der jeweiligen Teilcyclen das im Einzelfall tatsächlich sind, muß im jeweiligen Fall dann noch gesondert untersucht werden.

dieser Teilcyclen hin. Weitergehende Interpretationen sollten mit Hilfe kinetischer Messungen möglich sein.

Wie die vorliegende Analyse des Systems Nickel/Butadien/Diphenylphenoxiphosphan zeigt, ermöglicht die Aufstellung der Ligandkonzentrations-Steuerungskarten eine Mechanismenanalyse unter besonderer Berücksichtigung der thermodynamischen Selektivität. Es ergeben sich Aussagen über die Minimalzahl der Zwischenkomplexe und deren Kopplung. Eine vorherige Kenntnis der Struktur der auftretenden Zwischenkomplexe wie des Reaktionsmechanismus ist nicht erforderlich. Für einen gezielten Eingriff in das System (z. B. Erweiterung auf katalytische Mehrkomponentensysteme) ergeben sich wertvolle Informationen ebenso wie für eine Optimierung einzelner Produkte.

Experimenteller Teil

Alle Operationen wurden unter Schutzgas (Argon) durchgeführt. Die verwendeten Lösungsmittel, inneren Standards und Butadien wurden mit Na/K-Legierung bzw. $AlOC_2H_5(C_2H_5)_2$ absolutiert. Der Ligand $POC_6H_5(C_6H_5)_2$ wurde aus $PCl(C_6H_5)_2$ entsprechend der Literatur [8] hergestellt (Reinheit lt. ^{31}P-NMR-Spektrum 97%).

Ni-Standardlösung

Zu 5,36 g (19,5 mMol) $[Ni(COD)_2]$ wurden bei −78 °C in einer 500 ml-Ampulle 200 ml Toluol, 40 ml Tetralin (innerer Standard) und 250 ml flüssiges Butadien gegeben. Das Gemisch wurde bis zur völligen Auflösung des Ausgangskomplexes bei −15 °C gerührt, die orange-rote Lösung anschließend über Nacht bei −30 °C getempert.

Ligand-Standardlösung

Zur Variation des Ligand/Nickel-Verhältnisses (von 10^{-5} bis 1) wurden von einer molaren Lösung von $POC_6H_5(C_6H_5)_2$ in Toluol/Dodecan (2 : 1) Verdünnungen in Zehnerpotenzen angefertigt. Dazu wurde das gleiche Lösungsmittelgemisch Toluol/Dodecan (2 : 1) verwandt.

Für $[L]_0/[Ni]_0$-Verhältnisse größer 1 wurde der Ligand mit der entsprechenden Menge des inneren Standards Dodecan direkt in Katalyse-Ampullen (s. o.) eingewogen.

Versuchsdurchführung

Die Katalysen wurden in graduierten 10 ml-Ampullen durchgeführt. Nach der Eingabe der entsprechenden Mengen Ligand-Standard-Lösung wurden die Ampullen bei −78 °C mit der entsprechenden Nickel-Standardlösung versetzt, wobei sich eine Gesamtreaktionslösung von bis zu 8—9 ml ergab. Nach sorgfältigem Verschließen wurde ausgewogen und anschließend 15 h bei 60 °C thermostatisiert.

Die Stopfen und Hähne mußten wegen des sich bei der Reaktionstemperatur entwickelnden erheblichen Butadien-Überdrucks gut gefettet und gesichert sein.

GC-Analyse

Das gekühlte Reaktionsgemisch wurde nach Kontrollwägung direkt in einem Siemens L 350-Gaschromatographen aufgetrennt. Zur Abscheidung des Katalysators war als Vorsäule ein mit Glaswolle gefülltes 16 cm Glasrohr eingebaut.

GC-Bedingungen: 70 m Glas-Kapillarsäule (OV 101),
Trägergas N_2 1,5 bar
Temperaturprogramm 230 °C/140 °C/230 °C

Kontrollversuche, Korrekturen

Die eingesetzte Metallverbindung $[Ni(COD)_2]$ enthält komplex gebundenes (**3**), das die katalytischen Ergebnisse verfälscht. Bei der Herstellung der Nickel-Standardlösung entsteht während des Lösungsprozesses des $[Ni(COD)_2]$ ein katalytischer Zwischenkomplex mit einer C_{12}-Kette, gebildet aus drei Butadien-Molekülen. Zu Beginn der anschließenden Katalysen reagiert diese zu CDT ab [4].

Um diese Korrekturen berücksichtigen zu können, wurde die Nickel-Standardlösung mit $P(OC_6H_5)C_6H_5)_2$ in einem Molverhältnis $[L]_0/[Ni]_0$ von sechs versetzt und direkt der GC-Analyse unterworfen. Diese ergab ein Verhältnis [Ni] : [(3)] : [1a)] von 1 : 2 : 1. Dementsprechend wurden alle mit der Nickel-Standardlösung angesetzten Versuche korrigiert.

Die Eliminierung systematischer Fehler in den Ligand-Verdünnungsserien durch entsprechende Kontrollkatalysen über Direkteinwaagen wurde an anderer Stelle im Detail publiziert [4].

*

Einer der Autoren (A. S.) dankt der Max-Planck-Gesellschaft zur Förderung der Wissenschaften für ein Forschungsstipendium.

LITERATUR

[1] Busch, H., Heimbach, P., Meyer, R—V., Schenkluhn, H.: J. Chem. Res. (S), **1979,** 228; J. Chem. Res. (M), **1979,** 2601
[2] Heimbach, P.: Angew. Chem., **85,** 1035 (1973); Angew. Chem. Internat. Edit., **12,** 975 (1973)
[3] Jolly, P. W., Wilke, G.: The Organic Chemistry of Nickel Bd. 2., Academic Press, New York, San Francisco, London, 1975
[4] Brille, F., Kluth, J., Schenkluhn, H.: J. Molecular. Catal., **5,** 27 (1979)
[5] Kluth, J.: Dissertation, Gesamthochschule Essen, 1980
[6] Brille, F., Heimbach, P., Kluth, J, Schenkluhn, H.: Angew. Chem. **91,** 428(1979); Angew. Chem. Internat. Ed. English, **18,** 400 (1979)
[7] Seel, F.: Grundlagen der analytischen Chemie, Verlag Chemie, Weinheim 1960, S. 119
[8] Michaelis, A., La Coste, W.: Ber., **18,** 2109 (1885)

Attila Sisak H-8201 Veszprém, Postfach 28.

Hartmut Schenkluhn, Paul Heimbach } D-4300 Essen 1, Postfach 6843, BRD

Acta Chimica Academiae Scientiarum Hungaricae, Tomus 103 (4), pp. 387—395 (1980)

APPARATUS FOR THE MEASUREMENT OF THE MECHANICAL–RHEOLOGICAL PROPERTIES OF GELS

F. HORKAY[1], M. NAGY[2] and M. ZRINYI[2]

([1] National Institute of Occupational Health, Budapest, [2] Department of Colloid Science, L. Eötvös University, Budapest)

Received February 19, 1979
Accepted for publication May 31, 1979

An apparatus suitable for the determination of the mechanical–rheological properties of elastic specimens of low mechanical strength (*e.g.* of swollen polymer gels) has been developed, which makes possible at unidirectional compression the simultaneous measurement of force and deformation belonging to it at a high accuracy ($\pm 1 \times 10^{-4}$ N and ± 6 μm, resp.) and in a wide range (from 1×10^{-4} N to 2.000 N, and from 6 μm to 3.333 mm, resp.). Using stress deformation functions determined for gels of various degree of cross-linking prepared from polyvinyl alcohol, the molecular parameter characteristic of the structure of networks, the quantity of elastically active network chains has been calculated. It was found that values obtained experimentally considerably differ from data calculated for ideal model systems.

1. Introduction

One of the most important preconditions of reliable mechanical-rheological measurements is to produce homogeneous, isotropic deformation. In the case of a given body this can be realized by unidirectional tension or compression, and by simple shearing. In the former cases the hydrostatic components of the tensile or compressive force are also active, and can not be always neglected. In simple shearing this has not to be taken into consideration.

Depending on the mechanical properties of the test systems, various difficulties may arise in the carrying out of the measurements. For homogeneous, isotropic specimens of high strength and high elastic modulus (*e.g.* for metals) the type of deformation most often used is stretching, because the clamping of the sample is relatively easy. This is difficult to realize in rubber-elastic systems, due to the inhomogeneous stress field developing in the sample in the environment of the clamping neads holding the sample. However, difficulties can be eliminated by an appropriate technical arrangement and by the suitable selection of the form of the sample.

With soft systems, *i.e.* with systems of low mechanical strength and low elastic modulus, often already the clamping of the sample is problematic, thus the investigation of their mechanical–rheological properties can be usually realized only in a special apparatus. One of the possibilities is to expose the test sample to shearing stress in the gap of concentric cylinders as used in

rotation viscometry. Though permitting measurements of high accuracy, this experimental arrangement has two disadvantages, restricting its applicability in several respects. On the one hand, it is suitable only for the investigation of lio-gels formed in the gap, and on the other hand, for certain samples the dependence of mechanical properties on the degree of swelling of the system can not be studied.

It can be established on the basis of the aforesaid that of the simple types of deformation primarily unidirectional compression is suitable for the investigation of soft systems, because no clamping of the sample is needed in this case, and the determination of the mechanical properties of the specimen becomes possible even when there is a change in volume.

The present communication reports on an experimental apparatus of our own construction, which makes possible the rapid and accurate determination of the stress-deformation relationship of soft, elastic specimen.

2. Principle of operation of the apparatus

The instrument (Fig. 1) is a modification of the analytical balance. The vertical glass rod with flat end (1), fastened to the holding frame of the balance pan serves for the compression of the test sample. The sample (2) is located in the double-walled thermostable sample holder (4), fastened to the support (3), between two parallel glass plates (5). The force acting on the sample is equal to the difference of the weight placed on the balance pan and the weight set on the dial. Change in height occurring during deformation can be followed on the balance indicator (1 scale division is 27.4 μm). The apparatus makes

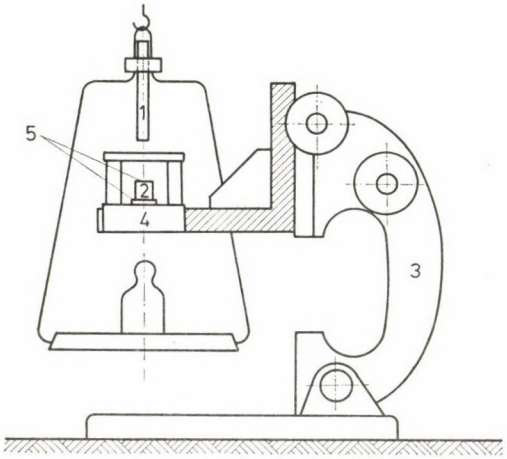

Fig. 1. Modulus measuring apparatus

possible a very accurate measurement of deformation and stress (± 6 μm and $\pm 1 \times 10^{-4}$ N) within a rather wide range (from 6 μm to 3.333 mm, and from 1×10^{-4} N to 2.000 N, respectively). The height regulating disc arranged on the support permits the determination of the undeformed sample at a high accuracy (± 0.005 mm). (Since a knowledge of the latter is of fundamental importance on account of its role in the theoretical relationships discussed in the following, its value has been determined for all the systems investigated also by an independent method, with a one-dimensional comparator of type Zeiss-Abbe. Values measured agreed within 0.1%.)

3. Gel preparation

Investigations of most of the authors were carried out on gels prepared by cross-linking polymerization [1]. In systems of this kind segment distribution is generally not homogeneous, the structure of the gel may be considerably affected during cross-linking already by small changes in external conditions, and the reproduction of the process is very difficult.

Cross-linking of a polymer in solution has the advantage that by changing the concentration of the solution and the quantity of the cross-linking agent introduced into the system makes possible the preparation of gels of different mechanical properties and of different liquid content. Moreover, the cross-linking process is generally easier to control, and reproducibility improves.

Investigations were carried out on polyvinyl alcohol (PVA, Poval 420, Japan) gels, cross-linked at 6w% polymer concentration and at four kinds (50, 100, 200, 400) of degrees of cross-linking (dc, the molar ratio of the monomer of the polymer and of the cross-linking agent). Cross-linking was carried out with glutaric aldehyde (GDA. Merck, GFR).

Gels were prepared by filling the solution (pH = 1.5) of the polymer, the cross-linking agent and the catalyst (2*n* HCl solution), homogenized by stirring, into a demountable gel pouring frame (Fig. 2), suitable for the preparation of cylindrical gel pieces. Gel formation proceeded under isothermal conditions, in a thermostat, at 298 $\pm$ 0.1 K in about 2 hours. The cylinders

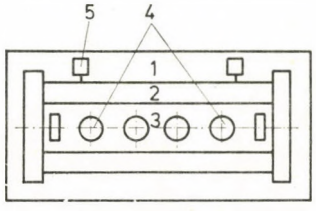

Fig. 2. Gel pouring frame. 1. Base plate, 2. gel pouring form, 3. sliding lid, 4. sample, 5. fixing screw

were placed after a day into weighting bottles with ground lid, and were left standing for two days for the complete proceeding of the processes. Next the medium of the gels was exchanged for distilled water, and the samples were stored until use in a refrigerator at 278 K.

4. Experimental results and their evaulation

Since an apparatus of new type and a novel gel preparing process were used in our investigations, a study of the reproducibility of measurement and sample preparation were thought to be necessary. Relevant results are summarized in Table I.

It can be seen from the table that the reproducibility of both gel preparation and mechanical measurement is within 2—3%.

Moreover, investigations were undertaken to establish the change in shape of the gel cylinders under stress (Fig. 3). It can be seen also from the figure that no so-called barrelling, indicative of inhomogeneous stress distribution, occurs during deformation, the gel cylinders are uniformly flattened between the glass plates well wetted by the medium (see Fig. 1). It has been further established that on relieving compression the samples regain their original shape, permanent deformation could not be detected in any of the systems.

The possible change in the degree of swelling of the gel samples by deformation has also been studied. Owing to thermodynamical reasons, a change in degree of swelling by deformation is namely to be expected. During our measurements carried out in a relatively narrow deformation range, no change in degree of swelling has been observed in any of the systems.

Table I

Reproducibility test

(Polymer concentration at cross-linking: 6w%, degree of cross-linking: 200, $T = 298$ K)

	Gel 1			Gel 2			Gel 3*		
$L_{0z'}$, mm	11.33			11.32			11.32		
Force, N	deformation, mm								
0.0196	0.43	0.43	0.42	0.42	0.42	0.42	0.43	0.43	0.42
0.0490	1.02	1.02	1.02	1.02	1.02	1.01	1.02	1.02	1.01
0.0784	1.51	1.52	1.51	1.51	1.51	1.51	1.51	1.52	1.51
0.0980	1.83	1.83	1.83	1.82	1.82	1.81	1.83	1.83	1.82
0.1176	2.13	2.14	2.13	2.13	2.12	2.12	2.14	2.14	2.12
0.1470	2.49	2.50	2.49	2.49	2.49	2.48	2.50	2.50	2.49

* Sample 3 was prepared at a different time than the other samples

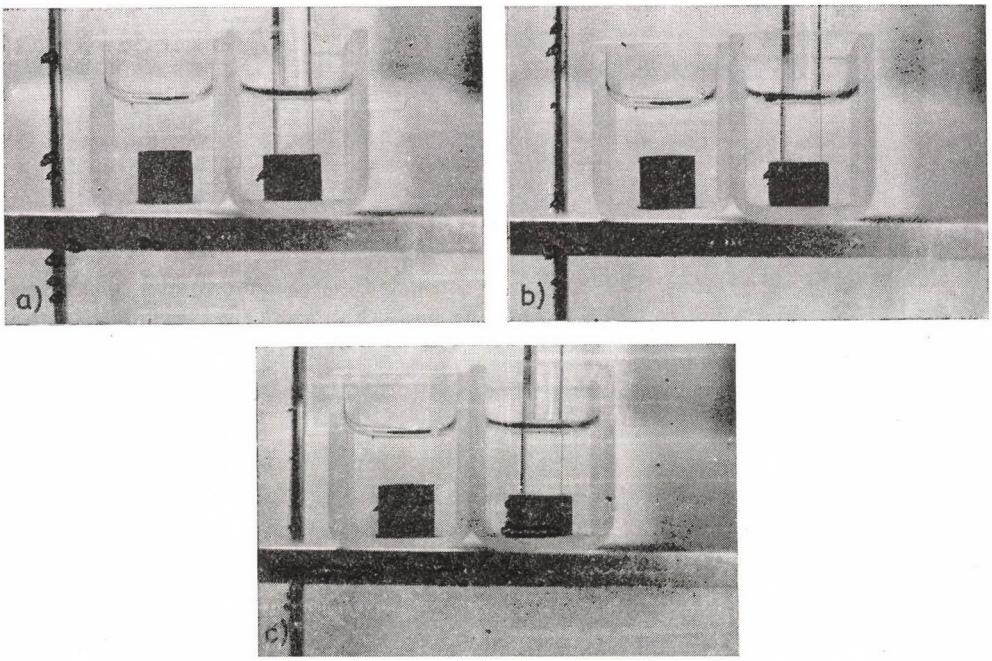

Fig. 3. Shape of the deformed and undeformed gel cylinders (a. $\Lambda_x = 0.85$ b. $\Lambda_x = 0.80$ c. $\Lambda_x = 0.75$)

For the evaluation of the mechanical tests the arithmetic mean of 3 parallel measuring data was used in each case. The systems were kept at a temperature of 298 $\pm$ 0.1 K.

The stress-deformation function was determined for each system. Since the degree of swelling of the gels was different, to facilitate comparison, the deformation ratio $\Lambda_x = L_x/L_{0x}$ (L_{0x} being the length of the undeformed, L_x that of the deformed sample in the direction of the x axis) has been used in the figure for the characterization of deformation (Fig. 4). It can be established on the basis of the figure that the mechanical properties of the gels considerably change with the degree of cross-linking. At the same time, in the case of systems of higher degree of cross-linking a substantially larger force is needed to produce the same deformation.

When the mechanical properties of the networks are known, informations on the structure of the systems can be obtained by determining on the basis of calculations for suitable model systems the relationship between the macroscopic parameters measured experimentally and the molecular quantities relevant to the model.

According to the generally used theories based on different idealized models, the change in Helmholtz energy accompanying the deformation of a cross-linked polymer [1, 2] is:

$$\Delta A = \frac{K_1 kT \nu_{el}}{2}(\Lambda_x^2 + \Lambda_y^2 + \Lambda_z^2 - 3) - \frac{K_2 kT \nu_{el}}{2}(\ln \Lambda_x \Lambda_x \Lambda_z)$$

and the force needed for deformation at constant volume V:

$$f = \left(\frac{\partial \Delta A}{\partial L}\right)_{T,V} = \frac{K_1 \nu_{el} kT}{L_{0x}}(\Lambda_x - \Lambda_x^{-2}),$$

where K_1 and K_2 are constants, ν_{el} is the number of the elastically active network chains, Λ_x, Λ_y and Λ_z are deformation ratios measured in different directions, k is Boltzman's constant, and T is the temperature.

For swollen networks the force referred to the unit initial cross section (at $q_i = 1$), σ_d, is in the following relationship with deformation ratio [1]:

$$\sigma_d = K_1 RT \nu_{el}^x q_i^{1/3} q_0^{-2/3}(\Lambda_x - \Lambda_x^{-2}), \tag{1}$$

where q_i is the degree of isotropic volumetric swelling, q_0 the so-called memory parameter, ν_{el}^x the quantity in moles of the elastically active network chains in the dry network of unit volume, and R the gas constant

On the other hand, independently of any molecular model, the density of stored Helmholtz energy $\left(\varrho_A = \frac{A}{V}\right)$ can be given in a completely general form for the deformation of elastic, homogenous, isotropic and incompressible bodies, as a function of the scalar invariants formed from the main deformation ratios [3]:

$$\varrho_A = \sum_{i=0,\, j=0}^{\infty} C_{ij}(I_1 - 3)^i \; (I_2 - 3)^j, \tag{2}$$

where I_1 and I_2 are the first and the second scalar invariants, while the C_{ij} values are material constants. I_1 and I_2 can be expressed with the deformation ratios, thus:

$$I_1 = \Lambda_x^2 + \Lambda_y^2 + \Lambda_z^2 \tag{3}$$

$$I_2 = \Lambda_x^2 \Lambda_y^2 + \Lambda_x^2 \Lambda_z^2 + \Lambda_y^2 \Lambda_z^2$$

The equality $I_3 = \Lambda_x^2 \Lambda_y^2 \Lambda_z^2 = 1$ represents the constancy of the volume. When only the first two terms of the summation according to Eq. (2) are taken into consideration, the so-called MOONEY—RIVLIN equation is obtained [4]:

$$\varrho_A = C_{1,0}(I_1 - 3) + C_{0,1}(I_2 - 3) = C_1(I_1 - 3) + C_2(I_2 - 3). \tag{4}$$

From relationships (3) and (4) the expression

$$f = 2\, C_1(\Lambda_x - \Lambda_x^{-2}) + 2\, C_2(\Lambda_x - \Lambda_x^{-2})\Lambda_x^{-1} \tag{5}$$

is obtained for the force. It can be clearly seen from Eq. (5) that if $C_2 = 0$, then $2C_1$ is identical with the factor in Eq. (1), containing the molecular

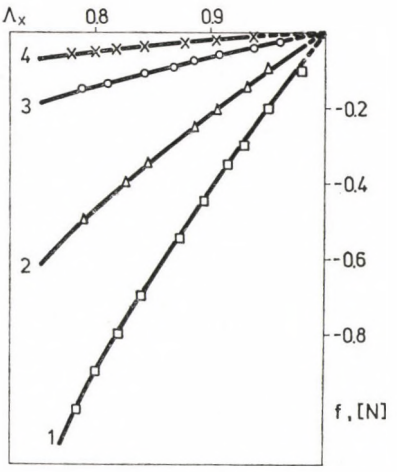

Fig. 4. Force deformation ratio functions (dc: (1) 50; (2) 100; (3) 200; (4) 400)

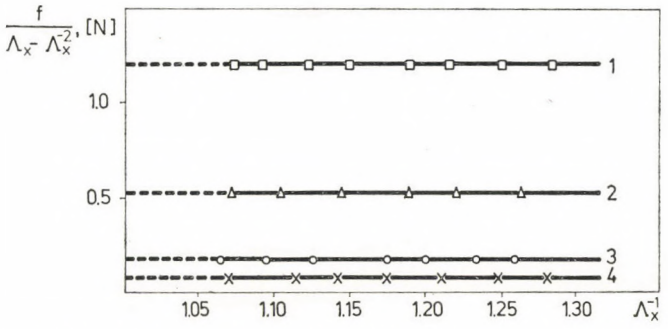

Fig. 5. MOONEY—RIVLIN plots (dc: (1) 50; (2) 100; (3) 200; (4) 400)

characteristics relevant to the network. When $C_2 \neq 0$, this may give information on the deviation from the model system selected.

Under consideration of the above said, it becomes possible to calculate from the experimentally determined force (or stress) — deformation ratio functions the constants C_1 and C_2 in Eq. (5), and when C_2 is zero, to calculate from C_1 the molecular parameters characteristic of the structure of the network.

On the basis of the $f - \Lambda_x$ functions for various PVA gels (Fig. 4), examples are shown for the application of Eqs (5) and (1). Functions according to relationship (5) are shown in Fig. 5. From the axial section of the straight lines extrapolated to $\Lambda_x^{-1} = 1$, from their slope, C_1 and C_2 can be determined. According to our experiences, a value of $C_2 = 0$ was obtained within experimental errors for all four systems. This is consistent with the result accepted in the literature that in unidirectional compression C_2 generally does not play a substantial role [5, 6].

In Fig. 6 the force referred to unit initial cross section ($q_i = 1$) was plotted as a function of $\Lambda_x - \Lambda_x^{-2}$. The slope of the straight lines obtained gives information on the molecular parameters in Eq. (1). Thus, if certain assumptions are made concerning the values of K_1 and q_0, ν_{el}^x can be determined.

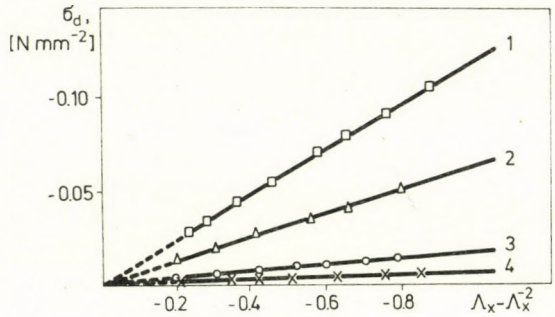

Fig. 6. Application of Eq. (1) to PVA gels (dc: (1) 50; (2) 100; (3) 200; (4) 400)

The quantity of elastically active network chains in the dry network of unit volume can be calculated also on the basis of the chemical reaction, when the number of cross-linking molecules introduced into the system is known. Under consideration of the fact that the network contains free (terminal) chains, which are linked only at one end to the net nodes, and probably do not play an active part during deformation, the quantity of elastically active network chains can be calculated from the following equation [2]:

$$\nu_{el}^x = \nu^x \left(1 - \frac{2\, d_2}{\nu^x \overline{M}_n}\right), \tag{6}$$

where ν^x is the quantity in mole of the total network chains referred to unit volume, $\overline{M}_n$ is the arithmetic mean relative molecular mass of the polymer chains in the initial solution, and d_2 is the density of the pure polymer.

In Table II ν_{el}^x values calculated on the basis of the chemical reaction and those determined experimentally are summarized.

It can be seen from the data that values measured and calculated differ considerably. This deviation decreases with increasing degree of cross-linking.

The difference between the values found experimentally and the values calculated can be probably attributed to reasons of solution structure.

It should be mentioned finally that when the establishing of equilibrium deformation is instantaneous in the mechanical measurements, the stress-deformation function can be determined for the single gel samples within 10—15 minutes. We call the attention to the fact that the apparatus is suitable

Table II

ν_{el}^{x} values of PVA gels

(Polymer concentration at cross-linking: 6 w%, $T = 298$ K)

Degree of cross-linking	ν_{el}^{x}, mol · m^{-3}	
	values calculated on the basis of Eq. (6)	values determined experimentally ($K_1 = 1, q_s = q_c$)
50	701	174
100	338	64
200	159	21
400	70	6

without any modification for the recording of thermomechanical curves, and with a slight modification it can be used also as penetrometer or as viscometer.

*

We wish to thank Prof. Ervin WOLFRAM for valuable advice and for the reading of the manuscript. Thanks are due to Mr. István KÁNTOR, mechanician to the Department of Colloid Science, for his expert work in realizing of the measuring apparatus and the gel pouring frame.

REFERENCES

[1] DUŠEK, K., PRINS. W.: Fortschr. Hochpolym. Forschung, **6**, 1 (1969)
[2] FLORY, P. J.: Principles of Polymer Chemistry. Cornell University Press, Ithaca, New York 1953
[3] RIVLIN, R. S.: Phil. Trans., **A 241**, 379 (1948)
[4] MOONEY, M.: J. Appl. Phys., **11**, 582 (1940)
[5] RIETSCH, F., FROEHLICH, D.: Polymer, **16**, 873 (1975)
[6] DE CANDIA, F., CIFERRI, A.: Makromol. Chem., **134**, 335 (1970)

Ferenc HORKAY H-1096 Budapest, Nagyvárad tér 2.

Miklós NAGY, Miklós ZRINYI H-1088 Budapest, Puskin u. 11—13.

Acta Chimica Academiae Scientiarum Hungaricae, Tomus 103 (4), pp. 397—403 (1980)

COMPUTERIZED CALCULATIONS OF COMPLEX EQUILIBRIA, II

THE CALCULATION OF THE PROTONATION CONSTANTS OF POLYFUNCTIONAL LIGANDS AND THE STABILITY CONSTANTS OF METAL COMPLEXES FROM POTENTIOMETRIC DATA

F. GAIZER

(College of Food Technology, Department of Chemistry, Hódmezővásárhely, Hungary)

Received January 5, 1979
Accepted for publication May 31, 1979

A computer programme has been constructed for the calculation of the protonation constants of large molecules able to bind (release) a great number of hydrogen ions and for the calculation of the stability constants of metal complexes with the composition M_qL_p. The present PH-POT programme is a variant of the author's SPEF-3 programme to evaluate potentiometric measurements. With the programme the values of equilibrium constants resulting in the minimum value of $\Sigma(\Delta E)^2$ can be calculated from experimental data T_H, T_{OH}, T_L and E, or T_M, T_L and E resp., and the constants of a blank pH-metric titration curve.

Introduction

For the calculation of protonation–deprotonation constants of polyprotic acids and polyhydroxyl bases a great number of numerical and graphical methods are known [1, 2]. However, these methods are insufficient in the case of large molecules which are able to bind or dissociate many protons (*e.g.* proteins). In such cases the only powerful method for the evaluation of experimental data is the application of computers. This is also necessitated by the large number of constants and by the fact that to draw unambiguous conclusions a large amount of experimental data must be evaluated and very often several possible models must be examined. The computer programme PH-POT* introduced in the present paper has been successfully applied for the evaluation of some complicated systems [3, 4]. It has a similarity to several published programmes [5—15], *i.e.* supposing a model it calculates the values of stability constants which give the best agreement between measured and calculated quantities. This programme is based on the principle of SPEFCA [18] and SPEF-3 [19] programmes and is able to calculate the optimal value of any constants. The programmes have some parts in common.

* The programme, with the necessary information, is available upon request.

The problems to be solved

For the protonation ($+r$) or deprotonation ($-r$) equilibria of a compound able to bind or release hydrogen ions (= release/bind hydroxyl ions) it can be written:

$$\pm r\,H^+ + p\,L \rightleftharpoons H_rL_p\ (\equiv c_{rp} \text{ or } c_j)$$

$$\beta_{rp} = \frac{[H_rL_p]}{[H^+]^{\pm r} \cdot [L]^p} \tag{1}$$

From mathematical point of view the choice of the protonating or deprotonating species is optional: it can be either the neutral molecule (H_NL) or one of the partly protonated species or the completely deprotonated molecule (L). In the last case only protonation constants are to be calculated, but in the previous one acidic dissociation constants are also to be calculated.

Equation (1) is valid also for the formation of metal complexes with the composition M_qL_p, if the free metal ion concentration is substituted for $[H^+]$.

The determination of equilibrium constants determined by Eq. (1) can be made from potentiometric measurements in either of two cases: 1.) the change in hydrogen ion concentration is measured by titrating the solution of the compound under investigation with strong acid or base, or 2.) the change in metal ion concentration is measured at addition of ligand. Restricting the further discussion for the somewhat complicated pH-metric case, when each reaction mixture can contain both strong acid (T_H) and strong base (T_{OH}) in known amount, as a result of titrations the E or $[H^+]$ versus ($T_H - T_{OH}$) curves are available. From these experimental data the number of protons bound or dissociated per molecule (Z_H) can be calculated by the following equation:

$$Z_H = \frac{(T_H - T_{OH}) + (K_s/[H^+]) - [H^+]}{T_L} \tag{2}$$

Here T_L is the concentration of the protonating molecule (*e.g.* protein) in each reaction mixture and K_s is the ionic product of water (solvent). The task of an evaluation process is to determine the most probable values of protonation constants from the T_H, T_{OH}, T_L and E (or $[H^+]$ or Z_H) experimental data.

The refinement of the parameters and the choice of error square sum

For the refinement of parameters the procedure based on Gauss' method is used, which was discussed in the previous papers [18, 19].

The best choice for the calculation of the error square sum to be minimized is a quantity the deviations of which can be summed up with the same (unit)

weighting factors, even if the titration is carried out in a large pH range. According to literature data [20] the E and Z_H values fulfil this requirement. However, we have found that these quantities do not have the same relation to the measured hydrogen ion concentration: minimizing $\Sigma(\Delta E)^2$ values, the error square sum depends on $\log([H^+]_{meas}/[H^+]_{calc})$, but if the $\Sigma(\Delta Z_H)^2$ is minimized, it is determined by $([H^+]_{meas} - [H^+]_{calc})$ in acidic medium and by $([OH^-]_{meas} - [OH^-]_{calc})$ in alkaline medium. From the two possibilities the minimization of $\Sigma(\Delta E)^2$ gives better convergence and is used in the programme. Thus the aim of the calculations carried out by the present programme is to find the values for parameters for which:

$$U = \sum^{expts} (E_{meas,i} - E_{calc,i})^2 = \text{minimum} \tag{3}$$

The calculation of E_{calc} values

If a pH-metric titration is made in a broad pH range, the e.m.f. (E) of a cell consisting of a hydrogen ion sensitive and a reference electrode can be given by the following equation:

$$E = E^0 + g \cdot \log [H^+] - j_H \cdot [H^+] - j_{OH} \cdot (K_s/[H^+]) \tag{4}$$

E^0 is the normal potential of measuring (glass) electrode, $g = 59.16$ mV (at 25 °C), j_H and j_{OH} are constants to take into account the diffusion potentials.

In Eq. (4) E^0, j_H and j_{OH} are unknown parameters, but it is advisable to treat also the constants K_s and g as adjustable parameters. This makes possible a check on the reliability of experimental data. Further, it may sometimes be necessary to determine the value of K_s corresponding to the ionic strength used. Therefore, before the calculation of equilibrium constants there is a further problem to be solved, the determination of the value of E^0, j_H, j_{OH} and occasionally of K_s and g constants. This can be made from the data of a blank titration curve carrying out the minimization according to Eq. (3) by the refinement process of the programme. To calculate E_{calc} by Eq. (4), the knowledge of the free hydrogen ion concentration is necessary at every point of the blank titration, in addition to guessed values of the above five parameters. This can be calculated by the equation expressing the electroneutrality as well as the T_H and T_{OH} values with the following formulas:

if $T_H > T_{OH}$:

$$[H^+] = \frac{(T_H - T_{OH}) + [(T_H - T_{OH})^2 + 4K_s]^{1/2}}{2K_s} \tag{5a}$$

if $T_{OH} > T_H$:

$$[H^+] = \frac{2K_s}{(T_{OH} - T_H) + [(T_{OH} - T_H)^2 + 4K_s]^{1/2}} \tag{5b}$$

At the refinement of the values of equilibrium constants also the calculation of E^{calc} values is carried out according to Eq. (4) using the values obtained by the previous calculation. The calculated free hydrogen ion concentrations, however, are those which can be calculated with a given set of β's. From the mass balance equations (6) and (7) it can be seen that one of the unknowns is the necessary $[H^+]$, and the other one, [L] is the concentration of the protonating/deprotonating free species:

$$(T_H - T_{OH}) = [H^+] - (K_s/[H^+]) + \Sigma r_j \cdot c_j$$
$$= [H^+] - (K_s/[H^+]) + \Sigma r_j \beta_j [H^+]^{r_j} [L]^{p_j} \quad (6)$$

$$T_L = [L] + \Sigma p_j \cdot c_j$$
$$= [L] + \Sigma p_j \beta_j [H^+]^{r_j} [L]^{p_j} \quad (7)$$

The description of the programme

The PH-POT programme in present form is applicable for the formation of a maximum of 12 complex species, but it can be extended to treat any number of complexes. In addition to the discussed pH-metric application, the formation constants of M_qL_p type metal complexes can be calculated from potentiometric measurements, if the free metal ion concentration is measured. In this latter case the T_M values form the T_H array, the elements of the T_{OH} array are equal to zero, and K_s is a suitable small number which makes $K_s/[M]$ in Eq. (4) and (6) negligible.

The parameter refining part of the programme is the same as that of the SPEF-3. The only difference is that the subroutine EXTCALC is omitted and the sum of square of residuals is calculated in subroutine PRINTING.

The calculation of E_{calc} values is carried out in the subroutine EQUSOLV. If the five parameters are to be calculated, the $[H^+]$ values calculated by Eq. (5) must be substituted into Eq. (4), but if the optimal values of equilibrium constants are to be determined, the necessary $[H^+]$ values are obtained by solving mass balance equations (6) and (7).

The solvation of the mass balance equations, which determines the running time of the programme, is carried out either by the Newton—Raphson method or, if this does not yield a satisfactory solution, by an increment-alternating iteration procedure [18, 21]. The running time of the first method is from one hundredth to one tenth of the second one, if the partial derivatives necessary to the calculation of the correction values of roots are made as follows. Assume for the roots $[H^+]$ and [L] of Eq. (6) and (7) chemically reasonable starting values and denote by $(T_H - T_{OH})_{calc}$ and $T_{L,calc}$ the terms calculated by substituting these values. Define the following quantities: $T_A = (T_H - T_{OH})_{calc} - (T_H - T_{OH})$ and $T_B = (T_{L,calc} - T_L)$. If the concentra-

tion of the individual species is calculated separately ($c_j = \beta_j[H^+]^{r_j}[L]^{p_j}$), the partial derivatives of T_A and T_B with respect to the unknowns can be obtained as follows:

$$\partial T_A/\partial[H^+] = 1 + K_s[H^+]^{-2} + \Sigma r_j^2 \cdot c_j/[H^+],$$

$$\partial T_A/\partial[L] = \Sigma r_j \cdot p_j \cdot c_j/[L], \textit{ etc.}$$

In this programme there is also included a short part to find the starting values of parameters. This practically eliminates the necessity for other methods for their determination.

Discussion

By the present programme the optimal values and errors of parameters of a supposed model can be calculated. To demonstrate the applicability of the programme, the evaluation of our experiments [22] determining the proto-

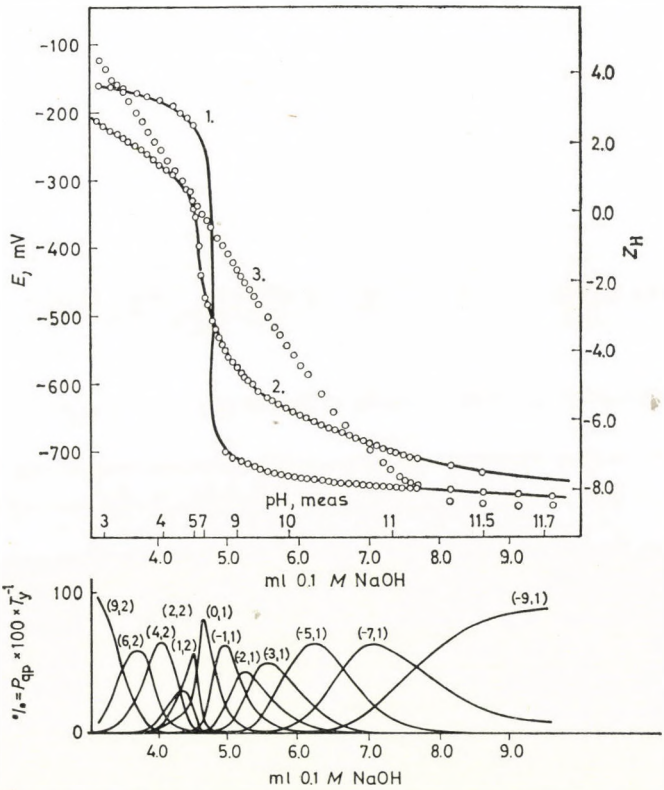

Fig. 1. The pH metric titration of the polypeptide gordox. Total gordox = 3.2×10^{-3} mol/dm^3, $T_H = 4.8 \times 10^{-2}$ mol/dm^3. 1. = blank curve, 2. = peptide containing solution, 3. = Z_H. The curves are the calculated ones with the best constants (Table I). Every third experimental point is plotted in the Figure

nation constants of the polypeptide gordox consisting of 59 amino acids is introduced. As can be seen in Fig. 1, the value of Z_H varies from 4.5 to −8.5 in the measured range. To describe the experimental curves, calculations have been carried out according to the models summarized in Table I. It can be seen

Table I

The evaluation of the pH-metric titration curve of the polypeptide gordox according to various models

(r, p)	log β-values							
(6, 1)	22.21							
(5, 1)		19.30						
(9, 2)			38.7	38.55	38.66	38.69	38.69	38.71
(3, 1)	13.04	12.98						
(6, 2)			28.86	28.83	28.86	28.76	28.76	28.77
(4, 2)			21.14			21.35	21.35	21.38
(3, 2)					17.34			
(1, 1)	5.11	5.11						
(2, 2)			13.12	12.84		12.63	12.63	12.63
(1, 2)				8.09	8.2	8.23	8.24	8.27
(−1, 2)						− 5.36	− 5.36	
(−2, 2)			−13.01	−12.93	−12.92	−12.94	−13.00	
(−1, 1)	− 7.98	− 7.98						− 7.98
(−2, 1)	−16.78	−16.78	−16.7	−16.7	−16.7	−16.75	−16.67	−16.89
(−3, 1)						−26.4		−26.3
(−4, 1)	−35.98	−35.98	−35.96	−35.99	−35.99		−35.99	
(−5, 1)						−46.23		−46.24
(−7, 1)	−67.27	−67.27	−67.27	−67.27	−67.27	−67.39	−67.26	−67.38
(−9, 1)	−89.82	−89.82	−89.82	−89.82	−89.82	− 89.67	−89.82	−89.68
$\sigma(E)$, mV	4.77	4.56	6.7	4.8	2.8	1.79	2.06	1.82

that there are three models which give formally satisfactory fit. The acceptance of any of them can be made only on the bases of chemical reasons or evidences.

Our experiences obtained by the application of this programme are very favorable: even if 12 equilibrium constants are calculated, it has a rather short running time and a relatively low memory requirement. The convergence, if 2—5 parameters are refined simultaneously, is reliable and fast. During the refinements the only stability constants requiring special attention are those which belong to complexes the formation of which is small relative to those of other complexes. Instead of the refinement of such constants, it is advisable to use the programme part written to search the value of a given parameter.

To find the optimal conditions of convergence we have found that the minimization of $\Sigma(\Delta E)^2$ is more advantageous than that of $\Sigma(\Delta Z_H)^2$ and never fails. We have also found that it is much better to calculate the elements of matrix G by numerical differentiation according to $\log \beta$ values, because the elements of the matrix are the same order of magnitude. The favorable running time using numerical differentiation is due to the fact that, as can be seen from the distribution of species in Fig. 1, the change in the value of a parameter influences only one part (here about one tenth) of the experimental points. However, this influence, especially if the value of parameter is not far from its optimal value, is not so large that one or two Newton—Raphson iterations would yield a satisfactory solution, if the roots of the previous solution are taken as starting values.

Finally, it must be emphasized that in the present system the calculation of parameter errors using only those experimental points where the formation of the corresponding species is considerable, is especially justified and results in more reliable parameter errors.

REFERENCES

[1] ROSSOTTI, F. J. C., ROSSOTTI, H. S.: The Determination of Stability Constants, McGraw Hill, New York 1961
[2] BECK, M. T.: Chemistry of Complex Equilibria, Akadémiai Kiadó, Budapest 1970
[3] BURGER, K., GAIZER, F., NOSZÁL, B., PÉKLI, M., TAKÁCSI-NAGY, G.: Bioinorg. Chem., **7,** 335 (1977)
[4] BURGER, K., GAIZER, F., ZAY, I., PÉKLI, M., NOSZÁL, B.: J. Inorg. Nucl. Chem., **40,** 725 (1978)
[5] TOBIAS, S. T., YASUDA, M.: Inorg. Chem., **2,** 1307 (1962)
[6] SILLÉN, L. G.: Acta Chem. Scand., **16,** 159 (1962)
[7] LANSBURY, R. C., PRICE, V. E., SMEETH, A. G.: J. Chem. Soc., **1965,** 1896
[8] VACCA, A., ARENARE, D., PAOLETTI, P.: Inorg. Chem., **5,** 1384 (1966)
[9] PERRIN, D. P., SAYCE, I. G.: J. Chem. Soc. *(A)*, **1967,** 82
[10] SAYCE, I. G.: Talanta, **15,** 1397 (1968)
[11] KARLSON, F., VESTIN, R.: Chem. Scr., **2,** 207 (1972)
[12] SABATINI, A., VACCA, A.: J. Chem. Soc., Dalton Trans., **1972,** 1693
[13] ZUR NEDDEN, P., MERCINY, E., DUYCKAERTS, G.: Anal. Chim. Acta, **64,** 197 (1973)
[14] SABATINI, A., VACCA, A., GANS. P.: Talanta, **21,** 53 (1974)
[15] MASSOUMI, A., OVERVOLL, P., LANGMYHR, F. J.: Anal. Chim. Acta, **68,** 103 (1974)
[16] GANS, P., VACCA, A.: Talanta, **21,** 45 (1974)
[17] GANS, P., SABATINI, A., VACCA, A.: Inorg. Chim. Acta, **18,** 327 (1976)
[18] GAIZER, F.: Magy. Kém. Foly., **83,** 250 (1977)
[19] GAIZER, F.: Acta Chim. Acad. Sci. Hung., **103,** 355 (1980)
[20] GAIZER, F.: Coord. Chem. Rev., **27,** 195 (1979)
[21] INGRI, N., SILLÉN, L. G.: Acta Chem. Scand., **16,** 173 (1962)
[22] BURGER, K., ZAY, I., GAIZER, F., NOSZÁL, B.: Inorg. Chim. Acta, **34,** L 339 (1979)

Ferenc GAIZER H-6801 Hódmezővásárhely, IV., Lenin u. 15.

Acta Chimica Academiae Scientiarum Hungaricae, Tomus 103 (4), pp. 405—413 (1980)

STUDIES IN THE FIELD OF PYRIDAZINE COMPOUNDS, II*

DERIVATIVES OF [1,2,4]TRIAZOLO[4,3-*b*]PYRIDAZINE-3-CARBOXYLIC ACID

J. KOSÁRY and P. SOHÁR**

(Institute for Drug Research, Budapest)

Received March 9, 1979
Accepted for publication June 1, 1979

Derivatives of [1,2,4]triazolo[4,3-*b*]pyridazine-3-carboxylic acid (**1b—d, 6a—f**) have been synthesized from new hydrazones (**2a—d**) prepared from 3-hydrazino-6--chloropyridazine and glyoxylic acid derivatives. Intermediates (**5a—c**) of the ring closure of **2** by bromine in acetic acid were isolated. Reductive dechlorination of **1c** gave the triazoles **7—9** besides **6d.**

The [1,2,4]triazolo[4,3-*b*]pyridazine ring system was first reported by TAKAYASHI in 1955 [2]. Later on several derivatives [3] were described, however, the 3-carboxylic acid remained unpublished. Now some representatives of this type **1b—d**, have been prepared.

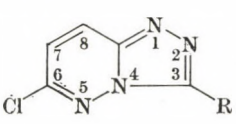

1

1a R=COOH
1b R=COOMe
1c R=COOEt
1d R=$CONH_2$
1e R=H

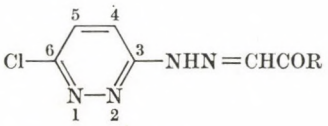

2

2a R=OH
2b R=OMe
2c R=OEt
2d R=NH_2

Compound **1c**, accompained by **2c**, was first isolated in our laboratory as a by-product from the following reaction:

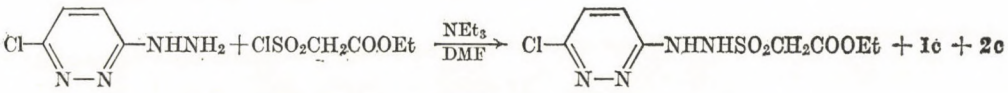

3 **4**

The structures **1b—d** are supported by their unambiguous synthesis. Condenzation of **3** with glyoxylic acid and ethyl glyoxalate yield **2a** and **2c**, respectively. Transesterification of **2c** gives **2b**, while treatment with methanolic ammonia of **2c** yields **2d**. Oxidative ring closure by bromine in acetic acid or by lead(IV) acetate [3] furnishes the compounds **1**. In the course of ring closure, **2a** underwent decarboxylation and, instead of **1a**, the known compound **1e** [2]

* For Part I, see Ref. [1]

** Present address: „EGYT" Pharmacochemical Works. Spectroscopic Department. H–1475 Budapest, P. O. Box 100

Table I

Characteristic IR and ^1H NMR data of compounds **1b—d, 2a—d, 4,**

Compound	IR (KBr)[b], cm^{-1}				^1H NMR,	
	νNH	νC=O	Skeletal vibr.[e]	Other bands	δCH_3[f] t (3H)	δCH_2[f] q a (2H)
1b[c]	—	1745 1735	840 830	—	—	—
1c[d]	—	1725	835	—	1.40	4.50
1d[d]	~ 3395 ~ 3305	1680[r]	830	βNH ~ 1630	—	—
2a[d]	~ 3240[i] ~ 2400[i] ~ 1880[i]	1695[i] 1575[i] 1415[i]	850	βNH ~ 1415	—	—
2b[d]	3200—2700	1735	850	—	—	—
2c[d]	3200—2700	1715	845	—	1.25	4.20
2d[d]	~3400, ~3360 3200—2700	1690[r]	845	βNH ~1600	—	—
4[d]	~3250 3200—2700	1725	845	ν_{as} SO_2 1350 ν_s SO_2 1150 δ SO_2 490	1.30	4.25
5b[c]	~3280	1725	845	βNH ~1490	1.40	4.40
6a[c]	~3320 ~3250	1660[r]	825	βNH 1560 ~1470	1.00[o]	—
6b[c]	—	1740 1730	825	νC—O[w] 1120 1115	—	—
6c[d]	3700—2700	1685[r]	830 810	ν C—O[w] 1120 βNH 1620	—	—
6d[c]	—	1725	820	—	1.50	4.60
6e[d]	~3380 3300—2700	1695[r]	820	βNH ~1620	—	—
6f[c]	—	1650[r]	810	ν C—O[w] 1110	—	—
7[d]	~3190 3300—2500	1705	—	νCN 2230 γ=CH[v] 720	1.40	4.45
8[d]	3300—2500	1740	—	νCN 2235	1.35	4.40
9[d]	~3220 3300—2500	1720	—	νCN 2260	1.35	4.40

5b, 6a—f, 7—9[a]

δ_{TMS} = 0 ppm[c,d]

δCH_3	δOCH_3 s (3H)	$\delta CH{=}N$ s (1H)	δH-6	δH-7 or H-5[g]	δH-8 or H-4[g]	δNH broad (1H)
—	4.15	—	—	7.40[h] (10)	8.30[h] (10)	—
—	—	—	—	7.70[h] (10)	8.65[h] (10)	—
—	—	—	—	7.65[h] (10)	8.60[h] (10)	~8.15 ~8.35
—	—	7.50	—	7.70*s* (2H)		~8.5[j]
—	3.80	7.55	—	7.80[h] (10)	7.65[h] (10)	?[k]
—	—	7.50	—	7.70[h] (10)	7.55 (10)	~12.3
—	—	7.40	—	8.05[h] (10)	7.75[h] (10)	~7.2[l] ~12.0
4.50[m]	—	—	—	7.70[h] (10)	7.30[h] (10)	~9.9[n]
—	—	—	—	7.70[h] (10)	7.55[h] (10)	~9.4
~1.7[p] ~3.6[q]	—	—	—	7.55[h] (10)	7.85[h] (10)	~8.1 ~9.1[r]
~3.6[s] ~3.9[t]	4.10	—	—	7.10[h] (10)	8.00[h] (10)	—
~3.6[s] ~3.8[t]	—	—	—	7.45[h] (10)	8.15[h] (10)	?[k]
—	—	—	8.75[u] (4, 2)	7.40[u] (9, 4)	8.35[u] (9, 2)	—
—	—	—	8.80[u] (5, 2)	7.50[u] (10, 5)	8.50[u] (10, 2)	~8.2[n,r]
~3.9[s,t]	—	—	8.55[u] (4, 2)	7.20[u] (10, 4)	8.20[u] (10, 2)	—
—	—	—	—	6.15[h] (12)	7.40[h] (12)	?[k]
—	—	—	—	6.65[h] (16)	7.65[h] (16)	?[k]
2.95[z] 3.15[z]	—	—	—	—	—	?[k]

was obtained. Treatment of **2b—d** with bromine first gives the intermediates **5a—c** from which the end-products can be obtained by short dehydrobromination with a base. By analogy with literature data [5, 6], TISLER [3b] proposed two alternative pathways for the cyclization with bromine.

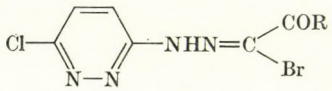

5

5a R=OMe

5b R=OEt

5c R=NH_2

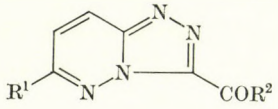

6

6a $R^1=R^2=n$-butilamino

6b R^1=morfolino, R^2=OMe

6c R^1=morfolino, $R^2=NH_2$

6d R^1=H, R^2=OEt

6e R^1=H, $R^2=NH_2$

6f R^1=H, R^2=morfolino

---

[a] Data for **5a** and **5c** are not included since, owing to their instability, the samples were always impure.

[b] νC—O type group frequencies of ester groups of compounds **1b,c**, **2b,c**, **4**, **5b**, **6b,d**, **7**, **8** and **9**, are in the ranges 1280—1150 and 1080—1020 cm^{-1}.

[c] In $CDCl_3$

[d] In DMSO-d_6

[e] Skeletal vibration bands of the pyridazine ring. Additional bands for the triazolopyridazines **1** and **6** were observed at 1580 ± 20, 1405 ± 15, 915 ± 10 and 750 ± 20 cm^{-1}, respectively

[f] $J = 7$ Hz

[g] Numbering H-7, H-8 is valid for **1** and **6**, numbering H-4, H-5 for **2**, **4** and **5**. With **7** and **8** the numbering of the parent pyridazine ring was retained; protons in alpha- and beta-position in respect to the triazole ring are identified as H-7 and H-8, respectively.

[h] The *A* and *B* part of an *AB* spectrum. Both *d* (1H), J_{AB} values [in Hz] are in parentheses.

[i] The IR spectrum of **2a** taken in KBr pellet showed that these molecules are partly present as zwitterions. The νNH (3240) and νC=O (1695) bands originate from molecules containing a carboxyl group, the νN^+H (2400, 1800) and νCO^- (1575, 1415) bands, in turn, from those present in the zwitterionic form.

[j] Overlapping broad signal (2H) for carboxylic—OH and amine—NH

[k] Overlapping signal for NH and water content of the solvent

[l] Amide —NH, *s* (2H)

[m] Signal for SO_2CH_2 group, *s* (2H)

[n] 2H

[o] 6H

[p] Signal for C—CH_2—CH_2—C group, *m* (4H)

[q] Signal for N—CH_2 group, *t* (2H)

[r] Amide group

[s] Signals for N—CH_2 group in the morpholine ring, *m* (4H)

[t] Signals for O—CH_2 group in the morpholine ring, *m* (4H)

[u] One of the three double dublets (3×1H) of the *AMX* spin system for H-6—8. Two coupling constants for each are given in parentheses [in Hz].

[v] γ(=CH) frequency, characteristic of *Z* 1,2-disubstituted ethylenes

[w] νC—O type band of the morpholine ring

[z] *A* and *B* part (2×2H) of the *AA'BB'*-type multiplet for the —CH_2—CH_2— group of the side chain.

The intermediacy of compounds **5** indicates that the first step is a substitution followed by the elimination of hydrogen bromide. The latter reaction requires a few days at room temperature, but it is very fast in the presence of base.

Since **1c** contains an ester group and an activated chlorine atom, it can be converted to **6a** by two moles of *n*-butylamine. With morpholine in methanol, the chlorine atom is substituted selectively, while the carbethoxy group only undergoes transesterification to give the methyl ester **6b**. Pure **1d** can only be prepared by ring closure from **2d**; aminolysis of the ester **1c** does not provide a homogeneous product.

Chlorine is readily removed from **1c** by reduction and the ethyl ester group in **6d** can then be smoothly subjected to aminolysis to obtain **6e** or **6f**.

In the course of the reductive dechlorination of **1c**, a series of interesting by-products (**7**—**9**) were formed whose structures were deduced from their IR and ^{1}H NMR spectra *(cf.* Table I).

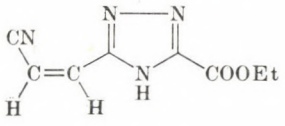

7

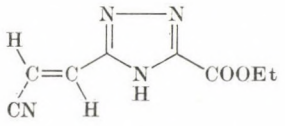

8

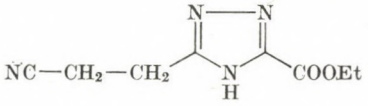

9

The formation of the nitriles **7**—**9** can be explained by cleavage of the N—N bond in the pyridazine ring to give **7** followed by isomerization or saturation of the double bond to yield **8** and **9**, respectively. An analogous photochemical cleavage of [1,2,4]triazolo[4,3-*b*]pyridazines (proceeding by free-radical mechanism) has been reported [7, 8]. The relative configurations of the geometrical isomers **7** and **8** are based on values of the vicinal coupling constants (12 Hz for **7** and 16 Hz for **8**), characteristic of *Z* and *E* olefins [9], respectively. Catalytic hydrogenation of both **7** and **8** gives **9**. In the course of the reduction **7** and **8** become equilibrated.

Experimental

M.p.'s are uncorrected. IR spectra were recorded in KBr pellets on a Perkin—Elmer 577 instrument. ^{1}H NMR spectra were taken on a VARIAN XL-100 FT and on a JEOL-60-HL instrument with TMS as internal standard, MS spectra on a VARIAN-MAT-SM-1 instrument.

Table II

	R_f	Molecular formula	Mol. weight	M.p., °C	Analyzis				
					C	H	N	Cl	Br
					Found (Calcd.)				
1b	0.35—0.40 (K—E, F)	$C_7H_5ClN_4O_2$	212.61	170	40.01 (39.54)	2.28 (2.37)	26.30 (26.35)	16.69 (16.67)	
1c	0.40—0.45 (E, F)	$C_8H_7ClN_4O_2$	226.64	168	42.35 (42.40)	3.20 (3.11)	24.68 (24.72)	15.65 (15.65)	
1d	0.25—0.30 (E, F)	$C_6H_4ClN_5O$	197.59	250			35.56 (35.45)	18.00 (17.94)	
1e	0.30—0.35 (K—E)	$C_5H_3ClN_4$	154.57	208 [1]			36.22 (36.24)	22.85 (22.93)	
2a	0.20—0.25 (M)	$C_6H_5ClN_4O_2$	200.59	248	35.91 (35.93)	2.55 (2.51)	28.01 (27.93)	17.66 (17.67)	
2b	0.60—0.65 (K—E)	$C_7H_7ClN_4O_2$	214.62	254	39.16 (39.17)	3.44 (3.29)	25.98 (26.11)	16.55 (16.52)	
2c	0.85—0.90 (E)	$C_8H_9ClN_4O_2$	228.65	224	42.00 (42.02)	4.05 (3.97)	24.47 (24.53)	15.49 (15.51)	
2d	0.25—0.30 (E)	$C_6H_6ClN_5O$	199.61	260			34.40 (35.20)	18.20 (17.80)	
3	0.70—0.75 (E)	$C_4H_5ClN_4$	144.57	140 [1]			38.74 (38.76)	24.01 (24.52)	
4	0.90—0.95 (E)	$C_8H_{11}ClN_4O_4S$	294.73	165	32.74 (32.55)	3.82 (3.72)	19.08 (19.00)	12.01 (12.05)	
5a		$C_7H_6BrClN_4O_2$	293.53	124			19.01 (19.09)	11.57 (12.08)	28.10 (27.22)
5b		$C_8H_8BrClN_4O_2$	307.57	125			18.10 (18.22)	11.10 (11.53)	26.00 (25.98)
5c		$C_6H_5BrClN_5O$	278.52	180	25.70 (25.87)	2.25 (1.80)	24.82 (25.14)	23.45 (25.46)	(Br+Cl, in Cl)
6a	0.50—0.55 (M)	$C_{14}H_{22}N_6O$	270.38	228			27.80 (28.94)		
6b	0.15—0.20 (E)	$C_{11}H_{13}N_5O_3$	263.26	222	50.02 (50.18)	4.98 (4.98)	26.40 (26.60)		
6c	0.45—0.50 (M)	$C_{10}H_{12}N_6O_2$	248.25	>260	48.52 (48.38)	5.01 (4.87)	32.92 (33.85)		
6d	0.60—0.65 (M, F)	$C_8H_8N_4O_2$	192.18	162	49.82 (49.83)	4.21 (4.19)	29.02 (29.15)		
6e	0.40—0.45 (M, F)	$C_6H_5N_5O$	163.15	245	45.01 (44.17)	4.17 (3.90)	41.47 (42.93)		
6f	0.50—0.55 (M)	$C_{10}H_{11}N_5O_2$	233.24	173			29.87 (30.03)		
7	0.65—0.70 (E)	$C_8H_8N_4O_2$	192.18	210	49.70 (49.83)	4.18 (4.19)	28.89 (29.15)		
8	0.60—0.65 (E)	$C_8H_8N_4O_2$	192.18	155	49.67 (49.83)	4.18 (4.19)	28.92 (29.15)		
9	0.40—0.45 (E)	$C_8H_{10}N_4O_2$	194.20	145	49.87 (49.47)	5.16 (5.19)	28.80 (28.85)		

Table III

Mass spectral data

Compound	$M+$ (rel. int.)	m/e (rel. int.)
1c	226 (17.5)	154 (100), 181 (39), 155 (25), 182 (22.5), 226 (17.5), 64 (10.5)
2c	228 (7)	155 (100), 73 (10), 228 (7), 20 (5), 183 (4), 129 (3.5), 75 (3.5)
6d	192 (23)	120 (100), 148 (26), 192 (23), 93 (21), 65 (16), 164 (2.5)
6e	163 (73)	120 (100), 163 (73), 147 (42), 93 (17), 65 (15), 64 (7), 135 (6)
8	192 (31)	120 (100), 147 (38), 192 (31), 79 (21), 148 (18), 149 (12)
9	194 (9.5)	122 (100), 81 (38), 149 (29), 150 (10), 126 (9.75), 194 (9.5), 148 (9), 154 (7.5)

TLC was performed on Kieselgel HF_{254} plates, with ethyl acetate (E), methanol (M), and chloroform–ethyl acetate (1 : 1) (K—E) as eluants; the spots were detected in UV light. Some of the substances showed violet fluorescence (F) when irradiated at 254 nm. Analytical data are compiled in Table II, the mass spectral data in Table III.

1-(Ethoxycarbonylmethylsulfonyl)-2-(6-chloro-3-pyridazinyl)hydrazine (4)

To a solution of **3** (28.9 g; 0.2 mole) [2] and dry triethylamine (20 g; 0.2 mole) in dichloromethane (400 ml), ethyl 2-chlorosulfonyl acetate (31.8 g; 0.17 mole) [10] was added dropwise at −5 °C. The mixture was stirred for 10 h at room temperature and boiled for 2 h. The solution was washed several times with water and evaporated. Trituration with isopropanol of the residue gave **4** (17.9 g; 30%)c.

1-Ethoxycarbonylmethylene-2-(6-chloro-3-pyridazinyl)hydrazine (2c)

(*a*) **2c** was isolated from the mother liquor of **4** by chromatography on a Kieselgel-40 column. First the contaminations were eluted with chloroform; **2c** (150 mg) was then the first fraction with ethyl acetate.

(*b*) A mixture of **3** (8.85 g; 0.061 mole), ethyl glyoxalate (3.08 g; 0.061 mole) [11] containing about 30% acetic acid and methanol (50 ml) was stirred at room temperature for 2 h. The product (10.1 g; 72.5%) crystallized directly, and it was in every respect identical with **2c**.

By the same method, **2a** was obtained in 80% yield.

1-Methoxycarbonylmethylene-2-(6-chloro-3-pyridazinyl)hydrazine (2b)

Compound **2c** (2.28 g; 0.01 mole) was refluxed for 2 h in methanol (100 ml) in the presence of triethylamine (0.02 mole); **2b** (2.1 g; 98%) crystallized on cooling overnight.

1-Aminocarbonylmethylene-2-(6-chloro-3-pyridazinyl)hydrazine (2d)

On stirring **2c** (2.28 g; 0.01 mole) in 7% methanolic ammonia (100 ml) for 3 days, **2d** (1.67 g; 84%) crystallized directly from the solution.

Ethyl 6-chloro-[1,2,4]triazolo[4,3-*b*]pyridazine-3-carboxylate (1c)

(*a*) **1c** (500 mg) was obtained as a second fraction on chromatography of the mother liquor of **4**.

(*b*) To a solution of **2c** (4.57 g; 0.02 mole) in acetic acid (40 ml) 90% lead (IV) acetate (5.6 g; 0.013 mole) was added in portions. Stirring was continued for 5 h, thereafter the solution was poured onto water (200 ml). Neutralization with solid $KHCO_3$, extraction with chloroform, evaporation and chromatography of the residue on Kieselgel-40 with chloroform–ethyl acetate (1 : 1) gave **1c** (1.19 g; 26%) besides unchanged **2c** (0.8 g).

(*c*) To a solution of **2c** (11.4 g; 0.05 mole) and sodium acetate (11 g), bromine (8 g; 0.05 mole) in acetic acid (10 ml) was added dropwise during 20 min. Stirring was continued for 3 h, the mixture diluted with water (1000 ml), the precipitated crystals were filtered off, washed with water and dried over phosphorus pentoxide to give 12.5 g (82%) of **5b**.

5b (12.5 g) was refluxed in isopropanol (200 ml) with triethylamine (5 ml) for 1 h. The solution was evaporated and the residue washed thoroughly with water to give a product (9.25 g; 77%) identical in every respect with **1c**.

Method (*c*) was applied to prepare **5a** (50%), **5c** (66%) and therefrom **1b** (41%) and **1d** (71%), respectively.

***N*-*n*-Butyl-6-*n*-butylamino-[1,2,4]triazolo[4,3-*b*]pyridazine-3-carboxamide (6a)**

1c (0.23 g; 1 mmole) was refluxed for 1 h with *n*-butylamine (1 ml) in methanol (10 ml). After evaporation in vacuum the residue was thoroughly washed with water to give **6a** (0.15 g; 52%).

Methyl 6-morpholino-[1,2,4]triazolo[4,3-*b*]pyridazine-3-carboxylate (6b)

1c (1.13 g; 5 mmoles) and morpholine (2 ml) were refluxed for 1 h in methanol (20 ml) of give **6b** (0.96 g; 73%) after workup as described for **6a**.

6-Morpholino-[1,2,4]triazolo[4,3-*b*]pyridazine-3-carboxamide (6c)

Refluxing of **1d** (100 mg; 0.5 mmole) and morpholine (0.2 ml) on isopropanol (5 ml) for 3 h gave **6c** (25 mg; 20%) after workup as described for **6a**.

Ethyl [1,2,4]triazolo[4,3-*b*]pyridazine-3-carboxylate (6d)

1c (6.75 g; 0.03 mole was hydrogenated in dimethylformamide (100 ml) in the presence of triethylamine (4.8 ml) and Pd-C catalyst. After evaporation of the solvent in vacuum the residue was chromatographed on Kieselgel-40 with ethyl acetate as eluant to give in this order **7** (0.50 g), **8** (0.37 g), **9** (0.96 g) and **6d** (2.82 g; 49%).

Ethyl 5-cyanoethyl-[1,3,4]triazole-2-carboxylate (9)

Hydrogenation of **8** (96 mg; 0.5 mmole) and subsequent chromatography as described for **6d**, gave **7** (25 mg), unchanged **8** (15 mg) and **9** (52 mg; 53%).

[1,2,4]Triazolo[4,3-*b*]pyridazine-3-carboxamide (6e)

Stirring of **6d** (0.96 g; 5 mmoles) in 7% methanolic ammonia (20 ml) for 3 h, evaporation in vacuum and trituration of the residue with acetone yielded **6e** (0.7 g; 86%).

[1,2,4]Triazolo[4,3-*b*]pyridazine-3-carboxylic acid morpholide (6f)

6d (0.37 g; 1.93 mmoles) was refluxed with morpholine (2 ml) and isopropanol (10 ml) for 5 h. Evaporation in vacuum and chromatography of the residue on Kieselgel-40 with methanol as eluant gave **6f** (0.35 g; 78%).

*

The authors are grateful to Mr. G. JERKOVICH for recording the mass spectra. Helpful discussions are acknowledged to Mr. E. KASZTREINER, technical assistance to Mrs. L. VASS, Miss É. RICHTER, Mrs. Zs. BIRÓ and Mr. A. FÜRJES.

REFERENCES

[1] KOSÁRY, J., BEHR, Á.: Magyar Kém. Folyóirat **85,** 469 (1979)
[2] TAKAHAYASHI, N.: J. Pharm. Soc. Jap., **75,** 1242 (1955)
[3a] MOSBY, W. L.: Heterocyclic Compounds. Systems with bridgehead nitrogen, II. pp. 870—873. Interscience Publishers, Inc. New York 1961
[3b] POLLAK, A., TISLER, M.: Tetrahedron, **22,** 2073 (1966)
[4] KRAMBERGER, L., LORENCAK, P., POLANC, S., VERCEK, B., STANOVNIK, B., TISLER, M., POVAZANEC, F.: J. Heterocycl. Chem., **12,** 337 (1975); BEZEG, A., STANOVNIK, B., SKET, B., TISLER, M.: J. Heterocycl. Chem., **9,** 1171 (1972); FRANCAVILLA, P., LAURIA, F.: J. Heterocycl. Chem., **8,** 415 (1971)
[5] GIBSON, M. S.: Tetrahedron, **19,** 1587 (1967)
[6] CHATTAWAY, F. D., WALKER, A. J.: J. Chem. Soc., **1925,** 975
[7] BRADSHAW, J. S. STANOVNIK, B., TISLER, M.: Tetrahedron Letters, **1973,** 2199
[8] BRADSHAW, J. S., TUELLER, J. E., BAXTER. S. L., MAAS, G. E., CARLOCK, J. T.: J. Heterocycl. Chem., **14,** 411 (1977)
[9] SOHÁR, P.: Mágneses Magrezonancia Spektroszkópia, p. 212. Akadémiai Kiadó, Budapest (1976)
[10] OLIVER, J. E., DEMIB, A. B.: Synthesis, **1975,** 321
[11] WOLF, F. J., WEIJLARD, J.: Organic Synthesis, Coll. Vol. **4,** 124 (1963)

Judit KOSÁRY H-1325 Budapest, P.O.Box 82.
Pál SOHÁR H-1475 Budapest, P.O.Box 100

Acta Chimica Academiae Scientiarum Hungaricae, Tomus 103 (4), pp. 415—420 (1980)

SYNTHESIS OF 7-[(HETEROARYL-THIO) ACETAMIDO]-3-DEACETOXYCEPHALOSPORANIC ACID DERIVATIVES, II*

LE NGOC PHAN[1], I. MISKOLCZI[2], F. SZTARICSKAI[1] and R. BOGNÁR[1]

([1] Research Group for Antibiotics, Hungarian Academy of Sciences and Institute of Organic Chemistry, Kossuth Lajos University, Debrecen, [2] Biogal Pharmaceutical Works, Debrecen)

Received April 13, 1979
Accepted for publication June 1, 1979

The ring-expansion reaction of 6-chloroacetamidopenicillanic acid-*S*-sulfoxide trichloroethyl ester (**I**) gave the corresponding deacetoxycephalosporin derivative (**II**). Removal of the trichloroethyl group of **II** with zinc–formic acid resulted in 7-chloroacetamido-3-deacetoxycephalosporanic acid (**III**).

By the reaction of mesyl- and tosyloxyacetic acid 8-quinolyl esters (**VIIIa, b**) with various heteroaryl-mercapto compounds the active esters **IXa—d** were synthesized. The latter compounds have been prepared and successfully used earlier for the acylation of 7-amino-3-deacetoxycephalosporanic acid (**IV**).

The nucleophilic replacement reaction of the mesyloxy- and tosyloxy group of 7-mesyloxy (**Va**)- or tosyloxyacetamido-3-deacetoxycephalosporanic acid (**Vb**) with heteroaryl-mercapto compounds offers a new route for synthesizing several 7-[(heteroaryl-thio)acetamido]-3-deacetoxycephalosporanic acids (**VIa—d**).

In our previous communication [1] the preparation and biological properties of some 7-[(heteroaryl-thio)acetamido]-3-deacetoxycephalosporanic acids were reported. For the synthesis of the latter compounds 7-chloroacetamido-3-deacetoxycephalosporanic acid (**III**), obtained by the acylation of 7-amino-3-deacetoxycephalosporanic acid (**IV**), was used. The preparation of **III** from penicillin sulfoxide esters has been known in the patent literature [2]; the ring expansion of 6-chloroacetamidopenicillanic acid-sulfoxide *p*-methoxybenzyl ester or of 6-trichloroacetamidopenicillanic acid-sulfoxide trichloroethyl ester led to the corresponding deacetoxycephalosporanic acid analogues. Removal of the *p*-methoxybenzyl group with trifluoroacetic acid or treatment of 7-trichloroacetamido-3-deacetoxycephalosporanic acid trichloroethyl ester with zinc–formic acid resulted in compound **III**.

In the present work 6-chloroacetamidopenicillanic acid sulfoxide trichloroethyl ester (**I**), prepared earlier in our laboratory [1], was used for the ring expansion reaction (Fig. 1). On refluxing **I** in benzene–dimethylacetamide in the presence of methanesulfonic acid, crystalline—7-chloroacetamido-3-deacetoxycephalosporanic acid trichloroethyl ester (**II**) was obtained in 41% yield. The physical properties (IR spectrum, decomposition point and TLC) of **II** were in good agreement with those of an authentic sample prepared earlier in an independent route [1]. Treatment of **II** with zinc–formic acid gave 7-chloro-

* Part I, see Ref. [1].

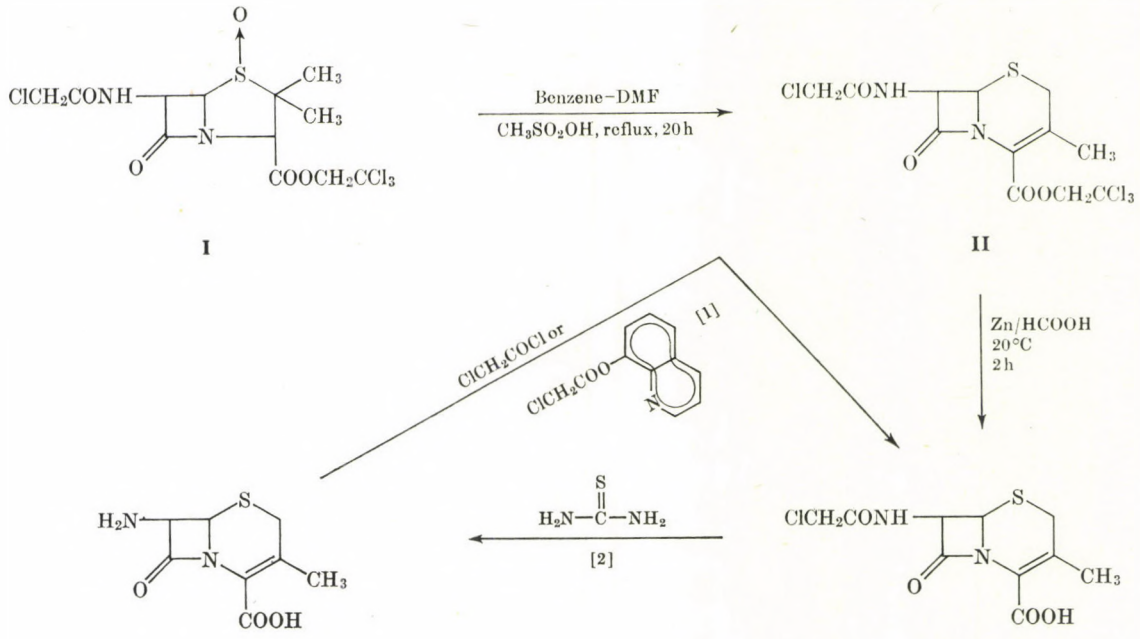

Fig. 1. Synthesis of 7-chloroacetamido-3-deacetoxycephalosporanic acid by ring expansion

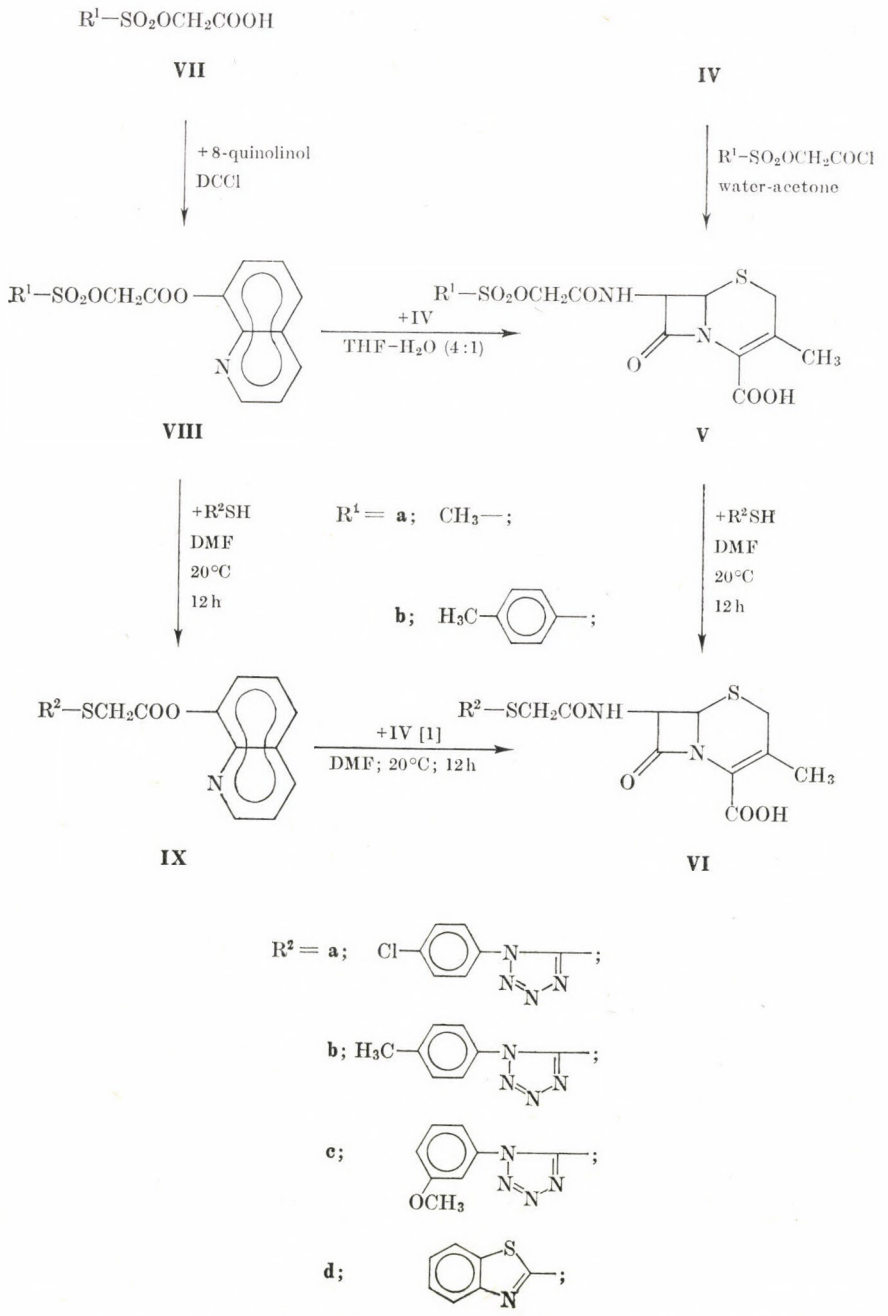

Fig. 2. **Synthesis of 7-[(heteroaryl-thio)acetamido]-3-deacetoxycephalosporanic acids**

acetamido-3-deacetoxycephalosporanic acid (**III**) in 60% yield. The reaction of **III** with thiourea, according to a known procedure [2], resulted in 75% of 7-amino-3-deacetoxycephalosporanic acid (**IV**).

Utilizing the commonly known high reactivity of the mesyl and tosyl esters of various organic compounds (*i.e.* carbohydrates, antibiotics or alkaloids) in nucleophilic replacement reactions, a new method was elaborated for the synthesis of 7-[(heteroaryl-thio)acetamido]-3-deacetoxycephalosporanic acid derivatives (**VIa—d**), as follows (Fig. 2).

Treatment of mesyl- or tosyloxyacetic acid (**VII**) [3] with 8-hydroxyquinoline in the presence of *N,N*-dicyclohexylcarbodiimide resulted in the active esters **VIIIa** and **VIIIb**, respectively. Reaction of **VIIIa** or **VIIIb** with several mercapto compounds (in *N,N*-dimethylformamide at room temperature) gave the corresponding heteroaryl-thioacetic acid quinolyl esters **IXa–d**. The physical characteristics of the prepared esters were in good agreement with those of the samples prepared earlier in an independent route [1], and the yields were also nearly the same.

Acylation of 7-amino-3-deacetoxycephalosporanic acid with the active esters **IXa, b, d** has been recently reported [1]. Acylation of **IV** with the ester **IXc** gave 37.7% of deacetoxycephalosporanic acid **VIc**.

The acylation of 7-amino-3-deacetoxycephalosporanic acid (**IV**) with either acyl chlorides or 8-quinolyl active esters gave 7-mesyloxy- (**Va**) and 7-tosyloxyacetamido-3-deacetoxycephalosporanic (**Vb**) acids. By nucleophilic replacement of the mesyloxy- or tosyloxy group in the latter compounds with heteroaryl-mercapto compounds, a new method was elaborated for the synthesis of several 7-[(heteroaryl-thio)acetamido]-3-deacetoxycephalosporanic acids (**VIa–d**). These compounds have been prepared earlier [1] starting with 7-chloroacetamido-3-deacetoxycephalosporanic acid (**III**).

On treatment of **Va** or **Vb** with several mercapto compounds in *N,N*-dimethylformamide at room temperature, the corresponding deacetoxycephalosporanic acid derivatives (**VIa—d**) were obtained in good yield. The structures of the prepared compounds were proved by comparison of their physical data (m.p. IR, TLC) with authentic samples.

Experimental

M. p.'s were determined in capillary tubes and were uncorrected. The IR spectra were recorded in KBr pellets with a UNICAM SP 200 G instrument. Thin-layer chromatography was carried out on DC-Alurolle Kieselgel 60 F 254 (Merck) layer, using (A) 7 : 3 : 1 benzene–ethyl acetate–acetic acid and (B) 1 : 1 benzene–ethyl acetate solvent mixtures. The spots were visualized with iodine vapour.

7-Chloroacetamido-3-deacetoxycephalosporanic acid trichloroethyl ester (II)

A solution of 6-chloroacetamidopenicillanic acid -*S*-sulfoxide trichloroethyl ester (**I**) (4.4 g; 0.01 mole) in benzene (450 ml) and *N,N*-dimethylacetamide (90 ml) was refluxed for 20 h. During this period (at 0, 6 and 12 h) 0.7 ml of methanesulfonic acid was added in portions,

and the mixture was continuously absolutized by the addition of "Klinosorb 4". The mixture was then distilled in vacuum to remove benzene, the dimethylacetamide solution was diluted with water to 200 ml and extracted with ethyl acetate. The organic layer was washed with water, dried over $MgSO_4$ and decolourized with carbon and Fuller's earth and finally evaporated to dryness. The residue was crystallized by the addition of ether (20 ml) to obtain 1.75 g (41.46%) of **II**, m.p. 120 °C, $R_f(A) = 0.9$, $R_f(B) = 0.88$.

The chromatographic mobility, m.p. and IR spectral data of the product were in good agreement with that of a sample prepared [1] by the acylation of 7-amino-3-deacetoxycephalosporanic acid trichloroethyl ester.

7-Chloroacetamido-3-deacetoxy-ceph-3-em-4-carboxylic acid (III)

To a solution of **II** (1.7 g; 0.004 mole) in 90% formic acid (30 ml) zinc dust (1.7 g) was added, and the mixture was stirred for 2 h at room temperature. The unchanged zinc dust was then removed by filtration, the filtrate was diluted with water to 100 ml and extracted with ethyl acetate. The organic layer was washed with water, dried over $MgSO_4$ and evaporated to dryness. The residue was crystallized from acetone–light petroleum to give **III** (0.7 g; 59.93%), m.p. 174 °C (dec.), $R_f(A) = 0.41$; $[\alpha]_D^{20} +127°$ ($c = 1$, dimethylformamide).

The physical characteristics (R_f, m.p., IR spectrum and $[\alpha]_D$) of **III** were in good agreement with that of an authentic sample prepared [1] by the acylation of **IV**.

7-Aminodeacetoxy-ceph-3-em-4-carboxylic acid (IV)

This compound was synthesized according to the patent procedure [2]. Re-acylation of the product **IV** with chloroacetyl chloride gave **III**.

Sulfonyloxyacetic acid 8-quinolyl esters (VIIIa,b)

A solution of 8-hydroxyquinoline (1.45 g; 0.01 mole) the sulfonyloxyacetic acid (**VIIa** or **VIIb**) (0.01 mole) and *N,N*-dicyclohexylcarbodiimide (2.06 g; 0.01 mole) in (*a*) ethyl acetate (50 ml) or (*b*) in dichloromethane (100 ml) was stirred at room temperature for 2 h. The precipitated dicyclohexylurea was removed by filtration and the filtrate evaporated to dryness in vacuum. The crystalline residue was recrystallized (*a*) from ether or (*b*) from ether–light petroleum to obtain pure **VIIIa** and **VIIIb**.

VIIIa 2.35 g (83.6%); m.p. 123 °C (dec.).

$C_{12}H_{11}O_5NS$ (281.28). Calcd. S 11.40; N 4.98. Found S 11.42, 11.32; N 5.09, 5.22%.

VIIIb 2.05 g (57.4%); m.p. 97–99 °C.

$C_{18}H_{15}O_5NS$ (357.37). Calcd. S 8.97; N 3.91. Found S 8.61, 8.47; N 3.97, 3.85%.

Heteroaryl-thioacetic acid 8-quinolyl esters (IXa—d)

A solution of 0.01 mole of the sulfonyloxyacetic acid 8-quinolyl ester (**VIIIa** or **VIIIb**), the required heteroaryl-mercapto compound (0.01 mole) and triethyl amine (1.4 ml) in *N,N*-dimethylformamide (20 ml) was allowed to stand at room temperature for 12 h. The reaction mixture was then diluted with water to 100 ml and extracted with ethyl acetate. The organic layer was washed with water, dried over $MgSO_4$ and concentrated. The residue was crystallized (**a**, **b**) from ether or (**c**, **d**) from ether–light petroleum.

IXa from **VIIIa**, 3.2 g (80.4%), m.p. 133 °C.
from **VIIIb**, 1.45 g (36.5%), m.p. 133 °C.

IXb from **VIIIa**, 2.0 g (53.19%), m.p. 130 °C.
from **VIIIb**, 1.29 g (34.2%), m.p. 130 °C.

IXc, prepared from chloroacetic acid 8-quinolyl ester [1], 2.05 g (72.1%), m.p. 88–91 °C.
$C_{19}H_{15}N_5O_3S$ (393.41). Calcd. S 8.15, N. 17.81. Found S 8.02, 7.93; N 17.72, 17.67%.

IXc, prepared from **VIIIa**, 1.8 g (45.8%), m.p. 88–91 °C.
from **VIIIb**, 1.6 g (40.7%), m.p. 88–91 °C.

IXb, prepared from **VIIIa**, 2.5 g (71.02%), m.p. 100–102 °C.
from **VIIIb**, 1.6 g (45.45%), m.p. 100–102 °C. The physical data (*i.e.* m.p., m.m.p. and *Rf*) of compounds **IXa—d** were in good agreement with that of authentic samples prepared [1] in an independent route.

7-(Sulfonyloxyacetamido)-3-deacetoxycephalosporanic acids (Va, b)

To a solution of **IV** (2.14 g; 0.01 mole), sodium hydrogen carbonate (2.5 g) in 2 : 3 water–acetone (250 ml), a solution of the corresponding acid chloride (0.011 mole) in acetone (10 ml) was added by drops. Acetone was then evaporated, the aqueous solution was acidified with dilute HCl to pH 2 and extracted with ethyl acetate. The organic layer was dried over $MgSO_4$ and evaporated to dryness in vacuum. The residue was crystallized (**a**) from methanol or (**b**) from acetone–water.

Va 1.8 g (51.4%), m.p. 163 °C (dec.).

$C_{11}H_{14}O_7N_2S_2$ (350.37). Calcd. S 18.30; N 7.99. Found S 18.31, 18.40 N 7.97, 7.85%.

IR (KBr): ν C=O (β-lactam) 1780; ν C=O (amide I) 1680; ν C=O (COOH) 1725; ν NH (amide) 3280 cm^{-1}.

Vb 2.02 g (47.41%), m.p. 162 °C (dec.).

$C_{17}H_{18}N_2O_7S_2$ (426.46). Calcd. S 15.03; N 6.57. Found S 15.00, 14.96; N 6.30, 6.22%.

IR (KBr): ν C=O (β-lactam) 1775; ν C=O (amide I) 1680; ν (COOH) 1725; NH (amide) 3285 cm^{-1}.

In the acylations of **IV** with the active esters (**VIII**), the yield of **Va** and **Vb** was 42.85 and 60.32% respectively.

7-[(Heteroaryl-thio)acetamido]-3-deacetoxyceph-3-em-4-carboxylic acids (VIa—d)

A solution of the 7-(sulfonyloxyacetamido)-3-deacetoxycephalosporanic acid (**Va** or **Vb**) (0.01 mole) and triethylamine (2.8 ml) in *N,N*-dimethylformamide (40 ml) was allowed to stand at room temperature for 12 h. The reaction mixture was then diluted with water to 100 ml and acidified to pH 2 with dilute hydrochloric acid. The solid precipitate was filtered off and recrystallized from the solvent given in Ref. [1].

VIa from **Va**, 2.0 g (42.90%), m.p. 185 °C (dec.).
from **Vb**, 2.3 g (49.3%), m.p. 185 °C (dec.).
VIb from **Va**, 2.8 g (62.90%), m.p. 185 °C (dec.).
from **Vb**, 1.6 g (36.10%), m.p. 185 °C (dec.).
VIc from **Va**, 2.6 g (56.50%), m.p. 178 °C (dec.).
from **Vb**, 2.0 g (43.5%), m.p. 178 °C (dec.).
VId from **Va**, 3.0 g (71.42%), m.p. 208 °C (dec.).
from **Vb**, 3.18 g (75.66%), m.p. 208 °C (dec.).

Compounds **VIa—d** were identical in every respect (m.p., m. m.p., chromatographic mobility, and IR spectrum) with the corresponding standard samples prepared earlier in an independent way.

*

The authors thank the Hungarian Academy of Sciences, the Biogal Pharmaceutical Works and also the CHINOIN Pharmaceutical Works for supporting this research.

REFERENCES

[1] Sztaricskai, F., Miskolczi, I., Bognár, R.: Acta Chim. Acad. Sci. Hung. **100,** 365 (1979)
[2] German Pat. 24. 42663 (1975); C. A., **83,** 43356a (1975) German Pat. 24. 42662 (1975); C. A., **83,** 43313k (1975)
[3] Lattrell, R., Lohaus, G.: Liebigs Ann. Chem., **1974,** 870
[4] Sztaricskai, F., Miskolczi, I., R., Farkas, E., Bognár, R.: Acta Chim. (Budapest) **94,** 169 (1977)

Rezső Bognár
Ferenc Sztaricskai
Le Ngoc Phan
H-4010 Debrecen, P.O.BOX 20.

István Miskolczi
H-4042 Debrecen, Pallagi út 13—15.

INDEX

PHYSICAL AND INORGANIC CHEMISTRY

ORGANIC CHEMISTRY

Printed in Hungary

A kiadásért felel az Akadémiai Kiadó igazgatója — Műszaki szerkesztő: Zacsik Annamária

A kézirat nyomdába érkezett: 1979. X. 10. — Terjedelem: 8,4 (A/5) ív, 37 ábra

80.7593 Akadémiai Nyomda, Budapest — Felelős vezető: Bernát György

ACTA CHIMICA

ТОМ 103 – ВЫП. 4

РЕЗЮМЕ

Окисление 3β-хлорохолест-5-ен-7-она по Бейер-Виллингеру

ШАФИУЛАХ и Э. А. ХАН

Окисление 3*β*-хлорохолест-5-ен-7-она (**1**) с помощью гидроперекиси бензоила (с 1 и 2 мольэквивалентами), используя моногидрат *п*-толуолсульфокислоты в качестве катализатора, дает 3*β*-хлоро-5,6 α-оксидо-5α-холестан-7-он (**2**), 3*β*-хлоро-7а-окса-В-хомохолест-5-ен-7-он (**3**), 3*β*-хлоро-5-формил-6-окса-5α-холестан-7-он (**4**) и 3*β*-хлоро-5-оксо-5,7-*секо*-6-норхолестан-7-кислоту (**5**). С тремя моль-эквивалентами гидроперекиси бензола **1** дает помимо 2—5, также 5-оксо-5,7-*секо*-6-норхолест-3-ен-7-кислоту (**6**). Кислоты **5** и **6** были превращены в их метиловые эфиры (**7**) и (**8**). Структура этих соединений была определена на основе их спектральных свойств, химических превращений и сравнения с подлинными образцами в известных случаях.

Стероидальные тетразолы конденсированные по кольцу А

ШАФИУЛЛАХ и М. А. ГАФФАРИ

Реакция 4-метилхолест-4-ен-3-она (**1**) с избытком гидразойной кислоты (BF_3-этерат в качестве катализатора) дает 3-аза-А-гомо-4а-метилхолест-4а-ен-4-он (**2**) и 3-аза-А-гомо-4а-метилхолест-4а-ено[3,4-*d*]тетразол (**3**). При подобных условиях реакции 4,4-диметилхолест-5-ен-3-он (**4**) дает 4,4-диметил-5α-холестан-3,6-дион (**5**) и 4-аза-А-гомо-4а,4*b*-диметилхолест-5-ено[4,3-*d*]тетразол (**6**). В реакции 4-моноэтильного аналога (**7**) соединения **1** были получены 3-аза-А-гомо-4а-этилхолест-4а-ено[3,4-*d*] тетразол · (**8**) и его 4-аза-изомер (8*a*), в то время как 4-диэтилхолест-5-ен-3-он аналог (**9**) соединения **4** дает 4,4-диэтил-3,4-*секо*-4*β*-азидохолест-5-ен-3-нитрил (**10**) и 4-аза-А-гомо-4а,4*b*-диэтилхолест-5-ено[4,3-*d*] тетразол (**11**). Структура этих соединений была определена, исходя из их спектральных свойств. Приводится механизм необычных первращений.

Отщепление фенольного гидроксила: превращение (-)-α-наркотина в (-)-β-гидрастин

П. КЕРЕКЕШ, ДЬ. ГААЛ и Р. БОГНАР

Природный (2)-α-наркотин был превращен в наркотолин-8-(1-фенил-5-тетразолил) эфир, который при каталитическом гидрировании дает (-)-*β*-гидрастин.

Реакции изомеров наркотина с бромистым цианом

П. КЕРЕКЕШ и ДЬ. ГААЛ

(-)-α-Наркотин (1*R*, 1'*S*) (**1**) и (+)-*β*-наркотин (1*S*, 1'*S*) (**4**) были подвергнуты взаимодействию с бромцианом в смеси растворителей тетрагидрофуран-вона, этанол-хлороформ и в присутствии окиси магния. Реакция обоих изомеров наркотина в смеси тетрагидрофуран-вода приводит к одинаковому продукту, а именно, к (-)-*N*-циано-1(*S*)-гидрокси-1,2-*секо*-1'(*S*)-наркотину (**5***a*). При использовании смеси этанол-хлороформ и, исходя из **1** и **4**, вновь был получен одинаковый продукт, а именно, (-)-*N*-циано-1(*S*)-этокси-1,2-*секо*-1'(*S*)-наркотин (**5***b*). Соответствующие знантомерные изомеры наркотина, а именно, (+)-α-наркотин (1S, 1'S) (*2*) и (-)-*β*-наркотин (1*R*, 1'*R*) (**3**) также дают знантомерные секо-соединения (**6***a* и **6***b*) в идентичных условиях реакции. Рефлексирование секосоединений с разбав-

ленной соляной кислотой приводит к циклизации, т. о. 5*a* и 5*b*, а также 6*a* и 6*b* были-первращены в основные продукты (+)-β-наркотин и (-)-β-наркотин, соответственно.

Была определена абсолютная конфигурация секо-соединений и были сделаны попытки интерпретации сетерохимического пути реакций раскрытия кольца и циклизации.

Оценка комплексных равновесий с помощью ЭВМ, I

Общая программа для оценки спектрофотометрических измерений равновесий

Ф. ГАЙЗЕР и М. МАТЭ

Для оценки спектрофотометрических измерений равновесий типа

$$qM + pL \pm rH^+ \rightleftharpoons M_qL_p(H^+)_{\pm r}$$

где r и/или q могут быть равными нулю, была разработана программа для ЭВМ, требующая малую меморию и с коротким временем пробега. Из экспериментальных данных T_L, T_M, $[H^+]$ и A программа рассчитывает, используя метод наименьших квадратов, константы образования и молярные коэффициенты экстинкции, дающие наилучшие совпадения с экспериментальными кривыми. Расчет оптимальных значений констант происходит с помощью метода Гаусса. Было найдено, что числовое дифференцирование по величинам 1 g β дает наилучшую конвергенцию.

Программа, составленная на языке AS A FORTRAN, в случае образования 9 комплексных частиц, способная и одновременному уточнению 2—5 параметров, исходя из данных, измеренных на трех длинах волн. Программа может быть легко расширена, и части ее в общей формулировке могут быть использованы также для оценки других измерений комплексных равновесий.

Исследование тозиловых и мезиловых производных в морфиновом ряду, XXII

Некоторые нуклеофильные реакции замещения 6-*O*-мезилнеопина

Ш. БЕРЕНИ, Ш. МАКЛЕЙТ, Р. БОГНАР и А. ТЕГДЕШ

Былсинтезирован 6-*O*-мезилнеопин, не известный в литературе, и исследованы его некоторые нуклеофильные реакции замещения. В результате были получены его 6β-хлор-, 6β-бром- и 6β-азидопроизводные, также не известные в литературе. Был получен простым путем и с хорошим выходом, упоминаемый в литературе лишь в качестве промежуточного продукта, 6-деметокситебаин, который, благодаря своему строению, имеет широкие возможности для целого ряда дальнейших ценных превращений. Для образования 6-деметокситебаина полагался механизм $_{SN}2$ + E. Строение полученных новых соединений было доказано с помощью ИК, ПМР, ЯМР—C^{13} исследований, а также на основе их химических превращений.

N-Деметилирование морфиновых алкалоидов. Получение норнеопина

Ш. ХОСТАФИ, Ш. МАКЛЕИТ и Р. БОГНАР

На основе анализа методов для *N*-деметилирования морфиновых алкалоидов были разработаны два пути получения до сих пор не известного норнеопина, исходя из неопина со строением аллиламина.

Был синтезирован не описанный до сих пор в литературе *N*-нитрозонорнеопин, гидролиз которого с помощью разбавленной соляной кислоты дает норнеопин. В связи с этим, снова было исследовано *N*-деметилирование кодеина и дегидрокодеина, описанное подобным образом.

Реакция неопина с диметиловым эфиром азодикарбоновой кислоты оказалась также пригодной для получения норнеопина. Последний метод обладает некоторыми преимуществами. Исследуя реакцию тебаина с диметиловым эфиром азодикарбоновой кислоты, описанную в литературе, были найдены те условия, при которых нортебаин может быть получен без тебаина.

Контроль реакций, катализированных металлами, VIII

Контрольная карта концентрации лиганда системы никель/бутадиен/дифенилфеноксифосфан

А. ШИШАК, Х. ШЕНКЛУН и П. ХЕЙМБАХ

Селективность гомогенной каталитической циклоолигомеризации бутадеина была исследована при изменении молярного отношения дифенилфеноксифосфан/никель ($[L]_0/[M]_0$) в интервале $10^{-5} \div 10^2$. При изображении распределения продуктов в зависимости от $lg([L]_0/[M]_0)$ (контрольная карта концентрации лиганда) были обанружены явления ассоциации лиганда для каталититечских промежуточных продуктов и связь каталитических циклов.

Прибор для исследования механо-реологических свойств гелей

Ф. ХОРКАИ, М. НАДЬ и М. ЗРИНИ

Был разработан прибор для определения механо-реологических параметров упругих тел с небольшой механической прочностью (напр., набухшие гели полимеров), который позволяет, в случае однонаправленного сжатия, одновременно и с высокой точностью ($\pm 1 \cdot 10^{-4}$ N, т. е. ± 6 м) измерять нагрузку и соответствующую ей деформацию в широком диапазоне (от $1 \cdot 10^{-4}$ N до 2 000 N, т. е. от 6 μм до 3,333 мм).

С помощью зависимостей нагрузка-деформация, определенных для гелей поливинилового спирта с различной степенью сшивки, были рассчитаны молекулярные параметры, характеризующие пространственную сетку, и количество цепей сшивки, действующих эластично. Было обнаружено, что экспериментально полученные величины значительно отличаются от результатов расчетов, соответствующих модели идеальной системы.

Расчет комплексных равновесий с помощью ЭВМ, II

Расчет констант протонитрования полифункциональных лигандов и констант стабильности металлистических комплексов из потенциометрических данных

Ф. ГАЙЗЕР

Была разработана программа ЭВМ для расчета констант протонирования больших молекул, способных связывать (выделять) большое число водородных ионов, а также для расчета констант стабильности металлических комплексов с составом M_qL_p. Настоящая программа PH—POT является вариантом программы автора SPEF-3 и предназначена для оценки потенциометрических измерений. С помощью этой программы из экспериментальных данных T_H, T_{OH}, T_L и E или T_M, T_L и E, соответственно, а также из констант кривой слепого pH-метрического титрования могут быть рассчитаны величины констант равновесия, получаемые при минимальной величине $\Sigma(\Delta E)^2$.

Исследования в области соединений с пиридазиновым кольцом, II

Производные [1,2,4]триазоло[4,3-*b*]пиридазин-3-карбоновой кислоты

Ю. КОШАРИ и П. ШОХАР

Были получено новые производные циклической системы [1,2,4] триазоло [4,3-*b*] пиридазина, содержащие функцию карбоновой кислоты в положении 3 (**1***b*—*d*; **6а**—*f*). Исходными соединениями служили до сих пор не известные гидразоны, образующиеся из 3-гидразино-6-хлорпиридазина с производными гликосальной кислоты (**2***a*—*d*). При циклизации 2 с помощью системы B_2—AcOH удалось изолировать также промежуточные продукты (**5***a*—*c*), которые в некоторой степени изменяют уже сложившиеся представления

относительно механизма циклизации. При восстановительном дегалогенировании 1*c* наряду с ожидаемым продуктом 6*d*, были изолированы неизвестные производные триазола **7—9**, строение которых было выяснено на основе их ИК и ЯМР—H^1 спектров.

Синтез 7-[(гетероарил-тио)ацетамидо]-3-деацетоксицефалоспорановой кислоты и ее производных, II

Л. Н. ФАН, И. МИШКОЛЬЦИ, Ф. СТАРИЧКАИ и Р. БОГНАР

С помощью реакции расширения кольца были получены трихлорэтильный эфир *S*-сулфоксида б-хлороацетамидопенициллановой кислоты (**I**) и соответствующее деацетоксицефалоспориновое производное (**II**). Удаление трихлороэтильной группы соединения **II** с помощью муравьинокислого цинка приводит к 7-хлороацетамидо-3-деацетоксицефалоспорановой кислоте (**III**).

За счет реакции 8-хинолиловых эфиров мезил- и тозилоксиуксусной кислоты (**VIIIa, b**) с различными гетероарилмеркаптановыми соединениями были синтезированы активные эфиры **IXa—d**. Последние соединения были получены и успешно использованы ранее для ацилирования 7-амино-3-деацетоксицефалоспорановой кислоты (**IV**).

Реакция нуклеофильного замещения мезилокси и тозилокси групп в 7-мезилокси- (**Va**) или в 7-тозилоксиацетамидо-3-деацетоксицефалоспорановой кислоте (**Vb**) с помощью гетероарилмеркаптановых соединений приводит к новому пути синтеза 7-[(гетероарилтио)-ацетамидо]-3-деацетоксицефалоспорановых кислот (**VIa—d**).

Les Acta Chimica paraissent en français, allemand, anglais et russe et publient des mémoires du domaine des sciences chimiques.

Les Acta Chimica sont publiés sous forme de fascicules. Quatre fascicules seront réunis en un volume (3 volumes par an).

On est prié d'envoyer les manuscrits destinés à la rédaction à l'adresse suivante:

Acta Chimica
Budapest, P.O.B. 67, H-1450, Hongrie

Toute correspondance doit être envoyée à cette même adresse.

La rédaction ne rend pas de manuscript.

Abonnement en Hongrie à l'Akadémiai Kiadó (1363 Budapest, P.O.B. 24, C. C. B. 215 11488), à l'étranger à l'Entreprise du Commerce Extérieur « Kultura » (H-1389 Budapest 62, P.O.B. 149 Compte-courant No. 218 10990) ou chez représentants à l'étranger.

Die Acta Chimica veröffentlichen Abhandlungen aus dem Bereich der chemischen Wissenschaften in deutscher, englischer, französischer und russischer Sprache.

Die Acta Chimica erscheinen in Heften wechselnden Umfanges. Vier Hefte bilden einen Band. Jährlich erscheinen 3 Bände.

Die zur Veröffentlichung bestimmten Manuskripte sind an folgende Adresse zu senden:

Acta Chimica
Budapest, Postfach 67, H-1450, Ungarn

An die gleiche Anschrift ist jede für die Redaktion bestimmte Korrespondenz zu richten:

Manuskripte werden nicht zurückerstattet.

Bestellbar für das Inland bei Akadémiai Kiadó (1363 Budapest, Postfach 24, Bankkonto Nr. 215 11488), für das Ausland bei »Kultura« Außenhandelsunternehmen (H-1389 Budapest 62, P.O.B. 149. Bankkonto Nr. 218 10990) oder seinen Auslandsvertretungen.

«Acta Chimica» издают статихи по химии на русском, английском, французском и немецком языках.

«Acta Chimica» выходит отдельными выпусками разного объекта, 4 выпуска составхяют один том и за год выподят 3 тома.

Предназначенные для публикации рукописи следует направлять по адресу:

Acta Chimica
Budapest, P.O.B. 67, H-1450, ВНР

Всякую корреспонденцию в редакцию направляйте по этому же адресу.

Редакция рукописей не возвращает.

Отечественные подписчики направляйте свои заявки по адресу Издательства Академии Наук (1363 Budapest, P.O.B. 24, Текущий счет 215 11488), а иностранные подписчики через организацию по внешней торговие «Kultura» (H-1389 Budapest 62, P.O.B. 149. Текущий счет 218 10990) или через ее заграничные представительства и уполномеченных.

Reviews of the Hungarian Academy of Sciences are obtainable at the following addresses:

AUSTRALIA
C.B.D. LIBRARY AND SUBSCRIPTION SERVICE, Box 4886, G.P.O., *Sydney N.S.W. 2001*
COSMOS BOOKSHOP, 145 Ackland Street, *St. Kilda (Melbourne), Victoria 3182*

AUSTRIA
GLOBUS, Höchstädtplatz 3, *1200 Wien XX*

BELGIUM
OFFICE INTERNATIONAL DE LIBRAIRIE, 30 Avenue Marnix, *1050 Bruxelles*
LIBRAIRIE DU MONDE ENTIER, 162 Rue du Midi, *1000 Bruxelles*

BULGARIA
HEMUS, Bulvar Ruski 6, *Sofia*

CANADA
PANNONIA BOOKS, P.O. Box 1017, Postal Station "B", *Toronto, Ontario M5T 2T*

CHINA
CNPICOR, Periodical Department, P.O. Box 50, *Peking*

CZECHOSLOVAKIA
MAD'ARSKÁ KULTURA, Národni třida 22, *115 33 Praha*
PNS DOVOZ TISKU, Vinohradská 46, *Praha 2*
PNS DOVOZ TLAČE, *Bratislava 2*

DENMARK
EJNAR MUNKSGAARD, Norregade 6, *1165 Copenhagen*

FINLAND
AKATEEMINEN KIRJAKAUPPA, P.O. Box 128, *SF-00101 Helsinki 10*

FRANCE
EUROPERIODIQUES S. A., 31 Avenue de Versailles, *78170 La Celle St.-Cloud*
LIBRAIRIE LAVOISIER, 11 rue Lavoisier, *75008 Pari*
OFFICE INTEHNATIONAL DE DOCUMENTATION ET LIBRAIRIE, 48 rue Gay-Lussac, *75240 Paris Cedex 05*

GERMAN DEMOCRATIC REPUBLIC
HAUS DER UNGARISCHEN KULTUR, Karl-Liebknecht-Strasse 9, *DDR-102 Berlin*
DEUTSCHE POST ZEITUNGSVERTRIEBSAMT, Strasse der Pariser Kommüne 3—4, *DDR-104 Berlin*

GERMAN FEDERAL REPUBLIC
KUNST UND WISSEN ERICH BIEBER, Postfach 46, *7000 Stuttgart 1*

GREAT BRITAIN
BLACKWELL'S PERIODICALS DIVISION, Hythe Bridge Street, *Oxford OX1 2ET*
BUMPUS, HALDANE AND MAXWELL LTD., Cowper Works, *Olney, Bucks MK46 4BN*
COLLET'S HOLDINGS LTD., Denington Estate. *Wellingborough, Northant NN8 2QT*
WM. DAWSON AND SONS LTD., Cannon House, *Folke tone, Kent CT19 5EE*
H. K. LEWIS AND CO., 136 Gower Street, *London WC1E 3BS*

GREECE
KOSTARAKIS BROTHERS, International Booksellers, 2 Hippokratous Street, *Athens-143*

HOLLAND
MEULENHOFF-BRUNA B.V., Beulingstraat 2, *Amsterdam*
MARTINUS NIJHOFF B.V., Lange Voorhout 9—11, *Den Haag*
SWETS SUBSCRIPTION SERVICE, 347b Heereweg, *Lisse*

INDIA
ALLIED PUBLISHING PRIVATE LTD., 13/14 Asaf Ali Road, *New Delhi 110001*
150 B-6 Mount Road, *Madras 600002*
INTERNATIONAL BOOK HOUSE PVT. LTD., Madame Cama Road, *Bombay 400039*
THE STATE TRADING CORPORATION OF INDIA LTD., Books Import Division, Chandralok, 36 Janpath, *New Delhi 110001*

ITALY
EUGENIO CARLUCCI, P.O. Box 252, *70100 Bari*
INTERSCIENTIA, Via Mazzé 28, *10149 Torino*
LIBRERIA COMMISSIONARIA SANSONI, Via Lamarmora 45, *50121 Firenze*
SANTO VANASIA, Via M. Macchi 58, *20124 Milano*
D. E. A., Via Lima 28, *00198 Roma*

JAPAN
KINOKUNIYA BOOK-STORE CO. LTD., 17-7 Shinjuku-ku 3 chome, Shinjuku-ku, *Tokyo 160-91*
MARUZEN COMPANY LTD., Book Department, P.O. Box 5050 Tokyo International, *Tokyo 100-31*
NAUKA LTD. IMPORT DEPARTMENT, 2-30-19 Minami Ikebukuro, Toshima-ku, *Tokyo 171*

KOREA
CHULPANMUL, *Phenjan*

NORWAY
TANUM-CAMMERMEYER, Karl Johansgatan 41—43, *1000 Oslo*

POLAND
WĘGIERSKI INSTYTUT KULTURY, Marszałkowska 80, *Warszawa*
CKP 1 W ul. Towarowa 28 *00-95 Warsawa*

ROUMANIA
D. E. P., *Bucureşti*
ROMLIBRI, Str. Biserica Amzei 7, *Bucureşti*

SOVIET UNION
SOJUZPETCHATJ — IMPORT, *Moscow*
and the post offices in each town
MEZHDUNARODNAYA KNIGA, *Moscow G-200*

SPAIN
DIAZ DE SANTOS, Lagasca 95, *Madrid 6*

SWEDEN
ALMQVIST AND WIKSELL, Gamla Brogatan 26, *101-20 Stockholm*
GUMPERTS UNIVERSITETSBOKHANDEL AB, Box 346, *401 25 Göteborg 1*

SWITZERLAND
KARGER LIBRI AG, Petersgraben 31, *4071 Basel*

USA
EBSCO SUBSCRIPTION SERVICES, P.O. Box 1943, *Birmingham, Alabama 35201*
F. W. FAXON COMPANY, INC., 15 Southwest Park, *Westwood, Mass, 02090*
THE MOORE-COTTRELL SUBSCRIPTION AGENCIES, *North Cohocton, N.Y. 14868*
READ-MORE PUBLICATIONS, INC., 140 Cedar Street, *New York, N. Y. 10006*
STECHERT-MACMILLAN, INC., 7250 Westfield Avenue, *Pennsauken N.J. 08110*

VIETNAM
XUNHASABA, 32, Hai Ba Trung, *Hanoi*

YUGOSLAVIA
JUGOSLAVENSKA KNJIGA, Terazije 27, *Beograd*
FORUM, Vojvode Mišića 1, *21000 Novi Sad*

30. V. 1980 HU ISSN 0001—5407 Index: 26.007